



**Università  
degli Studi  
di Ferrara**

**DOCTORAL COURSE IN  
"CHEMISTRY"**

CYCLE XXXI

DIRECTOR

Prof. Bignozzi Carlo Alberto

**Preparation and *in vitro* characterization  
of novel pharmaceutical and cosmetic formulations  
consisting of urea-crosslinked hyaluronic acid**

Scientific/Disciplinary Sector CHIM/08

**Candidate**

Dr. Fallacara Arianna

**Supervisor**

Prof. Manfredini Stefano

Years 2015/2018





*A mia madre e a mio padre*



*Per caso, ma non a caso?*

*“Questions of science, science and progress*

*Do not speak as loud as my heart”*

The Scientist, Coldplay



# ACKNOWLEDGMENTS

I miei ringraziamenti vanno, innanzitutto, al mio tutore accademico, il Professor Stefano Manfredini, per avermi dato la possibilità di fare un dottorato di ricerca presso l'Università degli Studi di Ferrara, e per avermi permesso di arricchirlo con un'esperienza all'estero, con un'esperienza aziendale, e con la partecipazione a tanti eventi, corsi di formazione e seminari in ambito farmaceutico e cosmetico.

Ringrazio la Professoressa Daniela Traini per avermi accolta durante il mio secondo anno di dottorato presso il suo brillante gruppo di ricerca del Woolcock Institute of Medical Research di Sydney, offrendomi così la possibilità di dare una sorprendente svolta al mio progetto di ricerca, e di vivere più serenamente un periodo difficile dal punto di vista lavorativo.

Ringrazio il Dottor Ugo Raffaello Citernesì dell'Istituto Ricerche Applicate (I.R.A. S.r.l.) per aver supportato con una borsa di studio il mio corso di dottorato, permettendomi così di continuare a lavorare sull'acido ialuronico in seguito alla mia tesi di laurea in CTF. Lo ringrazio anche per avermi permesso di fare uno stage, durante il mio terzo anno accademico, presso la sua azienda, facendo volgere il mio sguardo sugli ambiti aziendali: ricerca e sviluppo, regolatorio, produzione e controllo qualità.

Grazie alla Professoressa Paola Bergamini, che per me è un preziosissimo punto di riferimento, uno stimato esempio professionale e umano all'interno dell'Università degli Studi di Ferrara. Grazie per avermi ascoltata, incoraggiata e stimolata durante questi anni, per avermi supportata nel mio credere che fondamentali sono le qualità personali che vanno oltre la sfera professionale e deontologica, e che le ragioni del cuore superano tutte le altre.

Grazie alle belle persone che ho conosciuto nei laboratori dell'Università degli Studi di Ferrara, e che cito nell'ordine di incontro: Federica, Erika, Mattia, Filippo, Laura, Valentina, Piergiacomo ed Ernestine. In particolare, grazie ai miei laureandi, Filippo e Laura, che hanno avuto un ruolo importantissimo in questo mio percorso, e che oggi sono tra i miei più cari amici. Grazie Filippo e Laura per aver condiviso moltissimo con me; non avrei potuto avere "compagni di viaggio" migliori di voi.

Grazie al meraviglioso gruppo di ricerca del Woolcock Institute of Medical Research di Sydney per la calorosa e sorridente accoglienza. Grazie in particolare al Professore Paul M. Young, alla Dottoressa Hui Xin Ong e alla Dottoressa Maliheh Ghadiri. Grazie, soprattutto, al Dottor Michele Pozzoli, ricercatore che stimo tantissimo e che ha contribuito molto a questo lavoro di ricerca. Grazie, amico mio.

Grazie al personale di I.R.A. S.r.l. per avermi accolta positivamente in azienda.

Grazie alle Professoressa Rita Cortesi e Silvia Vertuani, e al Professore Alessandro Dalpiaz dell'Università degli Studi di Ferrara per avermi dato la possibilità di confrontarmi con loro quando ne ho avuto bisogno.

Grazie a Gabriele Bertocchi e alla Professoressa Paola Gilli dell'Università degli Studi di Ferrara per la loro gentilissima assistenza tecnica durante le analisi di diffrazione dei raggi X.

Un grazie speciale a tutti coloro che mi hanno sempre e da sempre supportata e amata.

Grazie alle mie amiche e ad i miei amici: in particolare, grazie a Krizia, Martina, Francesca, Bruna, Erika, Valeria, Marta, Shani, Sara Mariachiara, Sara, Stefano, Filomena, Claudia e Giorgio.

Grazie di cuore a Martina (Marti Parigi) per aver sempre creduto in me, e per avermi sempre mostrato stima, affetto e profonda amicizia. Dedico anche a te, con il cuore, questo lavoro.

Grazie a Michael, che ha un posto meraviglioso, unico ed assolutamente insostituibile nella mia vita, e che è sempre al mio fianco, nonostante tutto, e nonostante tutti.

Ringrazio le mie zie ed i miei zii, le mie cugine ed i miei cugini –in particolare zia Gianna e Rosalba- per l’interesse e l’affetto che hanno sempre mostrato nei miei confronti. Grazie per aver sempre creduto nelle mie capacità, e per aver sempre gioito dei miei successi, proprio come avrebbero fatto i nonni. Ringrazio i miei nonni perché mi hanno donato una famiglia tanto numerosa quanto unita e speciale.

Il mio più grande ringraziamento va ai miei genitori, Maria e Michele, e a mia sorella, Francesca, per l’amore incondizionato e la presenza costante. Grazie per avermi sostenuta in tutto ciò che ho dovuto affrontare intraprendendo questo percorso, e per avermi messa nelle condizioni di potercela fare. Grazie per avermi sempre ascoltata, e per aver fatto sì che alle mie paure rispondessi con il coraggio.

Infine, grazie a Dio per avermi dato il coraggio e la forza di affrontare questo percorso tanto entusiasmante quanto faticoso, e a me stessa, per aver saputo fare tesoro di questi doni.







# TABLE OF CONTENTS

LIST OF FIGURES AND TABLES .....	XIX
GLOSSARY AND ABBREVIATIONS.....	XXV
THESIS ABSTRACT.....	XXXI
RIASSUNTO DELLA TESI.....	XXXIII
CHAPTER 1 .....	1
1.1. General introduction and aims of the study .....	3
1.2. Structure of the thesis .....	4
1.2. References .....	6
CHAPTER 2 .....	9
2.0. Preface .....	11
2.1. Abstract.....	12
2.2. Introduction and historical background of HA.....	13
2.3. Physico-chemical, structural and hydrodynamic properties of HA .....	14
2.4. Biology of HA.....	17
2.4.1. <i>HA occurrence in living organism and diffusion in the human body</i> .....	17
2.4.2. <i>HA synthesis in the human body</i> .....	17
2.4.3. <i>HA degradation in the human body</i> .....	18
2.4.4. <i>Biological roles of HA in relation to its MW</i> .....	20
2.4.5. <i>Mechanisms of action of HA</i> .....	21
2.4.5.1. <i>HA cell surface receptors</i> .....	22
2.5. Industrial production of HA.....	24
2.6. Synthetic modifications of HA .....	25
2.6.1. <i>General introduction of the chemical approaches to modify HA</i> .....	25
2.6.2. <i>Modification of HA hydroxyl groups</i> .....	27
2.6.3. <i>Modification of HA carboxyl groups</i> .....	28
2.6.4. <i>Modification of HA N-acetyl groups</i> .....	29
2.7. Applications of HA and its derivatives.....	29
2.7.1. <i>Drug delivery systems</i> .....	30
2.7.2. <i>Cancer therapy</i> .....	32
2.7.3. <i>Wound treatment</i> .....	33
2.7.4. <i>Ophthalmologic surgery and ophthalmology</i> .....	33

2.7.5. <i>Arthrology</i> .....	34
2.7.6. <i>Rhinology and pneumology</i> .....	35
2.7.7. <i>Urology</i> .....	35
2.7.8. <i>Soft tissue regeneration</i> .....	35
2.7.9. <i>Cosmetics</i> .....	36
2.7.10. <i>Dietary</i> .....	36
2.7.11. <i>3D cell culture models</i> .....	38
<b>2.8. Conclusions, future trends and perspectives</b> .....	<b>40</b>
<b>2.9. Acknowledgments</b> .....	<b>41</b>
<b>2.10. Conflicts of interest</b> .....	<b>41</b>
<b>2.11. References</b> .....	<b>42</b>
<b>CHAPTER 3</b> .....	<b>63</b>
<b>3.0. Preface</b> .....	<b>65</b>
<b>3.1. Abstract</b> .....	<b>66</b>
<b>3.2. Introduction</b> .....	<b>67</b>
<b>3.3. Synthesis of HA-CL</b> .....	<b>68</b>
<b>3.4. Rheological characterization of HA-CL</b> .....	<b>69</b>
<b>3.5. References</b> .....	<b>71</b>
<b>CHAPTER 4</b> .....	<b>73</b>
<b>4.0. Preface</b> .....	<b>75</b>
<b>4.1. Abstract</b> .....	<b>76</b>
<b>4.2. Introduction</b> .....	<b>77</b>
<b>4.3. Materials and methods</b> .....	<b>78</b>
4.3.1. <i>Materials</i> .....	<b>78</b>
4.3.2. <i>Formulation of HA-CL solutions</i> .....	<b>78</b>
4.3.3. <i>Physical-chemical characterization and stability of HA-CL solutions</i> .....	<b>79</b>
4.3.4. <i>In vitro efficacy study</i> .....	<b>79</b>
4.3.4.1. <i>Experimental scheme</i> .....	<b>79</b>
4.3.4.2. <i>Cell cultures</i> .....	<b>79</b>
4.3.4.3. <i>Cell viability</i> .....	<b>80</b>
4.3.4.4. <i>IL-8 ELISA test</i> .....	<b>80</b>
4.3.4.5. <i>Epithelial corneal wound closure</i> .....	<b>80</b>
4.3.4.6. <i>Western blot analysis</i> .....	<b>81</b>

4.3.4.7. <i>Statistical analysis</i> .....	81
<b>4.4. Results and discussion</b> .....	<b>82</b>
4.4.1. <i>Synthesis of HA-CL</i> .....	82
4.4.2. <i>Physical-chemical characterization and stability of HA-CL solutions</i> .....	82
4.4.3. <i>Cell viability</i> .....	83
4.4.4. <i>Effect of HA-CL on IL-8 levels</i> .....	84
4.4.5. <i>Epithelial corneal wound closure</i> .....	85
4.4.6. <i>Cyclin D1 protein levels</i> .....	87
<b>4.5. Conclusions</b> .....	<b>87</b>
<b>4.6. Acknowledgments</b> .....	<b>88</b>
<b>4.7. Conflicts of interest</b> .....	<b>88</b>
<b>4.8. References</b> .....	<b>89</b>
<b>CHAPTER 5</b> .....	<b>93</b>
<b>5.0. Preface</b> .....	<b>95</b>
<b>5.1. Abstract</b> .....	<b>96</b>
<b>5.2. Introduction</b> .....	<b>97</b>
<b>5.3. Materials and methods</b> .....	<b>98</b>
5.3.1. <i>Preparation of hyaluronan and hyaluronan-SAP solutions (aqueous phases)</i> .....	99
5.3.2. <i>Characterization of hyaluronan and hyaluronan-SAP solutions: pH and     rheology</i> .....	99
5.3.3. <i>Formulation of HA and HA-CL microspheres containing or not SAP</i> .....	100
5.3.4. <i>MS yield, drug loading and encapsulation efficiency</i> .....	100
5.3.5. <i>Particle size analysis</i> .....	101
5.3.6. <i>SEM morphological analysis</i> .....	101
5.3.7. <i>X-ray powder diffraction</i> .....	101
5.3.8. <i>Thermal analysis (DSC and TGA)</i> .....	101
5.3.9. <i>Dynamic Vapour Sorption (DVS)</i> .....	102
5.3.10. <i>Solubility test</i> .....	102
5.3.11. <i>In vitro drug release studies</i> .....	102
5.3.11.1. <i>Dialysis</i> .....	102
5.3.11.2. <i>Franz cells</i> .....	103
5.3.12. <i>Drug release data analysis</i> .....	103
5.3.12.1. <i>Similarity and difference factors for SAP release profiles</i> .....	103

5.3.12.2. <i>Analysis of SAP release kinetics using mathematical models</i> .....	104
5.3.13. <i>Statistical analysis</i> .....	105
<b>5.4. Results and discussion</b> .....	<b>105</b>
5.4.1. <i>Preformulation study: evaluation and optimization of microspheres</i> .....	105
5.4.2. <i>Characterization of optimized microspheres</i> .....	109
5.4.2.1. <i>SEM morphological analysis</i> .....	109
5.4.2.2. <i>X-ray diffraction</i> .....	110
5.4.2.3. <i>Thermal analysis (DSC and TGA)</i> .....	111
5.4.2.4. <i>Dynamic Vapour Sorption (DVS)</i> .....	113
5.4.2.5. <i>SAP solubility</i> .....	114
5.4.2.6. <i>In vitro drug release studies and kinetic analysis</i> .....	114
<b>5.5. Conclusion</b> .....	<b>117</b>
<b>5.6. Patent resulting from the work reported in this manuscript</b> .....	<b>117</b>
<b>5.7. Authors contributions</b> .....	<b>117</b>
<b>5.8. Funding</b> .....	<b>118</b>
<b>5.9. Acknowledgements</b> .....	<b>118</b>
<b>5.10. Conflicts of interests</b> .....	<b>118</b>
The authors declare no conflict of interest. U.R.C. own stocks in I.R.A. srl. The funder had no role in the design of the study; in the collection, analyses, or interpretation of data; in the writing of the manuscript, and in the decision to publish the results. ....	118
<b>5.11. References</b> .....	<b>119</b>
<b>CHAPTER 6</b> .....	<b>127</b>
<b>6.0. Preface</b> .....	<b>129</b>
<b>6.1. Abstract</b> .....	<b>130</b>
<b>6.2. Introduction</b> .....	<b>131</b>
<b>6.3. Materials and methods</b> .....	<b>133</b>
6.3.1. <i>Materials</i> .....	133
6.3.2. <i>Preparation and physico-chemical characterization of hyaluronan and SAP samples</i> .....	133
6.3.3. <i>Cell culture</i> .....	134
6.3.4. <i>LDH and MTS cytotoxicity assays</i> .....	134
6.3.5. <i>Evaluation of epithelial barrier integrity</i> .....	136
6.3.6. <i>Pro-inflammatory markers expression</i> .....	136
6.3.7. <i>Analysis of intracellular reactive oxygen species (ROS)</i> .....	137

6.3.8. <i>Electric cell-substrate impedance sensing (ECIS) wound healing assay</i> .....	137
6.3.9. <i>Statistical analysis</i> .....	137
6.4. <b>Results and discussion</b> .....	138
6.4.1. <i>Physico-chemical properties of hyaluronan and SAP solutions</i> .....	138
6.4.2. <i>LDH and MTS cytotoxicity assays</i> .....	139
6.4.3. <i>Evaluation of epithelial barrier integrity</i> .....	140
6.4.4. <i>Pro-inflammatory markers expression</i> .....	141
6.4.5. <i>Analysis of intracellular ROS</i> .....	143
6.4.6. <i>Electric cell-substrate impedance sensing wound healing assay</i> .....	145
6.5. <b>Conclusions</b> .....	147
6.6. <b>Acknowledgements</b> .....	147
6.7. <b>Conflicts of interests</b> .....	147
6.8. <b>References</b> .....	148
CHAPTER 7 .....	159
7.0. <b>Preface</b> .....	161
7.1. <b>Abstract</b> .....	162
7.2. <b>Introduction</b> .....	163
7.3. <b>Materials and methods</b> .....	164
7.3.1. <i>Materials</i> .....	164
7.3.2. <i>Preparation of spray-dried hyaluronan–SAP formulations</i> .....	164
7.3.3. <i>Yield, encapsulation efficiency and drug loading of hyaluronan–SAP formulations</i> .....	165
7.3.4. <i>Morphological analysis</i> .....	165
7.3.5. <i>Particle size analysis</i> .....	165
7.3.6. <i>Thermal analysis</i> .....	166
7.3.7. <i>Moisture sorption and stability</i> .....	166
7.3.8. <i>In vitro aerosol performance</i> .....	166
7.3.9. <i>In vitro SAP release study</i> .....	167
7.3.10. <i>Cell culture and establishment of an air-interface Calu-3 cell model</i> .....	167
7.3.11. <i>In vitro SAP diffusion/transport study using air-interface Calu-3 cell culture</i> .....	167
7.3.12. <i>Statistical analysis</i> .....	168
7.4. <b>Results and discussion</b> .....	169

7.4.1. <i>Yield, drug loading and encapsulation efficiency of hyaluronan–SAP formulations</i> .....	169
7.4.2. <i>Morphological analysis</i> .....	170
7.4.3. <i>Particle size analysis</i> .....	170
7.4.4. <i>Thermal analysis</i> .....	171
7.4.5. <i>Moisture sorption and stability</i> .....	172
7.4.6. <i>In vitro aerosol performance</i> .....	173
7.4.7. <i>In vitro SAP release studies</i> .....	174
7.5. <b>Conclusions</b> .....	176
7.6. <b>Acknowledgements</b> .....	176
7.7. <b>Conflicts of interests</b> .....	176
7.8. <b>References</b> .....	177
<b>CHAPTER 8</b> .....	<b>183</b>
8.0. <b>Preface</b> .....	<b>185</b>
8.1. <b>Abstract</b> .....	<b>186</b>
8.2. <b>Introduction</b> .....	<b>187</b>
8.3. <b>Materials and Methods</b> .....	<b>188</b>
8.3.1. <i>Materials</i> .....	<b>188</b>
8.3.2. <i>Preparation of the freeze-dried formulation</i> .....	<b>189</b>
8.3.3. <i>Physico-chemical characterization</i> .....	<b>189</b>
8.3.3.1. <i>Chemical quantification of SAP by high-performance liquid chromatography</i> .....	189
8.3.3.2. <i>Morphological analysis</i> .....	190
8.3.3.3. <i>Particle size analysis</i> .....	190
8.3.3.4. <i>Thermal analysis</i> .....	190
8.3.3.5. <i>In vitro SAP release study</i> .....	190
8.3.3.6. <i>Aerosol performance by cascade impaction</i> .....	191
8.3.3.7. <i>In-line geometric aerosol laser diffraction analysis</i> .....	191
8.3.4. <i>In vitro biological studies on nasal cell models</i> .....	<b>191</b>
8.3.4.1. <i>Cultivation of RPMI 2650 cell line</i> .....	192
8.3.4.2. <i>MTS cytotoxicity assay on RPMI 2650 cells</i> .....	192
8.3.4.3. <i>Deposition/transport study on RPMI 2650 cells</i> .....	192
8.3.4.4. <i>Physical injury and wound healing assay on RPMI 2650 cells</i> .....	193

8.3.4.5. <i>Sampling, expansion and ALI cultivation of brushed nasal epithelial cells</i> .....	193
8.3.4.6. <i>Pro-inflammatory IL-8 expression in brushed nasal epithelial cells</i>	194
8.3.5. <i>Statistical analysis</i> .....	195
<b>8.4. Results and discussion</b> .....	<b>195</b>
8.4.1. <i>Physico-chemical characterization</i> .....	196
8.4.1.1. <i>Morphological analysis</i> .....	196
8.4.1.2. <i>Particle size analysis</i> .....	196
8.4.1.3. <i>Thermal analysis</i> .....	197
8.4.1.4. <i>In vitro aerosolization performance</i> .....	197
8.4.2. <i>In vitro studies on nasal cell models</i> .....	199
8.4.2.1. <i>MTS cytotoxicity assay on RPMI 2650 cells</i> .....	199
8.4.2.2. <i>Wound healing assay on RPMI 2650 cells</i> .....	199
8.4.2.3. <i>Pro-inflammatory IL-8 expression in brushed nasal epithelial cells</i>	200
8.4.3. <i>In vitro release study: release by Franz's cells and transport across RPMI 2650 cells</i> .....	201
<b>8.5. Conclusions</b> .....	<b>202</b>
<b>8.6. Disclosure</b> .....	<b>203</b>
<b>8.7. Acknowledgements</b> .....	<b>203</b>
<b>8.8. References</b> .....	<b>204</b>
<b>CHAPTER 9</b> .....	<b>213</b>
<b>9.1. General conclusions</b> .....	<b>215</b>
<b>9.2. Future perspectives</b> .....	<b>216</b>
<b>APPENDICES</b> .....	<b>219</b>
<b>A.1. Publications list</b> .....	<b>219</b>
<i>A.1.1. Journal articles included as thesis chapters</i> .....	219
<i>A.1.2. Other publications, patents and conference proceedings during candidacy</i>	311
<i>A.1.3. Copyrights permissions</i> .....	378





# LIST OF FIGURES AND TABLES

Figure 2.1. Chemical structures of HA disaccharide unit (A) and HA tetrasaccharide unit where the hydrophilic functional groups and the hydrophobic moieties are respectively evidenced in blue and yellow, while the hydrogen bonds are represented by green dashed lines (B). .....	15
Figure 2.2. Shear-thinning and non-thixotropic behavior of 0.5% HA solution (2 MDa) analyzed using the rotational rheometer AR2000 (TA instruments, New Castle, DE, USA), connected to the Rheology Advantage software (Version V7.20) and equipped with an aluminium cone/plate geometry (diameter 40 mm, angle 2°, 64- $\mu$ m truncation). The viscosity decreases in response to gradual increases of the shear rate over time (upward ramp), and then, the viscosity increases in response to gradual decreases of the shear rate over time (downward ramp). The initial viscosity is recovered through the same intermediate states of the breakdown process: the breakdown of the polymeric network is transient and reversible, and therefore, the original structure of HA is recovered. ....	16
Figure 2.3. Schematic diagram showing HA key steps from its synthesis to its degradation..	18
Figure 2.4. Summary of HA cell surface receptors and of the actions that they control when linked by HA. ....	22
Figure 2.5. Chemical modifications of HA: conjugation and crosslinking (A). HA forms used for pharmaceutical, medical, food and cosmetic applications: native, conjugated and crosslinked (B). ....	26
Figure 2.6. Medical, pharmaceutical, cosmetic and dietary applications of HA and its derivatives. ....	30
Table 2.1. Summary of the medical, pharmaceutical, cosmetic and dietary applications of HA and its derivatives, reporting some examples, the beneficial actions, the key features and the state of the art. ....	39
Table 2.2. Data on hyaluronan patents resulting from the database Questel (Paris, France)...	40
Figure 3.1. Synthesis of HA-CL with urea (Fallacara et al., 2017b). ....	68
Figure 3.2. Flow curves of HA-CL and lyophilized HA-CL, showing the viscosity ( $\eta$ ) as a function of the shear rate ( $\dot{\gamma}$ ). ....	69
Figure 3.3. Amplitude sweep test of HA-CL and lyophilized HA-CL, showing the storage ( $G'$ ) and loss ( $G''$ ) moduli as a function of the strain ( $\gamma$ ). ....	70
Figure 3.4. Frequency sweep test of HA-CL and lyophilized HA-CL, showing the storage ( $G'$ ) and loss ( $G''$ ) moduli as a function of the angular frequency ( $\omega$ ). ....	70
Figure 4.1. Synthesis of HA-CL with urea.....	82

Table 4.1. Stability of S1 and S2 during 6 months, at $23 \pm 2^\circ\text{C}$ and at $40 \pm 2^\circ\text{C}$ : pH and viscosity values. ....	82
Table 4.2. Cell viability (MTT test) of CTR-, CTR+, S1 and S2 at 48 and 72 h.....	83
Table 4.3. Anova and Tukey-Kramer test statistical analysis of cell viability (MTT test) of the conditions CTR-, CTR+, S1 and S2 at 48 and 72 h (statistically significant values in bold, $p < 0.05$ ). ....	84
Table 4.4. IL-8 levels in CTR-, CTR+, S1 and S2 tissues assessed at 48 and 72 h by ELISA test. ....	84
Table 4.5. Anova and Tukey-Kramer test statistical analysis of IL-8 levels in CTR-, CTR+, S1 and S2 tissues at 48 h (statistically significant values in bold, $p < 0.05$ ). ....	85
Figure 4.2. Histological analysis (HE staining) of 3D reconstructed tissues of human corneal epithelium. After wounding, HCE cells were incubated in growth medium with or without S1 and S2 for 72 h. Representative images from each group were recorded at 48 and 72 h post-wounding.....	85
Figure 4.3. In vitro wound healing assay of human corneal epithelial cells. After the scratch, HCEpiC cells were incubated in fresh medium with or without S1 and S2 for 36 h. Representative images from each group were recorded at 0, 12, 24 and 36 h post-scratching. The red lines indicate the wound borders.....	86
Figure 4.4. Quantification of wound healing in human corneal epithelial cells. The relative scratch gap was calculated as the percentage of the remaining wounded area at the given time point compared with the initially wounded area at 0 h. Data were expressed as mean $\pm$ SD ( $n = 3$ ). * $P < 0.05$ compared with control. ....	86
Figure 4.5. Effect of S1 and S2 on the proliferative marker cyclin D1 in HCEpiC cells. The graph shows the cyclin D1 protein levels in HCEpiC cells treated with S1 or S2 for 12 h. Data are means $\pm$ SD of triplicate. * indicates statistically significant difference from untreated control at 0 h; $^{\S}$ indicates statistically significant difference from untreated control at 12 h (one-way ANOVA, $P < 0.05$ ).....	87
Figure. 5.1. Shear-thinning behaviour of hyaluronan solutions: viscosity as a function of shear rate ( $n = 3$ , $\pm$ SD).....	106
Table 5.1. Main properties of HA solutions: pH, $\eta_0$ , $G'_{1\text{Hz}}$ , $C_f$ ( $n = 3$ , $\pm$ SD). ....	107
Table 5.2. Effect of emulsification time, polymer type and SAP presence on MS properties ( $n = 3$ , $\pm$ SD).....	108
Figure 5.2. Particle size distribution of hyaluronan MS produced after 60 minutes of emulsification ( $n = 3$ , $\pm$ SD).....	109

Figure 5.3. SEM micrographs of hyaluronan MS produced after 60 minutes of emulsification: HA (a), HA - SAP (b), HA-CL (c), HA-CL – SAP (d).....	110
Figure 5.4. X-ray diffraction patterns of: SAP (a), HA MS (b), HA-CL MS (c), HA – SAP MS (d), HA-CL – SAP MS (e). .....	111
Figure 5.5. DSC thermal profiles of: SAP (a), HA MS (b), HA-CL MS (c), HA – SAP MS (d), HA-CL – SAP MS (e). .....	112
Figure 5.6. TGA thermograms of: SAP (a), HA MS (b), HA-CL MS (c), HA – SAP MS (d), HA-CL – SAP MS (e). .....	113
Figure 5.7. DVS isotherms of the first cycle sorption-desorption for: SAP (a), HA MS and HA - SAP MS (b), HA-CL MS and HA-CL – SAP MS (c). .....	114
Figure 5.8. Diffusion profile of SAP as free drug and release profile of SAP from HA and HA-CL MS investigated by dialysis (a) and Franz diffusion cells (b).....	115
Table 5.3. Similarity factors ( $f_2$ ) and difference factors ( $f_1$ ) for free SAP and MS formulations. ....	116
Table 5.4. Correlation coefficient for Zero order, First order, Higuchi and Korsmeyer-Peppas models for SAP dissolution profiles obtained with Franz diffusion cell method. ....	117
Figure 6.1. Chemical structures of SAP, HA and HA-CL. ....	132
Table 6.1. Physico-chemical properties (pH, osmolality and viscosity) of: 0.15–0.45% (w/v) HA – SAP and HA-CL – SAP, 0.45% (w/v) SAP, 0.15% (w/v) HA and HA-CL solutions (n = 3 ± StDev). ....	139
Figure 6.2. Viabilities of Calu-3 cells evaluated using: (A) LDH assay and (B) MTS assay after 24 h of treatment with sample solutions. Data represent mean ± standard deviation (n = 3). Asterisks indicate significant difference from control untreated cells (****P < 0.0001). .....	139
Figure 6.3. Transepithelial electrical resistance (TEER, normalized resistance values) of Calu-3 cells after 4 h of treatment with 0.15–0.45% (w/v) hyaluronan-SAP, 0.45% (w/v) SAP, 0.15% (w/v) HA and HA-CL solutions compared to untreated cells (control). Data represent mean ± standard deviation (n = 3). .....	140
Figure 6.4. Concentration of IL-6 inflammatory cytokine in unstimulated Calu-3 cells supernatant after 24 h of exposure to 0.15–0.45% (w/v) hyaluronan-SAP, 0.45% (w/v) SAP, 0.15% (w/v) HA and HA-CL solutions, evaluated in comparison to untreated cells and cells treated with 10 ng/mL LPS (positive control). Data represent mean ± standard deviation (n = 3). Asterisks indicate significant difference from untreated cells control (****P < 0.0001). .....	142
Figure 6.5. Concentration of IL-6 inflammatory cytokine in Calu-3 cells supernatant stimulated with 10 ng/ mL LPS and then exposed for 24 h to 0.15–0.45% (w/v) hyaluronan-SAP, 0.45% (w/v) SAP, 0.15% (w/v) HA and HA-CL solutions, evaluated in comparison to	

untreated LPS-stimulated cells (control). Data represent mean  $\pm$  standard deviation (n = 3). Asterisks indicate significant difference from untreated cells control (\*P < 0.05 and \*\*P < 0.01)..... 143

Figure 6.6. Oxidative effects of 0.15–0.45% (w/v) hyaluronan-SAP, 0.45% (w/v) SAP, 0.15% (w/v) HA, 0.15% (w/v) HA-CL solutions, and controls (untreated cells, 0.03% H<sub>2</sub>O<sub>2</sub>, 1mM L-ascorbic acid) on intracellular ROS production (%) in Calu-3 cells. Data represent mean  $\pm$  standard deviation (n=3). Asterisks indicate significant differences from untreated cells control (A) and from HA-CL - SAP (B), with \*P < 0.05, \*\*P < 0.01, \*\*\*P < 0.001 and \*\*\*\*P < 0.0001..... 144

Figure 6.7. Intracellular ROS production (%) in Calu-3 cells stimulated with 10 ng/mL LPS and then exposed to 0.15–0.45% (w/v) hyaluronan- SAP, 0.45% (w/v) SAP, 0.15% (w/v) HA and HA-CL solutions, evaluated in comparison to untreated control (stimulated but untreated cells). Data represent mean  $\pm$  standard deviation (n=3). Asterisks indicate significant differences from untreated cells control (A) and from HA-CL – SAP (B), with \*P < 0.05, \*\*P < 0.01, \*\*\*P < 0.001 and \*\*\*\*P < 0.0001..... 145

Figure 6.8. Wound healing ability of 0.15–0.45% (w/v) hyaluronan-SAP, 0.45% (w/v) SAP, 0.15% (w/v) HA and HA-CL solutions on Calu-3 monolayers wounded with an electrical current (2000  $\mu$ A, 60 s, 100 kHz) applied using the ECIS system. For each sample, the time required for wound closure (vertical dashed line) was calculated as difference from the time employed by control cells (wounded but untreated –vertical dashed line in bold) (A) and additionally reported as absolute time to restore epithelial integrity (B)...... 146

Table 7.1. Yield (Y%), encapsulation efficiency (EE%) and drug loading (DL%) of hyaluronan-SAP formulations. Data represent mean  $\pm$  SD (n = 3)..... 170

Figure 7.1. Scanning electron microscope images of SD formulations: HA – SAP (A) and HA-CL – SAP (B)...... 170

Figure 7.2. Particle size distribution of SD HA – SAP (black line) and SD HA-CL – SAP (grey line) analyzed using dry dispersion system of laser diffraction. Data represent mean  $\pm$  SD (n = 3)...... 171

Figure 7.3. DSC thermograms of SD HA – SAP (continuous line) and SD HA-CL – SAP (dashed line)...... 172

Figure 7.4. DVS isotherms of the first (black lines) and second (grey lines) cycles of moisture sorption (continuous lines) and desorption (dashed lines) for SD HA – SAP (A) and HA - CL – SAP (B)...... 173

Figure 7.5. *In vitro* aerosol stage deposition of SD HA – SAP (black bars) and SD HA - CL - SAP (grey bars) using the MSLI at a flow rate of 60 L/min. Data represent mean  $\pm$  SD (n = 3)...... 174

Figure 7.6. <i>In vitro</i> SAP release profiles of SD HA – SAP (black curve) and SD HA - CL - SAP (grey curve) using Franz cells (A) air-interface Calu-3 cell model (B). Data represent mean $\pm$ SD (n = 3). .....	175
Figure 7.7. Percentage of total SAP remaining on the cell surface, inside the cells or transported to the basal compartment from SD HA – SAP (black bars) and SD HA - CL - SAP (grey bars), after 4 h. Data represent mean $\pm$ SD (n = 3). .....	176
Figure 8.1. SEM micrograph of LYO HA-CL – SAP. ....	196
Figure 8.2. Particle size distribution of LYO HA-CL – SAP. Data represent mean $\pm$ SD (n = 3). .....	196
Figure 8.3. DSC (A) and TGA (B) thermal profiles of LYO HA-CL – SAP. ....	197
Table 8.1. Percentage of SAP recovered in each stage of the apparatus E equipped with the 2-l glass EC for nasal delivery. Data are presented as mean $\pm$ SD (n = 3). .....	198
Table 8.2. Values of volumetric diameter, Span index and percentage of particles $\leq 10 \mu\text{m}$ obtained for LYO HA-CL – SAP with SprayTec <sup>TM</sup> system. Data represent mean $\pm$ SD (n = 3). .....	198
Figure 8.4. Viability of RPMI 2650 cells evaluated using MTS assay after 72 h of treatment with LYO HA-CL – SAP. Data represent mean $\pm$ SD (n = 3). .....	199
Figure 8.5. Wound images of untreated cells and cells treated with LYO HA-CL – SAP at different time points (0, 1, 8 h). .....	200
Figure 8.6. Concentration of IL-8 inflammatory cytokine in primary brushed ALI nasal cells supernatant after exposure to: LYO HA CL – SAP; LYO HA CL – SAP then LPS (LYO HA CL – SAP + LPS); LPS and then LYO HA CL – SAP (LPS + LYO HA CL – SAP). IL-8 levels were assessed in comparison to those of LPS-stimulated but untreated cells (positive control, i.e. cells exposed only to 10 ng/mL LPS), and unstimulated and untreated cells (control cells). Data represent mean $\pm$ standard deviation (n = 5). Asterisks indicate significant difference from LPS-stimulated but untreated cells (****P < 0.0001). .....	201
Figure 8.7. <i>In vitro</i> release profiles of SAP from LYO HA-CL – SAP: release by Franz’s cells (A) and transport across RPMI 2650 cells (B). Data represent mean $\pm$ SD (n = 3). .....	202



# GLOSSARY AND ABBREVIATIONS

ALI: air-liquid interface;

AR: allergic rhinitis;

ARDS: acute respiratory distress syndrome;

ATCC: American type cell culture collection;

BDDE: butanediol-diglycidyl ether;

BEGM: bronchial epithelial growth medium;

CD44: cluster of differentiation-44;

CDMT: 2-chloro-dimethoxy-1,3,5-triazine;

$C_f$ : Crossover Frequency;

COPD: chronic obstructive pulmonary disease;

CRS: chronic rhinosinusitis;

CTR-: negative control condition;

CTR+: positive control condition;

D[4,3]: Volume Weighted Mean Diameter;

DCF: dichlorofluorescein;

DCFH-DA: 2',7'-dichloro- fluorescein diacetate;

DFs: dermal fillers;

DL%: drug loading;

DMEM: Dulbecco modified eagle medium;

DMF: dimethylformamide;

DMSO: dimethylsulfoxide;

DMTMM: 4-(4,6-dimethoxy-1,3,5-triazin-2- yl)-4-methylmorpholinium;

DPI: dry powder inhaler;

DSC: differential scanning calorimetry;

Dv10: maximum particle size for 10% of the cumulative volume distribution of the sample;

Dv50: maximum particle size for 50% of the cumulative volume distribution of the sample, i.e. median Particle Size by Volume;

Dv90: maximum particle size for 90% of the cumulative volume distribution of the sample;

DVS: dynamic vapour sorption;

EC: 2-l glass expansion chamber;

ECM: extracellular matrix;

EDC: N-(3-dimethylaminopropyl)-N'-ethylcarbodiimide hydrochloride;

EE%: encapsulation efficiency;

ELISA: enzyme-linked immuno assay;

$f_1$ : difference factor;

$f_2$ : similarity factor;

FBS: foetal bovine serum;

FDA: Food and Drug Administration;

FPD: fine particle dose;

FPF<sub>LD</sub>: fine particle fraction of the loaded dose;

G': elastic (storage) modulus;

$G'_{1Hz}$ : Elastic Modulus at 1 Hz;

G": viscous (loss) modulus;

GAGs: glycosaminoglycans;

GRAS: generally regarded as safe;

H-bonds: hydrogen bonds;

H<sub>2</sub>O<sub>2</sub>: hydrogen peroxide;

HA: hyaluronic acid; hyaluronate; hyaluronan;

HA - SAP MS: native hyaluronic acid microspheres encapsulating sodium ascorbyl phosphate;

HA-CL: urea-crosslinked hyaluronic acid;



HA-CL - SAP MS: urea-crosslinked hyaluronic acid microspheres encapsulating sodium ascorbyl phosphate;

HARE: hyaluronan receptor for endocytosis;

HAS: hyaluronan synthases;

HBSS: Hank's balanced salt solution;

HCE: 3D reconstructed tissues of human corneal epithelium;

HCEpiC: 2D human corneal epithelial cells;

HE: hematoxylin and eosin;

HMW: high molecular weight;

HPLC: high-performance liquid chromatography;

HYAL: hyaluronidases;

IC50: half maximal inhibitory concentration;

IL-6: interleukin-6;

IL-8: interleukin-8;

KCS: keratoconjunctivitis sicca;

LDH: lactate dehydrogenase;

LMW: low molecular weight;

LPS: lipopolysaccharide;

LYO HA-CL – SAP: lyophilized formulation of urea-crosslinked hyaluronic acid and sodium ascorbyl phosphate;

LYVE1: lymphatic vessel endothelial hyaluronan receptor 1;

MC: modified expansion chamber;

MEM: minimum essential medium;

MS: Microspheres;

MSLI: multistage liquid impinger;

MTS: methyl tetrazolium salt;

MTT: 3(4,5-dimethylthiazol-2)2,5 difeniltetrazolium bromide;

MW: molecular weight;

MWCO: Molecular Weight Cut-off;

NGI: Next Generation Impactor;

NHS: N-hydroxysuccinimide;

oHA: oligosaccharides of hyaluronic acid;

PBS: phosphate buffer saline; phosphate buffered saline;

RH: relative humidity;

RHAMM: receptor for HA-mediated cell motility;

ROS: reactive oxygen species;

RPMI 2650: human nasal septum carcinoma-derived cells;

S1: solution 1, 0.02% (w/v) HA-CL;

S2, solution 2, 0.4% (w/v) HA-CL;

SAP: sodium ascorbyl phosphate;

SD: spray-dried;

SD HA – SAP: co-spray-dried native hyaluronic acid and sodium ascorbyl phosphate;

SD HA-CL – SAP: co-spray-dried urea-crosslinked hyaluronic acid and sodium ascorbyl phosphate;

SEM: scanning electron microscopy;

TBA: tetrabutylammonium;

TEER: transepithelial electrical resistance;

TGA: thermal gravimetric analysis;

TLRs: Toll-like receptors;

TSI: twin stage impinger;

UDS: unit dose system;

UV: ultraviolet;

Y%: yield.

$\gamma$ : strain;

$\dot{\gamma}$ : shear rate;

$\eta$ : viscosity;

$\eta_0$ : zero-shear rate viscosity;

$\omega$ : angular frequency.



# THESIS ABSTRACT

Hyaluronic acid (HA) is widely used in pharmaceuticals, medicine and cosmetics, as it is biocompatible, biodegradable, mucoadhesive, moisturizer, viscoelastic and biologically active. To slow down its degradation rate and implement its bioactivity, HA can be chemically modified to develop a number of customized and more performing derivatives tailored for different applications. The aim of the present PhD thesis was to investigate the possible pharmaceutical and dermatologic/cosmetic applications of the novel urea-crosslinked hyaluronic acid (HA-CL). First, an *in vitro* preliminary study showed the safety and the re-epithelialization efficacy of two prototypes of HA-CL eye drops, which could represent promising treatments of keratoconjunctivitis sicca. Secondly, HA-CL actual potentiality to prepare microspheres (MS) for sodium ascorbyl phosphate (SAP) dermal delivery was explored: a physico-chemical study displayed greater encapsulation efficiency and release properties for HA-CL – SAP MS compared to native HA – SAP MS (reference formulation). Then, in an *in vitro* study on pulmonary Calu-3 cells, the combination HA-CL - SAP showed greater anti-inflammatory, antioxidant and wound healing properties compared to the combination native HA – SAP, the single HA-CL, HA and SAP. This would support its possible use as co-adjuvant treatment of lung inflammatory diseases and encouraged the development and characterization of an inhalable dry powder formulation obtained by co-spray-drying of HA-CL and SAP. Finally, a freeze-dried powder formulation of HA-CL and SAP was prepared and showed its suitability for nasal delivery in terms of physico-chemical properties, *in vitro* aerosolization performance and bioactivity on RPMI 2650 nasal cells and brushed nasal epithelial cells. Overall, all these research works proved that the novel HA-CL could have interesting applications, improved the knowledge on this polymer and opened encouraging perspectives for future studies.

**Keywords:** anti-inflammatory; anti-oxidant; dermal application; dry powder; eye drops; hyaluronic acid; lung delivery; microspheres; nasal delivery; ophthalmic application; re-epithelializing; sodium ascorbyl phosphate; urea-crosslinked hyaluronic acid.



# RIASSUNTO DELLA TESI

L'acido ialuronico (AI) è ampiamente usato in ambito farmaceutico, medico e cosmetico, in quanto è biocompatibile, biodegradabile, mucoadesivo, idratante, viscoelastico e biologicamente attivo. Per rallentarne la velocità di degradazione ed implementarne la bioattività, si può modificare chimicamente l'AI, sviluppando così derivati più performanti e adatti a diverse applicazioni. Lo scopo della presente tesi di dottorato è stato studiare le possibili applicazioni farmaceutiche e dermatologiche/cosmetiche del nuovo acido ialuronico crosslinkato con urea (AI-CL). Innanzitutto, uno studio preliminare *in vitro* ha mostrato la sicurezza e l'attività riepitelizzante di due prototipi di gocce oculari di AI-CL, che potrebbero rappresentare promettenti trattamenti per la cheratocongiuntivite secca. In secondo luogo, è stata esplorata la possibilità di preparare microsfele (MS) di AI-CL per il rilascio dermico di sodio ascorbyl fosfato (SAF): uno studio fisico-chimico ha mostrato una più elevata efficienza di incapsulazione e migliori proprietà di rilascio per le MS di AI-CL e SAF, rispetto alle MS di AI nativo e SAF (formulazione controllo). Successivamente, in uno studio *in vitro* su cellule polmonari Calu-3, la combinazione AI-CL – SAF ha mostrato migliori proprietà antinfiammatorie, antiossidanti e cicatrizzanti rispetto alla combinazione AI – SAF, e ai singoli AI-CL, AI e SAF. Questo supporterebbe il suo possibile utilizzo come trattamento coadiuvante per i disturbi infiammatori polmonari, e ha incoraggiato lo sviluppo e la caratterizzazione di una formulazione costituita da una polvere secca inalabile ottenuta per co-spray-drying di AI-CL e SAF. Infine, è stata preparata un'altra formulazione a base di una polvere secca, ottenuta per liofilizzazione di AI-CL e SAF; essa è risultata adatta per uso nasale in termini di proprietà fisico-chimiche, performance aerodinamica *in vitro* e bioattività su cellule nasali RPMI 2650 e su cellule nasali epiteliali primarie. Nel complesso, questi lavori sperimentali hanno mostrato che il nuovo AI-CL può avere interessanti applicazioni, hanno ampliato le conoscenze relativamente all'AI-CL e hanno aperto incoraggianti prospettive per studi futuri.

**Parole chiave:** acido ialuronico; acido ialuronico crosslinkato con urea; antinfiammatorio; antiossidante; applicazione dermica; applicazione oftalmica; colliri; microsfele; polvere secca; riepitelizzante; rilascio nasale; rilascio polmonare; sodio ascorbil fosfato





# **CHAPTER 1**

*General introduction, aims of the study and structure of the thesis*



## 1.1. General introduction and aims of the study

As naturally-ubiquitous polymer, characterized by unique biological and physico-chemical properties, hyaluronic acid (HA) is relatively free from the risk of toxicity or immunogenicity and, therefore, has great clinical and commercial interest. Indeed, native HA can be used for a number of medical, pharmaceutical, cosmetic and dietary applications, which can also be extended through its chemical modifications –conjugation and crosslinking. Synthetic derivatives of HA are generally more performing polymers, which can satisfy specific demands and can be characterized by longer half-life. During the design of the more recent derivatives, particular attention has been paid to avoid the loss of native HA properties such as biocompatibility, biodegradability and mucoadhesivity (Fallacara et al., 2017a, 2018a).

The hyaluronan derivative object of the present thesis has been synthesized with this care, and is crosslinked with urea, a non-toxic biomolecule that can play its intrinsic activity once released from HA chains by degradation (Citernesi et al., 2015, WO/2015/007773 A1; Fallacara et al., 2017a). Due to the biocompatibility, the safety and the health effects of both urea and HA, urea-crosslinked hyaluronic acid (HA-CL) could represent a promising, versatile and multifunctional polymer with different possible uses.

For this reason, even if HA-CL was developed for the aesthetic field, (Citernesi et al., 2015, WO/2015/007773 A1; Fallacara et al., 2017a), the proprietor of its patent, I.R.A - Istituto Ricerche Applicate S.r.l.- financially supported a PhD scholarship in Chemistry at the University of Ferrara, with the aim to investigate the possible pharmaceutical and dermatologic/cosmetic applications of HA-CL. This represented an interesting and valiant research target considering that, in the future, the possible uses of HA derivatives are expected to increase as hyaluronan polymers, among their numerous advantages, can be multifunctional molecules, playing not only as drug delivery system, but also as active ingredients. More precisely, the following PhD research objectives have been accomplished:

- first of all, HA-CL was explored as possible treatment of dry eye syndrome. Hence, two different prototypes of HA-CL eye drops were formulated, characterized for their physico-chemical properties and tested for their stability and *in vitro* re-epithelialization ability (Fallacara et al., 2017b);
- secondly, HA-CL was investigated as dermal carrier of active ingredients. HA-CL microspheres were formulated and characterized for their physico-chemical properties, drug release profile and kinetic in comparison to native HA microspheres (Fallacara et al., 2018b);
- third, HA-CL, singularly or in combination with sodium ascorbyl phosphate (SAP), was explored *in vitro* as adjunctive treatment of lung inflammatory diseases. The aim was to understand if the combination HA-CL – SAP had improved biological activity with respect to the combination native HA – SAP and to the single SAP, HA and HA-CL components (Fallacara et al., 2018c);
- successively, an inhalable dry powder formulation consisting of co-spray-dried HA-CL and SAP was developed and evaluated with respect to a control formulation of co-spray-dried HA and SAP (Fallacara et al., submitted for publication);

- finally, a nasal freeze-dried powder containing HA-CL and SAP was formulated, characterized for its physico-chemical behaviour, *in vitro* cytotoxicity and bioactivity (Fallacara et al., 2019).

All the above mentioned experimental work has been performed by the PhD Student Arianna Fallacara, under the supervision of the Professor Stefano Manfredini of the Department of Life Sciences and Biotechnology (SVeB) - University of Ferrara. Three different host facilities have guaranteed access to all the necessary instrumentations and resources: the SVeB Department of the University of Ferrara; the Woolcock Institute of Medical Research and Discipline of Pharmacology -Sydney Medical School, University of Sydney (collaboration with the Respiratory Technology Group coordinated by the Professors Daniela Traini and Paul M. Young); the Istituto Ricerche Applicate –I.R.A. S.r.l. (collaboration with the R&D Group coordinated by the Doctor Ugo Raffaello Citernes).

## **1.2. Structure of the thesis**

The following diagram outlines the content of the thesis chapters, aligning them to the PhD research program. Completion of the previously mentioned research objectives was accomplished by performing a set of experiments presented in chapter 4, 5, 6, 7 and 8, as described in the diagram. Moreover, chapter 1 is a general introduction on the thesis, its aims and structure; chapter 2 consists of an overview on HA; chapter 3 describes the synthesis and rheology of the patented HA-CL; finally, chapter 8 includes a general conclusion and suggests future perspectives relatively to the possible uses of HA-CL.

**Chapter 1:** General introduction, aims of the study and structure of the thesis.

**Chapter 2:** An overview on hyaluronic acid.

**Chapter 3:** Synthesis and rheology of urea-crosslinked hyaluronic acid.

**Chapter 4:** Novel artificial tears containing crosslinked hyaluronic acid:  
an *in vitro* re-epithelialization study.

**Chapter 5:** Formulation and characterization of native and crosslinked hyaluronic acid microspheres for dermal delivery of sodium ascorbyl phosphate:  
a comparative study.

**Chapter 6:** Combination of urea-crosslinked hyaluronic acid and sodium ascorbyl phosphate for the treatment of inflammatory lung diseases: An *in vitro* study.

**Chapter 7:** Co-spray-dried urea cross-linked hyaluronic acid and sodium ascorbyl phosphate as novel inhalable dry powder formulation.

**Chapter 8:** *In vitro* characterization of physico-chemical properties, cytotoxicity, bioactivity of urea-crosslinked hyaluronic acid and sodium ascorbyl phosphate nasal powder formulation.

**Chapter 9:** General conclusions and future perspectives of urea-crosslinked hyaluronic acid.

## 1.2. References

- Citernes, U.R., Beretta, L., Citernes, L., 2015. Cross-Linked Hyaluronic Acid, Process for the Preparation Thereof and Use Thereof in the Aesthetic field. Patent number: WO/2015/007773 A1.
- Fallacara, A., Baldini, E., Manfredini, S., Vertuani, S., 2018a. Hyaluronic acid in the third millennium. *Polymers* (10)7, 701.
- Fallacara, A., Busato, L., Pozzoli, M., Ghadiri, M., Ong, H.X., Young, P.M., Manfredini, S., Traini, D., 2018c. Combination of urea-crosslinked hyaluronic acid and sodium ascorbyl phosphate for the treatment of inflammatory lung diseases: An in vitro study. *Eur. J. Pharm. Sci.*, 120, 96-106.
- Fallacara, A., Busato, L., Pozzoli, M., Ghadiri, M., Xin Ong, H., Young, P.M., Manfredini, S., Traini, D., Submitted to *J. Pharm. Sci.* Co-spray-dried urea cross-linked hyaluronic acid and sodium ascorbyl phosphate as novel inhalable dry powder formulation.
- Fallacara, A., Busato, L., Pozzoli, M., Ghadiri, M., Ong, H.X., Young, P.M., Manfredini, S., Traini, D., 2019. *In vitro* characterization of physico-chemical properties, cytotoxicity, bioactivity of urea-crosslinked hyaluronic acid and sodium ascorbyl phosphate nasal powder formulation. *Int. J. Pharm.*, 558, 341-350.
- Fallacara, A., Manfredini, S., Durini, E., Vertuani, S., 2017a. Hyaluronic acid fillers in soft tissue regeneration. *Facial Plast. Surg.* 33, 87-96.
- Fallacara, A., Marchetti, F., Pozzoli, M., Citernes, U.R., Manfredini, S., Vertuani, S., 2018b.. Formulation and characterization of native and crosslinked hyaluronic acid microspheres for dermal delivery of sodium ascorbyl phosphate: a comparative study. *Pharmaceutics*, 10 (4).
- Fallacara, A., Vertuani, S., Panozzo, G., Pecorelli, A., Valacchi, G., Manfredini, S., 2017b. Novel Artificial Tears Containing Cross-linked Hyaluronic Acid: An In Vitro Re-epithelialization study. *Molecules*, 22.







## CHAPTER 2

### *An overview on hyaluronic acid*

This chapter was published in *Polymers*, 10(7), 701 (2018) under the title  
“Hyaluronic acid in the third millennium”.

*Authors: Arianna Fallacara<sup>a</sup>, Erika Baldini<sup>a</sup>, Stefano Manfredini<sup>a,\*</sup>, Silvia Vertuani<sup>a</sup>.*

<sup>a</sup> Department of Life Sciences and Biotechnology, Master Course in Cosmetic Science and Technology (COSMAST), University of Ferrara, Via L. Borsari 46, 44121 Ferrara, Italy.

**\* Corresponding author:**

Prof. Stefano Manfredini: smanfred@unife.it; Tel.: +39-0532-455294; Fax: +39-0532-455378.

*DOI: 10.3390/polym10070701*



## **2.0. Preface**

Chapter 2 represents a general overview and an update regarding hyaluronic acid (HA): the key features of HA are described in terms of structure, physico-chemical and hydrodynamic properties, biology –occurrence, biosynthesis (by hyaluronan synthases), degradation (by hyaluronidases and oxidative stress), roles, mechanisms of action and receptors. Furthermore, both conventional and recently emerging methods developed for the industrial production of HA and its chemical derivatization are presented. Finally, the medical, pharmaceutical, cosmetic and dietary applications of HA and its derivatives are reviewed, reporting examples of HA-based products which are currently on the market or are undergoing further investigations. Therefore, the present chapter consents to critically approach the actual knowledge on HA and its state of art.

## 2.1. Abstract

Since its first isolation in 1934, hyaluronic acid (HA) has been studied across a variety of research areas. This unbranched glycosaminoglycan consisting of repeating disaccharide units of *N*-acetyl-D-glucosamine and D-glucuronic acid is almost ubiquitous in humans and in other vertebrates. HA is involved in many key processes, including cell signaling, wound repair, tissue regeneration, morphogenesis, matrix organization and pathobiology, and has unique physico-chemical properties, such as biocompatibility, biodegradability, mucoadhesivity, hygroscopicity and viscoelasticity. For these reasons, exogenous HA has been investigated as a drug delivery system and treatment in cancer, ophthalmology, arthrology, pneumology, rhinology, urology, aesthetic medicine and cosmetics. To improve and customize its properties and applications, HA can be subjected to chemical modifications: conjugation and crosslinking. The present review gives an overview regarding HA, describing its history, physico-chemical, structural and hydrodynamic properties and biology (occurrence, biosynthesis (by hyaluronan synthases), degradation (by hyaluronidases and oxidative stress), roles, mechanisms of action and receptors). Furthermore, both conventional and recently emerging methods developed for the industrial production of HA and its chemical derivatization are presented. Finally, the medical, pharmaceutical and cosmetic applications of HA and its derivatives are reviewed, reporting examples of HA-based products that currently are on the market or are undergoing further investigations.

**Keywords:** biological activity; crosslinking; drug delivery; cosmetic; food-supplement; functionalization; hyaluronan applications; hyaluronan derivatives; hyaluronan synthases; hyaluronic acid; hyaluronidases; physico-chemical properties.

## 2.2. Introduction and historical background of HA

Research on hyaluronic acid (HA) has expanded over more than one century.

The first study that can be referred to regarding HA dates from 1880: the French scientist Portes observed that mucin from vitreous body was different from other mucoids in cornea and cartilage and called it “hyalomucine” (Boeriu et al., 2013). Nevertheless, only in 1934, Meyer and Palmer isolated from bovine vitreous humor a new polysaccharide containing an amino sugar and a uronic acid and named it HA, from “hyaloid” (vitreous) and “uronic acid” (Meyer and Palmer, 1934). During the 1930s and 1950s, HA was isolated also from human umbilical cord, rooster comb and streptococci (Boas, 1949; Kendall et al., 1937).

The physico-chemical properties of HA were widely studied from the 1940s (Blumberg et al., 1958; Fletcher et al., 1955; Kaye and Stacey, 1950; Meyer, 1948; Varga, 1955), and its chemical structure was solved in 1954 by Meyer and Weissmann (Weissmann and Meyer, 1934). During the second half of the Twentieth Century, the progressive understanding of HA’s biological roles (Meyer, 1947; Ogston and Stanier, 1953; Pinkus and Perry, 1953) determined an increasing interest in its production and development as a medical product for a number of clinical applications. Hence, the extraction processes from animal tissues were progressively optimized, but still carried several problems of purification from unwanted contaminants (i.e., microorganisms, proteins). The first studies on HA production through bacterial fermentation and chemical synthesis were carried out before the 1970s (Boeriu et al., 2013).

The first pharmaceutical-grade HA was produced in 1979 by Balazs, who developed an efficient method to extract and purify the polymer from rooster combs and human umbilical cords (Balazs, US4141973, 1979). Balazs’ procedure set the basis for the industrial production of HA (Balazs, US4141973, 1979). Since the early 1980s, HA has been widely investigated as a raw material to develop intraocular lenses for implantation, becoming a major product in ophthalmology for its safety and protective effect on corneal endothelium (Binkhorst, 1980, 1981; Graue et al., 1980; Kanski, 1975; Miller and Stegmann, 1980; Percival, 1981, 1985; Regnault and Bregeat, 1974). Additionally, HA was found to be beneficial also for the treatment of joint (Auer et al., 1980; Dougados et al., 1993; Jones et al., 1995; Leardini et al., 1988; Namiki et al., 1982) and skin diseases (Juhlin, 1997; Pavicic et al., 2011), for wound healing (Abatangelo et al., 1983; Doillon and Silver, 1986; Hellström and Laurent, 1987; King et al., 1991) and for soft tissue augmentation (Duranti et al., 1998; Lin et al., 1994). Since the late 1980s, HA has also been used to formulate drug delivery systems (Camber and Edman, 1989; Benedetti et al., 1990; Lim et al., 2000; Moreira et al., 1991; Morimoto et al., 1991; Yerushalmi et al., 1994), and efforts continue still to today to develop HA-based vehicles to improve therapeutic efficacy (Egbu et al., 2018; El Kechai et al., 2016, 2017; Xie et al., 2011). During the 1990s and 2000s, particular attention was paid to identifying and characterizing the enzymes involved in HA metabolism, as well as developing bacterial fermentation techniques to produce HA with controlled size and polydispersity (Boeriu et al., 2013). Nowadays, HA represents a key molecule in a variety of medical, pharmaceutical, nutritional and cosmetic applications. For this reason, HA is still widely studied to elucidate its biosynthetic pathways and molecular biology, to optimize its biotechnological production, to synthesize derivatives with improved properties and to optimize and implement its therapeutic and aesthetic uses (Adamia et al., 2005, 2013; Boeriu

et al., 2013; Cyphert et al., 2015; De Oliveira et al., 2016; Ebid et al., 2014; Egbu et al., 2018; El Kechai et al., 2016, 2017; Fallacara et al., 2017a, b; Gao et al., 2008; Heldin et al., 2018; Knopf-Marques et al., 2016; Larrañeta et al., 2018; Mattheolabakis et al., 2015; Supp et al., 2014).

Considering the great interest in HA from different fields and the fast growing number of studies, the present chapter provides a comprehensive overview regarding HA and its potentialities, giving a concise update on the latest progress. As an example, a search on the most common public databases (i.e. Pubmed, Scopus, Isi Web of Science, ScienceDirect, Google Scholar, ResearchGate and Patent Data Base Questel) with the keyword “hyaluron\*”, gave a total of 161,863 hits: 142,575 papers and 19,288 patents. This huge amount of data is continuously growing. Thus, with the aim to give a clearer picture about where researches and applications in the field are going, the present chapter starts with an update of HA’s physico-chemical, structural and hydrodynamic properties and proceeds with the discussion of HA biology: occurrence, biosynthesis (by hyaluronan synthases), degradation (by hyaluronidases and oxidative stress), roles, mechanisms of action and receptors. Furthermore, both conventional and recently-emerging methods developed for the industrial production of HA and its chemical derivatization are described. Finally, the medical, pharmaceutical, cosmetic and dietary applications of HA and its derivatives are reviewed, reporting examples of HA-based products that currently are on the market or are undergoing further investigations.

Literature search: the Cochrane Controlled Trials Register (Central), Medline, EMBase and Cinahl from inception to November 2006 were consulted using truncated variations of preparation names, including brand names combined with truncated variations of terms related to osteoarthritis, all as text. No methodologic filter for controlled clinical trials was applied (the exact search strategy is available from the authors). Relevant articles into the Science Citation Index were entered to retrieve reports that have cited these articles, manually searched conference proceedings and textbooks, screened reference lists of all obtained articles and checked the proceedings of the U.S. Food and Drug Administration advisory panel related to relevant approval applications.

### **2.3. Physico-chemical, structural and hydrodynamic properties of HA**

HA is a natural and unbranched polymer belonging to a group of heteropolysaccharides named glycosaminoglycans (GAGs), which are diffused in the epithelial, connective and nervous tissues of vertebrates (Fraser et al., 1997; Girish and Kemparaju, 2007; Knopf-Marques et al., 2016). All the GAGs (i.e. HA, chondroitin sulfate, dermatan sulfate, keratin sulfate, heparin sulfate and heparin) are characterized by the same basic structure consisting of disaccharide units of an amino sugar (*N*-acetyl-galactosamine or *N*-acetyl-glucosamine) and an uronic sugar (glucuronic acid, iduronic acid or galactose). However, HA differs as it is not sulfated and it is not synthesized by Golgi enzymes in association with proteins (Fraser et al., 1997; Girish and Kemparaju, 2007; Knopf-Marques et al., 2016). Indeed, HA is produced at the inner face of the plasma membrane without any covalent bond to a protein core. Additionally, HA can reach a very high molecular weight (HMW,  $10^8$  Da), while the other GAGs are relatively smaller in size ( $<5 \times 10^4$  Da, usually  $1.5\text{--}2 \times 10^4$  Da) (Fraser et al., 1997; Girish and Kemparaju, 2007; Knopf-Marques et al., 2016).

The primary structure of HA is a linear chain containing repeating disaccharide units linked by  $\beta$ -1,4-glycosidic bonds. Each disaccharide consists of *N*-acetyl-D-glucosamine and D-glucuronic acid connected by  $\beta$  1,3-glycosidic bonds (Figure 2.1) (Laurent and Fraser, 1992; Weissmann and Meyer, 1934). When both the monosaccharides are in the  $\beta$  configuration, a very energetically-stable structure is formed, as each bulky functional group (hydroxyl, carboxyl, acetamido, anomeric carbon) is in the sterically-favorable equatorial position, while each small hydrogen atom occupies the less energetically-favorable axial position (Hascall and Laurent, 1997). Thus, the free rotation around the glycosidic bonds of HA backbone is limited, resulting in a rigid conformation where hydrophobic patches (CH groups) are alternated with polar groups (Scott, 1989; Scott et al., 1991), which are linked by intra- and inter-molecular hydrogen bonds (H-bonds) (Figure 2.1) (Scott and Heatley, 1999). At physiological pH, each carboxyl group has an anionic charge, which can be balanced with a mobile cation such as  $\text{Na}^+$ ,  $\text{K}^+$ ,  $\text{Ca}^{2+}$  and  $\text{Mg}^{2+}$ . Hence, in aqueous solution, HA is negatively charged and forms salts generally referred to as hyaluronan or hyaluronate (Balazs et al., 1986; Laurent, 1989), which are highly hydrophilic and, consequently, surrounded by water molecules. More precisely, as displayed in Figure 2.1, water molecules link HA carboxyl and acetamido groups with H-bonds that stabilize the secondary structure of the biopolymer, described as a single-strand left-handed helix with two disaccharide residues per turn (two-fold helix) (Heatley and Scott, 1988). In aqueous solution, HA two-fold helices form duplexes, i.e., a  $\beta$ -sheet tertiary structure, due to hydrophobic interactions and inter-molecular H-bonds, which enable the aggregation of polymeric chains with the formation of an extended meshwork (Scott et al., 1991; Scott and Heatley, 1999).

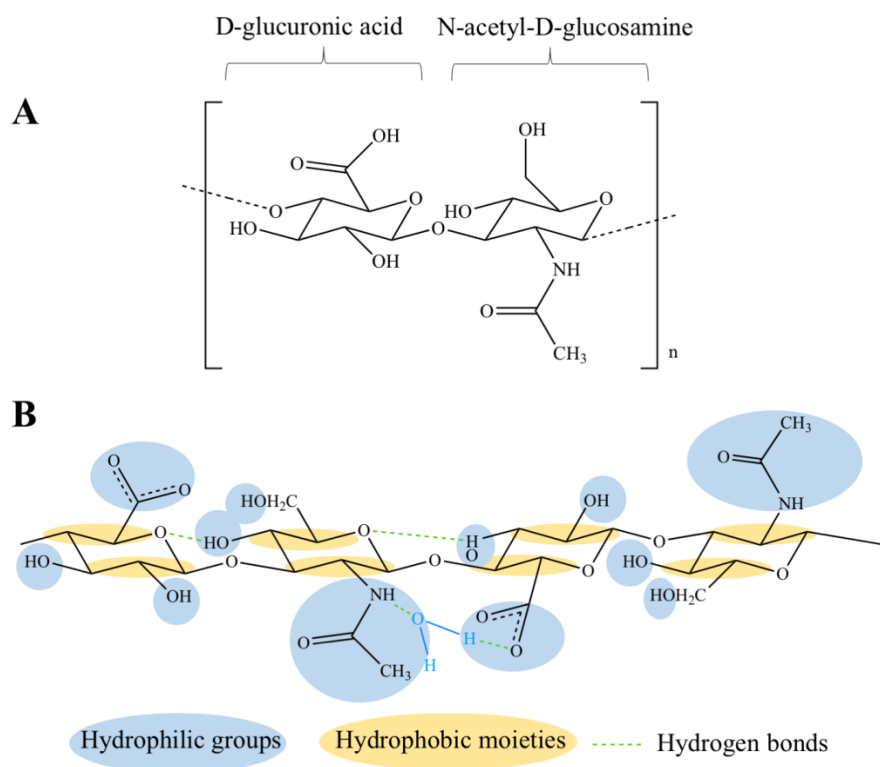


Figure 2.1. Chemical structures of HA disaccharide unit (A) and HA tetrasaccharide unit where the hydrophilic functional groups and the hydrophobic moieties are respectively evidenced in blue and yellow, while the hydrogen bonds are represented by green dashed lines (B).

The establishment of this network depends on HA molecular weight (MW) and concentration; for example, HMW native HA ( $>10^6$  Da) forms an extended network even at a very low concentration of 1  $\mu\text{g/mL}$  (Scott et al., 1991, 1992). With increasing MW and concentration, HA networks are strengthened, and consequently, HA solutions display progressively increased viscosity and viscoelasticity (Kobayashi et al., 1994). Since hyaluronan is a polyelectrolyte (Cleland, 1968), its rheological properties in aqueous solutions are influenced also by ionic strength, pH and temperature (Knopf-Marques et al., 2016; Kobayashi et al., 1994; Balazs et al., 1974): as these factors increase, HA viscosity declines markedly, suggesting a weakening of the interactions among the polymer chains (Rwei et al., 2008). In particular, HA is highly sensitive to pH alterations: in acidic and alkaline environments, a critical balance between repulsive and attractive forces occurs (Lapcik et al., 1998) and when the pH is lower than four or higher than 11, HA is degraded by hydrolysis (Maleki et al., 2008). In alkaline conditions, this effect is more pronounced, due to the disruption of H bonds, which take part in the structural organization of HA chains (Ghosh et al., 1993; Lapcik et al., 1998; Morris et al., 1980). Therefore, both the structural properties and the polyelectrolyte character of HA determine its rheological profile (Gura et al., 1998; Rwei et al., 2008; Pisárčik et al., 1995; Scott and Heatley, 1999). HA solutions are characterized by a non-Newtonian, shear-thinning and viscoelastic behavior. The shear-thinning (or pseudoplastic) profile of HA is due to the breakdown of the inter-molecular hydrogen bonds and hydrophobic interactions under increasing shear rates: HA chains deform and align in the streamlines of flow, and this results in a viscosity decrease (Lapcik et al., 1998; Pisárčik et al., 1995) (Figure 2.2.).

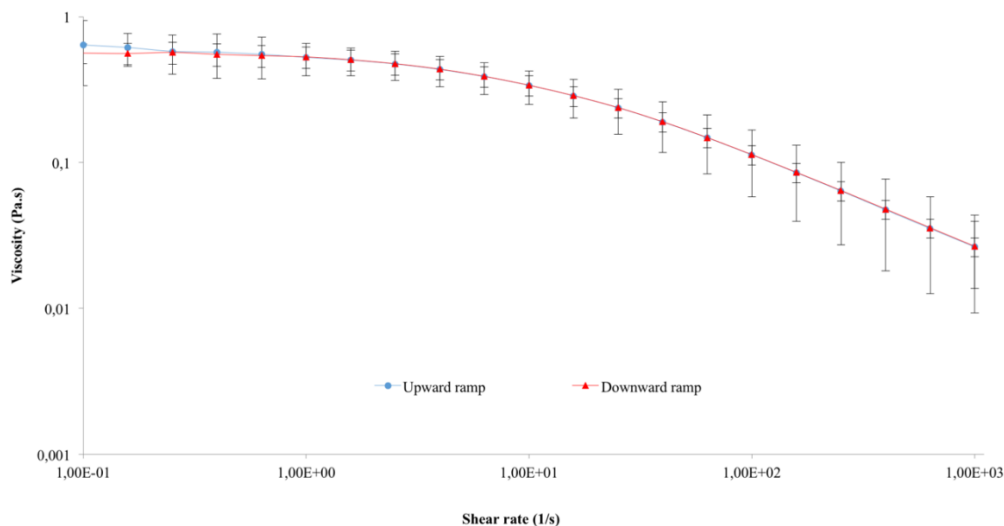


Figure 2.2. Shear-thinning and non-thixotropic behavior of 0.5% HA solution (2 MDa) analyzed using the rotational rheometer AR2000 (TA instruments, New Castle, DE, USA), connected to the Rheology Advantage software (Version V7.20) and equipped with an aluminium cone/plate geometry (diameter 40 mm, angle 2°, 64- $\mu\text{m}$  truncation). The viscosity decreases in response to gradual increases of the shear rate over time (upward ramp), and then, the viscosity increases in response to gradual decreases of the shear rate over time (downward ramp). The initial viscosity is recovered through the same intermediate states of the breakdown process: the breakdown of the polymeric network is transient and reversible, and therefore, the original structure of HA is recovered.



Additionally, HA solutions are non-thixotropic: as the shear rate decreases and ends, they recover their original structure and viscosity proceeding through the same intermediate states of the breakdown process (Rwei et al., 2008) (Figure 2.2.). Hence, the breakdown of the polymeric network is transient and reversible. This unique rheological behavior is peculiar and extremely important, as it determines many physiological roles and pharmaceutical, medical, food and cosmetic applications of hyaluronan.

## **2.4. Biology of HA**

### ***2.4.1. HA occurrence in living organism and diffusion in the human body***

Hyaluronan is widely diffused in nature: it is present in humans, animals, such as, rabbits, bovines, roosters, bacteria, such as *Streptococcus equi*, *Streptococcus zooepidermicus*, *Streptococcus equisimilis*, *Streptococcus pyogenes*, *Streptococcus uberis*, *Pasteurella multocida* (Balazs et al., 1993; DeAngelis et al., 1998; De Oliveira et al., 2016; Schiraldi et al., 2010), algae, such as the green algae *Chlorella* sp. infected by the *Chlorovirus* (DeAngelis, 1999; De Oliveira et al., 2016), yeasts, such as *Cryptococcus neoformans* (De Oliveira et al., 2016), and mollusks (Volpi and Maccari, 2003). However, it is not found in fungi, plants and insects (Kogan et al., 2007).

In the human body, the total content of HA is about 15 g for a 70-kg adult (Volpi et al., 2009). HA is prevalently distributed around cells, where it forms a pericellular coating, and in the extracellular matrix (ECM) of connective tissues (Laurent and Fraser, 1992; Schiraldi et al., 2010). Approximately 50% of the total HA resides in the skin, both in the dermis and the epidermis (Schiraldi et al., 2010). Synovial joint fluid and eye vitreous body, being mainly composed of ECM, contain important amounts of hyaluronan: 3–4 mg/mL and 0.1 mg/mL (wet weight), respectively (Laurent and Fraser, 1992; Schiraldi et al., 2010). Moreover, HA is also abundant in the umbilical cord (4 mg/mL), where it represents the major component of Wharton's jelly together with chondroitin sulfate (Robert et al., 2010; Sobolewski et al., 1997). The turnover of HA is fast (5 g/day) and is finely regulated through enzymatic synthesis and degradation (Volpi et al., 2009).

### ***2.4.2. HA synthesis in the human body***

In the human body, HA is synthesized as a free linear polymer by three transmembrane glycosyltransferase isoenzymes named hyaluronan synthases, HAS: HAS1, HAS2 and HAS3, whose catalytic sites are located on the inner face of the plasma membrane. HA growing chains are extruded onto the cell surface or into the ECM through the plasma membrane and HAS protein complexes (Itano and Kimata, 2002; Weigel et al., 1997) (Figure 2.3). The three HAS isoforms share the 50–71% of their amino acid sequences (55% HAS1/HAS2, 57% HAS1/HAS3, 71% HAS2/HAS3), and indeed, they are all characterized by seven membrane-spanning regions and a central cytoplasmic domain (Heldin et al., 2018; Volpi et al., 2009; Weigel et al., 1997). However, HAS gene sequences are located on different chromosomes (hCh19-HAS1, hCh8-HAS2 and hCh16-HAS3) (Itano et al., 1999; Spicer and McDonald, 1998), and the expression and the activity of HAS isoforms are controlled by growth factors, cytokines and other proteins such as kinases in different fashions, which appear cell and tissue

specific (Heldin et al., 2018; Itano and Kimata, 2002; Jiang et al., 2007; Vigetti et al., 2014a). Hence, the three HAS genes may respond differently to transcriptional signals: for example, in human fibroblasts like synoviocytes, transforming growth factor  $\beta$  upregulates HAS1 expression, but downregulates HAS3 expression (Stuhlmeier and Pöllascheck, 2004). Moreover, HAS biochemical and synthetic properties are different: HAS1 is the least active isoenzyme and produces HMW hyaluronan (from  $2 \times 10^5$  to  $2 \times 10^6$  Da). HAS2 is more active and synthesizes HA chains greater than  $2 \times 10^6$  Da. It represents the main hyaluronan synthetic enzyme in normal adult cells, and its activity is finely regulated (Vigetti et al., 2014b). HAS2 also regulates the developmental and reparation processes of tissue growth, and it may be involved in inflammation, cancer, pulmonary fibrosis and keloid scarring (Li et al., 2016; Supp et al., 2014; Volpi et al., 2009; Zhang et al., 2016a, b). HAS3 is the most active isoenzyme and produces HA molecules with MW lower than  $3 \times 10^5$  Da (Girish and Kemparaju, 2007).

Dysregulation and misregulation of HAS genes' expression result in abnormal production of HA and, therefore, in increased risk of pathological events, altered cell responses to injury and aberrant biological processes such as malignant transformation and metastasis (Adamia et al., 2005, 2013; Heldin et al., 2018; Toole, 2004).

Even if the exact regulation mechanisms and functions of each HAS isoenzyme have not been fully elucidated yet (Vigetti et al., 2014b), all the aforementioned studies suggest that HAS are critical mediators of physiological and pathological processes, as they are involved in development, injury and disease.

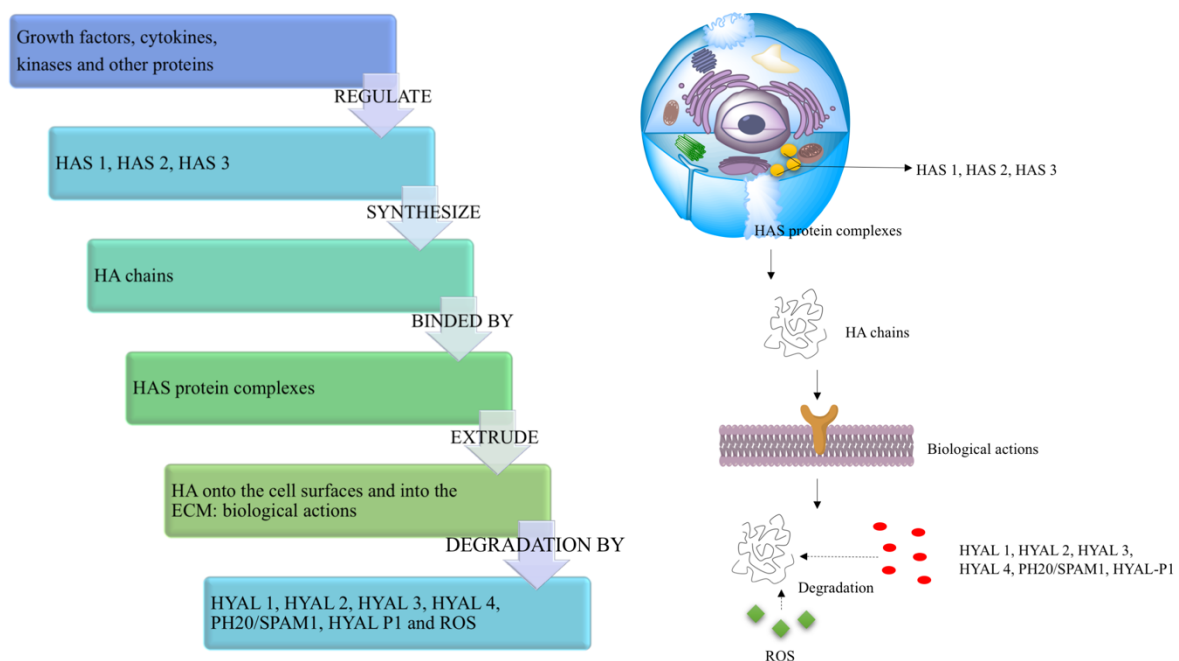


Figure 2.3. Schematic diagram showing HA key steps from its synthesis to its degradation.

### 2.4.3. HA degradation in the human body

HA degradation in the human body is accomplished by two different mechanisms: one is specific, mediated by enzymes (hyaluronidases (HYAL)), while the other is nonspecific,

determined by oxidative damage due to reactive oxygen species (ROS) (Figure 2.3.). Together, HYAL and ROS locally degrade roughly 30% of the 15 g HA present in the human body. The remaining 70% is catabolized systemically: hyaluronan is mostly transported by the lymph to the lymph nodes, where it is internalized and catabolized by the endothelial cells of the lymphatic vessels. Additionally, a small part of HA is carried to the bloodstream and degraded by liver endothelial cells (Heldin et al., 2018).

HYAL have a pivotal regulatory function in the metabolism of hyaluronan. These enzymes predominantly degrade HA, even if they are able to catabolize also chondroitin sulfate and chondroitin (Stern and Jedrzejewski, 2006). Randomly cleaving the  $\beta$ -*N*-acetyl-D-glucosaminidic linkages ( $\beta$ -1,4 glycosidic bonds) of HA chains, HYAL are classified as endoglycosidases. In the human genome, six HYAL gene sequences have been identified in two linked triplets: HYAL 1, HYAL 2, HYAL 3 genes, clustered on chromosome 3p21.3; HYAL-4 and PH20/SPAM1 genes, similarly located on chromosome 7p31.3, together with HYAL-P1 pseudogene (Csoka et al., 2001). HYAL have a consistent amino acid sequence in common: in particular, HYAL 1, HYAL 2, HYAL 3, HYAL 4 and PH20/SPAM1 share about 40% of their identity (Stern and Jedrzejewski, 2006). The expression of HYAL appears tissue specific. Nowadays, much is still unknown about HYAL activity, functions and posttranslational processing. HYAL-1, HYAL 2 and PH20/SPAM1 are the most characterized human HYAL. Both HYAL-1 and HYAL 2 have an optimal activity at acidic pH ( $\leq 4$ ) (Lepperdinger et al., 1998; Lokeshwar et al., 2001) and are highly expressed in human somatic tissues (Csoka et al., 2001). HYAL 1 was the first human HYAL to be isolated: it was purified from serum (60 ng/mL) (Frost et al., 1997) and, successively, from urine (Csoka et al., 1997). HYAL 1 was found to regulate cell cycle progression and apoptosis: it is the main HYAL expressed in cancers, and therefore, it may regulate tumor growth and angiogenesis (Stern, 2008). HYAL 1 works together with HYAL 2 to degrade HA, possibly according to the following mechanism, which is still the object of study. HYAL 2 is anchored on the external side of the cell surface: here, it cleaves into oligosaccharides (approximately 25 disaccharide units,  $2 \times 10^4$  Da) and the extracellular HMW HA ( $\geq 10^6$  Da), which is linked to its receptor cluster of differentiation-44 (CD44). These intermediate fragments are internalized, transported first to endosomes and then to lysosomes, where they are degraded into tetrasaccharide units (800 Da) by HYAL-1 (Cyphert et al., 2015). Differently from HYAL-1 and HYAL-2, PH20/SPAM1 shows not only endoglycosidase activity both at acidic and neutral pH, but also a role in fertilization (Cherr et al., 2001). Hence, PH20/SPAM1 is unique among HYAL, as it behaves as a multifunctional enzyme.

HMW hyaluronan can also be naturally degraded in the organism by ROS, including superoxide, hydrogen peroxide, nitric oxide, peroxyxynitrite and hypohalous acids, which are massively produced during inflammatory responses, tissue injury and tumorigenesis (Girish and Kemparaju, 2007; Soltés et al., 2006). The depolymerization of HA occurs through mechanisms of the reaction that are dependent on the ROS species, but always involve the scission of the glycosidic linkages (Volpi et al., 2009). Studies have shown that oxidation-related inflammatory processes, determining HA fragmentation, can increase the risk of injury in the airways and determine loss of viscosity in synovial fluid, with consequent cartilage degeneration, joint stiffness and pain (Monzon et al., 2010; Schiller et al., 1995, 2003). ROS-induced degradation of HA might suggest why its antioxidant activity is one of its possible

roles in reducing inflammation; however, so far, this biological function of HA has only been hypothesized, as it is not sufficiently supported by experimental data.

Due to these degradation mechanisms, which continuously occur *in vivo*, it has been estimated that the half-life of HA in the skin is about 24 h, in the eye 24–36 h, in the cartilage 1–3 weeks and in the vitreous humor 70 days (Schiraldi et al., 2010).

#### **2.4.4. Biological roles of HA in relation to its MW**

The equilibrium between HA synthesis and degradation plays a pivotal regulatory function in the human body, as it determines not only the amount, but also the MW of hyaluronan. Molecular mass and circumstances of synthesis/degradation are the key factors defining HA's biological actions (Cyphert et al., 2015; Heldin et al., 2018; Toole, 2004). Indeed, high molecular weight (HMW) and low molecular weight (LMW) hyaluronan can even display opposite effects (Cyphert et al., 2015; Girish and Kemparaju, 2007) and when they are simultaneously present in a specific tissue, they can exert actions different from the simple sum of those of their separate size-related effects (Cyphert et al., 2015).

Extracellular HMW HA ( $\geq 10^6$  Da) is anti-angiogenic, as it is able to inhibit endothelial cell growth (Cyphert et al., 2015; Girish and Kemparaju, 2007; Jiang et al., 2011). Additionally, due its viscoelasticity, it acts as a lubricating agent in the synovial joint fluid, thus protecting the articular cartilage (Tamer, 2013). HMW HA has also important and beneficial roles in inflammation, tissue injury and repair, wound healing and immunosuppression: it binds fibrinogen and controls the recruitment of inflammatory cells, the levels of inflammatory cytokines and the migration of stem cells (Girish and Kemparaju, 2007; Jiang et al., 2007, 2011).

During some environmental and pathological conditions, such as asthma, pulmonary fibrosis and hypertension, chronic obstructive pulmonary disease and rheumatoid arthritis, HMW HA is cleaved into LMW HA ( $2 \times 10^4$ – $10^6$  Da), which has been shown to possess pro-inflammatory and pro-angiogenic activities (Cyphert et al., 2015; Toole, 2004). Indeed, LMW hyaluronan is able to stimulate the production of proinflammatory cytokines, chemokines and growth factors (Cyphert et al., 2015) and to promote ECM remodeling (Heldin et al., 2018). Moreover, LMW HA can also induce tumor progression, exerting its influence on cells (Cyphert et al., 2015; Wu et al., 2015) and provoking ECM remodeling.

Both anti- and pro-inflammatory properties have been displayed by oHA and HA fragments ( $\leq 2 \times 10^4$  Da), depending on cell type and disease. Certain studies have shown that oHA are able to reduce Toll-like receptors (TLRs)-mediated inflammation (Kim et al., 2013), inhibit HA-CD44 activation of kinases (Misra et al., 2006) and retard the growth of tumors (Toole et al., 2008). However, oHA have been also found to promote inflammation in synovial fibroblasts (Campo et al., 2013), stimulate cell adhesion (Yang et al., 2012) and enhance angiogenesis during wound healing (Gao et al., 2008).

Therefore, HA is clearly a key molecule involved in a number of physiological and pathological processes. However, despite the intensive studies carried out so far, still little is known about HA's biological roles, the factors determining HA accumulation in transformed connective tissues and the consequent cancer progression, and much less is known about their dependence on hyaluronan molecular size and localization (intra- or extra-cellular). Further

researches focusing on HA molecular biology and mechanisms of action are necessary to clarify all these aspects and may facilitate the development of novel HA-based therapies.

#### ***2.4.5. Mechanisms of action of HA***

HA performs its biological actions (Section 3.4.) according to two basic mechanisms: it can act as a passive structural molecule and as a signaling molecule. Both of these mechanisms of action have been shown to be size-dependent (Cyphert et al., 2015; Volpi et al., 2009).

The passive mechanism is related to the physico-chemical properties of HMW HA. Due to its macromolecular size, marked hygroscopicity and viscoelasticity, HA is able to modulate tissue hydration, osmotic balance and the physical properties of ECM, structuring a hydrated and stable extracellular space where cells, collagen, elastin fibers and other ECM components are firmly maintained (Fraser et al., 1997; Robert et al., 2010; Volpi et al., 2009).

HA also acts as a signaling molecule by interacting with its binding proteins. Depending on HA MW, location and on cell-specific factors (receptor expression, signaling pathways and cell cycle), the binding between HA and its proteins determines opposite actions: pro- and anti-inflammatory activities, promotion and inhibition of cell migration, activation and blockage of cell division and differentiation. All the factors that determine HA activities as a signaling molecule could be related: MW may influence HA uptake by cells and may affect receptor affinity. Additionally, receptor complexes may cluster differently depending on HA MW (Cyphert et al., 2015).

HA binding proteins can be distinguished into HA-binding proteoglycans (extracellular or matrix hyaladherins) and HA cell surface receptors (cellular hyaladherins) (Cyphert et al., 2015). HA has shown two different molecular mechanisms of interaction with its hyaladherins. First, HA can interact in an autocrine fashion with its receptors on the same cell (Girish and Kemparaju, 2007). Second, it can behave as a paracrine substance, which binds its receptors on neighboring cells and thus activates different intracellular signal cascades. If HA has an HMW, a single chain can interact simultaneously with several cell surface receptors and can bind multiple proteoglycans. These structures, in turn, can aggregate with additional ECM proteins to form complexes, which can be linked to the cell surface through HA receptors (Girish and Kemparaju, 2007; Toole, 2004). Hence, HA acts as a scaffold that stabilizes the ECM structure not only through its passive structural action, but also through its active interaction with several extracellular hyaladherins, such as aggrecan (prominent in the cartilage), neurocan and brevican (prominent in the central nervous system) and versican (present in different soft tissues) (Girish and Kemparaju, 2007). For these reasons, pericellular HA is involved in the preservation of the structure and functionality of connective tissues, as well as in their protection from environmental factors (Robert et al., 2010).

### 2.4.5.1. HA cell surface receptors

HA interactions with its cell surface receptors mediate three biological processes: signal transduction, formation of pericellular coats and receptor-mediated internalization (Girish and Kemparaju, 2007). The present subsection describes HA cell surface receptors and the biological actions that they control when linked by HA (Figure 2.4.).

The principal receptor for HA is CD44, which is a multifunctional transmembrane glycoprotein. It is expressed in many isoforms diffused in almost all human cell types. CD44 can interact not only with HA, but also with different growth factors, cytokines and extracellular matrix proteins as fibronectin (Vigetti et al., 2014b). CD44 intracellular domain interacts with cytoskeleton; hence, when its extracellular domain binds ECM hyaluronan, a link between the cytoskeletal structures and the biopolymer is created (Knopf-Marques et al., 2016). HA-CD44 interaction is involved in a variety of intracellular signaling pathways that control cell biological processes: receptor-mediated hyaluronan internalization/degradation, angiogenesis, cell migration, proliferation, aggregation and adhesion to ECM components (Cyphert et al., 2015; Girish and Kemparaju, 2007; Knopf-Marques et al., 2016; Toole, 2004; Turley et al., 2002). Hence, CD44 plays a critical role in inflammation and wound healing (Knopf-Marques et al., 2016; Vigetti et al., 2014b). However, abnormal activation of HA-CD44 signaling cascades, as well as overexpression and upregulation of CD44 (due to pro-inflammatory cytokines such as interleukin-1, and growth factors such as epidermal growth factors) can result into development of pathological lesions and malignant transformation (Girish and Kemparaju, 2007; Toole, 2004). Indeed, CD44 is overexpressed in many solid tumors, such as pancreatic, breast and lung cancer (Mattheolabakis et al., 2015).

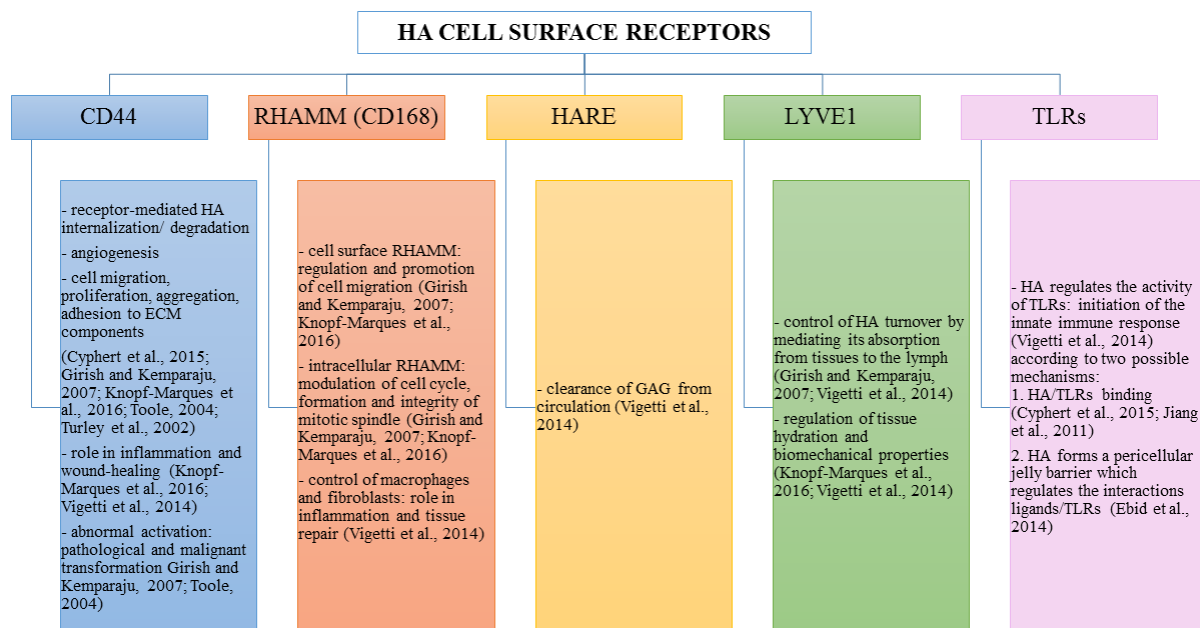


Figure 2.4. Summary of HA cell surface receptors and of the actions that they control when linked by HA.

The receptor for HA-mediated cell motility (RHAMM) is also known as CD168, and it was the first isolated cellular hyaloadherin. It exists in several isoforms, which can be present not only in the cell membrane, but also in the cytoplasm and in the nucleus (Vigetti et al., 2014b). When liked by HA, cell surface RHAMM mediates and promotes cell migration, while intracellular RHAMM modulates the cell cycle, the formation and the integrity of mitotic spindle (Girish and Kemparaju, 2007; Knopf-Marques et al., 2016). Interactions of HA with RHAMM play important roles in inflammation and tissue repair, by triggering a variety of signaling pathways and thus controlling cells such as macrophages and fibroblasts (Vigetti et al., 2014b).

Hyaluronan receptor for endocytosis (HARE) was initially isolated from endothelial cells in the liver, lymph nodes and spleen and successively found also in endothelial cells of eye, brain, kidney and heart (Vigetti et al., 2014b). It is able to bind not only HA, but also other GAGs, with the exception of keratin sulfate, heparin sulfate and heparin. It is involved in the clearance of GAGs from circulation (Vigetti et al., 2014b).

Furthermore, lymphatic vessel endothelial hyaluronan receptor 1 (LYVE1, a HA-binding protein expressed in lymph vascular endothelium and macrophages) controls HA turnover by mediating its adsorption from tissues to the lymph (Girish and Kemparaju, 2007; Vigetti et al., 2014b). In this way, LYVE1 is involved in the regulation of tissue hydration and their biomechanical properties (Knopf-Marques et al., 2016; Vigetti et al., 2014b). Additionally, LYVE1 forms complexes with growth factors, prostaglandins and other tissue mediators, which are implicated in the regulation of lymphangiogenesis and intercellular adhesion (Knopf-Marques et al., 2016; Vigetti et al., 2014b).

Finally, HA is involved in the regulation of the activity of TLRs that, recognizing bacterial lipopolysaccharides and lipopeptides, are able to initiate the innate immune response (Vigetti et al., 2014b). Two possible mechanisms have been proposed to explain how HA can influence TLRs. According to the first theory, LMW hyaluronan acts as an agonist for TLR2 and TLR4, thus provoking an inflammatory reaction (Cyphert et al., 2015; Jiang et al., 2011). On the contrary, according to the second theory, hyaluronan does not bind to TLRs, but it is able to regulate TLRs interactions with their ligands through the pericellular jelly barrier that it forms (Ebid et al., 2014). Indeed, in physiological conditions, HMW HA creates a dense and viscous protective coat around the cells, thus covering surface receptors such as TLRs and limiting their interactions with ligands. During inflammation, an imbalance between HA synthesis and degradation occurs, and this alters the thickness and the viscosity of HA pericellular barrier (Ebid et al., 2014). More precisely, HA is rapidly degraded due to pH reduction, ROS increase and the possible presence of pathogens producing HYAL (Knopf-Marques et al., 2016; Soltés et al., 2006). Hence, HA MW decreases, reducing the polymer water binding ability and the thickness and the viscosity of its pericellular shield (Ebid et al., 2014). This results in an increased accessibility of the cell receptors to their ligands, in the initiation of the innate immune response and in the enhancement of the inflammatory reaction (Ebid et al., 2014). For this reason, HA can also be involved in the pathogenesis of diseases sustained by immunological processes (Knopf-Marques et al., 2016).

## 2.5. Industrial production of HA

The plethora of activities of a food-contained molecule has raised important interest for public health: the global market of HA was USD 7.2 billion in 2016, and it is expected to reach a value of USD 15.4 billion by 2025 (Research, 2018). Indeed, hyaluronan is gaining an exponentially growing interest for many pharmaceutical, medical, food and cosmetic applications, due to its important activities—anti-inflammatory, wound healing and immunosuppressive—and its numerous and incomparable biological and physico-chemical properties, such as biocompatibility, biodegradability, non-immunogenicity, mucoadhesivity, hygroscopicity, viscoelasticity and lubricity. Hence, there is a strong interest in optimizing HA production processes to obtain products that fulfill high quality standards and are characterized by great yield and accessible costs. Both the source and the purification process co-occur to determine the characteristics of the produced HA in terms of purity, MW, yield and cost (Rangaswamy and Jain, 2008; Shiedlin et al., 2004). Therefore, producing high quality HA with high yield and less costly methods represents one of the biggest challenges in the field of hyaluronan applied research.

The first production process applied at an industrial scale consisted of HA extraction from animal sources, such as bovine vitreous and rooster combs (De Oliveira et al., 2016; Knopf-Marques et al., 2016) (Shiedlin et al., 2004). Despite the extraction protocols being improved over the years, this methodology was always hampered by several technical limitations, which led to the production of highly polydispersed HA ( $MW \geq 10^6$  Da) with a low yield (Boeriu et al., 2013; Knopf-Marques et al., 2016). This was due to the polymer intrinsic polydispersity, its low concentration in tissues and its uncontrolled degradation caused by the endogenous HYAL and the harsh isolation conditions (De Oliveira et al., 2016; Knopf-Marques et al., 2016). Additional disadvantages of animal-derived HA were represented by the risk of biological contamination—the presence of proteins, nucleic acids and viruses—and by the high purification costs (De Oliveira et al., 2016; Knopf-Marques et al., 2016; Shiedlin et al., 2004). Therefore, alternative methodologies for the industrial production of HA have been developed.

Currently, commercial hyaluronan is principally produced with biotechnology (microbial fermentation). Microorganism-derived HA is biocompatible with the human body because the HA structure is highly conserved among the different species (Boeriu et al., 2013; De Oliveira et al., 2016). Streptococci strains A and C were the first bacteria used for HA production, and nowadays, many commercial products are derived from *Streptococcus equi* (such as Restylane<sup>®</sup> by Q-med AB and Juvederm<sup>®</sup> by Allergan). Optimum bacterial culture conditions to obtain HMW HA ( $3.5\text{--}3.9 \times 10^6$  Da) have been determined at 37 °C, pH 7, in the presence of lactose or sucrose (Kim et al., 1996; Rangaswamy and Jain, 2008). Hyaluronan yield has been optimized up to 6–7 g/L, which is the upper technical limit of the process due to mass transfer limitation caused by the high viscosity of the fermentation broth (Boeriu et al., 2013). As streptococci genera include several human pathogens, an accurate and expensive purification of the produced HA is necessary (De Oliveira et al., 2016; Knopf-Marques et al., 2016). Hence, other microorganisms have been and are currently investigated to synthesize HA. An ideal microorganism for HA biosynthesis should be generally regarded as safe (GRAS), not secrete any toxins and be able to produce at least  $10^6$  Da HA, as the polymer



quality and market value increase with its purity and MW, which affect rheological and biological properties and define suitable applications (De Oliveira et al., 2016; Liu et al., 2011). Since the natural hyaluronan-producing organisms are mostly pathogenic, metabolic engineering currently represents an interesting opportunity to obtain HA from non-pathogenic, GRAS microorganisms. Endotoxin-free HA has already been synthesized by recombinant hosts including *Lactococcus lactis* (Kaur and Jayaraman, 2016), *Bacillus subtilis* (Chien and Lee, 2007), *Escherichia coli* (Yu and Stephanopoulos, 2008) and *Corynebacterium glutamicum* (Cheng et al., 2016). However, up to now, there has been no heterologous bacterial host producing as much HA as the natural ones. Hence, there is an increasing effort to find an ideal bioreactor for HA production: in addition to bacteria, also eukaryotic organisms such as yeasts, like *Saccharomyces cerevisiae* (DeAngelis and Achyuthan, 1996) and *Pichia pastoris* (Jeong et al., 2014), and plant cell cultures, like transformed tobacco-cultured cells (Rakkhumkaew et al., 2013), have been explored in the last few years.

Finally, to obtain HA of defined MW and narrow polydispersity, other approaches have been used. For example, to produce monodisperse oHA, chemoenzymatic synthesis has been performed (DeAngelis, 2008). This technique has successfully led to a product commercialized under the name Select HA™ (Hyalose LLC), characterized by a low polydispersity index value. Moreover, other studies have shown the possibility to prepare HA monodisperse fragments by controlling the degradation of HMW hyaluronan using different methods, including acidic, alkaline, ultrasonic and thermal degradation (Stern et al., 2007).

## **2.6. Synthetic modifications of HA**

HA has several interesting medical, pharmaceutical, food and cosmetic uses in its naturally-occurring linear form. However, chemical modifications of the HA structure represent a strategy to extend the possible applications of the polymer, obtaining better performing products that can satisfy specific demands and can be characterized by a longer half-life. During the design of novel synthetic derivatives, particular attention is paid to avoiding the loss of native HA properties such as biocompatibility, biodegradability and mucoadhesivity (Knopf-Marques et al., 2016).

### **2.6.1. General introduction of the chemical approaches to modify HA**

HA chemical modifications mainly involve two functional sites of the biopolymer: the hydroxyl (probably the primary alcoholic function of the *N*-acetyl D glucosamine) and the carboxyl groups. Furthermore, synthetic modifications can be performed after the deacetylation of HA *N*-acetyl groups, a strategy that allows one to recover amino functionalities (Schanté et al., 2011). All these functional groups of HA can be modified through two techniques, which are based on the same chemical reactions, but lead to different products: conjugation and crosslinking (Figure 2.5.). Conjugation consists of grafting a monofunctional molecule onto one HA chain by a single covalent bond, while crosslinking employs polyfunctional compounds to link together different chains of native or conjugated HA by two or more covalent bonds (Schanté et al., 2011). Crosslinked hyaluronan can be prepared from native HA (direct crosslinking) (Fallacara et al., 2017a, b; Malson and

Lindqvist, 1986) or from its conjugates (see below). Conjugation and crosslinking are generally performed for different purposes. Conjugation permits crosslinking with a variety of molecules; to obtain carrier systems with improved drug delivery properties with respect to native HA; to develop pro-drugs by covalently linking active molecules to HA (Schanté et al., 2011). On the other hand, crosslinking is normally intended to improve the mechanical, rheological and swelling properties of HA and to reduce its degradation rate, in order to develop derivatives with a longer residence time in the site of application and greater release properties (Collins and Birkinshaw, 2008; Fallacara et al., 2017a; Shimojo et al., 2015). A recent trend is to conjugate and crosslink HA chains using bioactive molecules in order to develop derivatives with improved and customized activities (Fallacara et al., 2017a) for a variety of applications in medicine, aesthetics and bioengineering, including cell and molecule delivery, tissue engineering and the development of scaffolds (Bowman et al., 2018; Fallacara et al., 2017a, b; Gelardi et al., 2013a, b; Kaur et al., 2006; Knopf-Marques et al., 2016; Nobile et al., 2014).

A number of synthetic approaches have been developed to produce conjugated or crosslinked hyaluronan (Schanté et al., 2011).

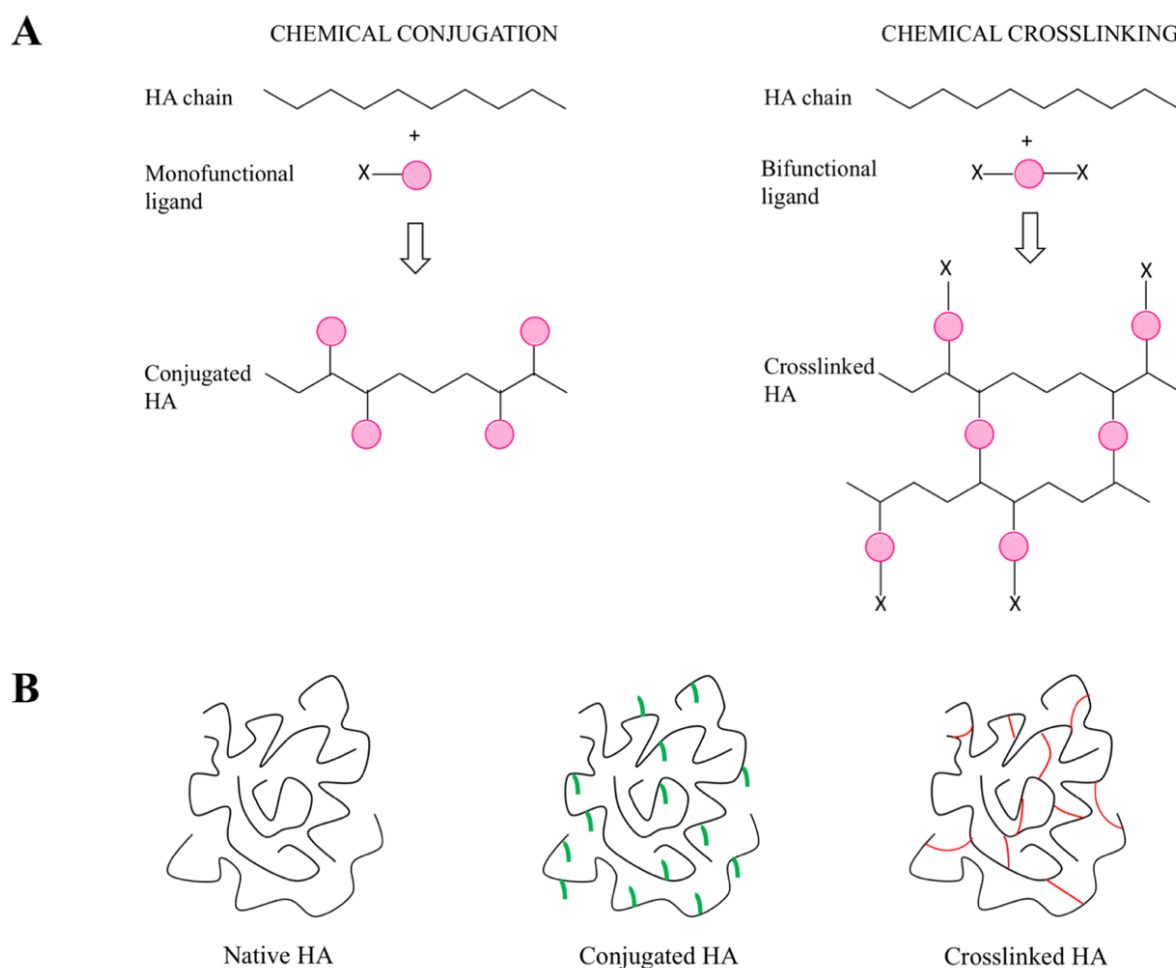


Figure 2.5. Chemical modifications of HA: conjugation and crosslinking (A). HA forms used for pharmaceutical, medical, food and cosmetic applications: native, conjugated and crosslinked (B).

Generally, HA is chemically modified in the liquid phase. Since it is hydrophilic, several reactions are performed in aqueous media also from its conjugates (Bulpitt and Aeschlimann, 1999; Lim et al., 2018; Maleki et al., 2007): however, they are pH dependent and, therefore, require acidic or alkaline conditions, which if too strong, can determine HA degradation (Maleki et al., 2007, 2008). Other synthetic methods, involving the use of reagents sensitive to hydrolysis, are performed in anhydrous organic solvents such as dimethylsulfoxide (DMSO) (Bulpitt and Aeschlimann, 1999) or dimethylformamide (DMF) (Magnani et al., 2000). These approaches necessarily introduce a preparation step to convert native HA into tetrabutylammonium (TBA) salt, soluble in organic ambient (Magnani et al., 2000): this increases the reaction time and cost, as well as the chances of HA chain fragmentation due to physico-chemical treatments. Additionally, when HA modifications take place in organic solvents, longer final purification processes are necessary (Schanté et al., 2011). The basic and classic chemistry that underlies the possible modifications of HA functional groups in the liquid phase is overviewed in the following Sections 5.2–5.4.

Since HA derivatives of high quality and purity are necessary to develop injectable products, implantable scaffolds, drug delivery systems and 3D hydrogel matrices encapsulating living cells, techniques for efficient, low-cost and safe modification of HA are continuously being explored (Knopf-Marques et al., 2016; Lim et al., 2018; Sigen et al., 2018). Hence, in the last few years, several efforts have been made to introduce one-pot reactions that preferably proceed in an aqueous environment, under mild and, possibly, environmentally-friendly conditions, without the use of toxic catalysts and reagents (Lim et al., 2018; Sigen et al., 2018). Additionally, alternative approaches to efficiently modify HA have been introduced: solvent-free methods, i.e., reactions in solid phase (Larrañeta et al., 2018), “click chemistry” syntheses, which are simple and chemoselective, proceeding with fast kinetics in an aqueous environment, under mild conditions, leading to quantitative yields, without appreciable amounts of side products, i.e., the thiol-ene reaction (Felgueiras et al., 2017), the Dies–Alder cycloaddition (Smith et al., 2018) and the azide-alkyne cycloaddition (Fu et al., 2017); in situ crosslinking of functionalized HA through air oxidation (Shu et al., 2002); photo-crosslinking of functionalized HA in the presence of photosensitizers (Bencherif et al., 2008; Donnelly et al., 2017).

### ***2.6.2. Modification of HA hydroxyl groups***

By modifying HA’s hydroxyl groups, the carboxyl groups remain unchanged, thus preserving HA’s natural recognition by its degradative enzymes (Schanté et al., 2011). Over the years, different derivatives of HA (ethers, hemiacetals, esters and carbamates) have been produced through reactions that occur between the polymeric hydroxyl groups and mono- or bi-functional agents.

Epoxides and bisepoxides like butanediol-diglycidyl ether (BDDE) (Malson and Lindqvist, 1986), ethylene glycol-diglycidyl ether, polyglycerol polyglycidyl ether (Yui et al., 1992), epichlorohydrin and 1,2,7,8 diepoxyoctane (Zhao, 2000) have been widely used to synthesize ether derivatives of hyaluronan in alkaline aqueous solution. Currently, HA-BDDE ether represents one of the most marketed HA derivative: it can be obtained through simple synthetic procedures in an aqueous environment, and it is degraded into non-cytotoxic fragments (Schanté et al., 2011). Other efficient methods to form ether derivatives of HA

involve the use of divinyl sulfone (Collins and Birkinshaw, 2007) or ethylene sulfide (Serban et al., 2008) in basic water.

Many studies showed that hemiacetal bonds can be formed between the hydroxyl groups of HA and glutaraldehyde in an acetone-water medium. Since glutaraldehyde is toxic, particular handling is required during the reaction and purification of the final product (Crescenzi et al., 2003; Tomihata and Ikada, 1997).

The hydroxyl groups of HA can be also esterified by reacting with octenyl succinic anhydride (Toemmeraas and Eenschooten, 2007) or methacrylic anhydride (Seidlits et al., 2010) under alkaline conditions. Alternatively, HA can be converted into a DMSO-soluble salt, which can undergo esterification with activated compounds such as acyl-chloride carboxylates (Pravata et al., 2008).

Finally, the activation of HA hydroxyl groups to cyanate esters, and the subsequent reaction in basic water with amines, allows one to synthesize carbamate derivatives with high degrees of substitution, in a reaction time of only 1 h (Mlcochová et al., 2006).

### **2.6.3. Modification of HA carboxyl groups**

Strategies for the derivatization of HA also involve esterification and amidation, which can be performed after the activation of the polymeric carboxyl groups using different reagents. By modifying HA's carboxyl groups, derivatives more stable to HYAL degradation can be synthesized: hence, if a drug is conjugated on the carboxyl groups of HA, a slow drug release may occur (Schanté et al., 2011).

Esterification can be performed by alkylation of HA carboxyl groups using alkyl halides (Della Valle and Romeo, 1989) or tosylate activation (Huin-Amargier et al., 2006). Moreover, HA esters can be synthesized using diazomethane as the activator of the carboxyl groups (Hirano et al., 2005). All these reactions proceed in DMSO from the TBA salt of HA. Alternatively, HA can undergo esterification also in water using epoxides such as glycidyl methacrylate and excess trimethylamine as a catalyst (Prata et al., 2010). The conversion of HA carboxyl groups into less hydrophilic esters represents a strategy to decrease the water solubility of HA, with the aim to reduce its susceptibility to HYAL degradation and enhance its in situ permanence time (Knopf-Marques et al., 2016). A well-known biopolymer synthesized to this end is HA benzyl ester (HYAFF 11), the properties of which are finely regulated by its degree of functionalization (Benedetti et al., 1990, 1993).

Amidation represents a further approach to modify HA: over the years, several synthetic procedures have been developed. However, some of these present important drawbacks: for example, Ugi condensation (useful to crosslink HA chains through diamide linkages) requires a strongly acidic pH (3), the use of formaldehyde, which is carcinogenic, and cyclohexyl isocyanide, which determines a pending undesired cyclohexyl group in the final product (Crescenzi et al., 2003; Maleki et al., 2007). HA amidation with 1,1'-carbonyldiimidazole (Bellini and Topai, 2000) or 2-chloro-1-methylpyridinium iodide (Magnani et al., 2000) as activating agents are performed in DMSO and DMF, respectively: hence, HA conversion into TBA salt and longer purification steps are needed. On the contrary, other methods are based on reaction conditions that meet the modification requirements for HA. Particularly efficient is the activation of HA carboxyl groups by carbodiimide (i.e., *N*-(3-dimethylaminopropyl)-*N'*-ethylcarbodiimide hydrochloride) (EDC) and co-activators such are *N*-hydroxysuccinimide

(NHS) or 1-hydroxybenzotriazole in water: proceeding under mild conditions, this reaction does not lead to HA chains' cleavage, and it is suitable also for the derivatization with biopolymers easily susceptible to denaturation, such as protein or peptides (Bulpitt and Aeschlimann, 1999; Kaczmarek et al., 2018; Kirk et al., 2013). Another promising method to synthesize HA derivatives with high grafting yields, in mild conditions, is based on triazine-activated amidation, typically performed with 2-chloro-dimethoxy-1,3,5-triazine (Bergman et al., 2007) or (4-(4,6-dimethoxy-1,3,5-triazin-2-yl)-4-methylmorpholinium (DMTMM) (D'Este et al., 2014). A recent study made a systematic comparison of EDC/NHS and DMTMM activation chemistry for modifying HA via amide formation in water (D'Este et al., 2014). The results showed that DMTMM is more efficient than EDC/NHS for ligation of amines to HA and does not require accurate pH control during the reaction to be effective (D'Este et al., 2014). Using these mild conditions of amidation, it is possible to synthesize highly hydrophilic and biocompatible derivatives, such as urea-crosslinked HA, which has already shown interesting applications in the ophthalmic and aesthetics field (Fallacara et al., 2017a, b).

#### **2.6.4. Modification of HA *N*-acetyl groups**

The deacetylation of the *N*-acetyl groups of HA recovers amino functionalities, which can then react with activated acids using the same amidation methods described above. However, this approach is not frequently used to synthesize HA derivatives for two main reasons: first of all, even the mildest deacetylation techniques have been shown to induce chain fragmentation (Bellini and Topai, 2000; Bulpitt and Aeschlimann, 1999; Crescenzi et al., 2002). Moreover, the deacetylation is a strong structural modification, which could importantly change the unique biological properties typical of native HA: indeed, it has been recently found that it reduces the interactions with the receptor CD44 (Bhattacharya et al., 2017).

#### **2.7. Applications of HA and its derivatives**

Due to their unique biological and physico-chemical properties and to their safety profile, native HA and many of its derivatives represent interesting biomaterials for a variety of medical, pharmaceutical, food and cosmetic applications (Figure 2.6). Some HA-based products are already on the market and/or have already a consolidated clinical practice, while others are currently undergoing further investigations to confirm their effectiveness. Since the literature concerning HA derivatives and their applications is very extensive, only some examples are reported hereafter.

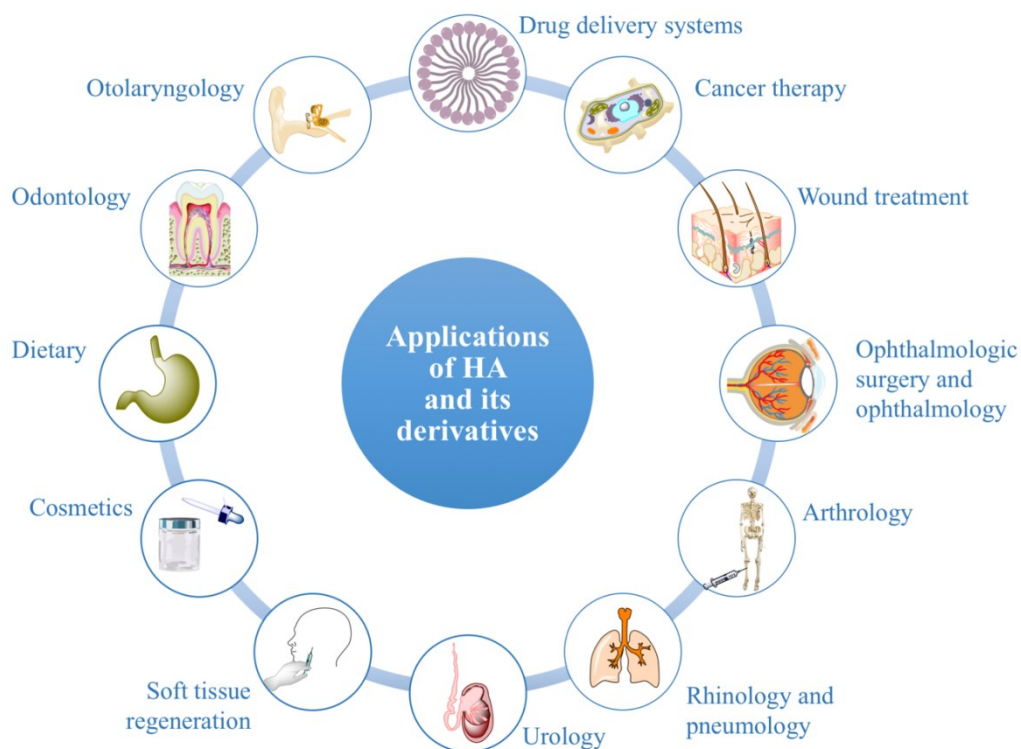


Figure 2.6. Medical, pharmaceutical, cosmetic and dietary applications of HA and its derivatives.

### 2.7.1. Drug delivery systems

HA and its derivatives of synthesis represent useful and emerging tools to improve drug delivery. They have been used alone or in combination with other substances to develop pro-drugs, surface-modified liposomes, nanoparticles, microparticles, hydrogel and other drug carriers. All these delivery systems are undergoing a continuous optimization as they are the object of intensive research. However, the industrialization and extensive clinical application of HA and its derivatives as drug carriers still have a long way to go, as many scientific studies are only at an *in vitro* experimental stage.

The conjugation of active ingredients to HA is intended to develop pro-drugs with improved physico-chemical properties, stability and therapeutic efficacy compared to free drugs. Considering that hyaluronan has several biological functions, HA-drug conjugates can exert their activities as such. Alternatively, their therapeutic actions are accomplished when the drugs are released, i.e., when the covalent bonds, which link drugs and HA, are broken down in the organism, ideally at the specific target sites. A variety of active ingredients can be conjugated to HA for topical or systemic uses. For example, HA can be conjugated with antidiabetic peptides such as exendin 4: this derivative shows a prolonged half-life, a protracted hypoglycemic effect and improved insulinotropic activity compared to the free exendin 4 in type 2 diabetic mice (Kong et al., 2010). However, since HA has a short half-life in the blood, the majority of HA-drug conjugates have been developed for local, i.e., intraarticular, intratumoral, subcutaneous, intravesical and intraperitoneal, rather than systemic administration (Mero and Campisi, 2014). For instance, a variety of anti-inflammatory drugs, including hydrocortisone, prednisone, prednisolone and dexamethasone, have been conjugated to HA and investigated for intraarticular therapy of arthritis (Della

Valle and Romeo, 1989). Furthermore, a recent study has displayed the potential of an emulsion containing a novel HA-P40 conjugate to treat a mouse model of dermatitis induced by oxazolone (Mangano et al., 2017). P40 is a particulate fragment isolated from *Corynebacterium granulosum* (actually known as *Propionibacterium acnes*), which has immunomodulatory, antibacterial, antiviral and antitumor properties. The conjugation of P40 to HA successfully prevents its systemic absorption and, therefore, improves its topical therapeutic effect (Mangano et al., 2017). Other research has shown that conjugation of curcumin with HA represents a strategy to enhance the water solubility and stability of curcumin (Manju and Sreenivasan, 2011). Moreover, the HA-curcumin conjugate displays improved healing properties compared to free curcumin and free HA, both *in vitro* (wound model of human keratinocytes) and *in vivo* (wound model of diabetic mouse). Hence, HA-conjugated curcumin may be useful to treat diabetic wounds (Sharma et al., 2018). Finally, the most promising and thoroughly studied conjugations of active ingredients to HA involve antitumoral agents, which can be strategically carried to malignant cells by hyaluronan, as explained in Section 6.2 (Chen et al., 2018; Mero and Campisi, 2014).

HA can also be conjugated to phospholipids in order to develop surface-modified liposomes: the chemical modification can be performed prior to liposome formulation (Nguyen et al., 2017) or after, on the outside shell (Hayward et al., 2016; Han et al., 2016). Moreover, HA can also be non-covalently linked on the liposome surface: indeed, liposomes can be covered by HA through ionic interaction mechanism (Chi et al., 2017; Negi et al., 2015) or the simple lipid film hydration technique (Moustafa et al., 2017). HA-modified liposomes appear to be promising carriers, as they have been shown to enhance the stability of drugs in the bloodstream, prolong their half-life, reduce their systemic toxicity (Han et al., 2016), enhance their tissue permeability, sustain their prolonged release (Moustafa et al., 2017) and ameliorate their therapeutic effects through synergistic actions (Manconi et al., 2017). HA-coated liposomes could improve the safety and the efficacy of antitumoral therapies: they appear proficient in mediating site-specific delivery of siRNA (Leite Nascimento et al., 2016) and anticancer drugs such as doxorubicin (Hayward et al., 2016), gemcitabine (Han et al., 2016), imatinib mesylate (Negi et al., 2015) and docetaxel (Nguyen et al., 2017), via CD44 cell receptors. Additionally, HA-surface-modified liposomes have been investigated as delivery systems also in ophthalmology (Moustafa et al., 2017), pneumology (Manconi et al., 2017) and topical treatment of wounds and burns (Yerushalmi et al., 1994).

Another promising type of drug delivery system, which can be formulated with HA and its derivatives of synthesis, is represented by nanoparticles. Hyaluronan can be a constituent element of nanoparticles (Maudens et al., 2018; Kim et al., 2013), but can also be used to cover nanoparticles, in order to improve the targeting efficiency and the therapeutic action of the encapsulated drugs (Pandey et al., 2018). HA-nanoparticles are being investigated for a number of administration routes and customized applications: for example, HA-Flt1 peptide conjugate nanoparticles might represent a next-generation pulmonary delivery carrier for dexamethasone in the management of asthma (Kim et al., 2013), while chitosan nanoparticles coated with HA and containing betamethasone valerate have displayed a great potential for the topical treatment of atopic dermatitis (Pandey et al., 2018). Hyaluronan nanoparticles included in polymeric films have shown potential as innovative therapeutic system for the prolonged release of vitamin E for the management of skin wounds (Pereira et al., 2016).

Moreover, the HA-poly(*N*-isopropylacrylamide) conjugate appears to be a promising candidate to treat osteoarthritis: once injected subcutaneously or intra-articularly, it spontaneously forms biocompatible nanoparticles able to control inflammation with a long-lasting action (Maudens et al., 2018). Finally, other HA surface-modified nanoparticles have been investigated for cancer-targeted therapies (Cho et al., 2011; Parashar et al., 2018; Wang et al., 2017).

Additionally, over the years, HA microspheres and microparticles have been explored as formulations to improve the biomucoadhesive property and the drug release profile and to ameliorate the texturing feeling in the case of dermal formulations. For example, it has been shown that spray-dried HA microspheres allow favorable ofloxacin delivery to the lung via inhalation, determining a superior pharmacological effect compared to free ofloxacin and to other routes of ofloxacin administration (Hwang et al., 2008). Similarly, inhaled HA microparticles have displayed prolonged pulmonary retention of salbutamol sulfate and reduced systemic exposure and side effects in a rat model (Li et al., 2017). HA microspheres have been evaluated also as possible materials for bone supplementation: indeed, they could be introduced in mineral bone cements to extend the release of active compounds (Fatnassi et al., 2014). A recent work has shown the potential of caffeine-loaded HA microparticles dispersed in a lecithin organogel as a dermal formulation for the long-term treatment of cellulite: this drug delivery system is not only effective at repairing cellulite tissue damage, but has also an intrinsic moisturizing action (Simsolo et al., 2018). Besides the microparticles prepared from native HA, the scientific literature also describes microspheres formulated from HA derivatives of synthesis such as hyaluronan benzyl esters (Esposito et al., 2005) and divinyl sulfone-crosslinked hyaluronan (Shimojo et al., 2015) as topical drug delivery systems.

Finally, hydrogels prepared from linear HA and its chemical derivatives are 3D polymeric networks, which can be well-suited systems for topical delivery of cells (Koivusalo et al., 2018) and many active ingredients, such as anti-inflammatories (El Kechai et al., 2016), anti-bacterials (Luo et al., 2000), antibodies and proteins in general (Egbu et al., 2018). To implement the mechanical and release properties, HA hydrogels can incorporate thermoresponsive polymers (Egbu et al., 2018) or other drug carriers such as liposomes (El Kechai et al., 2016, 2017). Up to now, HA hydrogels have shown a great potential for intraocular (Egbu et al., 2018; Koivusalo et al., 2018), intratympanic (El Kechai et al., 2016), intraarticular (Kroin et al., 2016) and dermal delivery (Pirard et al., 2005). A topical 2.5% HA hydrogel containing 3% diclofenac has been commercialized for the treatment of actinic keratosis under the tradename of Solaraze<sup>®</sup> (Pharmaderm) in Europe, USA and Canada (Pirard et al., 2005).

### **2.7.2. Cancer therapy**

It has been shown that the receptor CD44 is overexpressed in a variety of tumor cells, which consequently, display an increase of HA binding and internalization (Gao et al., 2015; Knopf-Marques et al., 2016; Mattheolabakis et al., 2015). Hence, the receptor CD44 has been identified as a potential target in cancer therapy, and hyaluronan, its primary ligand, has been recognized as a powerful tool to develop targeted therapies (Mattheolabakis et al., 2015; Parashar et al., 2018). Many research works have shown that HA can act as a drug carrier and



targeting agent at the same time, under the form of polymer-antitumoral conjugates or delivery systems encapsulating anticancer drugs (Mero and Campisi, 2014). Additionally, hyaluronan can be employed to design surface-modified nanoparticles (Cho et al., 2011; Parashar et al., 2018; Wang et al., 2017) or liposomes (Chi et al., 2017; Han et al., 2016; Hayward et al., 2016; Negi et al., 2015; Nguyen et al., 2017). After CD44 receptor-mediated cell internalization, all these HA derivatives are hydrolyzed by intracellular enzymes, and therefore, drugs are released inside the cancer target cells (Mero and Campisi, 2014). This should improve the pharmacokinetic profile and the delivery process of many anticancer drugs, overcoming the limitations that reduce their clinical potential, such as low solubility, short *in vivo* half-life, lack of discrimination between healthy and malignant tissues, consequent off-target accumulation and side effects (Mattheolabakis et al., 2015; Mero and Campisi, 2014). Up to now, there are no HA-antitumoral conjugates and anticancer loaded carriers of HA on the market; however, the promising results of many research works and clinical trials outline their potential and encourage further studies (Mattheolabakis et al., 2015; Mero and Campisi, 2014). For example, it has been shown that HA-modified polycaprolactone nanoparticles encapsulating naringenin enhance drug uptake by cancer cells *in vitro* and inhibit tumor growth in rat with urethane-induced lung cancer (Parashar et al., 2018). Additionally, HA-coated chitosan nanoparticles have been found to promote 5-fluorouracil delivery into tumor cells that overexpress the CD44 receptor (Wang et al., 2017). Further studies have displayed that a novel unsaturated derivative of HA (Buffa et al., 2017) and different types of HA-paclitaxel conjugates (Chen et al., 2018; Mero and Campisi, 2014) have a great potential as anticancer therapies.

### **2.7.3. Wound treatment**

As previously explained (Section 3.4.), endogenous HA sustains wound healing and re-epithelialization processes thanks to several actions including the promotion of fibroblast proliferation, migration and adhesion to the wound site, as well as the stimulation of collagen production (Aya and Stern, 2014). For this reason, HA is used in topical formulations (such as Connettivina<sup>®</sup> by Fidia) to treat skin irritations and wounds such as abrasions, post-surgical incisions, metabolic and vascular ulcers and burns (Aya and Stern, 2014; Neuman et al., 2015; Rueda Lopéx et al., 2005; Schiraldi et al., 2010; Tagliagambe et al., 2017). Currently, HA derivatives (Kirk et al., 2013; Li et al., 2018; Sharma et al., 2018; Shi et al., 2018) and HA-based wound dressings, films or hydrogels enriched with other therapeutic agents (Berce et al., 2018; Sanad and Abdel-Bar, 2017) are being evaluated in order to understand if the cicatrization process could be further enhanced. The wound healing properties of HA and its derivatives are being explored not only in dermatology, but also in other medical fields such as ophthalmology (Fallacara et al., 2017b; Wirostko et al., 2014), otolaryngology (Kaur et al., 2006), rhinology (Cassano et al., 2016) and odontology (Dahiya and Kamal, 2013).

### **2.7.4. Ophthalmologic surgery and ophthalmology**

HA is a natural component of the human eye: it has been found in vitreous body, lacrimal gland, corneal epithelium and conjunctiva and tear fluid (Fallacara et al., 2017b). Therefore,

ophthalmic products based on HA are fully biocompatible and do not trigger foreign body reactions (Schanté et al., 2011).

HA solutions are the most used viscosurgical devices to protect and lubricate the delicate eye tissues, replace lost vitreous fluid and provide space for manipulation during ophthalmic interventions (Neumayer et al., 2008). Indeed, the viscosity of HA permits keeping the tissues in place, reducing the risk of displacement, which can potentially compromise both the surgery and the repairing process (Knopf-Marques et al., 2016). The first ophthalmic viscosurgical device containing HA was approved by the FDA in 1980 and is still marketed under the trademark Healon<sup>®</sup> (Abbott).

Moreover, HA is the active ingredient of many eye drops, such as DropStar<sup>®</sup> by Bracco and Lubristil<sup>®</sup> by Eyelab, which, hydrating the ocular surface and improving the quality of vision, are the mainstay to treat diseases such as dry eye syndrome and are useful at increasing the comfortability of contact lenses (Carracedo et al., 2017; Fallacara et al., 2017b; Vandermeer et al., 2018). Many studies have proven the safety and the efficacy of native HA solutions as artificial tears (Aragona et al., 2002; Ho et al., 2013; Johnson et al., 2006; Vandermeer et al., 2018). More recently, also novel derivatives of hyaluronan with improved mechanical and biological properties are being investigated to formulate eye drops with enhanced ocular residence times. For example, promising preliminary results have been obtained with solutions of HA-cysteine ethyl ester (Laffleur and Dachs, 2015) and urea-crosslinked HA (HA-CL) (Fallacara et al., 2017b).

### **2.7.5. Arthrology**

HA is one of the major lubricating agents of the ECM of synovial joint fluid: due to its viscoelasticity, it absorbs mechanical impacts and avoids friction between the bone-ends (Laurent and Fraser, 1992; Schiraldi et al., 2010; Tamer, 2013). When the synovial fluid is reduced or inflamed, and the HA level decreases, disorders such as rheumatoid arthritis and osteoarthritis occur. Viscosupplementation represents an approach to treat and slow down the progression of these conditions: intraarticular injections of HMW HA, such as Supartz FX<sup>®</sup> by Bioventus and Hyalgan<sup>®</sup> by Fidia, allow maximizing the topical effect and the reduction of pain, as well as minimizing systemic adverse effects (Bowman et al., 2018). Locally-injected HA has been shown to provide long-term clinical benefits, suggesting that it acts with more than one mechanism (Bowman et al., 2018; Ghosh and Guidolin, 2002), as the restoration of synovial fluid viscoelasticity is only temporary because HA is degraded within 24 h (Brown et al., 1991). Hence, the therapeutic effect of HA intra-articular injection appears prevalently due to biological activities: induction of the synthesis of new HA in synovial cells, stimulation of chondrocyte proliferation and resulting reduction of cartilage degradation (Bowman et al., 2018; Ghosh and Guidolin, 2002; Greenberg et al., 2006). In order to increase the half-life after injection and, consequently, the therapeutic efficacy, crosslinked HA derivatives have been investigated and introduced on the market (such as Synvisc<sup>®</sup> by Genzyme) as viscosupplementation agents (Bowman et al., 2018; Sun et al., 2017).

### ***2.7.6. Rhinology and pneumology***

Endogenous HMW HA plays a pivotal role in the homeostasis of the upper and the lower airways: it is an important component of the normal airway secretions, exerts anti-inflammatory and anti-angiogenic actions, promotes cell survival and mucociliary clearance, organizes extracellular matrix, stabilizes connective tissues, sustains healing processes and regulates tissues hydration (Garantziotis et al., 2016; Gelardi et al., 2013b; Gerdin and Hällgren, 1997; Monzon et al., 2006). Hence, exogenous HMW HA represents a promising therapeutic agent for the treatment of nasal and lung diseases that involve inflammation, oxidative stress and epithelial remodeling, such as allergic and non-allergic rhinitis, asthma, chronic obstructive pulmonary disease and cystic fibrosis (Furnari et al., 2012; Garantziotis et al., 2016; Gavina et al., 2013; Gelardi et al., 2013a; Petrigini and Allegra, 2006; Turino et al., 2017). Examples of marketed formulations containing HA to treat respiratory diseases are Ialoclean<sup>®</sup> (Farma-Derma), a nasal spray to treat nasal dryness and rhinitis and to promote nasal wound healing, Hyaneb<sup>®</sup> (Chiesi Farmaceutici), a hypertonic saline solution containing HA to hydrate and reduce mucus viscosity in cystic fibrosis patients (Nenna et al., 2011), and Yabro<sup>®</sup> (Ibsa Farmaceutici), a high viscosity nebulizer solution of HA to treat bronchial hyper-reactivity (Gelardi et al., 2013a).

### ***2.7.7. Urology***

Recently, the possible therapeutic uses of HA in urology have been explored. Preliminary evidence has shown that intravesical HA, administered alone or in combination with chondroitin sulfate or alpha blockers, could be able to reduce the recurrence of urinary tract infections such as bacterial cystitis, to alleviate the symptoms of these diseases and to protect the mucosa of urinary bladder (Goddard and Janssen, 2017; Ząbkowski et al., 2015). However, further clinical studies are necessary to confirm the effectiveness of HA treatment in urology.

### ***2.7.8. Soft tissue regeneration***

HA skin content decreases with aging, and the most visible effects are the loss of facial skin hydration, elasticity and volume, which are responsible for wrinkles (Robert et al., 2010). Over the last few years, HA has been widely used as a biomaterial to develop dermal fillers (DFs), which are class III medical devices that, injected into or under the skin, restore lost volumes and correct facial imperfections such as wrinkles or scars (Fallacara et al., 2017a). Being characterized by most of the properties that an ideal DF should have—biocompatibility, biodegradability, viscoelasticity, safety, versatility—HA DFs have become the most popular agents for viscoaugmentation, i.e., for soft tissue contouring and volumizing (Fallacara et al., 2017a). Indeed, according to data from the American Society of Plastic Surgeons (ASPS), in 2017, out of a total of 2,691,265 treatments with soft tissue fillers, 2,091,476 were performed with HA DFs (American Society of Plastic Surgeons, 2017). One of the reasons for this success resides in the reversibility of the HA DF effect: they correct wrinkles in a reversible manner, as a hypothetical medical error or complication can be remedied through the injection of HYAL (Vitrace<sup>®</sup>, ISTA Pharmaceuticals; Hylenex<sup>®</sup>,

Halozyme Therapeutics) (Fallacara et al., 2017a). The duration of the corrective effect of HA DFs varies between three and 24 months, depending prevalently on HA concentration, crosslinking (degree and type), the treated area and the individual (Fallacara et al., 2017a; Muhn et al., 2012). For example, Hylaform<sup>®</sup> (Genzyme Biosurgery) contains 4.5–6 mg/mL HA crosslinked with divinyl sulfone (20% degree), and its effect lasts 3–4 months, while the Juvederm<sup>®</sup> DFs family (Allergan) contains 18–30 mg/mL HA crosslinked with 9–11% BDDE, and its effect lasts 6–24 months (Fallacara et al., 2017a). Finally, DFs that combine BTX-A and HA have been developed to ensure an optimal correction even in patients with extremely deep wrinkles (Fallacara et al., 2017a).

### **2.7.9. Cosmetics**

HA represents a moisturizing active ingredient widely used in cosmetic formulations (gels, emulsions or serums) to restore the physiological microenvironment typical of youthful skin.

HA-based cosmetics such as Fillerina<sup>®</sup> (Labo Cosprophar Suisse) claims to restore skin hydration and elasticity: this is reported to exert an anti-wrinkle effect, although no rigorous scientific proof is able to fully substantiate this claim (Janiš et al., 2017; Nobile et al. 2014; Schiraldi et al., 2010). It has to be considered that HA's hydrating effect largely depends on its MW, and its longevity depends on HA stability to hyaluronidases. Indeed, HMW HA mainly works as a film-forming polymer: it reduces water evaporation, with an occlusive-like action. On the other hand, medium MW and LMW HA mainly work by binding moisture from the environment, do to their high hygroscopicity (Janiš et al., 2017; Nobile et al. 2014). In some cases, this capacity may reverse HA's expected hydrating activity as at a high concentration, HA may even extract humidity from the skin. Furthermore, also sunscreens containing hyaluronan may contribute to maintaining a youthful skin, protecting it against the harmful effects of ultraviolet irradiation, due to the possible free radical scavenging properties of HA (Hašová et al., 2011; Trommer et al., 2003). The same capability has been demonstrated by dietary intake of HA (Section 6.10).

### **2.7.10. Dietary**

HA can also represent an interesting ingredient in enriched food and food supplements: it has gained the unofficial designation as a nutri-cosmetic because of its capability to improve skin appearance (Drealos, 2010). For a long time, the fact that HA can cross in its “intact” form the intestinal barrier has been debated; recently, a few studies have appeared in the literature to highlight this question. Kimura et al. have evaluated the degradation and absorption of HA (300 KDa and 2 KDa) after oral ingestion in rats, demonstrating intestinal degradation to oligosaccharides, which are subsequently absorbed in the large intestine, translocated into the blood and distributed in the skin (Kimura et al., 2016). Orally-ingested LMW HA has shown the opposite effects: some studies have reported inflammatory properties with the activation of the immune response (Zgheib et al., 2014), while other research has highlighted the efficacy in reducing knee joint pain without inflammation (Sato and Iwaso, 2009). Nowadays, the mechanisms at the base of these different actions of LMW ingested HA remain still unclear. In another study, the absorption, distribution and excretion

of HMW-labeled (1 MDa) HA were evaluated after oral administration in rats and dogs: for the first time, it was shown that dietary HMW HA can be distributed to connective tissues (Balogh et al., 2008). In particular, these reproducible results suggest that orally-administered HMW HA may reach joints, bones and skin, even if in small amounts (Balogh et al., 2008), thus highlighting that a rationale may exist in the use of HA-based food supplements designed for joint and skin health.

In these regards, several studies have reported on the safety of HA as a food supplement, confirming its possible use as a food ingredient itself. HA is marketed as a food supplement in the USA, Canada, Europe and Asia (particularly in Korea and Japan) with some difference in the suggested use: to treat joint pain in the USA and in Europe; to treat wrinkles and to moisturize in Japan, even if the involvement of this polymer in the skin moisture retention effect needs to be further elucidated in the future (Oe et al., 2014). The attention was focused prevalently on studies that exclude complex mixtures, in order to evidence the effects of HA alone; however, several research works describe the use of HA as a food ingredient in enriched extracts or mixtures with collagen and other supplements. For example, in a preliminary double-blind, controlled, randomized, parallel trial over 12 weeks, rooster comb extract was added to low fat yoghurt, which was given to mild knee pain patients (n: 40), resulting in significative improvement in muscle strength in men (Solà et al., 2015). In another recent clinical study, an oral HA preparation diluted in a cascade fermented organic whole food concentrate supplemented with biotin, vitamin C, copper and zinc (Regulatpro<sup>®</sup> Hyaluron, Dr. Niedermaier<sup>®</sup>) led to a significant cutaneous antiaging effect in twenty female subjects after 40 days of daily consumption (Göllner et al., 2017). From such mixtures, it is difficult to elucidate HA's specific contribution.

Regarding supplementation with HA alone, some studies have demonstrated a direct correlation between ingestion and body effects. In a recent review, Kawada et al. underlined a number of studies in support of the contribution of ingested HA to hydrate skin, thus improving the quality of life for people who suffer from skin dryness induced by UV, smoking and pollutants, responsible for cutaneous reduction of HA (Kawada et al., 2014). Indeed, the review of Kawada and coworkers reported that, in different randomized, double-blind, placebo-controlled trials, the amounts of HA ranging from 37.52–240 mg per day, ingested in a period comprised between four and six weeks, significantly improved cutaneous moistness (Kawada et al., 2014). These results, as always happens with biopolymers as food supplements, are difficult to correlate with quantitative effects, as polymer sources and MW always vary. However, qualitatively, the correlation between HA consumption and the decrease of skin dryness is evident. The authors suggest that partially-digested HA, regardless of its MW, is adsorbed in the gut, while intact HA is absorbed by the lymphatic system; both are distributed to the skin, where they can work as inducers of fibroblast proliferation and endogenous HA synthesis (Kawada et al., 2014). In a more recent study, the same authors have investigated, in a double blind, placebo controlled, randomized study of 61 subjects with dry skin, the effects of HA (120 mg/day) of two different MW (800 KDa and 300 KDa) over six weeks (Kawada et al., 2015a). Both the HAs were effective, but the 300-KDa group showed the best improvements in skin dryness and moisture content (Kawada et al., 2015a). Again, Kawada et al., in an experiment on hairless mice, demonstrated that the oral administration of 200 mg/kg body weight per day of two different MW HA (300 KDa and less than 10 KDa) for six weeks reduced epidermal thickness and improved skin hydration

upon UV irradiation (Kawada et al., 2015b). The effect was stronger for the less than 10-KDa HA (Kawada et al., 2015b). The authors also demonstrated that the less than 10 KDa orally-administered HA also stimulated HAS2 expression, thus highlighting an overall role of LMW HA in the prevention of skin photoageing with different mechanisms (Kawada et al., 2015b). Thus, combining HA oral treatment with HA topical and injective administration could be very successful in the control of skin ageing. A further study suggesting that orally-administered HA can migrate into the skin of rats, thus possibly reducing skin dryness, was conducted by Oe et al., who demonstrated that about 90% of the ingested HA was absorbed from the digestive tract and was used as an energy source or a structural component (Oe et al., 2014).






Dietary HA can be beneficial not only for skin, but also for joints, as evidenced by a number of randomized, double-blinded, placebo-controlled studies relative to the treatment of knee pain, relief of synovial effusion or inflammation and improvement of muscular knee strength (Oe et al., 2016).

### **2.7.11. 3D cell culture models**

HA and its synthetic derivatives can be used as 3D scaffold structures, which represent physical support systems for *in vitro* cell culture (Larson, 2015). Indeed, 3D tissue models can be obtained by culturing cells on pre-fabricated polymeric scaffolds or matrices, designed to simulate the *in vivo* ECM (Larson, 2015). Cells attach, migrate and fill the interstices within the scaffold to form 3D cultures (Larson, 2015). 3D scaffolds can be promising also for *in vivo* tissue regeneration, reproducing the natural physical and structural environment of living tissue (Larson, 2015). An example of a cell substrate suitable for a 3D environment, for both *in vitro* and *in vivo* research, is represented by HyStem<sup>®</sup> Hydrogels (ESI·BIO<sup>™</sup>).

For example, HA derivatives characterized by aldehyde and hydrazide groups have been used to develop a biomimetic, 3D culture system for poorly-adherent metastatic prostate cancer cells, employed as an *in vitro* platform to test the efficacy of anticancer drugs (Gurski et al., 2009). The hyaluronan-3D cell culture system provided a useful interesting alternative to study antineoplastic drugs, with results superior compared to those from conventional 2D monolayers (Gurski et al., 2009). Another work showed that methacrylated HA is useful to develop *in vitro* 3D culture models to assess glial scarring in a robust and repeatable way, in order to evaluate, for example, the foreign body response to implants such as electrodes in the central nervous system (Jeffery et al., 2014). Additionally, a recent study highlighted the importance of ink formulation and crosslinking on the printing of stable structures: a dual-crosslinking HA system was evaluated as printable hydrogel ink in biomedicine (Ouyang et al., 2016). It encompassed shear-thinning and self-healing properties through guest-host bonding, and showed an improved cell adhesion after further functionalization (i.e., peptides) (Ouyang et al., 2016).

Table 2.1. Summary of the medical, pharmaceutical, cosmetic and dietary applications of HA and its derivatives, reporting some examples, the beneficial actions, the key features and the state of the art.

Application	Examples	Beneficial actions and key advantages	State of the art
 <p><b>DRUG DELIVERY SYSTEMS</b></p>	<p>- Pro-drugs: HA-exedin 4 (Kong et al., 2010), HA-hydrocortisone, HA-prednisone, HA-prednisolone, HA-dexamethasone (Della Valle and Romeo, 1989), HA-P40 (Mangano et al., 2017), HA-curcumin (Manju and Sreenivasan, 2011) conjugates.</p> <p>- Surface modified liposomes: for the delivery of siRNA (Leite Nascimento et al., 2016), doxorubicin (Hayward et al., 2016), gembicicabine (Han et al., 2016), imatinib masylate (Negi et al., 2015), docetaxel (Nguyen et al., 2017); for ophthalmology (Moustafa et al., 2017), pneumology (Manconi et al., 2017) and topical treatments of wounds and burns (Yerushalmi et al., 1994).</p> <p>- Nanoparticles: consisting of HA (Kim et al., 2013; Maudens et al., 2018) or covered with HA (Pandey et al., 2018). Pulmonary delivery of dexamethasone to treat asthma (Negi et al., 2015), skin delivery of betametasone valerate for atopic dermatitis (Pandey et al., 2018), skin delivery of vitamin E for the management of wounds (Pereira et al., 2016), treatment of osteoarthritis (Maudens et al., 2018), cancer targeted therapies (Cho et al., 2011; Parashar et al., 2018; Wang et al., 2017).</p> <p>- Microspheres and microparticles: pulmonary delivery of ofloxacin (Hwang et al., 2008) and salbutamol sulphate (Li et al., 2017), bone supplementation (Fatnassi et al., 2014), skin delivery of caffeine (Simsolo et al., 2018). Microspheres can be formulated from native HA or from its synthetic derivatives such as HA benzyl esters (Esposito et al., 2005) and DVS-crosslinked HA (Shimajo et al., 2015).</p> <p>- Hydrogel: topical delivery of anti-inflammatories (El Kechai et al., 2016), anti-bacterials (Luo et al., 2000), antibodies and proteins (Egbu et al., 2018). Great potential for intraocular (Egbu et al., 2018; Koivusalo et al., 2018), intratympanic (El Kechai et al., 2016), intraarticular (Kroin et al., 2016) and dermal delivery (Pirard et al., 2005).</p>	<p>- Development of pro-drugs and derivatives with improved physico-chemical properties, stability, half-life time, and therapeutic efficacy compared to free drugs. Reduction of toxicity.</p> <p>- Development of biocompatible and biodegradable drug delivery systems with intrinsic moisturizing activity.</p>	<p>Except for gels, the industrialization and extensive clinical application are still a long way to go; many scientific studies are only at an <i>in vitro</i> experimental stage. Example of commercialized hydrogel: Solaraze® (Pharmaderm).</p>
 <p><b>CANCER THERAPY</b></p>	<p>Polymer-antitumoral conjugates and delivery systems encapsulating anticancer drugs:</p> <p>- HA-modified polycaprolactone nanoparticles encapsulating naringenin (Parashar et al., 2018).</p> <p>HA-coated chitosan nanoparticles encapsulating 5-fluorouracil (Wang et al., 2017).</p> <p>- novel unsaturated derivative of HA (Buffa et al., 2017).</p> <p>- HA-paclitaxel conjugates (Chen et al., 2018; Mero and Campisi, 2014).</p>	<p>HA can act as drug carrier and targeting agent (for CD44 receptor) at the same time (Mattheolabakis et al., 2015; Mero and Campisi, 2014; Parashar et al., 2018).</p>	<p>Promising results of many researches and clinical trials; further studies are strongly encouraged to develop marketable products.</p>
 <p><b>WOUND TREATMENT</b></p>	<p>- HA based wound dressings, films and hydrogels, eventually enriched with other therapeutic agents (Berce et al., 2018; Sanad and Abdel-Bar, 2017).</p> <p>- Applications in: dermatology, ophthalmology (Fallacara et al., 2017b; Wirostko et al., 2014), otolaryngology (Kaur et al., 2006), rhinology (Cassano et al., 2016), odontology (Dahiya and Kamal, 2013).</p>	<p>- Promotion of fibroblast proliferation, migration and adhesion to the wound site.</p> <p>- Stimulation of collagen production.</p> <p>- Improvement and acceleration of wound healing and re-epithelialization processes: treatment of skin irritations and wounds such as abrasion, post-surgical incisions, metabolic and vascular ulcers, burns (Aya and Stern, 2014; Neuman et al., 2015; Rueda López et al., 2005; Tagliagambe et al., 2017; Volpi et al., 2009).</p>	<p>Several products already marketed, such as Connettivina® (Fidia).</p>
 <p><b>OPHTHALMOLOGIC SURGERY AND OPHTHALMOLOGY</b></p>	<p>Solutions as viscosurgical devices and eye drops, consisting of native HA or its derivatives, such as HA-cysteine ethyl ester (Laffleur and Dachs, 2015) and urea-crosslinked HA (Fallacara et al., 2017b).</p>	<p>- Protection and lubrication of eye tissues, replacement of lost vitreous fluid and creation of space for manipulation during ophthalmic interventions (Knopf-Marques et al., 2016; Neumayer et al., 2008).</p> <p>- Hydration of the ocular surface, treatment of dry eye syndrome (Carracedo et al., 2017; Fallacara et al., 2017b; Vandermeer et al., 2018).</p>	<p>Several products already marketed, such as the viscosurgical device Healon® (Abbott) and the eye drops DropStar® (Bracco) and Lubristil® (Eyelab). Many studies show the safety and the efficacy of these formulations (Aragona et al., 2002; Ho et al., 2013; Johnson et al., 2006; Vandermeer et al., 2018).</p>
 <p><b>ARTHROLOGY</b></p>	<p>Intraarticular injections of native HMW HA and its crosslinked derivatives as viscosupplementation agents (Bowman et al., 2018; Brown et al., 1991; Sun et al., 2017).</p>	<p>- Absorption of mechanical impacts and avoidance of frictions between the bone-ends (Laurent and Fraser, 1992; Schiraldi et al., 2010; Tamer, 2013).</p> <p>Restoration of synovial fluid viscoelasticity (Brown et al., 1991).</p> <p>- Induction of HA synthesis in synovial cells stimulation of chondrocyte proliferation and resulting reduction of cartilage degradation (Bowman et al., 2018; Ghosh and Guidolin, 2002; Greenberg et al., 2006).</p> <p>- Treatment of rheumatoid arthritis and osteoarthritis, with reduction of pain and adverse effects (Bowman et al., 2018).</p>	<p>Many studies display the safety and the efficacy of HA intraarticular injections.</p> <p>Marketed products: Supartz FX® (Bioventus), Hyalgan® (Fidia) and Synvisc® (Genzyme).</p>

## 2.8. Conclusions, future trends and perspectives

Table 2.1. summarizes some of the most common medical, pharmaceutical, cosmetic and dietary applications of HA and its derivatives. The present review underlines the interest of academic and industrial research on HA: a comprehensive overview of this polymer is provided through the description of its structural, physico-chemical and hydrodynamic properties, occurrence, metabolism, biological roles, mechanisms of action, methods of production and derivatization, pharmaceutical, biomedical, food supplement and cosmetic applications.

During the last few decades, HA has shown great success due to its numerous and unique properties, such as biodegradability, biocompatibility, mucoadhesivity, hygroscopicity and viscoelasticity, and to the broad spectrum of chemical modifications that it can undergo, allowing the development of derivatives with specific targeting and long-lasting drug delivery. Several *in vitro* and *in vivo* studies have shown the beneficial actions of HA treatment, with anti-inflammatory, wound healing, chondroprotective, antiangiogenic, anti-ageing and immunosuppressive effects, among others (Cyphert et al., 2015; Fallacara et al., 2017b; Girish and Kemparaju, 2007; Tamer, 2013). This supported the development of a great number of HA-based commercial products: from native HA for ophthalmic and arthritic therapies, to food supplement, esthetic and cosmetic formulations. More recently, also some chemical derivatives of HA have received FDA approval and have been successfully introduced on the market, especially as DFs. As a proof of the great potential of this molecule in terms of real benefits for health, a search on the patent database Questel (Paris, France) was conducted (on 20 April 2018) and resulted in Table 2.2. that illustrates the interest toward HA.

Table 2.2. Data on hyaluronan patents resulting from the database Questel (Paris, France).

<b>Total</b>	<b>13,684</b>
Alive	8749
Dead	4935
<b>1st application year</b>	<b>unknown</b>
After 2015	2717
2011–2015	4568
2006–2010	2647
2001–2005	1694
Before 2001	2058

Although hyaluronan displays a great number of potential applications, further investigations and technological improvements are required, as there are still some questions to be answered and some issues to be addressed. First of all, many aspects of HA metabolism, receptor clustering and affinity still need to be explored to understand the different biological actions that hyaluronan has through changes in MW fully. Additional insight needs to be gained in understanding whether there is a relation between HA size and localization and how concomitant use of different HA sizes may modulate signaling. The comprehension of all these mechanisms could provide opportunities to extend and improve hyaluronan pharmaceutical, biomedical, cosmetics and food supplements applications, obtaining more



targeted effects. Towards this aim, the key mechanisms that control MW during HA biotechnological synthesis should be clarified to develop methods to produce more uniform size-defined HA. Additionally, progresses in metabolic engineering are necessary to improve HA yield and find biosynthetic strategies with good sustainability and acceptable production cost. Furthermore, the preparation of hyaluronan chemical derivatives needs to be optimized, using strategies such as one-pot reactions, chemo-selective synthesis, solvent-free methods and “click chemistry” approaches. Furthermore, the reproducibility of HA derivatives during scale-up, their pharmacokinetic and pharmacodynamic properties must be improved to allow their successful commercialization. Finally, all the HA-based next generation products, such as innovative crosslinked derivatives, polymer-drug conjugates and delivery systems, should be developed, enabling high biocompatibility, prolonged half-life and improved in situ permanence: hence, *in vivo* and clinical studies are required to characterize their safety and efficacy fully. Nevertheless, to date, recent *in vitro* research works have shown promising results, which open encouraging perspectives for safe and health uses of these novel derivatives: for example, HA-CL has displayed high biocompatibility towards human corneal and lung epithelial cell, as well as interesting anti-inflammatory, antioxidant and wound healing properties (Fallacara et al., 2017b, 2018).

## **2.9. Acknowledgments**

This work was supported by a PhD grant (to Arianna Fallacara) from I.R.A. Srl (Istituto Ricerche Applicate, Usmate-Velate, Monza-Brianza, Italy) and by Ambrosialab Srl (Ferrara, Italy, Grant 2017 to Stefano Manfredini and Silvia Vertuani).

## **2.10. Conflicts of interest**

The authors declare no conflict of interest.

## 2.11. References

- Abatangelo, G., Martelli, M., Vecchia, P., 1983. Healing of hyaluronic acid-enriched wounds: histological observations. *J. Surg. Res.* 35, 410-416.
- Adamia, S., Maxwell, C.A., Pilarski, L.M., 2005. Hyaluronan and hyaluronan synthases: potential therapeutic targets in cancer. *Curr. Drug Targets Cardiovasc. Haematol. Disord.* 5, 3-14.
- Adamia, S., Pilarski, P.M., Belch, A.R., Pilarski, L.M., 2013. Aberrant splicing, hyaluronan synthases and intracellular hyaluronan as drivers of oncogenesis and potential drug targets. *Curr. Cancer Drug Targets* 13, 347-361.
- American Society of Plastic Surgeons, A., 2017. 2017 Plastic surgery statistics report. <https://www.plasticsurgery.org/documents/News/Statistics/2017/plastic-surgery-statistics-report-2017.pdf> Accessed on March 2018.
- Aragona, P., Papa, V., Micali, A., Santocono, M., Milazzo, G., 2002. Long term treatment with sodium hyaluronate-containing artificial tears reduces ocular surface damage in patients with dry eye. *Br. J. Ophthalmol.* 86, 181–184.
- Auer, J.A., Fackelman, G.E., Gingerich, D.A., Fetter, A.W., 1980. Effect of hyaluronic acid in naturally occurring and experimentally induced osteoarthritis. *Am. J. Vet. Res.* 41, 568-574.
- Aya, K.L., Stern, R., 2014. Hyaluronan in wound healing: rediscovering a major player. *Wound Repair Regen.* 22, 579-593.
- Balazs, E.A., 1974. The physical properties of synovial fluid and the special role of hyaluronic acid. In: Helfet, A. (ed.) *Disorders of the Knee*. T.B. Lippincott Company, Philadelphia., pp. 63-75.
- Balazs, E.A., 1979. Ultrapure hyaluronic acid and the use thereof. U.S. Patent, US4141973.
- Balazs, E.A., Laurent, T.C., Jeanloz, R.W., 1986. Nomenclature of hyaluronic acid. *Biochem. J.* 235, 903.
- Balazs, E.A., Leshchiner, E., Larsen, N.E., Band, P., 1993. Applications of hyaluronan and its derivatives. In: Gebelein, C.G. (ed) *Biotechnological polymers*. Technomic, Lancaster., 41-65.
- Balogh, L., Polyak, A., Mathe, D., Kiraly, R., Thuroczy, J., Terez, M., Janoki, G., Ting, Y., Bucci, L.R., Schauss, A.G., 2008. An effectiveness study of hyaluronic acid [Hyabest® (J)] in the treatment of osteoarthritis of the knee on the patients in the United States. *J. Agric. Food Chem.* 56, 10582–10593.
- Bellini, D., Topai, A., 2000. Amides of hyaluronic acid and the derivatives thereof and a process for their preparation. WO 2000001733 A1.

- Bencherif, S.A., Srinivasan, A., Horkay, F., Hollinger, J.O., Matyjaszewski, K., Washburn, N.R., 2008. Influence of the degree of methacrylation on hyaluronic acid hydrogels properties. *Biomaterials*. 29, 1739-1749.
- Benedetti, L., Cortivo, R., Berti, T., Berti, A., Pea, F., Mazzo, M., Moras, M., Abatangelo, G., 1993. Biocompatibility and biodegradation of different hyaluronan derivatives (Hyaff) implanted in rats. *Biomaterials*. 14, 1154-1160.
- Benedetti, L.M., Topp, E.M., Stella, V.J., 1990. Microspheres of hyaluronic acid esters—Fabrication methods and in vitro hydrocortisone release. *J. Control. Release* 13, 33-41.
- Berce, C., Muresan, M.S., Soritau, O., Petrushev, B., Tefas, L., Rigo, I., Ungureanu, G., Catoi, C., Irimie, A., Tomuleasa, C., 2018. Cutaneous wound healing using polymeric surgical dressings based on chitosan, sodium hyaluronate and resveratrol. A preclinical experimental study. *Colloids Surf. B. Biointerfaces*. 163, 155-166.
- Bergman, K., Elvingson, C., Hilborn, J., Svensk, G., Bowden, T., 2007. Hyaluronic acid derivatives prepared in aqueous media by triazine-activated amidation. *Biomacromolecules*. 8, 2190-2195.
- Bhattacharya, D., Svehkarev, D., Soucek, J.J., Hill, T.K., Taylor, M.A., Natarajan, A., Mohs, A.M., 2017. Impact of structurally modifying hyaluronic acid on CD44 interaction. *J. Mater. Chem. B*. 5, 8183-8192.
- Binkhorst, C.D., 1980. Inflammation and intraocular pressure after the use of Healon in intraocular lens surgery. *J. Am. Intraocul. Implant. Soc.* 6, 340-341.
- Binkhorst, C.D., 1981. Advantages and disadvantages of intracameral Na-hyaluronate (Healon) in intraocular lens surgery. *Doc. Ophthalmol.* 50, 233-235.
- Blumberg, B.S., Ogston, A.G., Lowther, D.A., Rogers, H.J., 1958. Physicochemical properties of hyaluronic acid formed by *Streptococcus haemolyticus*. *Biochem J.* 70, 1-4.
- Boas, N.F., 1949. Isolation of hyaluronic acid from the cock's comb. *J. Biol. Chem.* 181, 573-575.
- Boeriu, C.G., Springer, J., Kooy, F.K., van den Broek, L.A.M., Eggink, G., 2013. Production methods for hyaluronan. *Int. J. Carbohydr. Chem.* 2013, 14, doi:10.1155/2013/624967.
- Bowman, S., Awad, M.E., Hamrick, M.W., Hunter, M., Fulzele, S., 2018. Recent advances in hyaluronic acid based therapy for osteoarthritis. *Clin. Transl. Med.* 7, 6.
- Brown, T.J., Laurent, U.B., Fraser, J.R., 1991. Turnover of hyaluronan in synovial joints: elimination of labelled hyaluronan from the knee joint of the rabbit. *Exp Physiol.* 76, 125-134.
- Buffa, R., Šedová, P., Basarabová, I., Bobula, T., Procházková, P., Vágnerová, H., Dolečková, I., Moravčíková, S., Hejlová, L., Velebný, V., 2017. A new unsaturated derivative of hyaluronic acid - Synthesis, analysis and applications. *Carbohydr. Polym.* 163, 247-253.

- Bulpitt, P., Aeschlimann, D., 1999. New strategy for chemical modification of hyaluronic acid: preparation of functionalized derivatives and their use in the formation of novel biocompatible hydrogels. *J. Biomed. Mater. Res.* 47, 152-169.
- Campo, G.M., Avenoso, A., D'Ascola, A., Prestipino, V., Scuruchi, M., Nastasi, G., Calatroni, A., Campo, S., 2013. 4-mer hyaluronan oligosaccharides stimulate in ammation response in synovial broblasts in part via TAK-1 and in part via p38-MAPK. *Curr. Med. Chem.* 20, 1162-1172.
- Carracedo, G., Villa-Collar, C., Martin-Gil, A., Serramito, M., Santamaría, L., 2017. Comparison Between Viscous Teardrops and Saline Solution to Fill Orthokeratology Contact Lenses Before Overnight Wear. *Eye Contact Lens.* doi: 10.1097/ICL.0000000000000416.
- Cassano, M., Russo, G.M., Granieri, C., Cassano, P., 2016. Cytofunctional changes in nasal ciliated cells in patients treated with hyaluronate after nasal surgery. *Am. J. Rhinol. Allergy.* 30, 83-88.
- Chen, Y., Peng, F., Song, X., Wu, J., Yao, W., Gao, X., 2018. Conjugation of paclitaxel to C-6 hexanediamine-modified hyaluronic acid for targeted drug delivery to enhance antitumor efficacy. *Carbohydr. Polym.* 181, 150-158.
- Cheng, F., Gong, Q., Yu, H., Stephanopoulos, G., 2016. High-titer biosynthesis of hyaluronic acid by recombinant *Corynebacterium glutamicum*. *Biotechnol J.* 11, 574-584.
- Cherr, G.N., Yudin, A.I., Overstreet, J.W., 2001. The dual functions of GPI-anchored PH-20: hyaluronidase and intracellular signaling. *Matrix Biol.* 20, 515-525.
- Chi, Y., Yin, X., Sun, K., Feng, S., Liu, J., Chen, D., Guo, C., Wu, Z., 2017. Redox-sensitive and hyaluronic acid functionalized liposomes for cytoplasmic drug delivery to osteosarcoma in animal models. *J. Control Release.* 261, 113-125.
- Chien, L.J., Lee, C.K., 2007. Enhanced hyaluronic acid production in *Bacillus subtilis* by coexpressing bacterial hemoglobin. *Biotechnol. Prog.* 23, 1017-1022.
- Cho, H.J., Yoon, H.Y., Koo, H., Ko, S.H., Shim, J.S., Lee, J.H., Kim, K., Kwon, I.C., Kim, D.D., 2011. Self-assembled nanoparticles based on hyaluronic acid-ceramide (HA-CE) and Pluronic® for tumor-targeted delivery of docetaxel. *Biomaterials.* 32, 7181-7190.
- Collins, M., Birkinshaw, C., 2007. Comparison of the effectiveness of four different crosslinking agents with hyaluronic acid hydrogel films for tissue-culture applications. *J. Appl. Polym. Sci.* 104, 3183–3191.
- Collins, M.N., Birkinshaw, C., 2008. Physical properties of crosslinked hyaluronic acid hydrogels. *J. Mater. Sci. Mater. Med.* 19, 3335-3343.
- Crescenzi, V., Francescangeli, A., Segre, A., Capitani, D., Mannina, L., Renier, D., Bellini, D., 2002. NMR structural study of hydrogels based on partially deacetylated hyaluronan. *Macromol. Biosci.* 2, 272–279.

- Crescenzi, V., Francescangeli, A., Taglienti, A., Capitani, D., Mannina, L., 2003. Synthesis and partial characterization of hydrogels obtained via glutaraldehyde crosslinking of acetylated chitosan and of hyaluronan derivatives. *Biomacromolecules*. 4, 1045–1054.
- Csoka, A.B., Frost, G.I., Stern, R., 2001. The six hyaluronidase-like genes in the human and mouse genomes. *Matrix Biol.* 20.
- Csoka, A.B., Frost, G.I., Wong, T., Stern, R., 1997. Purification and microsequencing of hyaluronidase isozymes from human urine. *FEBS Lett.* 417, 307–310.
- Cyphert, J.M., Trempus, C.S., Garantziotis, S., 2015. Size matters: molecular weight specificity of hyaluronan effects in cell biology. *Int. J. Cell Biol.*, 563818.
- Dahiya, P., Kamal, R., 2013. Hyaluronic acid: a boon in periodontal therapy. *N. Am. J. Med. Sci.* 5, 309-315.
- De Oliveira, J.D., Carvalho, L.S., Gomes, A.M., Queiroz, L.R., Magalhães, B.S., Parachin, N.S., 2016. Genetic basis for hyper production of hyaluronic acid in natural and engineered microorganisms. *Microb. Cell Fact.* 15, 119.
- DeAngelis, P.L., 1999. Hyaluronan synthases: fascinating glycosyltransferases from vertebrates, bacterial pathogens, and algal viruses. *Cell. Mol. Life Sci.* 56, 670-682.
- DeAngelis, P.L., 2008. Monodisperse hyaluronan polymers: synthesis and potential applications. *Curr. Pharm. Biotechnol.* 9, 246–248.
- DeAngelis, P.L., Achyuthan, A.M., 1996. Yeast-derived recombinant DG42 protein of *Xenopus* can synthesize hyaluronan in vitro. *J. Biol. Chem.* 271, 23657–23660.
- DeAngelis, P.L., Jing, W., Drake, R.R., Achyuthan, A.M., 1998. Identification and molecular cloning of a unique hyaluronan synthase from *Pasteurella multocida*. *J. Biol. Chem.* 273, 8454-8458.
- Della Valle, F., Romeo, A., 1989. Esters of hyaluronic acid. US4851521.
- D'Este, M., Eglin, D., Alini, M., 2014. A systematic analysis of DMTMM vs EDC/NHS for ligation of amines to hyaluronan in water. *Carbohydr. Polym.* 108, 239-246.
- Doillon, C.J., Silver, F.H., 1986. Collagen-based wound dressing: effects of hyaluronic acid and fibronectin on wound healing. *Biomaterials*. 7, 3-8.
- Donnelly, P.E., Chen, T., Finch, A., Brial, C., Maher, S.A., Torzilli, P.A., 2017. Photocrosslinked tyramine-substituted hyaluronate hydrogels with tunable mechanical properties improve immediate tissue-hydrogel interfacial strength in articular cartilage. *J. Biomater. Sci. Polym. Ed.* 28, 582-600.

- Dougados, M., Nguyen, M., Listrat, V., Amor, B., 1993. High molecular weight sodium hyaluronate (hyalectin) in osteoarthritis of the knee: a 1 year placebo-controlled trial. *Osteoarthritis Cartilage*. 1, 97-103.
- Drealos, Z.D., 2010. Nutrition and enhancing youthful-appearing skin. *Clin. Dermatol.* 28, 400–408.
- Duranti, F., Salti, G., Bovani, B., Calandra, M., Rosati, M.L., 1998. Injectable hyaluronic acid gel for soft tissue augmentation. A clinical and histological study. *Dermatol. Surg.* 24, 1317-1325.
- Ebid, R., Lichtnekert, J., Anders, H.J., 2014. Hyaluronan is not a ligand but a regulator of toll-like receptor signaling in mesangial cells: role of extracellular matrix in innate immunity. *ISRN Nephrol.* 2014:714081.
- Egbu, R., Brocchini, S., Khaw, P.T., Awwad, S., 2018. Antibody loaded collapsible hyaluronic acid hydrogels for intraocular delivery. *Eur. J. Pharm. Biopharm.* 124, 95-103.
- El Kechai, N., Geiger, S., Fallacara, A., Cañero Infante, I., Nicolas, V., Ferrary, E., Huang, N., Bochot, A., Agnely, F., 2017. Mixtures of hyaluronic acid and liposomes for drug delivery: Phase behavior, microstructure and mobility of liposomes. *Int. J. Pharm.* 523, 246-259.
- El Kechai, N., Mabelle, E., Nguyen, Y., Huang, N., Nicolas, V., Chaminade, P., Yen-Nicolaÿ, S., Gueutin, C., Granger, B., Ferrary, E., Agnely, F., Bochot, A., 2016. Hyaluronic acid liposomal gel sustains delivery of a corticoid to the inner ear. *J. Control. Release.* 226, 248-257.
- Esposito, E., Menegatti, E., Cortesi, R., 2005. Hyaluronan-based microspheres as tools for drug delivery: a comparative study. *Int. J. Pharm.* 288, 35-49.
- Fallacara, A., Manfredini, S., Durini, E., Vertuani, S., 2017a. Hyaluronic acid fillers in soft tissue regeneration. *Facial Plast. Surg.* 33, 87-96.
- Fallacara, A., Vertuani, S., Panozzo, G., Pecorelli, A., Valacchi, G., Manfredini, S., 2017b. Novel Artificial Tears Containing Cross-Linked Hyaluronic Acid: An In Vitro Re-Epithelialization Study. *Molecules.* 22.
- Fallacara, A., Busato, L., Pozzoli, M., Ghadiri, M., Ong, H.X., Young, P.M., Manfredini, S., Traini, D., 2018. Combination of urea-crosslinked hyaluronic acid and sodium ascorbyl phosphate for the treatment of inflammatory lung diseases: An in vitro study. *Eur. J. Pharm. Sci.* 120, 96–106.
- Fatnassi, M., Jacquart, S., Brouillet, F., Rey, C., Combes, C., Girod Fullana, S., 2014. Optimization of spray-dried hyaluronic acid microspheres to formulate drug-loaded bone substitute materials. *Powder Technol.* 255, 44–51.

- Felgueiras, H.P., Wang, L.M., Ren, K.F., Querido, M.M., Jin, Q., Barbosa, M.A., Ji, J., Martins, M.C., 2017. Octadecyl chains immobilized onto hyaluronic acid coatings by thiol-ene "click chemistry" increase the surface antimicrobial properties and prevent platelet adhesion and activation to polyurethane. *ACS Appl. Mater. Interfaces*. 9, 7979-7989.
- Fletcher, E., Jacobs, J.H., Markham, R.L., 1955. Viscosity studies on hyaluronic acid of synovial fluid in rheumatoid arthritis and osteoarthritis. *Clin. Sci*. 14, 653-660.
- Fraser, J.R., Laurent, T.C., Laurent, U.B., 1997. Hyaluronan: its nature, distribution, functions and turnover. *J. Intern. Med*. 242, 27-33.
- Frost, G.I., Csóka, A.B., Wong, T., Stern, R., 1997. Purification, cloning, and expression of human plasma hyaluronidase. *Biochem. Biophys. Res. Commun*. 236, 10-15.
- Fu, S., Dong, H., Deng, X., Zhuo, R., Zhong, Z., 2017. Injectable hyaluronic acid/poly(ethylene glycol) hydrogels crosslinked via strain-promoted azide-alkyne cycloaddition click reaction. *Carbohydr. Polym*. 169, 332-340.
- Furnari, M.L., Termini, L., Traverso, G., Barrale, S., Bonaccorso, M.R., Damiani, G., Piparo, C.L., Collura, M., 2012. Nebulized hypertonic saline containing hyaluronic acid improves tolerability in patients with cystic fibrosis and lung disease compared with nebulized hypertonic saline alone: a prospective, randomized, double-blind, controlled study. *Ther. Adv. Respir. Dis*. 6, 315-322.
- Gao, F., Yang, C.X., Mo, W., Liu, Y.W., He, Y.Q., 2008. Hyaluronan oligosaccharides are potential stimulators to angiogenesis via RHAMM mediated signal pathway in wound healing. *Clin. Invest. Med*. 31, E106-E116.
- Gao, Y., Foster, R., Yang, X., Feng, Y., Shen, J.K., Mankin, H.J., Hornicek, F.J., Amiji, M.M., Duan, Z., 2015. Up-regulation of CD44 in the development of metastasis, recurrence and drug resistance of ovarian cancer. *Oncotarget*. 6, 9313-9326.
- Garantziotis, S., Brezina, M., Castelnovo, P., Drago, L., 2016. The role of hyaluronan in the pathobiology and treatment of respiratory disease. *Am. J. Physiol. Lung Cell Mol. Physiol*. 310, L785-L795.
- Gavina, M., Luciani, A., Vilella, V.R., Esposito, S., Ferrari, E., Bressani, I., Casale, A., Bruscia, E.M., Maiuri, L., Raia, V., 2013. Nebulized hyaluronan ameliorates lung inflammation in cystic fibrosis mice. *Pediatr. Pulmonol*. 48, 761-771.
- Gelardi, M., Guglielmi, A.V., De Candia, N., Maffezzoni, E., Berardi, P., Quaranta, N., 2013a. Effect of sodium hyaluronate on mucociliary clearance after functional endoscopic sinus surgery. *Eur. Ann. Allergy Clin. Immunol*. 45, 103-108.
- Gelardi, M., Iannuzzi, L., Quaranta, N., 2013b. Intranasal sodium hyaluronate on the nasal cytology of patients with allergic and nonallergic rhinitis. *Int. Forum Allergy Rhinol*. 3, 807-813.

- Gerdin, B., Hällgren, R., 1997. Dynamic role of hyaluronan (HYA) in connective tissue activation and inflammation. *J. Intern. Med.* 242, 49-55.
- Ghosh, P., Guidolin, D., 2002. Potential mechanism of action of intra-articular hyaluronan therapy in osteoarthritis: are the effects molecular weight dependent? *Semin. Arthritis Rheum.* 32, 10-37.
- Ghosh, S., Kobal, I., Zanette, D., Reed, W.F., 1993. Conformational contraction and hydrolysis of hyaluronate in sodium hydroxide solutions. *Macromolecules* 26, 4685–4693.
- Girish, K.S., Kemparaju, K., 2007. The magic glue hyaluronan and its eraser hyaluronidase: a biological overview. *Life Sci.* 80, 1921-1943.
- Goddard, J.C., Janssen, D.A.W., 2017. Intravesical hyaluronic acid and chondroitin sulfate for recurrent urinary tract infections: systematic review and meta-analysis. *Int. Urogynecol. J.*, doi: 10.1007/s00192-00017-03508-z.
- Göllner, I., Voss, W., von Hehn, U., Kammerer, S., 2017. Ingestion of an Oral Hyaluronan Solution Improves Skin Hydration, Wrinkle Reduction, Elasticity, and Skin Roughness: Results of a Clinical Study. *J. Evid. Based Complement. Altern. Med.* 22, 816–823.
- Graue, E.L., Polack, F.M., Balazs, E.A., 1980. The protective effect of Na-hyaluronate to corneal endothelium. *Exp. Eye. Res.* 31, 119-127.
- Greenberg, D.D., Stoker, A., Kane, S., Cockrell, M., Cook, J.L., 2006. Biochemical effects of two different hyaluronic acid products in a co-culture model of osteoarthritis. *Osteoarthritis Cartilage.* 14, 814-822.
- Gura, E., Hüchel, M., Müller, P.J., 1998. Specific degradation of hyaluronic acid and its rheological properties. *Polym. Degrad. Stab.* 59, 297-302.
- Gurski, L.A., Jha, A.K., Zhang, C., Jia, X., Farach-Carson, M.C., 2009. Hyaluronic acid-based hydrogels as 3D matrices for in vitro evaluation of chemotherapeutic drugs using poorly adherent prostate cancer cells. *Biomaterials.* 30, 6076–6085.
- Han, N.K., Shin, D.H., Kim, J.S., Weon, K.Y., Jang, C.Y., Kim, J.S., 2016. Hyaluronan-conjugated liposomes encapsulating gemcitabine for breast cancer stem cells. *Int. J. Nanomedicine* 11, 1413-1425.
- Hascall, V., Laurent, T., 1997. Hyaluronan: structure and physical properties. *GlycoForum - Hyaluronan Today Website.* Available online: <http://glycoforum.gr.jp/science/hyaluronan/HA01/HA01E.html> (accessed on 22 February 2018).
- Hašová, M., Crhák, T., Safránková, B., Dvořáková, J., Muthný, T., Velebný, V., Kubala, L., 2011. Hyaluronan minimizes effects of UV irradiation on human keratinocytes. *Arch. Dermatol. Res.* 303, 277-284.



- Hayward, S.L., Wilson, C.L., Kidambi, S., 2016. Hyaluronic acid-conjugated liposome nanoparticles for targeted delivery to CD44 overexpressing glioblastoma cells. *Oncotarget*. 7, 34158-34171.
- Heatley, F., Scott, J.E., 1988. A water molecule participates in the secondary structure of hyaluronan. *Biochem J*. 254, 489-493.
- Heldin, P., Lin, C.Y., Kolliopoulos, K., Chen, Y.H., Skandalis, S.S., 2018. Regulation of hyaluronan biosynthesis and clinical impact of excessive hyaluronan production. *Matrix Biol.*, doi: 10.1016/j.matbio.2018.1001.1017.
- Hellström, S., Laurent, C., 1987. Hyaluronan and healing of tympanic membrane perforations. An experimental study. *Acta Otolaryngol. Suppl.* 442, 54-61.
- Hirano, K., Sakai, S., Ishikawa, T., Avci, F.Y., Linhardt, R.J., Toida, T., 2005. Preparation of the methyl ester of hyaluronan and its enzymatic degradation. *Carbohydr. Res.* 340, 2297-2304.
- Ho, W.T., Chiang, T.H., Chang, S.W., Chen, Y.H., Hu, F.R., Wang, I.J., 2013. Enhanced corneal wound healing with hyaluronic acid and high-potassium artificial tears. *Clin. Exp. Optom.* 96, 536-541.
- Huin-Amargier, C., Marchal, P., Payan, E., Netter, P., Dellacherie, E., 2006. New physically and chemically crosslinked hyaluronate (HA)-based hydrogels for cartilage repair. *J. Biomed. Mater. Res. A* 76, 416-424.
- Hwang, S.M., Kim, D.D., Chung, S.J., Shim, C.K., 2008. Delivery of ofloxacin to the lung and alveolar macrophages via hyaluronan microspheres for the treatment of tuberculosis. *J. Control Release.* 129, 100-106.
- Itano, N., Kimata, K., 2002. Mammalian hyaluronan synthases. *IUBMB Life.* 54, 195-199.
- Itano, N., Sawai, T., Yoshida, M., Lenas, P., Yamada, Y., Imagawa, M., Shinomura, T., Hamaguchi, M., Yoshida, Y., Ohnuki, Y., Miyauchi, S., Spicer, A.P., McDonald, J.A., Kimata, K., 1999. Three isoforms of mammalian hyaluronan synthases have distinct enzymatic properties. *J. Biol. Chem.* 274, 25085-25092.
- Janiš, R., Pata, V., Egner, P., Pavlačková, J., Zapletalová, A., Kejlová, K., 2017. Comparison of metrological techniques for evaluation of the impact of a cosmetic product containing hyaluronic acid on the properties of skin surface. *Biointerphases.* 12, 021006.
- Jeffery, A.F., Churchward, M.A., Mushahwar, V.K., Todd, K.G., Elias, A.L., 2014. Hyaluronic acid-based 3D culture model for in vitro testing of electrode biocompatibility. *Biomacromolecules.* 15, 2157-2165.
- Jeong, E., Shim, W.Y., Kim, J.H., 2014. Metabolic engineering of *Pichia pastoris* for production of hyaluronic acid with high molecular weight. *J. Biotechnol.* 185, 28-36.

- Jiang, D., Liang, J., Noble, P.W., 2007. Hyaluronan in tissue injury and repair. *Annu. Rev. Cell. Dev. Biol.* 23, 435-461.
- Jiang, D., Liang, J., Noble, P.W., 2011. Hyaluronan as an immune regulator in human diseases. *Physiol. Rev.* 91, 221-264.
- Johnson, M.E., Murphy, P.J., Boulton, M., 2006. Effectiveness of sodium hyaluronate eyedrops in the treatment of dry eye. *Graefes Arch. Clin. Exp. Ophthalmol.* 244, 109-112.
- Jones, A.C., Patrick, M., Doherty, S., Doherty, M., 1995. Intra-articular hyaluronic acid compared to intra-articular triamcinolone hexacetonide in inflammatory knee osteoarthritis. *Osteoarthritis Cartilage.* 3, 269-273.
- Juhlin, L., 1997. Hyaluronan in skin. *J. Intern. Med.* 242, 61-66.
- Kaczmarek, B., Sionkowska, A., Kozłowska, J., Osyczka, A.M., 2018. New composite materials prepared by calcium phosphate precipitation in chitosan/collagen/hyaluronic acid sponge cross-linked by EDC/NHS. *Int. J. Biol. Macromol.* 107, 247-253.
- Kanski, J.J., 1975. Intravitreal hyaluronic acid injection. A long-term clinical evaluation. *Br. J. Ophthalmol.* 59, 255-256.
- Kaur, K., Singh, H., Singh, M., 2006. Repair of tympanic membrane perforation by topical application of 1% sodium hyaluronate. *Indian J. Otolaryngol. Head Neck Surg.* 58, 241-244.
- Kaur, M., Jayaraman, G., 2016. Hyaluronan production and molecular weight is enhanced in pathway-engineered strains of lactate dehydrogenase-deficient *Lactococcus lactis*. *Metab. Eng. Commun.* 3.
- Kawada, C., Kimura, M., Masuda, Y., Nomura, Y., 2015b. Oral administration of hyaluronan prevents skin dryness and epidermal thickening in ultraviolet irradiated hairless mice. *J. Photochem. Photobiol. B.* 153, 215-221.
- Kawada, C., Yoshida, T., Yoshida, H., Matsuoka, R., Sakamoto, W., Odanaka, W., Sato, T., Yamasaki, T., Kanemitsu, T., Masuda, Y., Urushibata, O., 2014. Ingested hyaluronan moisturizes dry skin. *Nutr. J.* 13, 70.
- Kawada, C., Yoshida, T., Yoshida, H., Sakamoto, W., Odanaka, W., Sato, T., Yamasaki, T., Kanemitsu, T., Masuda, Y., Urushibata, O., 2015a. Ingestion of hyaluronans (molecular weights 800 k and 300 k) improves dry skin conditions: A randomized, double blind, controlled study. *J. Clin. Biochem. Nutr.* 56, 66-73.
- Kaye, M.A., Stacey, M., 1950. Observations on the chemistry of hyaluronic acid. *Biochem. J.* 2, 13.
- Kendall, F.E., Heidelberger, M., Dawson, M.H., 1937. A serologically inactive polysaccharide elaborated by mucoid strains of group a hemolytic streptococcus. *J. Biol. Chem.* 118, 61-69.

- Kim, H., Park, H.T., Tae, Y.M., Kong, W.H., Sung, D.K., Hwang, B.W., Kim, K.S., Kim, Y.K., Hahn, S.K., 2013a. Bioimaging and pulmonary applications of self-assembled Flt1 peptide-hyaluronic acid conjugate nanoparticles. *Biomaterials*. 34, 8478-8490.
- Kim, J.H., Yoo, S.J., Oh, D.K., Kweon, Y.G., Park, D.W., Lee, C.H., Gil, G.H., 1996. Selection of a *Streptococcus equi* mutant and optimization of culture conditions for the production of high molecular weight hyaluronic acid. *Enzyme Microb. Technol.* 19, 440-445.
- Kim, M.Y., Muto, J., Gallo, R.L., 2013a. Hyaluronic acid oligosaccharides suppress TLR3-dependent cytokine expression in a TLR4-dependent manner. *PLoS ONE* 8, Article ID e72421.
- Kimura, M., Maeshima, T., Kubota, T., Kurihara, H., Masuda, Y., Nomura, Y., 2016. Adsorption of orally administered hyaluronan. *J. Med. Food*. 19, 1172–1179.
- King, S.R., Hickerson, W.L., Proctor, K.G., 1991. Beneficial actions of exogenous hyaluronic acid on wound healing. *Surgery*. 109, 76-84.
- Kirk, J.F., Ritter, G., Finger, I., Sankar, D., Reddy, J.D., Talton, J.D., Nataraj, C., Narisawa, S., Millán, J.L., Cobb, R.R., 2013. Mechanical and biocompatible characterization of a cross-linked collagen-hyaluronic acid wound dressing. *Biomater*. 3, pii: e25633.
- Knopf-Marques, H., Pravda, M., Wolfova, L., Velebny, V., Schaaf, P., Vrana, N.E., Lavallo, P., 2016. Hyaluronic Acid and Its Derivatives in Coating and Delivery Systems: Applications in Tissue Engineering, Regenerative Medicine and Immunomodulation. *Adv. Healthc. Mater.* 5, 2841-2855.
- Kobayashi, Y., Okamoto, A., Nishinari, K., 1994. Viscoelasticity of hyaluronic acid with different molecular weights. *Biorheology*. 31, 235-244.
- Kogan, G., Soltés, L., Stern, R., Gemeiner, P., 2007. Hyaluronic acid: a natural biopolymer with a broad range of biomedical and industrial applications. *Biotechnol. Lett.* 29, 17-25.
- Koivusalo, L., Karvinen, J., Sorsa, E., Jönkkäri, I., Väliäho, J., Kallio, P., Ilmarinen, T., Miettinen, S., Skottman, H., Kellomäki, M., 2018. Hydrazone crosslinked hyaluronan-based hydrogels for therapeutic delivery of adipose stem cells to treat corneal defects. *Mater. Sci. Eng. C. Mater. Biol. Appl.* 85, 68-78.
- Kong, J.H., Oh, E.J., Chae, S.Y., Lee, K.C., Hahn, S.K., 2010. Long acting hyaluronate--exendin 4 conjugate for the treatment of type 2 diabetes. *Biomaterials*. 31, 4121-4128.
- Kroin, J.S., Kc, R., Li, X., Hamilton, J.L., Das, V., van Wijnen, A.J., Dall, O.M., Shelly, D.A., Kenworth, T., Im, H.J., 2016. Intraarticular slow-release triamcinolone acetate reduces allodynia in an experimental mouse knee osteoarthritis model. *Gene*. 591, 1-5.
- Laffleur, F., Dachs, S., 2015. Development of novel mucoadhesive hyaluronic acid derivative as lubricant for the treatment of dry eye syndrome. *Ther. Deliv.* 6, 1211-1219.

- Lapčík, L.J., Lapčík, L., De Smedt, S., Demeester, J., Chabreck, P., 1998. Hyaluronan: Preparation, Structure, Properties, and Applications. *Chem. Rev.* 98, 2663-2684.
- Larrañeta, E., Henry, M., Irwin, N.J., Trotter, J., Perminova, A.A., Donnelly, R.F., 2018. Synthesis and characterization of hyaluronic acid hydrogels crosslinked using a solvent-free process for potential biomedical applications. *Carbohydr. Polym.* 181, 1194-1205.
- Larson, B., 2015. 3D Cell Culture: A Review of Current Techniques. Available online: <http://mktg.biotech.com/news/2015/Fall/featured-application.html> (accessed on 14 June 2018).
- Laurent, T., 1989. The biology of hyaluronan. Introduction. *Ciba Found. Symp.* 143, 1-20.
- Laurent, T.C., Fraser, J.R., 1992. Hyaluronan. *FASEB J.* 6, 2397-2404.
- Leardini, G., Perbellini, A., Franceschini, M., Mattara, L., 1988. Intra-articular injections of hyaluronic acid in the treatment of painful shoulder. *Clin. Ther.* 10, 521-526.
- Leite Nascimento, T., Hillaireau, H., Vergnaud, J., Rivano, M., Deloménie, C., Courilleau, D., Arpicco, S., Suk, J.S., Hanes, J., Fattal, E., 2016. Hyaluronic acid-conjugated lipoplexes for targeted delivery of siRNA in a murine metastatic lung cancer model. *Int. J. Pharm.* 514, 103-111.
- Lepperdinger, G., Strobl, B., Kreil, G., 1998. HYAL2, a human gene expressed in many cells, encodes a lysosomal hyaluronidase with a novel type of specificity. *J. Biol. Chem.* 273, 22466-22470.
- Li, H., Xue, Y., Jia, B., Bai, Y., Zuo, Y., Wang, S., Zhao, Y., Yang, W., Tang, H., 2018. The preparation of hyaluronic acid grafted pullulan polymers and their use in the formation of novel biocompatible wound healing film. *Carbohydr. Polym.* 188.
- Li, Y., Han, M., Liu, T., Cun, D., Fang, L., Yang, M., 2017. Inhaled hyaluronic acid microparticles extended pulmonary retention and suppressed systemic exposure of a short-acting bronchodilator. *Carbohydr. Polym.* 172, 197-204.
- Li, Y., Liang, J., Yang, T., Monterrosa Mena, J., Huan, C., Xie, T., Kurkciyan, A., Liu, N., Jiang, D., Noble, P.W., 2016. Hyaluronan synthase 2 regulates fibroblast senescence in pulmonary fibrosis. *Matrix Biol.* 55, 35-48.
- Lim, D.G., Prim, R.E., Kang, E., Jeong, S.H., 2018. One-pot synthesis of dopamine-conjugated hyaluronic acid/polydopamine nanocomplexes to control protein drug release. *Int. J. Pharm.* doi: <https://doi.org/10.1016/j.ijpharm.2018.03.007>.
- Lim, S.T., Martin, G.P., Berry, D.J., Brown, M.B., 2000. Preparation and evaluation of the in vitro drug release properties and mucoadhesion of novel microspheres of hyaluronic acid and chitosan. *J. Control. Release.* 66, 281-292.

- Lin, K., Bartlett, S.P., Matsuo, K., LiVolsi, V.A., Parry, C., Hass, B., Whitaker, L.A., 1994. Hyaluronic acid-filled mammary implants: an experimental study. *Plast. Reconstr. Surg.* 94, 306-315.
- Liu, L., Liu, Y., Li, J., Du, G., Chen, J., 2011. Microbial production of hyaluronic acid: current state, challenges, and perspectives. *Microb. Cell Fact.* 10, 99.
- Lokeshwar, V.B., Rubinowicz, D., Schroeder, G.L., Forgacs, E., Minna, J.D., Block, N.L., Nadji, M., Lokeshwar, B.L., 2001. Stromal and epithelial expression of tumor markers hyaluronic acid and HYAL1 hyaluronidase in prostate cancer. *J. Biol. Chem.* 276, 11922–11932.
- Luo, Y., Kirker, K.R., Prestwich, G.D., 2000. Cross-linked hyaluronic acid hydrogel films: new biomaterials for drug delivery. *J. Control Release.* 69, 169-184.
- Magnani, A., Rappuoli, R., Lamponi, S., Barbucci, R., 2000. Novel polysaccharide hydrogels: characterization and properties *Polym. Adv. Technol.* 11, 488-495.
- Maleki, A., Kjøniksen, A.L., Nystrom, B., 2008. Effect of pH on the behavior of hyaluronic acid in dilute and semidilute aqueous solutions. *Macromol. Symp.* 274, 131–140.
- Maleki, A., Kjøniksen, A.L., Nystrom, B., 2008. Effect of pH on the behavior of hyaluronic acid in dilute and semidilute aqueous solutions. *Macromol. Symp.* 274, 131–140.
- Malson, T., Lindqvist, B., 1986. Gels of crosslinked hyaluronic acid for use as a vitreous humor substitute. WO1986000079.
- Manconi, M., Manca, M.L., Valenti, D., Escribano, E., Hillaireau, H., Fadda, A.M., Fattal, E., 2017. Chitosan and hyaluronan coated liposomes for pulmonary administration of curcumin. *Int. J. Pharm.* 525, 203-210.
- Mangano, K., Vergalito, F., Mammana, S., Mariano, A., De Pasquale, R., Meloscia, A., Bartollino, S., Guerra, G., Nicoletti, F., Di Marco, R., 2017. Evaluation of hyaluronic acid-P40 conjugated cream in a mouse model of dermatitis induced by oxazolone. *Exp. Ther. Med.* 14, 2439-2444.
- Manju, S., Sreenivasan, K., 2011. Conjugation of curcumin onto hyaluronic acid enhances its aqueous solubility and stability. *J. Colloid Interface Sci.* 359, 318–325.
- Mattheolabakis, G., Milane, L., Singh, A., Amiji, M.M., 2015. Hyaluronic acid targeting of CD44 for cancer therapy: from receptor biology to nanomedicine. *J. Drug Target.* 23, 605-618.
- Maudens, P., Meyer, S., Seemayer, C.A., Jordan, O., Allémann, E., 2018. Self-assembled thermoresponsive nanostructures of hyaluronic acid conjugates for osteoarthritis therapy. *Nanoscale.* 10, 1845-1854.

- Mero, A., Campisi, M., 2014. Hyaluronic acid bioconjugates for the delivery of bioactive molecules. *Polymers* 6, 346-369.
- Meyer, K., 1947. The biological significance of hyaluronic acid and hyaluronidase. *Physiol Rev.* 27, 335-359.
- Meyer, K., 1948. Highly viscous sodium hyaluronate. *J. Biol. Chem.* 176, 993.
- Meyer, K., Palmer, J.W., 1934. The polysaccharide of the vitreous humor. *J. Biol. Chem.* 107, 629-634.
- Miller, D., Stegmann, R., 1980. Use of Na-hyaluronate in anterior segment eye surgery. *J. Am. Intraocul. Implant. Soc.* 6, 13-15.
- Misra, S., Toole, B.P., Ghatak, S., 2006. Hyaluronan constitutively regulates activation of multiple receptor tyrosine kinases in epithelial and carcinoma cells. *J. Biol. Chem.* 281, 34936–34941.
- Mlcochová, P., Bystrický, S., Steiner, B., Machová, E., Koós, M., Velebný, V., Krcmár, M., 2006. Synthesis and characterization of new biodegradable hyaluronan alkyl derivatives. *Biopolymers.* 82, 74-79.
- Monzon, M.E., Casalino-Matsuda, S.M., Forteza, R.M., 2006. Identification of glycosaminoglycans in human airway secretions. *Am. J. Respir. Cell. Mol. Biol.* 34, 135-141.
- Monzon, M.E., Fregien, N., Schmid, N., Falcon, N.S., Campos, M., Casalino-Matsuda, S.M., Forteza, R.M., 2010. Reactive oxygen species and hyaluronidase 2 regulate airway epithelial hyaluronan fragmentation. *J. Biol. Chem.* 285, 26126-26134.
- Moreira, C.A.J., Armstrong, D.K., Jelliffe, R.W., Moreira, A.T., Woodford, C.C., Liggett, P.E., Trousdale, M.D., 1991. Sodium hyaluronate as a carrier for intravitreal gentamicin. An experimental study. *Acta Ophthalmol. (Copenh).* 69, 45-49.
- Morimoto, K., Yamaguchi, H., Iwakura, Y., Morisaka, K., Ohashi, Y., Nakai, Y., 1991. Effects of viscous hyaluronate-sodium solutions on the nasal absorption of vasopressin and an analogue. *Pharm. Res.* 8, 471-474.
- Morris, E.R., Rees, D.A., Welsh, E.J., 1980. Conformation and dynamic interactions in hyaluronate solutions. *J. Mol. Biol.* 138, 383-400.
- Moustafa, M.A., Elnaggar, Y.S.R., El-Refaie, W.M., Abdallah, O.Y., 2017. Hyalugel-integrated liposomes as a novel ocular nanosized delivery system of fluconazole with promising prolonged effect. *Int. J. Pharm.* 534, 14-24.
- Muhn, C., Rosen, N., Solish, N., Bertucci, V., Lupin, M., Dansereau, A., Weksberg, F., Remington, B.K., Swift, A., 2012. The evolving role of hyaluronic acid fillers for facial volume restoration and contouring: a Canadian overview. *Clin. Cosmet. Investig. Dermatol.* 5, 147-158.

- Namiki, O., Toyoshima, H., Morisaki, N., 1982. Therapeutic effect of intra-articular injection of high molecular weight hyaluronic acid on osteoarthritis of the knee. *Int. J. Clin. Pharmacol. Ther. Toxicol.* 20, 501-507.
- Negi, L.M., Jaggi, M., Joshi, V., Ronodip, K., Talegaonkar, S., 2015. Hyaluronan coated liposomes as the intravenous platform for delivery of imatinib mesylate in MDR colon cancer. *Int. J. Biol. Macromol.* 73, 222-235.
- Nenna, R., Papasso, S., Battaglia, M., De Angelis, D., Petrarca, L., Felder, D., Salvadei, S., Berardi, R., Roberti, M., Papoff, P., Moretti, C., Midulla, F., 2011. 7% hypertonic saline and hyaluronic acid and in the treatment of infants mild-moderate bronchiolitis. *Eur. Respir. J.* 38, 1717.
- Neuman, M.G., Nanau, R.M., Oruña-Sánchez, L, Coto, G., 2015. Hyaluronic acid and wound healing. *J. Pharm. Pharm. Sci.* 18, 53-60.
- Neumayer, T., Prinz, A., Findl, O., 2008. Effect of a new cohesive ophthalmic viscosurgical device on corneal protection and intraocular pressure in small-incision cataract surgery. *J. Cataract Refract. Surg.* 34, 1362-1366.
- Nguyen, V.D., Zheng, S., Han, J., Le, V.H., Park, J.O., Park, S., 2017. Nanohybrid magnetic liposome functionalized with hyaluronic acid for enhanced cellular uptake and near-infrared-triggered drug release. *Colloids Surf. B. Biointerfaces.* 154, 104-114.
- Nobile, V., Buonocore, D., Michelotti, A., Marzatico, F., 2014. Anti-aging and filling efficacy of six types hyaluronic acid based dermo-cosmetic treatment: double blind, randomized clinical trial of efficacy and safety. *J. Cosmet. Dermatol.* 13, 277-287.
- Oe, M., Mitsugi, K., Odanaka, W., Yoshida, H., Matsuoka, R., Seino, S., Kanemitsu, T., Masuda, Y., 2014. Dietary hyaluronic acid migrates into the skin of rats. *Sci. World J.* 2014, 378024.
- Oe, M., Tashiro, T., Yoshida, H., Nishiyama, H., Masuda, Y., Maruyama, K., Koikeda, T., Maruya, R., Fukui, N., 2016. Oral hyaluronan relieves knee pain: A review. *Nutr. J.* 15, 11.
- Ogston, A.G., Stanier, J.E., 1953. The physiological function of hyaluronic acid in synovial fluid; viscous, elastic and lubricant properties. *J. Physiol.* 119, 244-252.
- Ouyang, L., Highley, C.B., Rodell, C.B., Sun, W., Burdick, J.A., 2016. 3D Printing of Shear-Thinning Hyaluronic Acid Hydrogels with Secondary Cross-Linking. *ACS Biomater. Sci. Eng.* 2, 1743–1751.
- Pandey, M., Choudhury, H., Gunasegaran, T.A.P., Nathan, S.S., Md, S., Gorain, B., Tripathy, M., Hussain, Z., 2018. Hyaluronic acid-modified betamethasone encapsulated polymeric nanoparticles: fabrication, characterisation, in vitro release kinetics, and dermal targeting. *Drug Deliv. Transl. Res.* doi: 10.1007/s13346-018-0480-1.

- Parashar, P., Rathor, M., Dwivedi, M., Saraf, S.A., 2018. Hyaluronic acid decorated naringenin nanoparticles: appraisal of chemopreventive and curative potential for lung cancer. *Pharmaceutics*. 10, doi: 10.3390/pharmaceutics10010033.
- Pavicic, T., Gauglitz, G.G., Lersch, P., Schwach-Abdellaoui, K., Malle, B., Korting, H.C., Farwick, M., 2011. Efficacy of cream-based novel formulations of hyaluronic acid of different molecular weights in anti-wrinkle treatment. *J. Drugs Dermatol*. 10, 990-1000.
- Pereira, G.G., Detoni, C.B., Balducci, A.G., Rondelli, V., Colombo, P., Guterres, S.S., Sonvico, F., 2016. Hyaluronate nanoparticles included in polymer films for the prolonged release of vitamin E for the management of skin wounds. *Eur. J. Pharm. Sci.* 83, 203-211.
- Petrigni, G., Allegra, L., 2006. Aerosolised hyaluronic acid prevents exercise-induced bronchoconstriction, suggesting novel hypotheses on the correction of matrix defects in asthma. *Pulm. Pharmacol. Ther.* 19, 166–171.
- Pinkus, H., Perry, E.T., 1953. The influence of hyaluronic acid and other substances on tensile strength of healing wounds. *J. Invest. Dermatol.* 21, 365-374.
- Pirard, D., Vereecken, P., Mélot, C., Heenen, M., 2005. Three percent diclofenac in 2.5% hyaluronan gel in the treatment of actinic keratoses: a meta-analysis of the recent studies. *Arch. Dermatol. Res.* 297, 185-189.
- Pisárčik, M., Bakoš, D., Čeppan, M., 1995. Non-Newtonian properties of hyaluronic acid aqueous solution. *Colloids Surf. A Physicochem. Eng. Asp.* 97, 197-202.
- Prata, J.E., Barth, T.A., Bencherif, S.A., Washburn, N.R., 2010. Complex fluids based on methacrylated hyaluronic acid. *Biomacromolecules*. 11, 769–775.
- Pravata, L., Braud, C., Boustta, M., El Ghzaoui, A., Tømmeraas, K., Guillaumie, F., Schwach-Abdellaoui, K., Vert, M., 2008. New amphiphilic lactic acid oligomer–hyaluronan conjugates: Synthesis and physicochemical characterization. *Biomacromolecules*. 9, 340–348.
- Rakkhumkaew, N., Shibatani, S., Kawasaki, T., Fujie, M., Yamada, T., 2013. Hyaluronan synthesis in cultured tobacco cells (BY-2) expressing a chlorovirus enzyme: cytological studies. *Biotechnol. Bioeng.* 110, 1174–1179.
- Rangaswamy, V., Jain, D., 2008. An efficient process for production and purification of hyaluronic acid from *Streptococcus equi* subsp. *zoepidemicus*. *Biotechnol. Lett.* 30, 493-496.
- Regnault, F., Bregeat, P., 1974. Treatment of severe cases of retinal detachment with highly viscous hyaluronic acid. *Mod. Probl. Ophthalmol.* 12, 378-383.
- Research, G.V., 2018. Hyaluronic Acid Market Size Worth USD 15.4 Billion by 2025 | CAGR: 8.8% <https://www.grandviewresearch.com/press-release/global-hyaluronic-acid-market> (Accessed March 8, 2018).



- Robert, L., Robert, A.M., Renard, G., 2010. Biological effects of hyaluronan in connective tissues, eye, skin, venous wall. Role in aging. *Pathol. Biol. (Paris)*. 58, 187-198.
- Rueda López, J., Segovia Gómez, T., Guerrero Palmero, A., Bermejo Martínez, M., Muñoz Bueno, A.M., 2005. [Hyaluronic acid: a new trend to cure skin injuries an observational study.]. *Rev. Enferm.* 28, 53-57.
- Rwei, S.P., Chen, S.W., Mao, C.F., Fang, H.W., 2008. Viscoelasticity and wearability of hyaluronate solutions. *Biochem. Eng. J.* 40, 211-217.
- Sanad, R.A., Abdel-Bar, H.M., 2017. Chitosan-hyaluronic acid composite sponge scaffold enriched with Andrographolide-loaded lipid nanoparticles for enhanced wound healing. *Carbohydr. Polym.* 173, 441-450.
- Sato, T., Iwaso, H., 2009. An effectiveness study of hyaluronic acid [Hyabest<sup>®</sup> (J)] in the treatment of osteoarthritis of the knee on the patients in the United States. *J. New Rem. Clin.* 58, 260–269.
- Schanté, C.E., Zuber, G., Herlin, C., Vandamme, T.F., 2011. Chemical modifications of hyaluronic acid for the synthesis of derivatives for a broad range of biomedical applications. *Carbohydr. Polym.* 85, 469-489.
- Schiller, J., Arnhold, J., Arnold, K., 1995. Action of hypochlorous acid on polymeric components of cartilage. Use of <sup>13</sup>C NMR spectroscopy. *Z. Naturforsch. C.* 50, 721-728.
- Schiller, J.F., B., Arnhold, J., Arnold, K., 2003. Contribution of reactive oxygen species to cartilage degradation in rheumatic diseases: molecular pathways, diagnosis and potential therapeutic strategies. *Curr. Med. Chem.* 10, 2123.
- Schiraldi, C., La Gatta, A., De Rosa, M., 2010. Biotechnological Production and Application of Hyaluronan. In: Elnashar, M. (ed.), *Biopolymers*, InTech, Available from: <https://www.intechopen.com/books/biopolymers/biotechnological-production-characterization-and-application-of-hyaluronan>.
- Scott, J.E., 1989. Secondary structures in hyaluronan solutions: chemical and biological implications. *Ciba Found. Symp.* 143:6-15; discussion 15-20, 281-285.
- Scott, J.E., 1992. Supramolecular organization of extracellular matrix glycosaminoglycans, in vitro and in the tissues. *FASEB J.* 6, 2639-2645.
- Scott, J.E., Cummings, C., Brass, A., Chen, Y., 1991. Secondary and tertiary structures of hyaluronan in aqueous solution, investigated by rotary shadowing-electron microscopy and computer simulation. Hyaluronan is a very efficient network-forming polymer. *Biochem J.* 274, 699-705.
- Scott, J.E., Heatley, F., 1999. Hyaluronan forms specific stable tertiary structures in aqueous solution: a <sup>13</sup>C NMR study. *Proc. Natl. Acad. Sci. U S A.* 96, 4850-4855.

- Seidlits, S.K., Khaing, Z.Z., Petersen, R.R., Nickels, J.D., Vanscoy, J.E., Shear, J.B., Schmidt, C.E., 2010. The effects of hyaluronic acid hydrogels with tunable mechanical properties on neural progenitor cell differentiation. *Biomaterials*. 31, 3930–3940.
- Serban, M., Yang, G., Prestwich, G., 2008. Synthesis, characterization and chondroprotective properties of a hyaluronan thioethyl ether derivative. *Biomaterials*. 29, 1388–1399.
- Sharma, M., Sahu, K., Singh, S.P., Jain, B., 2017. Wound healing activity of curcumin conjugated to hyaluronic acid: in vitro and in vivo evaluation. *Artif. Cells Nanomed. Biotechnol.* 1-9.
- Shi, L., Zhao, Y., Xie, Q., Fan, C., Hilborn, J., Dai, J., Ossipov, D.A., 2018. Moldable Hyaluronan Hydrogel Enabled by Dynamic Metal-Bisphosphonate Coordination Chemistry for Wound Healing. *Adv. Healthc. Mater.* 7.
- Shiedlin, A., Bigelow, R., Christopher, W., Arbabi, S., Yang, L., Maier, R.V., Wainwright, N., Childs, A., Miller, R.J., 2004. Evaluation of hyaluronan from different sources: *Streptococcus zooepidemicus*, rooster comb, bovine vitreous, and human umbilical cord. *Biomacromolecules*. 5, 2122-2127.
- Shimojo, A., A., Pires, A.M., Lichy, R., Rodrigues, A.A., Santana, M.H., 2015. The crosslinking degree controls the mechanical, rheological, and swelling properties of hyaluronic acid microparticles. *J. Biomed. Mater. Res. A*. 103, 730-737.
- Shu, X.Z., Liu, Y., Luo, Y., Roberts, M.C., Prestwich, G.D., 2002. Disulfide cross-linked hyaluronan hydrogels. *Biomacromolecules*. 3, 1304-1311.
- Sigen, A., Xu, Q., McMichael, P., Gao, Y., Li, X., Wang, X., Greiser, U., Zhou, D., Wang, W., 2018. A facile one-pot synthesis of acrylated hyaluronic acid. *Chem. Commun. (Camb)*. 54, 1081-1084.
- Simsolo, E.E., Eroğlu, İ., Tanrıverdi, S.T., Özer, Ö., 2018. Formulation and evaluation of organogels containing hyaluronan microparticles for topical delivery of caffeine. *AAPS PharmSciTech*. doi: 10.1208/s12249-018-0955-x.
- Smith, L.J., Taimoory, S.M., Tam, R.Y., Baker, A.E.G., Bintah Mohammad, N., Trant, J.F., Shoichet, M.S., 2018. Diels-Alder Click-Cross-Linked Hydrogels with Increased Reactivity Enable 3D Cell Encapsulation. *Biomacromolecules*. 19, 926-935.
- Sobolewski, K., Bańkowski, E., Chyczewski, L., Jaworski, S., 1997. Collagen and glycosaminoglycans of Wharton's jelly. *Biol. Neonate*. 71, 11-21.
- Solà, R., Valls, R.M., Martorell, I., Giralt, M., Pedret, A., Taltavull, N., Romeu, M., Rodríguez, À., Moriña, D., Lopez de Frutos, V., Montero, M., Casajuana, M.C., Pérez, L., Faba, J., Bernal, G., Astilleros, A., González, R., Puiggròs, F., Arola, L., Chetrit, C., Martínez-Puig, D., 2015. A low-fat yoghurt supplemented with a rooster comb extract on

muscle joint function in adults with mild knee pain: A randomized, double blind, parallel, placebo-controlled, clinical trial of efficacy. *Food Funct.* 6, 3531–3539.

Soltés, L., Mendichi, R., Kogan, G., Schiller, J., Stankovska, M., Arnhold, J., 2006. Degradative action of reactive oxygen species on hyaluronan. *Biomacromolecules.* 7, 659-668.

Spicer, A.P., McDonald, J.A., 1998. Characterization and molecular evolution of a vertebrate hyaluronan synthase gene family. *J. Biol. Chem.* 273, 1923-1932.

Stern, R., 2008. Hyaluronidases in cancer biology. *Semin. Cancer. Biol.* 18, 275-280.

Stern, R., Jedrzejewski, M.J., 2006. Hyaluronidases: their genomics, structures, and mechanisms of action. *Chem. Rev.* 106, 818-839.

Stern, R., Kogan, G., Jedrzejewski, M.J., Soltés, L., 2007. The many ways to cleave hyaluronan. *Biotechnol. Adv.* 25, 537-557.

Stuhlmeier, K.M., Pollaschek, C., 2004. Differential effect of transforming growth factor beta (TGF-beta) on the genes encoding hyaluronan synthases and utilization of the p38 MAPK pathway in TGF-beta-induced hyaluronan synthase 1 activation. *J. Biol. Chem.* 279, 8753-8760.

Sun, S.F., Hsu, C.W., Lin, H.S., Liou, I.H., Chen, Y.H., Hung, C.L., 2017. Comparison of single intra-articular injection of novel hyaluronan (HYA-JOINT Plus) with synvisc-one for knee osteoarthritis: a randomized, controlled, double-blind trial of efficacy and safety. *J. Bone Joint Surg. Am.* 99, 462-471.

Supp, D.M., Hahn, J.M., McFarland, K.L., Glaser, K., 2014. Inhibition of hyaluronan synthase 2 reduces the abnormal migration rate of keloid keratinocytes. *J. Burn Care Res.* 35, 84-92.

Tagliagambe, M., Elstrom, T.A., Ward, D.B., 2017. Hyaluronic Acid Sodium Salt 0.2% Gel in the Treatment of a Recalcitrant Distal Leg Ulcer: A Case Report. *J. Clin. Aesthet. Dermatol.* 10, 49-51.

Tamer, T.M., 2013. Hyaluronan and synovial joint: function, distribution and healing. *Interdiscip. Toxicol.* 6, 111-125.

Toemmeraas, K., Eenschooten, C., 2007. Aryl/alkyl succinic anhydride hyaluronan derivatives. WO/2007/033677.

Tomihata, K., Ikada, Y., 1997. Crosslinking of hyaluronic acid with glutaraldehyde. *J. Polym. Sci. Part A: Polym. Chem.* 35, 3553–3559.

Toole, B.P., 2004. Hyaluronan: from extracellular glue to pericellular cue. *Nat. Rev. Cancer.* 4, 528-539.

- Toole, B.P., Ghatak, S., Misra, S., 2008. Hyaluronan oligosaccharides as a potential anticancer therapeutic. *Curr. Pharm. Biotechnol.* 9, 249–252.
- Trommer, H., Wartewig, S., Böttcher, R., Pöppel, A., Hoentsch, J., Ozegowski, J.H., Neubert, R.H., 2003. The effects of hyaluronan and its fragments on lipid models exposed to UV irradiation. *Int. J. Pharm.* 254, 223-234.
- Turino, G.M., Ma, S., Lin, Y.Y., Cantor, J.O., 2017. The therapeutic potential of hyaluronan in COPD. *Chest*. doi: 10.1016/j.chest.2017.12.016.
- Turley, E.A., Noble, P.W., Bourguignon, L.Y., 2002. Signaling properties of hyaluronan receptors. *J. Biol. Chem.* 277, 4589-4592.
- Vandermeer, G., Chamy, Y., Pisella, P.J., 2018. Comparison of objective optical quality measured by double-pass aberrometry in patients with moderate dry eye: Normal saline vs. artificial tears: A pilot study. *J. Fr. Ophtalmol.* 41, e51-e57.
- Varga, L., 1955. Studies on hyaluronic acid prepared from the vitreous body. *J. Biol. Chem.* 217, 651-658.
- Vigetti, D., Karousou, E., Viola, M., Deleonibus, S., De Luca, G., Passi, A., 2014b. Hyaluronan: biosynthesis and signaling. *Biochim Biophys Acta.* 1840, 2452-2459.
- Vigetti, D., Viola, M., Karousou, E., De Luca, G., Passi, A., 2014a. Metabolic control of hyaluronan synthases. *Matrix Biol.* 35, 8-13.
- Volpi, N., Maccari, F., 2003. Purification and characterization of hyaluronic acid from the mollusc bivalve *Mytilus galloprovincialis*. *Biochimie* 85, 619-625.
- Volpi, N., Schiller, J., Stern, R., Soltés, L., 2009. Role, metabolism, chemical modifications and applications of hyaluronan. *Curr. Med. Chem.* 16, 1718-1745.
- Wang, T., Hou, J., Su, C., Zhao, L., Shi, Y., 2017. Hyaluronic acid-coated chitosan nanoparticles induce ROS-mediated tumor cell apoptosis and enhance antitumor efficiency by targeted drug delivery via CD44. *J Nanobiotechnology.* 15, 7.
- Weigel, P.H., Hascall, V.C., Tammi, M., 1997. Hyaluronan synthases. *J. Biol. Chem.* 272, 13997-14000.
- Weissmann, B., Meyer, K., 1954. The structure of hyalobiuronic acid and of hyaluronic acid from umbilical cord. *J. Am. Chem. Soc.* 76, 1753-1757.
- Wirostko, B., Mann, B.K., Williams, D.L., Prestwich, G.D., 2014. Ophthalmic Uses of a Thiol-Modified Hyaluronan-Based Hydrogel. *Adv. Wound Care (New Rochelle)* 3, 708-716.
- Wu, M., Cao, M., He, Y., Liu, Y., Yang, C., Du, Y., Wang, W., Gao, F., 2015. A novel role of low molecular weight hyaluronan in breast cancer metastasis. *FASEB J.* 29, 1290-1298.

- Xie, Y., Upton, Z., Richards, S., Rizzi, S.C., Leavesley, D.I., 2011. Hyaluronic acid: evaluation as a potential delivery vehicle for vitronectin: growth factor complexes in wound healing applications. *J. Control. Release* 153, 225-232.
- Yang, C., Cao, M., Liu, H., He, Y., Xu, J., Du, Y., Liu, Y., Wang, W., Cui, L., Hu, J., Gao, F., 2012. The high and low molecular weight forms of hyaluronan have distinct effects on CD44 clustering. *J. Biol. Chem.* 287, 43094-43107.
- Yerushalmi, N., Arad, A., Margalit, R., 1994. Molecular and cellular studies of hyaluronic acid-modified liposomes as bioadhesive carriers for topical drug delivery in wound healing. *Arch. Biochem. Biophys.* 313, 267-273.
- Yu, H., Stephanopoulos, G., 2008. Metabolic engineering of *Escherichia coli* for biosynthesis of hyaluronic acid. *Metab. Eng.* 10, 24–32.
- Yui, N., Okano, T., Sakurai, Y., 1992. Inflammation responsive degradation of crosslinked hyaluronic acid gels. *J. Control. Release* 22, 105-116.
- Ząbkowski, T., Jurkiewicz, B., Saracyn, M., 2015. Treatment of recurrent bacterial cystitis by intravesical instillations of hyaluronic acid. *Urol J.* 12, 2192-2195.
- Zgheib, C., Xu, J., Liechty, K.W., 2014. Targeting Inflammatory Cytokines and Extracellular Matrix Composition to Promote Wound Regeneration. *Adv. Wound Care.* 3, 344–355.
- Zhang, H., Tsang, J.Y., Ni, Y.B., Chan, S.K., Chan, K.F., Cheung, S.Y., Tse, G.M., 2016b. Hyaluronan synthase 2 is an adverse prognostic marker in androgen receptor-negative breast cancer. *J. Clin. Pathol.* 69, 1055-1062.
- Zhang, Z., Tao, D., Zhang, P., Liu, X., Zhang, Y., Cheng, J., Yuan, H., Liu, L., Jiang, H., 2016a. Hyaluronan synthase 2 expressed by cancer-associated fibroblasts promotes oral cancer invasion. *J. Exp. Clin. Cancer Res.* 35, 181.
- Zhao, X., 2000. Process for the production of multiple cross-linked hyaluronic acid derivatives. WO/2000/046253.



## CHAPTER 3

### *Synthesis and rheology of urea-crosslinked hyaluronic acid*

Part of this chapter was published as patent WO/2015/007773 A1 (2015) under the title  
“Cross-linked hyaluronic acid, process for the preparation thereof and  
use thereof in the aesthetic field”.

*Inventors: Ugo Raffaello Citernesi<sup>a</sup>, Lorenzo Beretta<sup>a</sup>, Lorenzo Citernesi<sup>a</sup>.*

*<sup>a</sup> I.R.A. Istituto Ricerche Applicate S.r.l., 20040, Usmate-Velate (MB), Italy.*

*Proprietor: I.R.A. Istituto Ricerche Applicate S.r.l., 20040, Usmate-Velate (MB), Italy.*





### **3.0. Preface**

Chapter 3 describes the synthesis of the patented urea-crosslinked hyaluronic acid (HA-CL), an innovative and high quality biopolymer intended for aesthetic and cosmetic applications. HA-CL has been developed to increase the rigidity of the polymer network (i.e., the gel viscoelasticity), thus obtaining a product with extended permanence in the site of application and reduced susceptibility to enzymatic degradation compared to native HA. This crosslinked biopolymer has been designed for the treatment of wrinkles and for the reconstitution of human tissues that have been removed after surgery, such as breast tissue. However, considering the safety and the health effects of both urea and HA, HA-CL can also be suitable to formulate cosmetic and pharmaceutical formulations.

### 3.1. Abstract

With ageing, hyaluronic acid (HA) skin content decreases and this determines the loss of dermal hydration and the appearance of wrinkles. The injection of HA dermal fillers (DFs) represents a non-surgical procedure to restore lost volumes and correct facial imperfection. The main limitation of HA, when used in its native form, is its short durability; hence, to obtain more long-lasting effects, the polymer is subjected to crosslinking, preferably with natural molecules which also hold intrinsic activity. In this context, a simple procedure to synthesize urea-crosslinked hyaluronic acid (HA-CL) in aqueous ambient has been developed. HA-CL has been characterized for its macroscopic appearance, pH and rheological properties. The rheological profile of the biopolymer was also assessed after terminal sterilization by means of autoclave for 20 minutes, at 121°C, and lyophilisation.

**Keywords:** aesthetic; cosmetic; crosslinking; dermal fillers; hyaluronic acid; physico-chemical properties; rheological properties; synthesis.

### 3.2. Introduction

As widely discussed in chapter 2, hyaluronic acid (HA) is an important component of the human skin (roughly, 7.5 g for a 70-kg adult), but its content decreases with ageing, provoking several undesired effects -the most visible are loss of skin hydration, elasticity and volume, which are responsible for wrinkles (Fallacara et al., 2018a). Therefore, over the last few years, HA has been widely used as a biomaterial to develop dermal fillers (DFs), which are class III medical devices that, injected into or under the skin, restore lost volumes and correct facial imperfections such as lines, wrinkles, folds, furrows or scars (Fallacara et al., 2017a, 2018a). Non-surgical procedures based on DFs injections are actually the most performed practices to reduce facial rhytides and restore facial volume and contours (Fallacara et al., 2017a). According to data from the American Society of Plastic Surgeons (ASPS), patients undergoing facial rejuvenation treatments with soft tissue fillers experience a continuous and important growth: 2017 marked 2,691,265 treatments -increase of 3% respect to 2016-: out of this total, 2,091,476 procedures were performed with hyaluronan DFs (American Society of Plastic Surgeons, 2017). Indeed, being characterized by most of the properties that an ideal DF should have -biocompatibility, biodegradability, viscoelasticity, safety, versatility-, HA DFs have become the most popular agents for soft tissue contouring and volumizing (Fallacara et al., 2017a, 2018a). The main limitation of HA, when used in its native form, is its short durability -about 1/2 days- due especially to the rapid enzymatic degradation (Fallacara et al., 2017a). To increase the rigidity of the polymer network (i.e., the gel viscoelasticity), extend its permanence in the site of application, and reduce its susceptibility to enzymatic degradation, HA is subjected to crosslinking (Fallacara et al., 2017a). HA classical crosslinkers are difunctional molecules of synthetic origin, for example divinyl sulfone and butanediol-diglycidyl ether (BDDE) (Fallacara et al., 2017a, 2018a). According to a recent trend, which aims to increase the biocompatibility and biodegradability of HA crosspolymers, and improve their beneficial effects, HA chains can be linked by natural crosslinkers that also hold intrinsic activity once released from HA by hydrolytic enzymes (Fallacara et al., 2017a). Thus, multifunctional polymers, consisting of complementary active agents, can be obtained (Fallacara et al., 2017a).

Toward this end, urea-crosslinked hyaluronic acid (HA-CL) has been synthesized from urea and native HA of bacterial origin, as high quality polymer intended for aesthetic and cosmetic applications. It can be applied in any area of the body, for example face, lips, periocular area, breasts and buttocks, and can be injected or implanted in the epidermis, dermis or hypodermis (Citernesi et al., 2015, WO/2015/007773 A1). Depending on the HA-CL concentration -on average from 15 to 30 mg/mL- it is possible to obtain DFs suitable for the treatment of wrinkles from fine to very deep, and with different duration of results -on average from 5 to 10 months (experimental study still ongoing) (Fallacara et al., 2017a). This crosslinked biopolymer is also suitable for the reconstitution of human tissues that have been removed after surgery, such as, for example, in the case of surgical removal of breast tissue or liposuction (Citernesi et al., 2015, WO/2015/007773 A1).

Urea, the crosslinker of HA-CL, is an organic compound chemically structured as a carbonyl group attached to two amine residues. It is physiologically present in the human body, and, therefore, it is extremely biocompatible. Urea has well-known keratolytic and moisturizing actions, due to its ability of water retention, that promotes cellular regeneration

and repair (Fallacara et al., 2017a). For these reasons, urea is safely and effectively used to treat a wide variety of diseases, such as dry and scaly skin (ichthyosis, xerosis, psoriasis, corns, calluses), damaged cutaneous annexes (ingrown, devitalized nails), non-infectious keratopathy, and injured corneal epithelium (Fallacara et al., 2017a, b).

Due to the safety and the health effects of both urea and HA (chapter 2), HA-CL can be suitable to formulate not only DFs and cosmetic products, but also pharmaceutical formulations. With the researches described in the present PhD thesis, it has been experimentally proved that this dualistic crosspolymer can be useful for the resolutions of tissue injuries due to its re-epithelialization and hydration effects (Fallacara et al., 2017a, b, 2018b), as well as for the formulations of microcarriers which act as delivery systems for pharmaceutical and cosmetic active ingredients (Fallacara et al., 2018c). Therefore, HA-CL could represent a promising, interesting, and versatile innovative polymer which finds multiple applications not only in the aesthetic and cosmetic fields, but also in the medical and pharmaceutical spheres (Fallacara et al., 2017a, b, 2018a, b, c).

### 3.3. Synthesis of HA-CL

The process of preparation of HA-CL (Figure 3.1.) has been invented and then patented by Citernesi and coworkers (2015, WO/2015/007773 A1).

Briefly, 8 g of native HA of bacterial origin were dissolved into 72 g of saline. Separately, 4 g of urea were dissolved into 16 g of 0.2 M HCl. Once completely homogenous, these two solutions were mixed to obtain a solution with a pH in the range from 3.5 to 4. The product was thermostated at  $35 \pm 2^\circ\text{C}$  for 24 h. Afterwards, the excess of urea was eliminated by dialysis, and the pH of the purified product was adjusted to reach a final value in the range 5.5-7.5 (Citernesi et al., 2015, WO/2015/007773 A1).

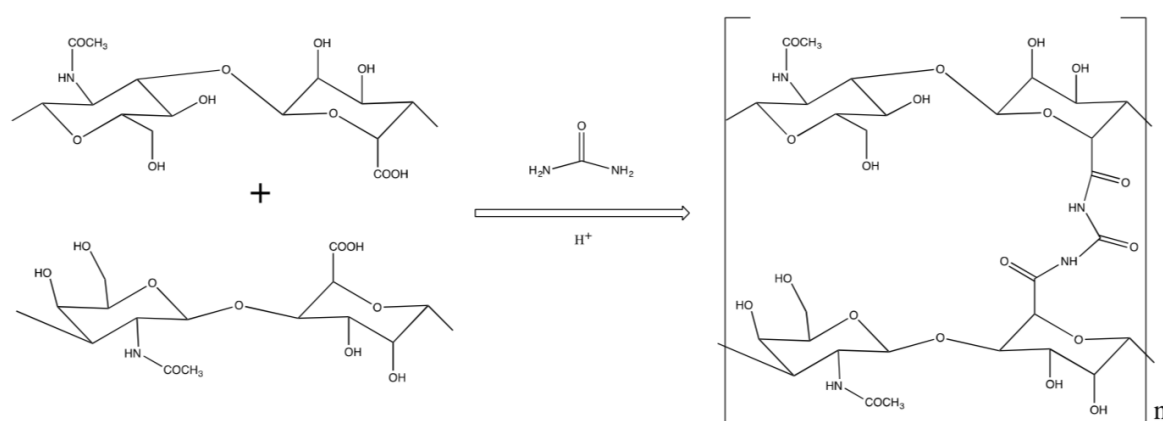


Figure 3.1. Synthesis of HA-CL with urea (Fallacara et al., 2017b).

According to some embodiments, the biopolymer newly formed from the polymerization reaction was in the form of a transparent, colorless and macroscopically homogenous hydrogel. In other embodiments, the HA-CL obtained with the method herein described was freeze-dried (Citernesi et al., 2015, WO/2015/007773 A1).

### 3.4. Rheological characterization of HA-CL

The rheological analyses were performed on the HA-CL hydrogel obtained according to the above described synthetic method, and on HA-CL hydrogel prepared by re-hydration of the freeze-dried product of synthesis (Citernes et al., 2015, WO/2015/007773 A1).

The rheological tests were performed using a Rheometer Physica MCR-101 from Anton Paar at  $23 \pm 0.05^\circ\text{C}$ . Tests were conducted both in continuous and oscillatory flow conditions using PP50-P2 sensor (50 mm parallel plates with serrated surfaces) with fixed gap (1 mm). The rheometer was connected to the Rheoplus software for data analysis.

The samples flow properties were measured in continuous flow conditions, with a controlled shear rate test, by recording viscosity values ( $\eta$ ) at increasing shear rate, ranging from  $0.001$  to  $1000 \text{ s}^{-1}$ .

The viscoelastic behaviour of HA-CL hydrogels was investigated through tests in oscillatory flow conditions. An amplitude sweep test was performed at a fixed frequency of 1 Hz, increasing the strain ( $\gamma$ ) from 0.01% to 1000% in order to identify the linear viscoelastic region of each product. Afterwards, a frequency sweep test was performed at a fixed strain (belonging to the linear viscoelastic region), with frequency ranging from 0.01 Hz to 10 Hz. This allowed the study of the inner structure of the samples and the trend of storage ( $G'$ ) and loss ( $G''$ ) moduli.

Flow measurements of the hydrogels showed superimposable flow curves for HA-CL and lyophilized HA-CL: both samples exhibited a shear-thinning behaviour, with comparable viscosity values (Figure 3.2.). For example, when the shear rate was  $0.001 \text{ s}^{-1}$ , the viscosity was 2316 Pa.s for HA-CL, and 2194 Pa.s for lyophilized HA-CL; when the shear rate was  $1000 \text{ s}^{-1}$ , the viscosity was 497 Pa.s for HA-CL, and 421 Pa.s for lyophilized HA-CL.

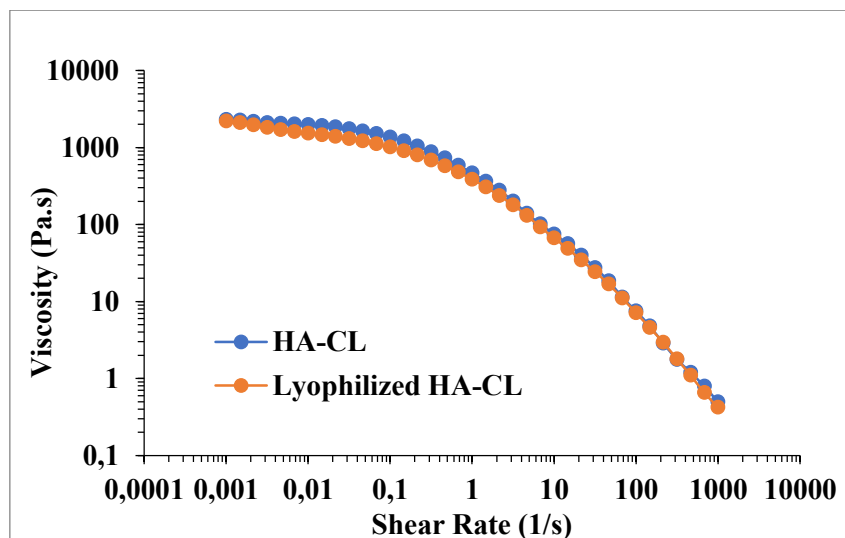


Figure 3.2. Flow curves of HA-CL and lyophilized HA-CL, showing the viscosity ( $\eta$ ) as a function of the shear rate ( $\dot{\gamma}$ ).

The results of the amplitude sweep test showed comparable values of storage ( $G'$ ) and loss ( $G''$ ) moduli, and comparable linear viscoelastic regions for both HA-CL and lyophilized HA-CL (Figure 3.3.)

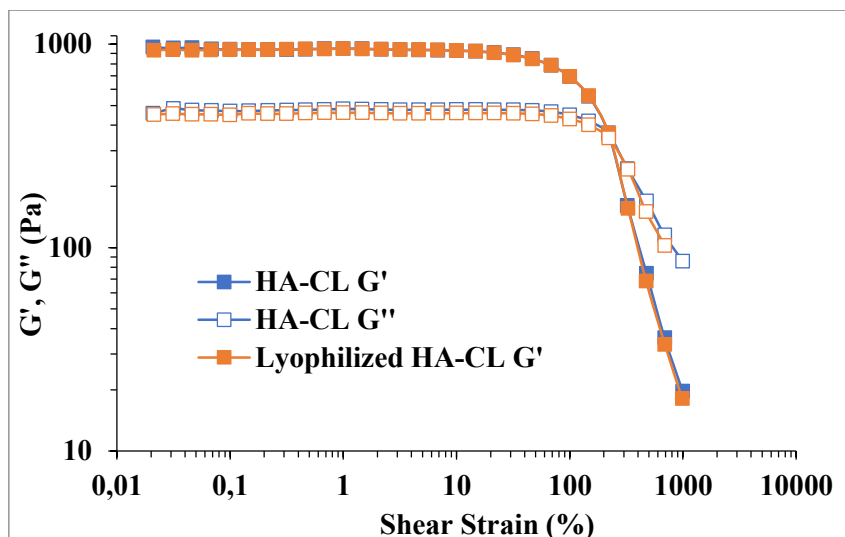


Figure 3.3. Amplitude sweep test of HA-CL and lyophilized HA-CL, showing the storage ( $G'$ ) and loss ( $G''$ ) moduli as a function of the strain ( $\gamma$ ).

Finally, oscillatory measurements (Figure 3.4.) showed that  $G'-G''$  crossover took place at a very similar value of angular frequency ( $\omega \sim 0.8$  rad/s) for HA-CL and lyophilized HA-CL, demonstrating that the lyophilization process did not impact on the polymer elastic properties (Citernesi et al., 2015, WO/2015/007773 A1).

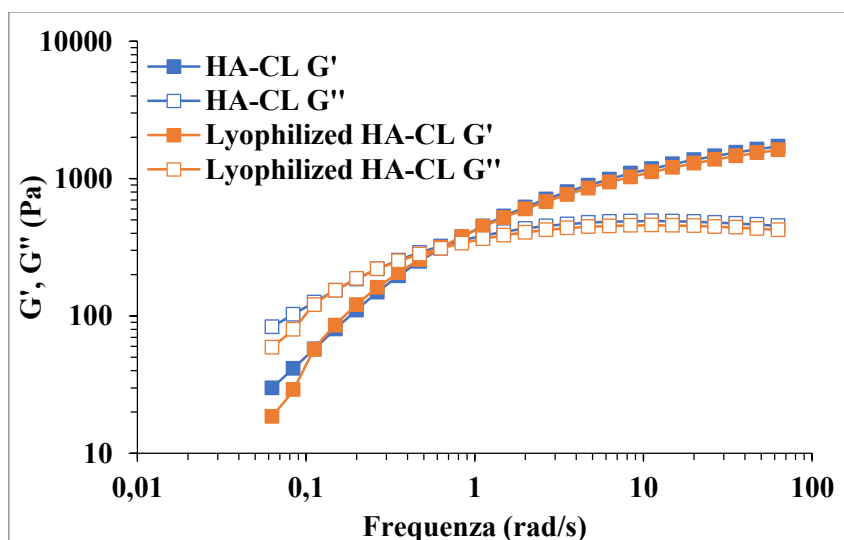


Figure 3.4. Frequency sweep test of HA-CL and lyophilized HA-CL, showing the storage ( $G'$ ) and loss ( $G''$ ) moduli as a function of the angular frequency ( $\omega$ ).

Hence, HA-CL exhibited a good resistance to freeze-drying. Indeed, after water removal and subsequent rehydration, it was possible to obtain a polymer with features similar to the one not subjected to freeze-drying (Figure 3.2., 3.3., 3.4.) (Citernesi et al., 2015, WO/2015/007773 A1).

### 3.5. References

American Society of Plastic Surgeons, A., 2017. 2017 Plastic surgery statistics report. <https://www.plasticsurgery.org/documents/News/Statistics/2017/plastic-surgery-statistics-report-2017.pdf> Accessed on March 2018.

Citernes, U.R., Beretta, L., Citernes, L., 2015. Cross-Linked Hyaluronic Acid, Process for the Preparation Thereof and Use Thereof in the Aesthetic field. Patent number: WO/2015/007773 A1.

Fallacara, A., Baldini, E., Manfredini, S., Vertuani, S., 2018a. Hyaluronic Acid in the Third Millennium. *Polymers*, 10, 701.

Fallacara, A., Busato, L., Pozzoli, M., Ghadiri, M., Ong, H.X., Young, P.M., Manfredini, S., Traini, D., 2018b. Combination of urea-crosslinked hyaluronic acid and sodium ascorbyl phosphate for the treatment of inflammatory lung diseases: An in vitro study. *Eur. J. Pharm. Sci.*, 120, 96-106.

Fallacara, A., Manfredini, S., Durini, E., Vertuani, S., 2017a. Hyaluronic acid fillers in soft tissue regeneration. *Facial Plast. Surg.* 33, 87-96.

Fallacara, A., Marchetti, F., Pozzoli, M., Citernes, U.R., Manfredini, S., Vertuani, S., 2018c. Formulation and characterization of native and crosslinked hyaluronic acid microspheres for dermal delivery of sodium ascorbyl phosphate: a comparative study. *Pharmaceutics*, 10 (4).

Fallacara, A., Vertuani, S., Panozzo, G., Pecorelli, A., Valacchi, G., Manfredini, S., 2017b. Novel Artificial Tears Containing Cross-linked Hyaluronic Acid: An In Vitro Re-epithelialization study. *Molecules*, 22.





## CHAPTER 4

### ***Novel artificial tears containing crosslinked hyaluronic acid: an in vitro re-epithelialization study***

This chapter was published in *Molecules*, 22(12), 2104 (2017) under the title  
“Novel artificial tears containing cross-linked hyaluronic acid:  
an *in vitro* re-epithelialization study”.

*Authors: Arianna Fallacara<sup>a</sup>, Silvia Vertuani<sup>a,\*</sup>, Giacomo Panozzo<sup>b</sup>, Alessandra Pecorelli<sup>c</sup>,  
Giuseppe Valacchi<sup>c</sup>, Stefano Manfredini<sup>a</sup>.*

<sup>a</sup> Department of Life Sciences and Biotechnology, Master Course in Cosmetic Science and Technology (COSMAST), University of Ferrara, Via L. Borsari 46, 44121 Ferrara, Italy.

<sup>b</sup> Ophthalmology Unit, Azienda ULSS n.22, 37012 Bussolengo, Italy.

<sup>c</sup> Department of Animal Sciences, Plants for Human Health Institute, North Carolina State University, NC Research Campus, 600 Laureate Way, Kannapolis, NC 28081, USA.

**\* Corresponding author:**

Prof. Silvia Vertuani: vrs@unife.it; Tel.: +39-0532-455294; Fax: +39-0532-455378.

DOI: 10.3390/molecules22122104



#### **4.0. Preface**

Hyaluronic acid (HA) is a natural component of the human eye and tear fluid. For this reason, artificial tears based on native HA are widely used to protect and lubricate the eye tissues, and to restore the ocular physiological conditions. Currently, to enhance the ocular residence time and the healthful effects, also novel derivatives of HA with improved mechanical and biological properties are being investigated as eye drops. In chapter 4, urea-crosslinked hyaluronic acid (HA-CL) is explored as novel biopolymer to formulate artificial tears with re-epithelialization properties.

#### 4.1. Abstract

Dry eye syndrome is a common disease which can damage the corneal epithelium. It is treated with eye drops to stimulate tear production and hydrate the corneal surface. The most prescribed artificial tear remedies contain hyaluronic acid (HA), which enhances epithelial wound healing, improving tissue health. To the best of our knowledge, only a few recent studies have investigated cross-linked HA (HA-CL) in eye drops for human applications. This work consists in an *in vitro* evaluation of the re-epithelialization ability of two different preparations containing a recently synthesized HA cross-linked with urea: 0.02% (w/v) HA-CL (solution 1, S1), and 0.4% (w/v) HA-CL (solution 2, S2). The study was conducted on both 2D human corneal cells (HCEpiC) and 3D reconstructed tissues of human corneal epithelium (HCE). Viability by 3-(4,5-dimethylthiazol-2-yl)-2,5-diphenyltetrazolium bromide (MTT) test, pro-inflammatory cytokine release (interleukin-8, IL-8) by ELISA, and morphology by hematoxylin and eosin (HE) staining were evaluated. In addition, to understand the molecular basis of the re-epithelialization properties, cyclin D1 levels were assessed by western blot. The results showed no cellular toxicity, a slight decrease in IL-8 release, and restoration of epithelium integrity when the wounded 3D model was treated with S1 and S2. In parallel, cyclin D1 levels increased in cells treated with both S1 and S2.

**Keywords:** anti-inflammatory; artificial tears; corneal epithelium; cyclin D1; dry eye syndrome; HA; HA-CL; IL-8; re-epithelialization.

## 4.2. Introduction

Dry eye syndrome or keratoconjunctivitis sicca (KCS) is a multifactorial disease of the tears and ocular surface, that results in symptoms of discomfort and visual disturbance, related to lacrimal film instability, with potential damage to the corneal epithelium (Lemp et al., 2007). It is accompanied by increased osmolarity of the tear film and inflammation of the ocular surface. When left untreated, this condition can provoke pain, ulcers, scars on the cornea, and even vision impairment (Lemp et al., 2007). Tear supplementation is the mainstay of the current therapy for the management of dry eye syndrome. This approach consists in the administration of artificial tears (which usually contain hydrophilic polymers) designed with a focus on physical properties relating to hydrating and lubricating of the ocular surface. Ideal tear replacement should recover and maintain a structurally and functionally normal ocular epithelium (Lemp et al., 2007) and consequently improve patient ocular comfort and quality of life by alleviating and eliminating both the signs (objective) and symptoms (subjective) of the disease.

Natural tears have a particular rheological profile; they are viscous under static conditions in the eye, while they are much less viscous during blinking. This behaviour could be well reproduced by hyaluronic acid (sodium salt) eye drops. HA is a biocompatible and biodegradable polymer. It is a vital component of human ocular physiology: it naturally occurs in the vitreous, lacrimal gland, corneal epithelium and conjunctiva (Berriaud et al., 2005; Lapcik et al., 1998; Stuart and Linn, 1985; Yoshida et al., 1996), and it has also been found in tear fluid (Berry et al., 1998; Frescura et al., 1994; Fukuda et al., 1996). HA has a unique viscoelastic profile. During blinks, shear stress causes HA molecules to align with each other. As a result, the solution momentarily loses its viscosity and spreads easily over the cornea surface. Between blinks, HA chains form a tangled meshwork, and the solution becomes more viscous. This stabilizes the pre-corneal tear film, and maximizes the solution residence time on ocular surface, where HA is able to improve eye hydration and lubrication, due to its hygroscopic and mucus-adhesive properties (Nakamura et al., 1993). Moreover, HA has been shown to stimulate corneal epithelial cell migration, and to possess anti-inflammatory and antioxidant properties: consequently, it might play a role in wound healing (Gomes et al., 2004; Inoue and Katakami, 1993; Nishida et al., 1991; Presti and Scott, 1994; Scott, 1995). The complete set of all these properties makes HA well suited for use in artificial tears. Many studies have been conducted to evaluate the safety and efficacy of HA solutions as eye drops. They have all highlighted appreciable improvements of KCS symptoms and signs, associated with HA concentration and molecular weight (generally 0.1–0.4% solutions of 0.8–1.4 MDa HA) (Aragona et al., 2002; Dumbleton et al., 2009; Hamano et al., 1996; Johnson et al., 2006; Prabhasawat et al., 2007; Sand et al., 1989; Stuart and Linn, 1985). All this explains why actually there are several HA-containing eye drops commercially available. However, most of the HA-containing artificial tears available on the market are characterized by the linear form of this polymer; there are only few and recent examples of eye drops consisting of HA-CL. Cross-linking is a chemical strategy with the aims to increase the rigidity of the polymer network (i.e., the gel viscoelasticity), extend its permanence in the site of application and decrease its susceptibility to enzymatic degradation, thus reducing the daily number applications of a formulation (Fallacara et al., 2017). To the best of our knowledge, only a few recent literature reports describe the effects of ophthalmic

formulations –hydrogels, films, artificial tears-containing HA-CL for veterinary (Williams and Mann, 2013, 2014; Williams et al., 2017; Wirostko et al., 2014; Yang et al., 2010) and human uses (Cagini et al., 2017; Calles et al., 2013, 2016; Postorini et al., 2017). These studies show promising results that open interesting perspectives to the ocular administration of cross-linked hyaluronans. Hence, the present work was devised with the aim to investigate the safety and the efficacy of eye drops based on a novel HA-CL to improve corneal re-epithelialization. More precisely, we examined the *in vitro* re-epithelialization capability of HA-CL preparations on both 2D and 3D human corneal epithelium model. In order to explore efficacy ranges, concentrations close to the ones of HA eye drops in the market, namely 0.02% and 0.4%, were assayed. The HA-CL used in this study is a recently patented polymer (Citernes et al., 2015, WO/2015/007773 A1), provided with greater consistency as compared to naturally occurring hyaluronic acid (Citernes et al., 2015, WO/2015/007773 A1; Fallacara et al., 2017). This polymer consists of HA chains cross-linked by urea acting as a multifunctional agent (Citernes et al., 2015, WO/2015/007773 A1; Fallacara et al., 2017). Indeed, urea is not only a cross-linking agent –which increases native HA viscosity by linking its chains, thus possibly determining a longer retention on the corneal epithelium. Urea is also a non-toxic molecule with intrinsic healthy activity (Citernes et al., 2015, WO/2015/007773 A1; Fallacara et al., 2017). Therefore, urea-cross-linked hyaluronic acid is a promising polymer, because it has been developed not only to improve the mechanical properties of native HA, but also its biological activities (Citernes et al., 2015, WO/2015/007773 A1; Fallacara et al., 2017). In fact, urea is well known to be a moisturizing agent, thanks to its ability of water retention, which promotes cellular regeneration and reparation (Fallacara et al., 2017). Charlton et al. (1996) found that topical urea is able to encourage corneal re-epithelialization and to limit epithelial damage after injury to corneal epithelium. Therefore, all the beforehand mentioned studies about the ophthalmic use of HA and urea suggest that HA cross-linked with urea (Citernes et al., 2015, WO/2015/007773 A1) could be an innovative promising ingredient for eye drops to induce corneal re-epithelialization. The herein described application of urea-crosslinked hyaluronan in the formulation of ophthalmic medicaments and medical devices is so far unprecedented.

### **4.3. Materials and methods**

#### **4.3.1. Materials**

HA-CL with urea ( $M_w$  2.0–4.0 MDa) was a patented raw material (Citernes et al., 2015, WO/2015/007773 A1) kindly provided by IRALab (Usmate Velate, Monza-Brianza, Italy). The solvent used for the preparation of HA-CL solutions was a saline-buffered solution consisting of Milli-Q water, NaCl,  $\text{Na}_2\text{HPO}_4 \cdot 12\text{H}_2\text{O}$ , and  $\text{NaH}_2\text{PO}_4 \cdot \text{H}_2\text{O}$  (pH 7.0). All the salts were in compliance with European or USP Pharmacopoeia.

#### **4.3.2. Formulation of HA-CL solutions**

Two different prototypes of solutions were formulated: 0.02% (w/v) HA-CL (solution 1, S1) and 0.4% (w/v) HA-CL (solution 2, S2). Each formulation was prepared by dissolving the polymer in the above described saline-buffered solution. The polymer was left to hydrate

under gentle magnetic stirring, at room temperature, for about 1 h, until reaching a transparent and homogeneous appearance. The solutions were sterilized through 0.2  $\mu\text{m}$  Stericup® vacuum driven sterile filters (Millipore, Canton-Schaffhausen, Switzerland), and then they were stored at room temperature ( $23 \pm 2$  °C) before being evaluated.

#### **4.3.3. Physical-chemical characterization and stability of HA-CL solutions**

Immediately after their preparation, the two prototypes of solutions were characterized by measuring in triplicate their pH and their viscosity ( $\eta$ , rotational viscometer VISCO-STAR equipped with TL5 spindle, Fungilab, Barcelona, Spain) at room temperature ( $23 \pm 2$  °C).

Moreover, pH,  $\eta$  and macroscopic appearance of HA-CL solutions were monitored during time to evaluate the physical-chemical stability of the eye drops prototypes. After the preparation, each formulation was divided into two aliquots, one stored for six months at ambient temperature ( $23 \pm 2$  °C, shelf life), and the other stored for six months in thermostatic oven ( $40 \pm 2$  °C, accelerate stability test). At selected time intervals (i.e., 1 week, 1, 2, 3, 6 months after the preparation), the samples were evaluated in triplicate for physical-chemical and organoleptic characteristics. Data were reported as mean values  $\pm$  standard deviations.

#### **4.3.4. In vitro efficacy study**

##### *4.3.4.1. Experimental scheme*

The adopted experimental scheme was:

- negative control condition: tissues not wounded and not treated (CTR-);
- positive control condition: tissues wounded but not treated (CTR+);
- treated conditions: tissues wounded and treated with the samples (S1 and S2).

Four tissues for each experimental condition were used.

##### *4.3.4.2. Cell cultures*

The *in vitro* evaluations of the safety and the re-epithelialization capability of HA-CL eye drops prototypes were performed on two different biological models: 3D reconstructed tissues of HCE and 2D HCEpiC.

The biological model consisting of 3D HCE, built from immortalized cells of human cornea (Model HCE–SkinEthic, Lyon, France) (Van Goethem et al., 2006), was used for the viability study (MTT test), the determination of IL-8 release (ELISA test), and the morphological investigations (HE staining). The 3D HCE was a 0.5 cm<sup>2</sup> corneal epithelium reconstructed by airlifted culture of transformed human corneal keratinocytes, placed for 5 days in chemically defined medium, on inert polycarbonate filter, at the air/liquid interface. After 6 days of reconstruction, corneal tissues were wounded by scalpel (with the exception of the negative control) and placed into plates with growth medium for the different treatments. 30  $\mu\text{L}$  of test solutions (S1 and S2) were applied on the wounded tissues and incubated for 48 and 72 h at 36.5 °C/5% CO<sub>2</sub>. No substance was applied to negative and

positive control tissues. Tissues were thus subjected to MTT test, ELISA test and HE staining.

The 2D biological model consisting of commercial HCEpiC cells was employed to confirm the wound healing properties of S1 and S2 (scratch assay), and to understand the molecular basis of the re-epithelialization in wound closure induced by S1 and S2 (cyclin D1 quantification by Western blot). HCEpiC cells grown in the corneal epithelial cell medium (ScienCell Research Laboratories, Inc., Carlsbad, CA, USA). Cells were incubated at 37 °C for 24 h in 95% air/5% CO<sub>2</sub> until 80% confluence. The medium was changed every 4 days, and cells from passages 2–4 were used for experiments. Tissues were thus subjected to scratch assays and western blot tests.

#### 4.3.4.3. Cell viability

To evaluate the suitability, the safety and the effect on corneal cells viability of HA-CL eye drops prototypes, an *in vitro* MTT assay was conducted. After the treatment of 3D HCE cells as above described (Section 2.4.2), the tissues were rinsed three times with 1 mL of PBS, arranged in 300 µL of 0.5 mg/mL MTT solution and then incubated for 3 h at 36.5 °C/5% CO<sub>2</sub>. Each tissue was transferred into a well containing 1.5 mL of isopropanol and incubated for 2 h at room temperature. Hereafter, the tissues were removed from the wells and homogenized to dissolve formazan salts. Two hundred µL of this solution were transferred in a 96 well-plate and absorbance reading was performed at 570 nm (isopropanol was used as blank for reading). For each test condition the ratio of the average optical density of the treated tissues on the average optical density of negative controls determined the viability rate. Data were reported as mean values ± standard deviations (expressed in %), and as mean % variations compared to the controls.

#### 4.3.4.4. IL-8 ELISA test

The inflammatory state of control and treated (S1 and S2) tissues was evaluated using ELISA test to quantify the pro-inflammatory marker interleukin-8 (IL-8). Therefore, after 3D HCE cells preparation as above described (Section 2.4.2), controls and treated tissues were undergone to IL-8 dosage using IL-8 ELISA commercial kit (ThermoFisher Scientific, Milano, Italy), according to the manufacturer's instructions. For the quantitative determination, it was used a previously plotted calibration curve made-up of standard known and growing concentrations of IL-8. The results of IL-8 dosage in cell culture CTR-, CTR+ and treated with the two solutions at 48 and 72 h were reported as mean values ± standard deviations (expressed in pg/mL), and as mean % variations compared to the controls.

#### 4.3.4.5. Epithelial corneal wound closure

Epithelial integrity and repair phenomena that followed wound induction were first of all studied on 3D HCE cells, and then confirmed on 2D HCEpiC.

Control and treated tissues of 3D HCE were cultured and prepared as previously described (Section 2.4.2), and after stained with hematoxylin-eosin (HE) (Fischer et al., 2008). Microscope examination permitted to investigate the histology of the tissues. Indeed,



hematoxylin, being a basic dye, coloured in blue/violet the negatively-charged cellular components principally located in the nucleus -nucleic acids, membrane proteins, cellular membranes, elastin-, while eosin, being an acid dye, stained in pink the positively charged cellular components predominantly situated in the cytoplasm and in the extracellular area - proteins, mitochondrial proteins, collagen fibers. The staining permitted to examine tissue integrity.

To confirm the wound healing properties of S1 and S2, HCEpiC cells were subjected to wound healing assay performed as previously described (Valacchi et al., 2009). Briefly, HCEpiC cells, grown to confluent monolayer on 48-well plates, were mechanically scratched with a 200- $\mu$ L sterile pipette tip, washed and then allowed to re-epithelialize for 36 h in the presence of S1 and S2. Serial bright-field images of scratches were captured at different time points (i.e., 0, 12, 24 and 36 h post-scratch). Then, changes in wound area at various time points for each treatment group were measured using Image-J software (National Institutes of Health, Bethesda, MD, USA), and compared to the wound area at 0 h, which was arbitrarily set as 100.

#### *4.3.4.6. Western blot analysis*

To evaluate cell proliferation, HCEpiC cells were seeded on cell culture dishes and, at subconfluence (50%), treated with the two solution S1 and S2. At 12 h, the cells were washed with ice-cold PBS and lysed in ice-cold lysis RIPA buffer. After centrifugation (15,000 $\times$  g, 15 min at 4 °C), the supernatants were collected. Protein concentrations were determined using the Bio-Rad protein assay kit (Bio-Rad Laboratories, Inc., Hercules, CA, USA). Total protein extracts (20  $\mu$ g) were loaded onto 10% sodium dodecyl sulphate–polyacrylamide electrophoresis gels and separated by molecular size. Gels were electro-blotted onto nitrocellulose membranes and then blots were blocked for 1 h in Tris-buffered saline, pH 7.5, containing 0.5% Tween 20% and 3% milk. Membranes were incubated overnight at 4 °C with Cyclin D1 antibody (Cell Signaling Technology, Inc., Danvers, MA, USA). The membranes were then incubated with horseradish peroxidase-conjugated secondary antibody for 1 h, and the bound antibodies were detected by chemiluminescence (Bio-Rad Laboratories, Inc.).  $\beta$ -actin (Cell Signaling Technology, Inc.) was used as loading control. Images of the bands were recorded with a ChemiDoc imaging system (Bio-Rad Laboratories, Inc.) and the densitometry analysis was performed using Image-J software. Results are expressed in arbitrary units as relative to  $\beta$ -actin expression.

#### *4.3.4.7. Statistical analysis*

Obtained data in the different experimental groups were subjected to statistical analysis and compared according to one-way ANOVA and Tukey-Kramer test. The variations were considered significant for  $p < 0.05$ .

## 4.4. Results and discussion

### 4.4.1. Synthesis of HA-CL

Hyaluronic acid cross-linked with urea (Figure 4.1.) was prepared as reported by Citerinesi and co-workers (2015, WO/2015/007773 A1).

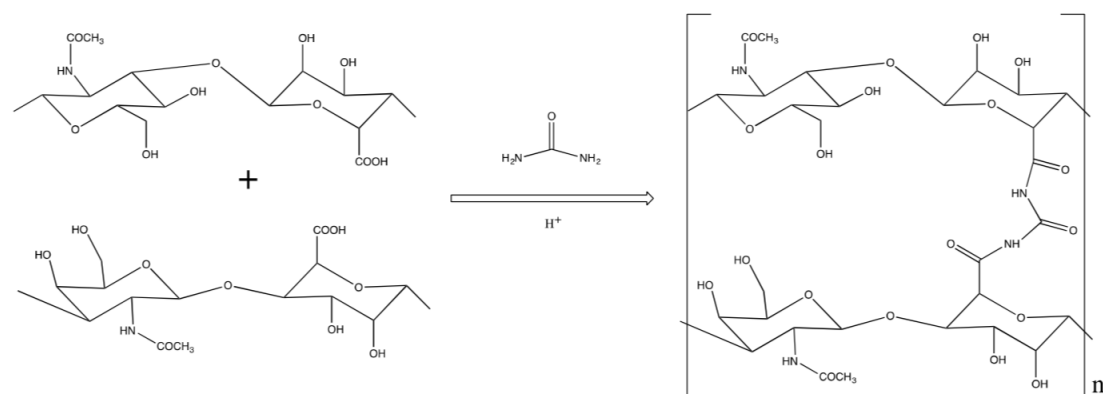


Figure 4.1. Synthesis of HA-CL with urea.

### 4.4.2. Physical-chemical characterization and stability of HA-CL solutions

In this study, two prototypes of eye drops were obtained by gently dissolving HA-CL into a saline-buffered aqueous solution. Immediately after their preparation, both the solutions displayed a transparent and homogenous appearance, and pH and viscosity ( $\eta$ ) values were respectively  $7.0 \pm 0.0$  and  $1.6 \pm 0.0$  mPa·s for S1, and  $7.1 \pm 0.0$  and  $85.9 \pm 0.0$  mPa·s for S2; therefore, suitable for ophthalmic formulations.

Table 4.1. Stability of S1 and S2 during 6 months, at  $23 \pm 2^\circ\text{C}$  and at  $40 \pm 2^\circ\text{C}$ : pH and viscosity values.

Time	T ( $^\circ\text{C}$ )	S1		S2	
		pH	$\eta$ (mPa·s)	pH	$\eta$ (mPa·s)
Day 7	$23 \pm 2$	$7.0 \pm 0.0$	$1.6 \pm 0.0$	$7.1 \pm 0.0$	$85.9 \pm 0.0$
	$40 \pm 2$	$7.0 \pm 0.0$	$1.6 \pm 0.0$	$7.1 \pm 0.0$	$85.8 \pm 0.0$
Month 1	$23 \pm 2$	$7.0 \pm 0.1$	$1.6 \pm 0.0$	$7.0 \pm 0.0$	$85.9 \pm 0.0$
	$40 \pm 2$	$7.0 \pm 0.0$	$1.6 \pm 0.0$	$7.0 \pm 0.0$	$85.8 \pm 0.2$
Month 2	$23 \pm 2$	$7.0 \pm 0.0$	$1.6 \pm 0.1$	$7.0 \pm 0.1$	$85.9 \pm 0.0$
	$40 \pm 2$	$7.0 \pm 0.0$	$1.6 \pm 0.2$	$7.0 \pm 0.2$	$85.8 \pm 0.1$
Month 3	$23 \pm 2$	$7.0 \pm 0.0$	$1.6 \pm 0.0$	$7.0 \pm 0.0$	$85.9 \pm 0.0$
	$40 \pm 2$	$7.1 \pm 0.1$	$1.5 \pm 0.0$	$7.0 \pm 0.0$	$85.6 \pm 0.3$
Month 6	$23 \pm 2$	$7.0 \pm 0.1$	$1.6 \pm 0.0$	$7.0 \pm 0.0$	$86.0 \pm 0.0$
	$40 \pm 2$	$7.1 \pm 0.0$	$1.5 \pm 0.2$	$7.0 \pm 0.0$	$85.7 \pm 0.0$

The stability study showed that the both S1 and S2 met the intended physical and chemical quality standards, as well as functionality and aesthetics, when stored under appropriate conditions. Indeed, both the formulations appeared homogeneous and perfectly transparent during the whole test, maintaining their initial appearance under all the conditions. The pH and viscosity values were pretty much constant during the whole study (Table 4.1.). Conservation at high temperature condition ( $40 \pm 2^\circ\text{C}$ ) provoked only extremely limited modifications of pH and viscosity parameters, which were more than acceptable (Table 4.1.).

#### 4.4.3. Cell viability

Tear supplementation is the treatment of choice to control signs and symptoms of dry eye syndrome (Lemp et al., 2007), and HA artificial tears eye drops are among the most studied (Aragona et al., 2002; Cagini et al., 2017; Dumbleton et al., 2009; Gomes et al., 2004; Hamano et al., 1996; Inoue and Katakami, 1993; Johnson et al., 2006; Nishida et al., 1991; Postorini et al., 2017; Prabhasawat et al., 2007; Sand et al., 1989; Stuart and Linn, 1985). Corneal re-epithelialization, recovery and maintenance of ocular epithelium physiological conditions can be promoted also by urea therapy (Charlton et al., 1996) Hence, the novel hyaluronan derivative cross-linked with urea could be a valid therapy for KCS. Prior to specific markers screenings, the effect of HA-CL on human corneal cells viability was assayed. Table 2 reports cell viability results (MTT test) at 48 and 72 h, under the experimental conditions CTR-, CTR+ and treated with S1 and S2 solutions. As reported in Table 2, the wound caused a decrease of cell viability in damaged untreated tissues (CTR+); however, cell viability increased during time (Table 2). The damaged and treated tissues showed a trend similar to the positive control at 48 h, while, after 72 h of exposure, the cell viability increased to reach values comparable to negative control (not damaged) (CTR-) (Table 4.2.).

Table 4.2. Cell viability (MTT test) of CTR-, CTR+, S1 and S2 at 48 and 72 h.

Condition	Cell Viability		% Variation vs CTR-		% Variation vs CTR+	
	48 H	72 H	48 H	72 H	48 H	72 H
CTR-	100.0 $\pm$ 0.5	100.0 $\pm$ 8.4	-	-	-	-
CTR+	72.4 $\pm$ 2.2	81.8 $\pm$ 4.4	-27.6	-18.2	-	-
S1	76.4 $\pm$ 2.1	107.2 $\pm$ 0.5	-23.6	+7.2	+4.0	+25.4
S2	74.4 $\pm$ 0.7	102.3 $\pm$ 2.0	-25.6	+2.3	+1.9	+20.5

Statistical analysis showed that after 72 h there were significant differences in cell viability between damaged untreated tissue (CTR+) and treated tissues (S1 and S2), and no significant differences between undamaged untreated tissue (CTR-) and treated tissues (S1 and S2) (Table 4.3.). The viability parameter is correlated to cell proliferation that it is an index of the degree of tissue repair. Based on the results obtained, it was possible to conclude that both HA-CL solutions completely restored cell viability, thus promoting the re-epithelialization of the studied cellular model after 72 h.

Table 4.3. Anova and Tukey-Kramer test statistical analysis of cell viability (MTT test) of the conditions CTR-, CTR+, S1 and S2 at 48 and 72 h (statistically significant values in bold,  $p < 0.05$ ).

Condition	vs CTR-		vs CTR+		vs S1		vs S2	
	48 H	72 H	48 H	72 H	48 H	72 H	48 H	72 H
CTR-	-	-	<b>0.00000</b>	<b>0.00983</b>	<b>0.00000</b>	0.41310	<b>0.00000</b>	0.97145
CTR+	<b>0.00000</b>	<b>0.00983</b>	-	-	0.07789	<b>0.00116</b>	0.58301	<b>0.00474</b>
S1	<b>0.00000</b>	0.41310	0.07789	<b>0.00116</b>	-	-	0.52885	0.72684
S2	<b>0.00000</b>	0.97145	0.58301	<b>0.00474</b>	0.52885	0.72684	-	-

#### 4.4.4. Effect of HA-CL on IL-8 levels

To understand if HA-CL solutions were able to modulate inflammation due to wound induction, IL-8 levels were quantified in human corneal control and treated cells. The chemokine IL-8 was chosen as pro-inflammatory marker as it is released in epithelial tissues in a pro-inflammatory status. Table 4.4. reports the results of IL-8 levels (ELISA test) at 48 and 72 h, in the experimental conditions CTR-, CTR+ and treated with S1 and S2 solutions. The wound caused an increased release, over time, of IL-8 in wounded untreated tissues (CTR+) (Table 4.4.). The treated tissues (conditions S1 and S2) showed a trend similar to the positive control (CTR+) throughout the exposure period, with an increase in IL-8 release compared to the negative control tissues (CTR-) (Table 4.4.).

Table 4.4. IL-8 levels in CTR-, CTR+, S1 and S2 tissues assessed at 48 and 72 h by ELISA test.

Condition	IL-8 pg/mL		% Variation vs CTR-		% Variation vs CTR+	
	48 H	72 H	48 H	72 H	48 H	72 H
CTR-	616.5 ± 37.7	595.7 ± 35.9	-	-	-	-
CTR+	762.2 ± 40.3	720.7 ± 49.5	+23.6	+21.0	-	-
S1	699.5 ± 32.4	701.5 ± 36.4	+13.5	+13.8	-8.2	-2.7
S2	664.3 ± 52.3	714.5 ± 58.2	+7.8	+15.9	-12.8	-0.9

Statistical analysis showed that there was not a significant difference in IL-8 levels between the positive control (CTR+) and the treated tissues (S1 and S2), and also between the two treated tissues at both 48 h (Table 4.5.) and 72 h post-treatment (data not shown).

Although no sample was able to significantly modulate IL-8 release in this particular experimental system, it was anyway possible to observe a slight reduction of IL-8 level in treated tissues compared to the positive control, especially at 48 h (-8.2% S1 vs CTR+, -12.8% S2 vs CTR+, Table 4.4.) suggesting a possible positive effect of S1 and S2.

Table 4.5. Anova and Tukey-Kramer test statistical analysis of IL-8 levels in CTR-, CTR+, S1 and S2 tissues at 48 h (statistically significant values in bold,  $p < 0.05$ ).

Condition	48 H			
	vs CTR-	vs CTR+	vs S1	vs S2
CTR-	-	<b>0.00625</b>	0.15548	0.61723
CTR+	<b>0.00625</b>	-	0.37554	0.07523
S1	0.15548	0.37554	-	0.82461
S2	0.61723	0.07523	0.82461	-

#### 4.4.5. Epithelial corneal wound closure

Histological analysis (HE staining) is a useful tool to study epithelial integrity and repair phenomena that follow the induction of mechanical damage. The histological images reported in Figure 4.2. represent the overtime wound closure of the different samples. The negative control CTR- had an intact and correct structure for the entire period of exposure. After wound, it is possible to appreciate a recovery of the damage overtime in the positive control CTR+ samples at 48 h and 72 h. The epitheliums treated with the two solutions S1 and S2 exhibited a clear improvement in the wound closure respect to the positive control.

To confirm the wound healing properties of S1 and S2, we also tested the two HA-CL solutions in a scratch assay on a 2D monolayer model of HCEpiC cells. Consistent with the 3D results, at 36 h post-scratch, treated HCEpiC cells displayed a nearly (S1) or complete (S2) wound closure compared to untreated control cells (Figure 4.3.). In particular, a significant difference in wound closure was observed between S2 treated HCEpiC and untreated control cells (Figure 4.4.), showing that S2 importantly improved epithelial corneal wound closure.

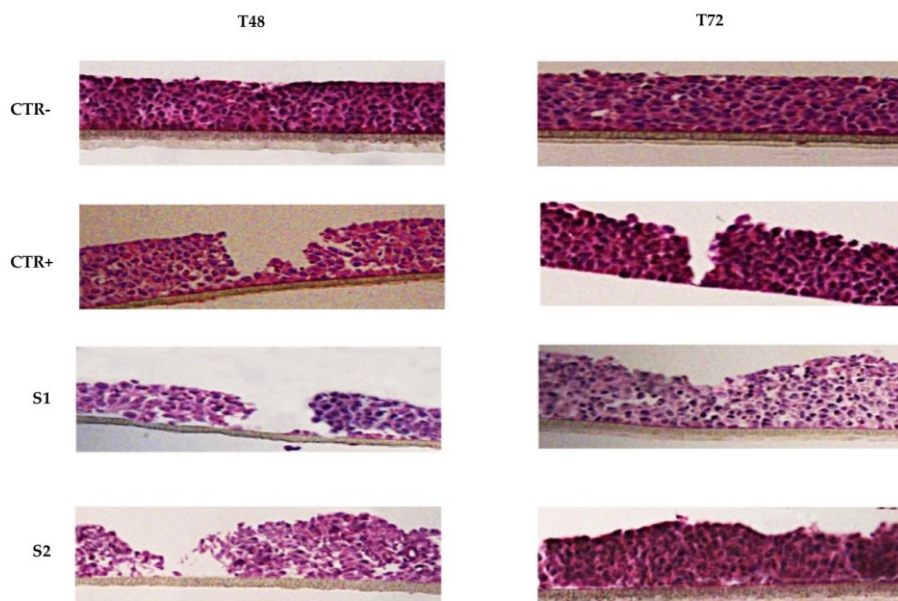


Figure 4.2. Histological analysis (HE staining) of 3D reconstructed tissues of human corneal epithelium. After wounding, HCE cells were incubated in growth medium with or without S1 and S2 for 72 h. Representative images from each group were recorded at 48 and 72 h post-wounding.

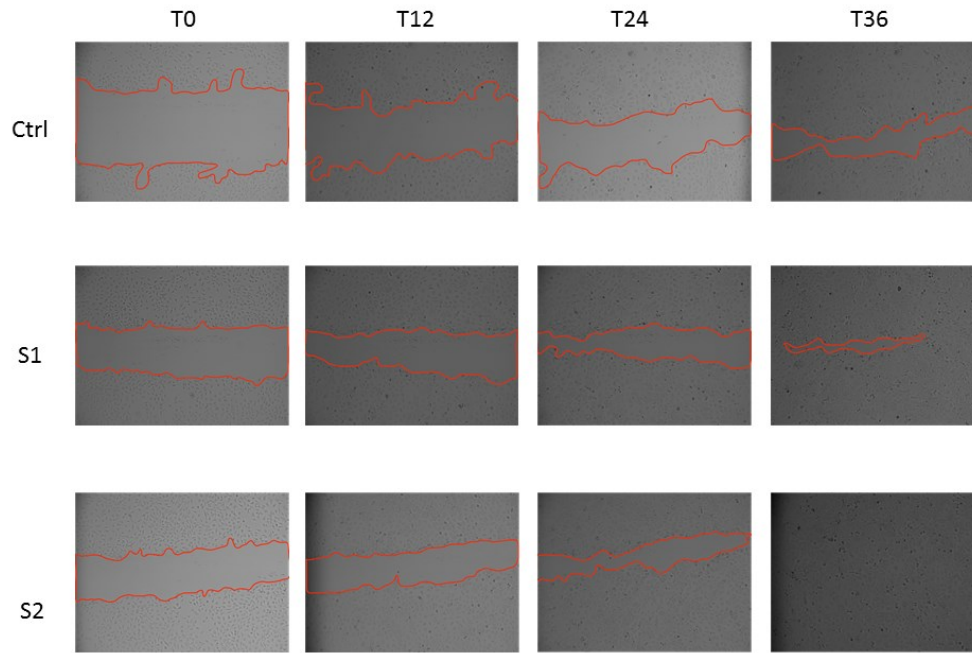


Figure 4.3. In vitro wound healing assay of human corneal epithelial cells. After the scratch, HCEpiC cells were incubated in fresh medium with or without S1 and S2 for 36 h. Representative images from each group were recorded at 0, 12, 24 and 36 h post-scratching. The red lines indicate the wound borders.

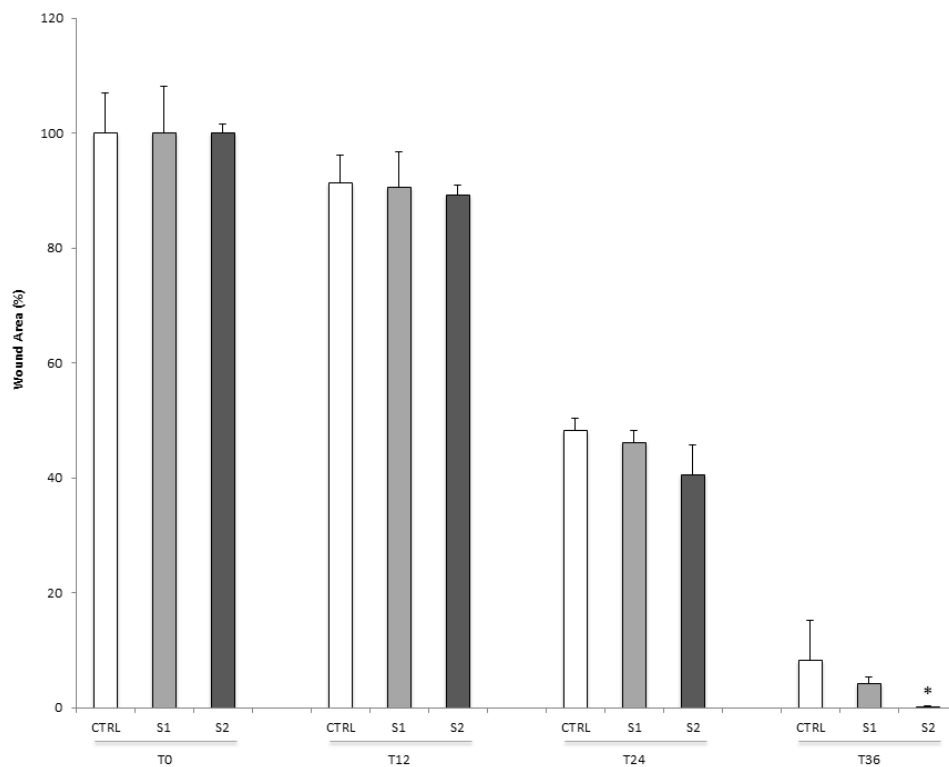


Figure 4.4. Quantification of wound healing in human corneal epithelial cells. The relative scratch gap was calculated as the percentage of the remaining wounded area at the given time point compared with the initially wounded area at 0 h. Data were expressed as mean  $\pm$  SD (n = 3). \*P < 0.05 compared with control.

#### 4.4.6. Cyclin D1 protein levels

To understand the molecular basis of the re-epithelialization properties of S1 and S2 in wound closure, the protein expression of cyclin D1, a cell-cycle regulator critical for G(1)-phase progression and S-phase entry, was also analyzed. As showed in Figure 4.5., both S1 and S2 treatments were able to induce a significant increase in cyclin D1 cellular levels after 12 h respect to the untreated control cells. This evidence suggested that S1 and S2 solutions might be able to accelerate epithelial wound closure by promoting a cyclin D1-induced cell proliferation.

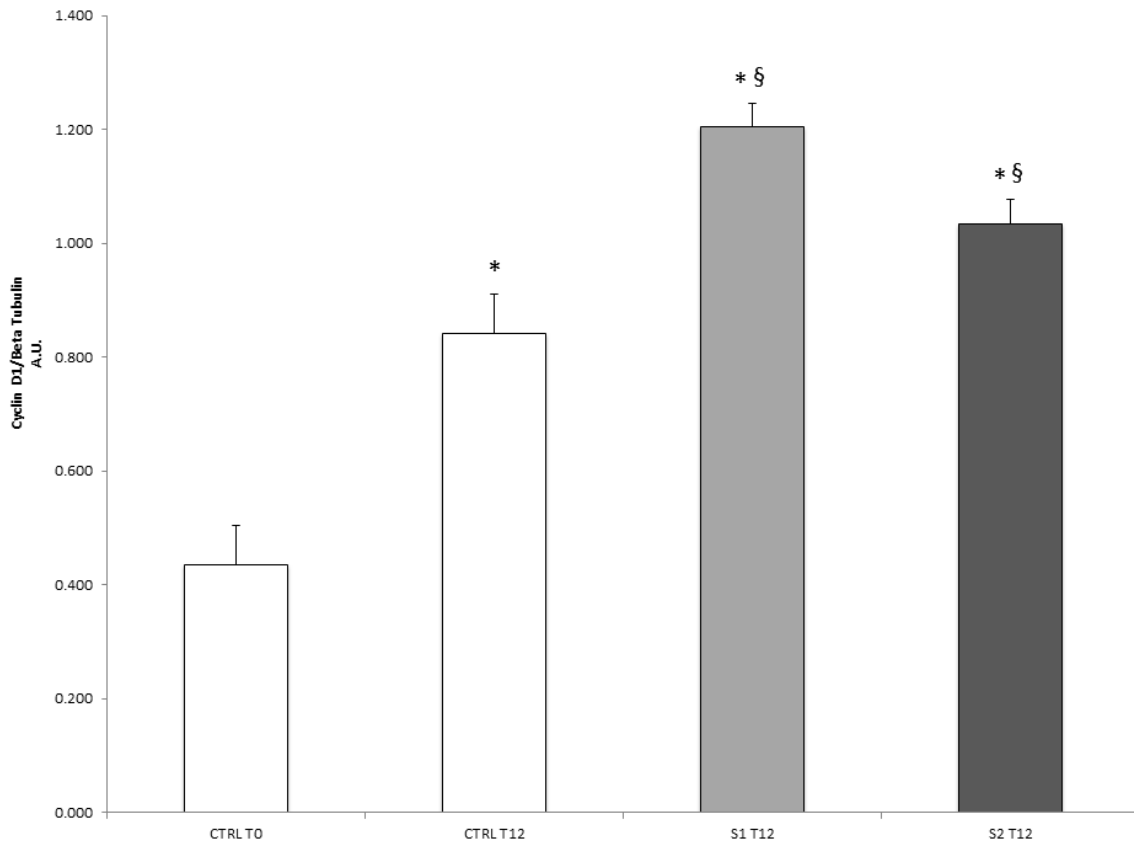


Figure 4.5. Effect of S1 and S2 on the proliferative marker cyclin D1 in HCEpiC cells. The graph shows the cyclin D1 protein levels in HCEpiC cells treated with S1 or S2 for 12 h. Data are means  $\pm$  SD of triplicate. \* indicates statistically significant difference from untreated control at 0 h; § indicates statistically significant difference from untreated control at 12 h (one-way ANOVA,  $P < 0.05$ ).

#### 4.5. Conclusions

Although the preliminary nature of this *in vitro* study, we have clearly shown, for the first time, promising results for the use of artificial tears containing HA-CL with urea for the treatment of dry eye disease and corneal injuries in human eyes. The two prototypes of eye drops developed were characterized by a good chemical-physical stability, and resulted safe for ophthalmic application. Despite both S1 and S2 were not able to significantly reduce IL-8 levels, they showed interesting wound healing properties. Indeed, according to the applied experimental protocol and to the data obtained, both the formulations showed a potential re-epithelialization efficacy on the cellular models analyzed: a clear recovery of the wound was

observed in the 2D model and also in the 3D model. This was confirmed also by histological analysis, which showed the restoring of microscopic epithelial structure after treatment with S1 and S2. Our findings were in agreement with the results of previous *in vitro* and *in vivo* studies, which showed that corneal epithelial wound healing is promoted by native HA (Condon et al., 1999; Gomes et al., 2004; Inoue and Katakami, 1993; Nishida et al., 1991; Papa et al., 2001; Williams et al., 2012) and others type of HA-CL (Cagini et al., 2017; Calles et al., 2013, 2016; Postorini et al., 2017; Williams and Mann, 2013, 2014; Williams et al., 2017; Wirostko et al., 2014; Yang et al., 2010). Moreover, Western blot analysis evidenced that, after the treatment with S1 and S2 eye drops, the level of the proliferative marker cyclin D1 was increased compared to the control. Therefore, the two HA-CL solutions accelerated the tissue proliferative process related to post-wound re-epithelialization. This study opens encouraging perspectives, since HA-CL with urea may promptly alleviate both signs and symptoms of dry eye syndrome, even if used at concentration lower (0.02% w/v) than the usually employed for native HA artificial tears (generally 0.1-0.4%) (Aragona et al., 2002; Condon et al., 1999; Dumbleton et al., 2009; Hamano et al., 1996; Johnson et al., 2006; Prabhasawat et al., 2007; Sand et al., 1989; Stuart and Linn, 1985). Therefore, HA-CL with urea eye drops could allow a rapid improvement of patient ocular comfort and quality of life through a therapy with absolutely acceptable costs. All these evidences and considerations strongly support further investigations, both *in vitro* and *in vivo*, for a deeper characterization of the biological activity of artificial tears containing HA-CL with urea. Moreover, further researches will be necessary to understand the ocular surface residence time and thus the required dose-frequency of eye drops containing HA-CL with urea, as well as their potential delivery through the membrane.

#### **4.6. Acknowledgments**

This work was supported by the University of Ferrara FAR Grant 2014; Ambrosialab Srl, Ferrara; COC Farmaceutici Srl, Rovereto (Modena); I.R.A. Srl (Istituto Ricerche Applicate, Usmate-Velate, Monza-Brianza, Italy). Authors wish to thank Farcoderm Srl (Milano) for the testing facilities.

#### **4.7. Conflicts of interest**

The authors declare no conflict of interest. The founding sponsors had no role in the design of the study; in the collection, analyses, or interpretation of data; in the writing of the manuscript, and in the decision to publish the results.



#### 4.8. References

- Aragona, P., Papa, V., Micali, A., Santocono, M., Milazzo, G., 2002. Long term treatment with sodium hyaluronate-containing artificial tears reduces ocular surface damage in patients with dry eye. *Br. J. Ophthalmol.* 86, 181–184.
- Berriaud, N., Milas, M., Rinaudo, M., 2005. Characterization and properties of hyaluronic acid (hyaluronan). In *Polysaccharides: Structural Diversity and Functional Versatility*, 2nd ed.; Dumitriu, S., Dekker, M., Eds.; CRC Press: New York, NY, USA; pp. 535–549.
- Berry, M., Pastis, K.W., Ellingham, R.B., Frost, L., Corfield, A.P., Easty, D.L., 1998. Hyaluronan in dry eye and contact lens wearers. In *Lacrimal Gland, Tear Film, and Dry Eye Syndromes 2*; Sullivan, D.A., Dartt, D.A., Meneray, M.A., Eds.; Plenum Press: New York, NY, USA; pp. 785–790.
- Cagini, C., Torroni, G., Fiore, T., Cerquaglia, A., Lupidi, M., Aragona, P., Iaccheri, B., 2017. Tear film stability in Sjogren syndrome patients treated with hyaluronic acid versus crosslinked hyaluronic acid-based eye drops. *J. Ocul. Pharmacol. Ther.* 33, 539–542.
- Calles, J.A., Lopez-García, A., Vallés, E.M., Palma, S.D., Diebold, Y., 2016. Preliminary characterization of dexamethasone-loaded cross-linked hyaluronic acid films for topical ocular therapy. *Int. J. Pharm.* 509, 237–243.
- Calles, J.A., Tàrtara, L.I., Lopez-García, A., Diebold, Y., Palma, S.D., Vallés, E.M., 2013. Novel bioadhesive hyaluronan-itaconic acid crosslinked films for ocular therapy. *Int. J. Pharm.* 455, 48–56.
- Charlton, J.F., Schwab, I.R., Stuchell, R., 1996. Topical urea as a treatment for non-infectious keratopathy. *Acta Ophthalmol. Scand.* 74, 391–394.
- Citernesi, U.R., Beretta, L., Citernesi, L., 2015. Cross-Linked Hyaluronic Acid, Process for the Preparation Thereof and Use Thereof in the Aesthetic Field. Patent WO/2015/007773 A1.
- Condon, P.I., McEwen, C.G., Wright, M., Mackintosh, G., Prescott, R.J., McDonald, C., 1999. Double blind, randomized, placebo controlled, crossover, multicenter study to determine the efficacy of a 0.1% (w/v) sodium hyaluronate solution (Fermavisc) in the treatment of dry eye syndrome. *Br. J. Ophthalmol.* 83, 1121–1124.
- Dumbleton, K., Woods, C., Fonn, D., 2009. An investigation of the efficacy of a novel ocular lubricant. *Eye Contact Lens.* 35, 149–155.
- Fallacara, A., Manfredini, S., Durini, E., Vertuani, S., 2017. Hyaluronic acid fillers in soft tissue regeneration. *Facial Plast. Surg.* 33, 87–96.
- Fischer, A.H., Jacobson, K.A., Rose, J., Zeller, R., 2008. Hematoxylin and eosin staining of tissue and cell sections. *CSH Protoc.* doi: 10.1101/pdb.prot4986.

- Frescura, M., Berry, M., Corfield, A., Carrington, S., Easty, D.L., 1994. Evidence of hyaluronan in human tears and secretions of conjunctival cultures. *Biochem. Soc. Trans.* 22, 228s.
- Fukuda, M., Miyamoto, Y., Miyara, Y., Mishima, H., Otori, T., 1996. Hyaluronic acid concentrations in human tear fluids. *Investig. Ophthalmol. Vis. Sci.* 37, 3916.
- Gomes, J.A.P., Amankwah, R., Powell-Richards, A., Dua, H.S., 2004. Sodium hyaluronate (hyaluronic acid) promotes migration of human corneal epithelial cells in vitro. *Br. J. Ophthalmol.* 88, 821–825.
- Hamano, T., Horimoto, K., Lee, M., Komemushi, S., 1996. Sodium hyaluronate eye drops enhance tear film stability. *Jpn. J. Ophthalmol.* 40, 62–65.
- Inoue, M., Katakami, C., 1993. The effect of hyaluronic acid on corneal epithelial cell proliferation. *Investig. Ophthalmol. Vis. Sci.* 34, 2313–2315.
- Johnson, M.E., Murphy, P.J., Boulton, M., 2006. Effectiveness of sodium hyaluronate eye drops in the treatment of dry eye. *Graefes Arch. Clin. Exp. Ophthalmol.* 244, 109–112.
- Lapcik, L.Jr., Lapcik, L., De Smedt, S., Demeester, J., Chabreček, P., 1998. Hyaluronan: Preparation, structure, properties, and applications. *Chem. Rev.* 98, 2663–2684.
- Lemp, M.A., Baudouin, C., Bau, J., Dogru, M., Foulks, G.N., Kinoshita, S., Laibson, P., Mc Culley, J., Murube, J., Pflugfelder, S.C., et al. 2007. DEWS definition and classification subcommittee of the international dry eye workshop. The definition and classification of dry eye disease: Report of the definition and classification subcommittee of the international dry eye workshop. *Ocular Surf.* 5, 75–92.
- Nakamura, M., Hikida, M., Nakano, T., Ito, S., Hamano, T., Kinoshita, S., 1993. Characterization of water retentive properties of hyaluronan. *Cornea.* 12, 433–436.
- Nishida, T., Nakamura, M., Mishima, H., Otori, T., 1991. Hyaluronan stimulates corneal epithelial migration. *Exp. Eye Res.* 53, 753–758.
- Papa, V., Aragona, P., Russo, S., Di Bella, A., Russo, P., Milazzo, G., 2001. Comparison of hypotonic and isotonic solutions containing sodium hyaluronate on the symptomatic treatment of dry eye patients. *Ophthalmology.* 215, 124–127.
- Postorino, E.I., Rania, L., Aragona, E., Mannucci, C., Alibrandi, A., Calapai, G., Puzzolo, D., Aragona, P., 2017. Efficacy of eye drops containing cross-linked hyaluronic acid and coenzyme Q10 in treating patients with mild to moderate dry eye. *Eur. J. Ophthalmol.* 28, 25–31.
- Prabhasawat, P., Tesavibul, N., Kasetsuwan, N., 2007. Performance profile of sodium hyaluronate in patients with lipid tear deficiency: Randomised, double-blind, controlled, exploratory study. *Br. J. Ophthalmol.* 91, 47–50.

- Presti, D., Scott, J.E., 1994. Hyaluronan-mediated protective effect against cell damage caused by enzymatically produced hydroxyl (OH.) radicals is dependent on hyaluronan molecular mass. *Cell Biochem. Funct.* 12, 281–288.
- Sand, B.B., Marnier, K., Norn, M.S., 1989. Sodium hyaluronate in the treatment of keratoconjunctivitis sicca. A double masked clinical trial. *Acta Ophthalmol.* 67, 181–183.
- Scott, J.E., 1995. Extracellular matrix, supramolecular organization and shape. *J. Anat.* 187, 259–269.
- Stuart, J.C., Linn, J.G., 1985. Dilute sodium hyaluronate (Healon) in the treatment of ocular surface disorders. *Ann. Ophthalmol.* 17, 190–192.
- Valacchi, G., Pecorelli, A., Mencarelli, M., Carbotti, P., Fortino, V., Muscettola, M., Maioli, E., 2009. Rottlerin: A multifaced regulator of keratinocyte cell cycle. *Exp. Dermatol.* 18, 516–521.
- Van Goethem, F., Adriaens, E., Alepee, N., Straube, F., De Wever, B., Cappadoro, M., Catoire, S., Hansen, E., Wolf, A., Vanparys, P., 2006. Prevalidation of a new in vitro reconstituted human cornea model to assess the eye irritating potential of chemicals. *Toxicol. In Vitro.* 20, 1–17.
- Williams, D., Middleton, S., Fattahian, H., Moridpour, R., 2012. Comparison of hyaluronic acid-containing topical eye drops with carbomer-based topical ocular gel as a tear replacement in canine keratoconjunctivitis sicca: a prospective study in twenty-five dogs. *Vet. Res. Forum.* 3, 229–232.
- Williams, D.L., Mann, B.K., 2013. A crosslinked HA-based hydrogel ameliorates dry eye symptoms in dogs. *Int. J. Biomater.* 2013, 460437.
- Williams, D.L., Mann, B.K., 2014. Efficacy of a crosslinked hyaluronic acid-based hydrogel as a tear film supplement: A masked controlled study. *PLoS ONE*, 9, e99766.
- Williams, D.L., Wirostko, B.M., Gum, G., Mann, B.K., 2017. Topical cross-linked HA-based hydrogel accelerates closure of corneal epithelial defects and repair of stromal ulceration in companion animals. *Investig. Ophthalmol. Vis. Sci.* 58, 4616–4622.
- Wirostko, B., Mann, K.B., Williams, D.L., Prestwich, G.D., 2014. Ophthalmic uses of a thiol-modified hyaluronan-based hydrogel. *Adv. Wound Care (New Rochelle)*. 3, 708–716.
- Yang, G., Espandar, L., Mamalis, N., Prestwich, G.D., 2010. A cross-linked hyaluronan gel accelerates healing of corneal epithelial abrasion and alkali burn injuries in rabbits. *Vet. Ophthalmol.* 13, 144–150.
- Yoshida, K., Nitatori, Y., Uchiyama, Y., 1996. Localization of glycosaminoglycans and CD44 in the human lacrimal gland. *Arch. Histol. Cytol.* 59, 505–513.



## CHAPTER 5

### ***Formulation and characterization of native and crosslinked hyaluronic acid microspheres for dermal delivery of sodium ascorbyl phosphate: a comparative study***

This chapter was published in *Pharmaceutics*, 10(4) (2018),  
under the title

“Formulation and characterization of native and crosslinked hyaluronic acid microspheres for dermal delivery of sodium ascorbyl phosphate: a comparative study”.

*Authors: Arianna Fallacara<sup>a,b,c</sup>, Filippo Marchetti<sup>a</sup>, Michele Pozzoli<sup>b</sup>, Ugo Raffaello Citernes<sup>c</sup>, Stefano Manfredini<sup>a,d,\*</sup>, Silvia Vertuani<sup>a,d</sup>*

<sup>a</sup> Department of Life Sciences and Biotechnology, Master Course in Cosmetic Science and Technology (COSMAST), University of Ferrara, Via L. Borsari 46, 44121 Ferrara, Italy.

<sup>b</sup> Respiratory Technology, Woolcock Institute of Medical Research and Discipline of Pharmacology, Faculty of Medicine and Health, The University of Sydney, 431 Glebe Point Road, Glebe, NSW 2037, Australia.

<sup>c</sup> I.R.A. Istituto Ricerche Applicate s.r.l. Via Del Lavoro 4a/6, 20865 Usmate Velate (MB), Italy.

<sup>d</sup> AmbrosiaLab Srl, Via Mortara 171, 44121, Ferrara, Italy.

**\* Corresponding author:**

Prof. Stefano Manfredini: smanfred@unife.it; Tel.: +39-0532-455294; Fax: +39-0532-455378.

DOI: 10.3390/pharmaceutics10040254



## 5.0. Preface

The central aim of the present PhD thesis was to develop novel pharmaceutical and cosmetic formulations containing urea-crosslinked hyaluronic acid (HA-CL), in order to investigate its potentialities in terms of bioactivity and delivery of active ingredients. Therefore, chapter 5 describes the formulation and the *in vitro* physico-chemical characterization of HA-CL microspheres (MS) intended for dermal delivery of sodium ascorbyl phosphate (SAP) -HA-CL – SAP MS. Considering that this was the first time that HA-CL – SAP MS were produced, reference formulations were also developed and characterized as terms of comparison: unloaded HA-CL MS, unloaded native hyaluronic acid (HA) microspheres (HA MS), SAP-loaded HA MS (HA – SAP MS). A systematic approach was employed to study the experimental features of the MS formulations, as well as their mechanisms of drug release.

## 5.1. Abstract

The present work evaluates for the first time the use of urea-crosslinked hyaluronic acid (HA-CL), a novel derivative of native hyaluronic acid (HA), to produce microspheres (MS) by emulsification-solvent evaporation, for dermal delivery of sodium ascorbyl phosphate (SAP). As the term of comparison, HA MS were prepared. A pre-formulation study – investigation of the effects of polymers solutions properties (pH, viscosity) and working conditions– led to the production of optimized HA-CL MS and HA-CL – SAP MS with: almost unimodal size distributions; mean diameter of  $13.0 \pm 0.7$  and  $9.9 \pm 0.8$   $\mu\text{m}$ , respectively; spherical shape and rough surface; high yield -similar to HA MS and HA – SAP MS ( $\approx 85\%$ ). SAP was more efficiently encapsulated into HA-CL MS ( $78.8 \pm 2.6\%$ ) compared to HA MS ( $69.7 \pm 4.6\%$ ). Physical state, thermal properties, relative moisture stability of HA-CL MS and HA-CL – SAP MS were comparable to those of HA MS and HA – SAP MS. However, HA-CL – SAP MS exhibited an extended drug release compared to HA – SAP MS, despite the same kinetic mechanism –contemporaneous drug diffusion and polymer swelling/dissolution. Therefore, HA-CL formulation showed a greater potential as microcarrier (for encapsulation efficiency and release kinetic), that could be improved, in future, using suitable excipients.

**Keywords:** dermal delivery; drug release; hyaluronic acid; urea-crosslinked hyaluronic acid; microspheres; sodium ascorbyl phosphate.



## 5.2. Introduction

Hyaluronic acid (HA) is a naturally occurring glycosaminoglycan, pervasively diffused in the human body: it is found in the extracellular matrix, skin dermis, eye vitreous, hyaline cartilage, synovial fluid, and umbilical cord. HA is well known for its numerous biological functions (Fallacara et al., 2018a; Laurent et al., 1995) and its interesting properties such as biocompatibility, biodegradability, and mucoadhesion (Liao et al., 2005; Mayol et al., 2008). Moreover, HA has moisturizing, lubricant, and filler actions, and it is involved in wound healing and anti-inflammatory processes (Fallacara et al., 2018a; Liao et al., 2005). For these reasons, hyaluronan has widespread applications in medical, pharmaceutical, and cosmetic fields, and represents an interesting starting material -frequently combined to other active ingredients or excipients- in tissue engineering, viscosupplementation and drug delivery (Benedetti et al., 1990; Casale et al., 2015; El Kechai et al., 2017; Esposito et al., 2005; Fallacara et al., 2017a, 2018a; Li et al., 2017; Liao et al., 2005; Lim et al., 2000; Mayol et al., 2008; Saadat et al., 2015). To design biomaterials with improved physical-chemical, viscoelastic and biological properties, native HA is often subjected to derivatization or crosslinking (Shimojo et al., 2015). Usually, HA is crosslinked with difunctional molecules of synthetic origin, for example, divinyl sulfone and diglycidyl ether (Ramamurthi and Vesely, 2002; Tomihata and Ikada, 1997). Nevertheless, the recent trend consists in crosslinking the polymer with substances characterized by lower toxicity and intrinsic health activity. The aim is to obtain cross-polymers that can act as multifunctional molecules able to deliver active ingredients and to exert, at the same time, a health action (Fallacara et al., 2018a). Toward this end, we are actually investigating the possible pharmaceutical, cosmetic, and aesthetic applications of the new HA crosslinked with urea (HA-CL) (Citernesi et al., 2015, WO/2015/007773 A1; Fallacara et al., 2017a, b, 2018b). HA-CL is a recently patented biocompatible and biodegradable polymer, provided with greater consistency and bioactivity with respect to native HA (Citernesi et al., 2015, WO/2015/007773 A1; Fallacara et al., 2017a, 2018b). This is due to hyaluronan crosslinking with urea, a molecule naturally present in the human body and also employed as active substance. Indeed, urea is widely and safely used in pharmaceutical and cosmetic formulations because it is keratolytic and moisturizing, and thus it enhances cellular regeneration and reparation. Urea is useful to treat different diseases, such as dry skin, damaged cutaneous annexes, non-infectious keratopathy, and injured corneal epithelium (Albèr et al., 2013; Charlton et al., 1996; Pan et al., 2013). Hence, HA-CL could be a promising biomaterial for topical treatments requiring simultaneous re-epithelialization and hydration for the resolution of aesthetic/functional skin and mucosae problems (Citernesi et al., 2015, WO/2015/007773 A1; Fallacara et al., 2017a, b).

Biodegradable and mucoadhesive polymers, in the form of microparticulate systems such as microspheres (MS), can accelerate skin wound healing (Degim, 2008) and extend the release of the encapsulated drugs (Abd El-Hameed and Kellaway, 1997; Esposito et al., 2005; Kulkarni et al., 2016). Acknowledging the aforementioned facts and properties of HA-CL, we decided to explore for the first time, with this work, the potentiality of HA-CL to formulate drug loaded MS intended for the dermal target. The preparative method chosen was a water-in-oil (w/o) emulsification solvent evaporation technique, and native HA was used as reference polymer, as it has been already employed to produce MS (Esposito et al., 2005; Lim et al., 2000). This study has as its goal the provision of the perfect case scenario: to have an

active molecule, never loaded before into hyaluronan microcarriers, which could be satisfyingly encapsulated and then freely released by the MS. Therefore, sodium ascorbyl phosphate (SAP) was selected as the model drug for its high hydrophilicity (Khan et al., 2017) and for its unprecedented encapsulation into hyaluronan MS. Moreover, SAP seemed to be an optimal candidate as it is characterized by good physical-chemical stability instead of ascorbic acid, and by several biological activities which go in synergy with those of HA. Indeed, SAP acts as a radical scavenger, with high capacity to reduce damages caused by photo-oxidation and lipid peroxidation, and it has strong antimicrobial activity on *Propionibacterium acnes*, the major bacterium responsible of *acne vulgaris* (Khan et al., 2017; Klock et al., 2005). The SAP is a non-irritating prodrug bioconverted by skin enzymes into ascorbic acid, which stimulates collagen synthesis and, therefore, increases skin elasticity (Amirlak et al., 2016; Spiclin et al., 2003). Hence, the combination of vitamin C derivatives and hyaluronan could open interesting perspectives. In fact, a recent study reported the safety of an HA sponge system containing a derivative of vitamin C used to reduce and treat scars (Amirlak et al., 2016). Additionally, the delivery of a combination of SAP and HA-CL showed enhanced anti-inflammatory and antioxidant activities with respect to the single SAP and HA-CL: hence, the association of SAP and HA-CL could be suitable as an adjunctive therapy for the treatment of inflammatory pulmonary disorders (Fallacara et al., 2018b).

In this study, SAP-loaded hyaluronan MS were formulated using the novel urea-crosslinked hyaluronic acid. A preformulation study was performed to obtain optimized MS: particle features such as mean diameter, size distribution, yield (Y%), drug loading (DL%) and encapsulation efficiency (EE%) were investigated in relation to the properties of the starting polymeric solutions and to the emulsification time. The optimized MS were then characterized more in detail for their physical-chemical properties - morphology, physical state, thermal behaviour and stability, moisture sorption and stability- and for their *in vitro* release profiles. An accurate and itemized theoretical study was carried out to understand and explain, with a systematic approach, the mechanisms of release and the experimental features of HA-CL formulations. Considering that this was the first research describing HA-CL MS, no excipients were added to the formulations, in order to investigate the actual polymer potentiality as microcarrier. Additionally, all the properties of SAP-loaded and unloaded MS of HA-CL were compared to SAP-loaded and unloaded MS of native HA (prepared as reference formulations).

### 5.3. Materials and methods

Native hyaluronic acid (sodium salt, molecular weight 1.2 MDa) and urea-crosslinked hyaluronic acid (molecular weight 2.0-4.0 MDa –raw material containing also pentylene glycol) were kindly given by I.R.A. Srl (Istituto Ricerche Applicate Srl, Usmate-Velate, Monza-Brianza, Italy). Sodium ascorbyl phosphate (known under the trade name STAY-C®50) was purchased from DSM Nutritional Products Ltd (Segrate, Milano, Italy). Phosphate buffered saline (PBS) and hexane were supplied by Sigma-Aldrich (Schnelldorf, Germany). Mineral oil was obtained from Fagron (Quarto Inferiore, Bologna, Italy). Sorbitan monooleate (Span 80) was provided by Acef (Fiorenzuola D'Arda, Piacenza, Italy).

### 5.3.1. Preparation of hyaluronan and hyaluronan-SAP solutions (aqueous phases)

HA 1% (w/v) solution and HA-CL 1% (w/v) solution were achieved through a progressive dispersion of the polymers in deionized water, under continuous magnetic stirring (300 rpm). Likewise, hyaluronan-SAP solutions 1% (w/v), 1:1- were prepared by dispersing the polymers into SAP water solutions, under constant magnetic stirring (300 rpm). The polymers were allowed to completely hydrate thus forming hydrogels, which were left to swell under moderate stirring, over 12 h, at room temperature, to reach homogeneous appearances. The gels were left at rest for 12 h prior to examinations or use as aqueous phases for MS formulation.

### 5.3.2. Characterization of hyaluronan and hyaluronan-SAP solutions: pH and rheology

Firstly, the pH of each hyaluronan aqueous phase was measured in triplicate using a digital pH meter (Docu pH+ meter, Sartorius Mechatronics, Goettingen, Germany).

Secondly, hyaluronan hydrogels were subjected to rheological analyses, performed in triplicate, at  $23 \pm 2$  °C, with a rotational rheometer AR2000 (TA Instruments, New Castle, Delaware, USA), equipped with an aluminum cone/plate geometry –diameter 40 mm, angle 2°, 64 μm truncation. A solvent trap was used in order to prevent samples dehydration. The rheometer was connected to the Rheology Advantage software (version V7.20) for data analysis.

Flow measurements were performed by a shear rate sweep, under steady state condition: after 1-min equilibration time, the shear rate ( $\dot{\gamma}$ ) was progressively increased from 0.01 to 1000 s<sup>-1</sup>. The gels were compared for their zero-shear-rate viscosity ( $\eta_0$ ), which was determined by fitting the viscosity curves according to the Cross equation (Wetton and Whorlow, 1968) (Eq. 5.1.):

$$\eta = \eta_{\infty} + \frac{\eta_0 - \eta_{\infty}}{1 + (C \cdot \dot{\gamma})^n} \quad (\text{Eq. 5.1.})$$

where  $\eta$  is the viscosity at a given shear rate (Pa.s),  $\dot{\gamma}$  is the shear rate (s<sup>-1</sup>),  $\eta_0$  is the zero-shear rate viscosity (Pa.s),  $\eta_{\infty}$  is the infinite-shear rate viscosity (Pa.s),  $C$  is a multiplicative parameter (s) and  $n$  is a dimensionless exponent.

where  $\eta$  is the viscosity at a given shear rate (Pa.s),  $\dot{\gamma}$  is the shear rate (s<sup>-1</sup>),  $\eta_0$  is the zero-shear-rate viscosity (Pa.s),  $\eta_{\infty}$  is the infinite-shear-rate viscosity (Pa.s),  $C$  is a multiplicative parameter (s) and  $n$  is a dimensionless exponent.

Oscillatory measurements were then taken under the constant stress value of 0.2 Pa, which belonged to the viscoelastic linear regime (defined by a strain sweep test), where the hydrogels could not be subjected to irreversible structural modifications. The experiments were carried out with oscillation frequencies ranging from 0.01 to 100 Hz. The elastic modulus ( $G'$ ) and the viscous modulus ( $G''$ ), measured as a function of the frequency of the stress applied, allowed to evaluate the viscoelastic properties of the gels (Couarraze and Grossiord, 2000). More precisely, the samples were compared for their elastic modulus at 1 Hz ( $G'_{1\text{Hz}}$ , quantitative index of elasticity), and for their crossover frequency ( $C_f$ , frequency where  $G'$  is equal to  $G''$ ).

### 5.3.3. Formulation of HA and HA-CL microspheres containing or not SAP

HA and HA-CL MS containing or not SAP were produced through a water-in-oil (w/o) emulsification solvent evaporation technique, adapted from the method described by Lim and co-workers (Lim et al., 2000).

The aqueous phase was added dropwise (flow rate: 0,91 mL/min) into 100 g of mineral oil (oil phase) containing 1 % (w/w) sorbitan monooleate as the emulsifying agent, under moderate magnetic stirring (200 rpm), at  $23 \pm 2^\circ\text{C}$ . The aqueous phase was then emulsified at 1000 rpm, at  $23 \pm 2^\circ\text{C}$ , into the oil phase, using a Silverson L5M A Laboratory Mixer (Silverson Machines, Buckinghamshire, United Kingdom), equipped with a fine emulsor screen workhead. Different emulsification times of 10, 30 and 60 min were investigated. Afterward, moderate magnetic stirring (200 rpm) and mild heating ( $37 \pm 2^\circ\text{C}$ ) were constantly maintained for 12 h to guarantee the complete evaporation of the dispersed aqueous phase. The MSs thus formed were separated from the oil phase by centrifugation at 4000 rpm, at  $23 \pm 2^\circ\text{C}$ , for 30 min (ALC Centrifuge PK110, OPTO-LAB, Concordia sulla Secchia, Modena, Italy). The pellets were resuspended in hexane and filtered under vacuum, at  $23 \pm 2^\circ\text{C}$ , using a Millipore glass filtration system, equipped with a polyamide membrane, pore size  $0.22 \mu\text{m}$  (Sartorius, Muggiò, Monza-Brianza, Italy). The collected MSs were finally dried in an oven at  $37 \pm 2^\circ\text{C}$  for 12 hours.

### 5.3.4. MS yield, drug loading and encapsulation efficiency

MS yield (Y%), drug loading (DL%) and drug encapsulation efficiency (EE%) were respectively calculated from Eqs. 5.2. – 5.4.:

$$Y\% = \frac{\text{weight of recovered MS}}{\text{weight of polymer* and drug fed initially}} \cdot 100 \quad (\text{Eq. 5.2.})$$

\* HA-CL was provided as a raw material containing pentylene glycol. Being hydrophilic, this excipient was taken into account for the determination of HA-CL MS Y%, because 1% (w/v) HA-CL solutions contained 0.75% (w/v) pentylene glycol.

$$DL\% = \frac{\text{weight of drug in MS}}{\text{weight of recovered MS}} \cdot 100 \quad (\text{Eq. 5.3.})$$

$$EE\% = \frac{\text{weight of drug in MS}}{\text{weight of drug fed initially}} \cdot 100 \quad (\text{Eq. 5.4.})$$

For each MS formulation, all the determinations were performed in triplicate and the results were reported as the mean  $\pm$  standard deviation (SD).

The amount of encapsulated drug was determined by completely dissolving 30 mg of SAP loaded MS in 300 mL of release medium. Drug concentration was then assayed by ultraviolet (UV) spectroscopy (SHIMADZU UV-2600 spectrophotometer, Kyoto, Japan), at 258 nm (wavelength value corresponding to SAP  $\lambda_{\text{max}}$ ), on the basis of a previously plotted

calibration curve. Unloaded HA and HA-CL MS were tested to ensure that other components of the formulations were not characterized by UV absorbance at the scanning wavelength.

### **5.3.5. Particle size analysis**

Particle size distributions of HA and HA-CL microspheres containing or not SAP were analyzed using laser diffraction (Malvern Mastersizer 2000, Malvern Instruments Ltd., UK). Samples of powder (ca. 10 mg) were dispersed through the Scirocco dry dispersion unit (Malvern, UK) with a feed pressure of 4 bars and a feed rate of 100%. Samples were analyzed in triplicate, with an obscuration value between 0.1% and 15% and a reference refractive index of 1.33. The volume weighted mean diameters ( $D[4,3]$ ) and the median particle size by volume  $Dv50$  were used to describe MS size. Size distributions were evaluated by calculation of samples Span values as follow (Eq. 5.5.):

$$Span = \frac{Dv90 - Dv10}{Dv50} \quad (\text{Eq. 5.5.})$$

where  $Dv90$ ,  $Dv10$ , and  $Dv50$  are respectively the 90%, 10% and 50% cumulative volume distributions. Thus, the Span values gave a measure of the ranges of the volume distributions relative to the median diameters.

### **5.3.6. SEM morphological analysis**

The morphology (shape and surface) of HA and HA-CL MS containing or not SAP was observed using a field emission scanning electron microscope (Zeiss EVO 40XVP, Carl Zeiss Pty Ltd., Oberkochen, Germany), with an acceleration voltage of 20 kV. Powder samples were deposited on carbon sticky tabs and sputter coated with a thin layer of gold-palladium, under an argon atmosphere, prior to analysis. The samples were then randomly scanned and photographed.

### **5.3.7. X-ray powder diffraction**

X-ray diffraction measurements on SAP and SAP-loaded and unloaded MS were performed at 40 kV, 40 mA, with the Bruker AXS D8 Advance Geiger counter equipped with a two-dimensional (2D) gas-filled sealed multiwire detector (scattering-angle resolution of  $0.02^\circ \text{ s}^{-1}$ ). Monochromatized Cu  $K\alpha$  radiation ( $\lambda = 1.54 \text{ \AA}$ ) was used. The analyses were performed in a  $5-45^\circ 2\theta$  range, at ambient temperature. The intensity vs. scattering angle spectra was obtained after the radial average of the measured 2D isotropic diffraction patterns. Bragg peaks were detected in the wide-angle X-ray diffraction region (WAXD).

### **5.3.8. Thermal analysis (DSC and TGA)**

The thermal profiles of SAP and MS formulations were studied using differential scanning calorimetry (DSC823e; Mettler-Toledo, Schwerzenbach, Switzerland). Roughly 5 mg of samples were weighted and crimp-sealed in DSC standard 40  $\mu\text{l}$  aluminum pans.

Samples were then subjected to a 10°C/min temperature ramp between -20 °C and 300 °C. The endothermic and exothermic peaks were determined using STARe software V.11.0x (Mettler Toledo, Greifensee, Switzerland).

Moreover, the temperature stability and solvent evaporation of each sample were determined using thermal gravimetric analysis (TGA; Mettler-Toledo, Schwerzenbach, Switzerland). Approximately 5 mg of samples were placed on aluminum crucible pans. The weight losses of the samples were assessed by heating the samples from 20 °C to 400 °C, with a scanning rate of 5 °C/min, under constant nitrogen gas. Data were analyzed using STARe software V.11.0x (Mettler Toledo, Greifensee, Switzerland) and expressed as the percentage of weight loss comparing to initial sample weight.

### **5.3.9. Dynamic Vapour Sorption (DVS)**

The relative moisture sorption and stability of SAP and MS formulations, with respect to humidity, were analyzed by Dynamic Vapour Sorption (DVS). Aluminum sample pans were loaded with 10 mg ca. of samples and then placed in the sample chamber of a DVS (DVS-1, Surface Measurement Systems Ltd., London, UK). Each sample was dried at 0% relative humidity (RH) before being exposed to 10% RH increments for two 0-90% RH cycles (25°C). Equilibrium of moisture sorption was determined, at each humidity step, by a change in mass to time ratio (dm/dt) of 0.0005% min<sup>-1</sup>.

### **5.3.10. Solubility test**

The solubility of SAP in a release medium (0.01 M PBS, pH = 7.4) was assessed in triplicate by solvent saturation method. An excess amount of SAP was added into tubes containing 2.5 mL of PBS. The tubes were sonicated into a water-bath sonicator at 32 KHz and 32°C, for 1 h, and then stirred on a thermostated orbital shaker at 120 rpm and 32°C, for 24 h. The tubes were then centrifuged at 2000 rpm for 5 minutes. The supernatants were withdrawn, filtered using 0.22 µm polyamide syringe filters, diluted with PBS and analyzed by UV spectroscopy.

### **5.3.11. In vitro drug release studies**

For topical microcarriers, there are no compendial or standard release methods and apparatuses (Balzus et al., 2016; Lusina Kregar et al., 2015). Therefore, in vitro release profiles of SAP from HA and HA-CL MS were evaluated with two different methodologies, under different experimental condition.

#### **5.3.11.1. Dialysis**

SAP release profiles were primarily obtained with dialysis method. A calculated amount of each test formulation containing ~10 mg of SAP was placed into a preconditioned dialysis bag (Slide-A-Lyzer G2, 10kDa MWCO, Thermo Fisher Scientific, Rodano, Milano, Italy), and dialyzed against 300 mL PBS (0.01 M, pH = 7.4), a release medium already described in the literature for drug release studies of dermal carriers (Balzus et al., 2016; Schlupp et al.,

2011; Zoubari et al., 2017). The whole set-up was continuously stirred at 150 rpm and maintained at  $32 \pm 1$  °C to reflect the physiological skin temperature (Balzus et al., 2016). At predefined time intervals, 1 mL of sample was withdrawn and replaced with an equal volume of warm PBS. The released SAP was quantified by UV spectroscopy. A minimum of three replicates was performed for each test formulation.

### 5.3.11.2. Franz cells

SAP release profiles from hyaluronan MS were also investigated by Franz's cells (25 mm internal diameter, PermeGear Inc., Hellertown, PA, USA). Polyamide filter membranes 0.45 µm pore size (Sartorius Biolab Products, Goettingen, Germany) were hydrated by sonication in deionized water for 30 min, and then cut and mounted between the receiver and donor compartments of the diffusion cells. The whole diffusion cells were put in a thermostatic bath, maintained at  $32 \pm 1$  °C. Test formulations were placed in the donor compartments -in order to have ~2 mg of SAP on the surface of the membranes -which were closed using a wax foil (Parafilm M, Bemis Company Inc., Oshkosh, WI, USA) to prevent evaporation. The receiver compartments were filled with 23 mL PBS (0.01 M, pH = 7.4) and kept under continuous magnetic stirring at 150 rpm. At selected time points, 0.5 mL of samples were withdrawn from the receptor compartment and replaced with equal volumes of warm PBS. Samples were assayed for SAP content using UV spectroscopy. A minimum of three replicates was performed for each formulation. The idea was to get preliminary indications which, if positive, will be used to support a request to the ethics committee for a human skin study.

### 5.3.12. Drug release data analysis

All the experimental release data were fitted to a series of statistical and kinetic models to evaluate formulations performances and to elucidate their drug release mechanisms, strictly related to the properties of the polymers. This detailed mathematical modeling study was carried out to develop and characterize our novel HA CL MS, in comparison to HA MS, with a systematic approach.

#### 5.3.12.1. Similarity and difference factors for SAP release profiles

For each release method used, SAP diffusion across the membranes and SAP release profiles from HA MS and HA CL MS were statistically analyzed and compared using Fit Factors described by Moore and Flanner (Moore and Flanner, 1996), adopted by the Food and Drug Administration guidance for dissolution testing in the industry (Food and Drug Administration, 1997). Fit factors are models widely applied by researchers (Cirri et al., 2016; Ong et al., 2011; Pozzoli et al., 2017; Salama et al., 2008) to directly compare the difference between percentage drug released per unit time between a reference and a test formulation. The difference factor ( $f_1$ ) and the similarity factor ( $f_2$ ) were calculated using Eqs. 5.6. and 5.7., respectively:

$$f_1 = \{[\sum_{t=1}^n |R_t - T_t| / \sum_{t=1}^n R_t]\} \cdot 100 \quad (\text{Eq. 5.6.})$$

$$f_2 = 50 \cdot \log\{[1 + (1/n) \sum(R_t - T_t)^2]^{-0.5} \cdot 100\} \quad (\text{Eq. 5.7.})$$

where  $R_t$  and  $T_t$  are percentages of drug released at a certain time point ( $t$ ) from the reference and the test formulation, respectively;  $n$  is the number of dissolution sampling times. The difference factor ( $f_1$ ) calculates the percent difference between the reference and the test curves at each time point thus measuring the relative error between the two curves. The similarity factor ( $f_2$ ) is a logarithmic reciprocal square root transformation of the sum of squared error and is a measurement of the similarity in percentage released between curves. For data analysis, arbitrary descriptors of difference and similarity need to be chosen: curves were considered different with  $f_1 \geq 10$  and  $f_2 \leq 50$ .

### 5.3.12.2. Analysis of SAP release kinetics using mathematical models

SAP release data acquired for HA and HA-CL MS were plotted into four mathematical models corresponding to the known release mechanisms. The linearized form of each function was evaluated using  $R^2$  regression analysis, in order to understand which was the best-fit mathematical model and, therefore, the kinetic process controlling SAP release from hyaluronan MS.

The first model used, called Zero-release kinetic, describes a release mechanism whose rate is independent of the active ingredient concentration, but it is time-dependent (Costa and Sousa Lobo, 2001). It is described by Eq. 5.8.:

$$Q_t/Q_\infty = Kt + Q_0 \quad (\text{Eq. 5.8.})$$

where  $Q_t/Q_\infty$  is the ratio between the cumulative percentage of drug released at time  $t$  and at infinite time,  $k$  is the zero-order release constant,  $t$  is the time, and  $Q_0$  is the initial quantity of drug in solution due to an immediate releasing process (most times  $Q_0 = 0$ ).

On the contrary, the First order model delineates a process where the release rate is concentration dependent (Costa and Sousa Lobo, 2001). It is represented by Eq. 5.9.:

$$\log \frac{Q_t}{Q_\infty} = \log Q_0 - kt/2.303 \quad (\text{Eq. 5.9.})$$

where  $Q_t/Q_\infty$  is the ratio between the cumulative percentage of drug released at time  $t$  and at infinite time,  $k$  is the first-order release constant,  $t$  is the time, and  $Q_0$  is the initial amount of drug in solution.

Also the Higuchi model was applied (Higuchi, 1961). It describes drug release from a matrix system whose swelling is negligible (Arifin et al., 2006; Costa and Sousa Lobo, 2001). Therefore, the release profile is governed by the properties of the polymeric matrix and by drug solubility, and it is described by the following equation (Eq. (10)):

$$Q_t/Q_\infty = k_H \sqrt{t} + Q_0 \quad (\text{Eq. 5.10.})$$

where  $Q_t/Q_\infty$  is the ratio between the cumulative percentage of drug released at time  $t$  and at infinite time,  $k$  is the Higuchi release rate constant,  $t$  is the time, and  $Q_0$  is the initial quantity of drug in solution due to an immediate releasing process (most times  $Q_0 = 0$ ).



Finally, the release data were fitted to Korsmeyer-Peppas model, which describes the drug release from swelling-controlled systems (Arifin et al., 2006; Costa and Sousa Lobo, 2001; Korsmeyer and Peppas, 1981; Peppas, 1985; Singhvi and Singh, 2011). In this polymeric systems, both diffusion and dissolution occur together, and they are quite indistinguishable. Korsmeyer-Peppas proposed the following semi-empirical equation (Eq. 5.11.):

$$Q_t/Q_\infty = kt^n + Q_0 \quad (\text{Eq. 5.11.})$$

where  $Q_t/Q_\infty$  is the ratio between the cumulative percentage of drug released at time  $t$  and at infinite time,  $k$  is a kinetic constant related to the structural and geometric properties of the system,  $t$  is the time,  $n$  is the release exponent (connected to geometric form), and  $Q_0$  is the initial amount of drug in solution. In this model, the  $n$  value characterizes the release mechanism: Fickian diffusion, i.e. drug diffusive process, is prevalent for  $n \approx 0.43$ ; Case-II transport, i.e. polymer dissolution process, for  $n \approx 0.89$ ; super Case-II transport for  $n > 0.89$ ; anomalous behaviour, i.e. a superposition of diffusion and dissolution, for  $0.43 < n < 0.89$ .

### **5.3.13. Statistical analysis**

Data are presented as mean  $\pm$  SD of three independent experiments ( $n = 3$ ). Statistical analysis was performed using GraphPad Prism software version 7.0b (GraphPad, San Diego, CA, USA). The tests used were one-way (characterization of hyaluronan solutions) or two-way (characterization of MS during the pre-formulation study) analysis of variance (ANOVA), followed by Tukey post hoc analysis for multiple comparisons. Differences between results were considered statistically significant at  $P < 0.05$ .

## **5.4. Results and discussion**

### **5.4.1. Preformulation study: evaluation and optimization of microspheres**

The present work describes the production and characterization of MS using two different hyaluronans: HA-CL (test polymer) and native HA (reference polymer already employed to formulate microspheres) (Li et al., 2017; Lim et al., 2000). The aim was to understand if the novel HA-CL could be a promising candidate to obtain MS intended for skin application. It is well known that particles features are affected by the properties of the starting polymer solutions and by factors related to the production method (Abd El-Hameed and Kellaway, 1997; Esposito et al., 2005; Liu et al., 2016). In this document, we correlated MS properties to the pH and the rheological behavior of HA aqueous phases, and to the emulsification time. This systematic approach was used in order to facilitate the development of our novel formulations, considering that this was the first study to investigate the novel HA-CL as microcarrier.

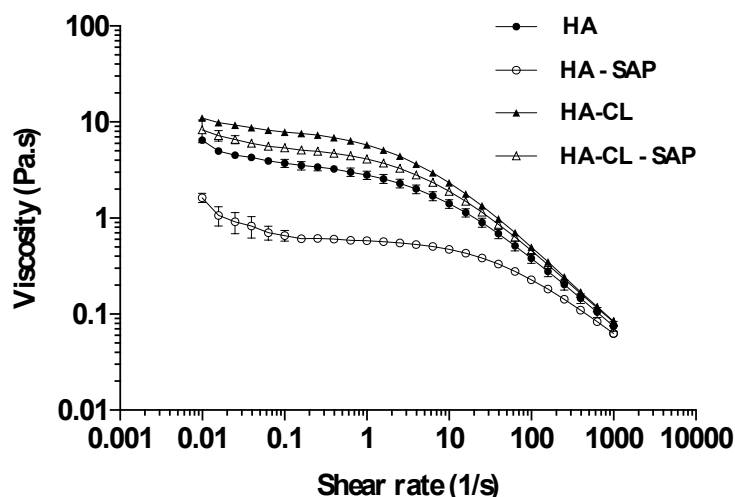


Figure. 5.1. Shear-thinning behaviour of hyaluronan solutions: viscosity as a function of shear rate ( $n = 3, \pm SD$ ).

All the hyaluronan solutions were characterized by a shear-thinning (Figure 5.1.) and viscoelastic behaviour. However, statistical analysis demonstrated that each solution was significantly different ( $P < 0.05$ ) from the others in terms of pH, zero-shear rate viscosity ( $\eta_0$ ), elastic modulus at 1 Hz ( $G'_{1Hz}$ ), and crossover frequency ( $C_f$ ). Indeed, HA type and SAP presence affected the values of pH,  $\eta_0$ ,  $G'_{1Hz}$ , and  $C_f$  (Table 5.1.).

As regarding the impact of polymer type, Table 5.1. shows implemented mechanical properties for HA-CL hydrogel with respect to HA hydrogel (i.e. higher  $\eta_0$  and  $G'_{1Hz}$ , lower  $C_f$ ). Considering, for example, simple polymeric solutions,  $\eta_0$ ,  $G'_{1Hz}$  and  $C_f$  were respectively  $9.1 \pm 0.3$  Pa.s,  $13.2 \pm 0.6$  Pa and  $1.8 \pm 0.0$  Hz for HA-CL, and  $4.2 \pm 0.2$  Pa.s,  $5.5 \pm 0.7$  Pa and  $6.2 \pm 1.8$  Hz for HA. This could be ascribed to the different molecular weight of the two polymers (1.2 MDa for native HA, 3.0 MDa for HA-CL), and to the crosslinking of the urea derivative. Indeed, it is well known that the viscosity and the viscoelasticity of hyaluronan solutions increase with increasing polymer molecular weight (Falcone et al., 2006) and crosslinking (Collins and Birkinshaw, 2008; Shimojo et al., 2015). For the shorter emulsification times investigated (10 and 30 minutes), the rheological behaviour of HA and HA-CL solutions seemed to be reflected in the mean size of the resulting particles. Certainly,  $Dv_{50}$  and  $D[4,3]$  values were significantly higher ( $P < 0.05$ ) for HA-CL MS with respect to HA MS produced after the same mixing time (Table 5.2.). After 10 minutes of emulsification,  $Dv_{50}$  and  $D[4,3]$  were respectively  $290.0 \pm 32.5$   $\mu\text{m}$  and  $311.0 \pm 32.5$   $\mu\text{m}$  for HA-CL MS, and  $117.7 \pm 20.0$   $\mu\text{m}$  and  $246.0 \pm 53.6$   $\mu\text{m}$  for HA MS. Moreover, after 30 minutes of emulsification,  $Dv_{50}$  and  $D[4,3]$  were respectively  $181.5 \pm 3.8$   $\mu\text{m}$  and  $208.7 \pm 6.7$   $\mu\text{m}$  for HA-CL MS, and  $113.7 \pm 19.6$   $\mu\text{m}$  and  $154.7 \pm 27.5$   $\mu\text{m}$  for HA MS. Similar findings have already been reported in literature: bigger particles are generally produced by larger droplets of the precursory w/o emulsion (Esposito et al., 2005), formed by increasing the solution viscosity (Ré et al., 2004).

Concerning the influence of SAP on the properties of HA and HA-CL solutions, it increased the pH, thus causing (as expected (Gatej et al., 2005; Maleki et al., 2008)) a statistically significant ( $P < 0.05$ ) decrease of  $\eta_0$  and  $G'_{1Hz}$ , and increase of  $C_f$  (Table 5.1.). In fact, the pH,  $\eta_0$ ,  $G'_{1Hz}$  and  $C_f$  of HA hydrogel, which were respectively  $6.8 \pm 0.1$ ,

4.2 ± 0.2 Pa.s, 5.5 ± 0.7 Pa and 6.2 ± 1.8 Hz, changed to 8.9 ± 0.1, 0.7 ± 0.0 Pa.s, 0.8 ± 0.0 Pa and 15.9 ± 0.4 Hz in presence of SAP. A similar trend was observed also for HA-CL solutions: without SAP, the pH,  $\eta_0$ ,  $G'_{1Hz}$  and  $C_f$  were respectively 7.2 ± 0.0, 9.1 ± 0.3 Pa.s, 13.2 ± 0.6 Pa and 1.8 ± 0.0 Hz; in presence of SAP, these values changed to 8.1 ± 0.1, 6.3 ± 0.5 Pa.s, 9.2 ± 0.4 Pa and 3.1 ± 0.1 Hz. Also in this case, the rheology of the initial solutions appeared correlated to the dimensional properties of the particles. Indeed, for the same HA type and emulsification time (10 or 30 minutes), SAP-loaded MS were smaller than unloaded MS (Table 5.2.), as highlighted by statistical analysis ( $P < 0.05$ ). For example, after 10 minutes' emulsification, Dv50 and D[4,3] of HA MS respectively decreased from 117.7 ± 20.0 µm and 246.0 ± 53.6 µm to 71.7 ± 4.2 µm and 121.0 ± 13.4 µm in presence of SAP. Similarly, Dv50 and D[4,3] of HA-CL MS respectively decreased from 290.0 ± 32.5 µm and 311.0 ± 32.5 µm to 245.5 ± 27.6 µm and 300.5 ± 24.7 µm in presence of SAP. In the same way, after 30 minutes of emulsification, HA and HA-CL MS mean size decreased when encapsulating SAP, as reported in Table 5.2..

Table 5.1. Main properties of HA solutions: pH,  $\eta_0$ ,  $G'_{1Hz}$ ,  $C_f$  (n = 3, ± SD).

<b>Solution</b>	<b>pH</b>	<b><math>\eta_0</math> (Pa.s)</b>	<b><math>G'_{1Hz}</math> (Pa)</b>	<b><math>C_f</math> (Hz)</b>
<b>HA</b>	6.8 ± 0.1	4.2 ± 0.2	5.5 ± 0.7	6.2 ± 1.8
<b>HA - SAP</b>	8.9 ± 0.1	0.7 ± 0.0	0.8 ± 0.0	15.9 ± 0.4
<b>HA-CL</b>	7.2 ± 0.0	9.1 ± 0.3	13.2 ± 0.6	1.8 ± 0.0
<b>HA-CL - SAP</b>	8.1 ± 0.1	6.3 ± 0.5	9.2 ± 0.4	3.1 ± 0.1

In summary, the effect of HA type and SAP presence on MS diameter appeared statistically significant ( $P < 0.05$ ) in the case of 10 and 30 minutes of emulsification. For MS produced after 60 minutes of mixing, this effect was negligible. Indeed, particles were all comparable in term of size, regardless of polymer type and SAP loading, with Dv50 ranging from 2.5 ± 0.1 to 13.0 ± 0.7 µm, and D[4,3] ranging from 3.1 ± 0.2 to 21.6 ± 4.0 µm (Table 5.2.). Therefore, after 60 minutes, the size effects due to the differences between hyaluronan solutions were levelled because of a more significative emulsification. Consequently, MS mean diameter and size distribution seemed to be affected not only by the rheology of the starting solution, but also by the emulsification time. For each MS formulation, particle diameter was found to be inversely proportional to the emulsification time in the range 10-60 minutes (Table 5.2.). This correlation was statistically significant ( $P < 0.05$ ), and it was in agreement with previously reported results (Liu et al., 2016). Indeed, the higher is the mixing time the smaller are the droplets produced during the emulsification, and, consequently, the final particles. On the contrary, the shorter is the emulsification time, the less fine is the w/o emulsion, and this normally determines the aggregation of aqueous droplets. As already observed (Esposito et al., 2005), also in our study bigger and less uniform-sized MS, with lower yield, were produced by droplets agglomeration -supposed to occur especially for 10 minutes' emulsification- (Table 5.2.). This drawback could be probably due to the bioadhesivity of the polymers which, when less dispersed, adhere more to the homogeniser workhead. However, by increasing the emulsification time from 10 to 60 minutes, MS mean size significantly decreased, while particle recovery (Y%) and encapsulation efficiency

(EE%) significantly increased ( $P < 0.05$ ) (Table 5.2.). For example, SAP-loaded HA MS could be considered: after 10 minutes of emulsification, Dv50, D[4,3], Span, Y% and EE% values were respectively  $71.7 \pm 4.2 \mu\text{m}$ ,  $121.0 \pm 13.4 \mu\text{m}$ ,  $4.3 \pm 0.1$ ,  $75.2 \pm 4.4 \%$  and  $59.0 \pm 4.0 \%$ . After 60 minutes of emulsification, these values became respectively  $2.5 \pm 0.1 \mu\text{m}$ ,  $3.1 \pm 0.2 \mu\text{m}$ ,  $2.2 \pm 0.0$ ,  $84.2 \pm 2.3 \%$  and  $69.7 \pm 4.6 \%$ . Considering the parallel increment of particles Y% and EE%, the drug loading (DL%) remained almost constant whatever the emulsification time (around 40% for SAP-loaded HA MS and 33% for SAP-loaded HA-CL MS) (Table 5.2.).

Table 5.2. Effect of emulsification time, polymer type and SAP presence on MS properties (n = 3,  $\pm$  SD).

<b>MS formulation</b>	<b>Dv50 (<math>\mu\text{m}</math>)</b>	<b>D[4,3] (<math>\mu\text{m}</math>)</b>	<b>Span</b>	<b>Y(%)</b>	<b>DL(%)</b>	<b>EE(%)</b>
<i>10 minutes</i>						
HA	$117.7 \pm 20.0$	$246.0 \pm 53.6$	$4.2 \pm 0.4$	$68.6 \pm 1.6$	-	-
HA - SAP	$71.7 \pm 4.2$	$121.0 \pm 13.4$	$4.3 \pm 0.1$	$75.2 \pm 4.4$	$39.2 \pm 0.4$	$59.0 \pm 4.0$
HA-CL	$290.0 \pm 32.5$	$311.0 \pm 32.5$	$1.5 \pm 0.2$	$56.7 \pm 5.4$	-	-
HA-CL - SAP	$245.5 \pm 27.6$	$300.5 \pm 24.7$	$2.4 \pm 0.5$	$70.6 \pm 1.1$	$32.5 \pm 1.4$	$65.3 \pm 3.5$
<i>30 minutes</i>						
HA	$113.7 \pm 19.6$	$154.7 \pm 27.5$	$2.9 \pm 0.1$	$79.4 \pm 2.9$	-	-
HA - SAP	$54.6 \pm 3.0$	$63.2 \pm 2.6$	$2.0 \pm 0.1$	$81.5 \pm 1.4$	$39.3 \pm 1.0$	$64.1 \pm 2.9$
HA-CL	$181.5 \pm 3.8$	$208.7 \pm 6.7$	$2.5 \pm 0.1$	$76.7 \pm 1.3$	-	-
HA-CL - SAP	$117.0 \pm 4.2$	$135.0 \pm 3.5$	$2.3 \pm 0.0$	$78.2 \pm 3.3$	$32.1 \pm 1.0$	$68.9 \pm 1.0$
<i>60 minutes</i>						
HA	$2.5 \pm 0.1$	$6.3 \pm 0.5$	$2.9 \pm 0.2$	$88.4 \pm 1.7$	-	-
HA - SAP	$2.5 \pm 0.1$	$3.1 \pm 0.2$	$2.2 \pm 0.0$	$84.2 \pm 2.3$	$41.3 \pm 1.6$	$69.7 \pm 4.6$
HA-CL	$13.0 \pm 0.7$	$21.6 \pm 4.0$	$2.5 \pm 0.3$	$85.8 \pm 4.4$	-	-
HA-CL - SAP	$9.9 \pm 0.8$	$15.2 \pm 4.0$	$2.6 \pm 0.2$	$85.0 \pm 4.8$	$33.6 \pm 2.3$	$78.8 \pm 2.6$

Taking into account the results of this pre-formulation study, the emulsification time of 60 minutes was chosen as the standard condition to produce optimized MS. Indeed, all the MS formulations produced after 60 minutes of emulsification were characterized by the highest Y%, ranging from  $84.2 \pm 2.3$  to  $88.4 \pm 1.7\%$  (comparable values). The EE% and DL% were satisfying, even if statistically different ( $P < 0.05$ ) for HA and HA-CL formulations: respectively  $69.7 \pm 4.6 \%$  and  $41.3 \pm 1.6\%$  for HA – SAP MS, and  $78.8 \pm 2.6\%$  and  $33.6 \pm 2.3\%$  for HA-CL – SAP MS (Table 2). Particle Dv50 ranging from  $2.5 \pm 0.1$  to  $13.0 \pm 0.7 \mu\text{m}$ , and D[4,3] ranging from  $3.1 \pm 0.2$  to  $21.6 \pm 4.0 \mu\text{m}$  (Table 5.2.) were suitable for dermal target (Bari et al., 2017; Ranjan et al., 2016). Indeed, to avoid palpable microspheres during application, mean size should be lower than  $50 \mu\text{m}$  ([No authors listed], 2009): this is essential both in the cosmetic and pharmaceutical field, as it determines the cosmetic elegance

of a product ([No authors listed], 2009) and the adherence to a therapy (Vertuani et al., 2013). A statistical comparison revealed no significant difference between the mean size of optimized MS ( $P > 0.05$ ). Moreover, all the optimized formulations showed almost unimodal size distributions (Figure 5.2.), with Span values lower than 3 (Table 5.2.).

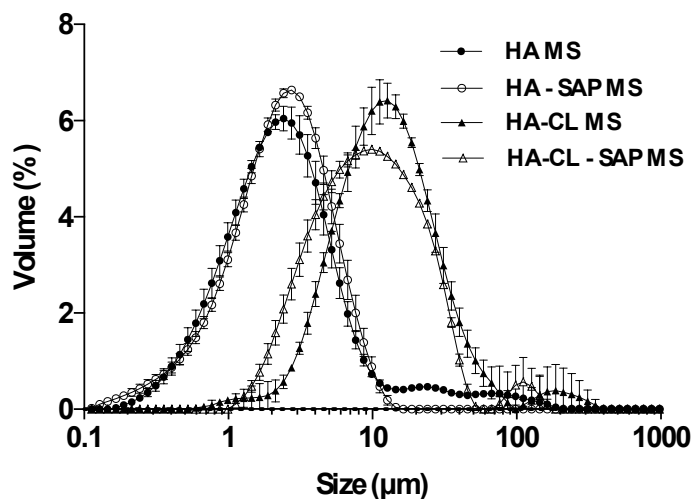


Figure 5.2. Particle size distribution of hyaluronan MS produced after 60 minutes of emulsification ( $n = 3, \pm SD$ ).

Optimized MS underwent a deeper physical-chemical characterization: analysis of morphology, physical and molecular state, thermal properties, relative moisture sorption and stability, stability, in vitro release properties and kinetic mechanisms.

#### 5.4.2. Characterization of optimized microspheres

##### 5.4.2.1. SEM morphological analysis

As regarding particle morphology, all hyaluronan MS encapsulating or not SAP showed a spherical shape. However, polymer typology (HA or HA-CL) influenced MS surface properties. Indeed, SAP-loaded and unloaded HA MS exhibited a regular and smooth surface, while SAP-loaded and unloaded HA-CL MS were characterized by an irregular and rough surface (Figure 5.3).

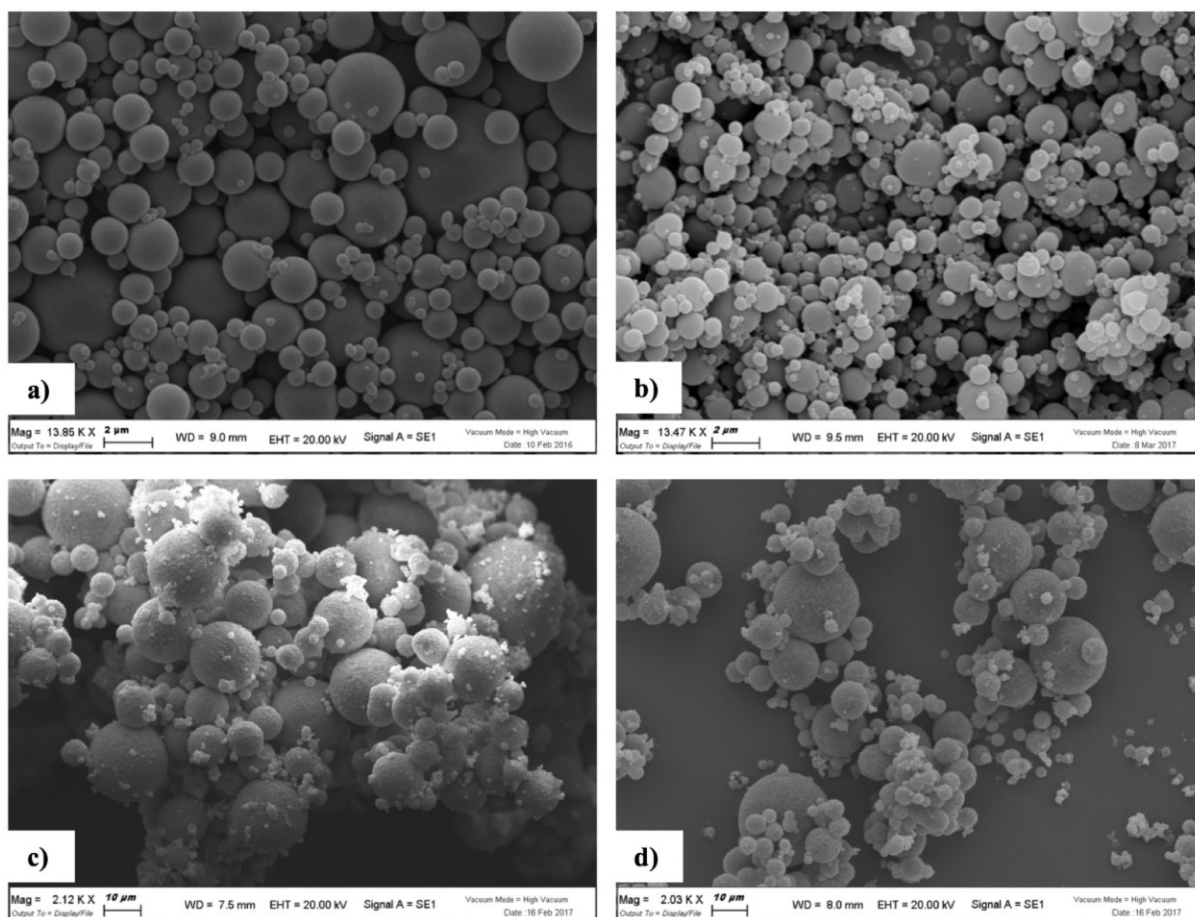


Figure 5.3. SEM micrographs of hyaluronan MS produced after 60 minutes of emulsification: HA (a), HA - SAP (b), HA-CL (c), HA-CL – SAP (d).

#### 5.4.2.2. X-ray diffraction

Wide angle X-ray diffractometry was performed to investigate the molecular states of MS formulations in comparison to SAP (Klug and Alexander, 1974) The diffraction patterns are reported in Figure 5.4. The WAXD pattern of unloaded HA and HA-CL MS exhibited humps typical of disordered structures, i.e. amorphous materials. SAP pattern was characterized by four low intense and broad peaks emerging from a hump at  $2\theta = 7.30, 20.00, 27.32,$  and  $33.12^\circ$ , which can be ascribed to small traits of crystallinity. Indeed, the diffraction intensity is defined by the crystal structure: the higher is the crystallinity degree, the higher is the intensity of the peaks (Klug and Alexander, 1974). The diffraction patterns of SAP-loaded MS showed both the main signals of the drug and of the carrier, indicating the permanence of SAP crystalline traits into the amorphous matrixes of HA and HA-CL. However, thermal analyses and DVS study provided evidence and confirmation that the crystallinity of SAP loaded MS was so low to be negligible.

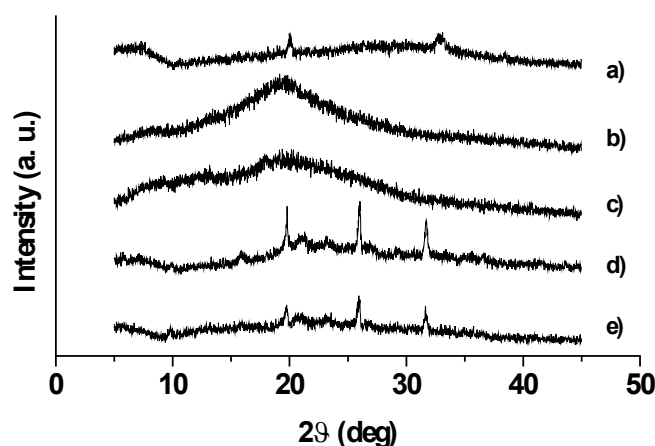


Figure 5.4. X-ray diffraction patterns of: SAP (a), HA MS (b), HA-CL MS (c), HA – SAP MS (d), HA-CL – SAP MS (e).

#### 5.4.2.3. Thermal analysis (DSC and TGA)

DSC and TGA were used to characterize the thermal behaviour and stability of the drug and the formulations, providing information on their hydration properties and their physical state (Siepmann and Peppas, 2001; Yang and Zhu, 2002). Figure 5.5. shows the DSC thermal profiles of SAP and MS formulations. SAP thermogram (a) was characterized by broad endothermic peaks around 67°C and 100°C, which could be associated with the loss of moisture after the initial drying procedure, and by a sharp exothermic peak at 233°C, due to the melting point with thermal decomposition (as reported in the literature for similar ascorbic acid derivatives (Moyano et al., 2010)). DSC thermal profile of HA MS (b) presented a wide endothermic peak, suggesting a dehydration process around 103°C, and a broad exothermic peak at 240°C ascribable to the polymer thermal decomposition and the formation of a carbonized residue. These results were in good agreement with previous observations for native HA (Collins and Birkinshaw, 2007, 2008; Kafedjiiski et al., 2007). DSC trace of HA-CL MS (c) exhibited a broad endothermic peak at 200°C, which could be attributed to pentylene glycol evaporation (boiling range 198-200°C). This was confirmed by pentylene glycol DSC thermal profile (trace not showed). Moreover, HA-CL MS curve showed a wide exothermic peak, due to polymer thermal degradation, at 250°C (shifted with respect to HA MS, indicating an altered structure due to crosslinking (Collins and Birkinshaw, 2007)). The thermograms of HA - SAP MS (d) and HA-CL - SAP MS (e) showed the same profile of the corresponding unloaded MS (DSC traces b and d, respectively), but the peaks shifted to lower temperatures (about 10-15°C of shift). This evidence, in addition to the reduced intensity of the exothermic peak, suggested an altered microstructure of the polymer matrix due to SAP presence (probable molecular dispersion of SAP inside the microspheres (Kulkarni et al., 2016)), and the superposition of SAP and hyaluronan thermal degradation phenomena.

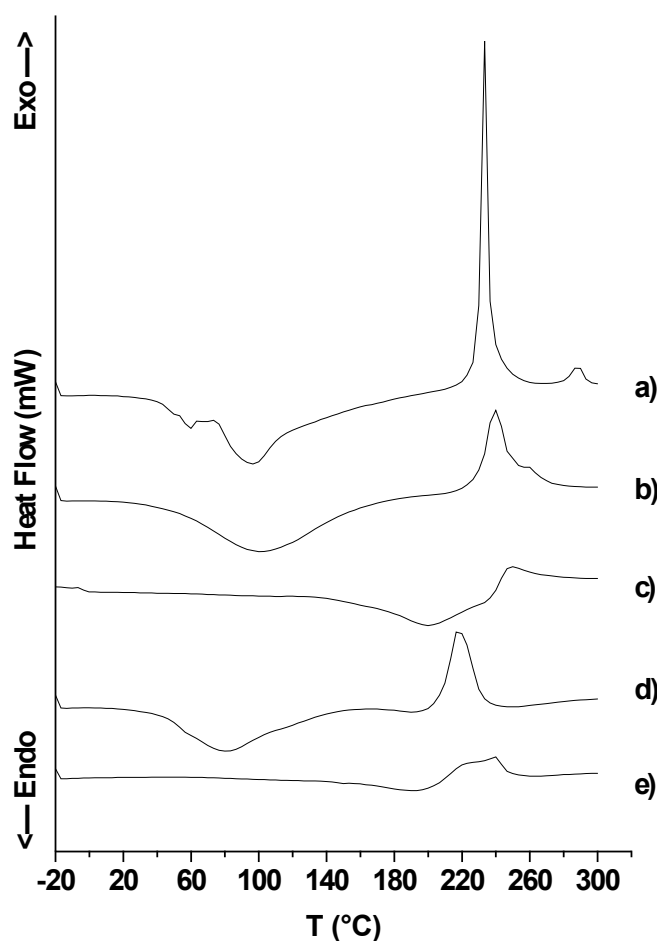


Figure 5.5. DSC thermal profiles of: SAP (a), HA MS (b), HA-CL MS (c), HA – SAP MS (d), HA-CL – SAP MS (e).

TGA thermal profiles of SAP and MS formulations are reported in Figure 5.6. SAP thermogram (a) showed the first region of weight loss (9.6% w/w) between ambient temperature and 223°C (moisture loss), and a second region (20.5% w/w) from 223 to 400°C (melting with decomposition and release of volatile degradation products). TGA curve of HA MS (b) consisted of three distinct degradation stages: the first one (20-223°C, showing 6.2% w/w of weight loss, due to water evaporation); the second (223-269°C) and the third stages (269-400°C), typical of a two-stages polysaccharide degradation. In the second stage, the 37.3% w/w of weight was lost due to a partial breakage of the molecular structure. Residues of hyaluronan were then degraded in the third stage, characterized by the 12.0% w/w of weight loss. Similar findings have already been described in the literature for native HA (Lapcik et al., 2014; Lewandowska et al., 2016; Réeff et al., 2013). A comparable TGA profile characterized HA - SAP MS (d), with 10.8% w/w of weight loss in the first region (20-208°C), 26.2% w/w in the second (208-258°C), and 12.0 % w/w in the third (258-400°C). For HA - SAP MS the decomposition of polymer and drug seemed to occur at once. TGA thermograms of HA-CL MS (c) and HA-CL - SAP MS (e) presented the two-stages polysaccharide degradation observed also for HA MS formulations (b and d), with an additive stage for pentylene glycol evaporation and more stages for water loss. The more gradual moisture evaporation was due to the water-binding action of pentylene glycol, humectant contained in HA-CL matrix. In detail, TGA trace of HA-CL MS (c) exhibited the following



weight loss regions: three stages for water and then pentylene glycol evaporation (20-97°C, 97-158°C, 158-223°C -total weight loss: 26.2% w/w), and two stages for HA degradation (223-265°C, 223-400°C -total weight loss: 29.5% w/w). TGA thermal profile of HA-CL -SAP MS (e) was characterized by two regions for moisture and then pentylene glycol loss (20-154°C, 154-212°C, a total weight loss of 21.5% w/w), and two regions for HA-CL and SAP decomposition (212-254°C, 254-400°C, a total weight loss of 30.3% w/w).

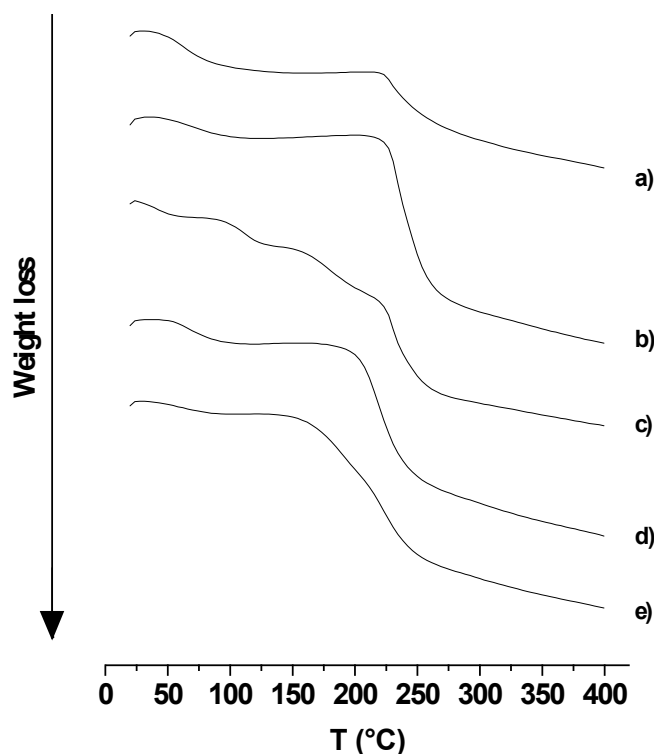


Figure 5.6. TGA thermograms of: SAP (a), HA MS (b), HA-CL MS (c), HA – SAP MS (d), HA-CL – SAP MS (e).

#### 5.4.2.4. Dynamic Vapour Sorption (DVS)

It is well known that HA is a highly hygroscopic macromolecule, therefore by nature susceptible to moisture sorption and elevated relative humidity (RH) (Albèr et al., 2015; Casale et al., 2015). To further characterize hyaluronan MS, and evaluate the effect of SAP encapsulation, the drug, and the formulations were subjected to two 0-90% RH cycles using a DVS. The isotherms of water sorption and desorption for the first humidity ramp (cycle 1) are shown in Figure 5.7. as a function of the RH %. Following the sorption data of SAP -panel a)-, there was a linear increase of water content starting from the dry powder up to an RH of 40%, where the moisture uptake was 6.6%. A steeper increase of water sorption (+ 9.6%) was observed in the RH range 40-50%. The final total humidity absorbed by SAP was 27.8%. The SAP desorption curve had a very different profile from the SAP sorption curve. A pronounced hysteresis was observed, and at the end of the desorption process, the final retained moisture was 15.4%. On the one hand, this suggested that SAP was not reversible in terms of humidity sorption/desorption, and that water molecules were not easily detached from it, perhaps because of their condensation among the hydrophobic skeleton of the drug. On the other hand,

MS formulations (panels b) and c)) showed, as previously observed for native HA (Panagopoulou et al., 2013; Servaty et al., 2001) similar trends for their sorption and desorption ramps, and high water-binding capacity due to H-bonds and electrostatic interaction with hyaluronan hydroxyl and carboxylic groups, respectively. Two-stages moisture sorption processes occurred for hyaluronan MS formulations, and this was in agreement with data already reported in the literature for native HA (Panagopoulou et al., 2013; Servaty et al., 2001). Indeed, in response to RH increment from 0 to 60%, water uptake slowly increased up to 20.9% for HA MS, 14.2% for HA – SAP MS, 16.4% for HA-CL MS, 23.0% for HA-CL – SAP MS (changes in mass similar to that of SAP (+ 17.8%) at 60% RH). However, the final water retention at the end of the sorption process was higher for MS formulations with respect to SAP, as moisture uptake was markedly enhanced for all the formulations in the RH range 60-90%. At 90% RH, the water content was 48.5% for HA MS, 41.9% for HA – SAP MS, 73.8% for HA-CL MS, 78.4% for HA-CL – SAP MS. The higher moisture sorptions observed for HA-CL formulations compared to HA formulations were most likely due to the water-binding ability of urea and pentylene glycol. All the MS formulations displayed hysteresis phenomena: for the same RH value, during the desorption process, samples were characterized by a higher moisture level than during the sorption procedure. However, the hysteresis was reduced with respect to SAP, as well as the final moisture level at the end of the desorption process (0% RH), which was 0.8% for HA MS, 4.9% for HA – SAP MS, 7.8% for HA-CL MS, 8.7% for HA-CL – SAP MS. Therefore, the encapsulation of SAP into hyaluronan MS produced formulations more reversible in terms of moisture sorption/desorption compared to the pure drug, even if more susceptible to high RH %.

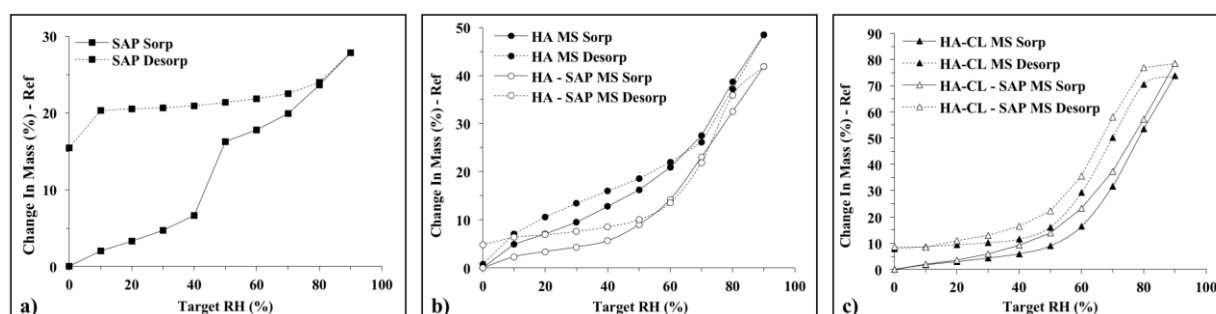


Figure 5.7. DVS isotherms of the first cycle sorption-desorption for: SAP (a), HA MS and HA - SAP MS (b), HA-CL MS and HA-CL – SAP MS (c).

#### 5.4.2.5. SAP solubility

The solubility of SAP in PBS (0.01 M, pH = 7.4) at 32°C was  $425.0 \pm 0.9$  mg/mL. This result displayed that sink conditions were guaranteed during the in vitro drug release studies, as SAP concentration, in the case of complete release, could reach values of 0.033 mg/mL in the dialysis tests, and 0.087 mg/mL in the Franz diffusion cell tests.

#### 5.4.2.6. In vitro drug release studies and kinetic analysis

One of the most important steps in the study of the efficacy of new delivery systems is

the *in vitro* drug release analysis. Topical carriers are an advanced form of powders for which, so far, there are no compendial or standard release techniques and apparatuses (Balzus et al., 2016; Lusina Kregar et al., 2015). Therefore, several *in vitro* drug release methods have been used: for example, dialysis (Balzus et al., 2016; Esposito et al., 2005; Montenegro et al., 2014; Saadat et al., 2015), Franz cells (Abd El-Hameed and Kellaway, 1997; Alves et al., 2016; Balzus et al., 2016; Salama et al., 2008), paddle or basket apparatuses (Dürriegl et al., 2011; Lim et al., 2000), flow through cells (Esposito et al., 2005; Salama et al., 2008). Variations in the release profiles between different methodologies could be observed (Balzus et al., 2016; Esposito et al., 2005; Salama et al., 2008), as the methods are different in their working principles. Therefore, during this study, SAP release from HA and HA-CL MS was evaluated with two different *in vitro* methods: dialysis and Franz diffusion cells. As the control, diffusion tests of free SAP across dialysis and polyamide filter membranes were performed.

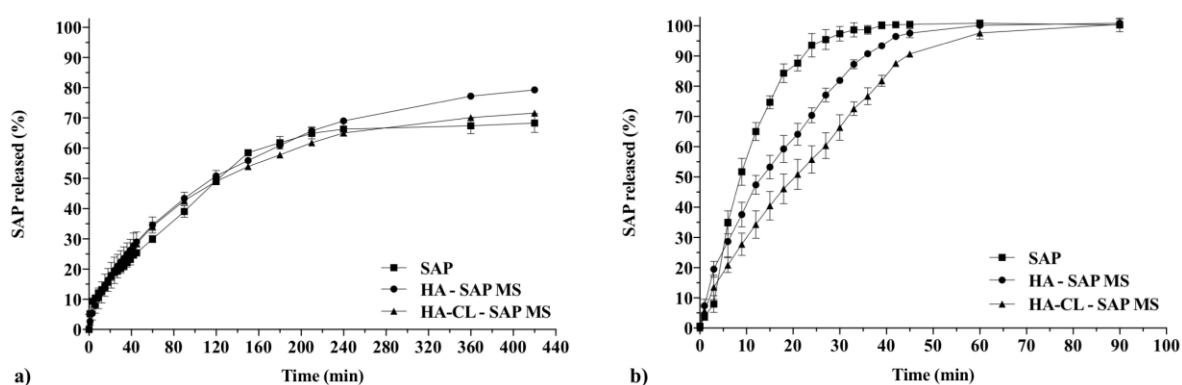


Figure 5.8. Diffusion profile of SAP as free drug and release profile of SAP from HA and HA-CL MS investigated by dialysis (a) and Franz diffusion cells (b).

Dialysis is a widely used release technique: microspheres are retained into a membrane, while the drug released diffuses firstly from the carrier to the media inside the membrane, and then to an external compartment. Inevitably, the membrane opposes a resistance to the diffusion of drug molecules. This resistance can be limited by using a membrane with a MWCO smaller than the microcarrier size, but importantly bigger than drug molecular weight (Moreno-Bautista and Tam, 2011). Considering hyaluronan MS size and SAP molecular weight (358.08 g/mol), 10kDa MWCO dialysis cassettes were employed in this study. Nevertheless, significant errors were introduced by this release method, as the experimental data did not seem to fully reflect the real release profile of SAP from hyaluronan MS. As previously reported in the literature (Moreno-Bautista and Tam, 2011; Zambito et al., 2012), the measured release kinetic seemed to be decreased with respect to the reality: the diffusion rate of free SAP, a highly hydrophilic drug, appeared extremely slow –after 420 minutes, only the  $68.3 \pm 3.1$  % of the drug diffused (Figure 5.8.a.). Moreover, SAP release profiles from MS appeared controlled by the membranes rather than by the microspheres, as they were almost identical to the diffusion profile of free SAP (Figure 5.8.a.). Indeed, a statistical comparison of dialysis data with Moore and Flanner Fit Factors confirmed that all the curves were similar, showing  $f_1 < 10$  and  $f_2 > 50$  (Table 5.3). Therefore, in this work, the precise release process and kinetic behavior could not be studied using dialysis release method. Similar drawbacks using dialysis technique have already been described in the literature for procaine

hydrochloride release from a polymeric carrier: the actual rate of drug release from the delivery system was faster than the rate of diffusion out of the membrane (Moreno-Bautista and Tam, 2011). These results confirm that dialysis could be an unreliable methodology to study drug release from microcarriers, especially when characterized by a rapid release kinetics (Moreno-Bautista and Tam, 2011; Zambito et al., 2012). Taken together, all these considerations and experimental pieces of evidence can be helpful to optimize, in future, the design of drug release studies for microsystems.

Table 5.3. Similarity factors ( $f_2$ ) and difference factors ( $f_1$ ) for free SAP and MS formulations.

Release method	Reference formulation	Test formulation	$f_1$	$f_2$
<i>Dialysis</i>	SAP	HA – SAP MS	7.9	71.4
	SAP	HA-CL – SAP MS	7.0	74.9
	HA – SAP MS	HA-CL – SAP MS	3.3	82.5
<i>Franz diffusion cell</i>	SAP	HA – SAP MS	15.4	42.7
	SAP	HA-CL – SAP MS	27.4	30.8
	HA – SAP MS	HA-CL – SAP MS	15.1	47.9

Franz diffusion cell tests are probably the most suitable and performed studies to investigate plain drug diffusion and drug release from microparticles intended for dermal and/or mucosal application. Indeed, this model reproduces the conditions encountered on skin and mucosae surface, consenting a slow hydration of the carrier in a humid environment. *In vitro* release profiles obtained with Franz diffusion cells method were different from those observed with dialysis technique, as displayed by Figure 5.8.. Free SAP diffusion was faster than SAP release from HA MS and HA-CL MS (Figure 5.8.b.). More precisely, SAP release from HA-CL MS was significantly extended not only compared to plain SAP but also with respect to HA MS, as proved by Moore and Flanner similarity and difference factors ( $f_1 > 10$  and  $f_2 < 50$ ) (Table 5.3.). For example, after 30 minutes, the amount of drug released was  $97.4 \pm 2.4$  % for plain SAP, versus  $81.9 \pm 0.4$  % and  $66.4 \pm 4.2$  % for HA MS and HA-CL MS, respectively (Fig. 5.8.b.). A slower drug release was expected with HA-CL MS, considering the higher molecular weight and the implemented mechanical properties of the crosslinked polymer compared to native HA (Citernes et al., 2015, WO/2015/007773 A1; Fallacara et al., 2017a; Garti, 2008). The influence of the polymer properties on the release profile was evident, and therefore Franz diffusion cell was found to be a discriminative method to study SAP release kinetic processes.

Among the mathematical templates used to analyse SAP release kinetic from hyaluronan MS, Korsmeyer-Peppas model resulted in the highest  $R^2$  values when compared to Zero order, First order and Higuchi models, for both the formulations (Table 5.4.). The values of the diffusional exponent  $n$  characterizing the release mechanism were 0.709 for HA – SAP MS and 0.712 for HA-CL – SAP MS, suggesting anomalous transport processes (Arifin et al., 2006; Singhvi and Singh, 2011). SAP release from hyaluronan MS was therefore governed not only by drug diffusion but also by polymer swelling and dissolution. Hyaluronan MS containing SAP behaved as swellable devices composed by hydrophilic polymeric matrixes

where a water-soluble drug was dispersed: water penetrated into the polymeric networks, causing their disentanglement and swelling. These phenomena decreased hyaluronan concentration, therefore enhancing its dissolution at the interface and SAP wettability and diffusion (Arifin et al., 2006; Singhvi and Singh, 2011). Thus, SAP release was completed in a time frame of about an hour for both the formulations (Figure 5.8.).

Table 5.4. Correlation coefficient for Zero order, First order, Higuchi and Korsmeyer-Peppas models for SAP dissolution profiles obtained with Franz diffusion cell method.

Formulation	Correlation coefficient R <sup>2</sup>			
	Zero order	First order	Higuchi	Korsmeyer-Peppas
HA - SAP MS	0.729	0.941	0.929	0.993
HA-CL - SAP MS	0.837	0.922	0.960	0.999

## 5.5. Conclusion

The present study showed, for the first time and with a systematic approach, that HA-CL could be a promising biopolymer to prepare drug-loaded microspheres with a water-in-oil (w/o) emulsification solvent evaporation technique. Appropriate working conditions led to the production of HA-CL MS and HA-CL – SAP MS characterized by almost unimodal size distributions (Span values lower than 3); mean diameter of  $13.0 \pm 0.7$  and  $9.9 \pm 0.8$   $\mu\text{m}$ , respectively (suitable for dermal application); spherical shape and rough surface; high yield - similar to that of HA MS and HA – SAP MS ( $\approx 85\%$ ). SAP could be more efficiently encapsulated into HA-CL MS ( $78.8 \pm 2.6\%$ ) compared to HA – SAP MS ( $69.7 \pm 4.6\%$ ). Physical and molecular state, thermal properties, relative moisture stability of HA-CL MS and HA-CL – SAP MS were comparable to those of HA MS and HA – SAP MS. However, a preliminary Franz diffusion cells test displayed a more extended drug release for HA-CL – SAP MS with respect to HA – SAP MS, despite the same kinetic mechanism (contemporaneous drug diffusion and polymer swelling and dissolution). This underlined that the implemented mechanical properties of the novel HA-CL could result in more efficient microsystems, which could be potentially improved, in future, by the addition of excipients able to further slow down drug release. In vitro studies on skin cells are currently performed to explore SAP release/transport across the cells and the bioactivity of HA-CL MS and HA-CL – SAP MS, in order to understand if they effectively improve hydration and re-epithelialization compared to HA MS and HA – SAP MS.

## 5.6. Patent resulting from the work reported in this manuscript

Fallacara, A.; Vertuani, S.; Manfredini, S.; Citernes, U.R. 2018c. Patent Appl. Filed, n. 102018000008192.

## 5.7. Authors contributions

A.F. and S.M. –corresponding author- conceived the study. A.F. designed and performed the experiments, acquired, analyzed and interpreted the data, wrote the manuscript. F.M. and M.P. contributed to carrying out the experiments, and S.M. participated in the interpretation

of the results. S.V. and U.R.C. contributed to revise the manuscript. All authors have given approval to the final version of the manuscript.

### **5.8. Funding**

This work was supported by a PhD grant (to Arianna Fallacara) from I.R.A. s.r.l. (Istituto Ricerche Applicate Srl, Usmate-Velate, Monza-Brianza, Italy). The authors thank the University of Ferrara and Ambrosialab s.r.l. (Ferrara, Italy, Grant 2016) for the financial support to the running costs of the study.

### **5.9. Acknowledgements**

Authors gratefully acknowledge the Woolcock Institute of Medical Research and Discipline of Pharmacology, Respiratory Technology -Faculty of Medicine and Health, The University of Sydney (431, Glebe, NSW 2037, Australia)- for the use of facilities and instrumentation. The technical assistance of Gabriele Bertocchi (University of Ferrara) for X-ray analysis is gratefully acknowledged, as well as the English revision of Luigi Mastroianni (State Language High School “Giosuè Carducci” Ferrara, Italy).

### **5.10. Conflicts of interests**

The authors declare no conflict of interest. U.R.C. own stocks in I.R.A. srl. The funder had no role in the design of the study; in the collection, analyses, or interpretation of data; in the writing of the manuscript, and in the decision to publish the results.

## 5.11. References

- [No authors listed], 2009. Benzoyl peroxide microsphere formulations: what is the science supporting microsphere vehicle technology and clinical use? *J. Clin. Aesthet. Dermatol.* 2, 46-54.
- Abd El-Hameed, M.D., Kellaway, I.W., 1997. Preparation and in vitro characterisation of mucoadhesive polymeric microspheres as intra-nasal delivery systems. *Eur. J. Pharm. Biopharm.* 44, 53-60.
- Albèr, C., Brandner, B.D., Björklund, S., Billsten, P., Corkery, R.W., Engblom, J., 2013. Effects of water gradients and use of urea on skin ultrastructure evaluated by confocal Raman microspectroscopy. *Biochim. Biophys. Acta* 1828, 2470-2478.
- Albèr, C., Engblom, J., Falkman, P., Kocherbitov, V., 2015. Hydration of hyaluronan: effects on structural and thermodynamic properties. *J. Phys. Chem. B.* 119, 4211-4219.
- Alves, A.C., Ramos, I.I., Nunes, C., Magalhães, L.M., Sklenářová, H., Segundo, M.A., Lima, J.L.F.C., Reis, S., 2016. On-line automated evaluation of lipid nanoparticles transdermal permeation using Franz diffusion cell and low-pressure chromatography. *Talanta* 146.
- Amirlak, B., Mahedia, M., Shah, N., 2016. A clinical evaluation of efficacy and safety of hyaluronan sponge with vitamin C versus placebo for scar reduction. *Plast. Reconstr. Surg. Glob. Open* 4, e792.
- Arifin, D.Y., Lee, L.Y., Wang, C.H., 2006. Mathematical modelling and simulation of drug release from microspheres: implication to drug delivery systems. *Adv. Drug Deliv. Rev.* 58, 1274-1325.
- Balzus, B., Colombo, M., Sahle, F.F., Zoubari, G., Staufenbiel, S., Bodmeier, R., 2016. Comparison of different in vitro release methods used to investigate nanocarriers intended for dermal application. *Int. J. Pharm.* 513, 247-254.
- Bari, E., Arciola, C.R., Vigani, B., Crivelli, B., Moro, P., Marrubini, G., Sorrenti, M., Catenacci, L., Bruni, G., Chlapanidas, T., Lucarelli, E., Perteghella, S., Torre, M.L., 2017. In vitro effectiveness of microspheres based on silk sericin and *Chlorella vulgaris* or *Arthrospira platensis* for wound healing applications. *Materials (Basel)*. 10, 1-17.
- Benedetti, L.M., Topp, E.M., Stella, V.J., 1990. Microspheres of hyaluronic acid esters - fabrication methods and in vitro hydrocortisone release. *J. Control. Release* 13, 33-41.
- Casale, M., Moffa, A., Sabatino, L., Pace, A., Oliveto, G., Vitali, M., Baptista, P., Salvinelli, F., 2015. Hyaluronic acid: perspectives in upper aero-digestive tract. A systematic review. *PLoS One* 10.
- Charlton, J.F., Schwab, I.R., Stuchell, R., 1996. Topical urea as a treatment for non-infectious keratopathy. *Acta Ophthalmol. Scand.* 74, 391-394.

Cirri, M., Roghi, A., Valleri, M., Mura, P., 2016. Development and characterization of fast-dissolving tablet formulations of glyburide based on solid self-microemulsifying systems. *Eur. J. Pharm. Biopharm.* 104, 19–29.

Citernesì, U.R., Beretta, L., Citernesì, L., 2015. Cross-linked hyaluronic acid, process for the preparation thereof and use thereof in the aesthetic field. Patent number: WO/2015/007773 A1.

Collins, M.N., Birkinshaw, C., 2007. Comparison of the effectiveness of four different crosslinking agents with hyaluronic acid hydrogel films for tissue-culture applications. *J. Appl. Polym. Sci.* 104, 3183-3191.

Collins, N.M., Birkinshaw, C., 2008. Physical properties of crosslinked hyaluronic acid hydrogels. *J. Mater. Sci.: Mater. Med.* 19, 3335-3343.

Costa, P., Sousa Lobo, J.M., 2001. Modeling and comparison of dissolution profiles. *Eur. J. Pharm. Sciences* 13, 123–133.

Couarraze, G.; Grossiord, J.L. *Initiation à la rhéologie*. TEC & DOC; 2000; ISBN: 2-7430-0285-9.

Degim, Z., 2008. Use of microparticulate systems to accelerate skin wound healing. *J. Drug Target.* 16, 437-448.

Dürriegl, M., Kwokal, A., Hafner, A., Šegvi Klari, M., Dumicic, A., Cetina-Cižmek, B., Filipovic-Grcic, J., 2011. Spray dried microparticles for controlled delivery of mupirocin calcium: process-tailored modulation of drug release. *J. Microencapsul.* 28, 108–121.

El Kechai, N., Geiger, S., Fallacara, A., Cañero Infante, I., Nicolas, V., Ferrary, E., Huang, N., Bochet, A., Agnely, F., 2017. Mixtures of hyaluronic acid and liposomes for drug delivery: Phase behavior, microstructure and mobility of liposomes. *Int. J. Pharm.* 523, 246-259.

Esposito, E., Menegatti, E., Cortesi, R., 2005. Hyaluronan-based microspheres as tools for drug delivery: a comparative study. *Int. J. Pharm.* 288, 35-49.

Falcone, S.J., Palmeri, D.M., Berg, R.A., 2006. Rheological and cohesive properties of hyaluronic acid. *J. Biomed. Mater. Res. A.* 76, 721-728.

Fallacara, A., Baldini, E., Manfredini, S., Vertuani, S., 2018a. Hyaluronic Acid in the Third Millennium. *Polymers*, 10, 701.

Fallacara, A., Busato, L., Pozzoli, M., Ghadiri, M., Ong, H.X., Young, P.M., Manfredini, S., Traini, D., 2018b. Combination of urea-crosslinked hyaluronic acid and sodium ascorbyl phosphate for the treatment of inflammatory lung diseases: An in vitro study. *Eur. J. Pharm. Sci.* 120, 96-106.



- Fallacara, A., Manfredini, S., Durini, E., Vertuani, S., 2017a. Hyaluronic acid fillers in soft tissue regeneration. *Facial Plast. Surg.* 33, 87-96.
- Fallacara, A., Vertuani, S., Panozzo, G., Pecorelli, A., Valacchi, G., Manfredini, S., 2017b. Novel Artificial Tears Containing Cross-Linked Hyaluronic Acid: An In Vitro Re-Epithelialization Study. *Molecules.* 22.
- Fallacara, A.; Vertuani, S.; Manfredini, S.; Citernes, U.R. 2018c. Patent Appl. Filed, n. 102018000008192.
- Food and Drug Administration, 1997. Guidance for Industry; Dissolution Testing on Immediate Release Solid Oral Dosage Forms.
- Garti, N. Delivery and Controlled Release of Bioactives in Foods and Nutraceuticals, 1st ed. Woodhead Publishing: Sawston, UK, 2008; pp: 496; ISBN: 978-1-84569-145-5.
- Gatej, I., Popa, M., Rinaudo, M., 2005. Role of pH on hyaluronan behavior in aqueous solution. *Biomacromolecules*, 61-67.
- Higuchi, T., 1961. Rate of release of medicaments from ointment bases containing drugs in suspension. *J. Pharm. Sci.* 50, 874.
- Kafedjiiski, K., Jetti, R.K., Föger, F., Hoyer, H., Werle, M., Hoffer, M., Bernkop-Schnürch, A., 2007. Synthesis and in vitro evaluation of thiolated hyaluronic acid for mucoadhesive drug delivery. *Int. J. Pharm.* 343, 48-58.
- Khan, H., Akhtar, N., Ali, A., 2017. Assessment of combined ascorbyl palmitate (AP) and sodium ascorbyl phosphate (SAP) on facial skin sebum control in female healthy volunteers. *Drug Res. (Stuttg)* 67, 52-58.
- Klock, J., Ikeno, H., Ohmori, K., Nishikawa, T., Vollhardt, J., Schehlmann, V., 2005. Sodium ascorbyl phosphate shows in vitro and in vivo efficacy in the prevention and treatment of acne vulgaris. *Int. J. Cosmet. Sci.* 27, 171-176.
- Klug, H.P., Alexander, L.E., 1974. X-Ray Diffraction Procedures for Polycrystalline and Amorphous Materials. 2nd ed. John Wiley and Sons, New York, USA; ISBN: 978-0-471-49369-3.
- Korsmeyer, R.W., Peppas, N.A., 1981. Effect of the morphology of hydrophilic polymeric matrices on the diffusion and release of water soluble drugs. *J. Membr. Sci.* 9, 211–227.
- Kulkarni, A.D., Bari, D.B., Surana, S.J., Pardeshi, C.V., 2016. In vitro, ex vivo and in vivo performance of chitosan-based spray-dried nasal mucoadhesive microspheres of diltiazem hydrochloride. *J Drug Deliv. Sci. Techno.* 31, 108-117.
- Lapcik, L.; Otyepková, E.; Lapčiková, B.; Otyepka, M.; Vlček, J.; Kupská, I. Physicochemical analysis of hyaluronic acid powder for cosmetic and pharmaceutical

processing, in: Collins, M.N. (Ed.), *Hyaluronic acid for biomedical and pharmaceutical applications*, 1 ed. Smithers Rapra Technology, 2014; pp. 89-101; ISBN-10: 9781909030770.

Laurent, T.C., Laurent, U.G.B., Fraser, J.R.E., 1995. Functions of hyaluronan. *Ann. Rheum. Dis.* 54, 429–432.

Lewandowska, K., Sionkowska, A., Grabska, S., Kaczmarek, B., 2016. Surface and thermal properties of collagen/hyaluronic acid blends containing chitosan. *Int. J. Biol. Macromol.* 92, 371-376.

Li, Y., Han, M., Liu, T., Cun, D., Fang, L., Yang, M., 2017. Inhaled hyaluronic acid microparticles extended pulmonary retention and suppressed systemic exposure of a short-acting bronchodilator. *Carbohydr. Polym.* 172, 197-204.

Liao, Y.H., Jones, S.A., Forbes, B., Martin, G.P., Brown, M.B., 2005. Hyaluronan: pharmaceutical characterization and drug delivery. *Drug Deliv.* 2, 327–342.

Lim, S.T., Martin, G.P., Berry, D.J., Brown, M.B., 2000. Preparation and evaluation of the in vitro drug release properties and mucoadhesion of novel microspheres of hyaluronic acid and chitosan. *J. Control. Release* 66, 281-292.

Liu, Z., Li, X., Xiu, B., Duan, C., Li, J., Zhang, X., Yang, X., Dai, W., Johnson, H., Zhang, H., Feng, X., 2016. A novel and simple preparative method for uniform-sized PLGA microspheres: preliminary application in antitubercular drug delivery. *Colloids Surf. B: Biointerfaces* 145, 679-687.

Lusina Kregar, M., Durrigl, M., Rozman, A., Jelcic, Z., Cetina-Cizmek, B., Filipovic-Grcic, J., 2015 Development and validation of an in vitro release method for topical particulate delivery systems. *Int. J. Pharm.* 485, 202-214.

Maleki, A., Kjoniksen, A., Nystrom, B., 2008. Effect of pH on the behavior of hyaluronic acid in dilute and semidilute aqueous solutions. *Macromol. Symp.* 274, 131-140.

Mayol, L., Quaglia, F., Borzacchiello, A., Ambrosio, L., La Rotonda, M.I., 2008. A novel poloxamers/hyaluronic acid in situ forming hydrogel for drug delivery: rheological, mucoadhesive and in vitro release properties. *Eur. J. Pharm. Biopharm.* 1, 199–206.

Montenegro, L., Trapani, A., Fini, P., Mandracchia, D., Latrofa, A., Cioffi, N., Chiarantini, L., Giusi, G.P., Brundu, S., Puglisi, G., 2014. Chitosan nanoparticles for topical co-administration of the antioxidants glutathione and idebenone: characterization and in vitro release. *Br. J. Pharm. Res.* 4, 2387-2406.

Moore, H.H., Flanner, J.W., 1996. Mathematical comparison of dissolution profiles. *Pharm. Technol.* 20, 64-74.

Moreno-Bautista, G., Tam, K.C., 2011. Evaluation of dialysis membrane process for quantifying the in vitro drug-release from colloidal drug carriers. *Colloids Surf. A Physicochem. Eng. Asp.* 389, 299-303.

- Moyano, M.A., Broussalis, A.M., Segall, A.I., 2010. Thermal analysis of lipoic acid and evaluation of the compatibility with excipients. *J. Therm. Anal. Calorim.* 99, 631-637.
- Ong, H.X., Traini, D., Bebawy, M., Young, P.M., 2011. Epithelial Profiling of Antibiotic Controlled Release Respiratory Formulations. *Pharm. Res.* 28, 2327-2338.
- Pan, M., Heinecke, G., Bernardo, S., Tsui, C., Levitt, J., 2013. Urea: a comprehensive review of the clinical literature. *Dermatol. Online J.* 19, 20392.
- Panagopoulou, A., Vázquez Molina, J., Kyritsis, A., Monleón Pradas, M., Vallés Lluch, A., Gallego Ferrer, G., Pissis, P., 2013. Glass Transition and Water Dynamics in Hyaluronic Acid Hydrogels. *Food Biophys.* 8, 192-202.
- Peppas, N.A., 1985. Analysis of fickian and non-fickian drug release from polymers. *Pharm. Acta Helv.* 60, 110-111.
- Pozzoli, M., Traini, D., Young, P.M., Sukkar, M.B., Sonvico, F., 2017. Development of a Soluplus busenoside freeze-dried powder for nasal drug delivery. *Drug Dev. Ind. Pharm.* 43, 1510-1518.
- Ramamurthi, A., Vesely, I., 2002. Smooth muscle cell adhesion on cross-linked hyaluronan gels. *J. Biomed. Mater. Res.* 60, 195–205.
- Ranjan, S., Fontana, F., Ullah, H., Hirvonen, J., Santos, H.A., 2016. Microparticles to enhance delivery of drugs and growth factors into wound sites. *Ther. Deliv.* 7, 711-732.
- Ré, M.A., Messias, L.S., Schettini, H., 2004. The influence of the liquid properties and the atomizing conditions on the physical characteristics of the spray-dried ferrous sulfate microparticles. *Drying B.*, 1174-1181.
- Réeff, J., Gaignaux, A., Goole, J., De Vriese, C., Amighi, K., 2013. New sustained-release intraarticular gel formulations based on monolein for local treatment of arthritic diseases. *Drug Dev. Ind. Pharm.* 39, 1731-1741.
- Saadat, E., Shakor, N., Gholami, M., Dorkoosh, F.A., 2015. Hyaluronic acid based micelle for articular delivery of triamcinolone, preparation in vitro and in vivo evaluation. *Int. J. Pharm.* 489, 218-225.
- Salama, R.O., Traini, D., Chan, H.K., Young, P.M., 2008. Preparation and characterisation of controlled release co-spray dried drug-polymer microparticles for inhalation 2: evaluation of in vitro release profiling methodologies for controlled release respiratory aerosols. *Eur. J Pharm. Biopharm.* 70, 145–152.
- Schlupp, P., Blaschke, T., Kramer, K.D., Höltje, H.D., Mehnert, W., Schäfer-Korting, M., 2011. Drug release and skin penetration from solid lipid nanoparticles and a base cream: a systematic approach from a comparison of three glucocorticoids. *Skin Pharmacol. Physiol.* 24, 199-209.

- Servaty, R., Schiller, J., Binder, H., Arnold, K., 2001. Hydration of polymeric components of cartilage--an infrared spectroscopic study on hyaluronic acid and chondroitin sulfate. *Int. J. Biol. Macromol.* 28, 121-127.
- Shimojo, A.A., Pires, A.M., Lichy, R., Rodrigues, A.A., Santana, M.H., 2015. The crosslinking degree controls the mechanical, rheological, and swelling properties of hyaluronic acid microparticles. *J. Biomed. Mater. Res. A.* 103, 730-737.
- Siepmann, J., Peppas, N.A., 2001. Modeling of drug release from delivery systems based on hydroxypropyl methylcellulose. *Adv. Drug. Deliv. Rev.* 48, 139-157.
- Singhvi, G., Singh, M., 2011. Review: in-vitro drug release characterization models. *Int. J. Pharm. Sci. Res.* 2, 77-84.
- Spiclin, P., Homar, M., Zupancic-Valant, A., Gasperlin, M., 2003. Sodium ascorbyl phosphate in topical microemulsions. *Int. J. Pharm.* 256, 65-73.
- Tomihata, K., Ikada, Y., 1997. Preparation of cross-linked hyaluronic acid films of low water content. *Biomaterials* 18, 189-195.
- Vertuani, S., Cvetkovska, A.D., Zauli, S., Virgili, A., Manfredini, S., Bettoli, V., 2013. The topical vehicle as a key factor in the management of the psoriatic patients' therapy. *G. Ital. Dermatol. Venereol.* 148, 679-685.
- Wetton, R.E., Whorlow, R.W. *Polymer systems: deformation and flow.* Macmillan, London, UK; 1968; ISBN-10: 0333062035.
- Yang, S.C., Zhu, J.B., 2002. Preparation and characterization of camptothecin solid lipid nanoparticles. *Drug Dev. Ind. Pharm.* 28, 265-274.
- Zambito, Y., Pedreschi, E., Di Colo, G., 2012. Is dialysis a reliable method for studying drug release from nanoparticulate systems? —A case study. *Int. J. Pharm.* 434, 28-34.
- Zoubari, G., Staufenbiel, S., Volz, P., Alexiev, U., Bodmeier, R., 2017. Effect of drug solubility and lipid carrier on drug release from lipid nanoparticles for dermal delivery. *Eur J Pharm Biopharm.*, 110, 39-46.





## CHAPTER 6

### ***Combination of urea-crosslinked hyaluronic acid and sodium ascorbyl phosphate for the treatment of inflammatory lung diseases: An in vitro study***

This chapter was published in *European Journal of Pharmaceutical Sciences*, 120, 96-106 (2018) under the title

“Combination of urea-crosslinked hyaluronic acid and sodium ascorbyl phosphate for the treatment of inflammatory lung diseases: An *in vitro* study”.

*Authors: Arianna Fallacara<sup>a,b</sup>, Laura Busato<sup>a,b</sup>, Michele Pozzoli<sup>a</sup>, Maliheh Ghadiri<sup>a</sup>, Hui Xin Ong<sup>a</sup>, Paul M. Young<sup>a</sup>, Stefano Manfredini<sup>b</sup>, Daniela Traini<sup>a</sup>, \**

<sup>a</sup> Respiratory Technology, Woolcock Institute of Medical Research and Discipline of Pharmacology, Sydney Medical School, The University of Sydney, 431 Glebe Point Road, Glebe, NSW 2037, Australia.

<sup>b</sup> Department of Life Sciences and Biotechnology, University of Ferrara, Via L. Borsari 46, 44121 Ferrara, Italy.

**\* Corresponding author:**

Prof. Daniela Traini: [daniela.traini@sydney.edu.au](mailto:daniela.traini@sydney.edu.au); Tel: +61 2 91140352.

DOI: 10.1016/j.ejps.2018.04.042





## 6.0. Preface

The treatment of respiratory pathologies -like asthma, chronic obstructive pulmonary disease, emphysema, acute respiratory distress syndrome and cystic fibrosis- represents a current emergency, as millions of people are affected and die every year. Furthermore, patients require more effective treatments, as numerous of them risk to become non-responsive to the conventional corticosteroid therapy. Naturally occurring biomolecules such as vitamins, biopolymers, polyphenols, and plant origin compounds have been recently investigated as they can deserve potential applications as adjunctive therapy for lung inflammatory diseases. Among these compounds, vitamin C and hyaluronic acid could represent a promising approach to restore and maintain the normal lung functions, as they have been shown to possess anti-inflammatory and antioxidant activities. Nevertheless, they have never been evaluated in combination on lung epithelial cells. Therefore, the content of chapter 6 consists in an *in vitro* study which investigated the safety and the efficacy of the novel association hyaluronic acid (HA) – vitamin C. More specifically, the bioactivity of sodium ascorbyl phosphate (SAP) -a more stable derivative of vitamin C- combined with the novel urea-crosslinked hyaluronic acid (HA-CL) was evaluated on Calu-3 lung carcinoma derived epithelia cells, in comparison to the association native HA – SAP, and to the single components SAP, native HA and HA-CL. The results of this study provide preliminary evidence that HA-CL and SAP, if delivered in combination, could be suitable as adjunctive therapy for inflammatory pulmonary disorders.

## 6.1. Abstract

This *in vitro* study evaluated, for the first time, the safety and the biological activity of a novel urea-crosslinked hyaluronic acid component and sodium ascorbyl phosphate (HA-CL – SAP), singularly and/or in combination, intended for the treatment of inflammatory lung diseases. The aim was to understand if the combination HA-CL – SAP had an enhanced activity with respect to the combination native hyaluronic acid (HA) – SAP and the single SAP, HA and HA-CL components. Sample solutions displayed pH, osmolality and viscosity values suitable for lung delivery and showed to be not toxic on epithelial Calu-3 cells at the concentrations used in this study. The HA-CL – SAP displayed the most significant reduction in interleukin-6 (IL-6) and reactive oxygen species (ROS) levels, due to the combined action of HA-CL and SAP. Moreover, this combination showed improved cellular healing (wound closure) with respect to HA – SAP, SAP and HA, although at a lower rate than HA-CL alone. These preliminary results showed that the combination HA-CL - SAP could be suitable to reduce inflammation and oxidative stress in lung disorders like acute respiratory distress syndrome, asthma, emphysema and chronic obstructive pulmonary disease, where inflammation is prominent.

**Keywords:** anti-inflammatory; antioxidant; hyaluronic acid; sodium ascorbyl phosphate; urea-crosslinked hyaluronic acid; wound healing.

## 6.2. Introduction

The airway epithelium is directly exposed to the external environment and, consequently, it is strongly responsive to exogenous toxic substances like cigarette smoke, biophysical and biological stresses. All these factors, in combination with genetic predisposition and age, are involved in the pathogenesis of bronchopulmonary diseases. Respiratory pathologies - like asthma, chronic obstructive pulmonary disease (COPD), emphysema, acute respiratory distress syndrome (ARDS) and cystic fibrosis - affect millions of people every year and are amongst the main causes of mortality (Burney et al., 2015; Crotty Alexander et al., 2015; Ferkol and Schraufnagel, 2014; World Health Organization, 2017; Yang et al., 2017). Furthermore, patients require more effective treatments, as numerous of them will become non-responsive to the conventional corticosteroid therapy (Barnes, 2013; Jiang and Zhu, 2016). Considering that inflammation and oxidative stress represent the principal mechanisms underlying the development and progression of many lung diseases (Kleniewska and Pawliczak, 2017; MacNee, 2001; Moldoveanu et al., 2009; Nichols and Chmiel, 2015; Oudijk et al., 2003), the use of anti-inflammatory and antioxidant compounds as adjunctive therapy could be a promising approach to restore and maintain normal lung functions, possibly by reducing drug resistant refractory phenomena. To this end, several recent researches have investigated the therapeutic value of naturally occurring biomolecules –such as vitamins, hyaluronan, polyphenols, and herbal active compounds - and of their derivatives (Bharara et al., 2016; Garantziotis et al., 2016; Li and Li, 2016; Park et al., 2016; Pincikova et al., 2017; Yeo et al., 2017; Zemmouri et al., 2017).

Vitamin C (i.e. ascorbic acid) is a physiological low-molecular weight antioxidant. In the lung, it is able to regulate the innate immune system, maintain host defence and function of the airway epithelial barrier (Li and Li, 2016). Indeed, vitamin C reduces the oxidative stress provoked by inhaled pollutants or irritants, thus limiting cellular damage induced by inflammatory-derived oxidants at the air-lung interface (Larsson et al., 2015). Moreover, vitamin C supplementation reduces acute lung inflammatory response, thus exhibiting a potential preventive and therapeutic role (Silva Bezerra et al., 2006). High doses of intravenous vitamin C with antioxidant and anti-inflammatory properties have been shown to be efficient as adjunctive therapy for recurrent ARDS (Bharara et al., 2016). Although the use of vitamin C to treat pulmonary impairments is still investigational, many studies have suggested its benefits against lung infections (Hemilä and Louhiala, 2007), COPD (Pirabbasi et al., 2016), asthma attacks, bronchial hypersensitivity (Hemilä, 2013) and smoke-induced pulmonary emphysema (Koike et al., 2014).

Sodium ascorbyl phosphate (SAP, Figure 6.1.) is a salt form of ascorbic acid 2-phosphate, and it is a hydrophilic derivative of vitamin C characterized by improved physico-chemical stability. SAP has already shown important antioxidant properties for dermal application (Klock et al., 2005; Spiclin et al., 2003). Additionally, even if to a lesser extent in comparison to magnesium ascorbyl phosphate (another salt of ascorbic acid 2-phosphate), SAP has been shown to stimulate collagen synthesis in cultures of human dermal fibroblasts (Geesin et al., 1993). Hence, SAP may be involved in wound healing processes like magnesium ascorbyl phosphate, which was found to be able not only to promote collagen synthesis (Amirlak et al., 2016; Geesin et al., 1993), but also to increase cell motility and fibroblast proliferation during skin reparation (Duarte et al., 2009; Stumpf et al., 2011).

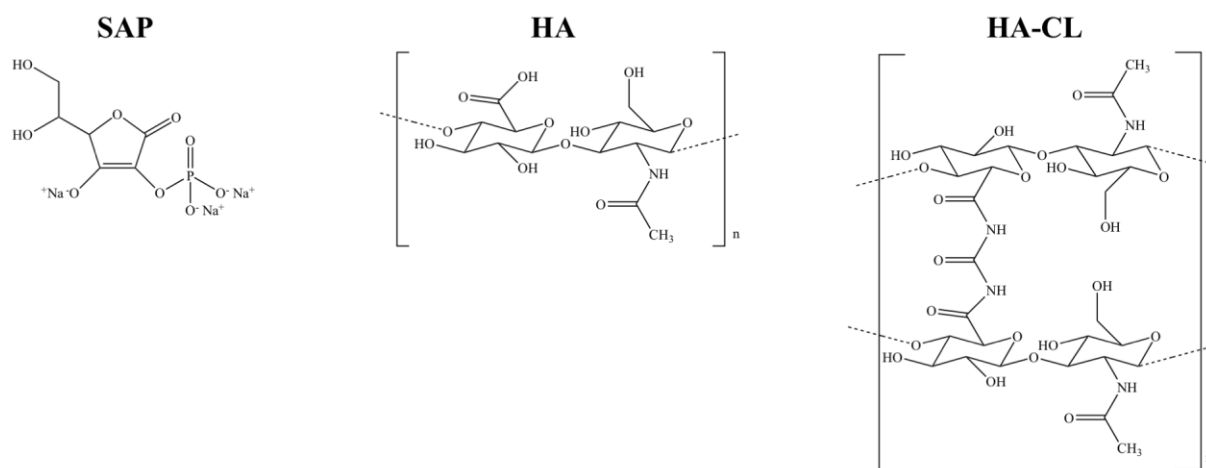


Figure 6.1. Chemical structures of SAP, HA and HA-CL.

Hyaluronic acid (HA, Figure 6.1.) is a biocompatible, biodegradable, visco-elastic and mucoadhesive glycosaminoglycan consisting of repeating dimeric units of D-glucuronic acid and N-acetyl-D-glucosamine (Fallacara et al., 2017a; Kakehi et al., 2003; Liao et al., 2005; Mayol et al., 2008; Toole, 2004). In humans, HA is ubiquitous, and in the lung its total content under physiological condition is approximately 160 mg (Turino and Cantor, 2003). Specifically, in the lung, the high-molecular-weight of HA exerts anti-inflammatory and anti-angiogenic actions, promotes cell survival, organizes extracellular matrix, stabilizes connective tissues, regulates hydration and water homeostasis (Garantziotis et al., 2016; Gerdin and Hällgren, 1997). Due to all these physico-chemical and biological properties, exogenous HA represents a promising multifunctional agent for the treatment of lung diseases, as it can be used as a drug carrier with intrinsic therapeutic potential (Garantziotis et al., 2016; Li et al., 2017; Martinelli et al., 2017; Surendrakumar et al., 2003). Emerging studies support the use of high- molecular-weight ( $> 1$  MDa) HA to treat airway diseases whose pathogenesis involves inflammation, oxidative stress and epithelial remodelling (Allegra et al., 2008; Buonpensiero et al., 2010; Cantor et al., 2005, 2011; Furnari et al., 2012; Garantziotis et al., 2016; Gavina et al., 2013; Jiang et al., 2005, 2010; Lennon and Singleton, 2011; Maiz Carro et al., 2012; Petrigni and Allegra, 2006; Savani et al., 2001; Souza-Fernandes et al., 2006; Venge et al., 1996). Two inhalation products containing HA as active ingredient are currently marketed: Hyaneb® (Chiesi Farmaceutici, IT) and Yabro® (Ibsa Farmaceutici, IT). Hyaneb® is a hypertonic saline solution containing HA (molecular-weight 0.5 MDa, 0.1% w/v) to hydrate and consequently, reduce mucus viscosity in cystic fibrosis patients (Nenna et al., 2011). Yabro®, on the other hand, is a high viscosity nebuliser solution of hyaluronan (molecular-weight 0.8–1MDa, 0.3% w/v) to treat bronchial hyper-re- activity due to irritants inhalation or physical stress (Gelardi et al., 2013).

To improve hyaluronan activity and potential for its use as therapeutic agent, several derivatives have been synthesized (Williams et al., 2017). In this study, a novel urea-crosslinked hyaluronic acid (HA-CL, Figure 6.1.) was investigated for pulmonary application. HA-CL is a patented (Citernesi et al., 2015, WO/2015/007773 A1) biocompatible and biodegradable polymer, with enhanced consistency in comparison to native HA (Citernesi et al., 2015, WO/2015/007773 A1; Fallacara et al., 2017a), due to its crosslinking with urea, a

molecule naturally occurring and therapeutically employed as hydrating and re-epithelializing agent (Albèr et al., 2013; Charlton et al., 1996; Pan et al., 2013).

In this context, the focus of the present *in vitro* bio-investigation was to evaluate the cytotoxicity and the bioactivity -anti-inflammatory, antioxidant and wound healing properties- of these components, vitamin C and hyaluronic acid (HA) derivatives, used singularly and in combination, on Calu-3 lung carcinoma derived epithelia cells.

### **6.3. Materials and methods**

#### **6.3.1. Materials**

Native hyaluronic acid (HA, i.e. sodium hyaluronate, molecular weight 1.2 MDa) and urea-crosslinked hyaluronic acid (HA-CL, molecular weight 2.0–4.0 MDa – raw material containing also pentylene glycol) were kindly donated by IRAlab (Usmate Velate, Monza-Brianza, Italy) and used as supplied. Sodium ascorbyl phosphate (SAP) was purchased from DSM Nutritional Products Ltd. (Segrate, Milano, Italy). Calu-3 cells were supplied by American Type Cell Culture Collection (ATTC, Rockville, USA). Transwell® polyester cell inserts (0.33cm<sup>2</sup> surface area, 0.4 µm pore size) were obtained from Corning by Sigma-Aldrich (Australia). Triton®X-100, L-ascorbic acid, 2',7'-dichloro- fluorescein diacetate (DCFH-DA), lipopolysaccharide (LPS) from Escherichia coli, non-essential amino acids solution, 200 mM L-glutamine solution were purchased from Sigma-Aldrich (Milan, Italy, and Sydney, Australia). Other cell culture reagents including Dulbecco's Modified Eagle's medium/F-12, phosphate buffer saline (PBS) and foetal bovine serum (FBS) were obtained from Gibco by ThermoFisher Scientific (Sydney, Australia). Hydrogen Peroxide (H<sub>2</sub>O<sub>2</sub>) 6% (w/v) was supplied by Gold Cross (Spring Hill, Australia). Methyl tetrazolium salt (MTS) reagent -CellTiter 96® Aqueous One Solution Cell Proliferation Assay- and lactate dehydrogenase (LDH) assay kit -RayBio LDH-Cytotoxicity assay kit II- for cell viability tests were purchased from Promega (Sydney, Australia) and RayBiotech (Kirrawee, Australia), respectively. Collagen Type I and enzyme-linked immuno assay (ELISA) kits for determination of the inflammation markers interleukin-6 (IL-6) and interleukin-8 (IL-8) were obtained from BD Bioscience (Sydney, Australia). Water was purified by Milli-Q reverse Osmosis (Molsheim, France).

#### **6.3.2. Preparation and physico-chemical characterization of hyaluronan and SAP samples**

To evaluate the *in vitro* cytotoxicity and biological activities of the novel combinations HA-CL – SAP and HA – SAP on Calu-3 lung cells, sample solutions were aseptically prepared. SAP was employed with a concentration of 0.45% (w/v), since high doses of ascorbate are necessary to obtain a significant therapeutic activity (Bharara et al., 2016; Li and Li, 2016). Hyaluronan was used at 0.15% (w/v), a concentration similar to those of commercially available products for inhalation (0.1–0.3% w/v) (Gelardi et al., 2013; Nenna et al., 2011), and ideal to improve drug bioavailability from lung compared to simple drug solutions (Morimoto et al., 2001). Thus, hyaluronan-SAP (0.15–0.45% w/v) solutions\* were formulated by dissolving polymers and drug into 10 mL of FBS-free cell culture medium that was kept under constant and gentle magnetic stirring overnight, at room temperature. In the

same way, 0.45% (w/v) SAP, 0.15% (w/v) HA and 0.15% (w/v) HA-CL\* solutions were prepared as comparison.

Before performing the biological study, all the solutions were subjected to physico-chemical characterization.

pH and osmolality were assessed using a Docu-pH+ meter (Sartorius Mechatronics, Goettingen, Germany) and a 5500 Vapor Pressure Osmometer (Wescor, Logan, United States). Viscosity analyses were carried out at  $37 \pm 2$  °C with a rotational rheometer AR2000 (TA instruments, New Castle, USA) connected to the Rheology Advantage software (version V7.20). The rheometer was equipped with an aluminium cone/plate geometry –diameter 40 mm, angle 2°, 64 µm truncation-, and with a solvent trap to prevent samples dehydration. Shear rate sweep tests were carried out under steady state condition: after 1- min equilibration time, the shear rate ( $\dot{\gamma}$ ) was progressively increased from 0.01 to 1000s<sup>-1</sup>. Zero-shear rate viscosity ( $\eta_0$ ) of the solutions was determined by fitting the viscosity curves according to the Cross equation (Cross, 1968) (Eq. 6.1.):

$$\eta = \eta_{\infty} + \frac{\eta_0 - \eta_{\infty}}{1 + (C \cdot \dot{\gamma})^n} \quad (\text{Eq. 6.1.})$$

where  $\eta$  is the viscosity at a given shear rate (Pa·s),  $\dot{\gamma}$  is the shear rate (s<sup>-1</sup>),  $\eta_0$  is the zero-shear rate viscosity (Pa·s),  $\eta_{\infty}$  is the infinite-shear rate viscosity (Pa·s), C is a multiplicative parameter (s) and n is a dimensionless exponent. Data are reported as mean  $\pm$  standard deviations of three independent analyses. As control, pH, osmolality and viscosity of cell culture medium alone were assayed as well.

\* Note: HA CL was provided as raw material containing pentylene glycol. Therefore, 0.15% (w/v) HA CL solutions contained also 0.11% (w/v) pentylene glycol.

### 6.3.3. Cell culture

The lung epithelia cancer derived Calu-3 cell line was chosen as *in vitro* respiratory model. This cell line has been well characterized and reflects the main characteristics and secretory activity of the airway epithelium when grown at an air-liquid interface (ALI) (Haghi et al., 2010). The ALI model allows for cell differentiation in terms of mucus secretion, tight junction generation and protein expressions to mimic the physiological conditions (Haghi et al., 2010).

Calu-3 cells were cultured between passages 38 to 43 in 75 cm<sup>2</sup> flasks containing Dulbecco's Modified Eagle's medium/F-12 enriched with 10% (v/v) foetal bovine serum (FBS), 1% (v/v) non-essential amino acids solution and 1% (v/v) L-glutamine solution. Cells were maintained in a humidified 95% air, 5% CO<sub>2</sub> atmosphere, at 37°C, until confluency was reached. The medium was replaced three times a week and cells were passaged according to American Type Culture Collection Recommendations - ATCC guidelines.

### 6.3.4. LDH and MTS cytotoxicity assays

The *in vitro* cytotoxicities of hyaluronan-SAP (0.15–0.45% w/v) solutions and their single

components - 0.45% (w/v) SAP, 0.15% (w/v) HA and 0.15% (w/v) HA-CL - were evaluated on Calu-3 cells by performing a LDH test. A commercial LDH assay kit was used to quantify the amount of LDH released into the cell culture medium, directly related to cell membrane damage. Extracellular LDH in the medium was measured by a coupled enzymatic reaction in which LDH catalysed lactate conversion into pyruvate, thus provoking the final production of formazan, a dye whose intensity was directly correlated with the number of cells lysed (Chan et al., 2013). Briefly, Calu-3 cells were seeded with a density of  $5 \times 10^4$  cells/well in a volume of 100  $\mu$ L into a 96 well-plate. Cells were incubated overnight at 37°C in a humidified atmosphere at 5% CO<sub>2</sub>. Supernatant was replaced with 100  $\mu$ L of pre-warmed treatments, and cells incubated at the same conditions for another 24 h. Background controls (medium), negative controls (untreated cells) and positive controls (cells treated with 1% w/v Triton<sup>®</sup>X-100) were included in the experiment. 10  $\mu$ L of cell culture supernatant was withdrawn and transferred into a new 96 well-plate, followed by the addition of 100  $\mu$ L of reaction mixture from LDH kit. After 30 min of light-protected incubation at room temperature, LDH activity was quantified by measuring the absorbance with a SpectraMax microplate reader at 450 nm. Experiments were performed in triplicate. Cytotoxicity was calculated according to the following equation (Eq. 6.2.), and presented as the percentage of LDH leakage of each treatment compared to the positive control:

$$LDH \text{ release (\% cell death)} = \frac{\text{Test sample} - \text{negative control}}{\text{Positive control} - \text{negative control}} \times 100 \quad (\text{Eq. 6.2.})$$

A MTS assay was also performed on Calu-3 cells to measure cytotoxicity on cellular metabolic activity as a function of HA – SAP and HA-CL – SAP solution concentrations. MTS assay is a colorimetric test based on tetrazolium reduction into formazan. This reaction occurs only in metabolic active cells (Riss et al., 2004). Briefly, 100  $\mu$ L of  $5 \times 10^4$  cells/well were seeded into a 96 well-plate. Cells were incubated overnight at 37 °C in a humidified atmosphere at 5% CO<sub>2</sub>. On the second day, 100  $\mu$ L of pre-warmed treatments were added to the seeded cells with progressively diluted concentration. Indeed, maintaining hyaluronan-SAP ratio constant to 1–3, a concentration range from 12.6 mM SAP (which corresponded to a solution containing 0.15% hyaluronan and 0.45% SAP) to 1.5 $\mu$ M SAP was tested. Background controls (medium) and untreated controls (untreated cells) were included in the experiment. After 24 h of incubation with treatments at 37°C, in a humidified atmosphere at 5% CO<sub>2</sub>, Calu-3 cells were incubated for another 4 h, in the same conditions, with 20  $\mu$ L of MTS solution. Finally, the 96 well-plate was read at 490 nm using a SpectraMax microplate reader. The absorbance values were directly proportional to cell viability (%). Experiments were performed in triplicate. Data were expressed as % cell viability relative to untreated control, and plotted against SAP concentration (nM) on a logarithmic scale.

Considering the results of the cytotoxicity tests, all the following biological assays were performed with the most concentrated solutions: 0.15–0.45% (w/v) HA – SAP and HA-CL – SAP, 0.45% (w/v) SAP, 0.15% (w/v) HA and (w/v) HA-CL.

### 6.3.5. Evaluation of epithelial barrier integrity

The epithelial barrier function was studied using an electrically-based method, consisting of transepithelial electrical resistance (TEER) measurements. Briefly, Calu-3 cells were seeded on Transwell polyester inserts at density of  $1.65 \times 10^5$  cell/insert, and maintained in a humidified 95% air, 5% CO<sub>2</sub> atmosphere, at 37 °C. After 24 h, the apical chamber medium was removed and the cells were maintained in the basolateral chamber, where the medium was replaced every alternate day with 600µL of fresh medium to establish an ALI model over 12–14 days. 200 µL of treatments -0.15–0.45% (w/v) hyaluronan-SAP, 0.45% (w/v) SAP, 0.15% (w/v) HA and 0.15% (w/v) HA-CL solutions- were added to the apical side, and after 4 h the resistance was measured using a EVOM voltohmmeter (World Precision Instrument, Sarasota, USA) connected to STX-2 chopstick electrodes. Blank controls (cell-free inserts containing medium) and untreated controls (inserts of cells in medium) were included in the study. Experiments were performed in triplicate. TEER ( $\Omega\text{cm}^2$ ) was calculated from the measured potential resistance difference ( $\Omega$ ) between the apical and basolateral sides, normalized by subtracting the blank insert and multiplying by the area of the Transwell inserts, according to the following equation (Eq. 6.3.):

$$TEER (\Omega\text{cm}^2) = (Resistance_{test} - Resistance_{blank}) \times 0.33 \quad (\text{Eq. 6.3.})$$

### 6.3.6. Pro-inflammatory markers expression

The expressions of the pro-inflammatory cytokines, IL-6 and IL-8, were evaluated in Calu-3 cells treated with 0.15–0.45% (w/v) hyaluronan-SAP, 0.45% (w/v) SAP, 0.15% (w/v) HA and 0.15% (w/v) HA-CL solutions.

The effects of test solutions were compared with untreated cells and positive controls, i.e. cells exposed to 10 ng/mL LPS. In this experiment, 1 mL of  $5 \times 10^5$  cells/well was seeded into a 24-well plate. Cells were incubated overnight at 37°C in a humidified atmosphere at 5% CO<sub>2</sub>. On the second day, cell culture medium was withdrawn and replaced with 1 mL of pre-warmed treatments. Calu-3 were then incubated for 24 h at 37°C, in a humidified atmosphere at 5% CO<sub>2</sub>, to allow for the production of IL-6 and IL-8. After that, cell culture supernatant was collected, centrifuged (5 min, 13,000 rpm, 4°C) and analysed for IL-6 and IL-8 levels using human IL-6 and IL-8 ELISA kits, according to the manufacturer's instructions. The amounts of cytokines released in the test samples were determined using standard calibration curves obtained with purified recombinant human IL-6 and IL-8 provided with the kit. The limits of detection were 4.7–300 pg/mL for IL-6 and 3.1–200 pg/mL for IL-8. Experiments were performed in triplicate.

The anti-inflammatory efficacy of the samples was evaluated by their ability to reduce inflammation in Calu-3 cells after induction of inflammatory cytokines production by LPS. Calu-3, seeded into a 24-well plate as previously described, were incubated with 10 ng/mL LPS for 24 h at 37°C, in a humidified atmosphere at 5% CO<sub>2</sub>. Cells were subsequently treated with hyaluronan and/or SAP solutions and, after 24 h of incubation, cell culture supernatant was withdrawn, centrifuged (5 min, 13,000 rpm, 4°C) and analysed for IL-6 and IL-8 levels as previously described.



### **6.3.7. Analysis of intracellular reactive oxygen species (ROS)**

Oxidative stress was evaluated by quantification of intracellular ROS produced by Calu-3 cells treated with 0.15–0.45% (w/v) hyaluronan-SAP, 0.45% (w/v) SAP, 0.15% (w/v) HA and 0.15% (w/v) HA-CL solutions, with and without LPS induction. ROS levels were determined by conversion of the non-fluorescent DCFH-DA into the fluorescent dichlorofluorescein (DCF).

Briefly, 100  $\mu$ L of Calu-3 cells were seeded with a density of  $5 \times 10^4$  cells/well into a 96 well-plate, incubated overnight at 37 °C in a humidified atmosphere at 5% CO<sub>2</sub>. Afterwards, Calu-3 were incubated in the dark for 30 min (37°C, 5% CO<sub>2</sub>) with 100  $\mu$ L of 5  $\mu$ M DCFH-DA (Wu and Yotnda, 2011). Then, DCFH-DA containing medium was removed and 100  $\mu$ L of treatment was added to DCFH-DA-loaded cells, protected from light. Background controls (medium), untreated and unlabelled controls (untreated and unlabelled cells), untreated controls (untreated cells), negative controls (cells treated with 1 mM L-ascorbic acid) and positive controls (cells treated with 0.03% H<sub>2</sub>O<sub>2</sub>) were included in the experiment. After 10 min of incubation (37°C, 5% CO<sub>2</sub>), cell supernatant was withdrawn and transferred into a 96-well plate for fluorescence analysis by a SpectraMax microplate reader with excitation filter set at 485 nm and emission filter set at 520 nm. Experiments were performed in triplicate and results were expressed as % of ROS production relative to untreated control.

The antioxidant activity of the samples was also investigated by their ability to reduce oxidative stress in Calu-3 cells after induction of ROS production by 10 ng/mL LPS.

### **6.3.8. Electric cell-substrate impedance sensing (ECIS) wound healing assay**

The ECIS system (ECIS Z $\theta$ , Applied Biophysics, NY, USA) was used to apply an electrical current to create a wound on the Calu-3 mono-layer and investigate the healing process over time. Briefly, 500  $\mu$ L of Calu-3 cells were seeded at  $5 \times 10^5$  cells/well in collagen coated 8W1E arrays (Applied Biophysics, NY, USA) and allowed to grow for 24 h, directly contacting the gold film surface of the microelectrode –250  $\mu$ m diameter. Culture medium was used as electrolyte. Once the cells reached confluency, an elevated electrical field (2000  $\mu$ A, 60 s, 100 kHz) was applied to wound the epithelial layer. Subsequently, cell debris were washed with sterile PBS and 300  $\mu$ L of the different pre-warmed treatments were added to each well: 0.15–0.45% (w/v) hyaluronan-SAP, 0.45% (w/v) SAP, 0.15% (w/v) HA and 0.15% (w/v) HA-CL solutions. Wounded but untreated cells were also included in the experiment as control. The study was carried out in an incubator at 37°C, with a humidified 5% CO<sub>2</sub> atmosphere. After wounding, resistance ( $\Omega$ ) across the cell layer was measured every 5 min for > 30 h, and data were collected and analysed using the ECIS software, according to the principle of ECIS measurements (Balasubramanian et al., 2008; Stolwijk et al., 2015). Resistance was normalized by dividing the resistance values from electrodes confluent with cells by the corresponding quantities for the cell-free electrodes.

### **6.3.9. Statistical analysis**

Data are presented as mean  $\pm$  standard deviation of three independent experiments. Statistical analysis was performed using GraphPad Prism software version 7.0 b (GraphPad, San

Diego, USA). One-way analysis of variance (ANOVA) followed by Tukey post hoc test for multiple comparisons was used to determine statistical significance (\*P < 0.05, \*\*P < 0.01, \*\*\*P < 0.001 and \*\*\*\*P < 0.0001).

## 6.4. Results and discussion

Both hyaluronic acid (Allegra et al., 2008; Buonpensiero et al., 2010; Cantor et al., 2005, 2011; Furnari et al., 2012; Garantziotis et al., 2016; Gavina et al., 2013; Jiang et al., 2005; Lennon and Singleton, 2011; Maiz Carro et al., 2012; Petrigni and Allegra, 2006; Savani et al., 2001; Souza-Fernandes et al., 2006; Venge et al., 1996) and vitamin C (Berger and Oudemans-van Straaten, 2015; Bharara et al., 2016; Bracher et al., 2012; Fisher et al., 2012; Garcia-Larsen et al., 2016; Gupta et al., 2016; Hemila, 2014; Jin et al., 2016; Li and Li, 2016; Park et al., 2016; Sawyer et al., 1989) have shown potential as adjunctive treatments for lung diseases with inflammatory and oxidative components. Therefore, the present *in vitro* study was devised to investigate the safety and efficacy of the novel hyaluronan – SAP on Calu-3 human epithelial cells. More specifically, the biological activity of SAP combined with HA-CL with urea, a recently synthesized promising polymer (Citernesi et al., 2015, WO/2015/007773 A1; Fallacara et al., 2017a; Fallacara et al., 2017b), has been investigated. This novel combination was evaluated in comparison to the native HA – SAP, and to the single components SAP, HA and HA-CL, to understand if an enhanced activity was present, and whether the crosslinked polymer had an added therapeutic value. Prior to any anti-inflammatory, antioxidant and wound healing tests, the potential cytotoxicity effect of hyaluronan and SAP (in combination and as single components) towards Calu-3 epithelia was evaluated. Moreover, the physico-chemical behaviour of the sample solutions was examined.

### 6.4.1. Physico-chemical properties of hyaluronan and SAP solutions

Prior to the biological study, the physico-chemical behaviour of the test solutions was analysed to evaluate the samples suitability for direct delivery on the lung epithelium (Forbes et al., 2000). To achieve optimal physico-chemical properties for airway tolerability, test formulations should have a pH close to neutrality (7.4) and an osmolality between 150 and 550 mosm/Kg, although small variations can be tolerated (Alhanout et al., 2011; Wong-Beringer et al., 2005).

As shown in Table 6.1., samples displayed an almost neutral pH for lung epithelium. More precisely, HA and HA-CL did not affect the pH of Calu-3 medium, which remained constant at 7.7. The addition of SAP to cell medium increased the pH to 8.1, regardless of the presence of hyaluronan. Nevertheless, these pH variations were not significant for Calu-3 tolerability, as all the solutions were biocompatible, as confirmed by the subsequent viability results. In regards to the sample's osmolality, all the test solutions showed values ranging between  $312.0 \pm 1.7$  (HA) and  $363.0 \pm 0.0$  mOsm/Kg (HA-CL – SAP) -Table 6.1.- that is also suitable for lung delivery.

Another important physico-chemical parameter that was assessed was viscosity, as it affects drug absorption rate. Previous studies reported that sodium hyaluronate solutions, being viscous and mucoadhesive, were able to control and enhance the absorption of drugs and, hence, improve their pharmacological availability from the lung, compared to the less viscous drugs solutions (Morimoto et al., 2001; Yamamoto et al., 2004). As shown in Table 6.1., 0.15–0.45% (w/v) HA –

SAP and HA-CL – SAP solutions were more viscous ( $4.5 \pm 0.2$  and  $5.5 \pm 1.0$  mPa·s, respectively) than 0.45% (w/v) SAP solution ( $1.0 \pm 0.0$  mPa·s) - $P < 0.0001$ . Indeed, HA and HA-CL acted as rheological agents, significantly increasing ( $P < 0.0001$ ) the viscosity of the cell culture medium from  $1.4 \pm 0.0$  to  $8.2 \pm 0.3$  and  $12.1 \pm 0.8$  mPa·s, respectively. Therefore, hyaluronate solutions seemed to be promising vehicle for pulmonary delivery of SAP, as they might be useful to guarantee high local drug concentration.

Table 6.1. Physico-chemical properties (pH, osmolality and viscosity) of: 0.15–0.45% (w/v) HA – SAP and HA-CL – SAP, 0.45% (w/v) SAP, 0.15% (w/v) HA and HA-CL solutions ( $n = 3 \pm \text{StDev}$ ).

Test solution	pH	Osmolality (mOsm/Kg)	Viscosity (mPa.s)
Calu-3-medium	$7.7 \pm 0.0$	$310.0 \pm 2.0$	$1.4 \pm 0.0$
HA - SAP	$8.1 \pm 0.0$	$347.0 \pm 1.0$	$4.5 \pm 0.2$
HA-CL - SAP	$8.1 \pm 0.0$	$363.0 \pm 0.0$	$5.5 \pm 1.0$
SAP	$8.1 \pm 0.0$	$351.0 \pm 1.0$	$1.0 \pm 0.0$
HA	$7.7 \pm 0.0$	$312.0 \pm 1.7$	$8.2 \pm 0.3$
HA-CL	$7.7 \pm 0.0$	$335.3 \pm 0.6$	$12.1 \pm 0.8$

#### 6.4.2. LDH and MTS cytotoxicity assays

The cytotoxicity of hyaluronan and/or SAP solutions on Calu-3 cells was evaluated via changes in cell membrane damage (LDH assay) and cell metabolic activity (MTS assay).

Sample solutions of HA – SAP, HA-CL – SAP, SAP, HA and HA-CL, at the selected concentrations of 0.15% (w/v) hyaluronan and 0.45% (w/v) SAP, respectively, were added to Calu-3 cells which underwent a LDH assay after 24 h. As displayed in Figure 6.2.A, none of these samples showed LDH release, thus indicating that treated Calu-3 cells maintained viability ( $P > 0.05$ ). On the contrary, cells exposure to 1% Triton®X-100, a toxic compound used as positive control, significantly increased LDH release in comparison with untreated cells control ( $P < 0.0001$ ), confirming cell death as expected. Thus, all the test samples, at the selected concentrations, showed to be non-toxic on the Calu-3 epithelial cells.

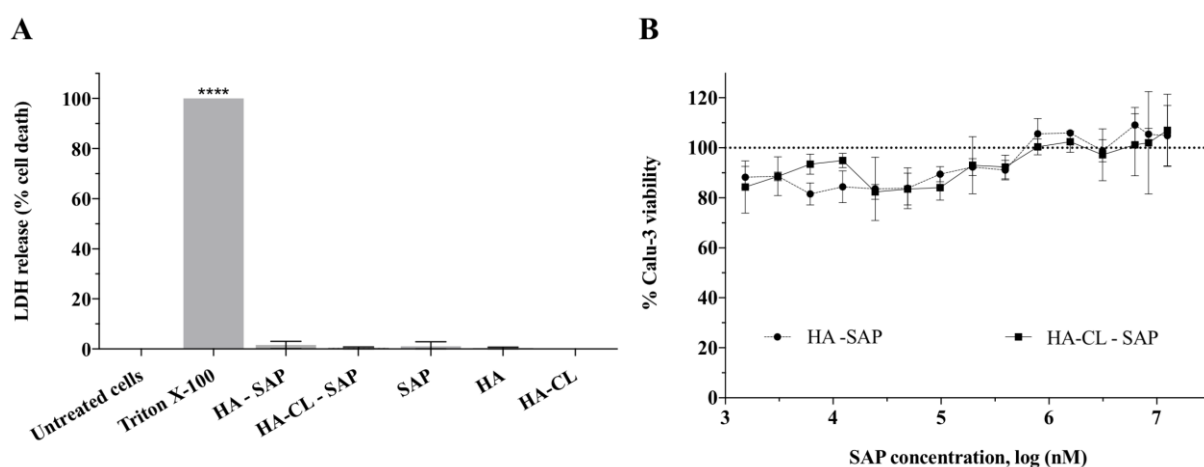


Figure 6.2. Viabilities of Calu-3 cells evaluated using: (A) LDH assay and (B) MTS assay after 24 h of treatment with sample solutions. Data represent mean  $\pm$  standard deviation ( $n = 3$ ). Asterisks indicate significant difference from control untreated cells (\*\*\*\* $P < 0.0001$ ).

To further confirm these results, Calu-3 cells were incubated for 24 h with HA – SAP and HA-CL – SAP solutions characterized by concentration ranging from 1.5  $\mu$ M to 12.6 mM SAP, and by a constant 1–3 polymer-drug ratio. Viability was assessed using a MTS assay. As shown in Figure 6.2.B., Calu-3 cells were viable after treatment with HA – SAP and HA-CL – SAP solutions within the wide range of concentrations investigated. The half maximal inhibitory concentration (IC<sub>50</sub>) values could not be determined across this concentration interval and, therefore, both the hyaluronan - SAP associations were considered safe for Calu-3 epithelium even with the highest concentration (Figure 6.2.B).

### 64.3. Evaluation of epithelial barrier integrity

A quantitative measurement of Calu-3 epithelium barrier integrity was performed after 4 h of exposure to 0.15–0.45% (w/v) HA – SAP and HA-CL – SAP, 0.45% (w/v) SAP, 0.15% (w/v) HA and HA-CL solutions. As displayed in Figure 6.3., TEER results obtained from the chopstick method showed no significant change ( $P > 0.05$ ) between control untreated cells ( $511 \pm 26 \Omega\text{cm}^2$ ) and cells treated with HA – SAP ( $500 \pm 15 \Omega\text{cm}^2$ ), HA-CL – SAP ( $519 \pm 32 \Omega\text{cm}^2$ ), SAP ( $545 \pm 28 \Omega\text{cm}^2$ ) and HA-CL ( $541 \pm 13 \Omega\text{cm}^2$ ), respectively. All the normalized resistance values were thus comparable and no treatment affected the integrity of Calu-3 epithelial monolayer under the time scale and the conditions studied. Hence, subsequent efficacy studies can be performed confidently within the concentrations evaluated.

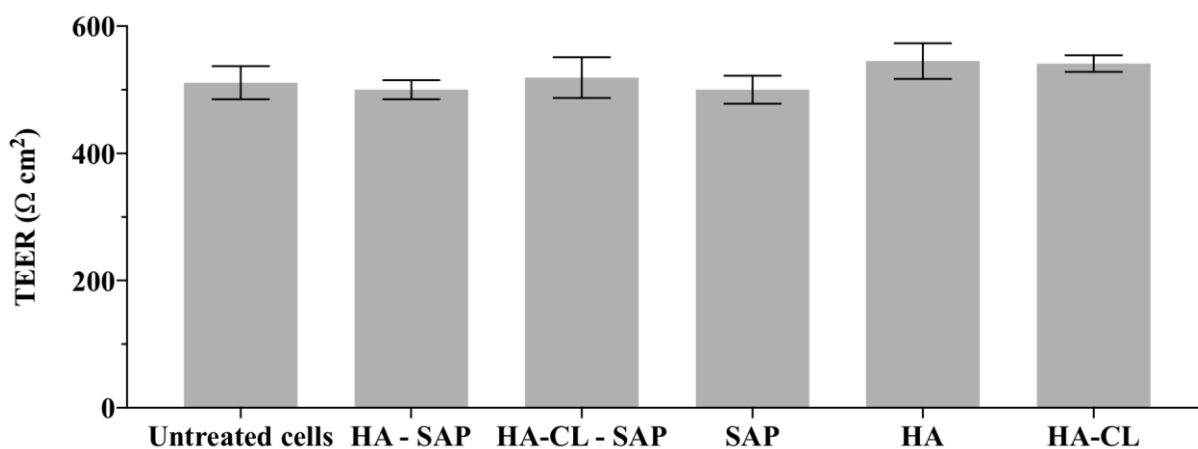


Figure 6.3. Transepithelial electrical resistance (TEER, normalized resistance values) of Calu-3 cells after 4 h of treatment with 0.15–0.45% (w/v) hyaluronan-SAP, 0.45% (w/v) SAP, 0.15% (w/v) HA and HA-CL solutions compared to untreated cells (control). Data represent mean  $\pm$  standard deviation ( $n = 3$ ).

#### 6.4.4. Pro-inflammatory markers expression

Airway inflammation is a biological response stimulated by several factors –such as genetic factors, endogenous substances, inhalation of exogenous irritants, cigarette smoke and pollutants, environmental factors-, and it represents the most important cause of the progression of acute and chronic lung disorders (MacNee, 2001; Oudijk et al., 2003; Wouters et al., 2007). During lung inflammation, different types of inflammatory cells are activated whereby cytokines, and inflammatory mediators such as IL-6 and IL-8 are released, exacerbating tissue irritations (Tulbah et al., 2016).

IL-6 is a pleiotropic cytokine, with important biological effects on inflammation, immunity and stress (Doganci et al., 2005). IL-6 was found to be overproduced during lung inflammatory processes in response to irritants and viruses, and in asthmatic and COPD patients (Rincon and Irvin, 2012). These evidences suggest that IL-6 plays an active role in the pathogenesis of inflammatory pulmonary diseases with different pathways, involving genetic mechanisms and an increased release of pro-inflammatory cytokines like interleukin-13 (responsible of mucus secretion) (Rincon and Irvin, 2012) and eotaxin (Ammit et al., 2007).

IL-8 is a potent neutrophil attractant and activator, which is overexpressed in lung diseases like ARDS (Allen and Kurdowska, 2014), COPD, cystic fibrosis and asthma (Mortaz et al., 2011; Ovreik et al., 2011). IL-8 is regulated via multiple signalling pathways which involve nuclear factor NF- $\kappa$ B, epidermal growth factor receptor, and MAP kinases, all implicated in the pathogenesis of lung inflammatory diseases (Ovreik et al., 2011).

As previously discussed, emerging data have shown that high-molecular weight hyaluronan can be used as therapeutic agent in inflammatory airway diseases (Allegra et al., 2008; Buonpensiero et al., 2010; Cantor et al., 2005, 2011; Furnari et al., 2012; Garantziotis et al., 2016; Gavina et al., 2013; Jiang et al., 2005; Lennon and Singleton, 2011; Maiz Carro et al., 2012; Petrigni and Allegra, 2006; Savani et al., 2001; Souza-Fernandes et al., 2006; Venge et al., 1996). Therefore, this *in vitro* study investigated if the novel HA-CL compound could provide enhanced anti-inflammatory activity than that of native HA, especially when in combination with SAP.

Results showed that HA-CL did not influence IL-8 production, even if combined with SAP, both in non-inflamed and inflamed Calu-3 cells (data not shown). Similarly, IL-6 release was not affected in non-inflamed Calu-3 cells treated with hyaluronan and/or SAP solutions (Figure 6.4.). On the contrary, exposure to 10 ng/mL LPS significantly increased ( $P < 0.0001$ ) IL-6 production from  $270.7 \pm 18.7$  pg/mL (untreated cells control) to  $1165.7 \pm 202.0$  pg/mL, as expected (Figure 6.4). This was due to the inflammatory effects of LPS, an endotoxin located on the outer membrane of bacteria -such as *Escherichia coli*, *Staphylococcus aureus* and *Pseudomonas aeruginosa*- (Pier, 2007; Rietschel et al., 1994), responsible of pathological processes, which aggravates chronic lung disorders during a respiratory infection (Cakir et al., 2003).

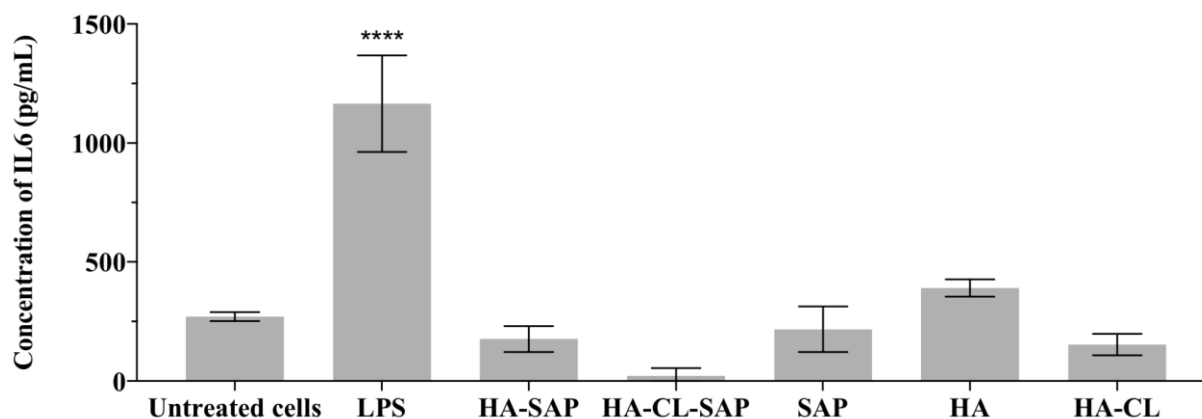


Figure 6.4. Concentration of IL-6 inflammatory cytokine in unstimulated Calu-3 cells supernatant after 24 h of exposure to 0.15–0.45% (w/v) hyaluronan-SAP, 0.45% (w/v) SAP, 0.15% (w/v) HA and HA-CL solutions, evaluated in comparison to untreated cells and cells treated with 10 ng/mL LPS (positive control). Data represent mean  $\pm$  standard deviation ( $n = 3$ ). Asterisks indicate significant difference from untreated cells control (\*\*\*\* $P < 0.0001$ ).

The anti-inflammatory properties of the test solutions were investigated after stimulation of Calu-3 cells with 10 ng/mL LPS 24 h prior to treatments exposure. IL-6 concentrations were determined 24 h after samples addition on the stimulated Calu-3 cells. With the exception of HA, which maintained an IL-6 level similar to that of non-treated LPS-induced Calu-3 cells ( $1165.7 \pm 202.0$  pg/mL), all other treatments showed the ability to reduce IL-6 release (Figure 6.5.). More specifically, HA – SAP reduced IL-6 concentration to  $808.3 \pm 90.7$  pg/mL, SAP to  $868.1 \pm 262.1$  pg/mL, HA-CL and HA-CL – SAP even to  $655.3 \pm 135.0$  and  $431.3 \pm 61.7$  pg/mL, respectively. Therefore, HA- CL was found to have a statistically significant anti-inflammatory activity towards inflamed Calu-3 cells ( $P < 0.05$ ), and an enhanced anti-inflammatory effect when combined with SAP (Figure 6.5.) - $P < 0.01$ .

As oxidative stress is responsible for lung inflammation, both directly and indirectly (Krishna et al., 1998; MacNee, 2001; Santus et al., 2014; Teramoto et al., 1996; Zuo et al., 2013), it was assumed that the antioxidant properties of SAP could improve the anti-inflammatory effect of hyaluronan. This enhanced effect was more evident in the case of HA-CL, probably due to its crosslinking with urea -an active molecule which enhances cellular regeneration and repairment (Albèr et al., 2013; Charlton et al., 1996; Pan et al., 2013)- and, therefore, to its higher molecular weight (2.0–4.0 MDa) in comparison to the native HA (1.2 MDa) from which it was synthesized. Indeed, the biological properties of hyaluronan depend on its size, where only high-molecular weight HA ( $> 1.0$  MDa) has shown anti-inflammatory properties (Garantziotis et al., 2016).

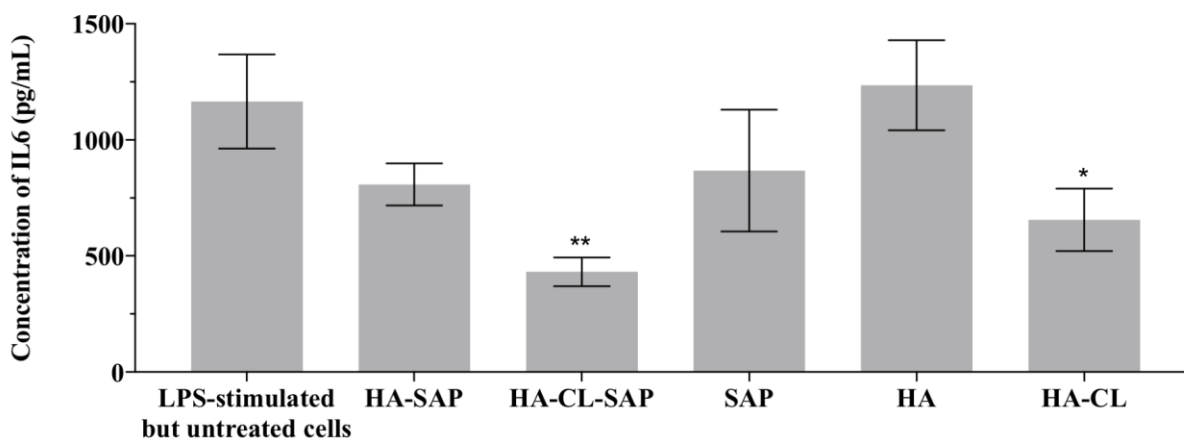


Figure 6.5. Concentration of IL-6 inflammatory cytokine in Calu-3 cells supernatant stimulated with 10 ng/ mL LPS and then exposed for 24 h to 0.15–0.45% (w/v) hyaluronan-SAP, 0.45% (w/v) SAP, 0.15% (w/v) HA and HA-CL solutions, evaluated in comparison to untreated LPS-stimulated cells (control). Data represent mean  $\pm$  standard deviation ( $n = 3$ ). Asterisks indicate significant difference from untreated cells control (\* $P < 0.05$  and \*\* $P < 0.01$ ).

#### 6.4.5. Analysis of intracellular ROS

The respiratory system is continually exposed to irritants, dusts, cigarette smoke, pollutants, viruses and bacteria, which cause the production of oxidant species (Holgate, 2011). When the imbalance between pro-oxidants and endogenous antioxidants moves in favour of pro-oxidant molecules, oxidative stress increases (Birben et al., 2012) and stimulates the production of pro-inflammatory mediators, responsible of ROS release by macrophages activation (Kirkham and Rahman, 2006). Thus, oxidative stress and inflammation engages in an endless cycle, which plays an important role in the pathogenesis of lung diseases (Corrigan and Kay, 1991; Kirkham and Rahman, 2006; MacNee, 2001). Considering that both HA and vitamin C seem to have potential as adjunctive treatments of lung diseases with inflammatory and oxidative components, and that SAP has good antioxidant properties when administered topically (Khan et al., 2017; Klock et al., 2005; Spiclin et al., 2003), this study investigated their ability to induce and reduce oxidative stress in Calu-3 cells. Intracellular ROS were quantified after cells treatment with combinations of 0.15–0.45% (w/v) hyaluronan-SAP, and were compared to ROS levels detected in cells exposed to 0.45% (w/v) SAP, 0.15% (w/v) HA and HA-CL, ascorbic acid (negative control),  $H_2O_2$  (positive control), and untreated cells control.

Results in Figure 6.6 showed that hyaluronan and/or SAP solutions did not induce oxidative stress in Calu-3 cells (without LPS stimulation). On the contrary, hyaluronan and/or SAP solutions reduced the basal level of intracellular ROS, compared to untreated cells. Indeed, both the hyaluronan-SAP combinations significantly decreased ROS concentrations compared to untreated cells: HA – SAP to  $57.9 \pm 2.4\%$  ( $P < 0.001$ ), and HA-CL – SAP to  $23.2 \pm 2.9\%$  ( $P < 0.0001$ ) (Figure 6.6.A), respectively. Thus, HA-CL – SAP displayed an activity comparable to that of the negative control ascorbic acid ( $41.3 \pm 3.4\%$ ), and an improved effect with respect to HA – SAP and of the single SAP ( $55.9 \pm 5.9\%$ ), HA ( $82.3 \pm 8.0\%$ ) and HA-CL ( $51.3 \pm 1.0\%$ ) (Figure 6.6.B), respectively. These data showed an

enhanced antioxidant effect due to HA-CL combination with SAP, with HA-CL – SAP appearing to be the best treatment to provide a potential preventive antioxidant action. On the other hand, the treatment with H<sub>2</sub>O<sub>2</sub> as a positive control resulted in a significant and damaging (Grommes et al., 2012) overproduction of ROS (139.1 ± 15.3%) (Figure 6.6.A).

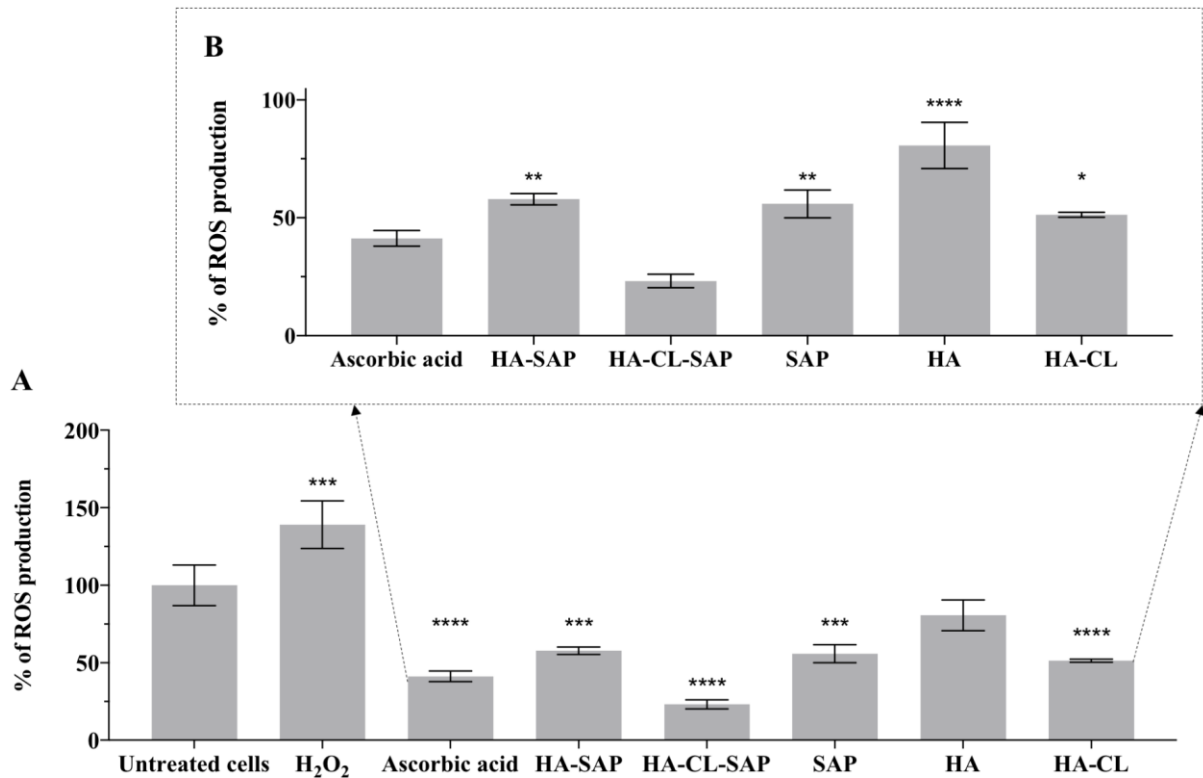


Figure 6.6. Oxidative effects of 0.15–0.45% (w/v) hyaluronan-SAP, 0.45% (w/v) SAP, 0.15% (w/v) HA, 0.15% (w/v) HA-CL solutions, and controls (untreated cells, 0.03% H<sub>2</sub>O<sub>2</sub>, 1mM L-ascorbic acid) on intracellular ROS production (%) in Calu-3 cells. Data represent mean ± standard deviation (n=3). Asterisks indicate significant differences from untreated cells control (A) and from HA-CL - SAP (B), with \*P < 0.05, \*\*P < 0.01, \*\*\*P < 0.001 and \*\*\*\*P < 0.0001.

The antioxidant activity of the samples was then studied for their ability to decrease ROS levels in inflamed Calu-3 cells that have been stimulated with 10 ng/mL LPS. All the test solutions significantly reduced ROS production in Calu-3 cells compared to untreated inflamed cells, as displayed in Figure 6.7.A. More precisely, the combination HA-CL – SAP showed a ROS release of 84.4 ± 0.6%, which was significantly lower than those of the association HA – SAP (93.2 ± 1.5%), and of the single SAP (95.7 ± 0.9%), HA (90.1 ± 0.4%) and HA-CL (87.9 ± 0.7%) (Figure 6.7.B), respectively. Hence, HA-CL – SAP showed to be the most promising treatment with the highest antioxidant activity.



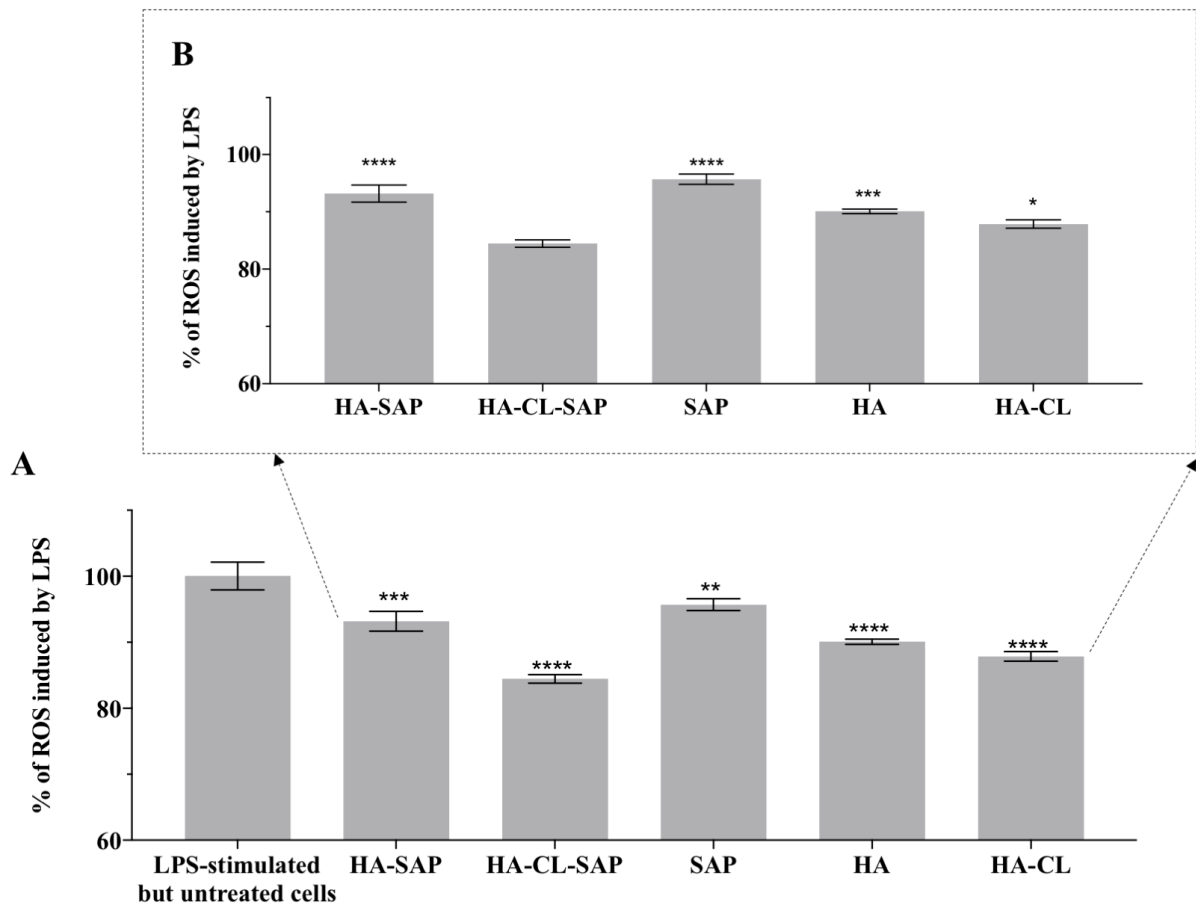


Figure 6.7. Intracellular ROS production (%) in Calu-3 cells stimulated with 10 ng/mL LPS and then exposed to 0.15–0.45% (w/v) hyaluronan- SAP, 0.45% (w/v) SAP, 0.15% (w/v) HA and HA-CL solutions, evaluated in comparison to untreated control (stimulated but untreated cells). Data represent mean  $\pm$  standard deviation (n=3). Asterisks indicate significant differences from untreated cells control (A) and from HA-CL – SAP (B), with \*P < 0.05, \*\*P < 0.01, \*\*\*P < 0.001 and \*\*\*\*P < 0.0001.

#### 6.4.6. Electric cell-substrate impedance sensing wound healing assay

Although the use of vitamin C and its derivatives to treat lung injury is still investigational, it has been shown that their antioxidant activity attenuates tissue damage and positively affects the functions of airway epithelial barrier (Bharara et al., 2016; Li and Li, 2016). Relative to HA, several studies reported that it plays a crucial role in the reparation and regeneration of lung (Jiang et al., 2005, 2010) and many other tissues, such as skin (Murphy et al., 2017; Papakonstantinou et al., 2012), tympanic membrane (Teh et al., 2012) and corneal epithelium (Gomes et al., 2004; Lee et al., 2015; Wu et al., 2013). Considering the strict correlation between tissue damage, inflammation and oxidative stress, hyaluronan's role in wound healing process cannot be precisely ascribed to any single one of its properties, but it is rather due to the combination of its protective effects (Chen and Abatangelo, 1999; Frenkel, 2014). Hence, the promising results of the anti-inflammatory and antioxidant tests performed during this *in vitro* study lead to the investigation of the wound healing ability. In a previous *in vitro* study, it was demonstrated that the novel HA-CL could induce tissue re-epithelialization (Fallacara et al., 2017b). Nevertheless, this was the first study to evaluate on Calu-3 cells the wound healing efficacy of the combinations

0.15–0.45% (w/v) HA – SAP and HA-CL – SAP, in comparison to the single 0.45% (w/v) SAP, 0.15% (w/v) HA and HA-CL.

As displayed in Figure 6.8., resistance decreased sharply upon wounding of the Calu-3 epithelia (after 24 h), and then progressively increased during the healing process to reach a plateau when tissues integrity was completely restored. Our results confirmed the importance of the wound healing activity of hyaluronan (Chen and Abatangelo, 1999; Frenkel, 2014; Jiang et al., 2005, 2010). Indeed, with the exception of SAP, all the treatments increased the rate of wound closure in comparison with untreated wounds (control), which showed a total re-epithelialization after 16.5 h. More precisely, HA – SAP and HA were able to heal the wound almost 4 h before control cells, while HA-CL – SAP and HA-CL 6.5 and 9 h before, respectively (Figure 6.8.). Therefore, although the combination HA-CL – SAP showed improved healing properties in comparison to HA, SAP and the association HA – SAP, the fastest wound closure ability was exhibited by the single HA-CL, which restored epithelial integrity in 7.7 h. This assay demonstrated that HA-CL had improved wound healing properties compared to native HA, and that hyaluronan and SAP, used in combination, did not enhance the re-epithelialization of Calu-3 wounded cells.

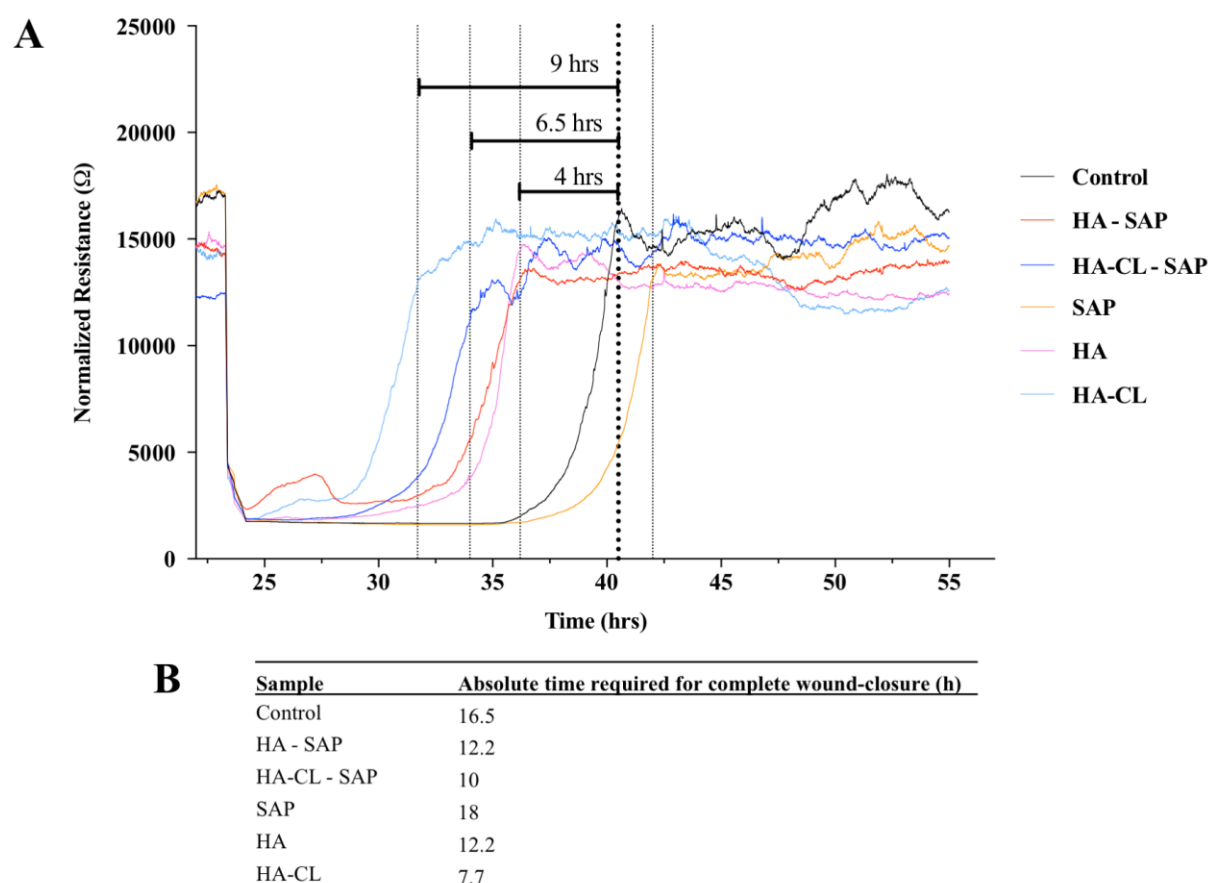


Figure 6.8. Wound healing ability of 0.15–0.45% (w/v) hyaluronan-SAP, 0.45% (w/v) SAP, 0.15% (w/v) HA and HA-CL solutions on Calu-3 monolayers wounded with an electrical current (2000  $\mu$ A, 60 s, 100 kHz) applied using the ECIS system. For each sample, the time required for wound closure (vertical dashed line) was calculated as difference from the time employed by control cells (wounded but untreated –vertical dashed line in bold) (A) and additionally reported as absolute time to restore epithelial integrity (B).

## 6.5. Conclusions

The present *in vitro* study investigated the safety and efficacy of the novel combination HA-CL – SAP in comparison to the association HA – SAP, intended for the treatment and possible prevention of lung diseases with inflammatory and oxidative components. To determine if the combination of the new HA-CL with SAP had an enhanced activity, and if the crosslinked polymer had an enhanced activity with respect to the native compound, the single SAP, HA and HA-CL components were tested. The samples displayed physico-chemical properties (pH, osmolality and viscosity) suitable for the airway, and showed to maintain viability and epithelial integrity of Calu-3 cells in the broad range of concentration explored (1.5  $\mu$ M to 12.6 mM). The association HA-CL – SAP showed the highest anti-inflammatory and antioxidant activity, indicating that polymer and drug worked in combination to reduce IL-6 and ROS levels, and that the crosslinked hyaluronan provided further benefits compared to the native one. Although the fastest kinetic of wound closure was exhibited by the single HA-CL, the combination HA-CL – SAP showed improved healing properties with respect to the association HA – SAP and to its single components. Therefore, these results provided preliminary evidence that HA-CL and SAP, if delivered in combination, could be suitable as adjunctive therapy for inflammatory pulmonary disorders.

## 6.6. Acknowledgements

This work was supported by a PhD grant (to Arianna Fallacara) from IRAlab Srl (Usmate-Verate, Monza-Brianza, Italy). The authors thank the University of Ferrara (Ferrara, Italy, Grant Fir 2016 to Silvia Vertuani) and Ambrosialab s.r.l. (Ferrara, Italy, Grant 2016 to Stefano Manfredini) for the financial support.

## 6.7. Conflicts of interests

The authors declare no conflict of interest.

## 6.8. References

- Albèr, C., Brandner, B.D., Björklund, S., Billsten, P., Corkery, R.W., Engblom, J., 2013. Effects of water gradients and use of urea on skin ultrastructure evaluated by confocal Raman microspectroscopy. *Biochim. Biophys Acta.* 1828, 2470-2478.
- Alhanout, K., Brunel, J.M., Dubus, J.C., Rolain, J.M., Andrieu, V., 2011. Suitability of a new antimicrobial aminosterol formulation for aerosol delivery in cystic fibrosis. *J. Antimicrob. Chemoter.* 66, 2797-2800.
- Allegra, L., Abraham, W.M., Fasano, V., Petrigni, G., 2008. Methacholine challenge in asthmatics is protected by aerosolised hyaluronan at high (1,000 kDa) but not low (300 kDa) molecular weight. *G. Ital. Mal. Torace* 62, 297–301.
- Allen, T.C., Kurdowska, A., 2014. Interleukin 8 and acute lung injury. *Arch. Pathol. Lab. Med.* 138, 266-269.
- Amirlak, B., Mahedia, M., Shah, N., 2016. A clinical evaluation of efficacy and safety of hyaluronan sponge with vitamin C versus placebo for scar reduction. *Plast. Reconstr. Surg. Glob. Open.* 4, e792.
- Ammit, A.J., Moir, L.M., Oliver, B.G., Hughes, J.M., Alkhouri, H., Ge, Q., Burgess, J.K., Black, J.L., Roth, M., 2007. Effect of IL-6 trans-signaling on the pro-remodeling phenotype of airway smooth muscle. *Am. J. Physiol. Lung Cell Mol Physiol.* 292, L199-L206.
- Balasubramanian, L., Yip, K.P., Hsu, T.H., Lo, C.M., 2008. Impedance analysis of renal vascular smooth muscle cells. *Am. J. Physiol. Cell Physiol.* 295, C954-C965.
- Barnes, P.J., 2013. Corticosteroid resistance in patients with asthma and chronic obstructive pulmonary disease. *J. Allergy Clin. Immunol.* 131, 636-645.
- Berger, M.M., Oudemans-van Straaten, H.M., 2015. Vitamin C supplementation in the critically ill patient. *Curr. Opin. Clin. Nutr. Metab. Care* 18, 193-201.
- Bharara, A., Grossman, C., Grinnan, D., Syed, A., Fisher, B., DeWilde, C., Natarajan, R., Fowler, A.A., 2016. Intravenous vitamin C administered as adjunctive therapy for recurrent acute respiratory distress syndrome. *Case Rep. Crit. Care.*
- Birben, E., Sahiner, U.M., Sackesen, C., Erzurum, S., Kalayci, O., 2012. Oxidative stress and antioxidant defense. *World Allergy Organ. J.* 5, 9-19.
- Bracher, A., Doran, S.F., Squadrito, G.L., Postlethwait, E.M., Bowen, L., Matalon, S., 2012. Targeted aerosolized delivery of ascorbate in the lungs of chlorine-exposed rats. *J. Aerosol Med. Pulm. Drug Deliv.* 25, 333-341.
- Buonpensiero, P., De Gregorio, F., Sepe, A., Di Pasqua, A., Ferri, P., Siano, M., Terlizzi, V., Raia, V., 2010. Hyaluronic acid improves “pleasantness” and tolerability of nebulized hypertonic saline in a cohort of patients with cystic fibrosis. *Adv. Ther.* 27, 870–878.

- Burney, P., Jarvis, D., Perez-Padilla, R., 2015. The global burden of chronic respiratory disease in adults. *Int. J. Tuberc. Lung Dis.* 19, 10-20.
- Cakir, O., Oruc, A., Eren, S., Buyukbayram, H., Erdinc, L., Eren, N., 2003. Does sodium nitroprusside reduce lung injury under cardiopulmonary bypass? *Eur. J. Cardiothorac. Surg.* 23, 1040–1045.
- Cantor, J.O., Cerreta, J.M., Ochoa, M., Ma, S., Chow, T., Grunig, G., Turino, G.M., 2005. Aerosolized hyaluronan limits airspace enlargement in a mouse model of cigarette smoke-induced pulmonary emphysema. *Exp. Lung. Res.* 31, 417–430.
- Cantor, J.O., Cerreta, J.M., Ochoa, M., Ma, S., Liu, M., Turino, G.M., 2011. Therapeutic effects of hyaluronan on smoke-induced elastic fiber injury: does delayed treatment affect efficacy? *Lung* 189, 51-56.
- Chan, F.K.M., Moriwaki, K., De Rosa, M.J., 2013. Detection of necrosis by release of lactate dehydrogenase (LDH) activity, methods in molecular biology. Clifton, N.J. 979, 65-70.
- Charlton, J.F., Schwab, I.R., Stuchell, R., 1996. Topical urea as a treatment for non-infectious keratopathy. *Acta Ophthalmol. Scand.* 74, 391-394.
- Chen, W.Y., Abatangelo, G., 1999. Functions of hyaluronan in wound repair. *Wound Repair Regen.* 7, 79-89.
- Citernes, U.R., Beretta, L., Citernes, L., 2015. Cross-linked hyaluronic acid, process for the preparation thereof and use thereof in the aesthetic field. Patent number: WO/2015/007773 A1.
- Corrigan, C., Kay, A., 1991. The roles of inflammatory cells in the pathogenesis of asthma and chronic obstructive pulmonary disease. *Am. Rev. Respir. Dis.* 143, 1165-1168.
- Cross, M.M., 1968. Polymer systems: deformation and flow. Wetton RE, Whorlow RW.
- Crotty Alexander, L.E., Shin, S., Hwang, J.H., 2015. Inflammatory diseases of the lung induced by conventional cigarette smoke: a review. *Chest.* 148, 1307-1322.
- Doganci, A., Sauer, K., Karwot, R., Finotto, S., 2005. Pathological role of IL-6 in the experimental allergic bronchial asthma in mice. *Clin. Rev. Allergy Immunol.* 28, 257-270.
- Duarte, T.L., Cooke, M.S., Jones, G.D., 2009. Gene expression profiling reveals new protective roles for vitamin C in human skin cells. *Free Radic. Biol. Med.* 46, 78-87.
- Fallacara, A., Manfredini, S., Durini, E., Vertuani, S., 2017a. Hyaluronic acid fillers in soft tissue regeneration. *Facial Plast. Surg.* 33, 87-96.
- Fallacara, A., Vertuani, S., Panozzo, G., Pecorelli, A., Valacchi, G., Manfredini S., 2017b. Novel Artificial Tears Containing Cross-Linked Hyaluronic Acid: An In Vitro Re-Epithelialization Study. *Molecules* 22.

Ferkol, T., Schraufnagel, D., 2014. The global burden of respiratory disease. *Ann. Am. Thorac. Soc.* 11, 404-406.

Fisher, B.J., Kraskauskas, D., Martin, E.J., Farkas, D., Wegelin, J.A., Brophy, D., Ward, K.R., Voelkel, N.F., Fowler, A.A.3rd, Natarajan, R., 2012. Mechanisms of attenuation of abdominal sepsis induced acute lung injury by ascorbic acid. *Am. J. Physiol. Lung Cell Mol. Physiol.* 303, L20-L32.

Forbes, B., Hashmi, N., Martin, G.P., Lansley, A.B., 2000. Formulation of inhaled medicines: effect of delivery vehicle on immortalized epithelial cells. *J. Aerosol Med.* 13, 281-288.

Frenkel, J.S., 2014. The role of hyaluronan in wound healing. *Int. Wound J.* 11, 159-163.

Furnari, M.L., Termini, L., Traverso, G., Barrale, S., Bonaccorso, M.R., Damiani, G., Piparo, C.L., Collura, M., 2012. Nebulized hypertonic saline containing hyaluronic acid improves tolerability in patients with cystic fibrosis and lung disease compared with nebulized hypertonic saline alone: a prospective, randomized, double-blind, controlled study. *Ther. Adv. Respir. Dis.* 6, 315-322.

Garantziotis, S., Brezina, M., Castelnuovo, P., Drago, L., 2016. The role of hyaluronan in the pathobiology and treatment of respiratory disease. *Am. J. Physiol. Lung Cell Mol. Physiol.* 310, L785-L795.

Garcia-Larsen, V., Del Giacco, S.R., Moreira, A., Bonini, M., Charles, D., Reeves, T., Carlsen, K.H., Haahtela, T., Bonini, S., Fonseca, J., Agache, I., Papadopoulos, N.G., Delgado, L., 2016. Asthma and dietary intake: an overview of systematic reviews. *Allergy* 71, 433-442.

Gavina, M., Luciani, A., Villella, V.R., Esposito, S., Ferrari, E., Bressani, I., Casale, A., Bruscia, E.M., Maiuri, L., Raia, V., 2013. Nebulized hyaluronan ameliorates lung inflammation in cystic fibrosis mice. *Pediatr. Pulmonol.* 48, 761-771.

Geesin, J.C., Gordon, J.S., Berg, R.A., 1993. Regulation of collagen synthesis in human dermal fibroblasts by the sodium and magnesium salts of ascorbyl-2-phosphate. *Skin Pharmacol.* 6, 65-71.

Gelardi, M., Iannuzzi, L., Quaranta, N., 2013. Intranasal sodium hyaluronate on the nasal cytology of patients with allergic and nonallergic rhinitis. *Int. Forum Allergy Rhinol.* 3, 807-813.

Gerdin, B., Hällgren, R., 1997. Dynamic role of hyaluronan (HYA) in connective tissue activation and inflammation. *J. Intern. Med.* 242, 49-55.

Gomes, J.A.P., Amankwah, R., Powell-Richards, A., Dua, H.S., 2004. Sodium hyaluronate (hyaluronic acid) promotes migration of human corneal epithelial cells in vitro. *Br. J. Ophthalmol.* 88.

Grommes, J., Vijayan, S., Drechsler, M., Hartwig, H., Morgelin, M., Dembinski, R., Jacobs, M., Koepfel, T.A., Binnebösel, M., Weber, C., Soehnlein, O., 2012. Simvastatin reduces endotoxin-

induced acute lung injury by decreasing neutrophil recruitment and radical formation. *PLoS One*. 7, e38917.

Gupta, I., Ganguly, S., Rozanas, C.R., Stuehr, D.J., Panda, K., 2016. Ascorbate attenuates pulmonary emphysema by inhibiting tobacco smoke and Rtp801-triggered lung protein modification and proteolysis. *Proc. Natl. Acad. Sci. USA* 113, E4208-E4217.

Haghi, M., Young, P.M., Traini, D., Jaiswal, R., Gong, J., Bebawy, M., 2010. Time-and passage-dependent characteristics of a Calu-3 respiratory epithelial cell model. *Drug Dev. Ind. Pharm.* 36, 1207–1214.

Hemila, H., 2014. The effect of vitamin C on bronchoconstriction and respiratory symptoms caused by exercise: a review and statistical analysis. *Allergy Asthma Clin. Immunol.* 10, 58.

Hemilä, H., 2013. Vitamin C and common cold-induced asthma: a systematic review and statistical analysis. *Allergy Asthma Clin. Immunol.* 9, 46.

Hemilä, H., Louhiala, P., 2007. Vitamin C may affect lung infections. *J. R. Soc. Med.* 100, 495-498.

Holgate, S.T., 2011. The sentinel role of the airway epithelium in asthma pathogenesis. *Immunol. Rev.* 242, 205-219.

Jiang, D., Liang, J., Fan, J., Yu, S., Chen, S., Luo, Y., Prestwich, G.D., Mascarenhas, M.M., Garg, H.G., Quinn, D.A., Homer, R.J., Goldstein, D.R., Bucala, R., Lee, P.J., Medzhitov, R., Noble, P.W., 2005. Regulation of lung injury and repair by Toll-like receptors and hyaluronan. *Nat. Med.* 11, 1173– 1179.

Jiang, D., Liang, J., Noble, P.W., 2010. Regulation of non-infectious lung injury, inflammation, and repair by the extracellular matrix glycosaminoglycan hyaluronan. *Anat. Rec. (Hoboken)*. 293, 982-985.

Jiang, Z., Zhu, L., 2016. Update on molecular mechanisms of corticosteroid resistance in chronic obstructive pulmonary disease. *Pulm. Pharmacol. Ther.* 37, 1-8.

Jin, X., Su, R., Li, R., Song, L., Chen, M., Cheng, L., Li, Z., 2016. Amelioration of particulate matter-induced oxidative damage by vitamin c and quercetin in human bronchial epithelial cells. *Chemosphere* 144, 459-466.

Takehi, K., Kinoshita, M., Yasueda, S., 2003. Hyaluronic acid: separation and biological implications. *J. Chromatogr. B. Analyt. Technol. Biomed Life Sci.* 797, 347-355.

Khan, H., Akhtar, N., Ali, A., 2017. Assessment of combined ascorbyl palmitate (AP) and sodium ascorbyl phosphate (SAP) on facial skin sebum control in female healthy volunteers. *Drug Res. (Stuttg)*. 67, 52-58.

Kirkham, P., Rahman, I., 2006. Oxidative stress in asthma and COPD: antioxidants as a therapeutic strategy. *Pharmacol. Ther.* 111, 476-494.

- Kleniewska, P., Pawliczak, R., 2017. The participation of oxidative stress in the pathogenesis of bronchial asthma. *Biomed. Pharmacother.* 94, 100-108.
- Klock, J., Ikeno, H., Ohmori, K., Nishikawa, T., Vollhardt, J. Schehlmann, V., 2005. Sodium ascorbyl phosphate shows in vitro and in vivo efficacy in the prevention and treatment of acne vulgaris. *Int. J. Cosmet. Sci.* 27, 171-176.
- Koike, K., Ishigami, A., Sato, Y., Hirai, T., Yuan, Y., Kobayashi, E., Tobino, K., Sato, T., Sekiya, M., Takahashi, K., Fukuchi, Y., Maruyama, N., Seyama, K., 2014. Vitamin C prevents cigarette smoke-induced pulmonary emphysema in mice and provides pulmonary restoration. *Am. J. Respir. Cell. Mol. Biol.* 50, 347-357.
- Krishna, M.T., Madden, J., Teran, L.M., Biscione, G.L., Lau, L.C., Withers, N.J., Sandström, T., Mudway, I., Kelly, F.J., Walls, A., Frew, A.J., Holgate, S.T., 1998. Effects of 0.2 ppm ozone on biomarkers of inflammation in bronchoalveolar lavage fluid and bronchial mucosa of healthy subjects. *Eur. Respir. J.* 11, 1294-1300.
- Larsson, N., Rankin, G.D., Bicer, E.M., Roos-Engstrand, E., Pourazar, J., Blomberg, A., Mudway, I.S., Behndig, A.F., 2015. Identification of vitamin C transporters in the human airways: a cross-sectional in vivo study. *BMJ Open.* 5, e006979.
- Lee, J.S., Lee, S.U., Che, C.Y., Lee, J.E., 2015. Comparison of cytotoxicity and wound healing effect of carboxymethylcellulose and hyaluronic acid on human corneal epithelial cells. *Int. J. Ophthalmol.* 8, 215-221.
- Lennon, F.E., Singleton, P.A., 2011. Role of hyaluronan and hyaluronan-binding proteins in lung pathobiology. *Am. J. Physiol. Lung Cell Mol. Physiol.* 301, L137–L147.
- Li, Y., Han, M., Liu, T., Cun, D., Fang, L., Yang, M., 2017. Inhaled hyaluronic acid microparticles extended pulmonary retention and suppressed systemic exposure of a short-acting bronchodilator. *Carbohydr. Polym.* 172, 197-204.
- Li, Y., Li, G., 2016. Is vitamin C beneficial to patients with CAP? *Curr. Infect Dis. Resp.* 18, 24.
- Liao, Y.H., Jones, S.A., Forbes, B., Martin, G.P., Brown, M.B., 2005. Hyaluronan: pharmaceutical characterization and drug delivery. *Drug Deliv.* 12, 327-342.
- MacNee, W., 2001. Oxidative stress and lung inflammation in airways disease. *Eur. J. Pharmacol.* 429, 195-207.
- Maiz Carro, L., Lamas Ferreiro, A., Ruiz de Valbuena Maiz, M., Wagner Struwing, C., Gabilondo Alvarez, G., Suarez Cortina, L., 2012. [Tolerance of two inhaled hypertonic saline solutions in patients with cystic fibrosis.]. *Med. Clin. (Barc)* 138, 57–59.
- Martinelli, F., Balducci, A.G., Kumar, A., Sonvico, F., Forbes, B., Bettini, R., Buttini, F., 2017. Engineered sodium hyaluronate respirable dry powders for pulmonary drug delivery. *Int. J. Pharm.* 517, 286-295.



- Mayol, L., Quaglia, F., Borzacchiello, A., Ambrosio, L., La Rotonda, M.I., 2008. A novel poloxamers/hyaluronic acid in situ forming hydrogel for drug delivery: rheological, mucoadhesive and in vitro release properties. *Eur. J. Pharm. Biopharm.* 70, 199-206.
- Moldoveanu, B., Otmishi, P., Jani, P., Walker, J., Sarmiento, X., Guardiola, J., Saad, M., Yu, J., 2009. Inflammatory mechanisms in the lung. *J. Inflamm. Res.* 2, 1-11.
- Morimoto, K., Metsugi, K., Katsumata, H., Iwanaga, K., Kakemi, M., 2001. Effects of low-viscosity sodium hyaluronate preparation on the pulmonary absorption of rh-insulin in rats. *Drug Dev. Ind. Pharm.* 27, 365-371.
- Mortaz, E., Henricks, P.A., Kraneveld, A.D., Givi, M.E., Garssen, J., Folkerts, G., 2011. Cigarette smoke induces the release of CXCL-8 from human bronchial epithelial cells via TLRs and induction of the inflammasome. *Biochim. Biophys. Acta.* 1812, 1104-1110.
- Murphy, S.V., Skardal, A., Song L., Sutton, K., Haug, R., Mack, D.L., Jackson, J., Soker, S., Atala, A., 2017. Solubilized Amnion Membrane Hyaluronic Acid Hydrogel Accelerates Full-Thickness Wound Healing. *Stem. Cells Transl. Med.* 6, 2020-2032.
- Nenna, R., Papasso, S., Battaglia, M., De Angelis, D., Petrarca, L., Felder, D., Salvadei, S., Berardi, R., Roberti, M., Papoff, P., Moretti, C., Midulla, F., 2011. 7% hypertonic saline and hyaluronic acid in the treatment of infants mild-moderate bronchiolitis. *Eur. Respir. J.* 38, 1717.
- Nichols, D.P., Chmiel, J.F., 2015. Inflammation and its genesis in cystic fibrosis. *Pediatr. Pulmonol.* 50, S539-56.
- Oudijk, E.D., Lammers, J.J., Koenderman, L., 2003. Systemic inflammation in chronic obstructive pulmonary disease. *Eur. Respir. J.* 22, 5s-13s.
- Ovrevik, J., Refsnes, M., Totlandsdal, A.I., Holme, J.A., Schwarze, P.E., Låg, M., 2011. TACE/TGF- $\alpha$ /EGFR regulates CXCL8 in bronchial epithelial cells exposed to particulate matter components. *Eur. Respir. J.* 38, 1189-1199.
- Pan, M., Heinecke, G., Bernardo, S., Tsui, C., Levitt, J., 2013. Urea: a comprehensive review of the clinical literature. *Dermatol. Online J.* 19.
- Papakonstantinou, E., Roth, M., Karakiulakis, G., 2012. Hyaluronic acid: a key molecule in skin aging. *Dermatoendocrinol.* 4, 253-258.
- Park, H.J., Byun, M.K., Kim, H.J., Kim, J.Y., Kim, Y.I., Yoo, K.H., Chun, E.M., Jung, J.Y., Lee, S.H., Ahn, C.M., 2016. Dietary vitamin C intake protects against COPD: the Korea National Health and Nutrition Examination Survey in 2012. *Int. J. Chron. Obstruct. Pulmon. Dis.* 11, 2721-2728.
- Petrigni, G., Allegra, L., 2006. Aerosolised hyaluronic acid prevents exercise-induced bronchoconstriction, suggesting novel hypotheses on the correction of matrix defects in asthma. *Pulm. Pharmacol. Ther.* 19, 166-171.

- Pier, G.B., 2007. Pseudomonas aeruginosa lipopolysaccharide: a major virulence factor, initiator of inflammation and target for effective immunity. *Int. J. Med. Microbiol.* 297, 277-295.
- Pincikova, T., Paquin-Proulx, D., Sandberg, J.K., Flodström-Tullberg, M., Hjelte, L., 2017. Vitamin D treatment modulates immune activation in cystic fibrosis. *Clin. Exp. Immunol.* 189, 359-371.
- Pirabbasi, E., Shahar, S., Manaf, Z.A., Rajab, N.F., Manap, R.A., 2016. Efficacy of ascorbic acid (vitamin C) and N-acetylcysteine (NAC) supplementation on nutritional and antioxidant status of male chronic obstructive pulmonary disease (COPD) patients. *J. Nutr. Sci. Vitaminol. (Tokyo)* 62, 54-61.
- Rietschel, E.T., Kirikae, T., Schade, F.U., Mamat, U., Schmidt, G., Loppnow, H., Ulmer, A.J., Zähringer, U., Seydel, U., Di Padova, F., Schreier, M., Brade, H., 1994. Bacterial endotoxin: molecular relationships of structure to activity and function. *FASEB J.* 8, 217-225.
- Rincon, M., Irvin, C.G., 2012. Role of IL-6 in asthma and other inflammatory pulmonary diseases. *Int. J. Biol. Sci.* 8, 1281-1290.
- Riss, T.L., Moravec, R.A., Niles, A.L., Duellman, S., Benink, H.A., Worzella, T.J., Minor, L., 2004. Cell viability assays, in: Sittampalam, G.S., Coussens, N.P., Brimacombe, K., Grossman, A., Arkin, M., Auld, D., Austin, C., Baell, J., Bejcek, B., Chung, T.D.Y., Dahlin, J.L., Devanaryan, V., Foley, T.L., Glicksman, M., Hall, M.D., Hass, J.V., Inglese, J., Iversen, P.W., Kahl, S.D., Kales, S.C., Lal-Nag, M., Li, Z., McGee, J., McManus, O., Riss, T., Trask, O.J. Jr., Weidner, J.R., Xia, M., Xu, X. (Ed.), *Assay guidance manual*, Bethesda (MD), pp. vol. 10.1590/S1806-83242009000300006 p.^pp.
- Santus, P., Corsico, A., Solidoro, P., Braido, F., Di Marco, F., Scichilone, N., 2014. Oxidative stress and respiratory system: pharmacological and clinical reappraisal of N-acetylcysteine. *COPD* 11, 705-717.
- Savani, R.C., Cao, G., Pooler, P.M., Zaman, A., Zhou, Z., DeLisser, H.M., 2001. Differential involvement of the hyaluronan (HA) receptors CD44 and receptor for HA-mediated motility in endothelial cell function and angiogenesis. *J. Biol. Chem.* 276, 36770–36778.
- Sawyer, M.A.J., Mike, J.J., Chavin, K., 1989. Antioxidant therapy and survival in ARDS. *Crit. Care Med.* 17.
- Silva Bezerra, F., Valença, S.S., Lanzetti, M., Pimenta, W.A., Castro, P., Gonçalves Koatz V.L., Porto, L.C., 2006. Alpha-tocopherol and ascorbic acid supplementation reduced acute lung inflammatory response by cigarette smoke in mouse. *Nutrition.* 22, 1192-1201.
- Souza-Fernandes, A.B., Pelosi, P., Rocco, P.R., 2006. Bench-to bedside review: the role of glycosaminoglycans in respiratory disease. *Crit. Care* 10, 237.
- Spiclin, P., Homar, M., Zupancic-Valant, A., Gasperlin, M., 2003. Sodium ascorbyl phosphate in topical microemulsions. *Int. J. Pharm.* 256, 65-73.

- Stolwijk, J.A., Matrougui, K., Renken, C.W., Trebak, M., 2015. Impedance analysis of GPCR-mediated changes in endothelial barrier function: overview and fundamental considerations for stable and reproducible measurements. *Pflugers Arch.* 467, 2193-2218.
- Stumpf, U., Michaelis, M., Klassert, D., Cinatl, J., Altrichter, J., Windolf, J., Hergenröther, J., Scholz, M., 2011. Selection of proangiogenic ascorbate derivatives and their exploitation in a novel drug-releasing system for wound healing. *Wound Repair Regen.* 19, 597-607.
- Surendrakumar, K., Martyn, G.P., Hodgers, E.C., Jansen, M., Blair, J.A., 2003. Sustained release of insulin from sodium hyaluronate based dry powder formulations after pulmonary delivery to beagle dogs. *J Control Release.* 91, 385-394.
- Teh, B.M., Shen, Y., Friedland, P.L., Atlas, M.D., Marano, R.J., 2012. A review on the use of hyaluronic acid in tympanic membrane wound healing. *Expert. Opin. Biol. Ther.* 12, 23-36.
- Teramoto, S., Shu, C.Y., Ouchi, Y., Fukuchi, Y., 1996. Increased spontaneous production and generation of superoxide anion by blood neutrophils in patients with asthma. *J. Asthma.* 33, 149-155.
- Toole, B.P., 2004. Hyaluronan: from extracellular glue to pericellular cue. *Nat. Rev. Cancer.* 4, 528-539.
- Tulbah, A.S., Ong, H.X., Lee, W.H., Colombo, P., Young, P.M., Traini, D., 2016. Biological effects of simvastatin formulated as pMDI on pulmonary epithelial cells. *Pharm. Res.* 33, 92-101.
- Turino, G.M., Cantor, J.O., 2003. Hyaluronan in respiratory injury and repair. *Am. J. Respir. Crit. Care Med.* 167, 1169-1175.
- Venge, P., Pedersen, B., Hakansson, L., Hallgren, R., Lindblad, G., Dahl, R., 1996. Subcutaneous administration of hyaluronan reduces the number of infectious exacerbations in patients with chronic bronchitis. *Am. J. Respir. Crit. Care Med.* 153, 312-316.
- World Health Organization, 2017. World health statistics 2017: monitoring health for the SDGs, sustainable development goals. World Health Organization, Geneva.
- Williams, D.L., Wirostko, B.M., Gum, G., Mann, B.K., 2017. Topical cross-linked HA-based hydrogel accelerates closure of corneal epithelial defects and repair of stromal ulceration in companion animals. *Invest. Ophthalmol. Vis. Sci.* 58, 4616-4622.
- Wong-Beringer, A., Lambros, M.P., Beringer, P.M., Johnson, D.L., 2005. Suitability of caspofungin for aerosol delivery: physicochemical profiling and nebulizer choice. *Chest.* 128, 3711-3716.
- Wouters, E.F., Groenewegen, K.H., Dentener, M.A., Vernooij, J.H., 2007. Systemic inflammation in chronic obstructive pulmonary disease: the role of exacerbations. *Proc. Am. Thorac. Soc.* 4, 626-634.

- Wu, C.L., Chou, H.C., Li, J.M., Chen, Y.W., Chen, J.H., Chen, Y.H., Chan, H.L., 2013. Hyaluronic acid-dependent protection against alkali-burned human corneal cells. *Electrophoresis*. 34, 388-396.
- Wu, D., Yotnda, P., 2011. Production and detection of reactive oxygen species (ROS) in cancers. *J. Vis. Exp.* 57, pii: 3357.
- Yamamoto, A., Yamada, K., Muramatsu, H., Nishinaka, A., Okumura, S., Okada, N., Fujita, T., Muranishi, S., 2004. Control of pulmonary absorption of water-soluble compounds by various viscous vehicles. *Int. J. Pharm.* 282, 141-149.
- Yang, I.V., Lozupone, C.A., Schwartz, D.A., 2017. The environment, epigenome, and asthma. *J. Allergy Clin. Immunol.* 140, 14-23.
- Yeo, S.C.M., Fenwick, P.S., Barnes, P.J., Lin, H.S., Donnelly, L.E., 2017. Isorhapontigenin, a bioavailable dietary polyphenol, suppresses airway epithelial cell inflammation through a corticosteroid-independent mechanism. *Br. J. Pharmacol.* 174, 2043-2059.
- Zemmouri, H., Sekiou, O., Ammar, S., El Feki, A., Bouaziz, M., Messarah, M., Boumendjel, A., 2017. *Urtica dioica* attenuates ovalbumin-induced inflammation and lipid peroxidation of lung tissues in rat asthma model. *Pharm. Biol.* 55, 1561-1568.
- Zuo, L., Otenbaker, N.P., Rose, B.A., Salisbury, K.S., 2013. Molecular mechanisms of reactive oxygen species-related pulmonary inflammation and asthma. *Mol. Immunol.* 56, 57-63.





## CHAPTER 7

### ***Co-spray-dried urea crosslinked hyaluronic acid and sodium ascorbyl phosphate as novel inhalable dry powder formulation***

This chapter has been submitted to *J. Pharm. Sci.* for publication with the title:  
“Co-spray-dried urea crosslinked hyaluronic acid and sodium ascorbyl phosphate  
as novel inhalable dry powder formulation”

*Authors: Arianna Fallacara<sup>a,b</sup>, Laura Busato<sup>a,b</sup>, Michele Pozzoli<sup>a</sup>, Maliheh Ghadiri<sup>a</sup>, Hui Xin Ong<sup>a</sup>, Paul M. Young<sup>a</sup>, Stefano Manfredini<sup>b</sup>, Daniela Traini<sup>a</sup>, \**

<sup>a</sup> Respiratory Technology, Woolcock Institute of Medical Research and Discipline of Pharmacology, Faculty of Medicine and Health, The University of Sydney, 431 Glebe Point Road, Glebe, NSW 2037, Australia.

<sup>b</sup> Department of Life Sciences and Biotechnology, University of Ferrara, Via L. Borsari 46, 44121 Ferrara, Italy.

**\* Corresponding author:**

Prof. Daniela Traini: [daniela.traini@sydney.edu.au](mailto:daniela.traini@sydney.edu.au); Tel: +61 2 91140352.





## 7.0. Preface

Chapter 6 has shown the safety and the bioactivity of the novel combination urea-crosslinked hyaluronic acid – sodium ascorbyl phosphate (HA-CL - SAP) on Calu-3 lung carcinoma derived epithelia cells. In detail, this study has provided preliminary evidences that the combination HA-CL - SAP could be suitable as adjunctive therapy for inflammatory pulmonary disorders. Therefore, chapter 7 describes the development of an inhalable dry powder formulation by co-spray-drying of HA-CL and SAP. As reference formulation, an inhalable dry powder consisting of native hyaluronic acid (HA) and SAP was also prepared by co-spray-drying. Both formulations underwent a physico-chemical characterization in order to prove their suitability for lung delivery in terms of morphology, size, thermal behaviour, moisture sorption, SAP release and transport across Calu-3 cells and *in vitro* aerosol performance.

## 7.1. Abstract

The pathogenesis and progression of several lung disorders is propagated by inflammatory and oxidative processes which can be controlled by adjunctive inhaled therapies. The present study aimed to develop an inhalable dry powder formulation consisting of co-spray-dried urea-crosslinked hyaluronic acid and sodium ascorbyl phosphate (SD HA-CL – SAP), a novel combination which was recently shown to possess anti-inflammatory, antioxidant and wound healing properties. Native HA and SAP were co-spray dried (SD HA – SAP) and evaluated as control formulation. Yield (Y%) and encapsulation efficiency (EE%) were  $67.0 \pm 4.8\%$  and  $75.5 \pm 7.2\%$  for SD HA – SAP,  $70.0 \pm 1.5\%$  and  $66.5 \pm 5.7\%$  for SD HA-CL – SAP, respectively. Both formulations were shown to be suitable for lung delivery in terms of morphology, particle size (median volumetric diameter  $\sim 3.4 \mu\text{m}$ ), physical and thermal stability, in vitro aerosol performance -respirable fraction:  $30.5 \pm 0.7\%$  for SD HA – SAP,  $35.3 \pm 0.3\%$  for SD HA CL – SAP. SAP release was investigated using Franz cells and air-interface Calu-3 cell model ( $> 90\%$  of SAP transported within 4 hours). In conclusion, the innovative SD HA-CL – SAP formulation holds much potential as inhalable dry powder for the treatment of inflammatory lung disorders.

**Keywords:** aerosol performance; inhalable dry powder; hyaluronic acid; pulmonary drug delivery; sodium ascorbyl phosphate; urea-crosslinked hyaluronic acid.

## 7.2. Introduction

Inflammation and oxidative stress are the principal mechanisms underlying the development and the progression of many lung diseases (Kleniewska and Pawliczak, 2017; MacNee, 2001; Moldoveanu et al., 2009; Nichols and Chmiel, 2015; Oudijk et al., 2003) which currently represent a leading cause of morbidity and mortality worldwide (Burney et al., 2015; Crotty Alexander et al., 2015; Ferkol and Schraufnagel, 2014; World Health Organization, 2017; Yang et al., 2017). The treatment of pathologies like acute respiratory distress syndrome (ARDS), asthma, emphysema and chronic obstructive pulmonary disease (COPD) could be improved by adjunctive therapy consisting of anti-inflammatory and antioxidant compounds (MacNee, 2001).

In this context, two physiological biomolecules have attracted our attention: ascorbic acid, an antioxidant, and hyaluronic acid (HA), a high-molecular-weight (> 1 MDa) multifunctional polymer. Many experimental works suggested the therapeutic and preventive role of ascorbic acid in lung impairments, principally due to its antioxidant and anti-inflammatory properties (Bharara et al., 2016; Larsson et al., 2015; Li Y. and Li G., 2016; Pirabbasi et al., 2016). Other studies showed the potential of HA both as pulmonary drug carrier (Li et al., 2017) and as lung therapeutic agent to treat inflammation and oxidative stress, and to promote epithelial remodelling (Allegra et al., 2008; Buonpensiero et al., 2010; Garantziotis et al., 2016; Gavina et al., 2013; Jiang et al., 2005, 2010; Petrigni and Allegra, 2006). All these evidences have led us to explore the *in vitro* therapeutic value of sodium ascorbyl phosphate (SAP, a derivative of ascorbic acid), native HA and urea-crosslinked hyaluronic acid (HA-CL, a recently synthesized multifunctional hyaluronan derivative - Citernesi, WO/2015/007773 A1, 2015; Fallacara 2017 a, b), separately and in combination, on Calu-3 lung carcinoma derived epithelia cells (Fallacara et al., 2018). In this study, the novel combination HA CL – SAP displayed the most significant decrease in interleukin-6 and reactive oxygen species levels. Furthermore, it improved cellular healing (wound closure) (Fallacara et al., 2018). These preliminary results suggested that hyaluronan –especially HA - CL- and SAP, if delivered in combination, could represent a novel therapeutic approach to treat and potentially prevent airway diseases.

Therefore, the aim of the present study was to develop and characterize a multi-drug inhalable formulation containing both HA-CL and SAP for localised treatment of inflammatory lung diseases. This was compared with another dry powder formulation containing native HA and SAP. Spray-drying was chosen as manufacture technique to obtain hyaluronan-SAP dry powders. Up to now, despite the technological potential of dry powder formulations and the therapeutic value of hyaluronan, the development of excipient-free inhalable dry powders containing hyaluronan has been limited by the intrinsic cohesiveness of the polymer, which results in poor flowability and unsatisfactory aerodynamic performance (Martinelli et al., 2017). However, the development of efficient excipient-free formulations is important to limit the risk of potential toxicity effects and the rejection by regulatory authorities. Indeed, stringent safety requirements must be satisfied, because the excipient-drug combination composes a whole inhalable medication, whose *in vitro* performance and *in vivo* efficacy must be proved (Pilcer and Amighi, 2010). Even the use of biocompatible excipients naturally occurring in the lungs, such as cholesterol and dipalmitoylphosphatidylcholine (DPPC), must be carefully evaluated to guarantee a precise balance between exogenous and

endogenous components (Pilcer and Amighi, 2010). Hence, there is a strong need to develop pulmonary formulations using alternative strategies to additives in order to improve aerosol behaviour. During the design of the present work, it was hypothesized that SAP, co-spray-dried with hyaluronan, could reduce the polymer cohesiveness thus improving the aerosolization performance of the whole formulation, without the aid of any carrier or lubricant excipient. The following physico-chemical properties of the inhalable formulations were investigated: recovery, SAP encapsulation, surface morphology, particle size, moisture and thermal stability, *in vitro* lung deposition. In addition, the dry powders were analyzed for SAP release profile and SAP transport across Calu-3 epithelial monolayer.

### **7.3. Materials and methods**

#### **7.3.1. Materials**

Native hyaluronic acid (HA, i.e. sodium hyaluronate, molecular weight 1.2 MDa) and urea-crosslinked hyaluronic acid (HA-CL, molecular weight 2.0-4.0 MDa –raw material containing also pentylene glycol) were kindly donated by IRAlab (Usmate Velate, Monza-Brianza, Italy) and used as supplied. Sodium ascorbyl phosphate (SAP) was obtained from DSM Nutritional Products Ltd (Segrate, Milano, Italy). Phosphate buffered saline (PBS, pH = 7.4, 0.01 M) used for the physico-chemical characterization of the formulations was supplied by Sigma-Aldrich (Schnelldorf, Germany). Calu-3 cells were purchased from American Type Cell Culture Collection (ATTC, Rockville, Maryland, USA). Transwell<sup>®</sup> polyester cell inserts (0.33 cm<sup>2</sup> surface area, 0.4 µm pore size) were supplied by Corning (Sydney, Australia). Dulbecco's Modified Eagle's medium/F-12, phosphate buffered saline (PBS) and foetal bovine serum (FBS) were obtained from Gibco (Sydney, Australia). Non-essential amino acids solution and 200 mM L-glutamine solution were supplied by Sigma-Aldrich (Milan, Italy, and Sydney, Australia). Cell Lytic solution was purchased from Invitrogen (Sydney, Australia).

#### **7.3.2. Preparation of spray-dried hyaluronan–SAP formulations**

Inhalable hyaluronan–SAP dry powder formulations were produced using a Buchi spray dryer (Buchi B-290 Mini Spray Dryer, Buchi, Flawil, Switzerland). Hyaluronan-SAP solutions were prepared by progressively dissolving the polymers, 0.15% (w/v) HA or HA-CL, and SAP -0.45% (w/v)- in deionized water, under constant and gentle magnetic stirring. The polymers were allowed to completely hydrate and swell overnight, at room temperature. Once homogeneity was achieved, hyaluronan-SAP solutions were spray-dried using the following process parameters: inlet temperature 150°C, flow rate 3.0 mL/min, aspiration rate 100% and nozzle diameter of 1.4 mm. Under these conditions, an outlet temperature ranging from 78 to 82°C was observed. A dehumidifier B-296 was used to control the air humidity of the system.

### 7.3.3. Yield, encapsulation efficiency and drug loading of hyaluronan–SAP formulations

Yield (Y%), encapsulation efficiency (EE%) and drug loading (DL%) of the SD powders were calculated from Eqs. (7.1.) - (7.3.), respectively:

$$Y\% = \frac{\text{weight of recovered SD powder}}{\text{weight of polymer* and drug fed initially}} \cdot 100 \quad (\text{Eq. 7.1.})$$

\* HA-CL was provided as raw material containing pentylene glycol, and it was used as supplied. Therefore, the Y% of HA-CL – SAP spray-dried powder was calculated considering that 0.15-0.45% (w/v) HA-CL – SAP solution contained also 0.11% (w/v) pentylene glycol.

$$EE\% = \frac{\text{weight of drug in SD powder}}{\text{weight of drug fed initially}} \cdot 100 \quad (\text{Eq. 7.2.})$$

$$DL\% = \frac{\text{weight of drug in SD powder}}{\text{weight of recovered SD powder}} \cdot 100 \quad (\text{Eq. 7.3.})$$

For each SD formulation, all the determinations were performed in triplicate and results expressed as mean  $\pm$  standard deviation.

The amount of encapsulated SAP was determined by completely dissolving 10 mg of each SD powder in 300 mL of release medium (PBS, pH = 7.4, 0.01 M). Drug concentration was then assayed using ultraviolet (UV) spectroscopy (SpectraMax M2, Molecular devices, Orleans Drive Sunnyvale, California, USA) at the 258 nm (SAP  $\lambda_{\text{max}}$ ) wavelength, in the linearity range 1- 30  $\mu\text{g/ml}$  ( $R^2=0.999$ ).

### 7.3.4. Morphological analysis

Scanning electron microscopy (SEM) was used to visualise the morphology of the SD formulations. Prior to analysis, HA – SAP and HA-CL – SAP dry powders were deposited on carbon sticky tapes, placed onto aluminium stubs, and coated with a thin layer of gold using the sputter coater (JEOL USA Smart Coater). The samples were observed and imaged using a bench top SEM (JCM, 6000 JEOL, Japan) with an acceleration voltage of 10 kV.

### 7.3.5. Particle size analysis

Particle size distribution of both SD HA – SAP and SD HA-CL – SAP was determined by laser diffraction (Mastersizer 3000, Malvern, Worcestershire, United Kingdom). Roughly, 10 mg of formulations were dispersed in air through the Scirocco Aero-S dry dispersion unit (Malvern, Worcestershire, United Kingdom), with a feed pressure of 4 bars and a feed rate of 100%. Samples were analyzed in triplicate, with an obscuration value between 0.1% and 15% and a reference refractive index of 1.33. The maximum particle size for 10, 50 and 90% of the cumulative volume distribution of the sample (defined as Dv10, 50 and 90, respectively) were used to describe particle size. The width of the particle size distribution was expressed by the Span index.

### **7.3.6. Thermal analysis**

The thermal response of SD HA – SAP and SD HA-CL – SAP was investigated using differential scanning calorimetry (DSC -DSC823e; Mettler-Toledo, Schwerzenbach, Switzerland). Approximately 5 mg of powders were weighted and crimp-sealed in DSC standard 40 µl aluminium pans. Samples were heated at 10°C/min between -20 to 300 °C. The endothermic and exothermic peaks were determined using STARe software V.11.0x (Mettler Toledo, Greifensee, Switzerland).

### **7.3.7. Moisture sorption and stability**

The relative moisture sorption and stability of SD HA – SAP and SD HA-CL – SAP with respect to humidity were analyzed by dynamic vapour sorption (DVS). Roughly, 10 mg of samples were loaded into aluminium sample pans and placed in the sample chamber of DVS (DVS-1, Surface Measurement Systems Ltd., London, United Kingdom). Each formulation was dried at 0% relative humidity (RH) before being exposed to 10% RH increments for two 0-90% RH cycles (25°C). Equilibrium of moisture sorption at each humidity step was determined by a change in mass to time ratio (dm/dt) of 0.0005% min<sup>-1</sup>.

### **7.3.8. In vitro aerosol performance**

Both SD formulations were analyzed for aerosolization efficiency using a multistage liquid impinger (MSLI, European Pharmacopoeia, Chapter 2.9.18., Copley Scientific Ltd., Nottingham, United Kingdom). The flow rate through the MSLI was controlled by a GAST rotary vein pump (Copley Scientific). Prior to the experiments, the flow rate was set to 60 L/min using a calibrated flow meter (TSI, Shoreview, Minnesota, USA). At this flow rate, the cut-off aerodynamic diameters of each stage of the MSLI were 13, 6.8, 3.1, and 1.7 µm for stages 1, 2, 3 and 4, respectively. Particles less than 1.7 µm were collected by stage 5 containing a paper filter. Stages 1-4 of the MSLI were filled with 20 mL of deionized water. Approximately 28 mg of SD formulations were manually loaded in size 3 gelatine capsules (Capsugel<sup>®</sup>, Sydney, Australia) and placed into a standard-resistance RS01 DPI device (Plastiap<sup>®</sup>, Osnago, Lecco, Italy). The device was connected by a custom-built mouthpiece adaptor to a United State Pharmacopoeia induction port (throat), connected to the MSLI. Then the pump was activated for 4 s to disperse the sample. After actuation, device, capsule, adaptor, throat, all MSLI stages and filter were washed separately with deionized water into suitable beakers. SAP concentration was determined by UV spectroscopy at 258 nm (SpectraMax M2, Molecular devices, Orleans Drive Sunnyvale, California, USA). Each sample was analyzed in triplicate and data were expressed as the percentage (mean ± standard deviation) of SAP recovered in each stage of MSLI, throat, device -comprising RS01 inhalation device, capsule and mouthpiece adaptor- over the total mass calculated. The aerosolization efficiency was calculated as fine particle dose (FPD – amount of SAP recovered from stage 3 to filter, corresponding to the amount of particles with a diameter < 6.8 µm) and fine particle fraction of the loaded dose (FPF<sub>LD</sub> – percentage ratio of FPD with

respect to the total amount of SAP collected from device, capsule, adaptor, throat and all MSLI stages and filter).

### **7.3.9. *In vitro* SAP release study**

*In vitro* SAP release studies were performed using Franz diffusion cells (25 mm internal diameter, multi-station VB6 apparatus, PermeGear Inc., Hellertown, Pennsylvania, USA) according to previously published protocol (Ong et al., 2011). Briefly, polyamide membrane filters 0.45  $\mu\text{m}$  pore size (Sartorius Biolab Products, Goettingen, Germany) were sonicated in deionized water for 30 min, cut and mounted between the receiver and donor compartments of the diffusion cells, which were kept in a thermostatic bath at  $37 \pm 0.5$  °C. SD HA – SAP and SD HA-CL – SAP formulations were placed in the donor compartments, so as to have ~ 4 mg of SAP on the surface of the membranes-, which were sealed using a wax foil (Parafilm M, Bemis Company Inc., Oshkosh, Wisconsin, USA) to prevent evaporation. The receiver compartments contained 23 mL of PBS (pH = 7.4, 0.01 M) continuously stirred at 150 rpm. At selected time points (0, 2, 5, 7, 10, 12, 15, 20, 25, 30, 45, 60, 90 min), 0.5 mL of samples were withdrawn from the receptor compartments and replaced with equal volumes of pre-warmed PBS. Samples were assayed for SAP concentration by UV spectroscopy at 258 nm (SpectraMax M2, Molecular devices, Orleans Drive Sunnyvale, California, USA). A minimum of three independent experiments was performed for each formulation. Data were expressed and plotted as mean  $\pm$  standard deviation of the cumulative percentage of SAP released from the formulations over time.

### **7.3.10. *Cell culture and establishment of an air-interface Calu-3 cell model***

Calu-3 lung carcinoma derived epithelia cells were cultured between passages 38 to 43 in 75 cm<sup>2</sup> flasks containing Dulbecco's Modified Eagle's medium/F-12 enriched with 10% (v/v) FBS, 1% (v/v) non-essential amino acids solution and 1% (v/v) L-glutamine solution. Cells were maintained in a humidified 95% air, 5% CO<sub>2</sub> atmosphere, at 37°C, until confluency was reached. The medium was replaced three times a week and cells were passaged according to American Type Culture Collection Recommendations -ATCC recommended guidelines.

Calu-3 cells were seeded on Transwell polyester inserts at density of  $1.65 \times 10^5$  cell/insert, and kept in a humidified 95% air, 5% CO<sub>2</sub> atmosphere, at 37°C, as previously described (Haghi et al., 2010). After 24 h, the apical chamber medium was removed and the basolateral chamber's medium was replaced every 3 days with 600  $\mu\text{L}$  of fresh medium to establish an air-interface model over 12-14 days.

### **7.3.11. *In vitro* SAP diffusion/transport study using air-interface Calu-3 cell culture**

In a previous study, it was demonstrated that both HA – SAP and HA-CL – SAP combinations at a concentration of 0.15-0.45% (w/v) were non-toxic on Calu-3 cells, and maintained cell viability and integrity (Fallacara et al., 2018). Hence, the transport of SAP from the SD formulations was studied confidently using Calu-3 cells.

The mechanism of drug deposition, dissolution and diffusion/transport was investigated

using the glass twin stage impinger (TSI, Apparatus A, European Pharmacopoeia, Chapter 2.9.18.; Copley Scientific Ltd., Nottingham, United Kingdom), a modified *in vitro* aerosol testing apparatus adapted to fix a cell culture Transwell upon the connecting tube of its lower chamber (Haghi et al., 2012). The TSI divides the dose emitted from the inhaler into two fractions: the non-respirable one (collected in the back of the glass throat and in the upper impingement chamber -stage 1), and the respirable one (deposited on the Calu-3 monolayer, in the lower impingement chamber, with a particle cut-off of 6.4  $\mu\text{m}$  -stage 2). Prior to the experiments, the flow rate was set to 60 L/min using a GAST rotary vein pump (Copley Scientific) and a calibrated flow meter (TSI, Shoreview, Minnesota, USA). Approximately 28 mg of SD HA – SAP and SD HA-CL – SAP formulations were manually loaded in size 3 gelatine capsules and placed into a standard-resistance RS01 DPI device. The device was connected to a custom-built mouthpiece adaptor to the TSI, and then the pump was activated for 4 s to disperse the powder. The connected Transwell, with the deposited formulation, was removed and placed into a well of 24-well plate containing 600  $\mu\text{L}$  of pre-warmed PBS (receiver fluid) to measure transported SAP across Calu-3 cell layer. The 24-well plate was maintained in a humidified 95% air, 5%  $\text{CO}_2$  atmosphere, at 37°C, and at predetermined time points (up to 240 min) 200  $\mu\text{L}$  of receiver PBS were sampled and replaced with an equal volume of pre-warmed PBS. After 240 min, the Transwell was transferred into an empty well, and the apical chamber was gently washed twice with 200  $\mu\text{L}$  of PBS to account for remaining SAP on cell surface. Finally, cells were lysed with Cell Lytic solution to quantify intracellular SAP. The lysate was centrifuged at 10,000 x g, for 10 min, at 4°C, and the supernatant was collected. The initial amount of formulation deposited on the cell layer was calculated from the sum of SAP mass transported, remaining on the monolayer and recovered inside the cells at the end of the experiment. Experiments were repeated three times for each SD formulation. Data were plotted as mean  $\pm$  standard deviation of the cumulative percentage of SAP transported over time. Additionally, results were graphed as mean  $\pm$  standard deviation of the percentage of SAP transported, retained on the cells and recovered inside the cells at the end of the experiment.

SAP concentration in the samples was analyzed using a high-performance liquid chromatography (HPLC) method adapted from Foco et al. study (2005). A Shimadzu Prominence UFLC system equipped with DGU-20A5R Prominence degassing unit, LC-20 AD solvent delivery unit, SIL-20A HT autosampler and SPD-20A UV/VIS detector was employed (Shimadzu Corporation, Tokyo, Japan). The injection volume was 50  $\mu\text{L}$  and the detection wavelength was 258 nm. Quantification of SAP was conducted using acetonitrile:0.3 M phosphate buffer (pH = 4) 40:60 (% v/v) as mobile phase, at a flow rate of 2.0 mL/min, in isocratic mode with a Luna  $\text{NH}_2$  column (5  $\mu\text{m}$ , 4.6 x 150 mm) (Phenomenex, Sydney, Australia). The retention time of SAP was 6 min. The content of SAP was quantified from the peak area according with a predetermined standard curve over the range 0.1-1000  $\mu\text{g}/\text{ml}$  ( $R^2 = 1$ ).

### **7.3.12. Statistical analysis**

All the data are presented as mean  $\pm$  standard deviation of a minimum of three independent experiments. Statistical analysis was performed using GraphPad Prism software version 7.0b (GraphPad, San Diego, USA). Data were analyzed with unpaired *t*-test followed



by Holm-Sidak method for multiple comparison, considering differences statistically significant for  $P < 0.05$ .

To evaluate the formulations performances, SAP release profiles obtained using Franz cell apparatus and Calu-3 cell model were statistically analyzed with fit factors described by Moore and Flanner (1996) and adopted by the Food and Drug Administration (FDA) guidance for dissolution testing in the industry (Food and Drug Administration, 1997). Fit factors are models to directly compare the difference between percentage drug released per unit time between a reference and a test formulation. The difference factor ( $f_1$ ) and the similarity factor ( $f_2$ ) were calculated using Eqs. (7.4.) and (7.5.), respectively:

$$f_1 = \{[\sum_{t=1}^n |R_t - T_t| / \sum_{t=1}^n R_t]\} \times 100 \quad (\text{Eq. 7.4.})$$

$$f_2 = 50 \cdot \log\{[1 + (1/n) \sum (R_t - T_t)^2]^{-0.5} \times 100\} \quad (\text{Eq. 7.5.})$$

Where  $R_t$  and  $T_t$  are percentages of drug released at a specific time point ( $t$ ) from the reference and the test formulation, respectively;  $n$  is the number of dissolution sampling times. The difference factor ( $f_1$ ) calculates the percent difference between the reference and the test curves at each time point thus measuring the relative error between the two curves. The similarity factor ( $f_2$ ) is a logarithmic reciprocal square root transformation of the sum of squared error and is a measurement of the similarity in percentage released between curves. For curves to be considered different, arbitrary limits with  $f_1 \geq 10$  and  $f_2 \leq 50$  were selected for analysis.

## 7.4. Results and discussion

A previous *in vitro* study on Calu-3 cells demonstrated an enhanced efficacy of the novel combination HA-CL – SAP compared to the combination HA – SAP in regards to the anti-inflammatory, antioxidant and wound healing properties (Fallacara et al., 2018). HA-CL was shown to act synergistically with SAP, and to possess an enhanced bioactivity with respect to native HA. Hence, the association HA-CL – SAP can potentially be useful for the treatment and possible prevention of lung disorders like ARDS, asthma, emphysema and COPD, where inflammation and oxidative stress are prominent (Fallacara et al., 2018).

The aim of the present study was to develop an inhalable SD formulation containing both HA-CL and SAP, and to characterize its physico-chemical behaviour, aerosolization performance and release properties in comparison to a control SD formulation consisting of native HA and SAP.

### 7.4.1. Yield, drug loading and encapsulation efficiency of hyaluronan–SAP formulations

Table 7.1. summarizes production yield (Y%), encapsulation efficiency (EE%) and drug loading (DL%) of hyaluronan-SAP microparticles. Both formulations were produced by spray-drying technology, with similar Y% ( $P > 0.05$ ):  $67.0 \pm 4.8\%$  for SD HA – SAP, and  $70.0 \pm 1.5\%$  for SD HA-CL – SAP. Comparable ( $P > 0.05$ ) EE% were observed:  $75.5 \pm 7.2\%$  for SD HA – SAP, and  $66.5 \pm 5.7\%$  for SD HA-CL – SAP, respectively. However, the pentylene glycol associated with the crosslinked hyaluronan affected the DL% value of SD HA-CL – SAP ( $60.0 \pm 4.2\%$ ), which was lower ( $P < 0.05$ ) with respect to SD HA – SAP

(84.7 ± 6.8%).

Table 7.1. Yield (Y%), encapsulation efficiency (EE%) and drug loading (DL%) of hyaluronan-SAP formulations. Data represent mean ± SD (n = 3).

FORMULATION	Y%	EE%	DL %
SD HA - SAP	67.0 ± 4.8	75.5 ± 7.2	84.7 ± 6.8
SD HA-CL - SAP	70.0 ± 1.5	66.5 ± 5.7	60.0 ± 4.2

#### 7.4.2. Morphological analysis

Scanning electron micrographs of SD HA – SAP and SD HA-CL – SAP dry powders are shown in Figure 7.1.A and B, respectively. Both the formulations displayed similar diameters and a spherical geometry, which is a morphological characteristic typical of spray-dried products. HA – SAP microparticles presented several cavities probably due to particle collapse following the rapid drying process during manufacturing, a phenomenon already described in literature (Adi et al., 2010; Ong et al., 2011; Salama et al., 2009). On the contrary, HA-CL – SAP microparticles showed a smoother surface, with occasional formation of small holes. Reasonably, the enhanced consistency of the crosslinked polymer in comparison to the native one (Citernes, WO/2015/007773 A1, 2015; Fallacara et al., 2017a) reduced particle collapse during their production and limited roughness of their surface.

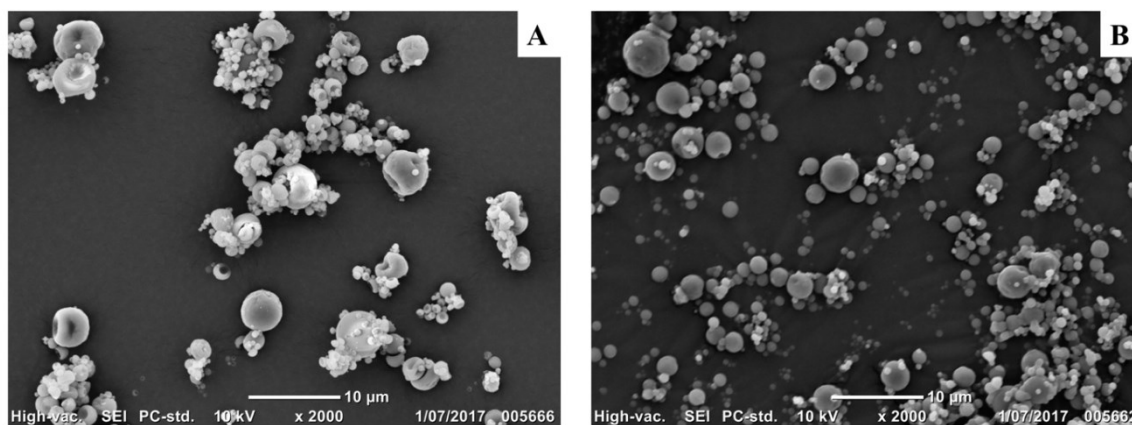


Figure 7.1. Scanning electron microscope images of SD formulations: HA – SAP (A) and HA-CL – SAP (B).

#### 7.4.3. Particle size analysis

Laser diffraction analysis showed that dry powders of HA – SAP and HA-CL – SAP were suitable for lung delivery (1-6 µm) (Chow et al., 2007; Patton, 1999; Sebti and Amighi, 2006). Both the hyaluronan-SAP formulations displayed almost unimodal size distributions within the inhalable range, with few agglomerations most likely due to hyaluronan cohesiveness and to the high surface area of the microparticles (Figure 7.2.). Nevertheless, 90% of HA – SAP microparticles had a diameter  $\leq 13.8 \pm 6.9$  µm, while HA-CL – SAP

microparticles exhibited a size of  $\leq 17.9 \pm 7.6 \mu\text{m}$ . The formulations showed similar ( $P > 0.05$ ) median volumetric diameters ( $Dv_{50}$ ) of  $3.4 \pm 2.4$  and  $3.4 \pm 0.3 \mu\text{m}$ , respectively. The Span index indicated a narrow particle size distribution for both the formulations, without significant differences ( $P > 0.05$ ):  $3.8 \pm 0.4$  for SD HA – SAP, and  $4.9 \pm 1.9$  for SD HA-CL – SAP, respectively.

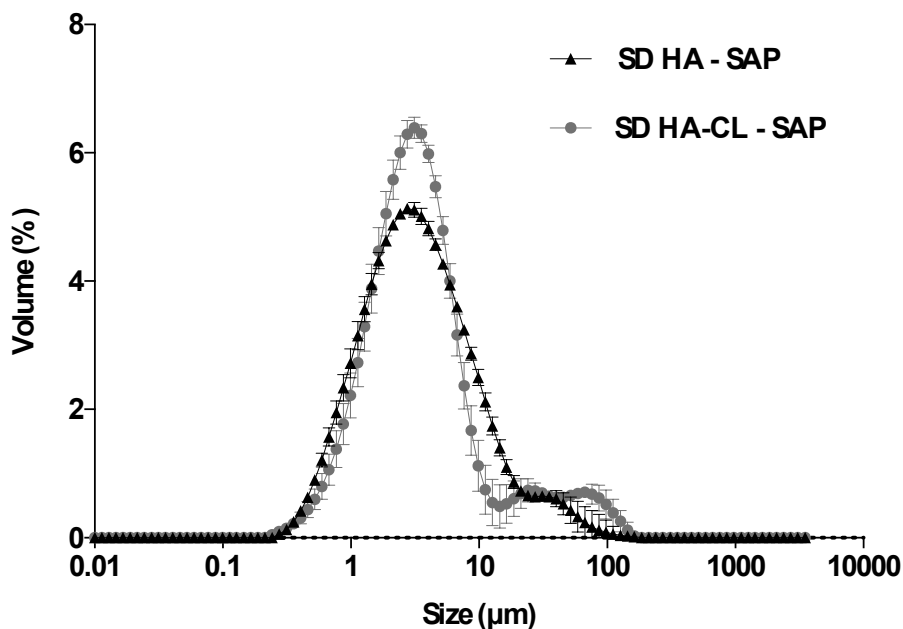


Figure 7.2. Particle size distribution of SD HA – SAP (black line) and SD HA-CL – SAP (grey line) analyzed using dry dispersion system of laser diffraction. Data represent mean  $\pm$  SD ( $n = 3$ ).

#### 7.4.4. Thermal analysis

DSC thermal responses of SD HA – SAP and SD HA-CL – SAP formulations were explored to determine the effect of heat flow on the microparticulate systems, and are shown in Figure 7.3. The DSC trace of SD HA – SAP displayed a wide endothermic peak around  $97^{\circ}\text{C}$ , due to a dehydration phenomenon, and an exothermic peak at  $237^{\circ}\text{C}$ , relative to HA and SAP thermal decomposition with the consequent formation of a carbonized residue (Figure 7.3.). This thermal profile was in agreement with the thermograms previously reported for native HA (Collins and Birkinshaw, 2007, 2008; Kafedjiiski, 2007) and ascorbic acid derivatives (Moyano et al., 2010). The DSC thermogram of SD HA-CL – SAP showed two broad endothermic peaks: the first at  $83^{\circ}\text{C}$ , related to water loss, and the second one at  $187^{\circ}\text{C}$ , attributed to pentylene glycol evaporation. This was confirmed by the DSC thermogram of pentylene glycol (trace not showed). The thermal degradation of HA-CL and SAP occurred at  $247^{\circ}\text{C}$ , where the DSC curve displayed a wide exothermic peak (Figure 7.3.). Hence, for both the formulations, the thermal degradation processes of polymer and drug occurred simultaneously.

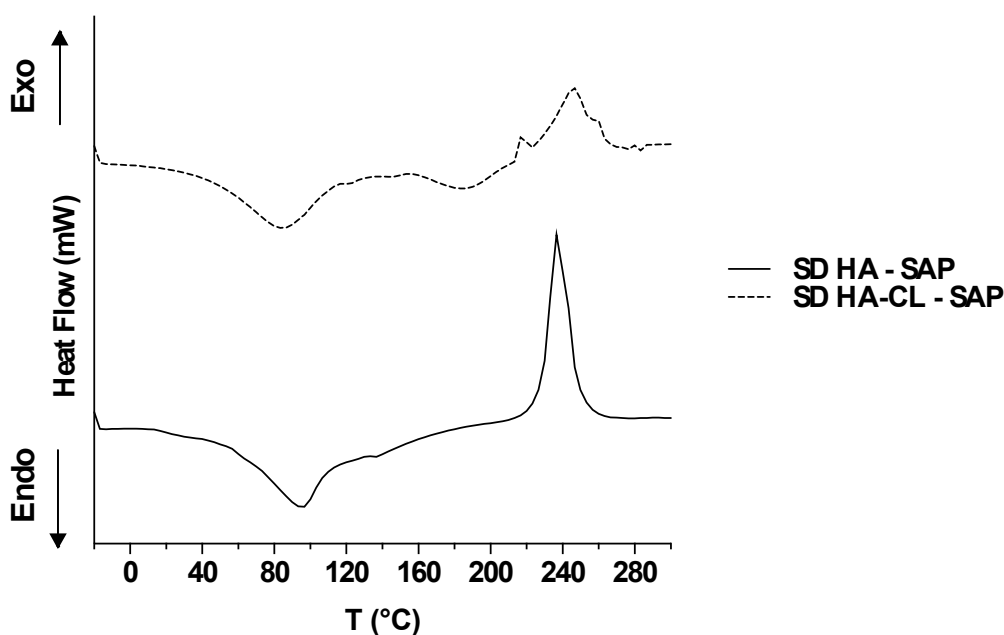


Figure 7.3. DSC thermograms of SD HA – SAP (continuous line) and SD HA-CL – SAP (dashed line).

#### 7.4.5. Moisture sorption and stability

Inhalable dry powders and hyaluronan, a hygroscopic polymer, are generally susceptible to moisture sorption and elevated RH (Albèr et al., 2015). Therefore, to further investigate the relative stability of the formulations' solid-state, both the SD powders underwent two 0-90% RH cycles using a DVS. Figure 7.4. depicts the isotherms of moisture sorption and desorption for the first and the second humidity ramps (cycle 1 and 2) as a function of the RH %.

The moisture sorption profiles of both the formulations were strongly affected by the pronounced water-binding capacity of hyaluronan, which is well-known to retain humidity through hydrogen bonds and electrostatic interaction (Panagopoulou et al., 2013; Servaty et al., 2001). Indeed, as already reported in literature for native HA, both the dry powders displayed intense moisture sorption (Panagopoulou et al., 2013; Servaty et al., 2001). More precisely, the first sorption curve of SD HA - SAP (Figure 7.4.A) was characterized by an increase of the water content up to 28.3% at 90%RH. A hysteresis was observed as the sorption and desorption traces of HA - SAP microparticles were very different. Indeed, SD HA - SAP lost water following an almost linear trend, retaining 11.6% of the humidity (Figure 7.4.A). During the second cycle, moisture content linearly increased up to 25.8% (sorption curve), and then decreased up to 11.7% (desorption curve), showing a less pronounced hysteresis compared to the first sorption-desorption cycle (Figure 7.4.A). This result suggested that SD HA - SAP adsorbed and desorbed humidity in an irreversible manner, and that water molecules were not completely released, probably because of their condensation among the hydrophobic skeleton of the polymer and the drug. A similar hypothesis was also supported by Panagopoulou and co-workers (2013), who studied water dynamics in hydrated HA hydrogels and postulated the formation of a water shell around the hydration sites and the hydrophobic patches of HA chains.

The isotherm of the first moisture sorption-desorption cycle for SD HA-CL – SAP is

shown in Figure 7.4.B. The water content of SD HA-CL – SAP slowly increased up to 26.0% in response to RH increment from 0 to 70%. Then, moisture uptake increased more rapidly in the RH range 70-90%, leading to a water content of 73.0%. It was hypothesized that the higher moisture sorption capacity observed for SD HA-CL - SAP compared to SD HA - SAP was due to the presence of urea and pentylene glycol -that are well known for their water-binding properties- in the formulation containing the crosslinked hyaluronan. At the end of the first desorption process, SD HA-CL - SAP showed a hysteresis phenomenon and a moisture level (1.1%) less significant compared to SD HA - SAP. Therefore, the formulation HA-CL – SAP, even if strongly influenced by high RH values, displayed a more reversible behaviour in terms of moisture sorption/desorption compared to the formulation HA - SAP. This was confirmed by the second cycle of humidity sorption-desorption, which showed a profile similar to the first cycle, leading to final water content of (1.8%) (Figure 7.4.B). These results excluded irreversible change or crystallisation phenomena in response to humidity variations, thus supporting the suitability of SD HA-CL – SAP as inhalable dry powder formulation more stable to moisture.

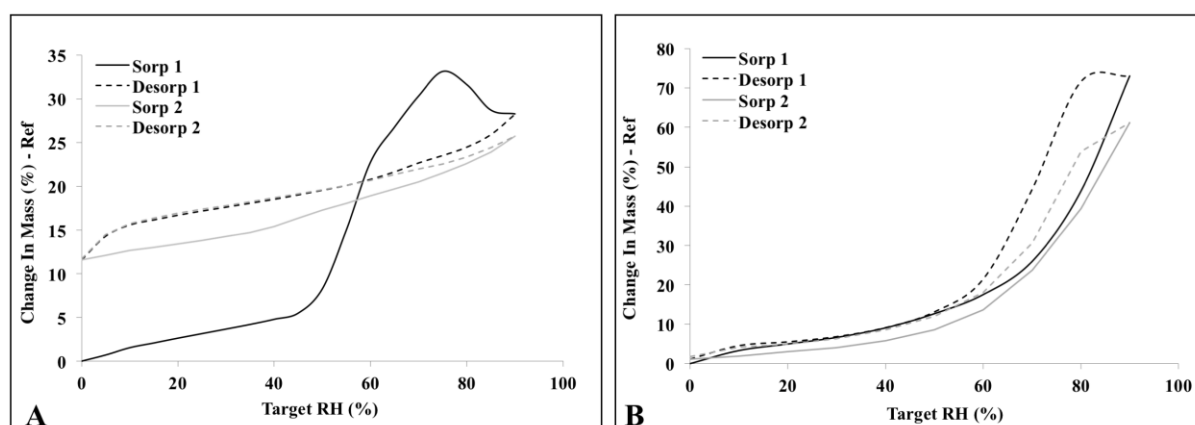


Figure 7.4. DVS isotherms of the first (black lines) and second (grey lines) cycles of moisture sorption (continuous lines) and desorption (dashed lines) for SD HA – SAP (A) and HA - CL – SAP (B).

#### 7.4.6. *In vitro* aerosol performance

Particle size is one of the most important parameters that determine the efficiency of drug delivery to the lung. More precisely, the deposition site of inhaled formulations in the respiratory system is governed by the particle aerodynamic diameter, which takes into account particle geometry, density and shape (Patton, 1999). Particles with an aerodynamic diameter between 1 and 6  $\mu\text{m}$  conventionally represent the “respirable particle fraction”, as they can reach the smaller airways, and this correlates with good therapeutic outcome (Chow et al., 2007; Patton, 1999; Sebti and Amighi, 2006). To predict the amount of inhalable microparticles and thus evaluate the aerosolization efficiency, both the hyaluronan-SAP formulations were aerosolized using RS01 device into the MSLI. Particles recovered from stage 3 to filter (aerodynamic diameter < 6.8  $\mu\text{m}$ ) were considered the respirable fraction.

Figure 7.5. shows the *in vitro* aerosol deposition of the SD samples. Analysis of data displayed that  $88.8 \pm 1.6\%$  and  $89.1 \pm 0.4\%$  of the loaded doses of SD HA – SAP and SD HA-CL – SAP were recovered across all the aerosolization system, falling within the

acceptable pharmacopoeia range of  $100 \pm 25\%$  (British Pharmacopoeia Commission, 2017). The FPD and the  $FPF_{LD}$  were calculated as  $5.9 \pm 0.1$  mg and  $30.5 \pm 0.7\%$  for SD HA – SAP, and  $4.9 \pm 0.1$  mg and  $35.3 \pm 0.3\%$  for SD HA-CL – SAP, respectively. Interestingly, although SD HA-CL – SAP showed a significantly higher ( $P < 0.001$ )  $FPF_{LD}$  in comparison to SD HA – SAP, it had a statistically lower ( $P < 0.001$ ) FPD due to its lower DL% (section 3.1.). Nevertheless, both the formulations displayed good aerosol performances, despite the electrostatic charge of hyaluronan and its resulting adhesive/cohesive nature. This is probably due to SAP partially reducing hyaluronan cohesiveness when co-spray-dried with it. Indeed, it is well-known that adhesive, cohesive and charged particles tend to adhere on the walls of the inhaler device and undergo an uncomplete de-aggregation upon actuation from the device (Karner and Urbanetz, 2011; Wong et al., 2015). This phenomenon could explain the reason behind why the  $11.1 \pm 0.5\%$  of SD HA – SAP and the  $20.8 \pm 1.9\%$  of SD HA-CL – SAP were retained inside the inhalation device and a significant portion of the samples deposited at the higher stages of the MSLI (Figure 7.5.). As a whole, this aerodynamic profile was in good agreement with the *in vitro* lung deposition observed by Li and coworkers (2017) for HA microparticles encapsulating salbutamol sulphate. Normally, the poor flowability of liquid-free HA formulations is improved only in presence of excipients that are able to reduce particle cohesiveness (Hwang et al., 2008; Martinelli et al., 2017). However, the present research aimed to develop excipient-free dry powders which could closely reflect the safety, the biocompatibility and the bioactivity showed by excipient-free solutions of HA – SAP and HA-CL – SAP during a previous *in vitro* study on Calu-3 epithelia (Fallacara et al., 2018).

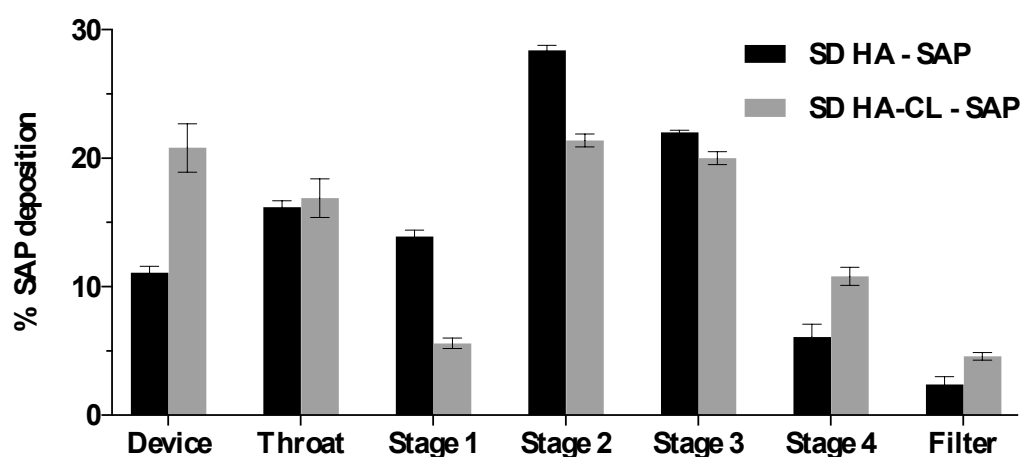


Figure 7.5. *In vitro* aerosol stage deposition of SD HA – SAP (black bars) and SD HA - CL - SAP (grey bars) using the MSLI at a flow rate of 60 L/min. Data represent mean  $\pm$  SD ( $n = 3$ ).

#### 7.4.7. *In vitro* SAP release studies

Figure 7.6. depicts SAP release profiles over time from SD HA – SAP and SD HA-CL – SAP formulations using two different *in vitro* methodologies, Franz diffusion cells and air-interface Calu-3 cell model. SAP concentrations were expressed in terms of percent total recovery through the experiments, and data were plotted as mean cumulative percentage ( $\pm$  standard deviation) of drug released over time.

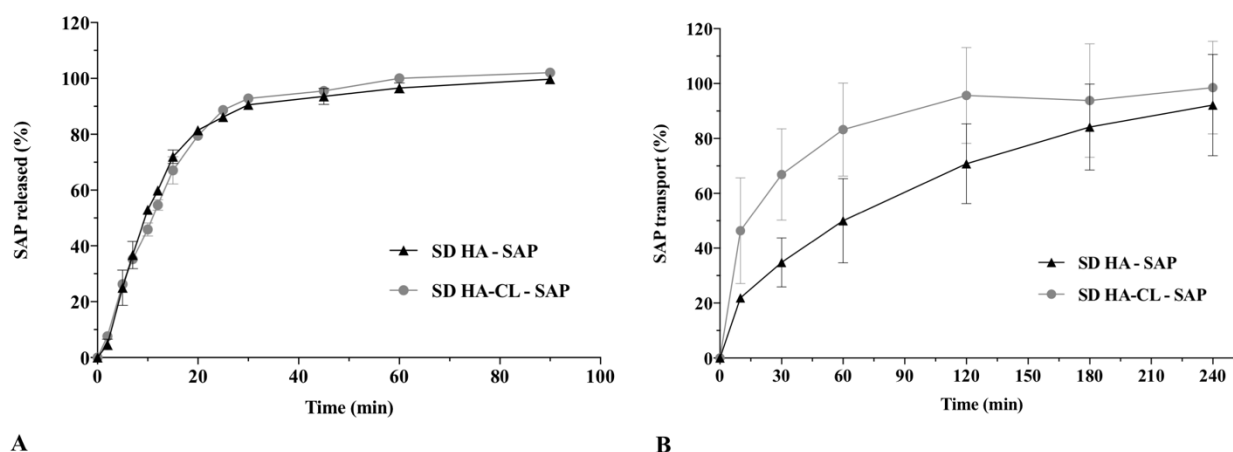


Figure 7.6. *In vitro* SAP release profiles of SD HA – SAP (black curve) and SD HA - CL - SAP (grey curve) using Franz cells (A) air-interface Calu-3 cell model (B). Data represent mean  $\pm$  SD (n = 3).

Using the Franz diffusion cells (Figure 7.6.A), hyaluronan-SAP dry powders displayed similar drug release profiles  $-f_1 = 4.7$  and  $f_2 = 72.5$ . Both the formulations were rapidly wetted when deposited on the filter membranes. This was expected as both hyaluronan and SAP are highly hydrophilic compounds. Hence, SAP quickly diffused into the media of the receptor compartment, showing a rapid release rate with  $>90\%$  of drug released within 30 min, regardless of the formulation.

The deposition of respirable dry powder aerosol formulations onto the air-interface Calu-3 cells using a modified TSI provides a more representative *in vitro* model of the *in vivo* state in terms of mucosae-particle interaction. Indeed, this system could potentially simulate the deposition of drugs to the tracheo-bronchiolar region of the lungs after inhalation. It allows particles to dissolve and diffuse into the thin aqueous layer of mucus and/or surfactant lining of the airway epithelial cells, which has been demonstrated to play an important role in determining the respiratory absorption rate (Ong et al., 2011). Therefore, this model allowed the evaluation of SAP release profile in a more physiological relevant manner. In general, the release rate of SAP from both the hyaluronan-SAP dry powders in the Calu-3 cell model was found to be slower compared to the Franz cell apparatus (Figure 7.6.B). For example, after 30 min, SD HA – SAP released  $34.8 \pm 9.0\%$  of SAP, and SD HA-CL – SAP released  $66.9 \pm 16.6\%$  of SAP. Moreover, the Calu-3 cell model was found to be a discriminative method to study SAP release process, as proved by Moore and Flanner similarity and difference factors, which evidenced different release profiles of SAP from the SD formulations  $-f_1 = 36.9$  and  $f_2 = 30.9$ . It was postulated that the water-binding ability of urea and pentylene glycol present within the HA-CL – SAP microparticulate system could have enhanced the formulation wettability and, therefore, SAP release and transport across the lung epithelium. However, the initial amount of SAP deposited on the cell layer was comparable for both formulations ( $P > 0.05$  -  $1184.6 \pm 256.0 \mu\text{g}$  for SD HA – SAP, and  $1236.7 \pm 207.2 \mu\text{g}$  for SD HA-CL – SAP), and at the end of the transport study, no significant difference ( $P > 0.05$ ) was detected between SD HA – SAP and SD HA-CL – SAP relatively to the percentage of SAP transported, remaining on the cells and trapped within the cells (Figure 7.7.). Indeed, after 240 min,  $92.2 \pm 18.4\%$  and  $98.5 \pm 16.9\%$  of SAP -from SD HA – SAP and SD HA-CL – SAP, respectively- were transported, while no drug was found trapped within

the cells. Only  $7.5 \pm 3.1\%$  of SAP from SD HA – SAP and  $1.4 \pm 0.6\%$  of SAP from SD HA-CL – SAP remained on the cells (Figure 7.7.). Therefore, SAP was almost all transported across the Calu-3 monolayer and was found in the basal compartment. Considering these results, it was hypothesized that *in vivo* SAP could exert its antioxidant and anti-inflammatory activity partly on the cell surface, and partly in the mesenchymal area, allowing for a systemic effect.

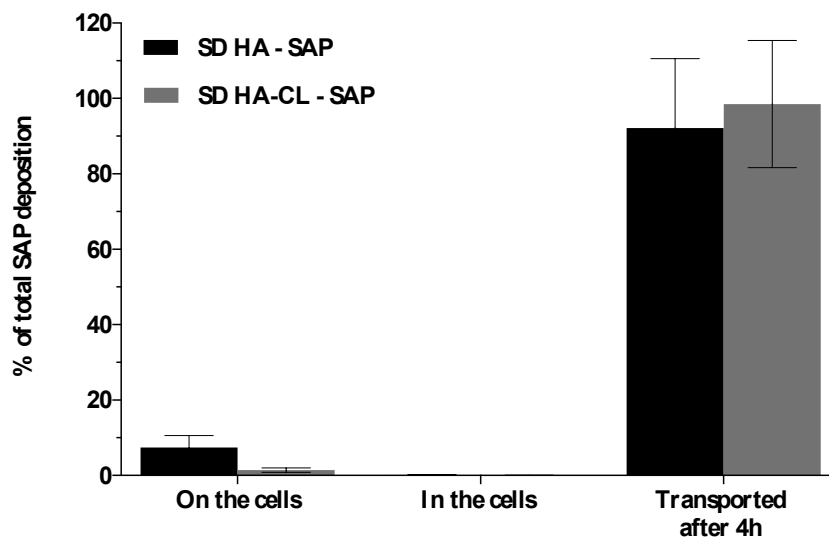


Figure 7.7. Percentage of total SAP remaining on the cell surface, inside the cells or transported to the basal compartment from SD HA – SAP (black bars) and SD HA - CL - SAP (grey bars), after 4 h. Data represent mean  $\pm$  SD (n = 3).

## 7.5. Conclusions

In this study, a novel SD HA-CL – SAP formulation was developed for the treatment of inflammatory respiratory diseases. As a control, a formulation consisting of co-spray-dried native HA and SAP was also prepared and characterized. HA-CL showed the same potential of native HA to form inhalable microparticles containing SAP. Indeed, both the reference (SD HA – SAP) and the test formulation (SD HA-CL – SAP) displayed suitable morphology, physico-chemical properties and aerosol performance for inhalation drug delivery. SAP was shown to be efficiently released and transported across an air-interface Calu-3 cell model. Future investigations will be performed to define the exact mechanism of SAP transport and the fate of such respiratory formulations *in vivo*. In conclusion, the present study provided preliminary evidence that SD HA-CL – SAP dry powder could be a promising adjunctive therapy for the treatment of pulmonary disorders like ARDS, asthma, emphysema and COPD.

## 7.6. Acknowledgements

This work was supported by a PhD grant (Arianna Fallacara) from Istituto Ricerche Applicate S.r.l. (I.R.A. S.r.l., Usmate-Velate, Monza-Brianza, Italy).

## 7.7. Conflicts of interests

The authors declare no conflict of interest.



## 7.8. References

- Adi, H., Young, P.M., Chan, H.K., Salama, R.O., Traini, D., 2010. Controlled release antibiotics for dry powder lung delivery. *Drug Dev. Ind. Pharm.* 36, 119–126.
- Albèr, C., Engblom, J., Falkman, P., Kocherbitov, V., 2015. Hydration of hyaluronan: effects on structural and thermodynamic properties. *J. Phys. Chem. B.* 119, 4211-4219.
- Allegra, L., Abraham, W.M., Fasano, V., Petrigni, G., 2008. Methacholine challenge in asthmatics is protected by aerosolised hyaluronan at high (1,000 kDa) but not low (300 kDa) molecular weight. *G. Ital. Mal. Torace* 62, 297–301.
- Bharara, A., Grossman, C., Grinnan, D., Syed, A., Fisher, B., DeWilde, C., Natarajan, R., Fowler, A.A., 2016. Intravenous vitamin C administered as adjunctive therapy for recurrent acute respiratory distress syndrome. *Case Rep. Crit. Care.*
- Buonpensiero, P., De Gregorio, F., Sepe, A., Di Pasqua, A., Ferri, P., Siano, M., Terlizzi, V., Raia, V., 2010. Hyaluronic acid improves “pleasantness” and tolerability of nebulized hypertonic saline in a cohort of patients with cystic fibrosis. *Adv. Ther.* 27, 870–878.
- Burney, P., Jarvis, D., Perez-Padilla, R., 2015. The global burden of chronic respiratory disease in adults. *Int. J. Tuberc. Lung Dis.* 19, 10-20.
- Chow, A.H., Tong, H.H., Chattopadhyay, P., Shekunov, B.Y., 2007. Particle engineering for pulmonary drug delivery. *Pharm. Res.* 24, 411-437.
- Citernesì, U.R., Beretta, L., Citernesì, L., 2015. Cross-linked hyaluronic acid, process for the preparation thereof and use thereof in the aesthetic field. Patent number: WO/2015/007773 A1.
- Collins, M.N., Birkinshaw, C., 2007. Comparison of the effectiveness of four different crosslinking agents with hyaluronic acid hydrogel films for tissue-culture applications. *J. Appl. Polym. Sci.* 104, 3183-3191.
- Collins, N.M., Birkinshaw, C., 2008. Physical properties of crosslinked hyaluronic acid hydrogels. *J. Mater. Sci. Mater. Med.* 19, 3335-3343.
- Commission, B.P., 2017. *British Pharmacopoeia*. Stationery Office, London.
- Crotty Alexander, L.E., Shin, S., Hwang, J.H., 2015. Inflammatory diseases of the lung induced by conventional cigarette smoke: a review. *Chest.* 148, 1307-1322.
- Fallacara, A., Busato, L., Pozzoli, M., Ghadiri, M., Ong, H.X., Young, P.M., Manfredini, S., Traini, D., 2018. Combination of urea-crosslinked hyaluronic acid and sodium ascorbyl phosphate for the treatment of inflammatory lung diseases: an in vitro study. *Eur. J. Pharm. Sci.* 120, 96–106.
- Fallacara, A., Manfredini, S., Durini, E., Vertuani, S., 2017a. Hyaluronic acid fillers in soft tissue regeneration. *Facial Plast. Surg.* 33, 87-96.

Fallacara, A., Vertuani, S., Panozzo, G., Pecorelli, A., Valacchi, G., Manfredini S., 2017b. Novel Artificial Tears Containing Cross-Linked Hyaluronic Acid: An In Vitro Re-Epithelialization Study. *Molecules* 22.

FDA, 1997. Guidance for Industry; Dissolution Testing on Immediate Release Solid Oral Dosage Forms.

Ferkol, T., Schraufnagel, D., 2014. The global burden of respiratory disease. *Ann. Am. Thorac. Soc.* 11, 404-406.

Foco, A., Gasperlin, M., Kristl, J., 2005. Investigation of liposomes as carriers of sodium ascorbyl phosphate for cutaneous photoprotection. *Int J Pharm.* 291, 21-29.

Garantziotis, S., Brezina, M., Castelnovo, P., Drago, L., 2016. The role of hyaluronan in the pathobiology and treatment of respiratory disease. *Am. J. Physiol. Lung Cell Mol. Physiol.* 310, L785-L795.

Gavina, M., Luciani, A., Vilella, V.R., Esposito, S., Ferrari, E., Bressani, I., Casale, A., Bruscia, E.M., Maiuri, L., Raia, V., 2013. Nebulized hyaluronan ameliorates lung inflammation in cystic fibrosis mice. *Pediatr. Pulmonol.* 48, 761–771.

Haghi, M., Young, P.M., Traini, D., Jaiswal, R., Gong, J., Bebawy, M., 2010. Time- and passage-dependent characteristics of a Calu-3 respiratory epithelial cell model. *Drug Dev. Ind. Pharm.* 36, 1207–1214.

Hwang, S.M., Kim, D.D., Chung, S.J., Shim, C.K., 2008. Delivery of ofloxacin to the lung and alveolar macrophages via hyaluronan microspheres for the treatment of tuberculosis. *J. Control. Release.* 129, 100-106.

Jiang, D., Liang, J., Fan, J., Yu, S., Chen, S., Luo, Y., Prestwich, G.D., Mascarenhas, M.M., Garg, H.G., Quinn, D.A., Homer, R.J., Goldstein, D.R., Bucala, R., Lee, P.J., Medzhitov, R., Noble, P.W., 2005. Regulation of lung injury and repair by Toll-like receptors and hyaluronan. *Nat. Med.* 11, 1173– 1179.

Jiang, D., Liang, J., Noble, P.W., 2010. Regulation of non-infectious lung injury, inflammation, and repair by the extracellular matrix glycosaminoglycan hyaluronan. *Anat. Rec. (Hoboken).* 293, 982- 985.

Kafedjiiski, K., Jetti, R.K., Föger, F., Hoyer, H., Werle, M., Hoffer, M., Bernkop-Schnürch, A., 2007. Synthesis and in vitro evaluation of thiolated hyaluronic acid for mucoadhesive drug delivery. *Int. J. Pharm.* 343, 48-58.

Karner, S., Urbanetz, N.A., 2011. The impact of electrostatic charge in pharmaceutical powders with specific focus on inhalation-powders. *J. Aerosol Sci.* 42, 428-445.

Kleniewska, P., Pawliczak, R., 2017. The participation of oxidative stress in the pathogenesis of bronchial asthma. *Biomed. Pharmacother.* 94, 100-108.

Larsson, N., Rankin, G.D., Bicer, E.M., Roos-Engstrand, E., Pourazar, J., Blomberg, A., Mudway, I.S., Behndig, A.F., 2015. Identification of vitamin C transporters in the human airways: a cross-sectional in vivo study. *BMJ Open*. 5, e006979.

Li, Y., Han, M., Liu, T., Cun, D., Fang, L., Yang, M., 2017. Inhaled hyaluronic acid microparticles extended pulmonary retention and suppressed systemic exposure of a short-acting bronchodilator. *Carbohydr. Polym.* 172.

Li, Y., Li, G., 2016. Is vitamin C beneficial to patients with CAP? *Curr. Infect Dis. Rep.* 18, 24.

MacNee, W., 2001. Oxidative stress and lung inflammation in airways disease. *Eur. J. Pharmacol.* 429, 195-207.

Martinelli, F., Balducci, A.G., Kumar, A., Sonvico, F., Forbes, B., Bettini, R., Buttini, F., 2017. Engineered sodium hyaluronate respirable dry powders for pulmonary drug delivery. *Int. J. Pharm.* 517, 286-295.

Moldoveanu, B., Otmishi, P., Jani, P., Walker, J., Sarmiento, X., Guardiola, J., Saad, M., Yu, J., 2009. Inflammatory mechanisms in the lung. *J. Inflamm. Res.* 2, 1-11.

Moore, H.H., Flanner, J.W., 1996. Mathematical comparison of dissolution profiles. *Pharm. Technol.* 20, 64-74.

Moyano, M.A., Broussalis, A.M., Segall, A.I., 2010. Thermal analysis of lipoic acid and evaluation of the compatibility with excipients. *J. Therm. Anal. Calorim.* 99, 631-637.

Nichols, D.P., Chmiel, J.F., 2015. Inflammation and its genesis in cystic fibrosis. *Pediatr. Pulmonol.* 50, S539-S556.

Ong, H.X., Traini, D., Bebawy, M., Young, P.M., 2011. Epithelial profiling of antibiotic controlled release respiratory formulations. *Pharm. Res.* 28, 2327-2338.

Organization, W.H., 2017. World health statistics 2017: monitoring health for the SDGs, sustainable development goals. World Health Organization, Geneva.

Oudijk, E.D., Lammers, J.J., Koenderman, L., 2003. Systemic inflammation in chronic obstructive pulmonary disease. *Eur. Respir. J.* 22, 5s-13s.

Panagopoulou, A., Vázquez Molina, J., Kyritsis, A., Monleón Pradas, M., Vallés Lluch, A., Gallego Ferrer, G., Pissis, P., 2013. Glass Transition and Water Dynamics in Hyaluronic Acid Hydrogels. *Food Biophys.* 8, 192-202.

Patton, J.S., 1999. Inhalation delivery of therapeutic peptides and proteins. *J. Aerosol Med.* 12, 45-46.

Petrigni, G., Allegra, L., 2006. Aerosolised hyaluronic acid prevents exercise-induced bronchoconstriction, suggesting novel hypotheses on the correction of matrix defects in asthma. *Pulm. Pharmacol. Ther.* 19, 166-171.

- Pilcer, G., Amighi, K., 2010. Formulation strategy and use of excipients in pulmonary drug delivery. *Int. J. Pharm.* 392, 1-19.
- Pirabbasi, E., Shahar, S., Manaf, Z.A., Rajab, N.F., Manap, R.A., 2016. Efficacy of ascorbic acid (vitamin C) and/N-acetylcysteine (NAC) supplementation on nutritional and antioxidant status of male chronic obstructive pulmonary disease (COPD) patients. *J. Nutr. Sci. Vitaminol. (Tokyo)* 62, 54-61.
- Salama, R.O., Traini, D., Chan, H.K., Sung, A., Ammit, A.J., Young, P.M., 2009. Preparation and evaluation of controlled release micro- particles for respiratory protein therapy. *J. Pharm. Sci.* 98, 2709–2717.
- Sebti, T., Amighi, K., 2006. Preparation and in vitro evaluation of lipidic carriers and fillers for inhalation. *Eur. J. Pharm. Biopharm.* 63, 51-58.
- Servaty, R., Schiller, J., Binder, H., Arnold, K., 2001. Hydration of polymeric components of cartilage--an infrared spectroscopic study on hyaluronic acid and chondroitin sulfate. *Int. J. Biol. Macromol.* 28, 121-127.
- Tulbah, A.S., Ong, H.X., Lee, W.H., Colombo, P., Young, P.M., Traini, D., 2016. Biological Effects of Simvastatin Formulated as pMDI on Pulmonary Epithelial Cells. *Pharm. Res.* 33, 92-101.
- Wong, J., Lin, Y.W., Kwok, P.C., Niemelä, V., Crapper, J., Chan, H.K., 2015. Measuring Bipolar Charge and Mass Distributions of Powder Aerosols by a Novel Tool (BOLAR). *Mol. Pharm.* 12, 3433-3440.
- Yang, I.V., Lozupone, C.A., Schwartz, D.A., 2017. The environment, epigenome, and asthma. *J. Allergy Clin. Immunol.* 140, 14-23.





## CHAPTER 8

### ***In vitro* characterization of physico-chemical properties, cytotoxicity, bioactivity of urea-crosslinked hyaluronic acid and sodium ascorbyl phosphate nasal powder formulation**

This chapter was published in *International Journal of Pharmaceutics*, 558, 341-350 (2019) under the title:

“Physico-chemical properties, *in vitro* cytotoxicity and bioactivity of urea-crosslinked hyaluronic acid and sodium ascorbyl phosphate nasal powder formulation”

*Authors: Arianna Fallacara<sup>a,b</sup>, Laura Busato<sup>a,b</sup>, Michele Pozzoli<sup>a</sup>, Maliheh Ghadiri<sup>a</sup>, Hui Xin Ong<sup>a</sup>, Paul M. Young<sup>a</sup>, Stefano Manfredini<sup>b</sup>, Daniela Traini<sup>a</sup>, \**

<sup>a</sup> Respiratory Technology, Woolcock Institute of Medical Research and Discipline of Pharmacology, Faculty of Medicine and Health, The University of Sydney, 431 Glebe Point Road, Glebe, NSW 2037, Australia.

<sup>b</sup> Department of Life Sciences and Biotechnology, University of Ferrara, Via L. Borsari 46, 44121 Ferrara, Italy.

**\* Corresponding author:**

Prof. Daniela Traini: [daniela.traini@sydney.edu.au](mailto:daniela.traini@sydney.edu.au); Tel: +61 2 91140352.

DOI: 10.1016/j.ijpharm.2019.01.012.





## 8.0. Preface

An integral part of the management of asthma is often represented by the treatment of inflammatory diseases of the upper airways, such as allergic rhinitis (AR) and chronic rhinosinusitis (CRS). Indeed, being upper and lower airways anatomically, histologically and immunologically linked, asthma, AR and CRS frequently coexist, as respiratory inflammation may start at one site and extend to another. The study described in chapter 6 has provided preliminary evidences that the combination urea-crosslinked hyaluronic acid – sodium ascorbyl phosphate (HA-CL - SAP) could be suitable as adjunctive therapy for inflammatory pulmonary disorders such as asthma. Considering all this, and the need to reduce the long-term use of the common treatments based on intranasal corticosteroids -that may involve the risk of epistaxis, nasal irritation and other complications-, a nasal freeze-dried formulation consisting of HA-CL and SAP (LYO HA-CL - SAP) was developed as novel therapy for inflammatory diseases of the upper airways. Hence, chapter 8 describes the preparation and the *in-vitro* characterization of LYO HA-CL – SAP in terms of physico-chemical properties and bioactivity.

## 8.1. Abstract

An innovative lyophilized dry powder formulation consisting of urea-crosslinked hyaluronic acid (HA-CL) and sodium ascorbyl phosphate (SAP) -LYO HA-CL – SAP- was prepared and characterized *in vitro* for physico-chemical and biological properties. The aim was to understand if LYO HA-CL – SAP could be used as adjuvant treatment for nasal inflammatory diseases. LYO HA-CL – SAP was suitable for nasal delivery and showed to be not toxic on human nasal septum carcinoma-derived cells (RPMI 2650 cells) at the investigated concentrations. It displayed porous, polygonal particles with unimodal, narrow size distribution, mean geometric diameter of  $328.3 \pm 27.5 \mu\text{m}$ , that is appropriate for nasal deposition with no respirable fraction and 88.7% of particles with aerodynamic diameter  $> 14.1 \mu\text{m}$ . Additionally, the formulation showed wound healing ability on RPMI 2650 cells, and reduced interleukin-8 (IL-8) level in primary nasal epithelial cells pre-induced with lipopolysaccharide (LPS). Transport study across RPMI 2650 cells showed that HA-CL could act not only as carrier for SAP and active ingredient itself, but potentially also as mucoadhesive agent. In conclusion, these results suggest that HA-CL and SAP had anti-inflammatory activity and acted in combination to accelerate wound healing. Therefore, LYO HA-CL – SAP could be a potential adjuvant in nasal anti-inflammatory formulations.

**Keywords:** anti-inflammatory; hyaluronic acid; nasal diseases; sodium ascorbyl phosphate; urea-crosslinked hyaluronic acid; wound healing.

## 8.2. Introduction

The nose is an olfactory organ, and also represents the first tract of the respiratory system, with pivotal functions: filtration, warming and moistening of the inhaled air; drainage of paranasal sinuses; sneezing; heat regulation; nasopulmonary reflexes. Hence, nasal mucosal health and proper nasal airflow are essential for the accomplishment of nasal functions (Elad et al., 2008; Jones, 2001; Patel, 2017).

Every day, the nasal passages are exposed to several pathogens that could enhance inflammation, oxidative stress, wounding and infection (Helms and Miller, 2006; Hong et al., 2016). Allergic rhinitis (AR) is one of the most common chronic disease of the nasal mucosa, induced by an Immunoglobulin-E-dependent inflammation due to allergens' exposure (Greiner et al., 2011; Montoro et al., 2007; Small and Kim, 2011). AR can evolve in chronic rhinosinusitis (CRS) (Fokkens et al., 2012; Helms and Miller, 2006; Licari et al., 2017a; Johansson et al., 2003), and AR and CRS frequently coexist with asthma. Indeed, respiratory inflammation may start at one site and extend to another, as upper and lower airways are anatomically, histologically and immunologically linked (Jarvis et al., 2012; Licari et al., 2017a, b; Marseglia et al., 2011). Therefore, the treatment of AR and CRS also represents an integral part of the management of asthma (Licari et al., 2017a; Marseglia et al., 2011). Intranasal corticosteroids are the mainstay therapy for AR and CRS, exerting an anti-inflammatory action and thus relieving symptoms (Helms and Miller, 2006; Licari et al., 2017a). However, their long-term use may have side effects (Campbell, 2018; Fokkens et al., 2012; Licari et al., 2017a). To limit these complications and drug resistant refractory phenomena, adjunctive therapeutic agents with anti-inflammatory, antioxidant and wound healing activity -like resveratrol, alpha-tocopherol (vitamin E), curcumin, N-acetyl-L-cysteine, bromelain, quercetin, beta-carotene (provitamin A), vitamin C (ascorbic acid) and hyaluronic acid (HA)- are currently being investigated for their ability to restore and maintain nasal mucosal health and functions (Albano et al., 2016; Baumeister et al., 2009; Bozdemir et al., 2016; Casale et al., 2014, 2016; Cassandro et al., 2015; Chauhan et al., 2016; Ciofalo et al., 2017; Emiroglu et al., 2017; Helms and Miller, 2006; Hong et al., 2016; Horváth et al., 2016; Podoshin et al., 1991; Sagit et al., 2011; Testa et al., 2017). The present study focused on vitamin C and HA derivatives.

Vitamin C represents a major low molecular weight antioxidant of the respiratory tract lining fluid (Bastacky et al., 1995; van der Vliet et al., 1999; Wu et al., 1996). Vitamin C has been shown to scavenge radical oxygen species (ROS), thus protecting the surface of the airway epithelium (Mudway and Kelly, 2000) and intracellular DNA, lipids and proteins from oxidative stress (Li and Schellhorn, 2007). Oral vitamin C supplementation, in combination with other oral antioxidants and intranasal steroids, was found to be beneficial in the management of AR (Chauhan et al., 2016) and nasal polyposis (Sagit et al., 2011). Additionally, intranasal vitamin C was shown to decrease nasal secretions, blockage and edema in patients with AR (Podoshin et al., 1991).

High-molecular weight ( $\geq 1$  MDa) hyaluronic acid (HA) is an important component of the normal airway secretions, produced by submucosal glands and by superficial airway epithelial cells (Basbaum and Finkbeiner, 1988; Fallacara et al., 2018a; Monzon et al., 2006). HA plays a central role in the homeostasis of the whole respiratory apparatus, influencing bio-mechanical forces, hydric balance, cellular functions, growth factors' activity and cytokines'

behaviour (Casale, 2016; Fallacara et al., 2018a; Petrigini and Allegra, 2006). In the nasal epithelium, HA promotes mucociliary clearance and sustains mucosal surface healing (Gelardi et al., 2013a). Hence, intranasal exogenous HA may represent an anti-inflammatory, antioxidant, and immuno-modulating agent highly beneficial to treat the inflammatory components of AR (Fallacara et al., 2018a; Gelardi et al., 2013b, 2016), CRS (Casale et al., 2014; Cassandro et al., 2015) and other upper respiratory diseases like acute rhinosinusitis (Ciofalo et al., 2017a, b) and bacterial acute rhinopharyngitis (Varricchio et al., 2014). Additionally, intranasal HA enhances the regeneration and the morphofunctional recovery of nasal ciliated cells in patients undergoing surgery, thus promoting rhino-sinusal remodeling (Cassano et al., 2016). The major limitations of HA are its fluid nature and rapid degradation, leading to a short residence time in the nose. Therefore, HA can be crosslinked in order to synthesize novel derivatives with improved mechanical properties and bioactivity (Chen, 2012).

The combination of sodium ascorbyl phosphate -SAP, a pro-drug of vitamin C with improved physico-chemical stability- and urea-crosslinked hyaluronic acid -HA-CL, a novel biopolymer with promising bioactivity (Citernesi et al., WO/2015/007773 A1, 2015; Fallacara et al., 2017a, b)- has recently shown potential to treat and prevent lung diseases sustained by inflammation and oxidative stress (Fallacara et al., 2018b, submitted for publication). Hence, the present work aimed to study if the combination of SAP and HA-CL could be beneficial as adjuvant therapy to treat inflammatory diseases of the upper airways. A novel nasal dry powder formulation containing SAP and HA-CL was developed using a freeze-dried technique, and characterized for its physico-chemical behaviour, *in vitro* cytotoxicity and bioactivity on human nasal epithelial cells.

### **8.3. Materials and Methods**

#### **8.3.1. Materials**

Urea-crosslinked hyaluronic acid (HA-CL, molecular weight 2.0-4.0 MDa –raw material containing also pentylene glycol) was kindly donated by I.R.A. Srl (Istituto Ricerche Applicate, Usmate-Velate, Monza-Brianza, Italy). HA-CL was provided as raw material containing pentylene glycol, and it was used as supplied. Therefore, a 1% (w/v) 1:1 HA-CL – SAP solution contained also 0.75% (w/v) pentylene glycol. Sodium ascorbyl phosphate (SAP) was purchased from DSM Nutritional Products Ltd (Segrate, Milano, Italy). Phosphate buffered saline (PBS, pH = 7.4, 0.01 M) used for the physico-chemical characterization of the formulation was supplied by Sigma-Aldrich (Sydney, NSW, Australia). Water was purified by Milli-Q reverse Osmosis (Molsheim, France). Polyamide membrane filters 0.45 µm pore size were obtained from Sartorius Biolab Products (Goettingen, Germany), while wax foils were provided by Parafilm M, Bemis Company Inc. (Oshkosh, WI, USA).

The unit dose system (UDS) powder device was purchased from Pfeiffer, Aptar Pharma division (Radolfzell, Germany).

Human nasal septum carcinoma-derived cells (RPMI 2650) were purchased from the American Type Cell Culture Collection (ATCC, Manassas, VA, USA). Snapwell™ cell culture inserts (1.13 cm<sup>2</sup> surface area, polyester, 0.4 µm pore size) and 96-well plates were obtained from Corning Costar (Lowell, MA, USA). Disposable cytology brushes (Model BC-

202D-2010) were provided by Olympus Australia Pty. Ltd. (Notting Hill, VIC, Australia). All other culture plastics were from Sarstedt (Adelaide, SA, Australia). Minimum essential medium (MEM), PBS for cell cultivation, Hank's balanced salt solution (HBSS), foetal bovine serum (FBS) and 0.25% trypsin-EDTA were all purchased from Gibco by Life Technologies (Sydney, NSW, Australia). Bronchial epithelial growth medium (BEGM) and SingleQuots™ kit were provided by Lonza (Walkersville, MD, USA). Lipopolysaccharide (LPS) from Escherichia coli, trans-retinoic acid, non-essential amino acids solution, 200 mM L-glutamine solution were purchased from Sigma-Aldrich (Sydney, NSW, Australia). CellLytic™ buffer was obtained from Invitrogen (Sydney, NSW, Australia). Methyl tetrazolium salt (MTS) reagent -CellTiter 96® Aqueous One Solution Cell Proliferation Assay- for cell viability test was purchased from Promega (Sydney, NSW, Australia). Bovine collagen was provided by Nutacon (Leimuiden, Netherlands). Rat collagen type I and enzyme-linked immuno assay (ELISA) kit for determination of the inflammation marker interleukin-8 (IL-8) were obtained from BD Bioscience (Sydney, NSW, Australia). All solvents were obtained from VWR Prolabo Chemicals (Milan, Italy) and were of HPLC grade.

### **8.3.2. Preparation of the freeze-dried formulation**

HA-CL and SAP were dissolved into 50 mL of milli-Q water kept under constant magnetic stirring, at room temperature, overnight. A 1% (w/v) 1:1 HA-CL - SAP solution was obtained and placed in a -80°C freezer for 24 h. Then, the solution was lyophilized for 24 h, at -100°C, with a vacuum degree of 0.1 mbar, using an Alpha 2-4 LSC plus freeze dryer (Martin Christ, Osterode am Harz, Germany) equipped with a rotary vane Vacuubrand R26 pump (Wertheim, Germany). No cryoprotectant was added to the formulation. At the end of the lyophilisation process, the sample was stored in a desiccator for 24 h, manually grinded with a spatula and passed through a stainless steel sieve (300 µm pore-size).

### **8.3.3. Physico-chemical characterization**

#### **8.3.3.1. Chemical quantification of SAP by high-performance liquid chromatography**

SAP was quantified using a high-performance liquid chromatography (HPLC) method that was adapted from literature (Foco et al., 2005). A Shimadzu Prominence UFLC system equipped with DGU-20A5R Prominence degassing unit, LC-20 AD solvent delivery unit, SIL-20A HT autosampler and SPD-20A UV/VIS detector was employed (Shimadzu Corporation, Tokyo, Japan). A volume of 50 µL of sample was injected using 40:60 (% v/v) acetonitrile:0.3 M phosphate buffer (pH = 4) as mobile phase, at a flow rate of 2.0 mL/min, in isocratic mode with a Luna NH<sub>2</sub> column (5 µm, 4.6 x 150 mm) (Phenomenex, Sydney, NSW, Australia). SAP retention time was 6 min. The concentration of SAP was measured at a wavelength of 258 nm from the peak area correlated with a predetermined standard curve over the range 0.1-1000 µg/mL ( $R^2 = 1$ ).

#### 8.3.3.2. Morphological analysis

Scanning electron microscopy (SEM) was used to investigate the morphology and surface properties of the lyophilized formulation containing HA-CL and SAP (LYO HA-CL – SAP). The analysis was carried out using a JCM-6000 benchtop scanning electron microscope (Jeol, Tokyo, Japan), operating at 10 kV. Prior to imaging, the sample was deposited on a carbon sticky tape, placed onto aluminium stubs, and gold-coated for 2 min using an automated sputter coater (Smart Coater, Jeol, Tokyo, Japan).

#### 8.3.3.3. Particle size analysis

Particle diameter and particle size distribution of LYO HA-CL – SAP were determined by laser diffraction (Mastersizer 3000, Malvern, Worcestershire, UK). Approximately 10 mg of sample were dispersed in air using the Scirocco Aero-S dry dispersion unit (Malvern, Worcestershire, UK), with a feed pressure of 4 bars, a feed rate of 100% and a total time of analysis set at 3 s. Measurements were carried out in triplicate, with an obscuration value between 0.1% and 15%, and a reference refractive index of 1.33. The maximum particle size for 10, 50 and 90% of the cumulative volume distribution of the sample (defined as Dv10, 50 and 90, respectively) were used to describe particle size. The width of the particle size distribution was expressed by the Span index. Data were reported as mean  $\pm$  standard deviation.

#### 8.3.3.4. Thermal analysis

The thermal response of LYO HA-CL – SAP was assessed using differential scanning calorimetry (DSC - DSC823e; Mettler-Toledo, Schwerzenbach, Switzerland). Roughly 5 mg of sample were weighed, crimp-sealed in DSC standard 40  $\mu$ L aluminium pans and heated at 10°C/min between -20 and 300°C. The endothermic and exothermic peaks were determined using STARe software V.11.0x (Mettler Toledo, Greifensee, Switzerland).

Additionally, the temperature stability and solvent evaporation of the freeze-dried formulation were investigated using the thermal gravimetric analysis (TGA - Mettler-Toledo, Switzerland). Approximately 5 mg of sample were placed onto aluminium crucible pans. The weight loss of the sample was evaluated over a temperature range of 20-400°C, with a scanning rate of 5°C/min, under constant nitrogen gas. Data were analyzed using STARe software V.11.0x (Mettler Toledo, Greifensee, Switzerland) and expressed as the percentage of weight loss with respect to initial sample weight.

#### 8.3.3.5. In vitro SAP release study

Franz's diffusion cells (25 mm internal diameter, multi-station VB6 apparatus, PermeGear Inc., Hellertown, PA, USA) were used to study SAP release profile from LYO HA-CL – SAP, according to a previously published protocol (Ong et al., 2011). Briefly, polyamide membrane filters (0.45  $\mu$ m pore size) were hydrated by sonication in PBS (pH = 7.4, 0.01 M) for 30 min, cut and placed between the receiver and donor compartments

of the diffusion cells that were maintained at  $37 \pm 0.5^\circ\text{C}$ . Samples were placed in the donor compartments in order to have  $\sim 5$  mg of SAP on the surface of the membranes, which were sealed using a wax foil to prevent evaporation. The receiver compartments were filled with 23 mL of PBS continuously stirred at 150 rpm. At defined time points (0, 5, 10, 15, 20, 30, 45, 60, 90, 120 min), 0.5 mL of samples were withdrawn from the receptor compartments and replaced with equal volumes of pre-warmed PBS. After 120 min, each filter was washed with 5 mL of PBS and then sonicated with another 5 mL of PBS for 10 min. Samples were assayed for SAP concentration using HPLC. Experiments were performed in triplicate and data were expressed and plotted as mean  $\pm$  standard deviation of the cumulative percentage of SAP released over time.

#### *8.3.3.6. Aerosol performance by cascade impaction*

The aerodynamic performance of LYO HA-CL – SAP delivered using the UDS device was investigated using a British Pharmacopoeia Apparatus E – Next Generation Impactor (NGI -Westech W7; Westech Scientific Instruments, Upper Stondon, UK), equipped with a 2-L glass expansion chamber (EC), according to the Food and Drug Administration (FDA) guidance for industry, and as previously reported in literature (FDA CDER, 2003; Pozzoli et al., 2016a, b, 2017).

Considering that the human nose can accommodate about 10-25 mg of powder *per nostril per shot* (Elmowafy et al., 2014), 16 mg of LYO HA-CL – SAP (corresponding to  $\sim 5$  mg of SAP) were loaded into the UDS device. Briefly, the device was connected to the inlet of the EC, that was assembled on the NGI. A rotary pump (Westech Scientific Instruments, Upper Stondon, UK) was connected to the NGI. The test was performed by actuating the device with an air flow of 15 L/min, calibrated using a flow meter (Model 4040, TSI Precision Measurement Instruments, Aachen, Germany), for 4 s. Each impactor stage was washed with the following volumes of deionized water: EC 25 mL; device, connection tube and first stage 10 mL; all other stages 5 mL. SAP was quantified using the HPLC method. Experiments were carried out in triplicate and data were expressed as mean  $\pm$  standard deviation.

#### *8.3.3.7. In-line geometric aerosol laser diffraction analysis*

Laser diffraction (SprayTec<sup>TM</sup>, Malvern Instruments, Worcestershire, UK) was used to measure the geometric particle size distribution of LYO HA-CL – SAP emitted from the UDS device (filled with 16 mg of formulation, corresponding to  $\sim 5$  mg of SAP). The device was connected to the measurement cell at a fixed angle of  $30^\circ$ , with an extraction flow of 15 L/min. Three independent analyses were performed for 4 s, with an acquisition rate of 2.5 kHz. Results were expressed as mean  $\pm$  standard deviation.

#### **8.3.4. *In vitro biological studies on nasal cell models***

Cytotoxicity, wound healing activity, drug deposition and transport were investigated using RPMI 2650 human nasal cell line. Additionally, anti-inflammatory activity was explored using primary brushed nasal epithelial cells.

#### 8.3.4.1. Cultivation of RPMI 2650 cell line

RPMI 2650 immortalized human nasal cell line were grown and passaged according to ATCC protocol and as previously described in literature (Bai et al., 2008; Kreft et al., 2015; Pozzoli, 2016a,b, 2017; Reichl and Becker, 2012). Briefly, cells between passages 17-25 were cultured in 75 cm<sup>2</sup> flasks containing MEM supplemented with 10% (v/v) FBS, 1% (v/v) non-essential amino acid solution and 2 mM L-glutamine, and maintained in a humidified atmosphere of 95% air, 5% CO<sub>2</sub>, at 37°C.

Liquid covered cultures were obtained by seeding RPMI 2650 cells ( $5 \times 10^4$  cells/well) in a volume of 100 µL into 96-well plates, and were used to perform cell viability assay within 24 h from the seeding.

Additionally, an air-liquid interface (ALI) nasal model was established using Snapwell<sup>TM</sup> cell culture inserts. In brief, inserts were coated with 250 µl of 1 µg/ml rat collagen type 1 solution in PBS and incubate overnight at 37°C to create the appropriate adherence of the cells to the membrane (Wengst and Reichl, 2010). 200 µl of RPMI 2650 nasal cells suspension ( $2.5 \times 10^6$  cell/ml) were seeded on Snapwell<sup>TM</sup> and after 24 h the medium from the apical compartment was withdrawn, resulting in an ALI model. The medium in the basolateral chamber was replaced 3 times per week. Wound healing and deposition/transport studies were performed 14 days after the seeding.

#### 8.3.4.2. MTS cytotoxicity assay on RPMI 2650 cells

The *in vitro* cytotoxicity of LYO HA-CL – SAP was assessed on a liquid covered culture of RPMI 2650 cells. Sample solutions with increasing concentrations of the formulation were aseptically prepared, added to the cells and, after 3 days, a MTS assay was performed to measure cellular metabolic activity.

Briefly,  $5 \times 10^4$  cells were seeded per well in a volume of 100 µL into 96-well plates. Cells were incubated overnight at 37°C in a humidified atmosphere with 5% CO<sub>2</sub>. On the second day, 100 µL of pre-warmed solutions of LYO HA-CL – SAP were added to each well. The lyophilized formulation was investigated in a SAP concentration range from 8.0 mM to 60.9 nM. Background controls (medium) and untreated controls (untreated cells) were included in the experiment. Plates were incubated for 72 h at 37°C in a humidified atmosphere with 5% CO<sub>2</sub>. Cells were then analysed for viability. Hence, 20 µL of MTS reagent were added to each well and the plates were incubated for another 3 h in the same conditions. Finally, the 96 well-plates were read at 490 nm using a SpectraMax microplate reader. The absorbance values were directly proportional to cell viability (%). Experiments were performed in triplicate. Data were expressed as mean ± standard deviation of the % cell viability relative to untreated control, and plotted against SAP concentration (nM) on a logarithmic scale.

#### 8.3.4.3. Deposition/transport study on RPMI 2650 cells

The aerosol deposition of LYO HA-CL – SAP on RPMI 2650 cell surface was studied using a custom-built 3D printed modified expansion chamber (MC) (Pozzoli et al., 2016a).



Prior to the experiment, three inserts were washed with pre-warmed HBSS and fitted into the upper hemisphere of the MC. As described above, a total dose of 16 mg of formulation (corresponding to ~ 5 mg of SAP, 1 shot/actuation) was delivered with the UDS device into the MC. The cell inserts were then removed from the MC and transferred into a 6-well plate, containing 1.5 mL/well of fresh pre-warmed HBSS. At defined time point (15, 30, 45, 60, 90, 120, 150, 180, 210, 240 min), 200 µL of samples were collected from the basal chamber and replaced with the same volume of fresh HBSS buffer. After 4 h, the apical surface of the epithelia was washed twice with 300 µL of HBSS in order to collect any remaining drug on the cells. At the end of the experiment, cells were washed with 300 µL of HBSS, scraped from the insert membrane, and lysed with 500 µL of CelLytic™ buffer in order to quantify intracellular SAP. Samples were centrifuged (10 min, 10,000 x g, 4°C) and the supernatants were analyzed for SAP concentration by HPLC. Experiments were performed in triplicate. The initial amount of SAP deposited on the cell layer was calculated as the sum of SAP mass transported, remaining on the epithelium and recovered inside the cells at the end of the experiment. Data were plotted as mean ± standard deviation of the cumulative percentage of SAP transported over time.

#### 8.3.4.4. *Physical injury and wound healing assay on RPMI 2650 cells*

Wound healing properties of LYO HA-CL – SAP were evaluated on ALI RPMI 2650 cell layer. The cells were mechanically scraped using a sterile 200 µl pipette tip to form three homogenous and parallel scratches. After scraping, the wells were allocated into the upper hemisphere of the MC, and the formulation was subsequently deposited on the cell layers as described above. The healing of the layers was monitored via a time-lapse microscopy. Immediately after wounding and deposition, the Snapwells™ plates were transferred to the built-in chamber of a Nikon Eclipse Ti (Nikon, Tokyo, Japan) equipped with Clear State Solution humidifier (Clear State Solution, Mount Waverly, VIC, Australia) and CO<sub>2</sub> controller which provided a humidified CO<sub>2</sub> atmosphere at 37°C. Images of the scratches were captured by a CoolSNAP ES2 high resolution digital camera (Photometrics, Tucson, AZ, USA) every 20 min over 24 h. Images were analysed with FIJI (NIH), wound edges were manually selected and wound area was automatically calculated. Experiments were performed in triplicate. Data were expressed as mean ± standard deviation of the percentage of wound closed according to the following equation (Eq. 8.1):

$$WC = \frac{W_i - W_t}{W_i} \times 100 \quad (\text{Eq. 8.1.})$$

where WC is the wound closure (%),  $W_i$  is the initial area of wound and  $W_t$  is the area of the wound at certain time.

#### 8.3.4.5. *Sampling, expansion and ALI cultivation of brushed nasal epithelial cells*

Nasal cells were obtained from 5 healthy volunteers between the ages of 20 and 30 through nasal brushing biopsies, and cultured according to methodologies as previously described (Müller et al., 2013). Brushings were performed only on volunteers without any

upper respiratory tract disease and infection for at least 4 weeks prior to sampling. Briefly, a cytology brush was inserted approximately 5 cm into the volunteers' naris, and the inferior turbinate and the nasal epithelium were gently brushed. Strips of ciliated nasal epithelium were obtained, with each brushing containing up to 10,000 cells.

Prior to cell seeding, the microwell plates, flasks, and Snapwell™ inserts were coated for 1 h with 0.5 mL, 1 mL, and 0.1 mL of 0.3 mg/mL of bovine collagen, respectively, and were air-dried. The strips of ciliated nasal epithelium were grown on collagen-coated tissue culture 12-well plates in BEGM hormonally supplemented with SingleQuots™ for approximately 1 week, changing cell medium every other day. The confluent basal cells were then expanded onto a collagen coated 25 cm<sup>2</sup> flask with the BEGM replaced three times per week. When cultures reached ~ 80% confluency, the basal cells were detached with 0.25% trypsin–EDTA and seeded with a density of 200,000–250,000 cells per well onto collagen-coated Snapwell™ cell culture inserts. At this stage, the cells were fed with ALI medium made up of 1:1 BEGM:DMEM 4.5 g/L D-glucose including SingleQuots until 100% confluent (into 1-2 days). Primary human basal epithelial cells were then exposed to an ALI interface: to allow for cell differentiation, ALI medium supplemented with additional 100 nM all-trans-retinoic acid was placed only in the basolateral chamber (Hirst et al., 2014; Lee et al., 2005; Yoo et al., 2003). The medium was changed three times per week, and any apical surface liquid or mucus was removed. Cilia started to re-generate after 12 days from the establishment of the ALI conditions, and become visible under the microscope from day 21 ALI.

#### *8.3.4.6. Pro-inflammatory IL-8 expression in brushed nasal epithelial cells*

The expression of the pro-inflammatory cytokine IL-8 was evaluated using the ALI primary nasal cells treated with LYO HA-CL – SAP (150 µg/mL), before, after and without LPS exposure. The effect of the formulation on cells was compared with unstimulated and untreated cells (control cells, i.e. cells in culture medium, without LPS and formulations) and LPS-stimulated but untreated cells (positive control, i.e. cells exposed only to 10 ng/mL LPS).

Firstly, LYO HA-CL – SAP was evaluated for its ability to influence IL-8 production in non-inflamed nasal cells. Subsequently, cells were incubated at 37 °C, 5% CO<sub>2</sub>, for 24 h, with a pre-warmed solution of LYO HA-CL – SAP. On the second day, cell culture medium was withdrawn, centrifuged (5 min, 13000 rpm, 4°C), and analyzed for IL-8 level using a human IL-8 ELISA kit, according to the manufacturer's protocol. The amount of IL-8 released in the samples was quantified using a standard calibration curve obtained with purified recombinant human IL-8 provided with the kit. The limit of detection was 3.1-200 pg/mL.

Then, to test the formulation ability to prevent inflammation, cells were exposed to a pre-warmed solution of LYO HA-CL – SAP, and incubated at 37 °C, 5% CO<sub>2</sub> for 24 h. Afterwards, cells were incubated again for another 24 h, at 37 °C, 5% CO<sub>2</sub>, with 10 ng/mL LPS. Subsequently, cell culture supernatant was withdrawn, centrifuged (5 min, 13000 rpm, 4°C), and analyzed for IL-8 level as previously described.

Finally, the anti-inflammatory efficacy of LYO HA-CL – SAP was evaluated by its ability to reduce inflammation in primary ALI nasal cells after induction of IL-8 production by LPS. Hence, cells were incubated with 10 ng/mL LPS for 24 h at 37°C, in a humidified atmosphere at 5% CO<sub>2</sub>. Subsequently, cells were exposed to a pre-warmed solution of LYO HA-CL – SAP, and after 24 h of incubation in the same conditions, cell culture supernatant

was withdrawn, centrifuged (5 min, 13000 rpm, 4°C), and analyzed for IL-8 concentration as previously described.

### **8.3.5. Statistical analysis**

All the data are presented as mean  $\pm$  standard deviation of a minimum of three independent experiments. Statistical analysis was performed using GraphPad Prism software version 7.0b (GraphPad, San Diego, USA). Wound healing data were analyzed with unpaired *t*-test, while anti-inflammatory response data were analyzed with one-way analysis of variance (ANOVA) followed by Tukey *post hoc* test for multiple comparisons. Differences were considered statistically significant for  $P < 0.05$  (\* $P < 0.05$ , \*\* $P < 0.01$ , \*\*\* $P < 0.001$  and \*\*\*\* $P < 0.0001$ ).

## **8.4. Results and discussion**

Previous studies showed that SAP and HA-CL, when delivered in combination, provide an enhanced effect in controlling lung inflammation and oxidative stress (Fallacara et al., 2018b, submitted for publication). Additionally, emerging data showed the beneficial role in nasal inflammatory diseases for the precursors of these substances –vitamin C (Chauhan et al., 2016; Podoshin et al., 1991; Sagit et al., 2011) and HA (Casale et al., 2014, 2016; Cassandro et al., 2015; Ciofalo et al., 2017a, b; Garantziotis et al., 2016; Gelardi et al., 2013b, 2016; Varricchio et al., 2014). All these evidences strongly supported the present study to develop a novel formulation containing both SAP and HA-CL to enhance treatments for nasal diseases, like AR and CRS. A dry powder formulation was prepared, as powders, being solid dosage forms, are chemically and microbiologically more stable than liquids, and require simpler compositions in excipients (if any) (Tiozzo Fasiolo et al., 2018). Moreover, compared to nasal liquids, nasal powders undergo slower clearances from the nasal cavity, and can be delivered more efficiently by insufflation devices that permit the deposition on a larger surface of the nasal mucosa (Tiozzo Fasiolo et al., 2018). All this can improve drug diffusion, adsorption across the mucosa, and bioavailability (Tiozzo Fasiolo et al., 2018).

### 8.4.1. Physico-chemical characterization

#### 8.4.1.1. Morphological analysis

In Figure 8.1. the morphology of LYO HA-CL – SAP observed by SEM is presented. The formulation was characterized by porous particles of polygonal shape, with size  $> 50 \mu\text{m}$  and  $< 600 \mu\text{m}$ , that is suitable for nasal delivery (Kippax et al., 2010).

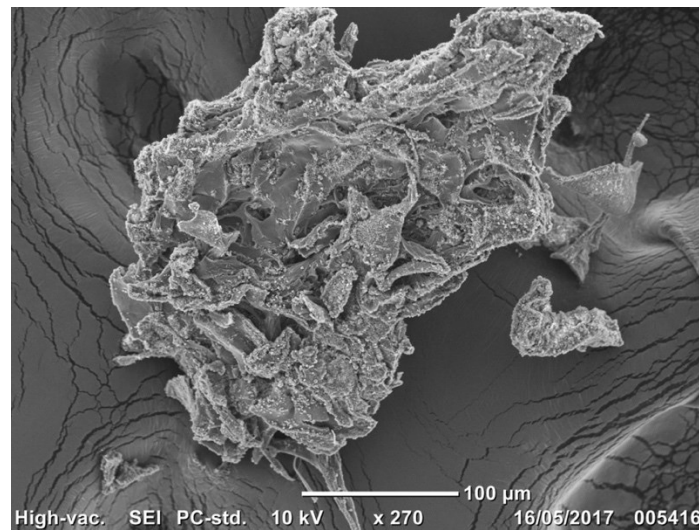


Figure 8.1. SEM micrograph of LYO HA-CL – SAP.

#### 8.4.1.2. Particle size analysis

Results of laser diffraction analysis of LYO HA-CL – SAP are shown in Figure 8.2. A unimodal and narrow dispersion (Span index:  $1.2 \pm 0.0$ ) was observed, with a  $Dv_{50}$  of  $328.3 \pm 27.5 \mu\text{m}$ . Moreover, 10% of LYO HA-CL – SAP particles had a diameter  $\leq 179.0 \pm 17.4 \mu\text{m}$  ( $Dv_{10}$ ), and 90%  $\leq 566.7 \pm 39.5 \mu\text{m}$  ( $Dv_{90}$ ). Hence, the freeze-dried formulation appeared to be suitable for nasal delivery as no particle fraction was found to be smaller than  $10 \mu\text{m}$  (Ozsoy et al., 2009; Tiozzo Fasiolo et al., 2018).

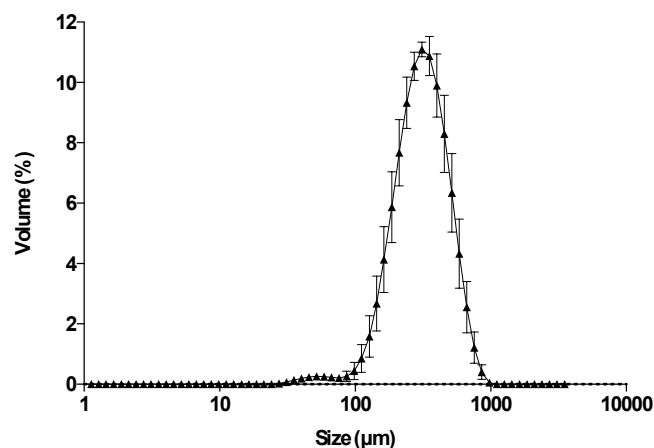


Figure 8.2. Particle size distribution of LYO HA-CL – SAP. Data represent mean  $\pm$  SD (n = 3).

#### 8.4.1.3. Thermal analysis

The thermal behaviour and physical stability of LYO HA-CL – SAP were investigated using DSC and TGA, as shown in Figure 8.3.

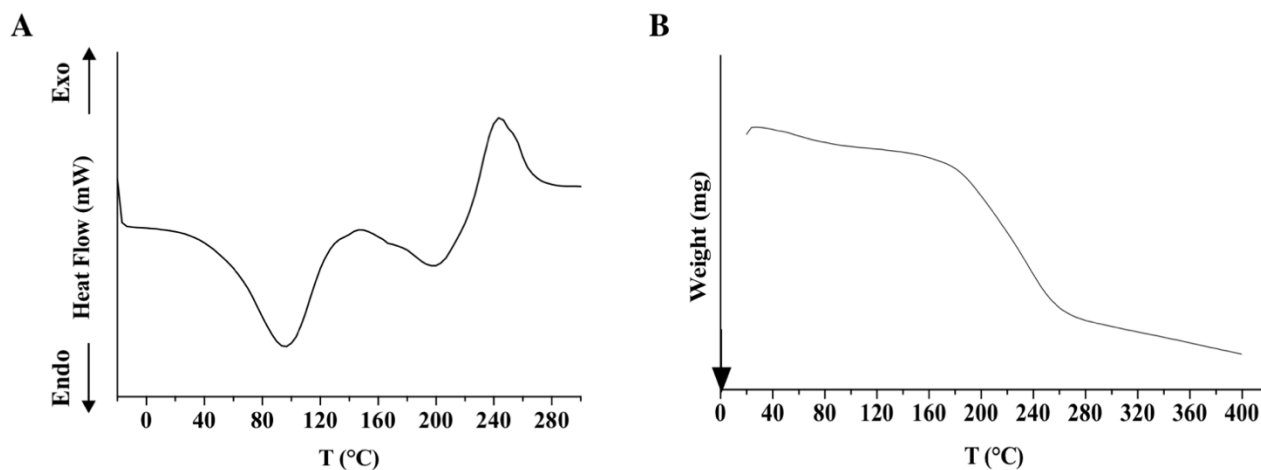


Figure 8.3. DSC (A) and TGA (B) thermal profiles of LYO HA-CL – SAP.

The DSC thermal profile of LYO HA-CL – SAP was characterized by two wide endothermic peaks: the first at 97°C, suggesting a dehydration process, and the second at 200°C, which was attributed to pentylene glycol evaporation (boiling range 198-200°C) (Figure 8.3.A). The thermal decomposition of LYO HA-CL – SAP and the formation of a carbonized residue occurred at 240°C, where a broad exothermic peak was observed. This DSC profile suggested that HA-CL and SAP formed a solid solution/amorphous solid dispersion in the freeze-dried formulation. Such result was in good agreement with previous observations reported for SAP raw material, HA-CL microspheres and other dry powder formulations containing both SAP and HA-CL (Fallacara et al., 2018c; submitted for publication).

TGA thermograph of LYO HA-CL – SAP is displayed in **Fig. 3B**. Three distinct degradation stages could be observed, with the first stage (20-181°C, 6.7% w/w of weight loss) that is characteristic of water evaporation; the second (181-246°C, 22.5% w/w of weight loss, including also the evaporation of pentylene glycol) and the third stages (246-400°C, 12.8% w/w of weight loss) that are typical of a two-stages polysaccharide degradation.

Hence, the thermal decomposition of HA-CL and SAP occurred simultaneously, as showed by DSC and TGA curves, and confirmed by data previously obtained for HA-CL microspheres containing SAP (Fallacara et al., 2018c).

#### 8.4.1.4. In vitro aerosolization performance

Particle size is a key parameter in defining the deposition pattern of formulations delivered to the nasal mucosa using nasal inhalers and pump sprays. To verify the absence of particles with aerodynamic diameter < 10 µm, that could reach the lower airways (Cheng et al., 2001; Doub et al., 2012), the FDA draft guidance for industry has suggested to perform impactor and laser diffraction analyses (FDA CDER, 2003). Hence, the aerodynamic

efficiency of LYO HA-CL – SAP, delivered with the UDS nasal device, was investigated using the Apparatus E equipped with a FDA 2-L glass EC (FDA CDER, 2003). Additionally, SprayTec™ laser diffraction technique was employed to assess the geometric particle size distribution of the emitted dose from the UDS nasal device.

In Table 8.1. the *in vitro* aerosolization performance of LYO HA-CL – SAP is presented. Results are presented as the percentage of the drug remaining in the device and deposited in the EC, connection tube, and each stage of the NGI, over the total theoretical amount of drug filled in the device. It was found that the LYO HA-CL – SAP formulation is suitable for nasal drug delivery, with 88.7% of the particles showing an aerodynamic diameter larger than 14.1 µm (78.3 ± 2.7% of the particles in the EC, plus 0.7 ± 0.5% in the connection tube and 9.7 ± 1.5% in the S1), while the remaining 11.3 ± 4.0% of SAP was recovered in the device. As no drug was detected in the lower stages of the NGI, there was no respirable fraction.

Table 8.1. Percentage of SAP recovered in each stage of the apparatus E equipped with the 2-l glass EC for nasal delivery. Data are presented as mean ± SD (n = 3).

	Amount of SAP recovered (%)	Cut off diameter (µm)
Device	11.3 ± 4.0	-
EC	78.3 ± 2.7	-
Connection tube	0.7 ± 0.5	-
S1	9.7 ± 1.5	> 14.1
S2-S8	-	< 14.1
Total recovery	100.0 ± 0.0	-

The aerosolization performance of the freeze-dried formulation was also characterised by SprayTec™ laser diffraction particle sizing. The SprayTec™ system ensures the characterization of the whole particle size distribution, and detects the dynamics of particle dispersion along with the device reproducibility, while cascade impaction provides information on the aerosol performance of the particles below 10 µm. Table 8.2. shows the results of SprayTec™ analyses carried out on LYO HA-CL – SAP, which exhibited a geometric diameter that is suitable for nasal delivery. Indeed, the size distribution was unimodal and narrow (Span index: 1.8 ± 0.0), with the 90% of particles below 537.8 ± 28.8 µm and a median diameter of 243.0 ± 13.0 µm. No particles below 10 µm were detected.

Table 8.2. Values of volumetric diameter, Span index and percentage of particles ≤ 10 µm obtained for LYO HA-CL – SAP with SprayTec™ system. Data represent mean ± SD (n = 3).

LYO HA-CL - SAP	
Dv(10)	100.5 ± 4.5
Dv(50)	243.0 ± 13.0
Dv(90)	537.8 ± 28.8
Span	1.8 ± 0.0
% V (≤ 10 µm)	0.0 ± 0.0

#### 8.4.2. *In vitro* studies on nasal cell models

##### 8.4.2.1. MTS cytotoxicity assay on RPMI 2650 cells

The *in vitro* cytotoxicity of LYO HA-CL – SAP was evaluated using the colorimetric MTS assay. RPMI 2650 cells were incubated for 72 h with solutions of the freeze-dried formulation with SAP concentration ranging from 8.0 mM to 60.9 nM. As displayed in Figure 8.4., cells maintained their metabolic activity and were viable after the exposure to the solution with the highest concentration. Since the half maximal inhibitory concentration value (IC<sub>50</sub>) could not be determined across all the concentration interval examined, LYO HA-CL – SAP could be considered non-toxic for RPMI 2650 cells at the wide concentration range tested. Hence, this study showed for the first time that the novel HA-CL polymer could be safely used for nasal formulations. In fact, HA-CL maintained the excellent safety profile of high molecular weight native HA, which was previously found to be non-toxic even at high concentration -1% on RPMI 2650 cells (Horváth et al., 2016), 3% on adult volunteers affected by rhinosinusitis (Ciofalo et al., 2017a).

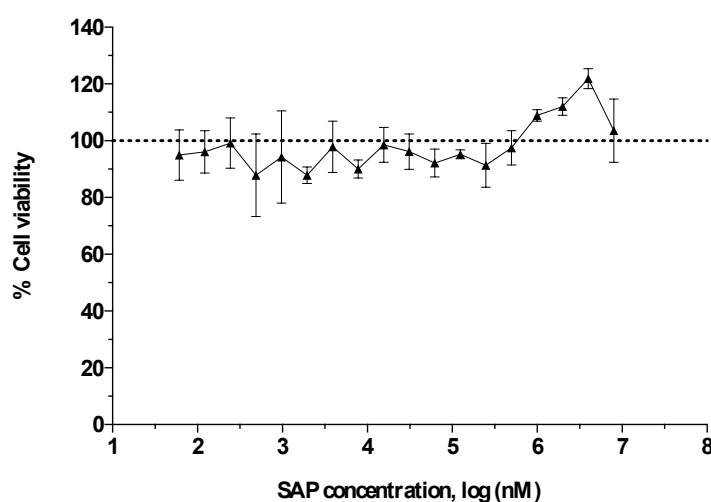


Figure 8.4. Viability of RPMI 2650 cells evaluated using MTS assay after 72 h of treatment with LYO HA-CL – SAP. Data represent mean  $\pm$  SD (n = 3).

##### 8.4.2.2. Wound healing assay on RPMI 2650 cells

Factors such as allergies, prolonged/chronic inflammation, virus and bacterial infections can alter the nasal mucosa homeostasis and therefore, can damage or destruct the epithelium. In order to assess the ability of LYO HA-CL - SAP to improve epithelia damage, wound healing assays were performed. Figure 8.5. shows images of the wound healing process without and with treatment (LYO HA-CL – SAP) at different time points (0, 1, 8 h). The freeze-dried powder formulation showed wound healing ability with significant improvement of the wound closure observed at 8 hours. Through image analysis, it was calculated that LYO HA-CL - SAP was able to close roughly the  $62 \pm 13$  % of the wound after 8 hours. This closure was significantly different compared to untreated cells ( $P < 0.0001$ ), where the wound closure was only  $13 \pm 4$ %. Hence, these results provided preliminary evidence that LYO

HA-CL – SAP was able to promote the re-epithelialization of RPMI 2650 wounded cells, demonstrating its potential use as adjuvant in nasal anti-inflammatory treatments.

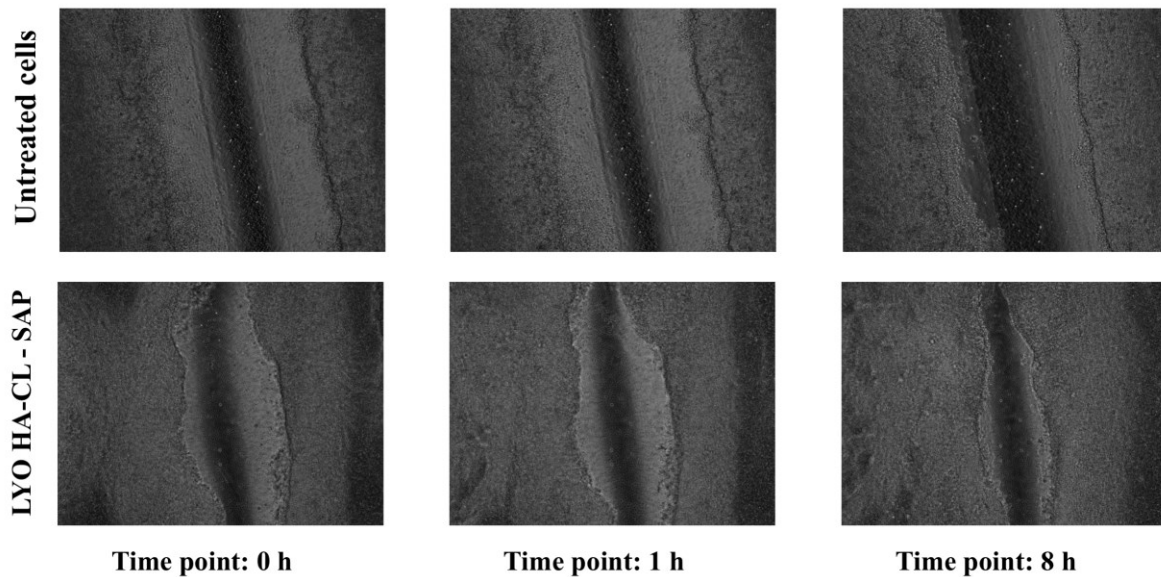


Figure 8.5. Wound images of untreated cells and cells treated with LYO HA-CL – SAP at different time points (0, 1, 8 h).

#### 8.4.2.3. Pro-inflammatory IL-8 expression in brushed nasal epithelial cells

IL-8 is a pro-inflammatory cytokine that is able to enhance allergic inflammation. It is highly expressed in many inflammatory diseases of the upper respiratory tract, including AR and CRS (Hu and Li, 2018; Lee et al., 2018). This *in vitro* study investigated the ability of the novel LYO HA-CL – SAP formulation in reducing the expression of IL-8 in primary ALI nasal cells, thus providing an anti-inflammatory activity.

Results showed that IL-8 production was not increased ( $P > 0.05$ ) by the exposure of non-stimulated primary nasal cells to LYO HA-CL – SAP, with IL-8 levels of  $15.2 \pm 3.3$  % in unstimulated and untreated cells and  $19.2 \pm 8.5$  % in LYO HA-CL – SAP treated cells (LYO HA-CL – SAP), as showed in Figure 8.6. On the contrary, cells exposed to 10 ng/mL LPS that remained untreated exhibited a significant inflammatory response ( $P < 0.0001$ ), with an IL-8 concentration that was 6.5 times higher with respect to unstimulated and untreated cells (Figure 8.6).

As depicted in Figure 8.6, cell exposure to LYO HA-CL – SAP treatment 24 h prior to stimulation with 10 ng/mL LPS significantly reduced IL-8 production to  $49.5 \pm 9.7$  % (LYO HA-CL – SAP + LPS), compared to LPS-stimulated but untreated cells ( $100.0 \pm 0.0$  %;  $P < 0.0001$ ). Hence, LYO HA-CL – SAP was shown to potentially play a preventive anti-inflammatory action.

Additionally, the anti-inflammatory property of LYO HA-CL – SAP was investigated after stimulation of primary nasal cells with 10 ng/mL LPS 24 h prior to treatment exposure. IL-8 concentration was determined 24 h after the sample addition on the LPS-stimulated cells. LYO HA-CL – SAP showed the ability to reduce IL-8 release compared to LPS-stimulated but untreated cells: more specifically, LYO HA-CL – SAP decreased IL-8 concentration to



68.8 ± 4.6 % (LPS + LYO HA-CL – SAP) (Figure 8.6). Therefore, LYO HA-CL – SAP was found to have a significant anti-inflammatory activity towards inflamed primary nasal cells ( $P < 0.0001$ ) (Figure 8.6). These results showed that the freeze-dried powder consisting of HA-CL and SAP could be a suitable formulation to reduce inflammation in upper airway diseases.

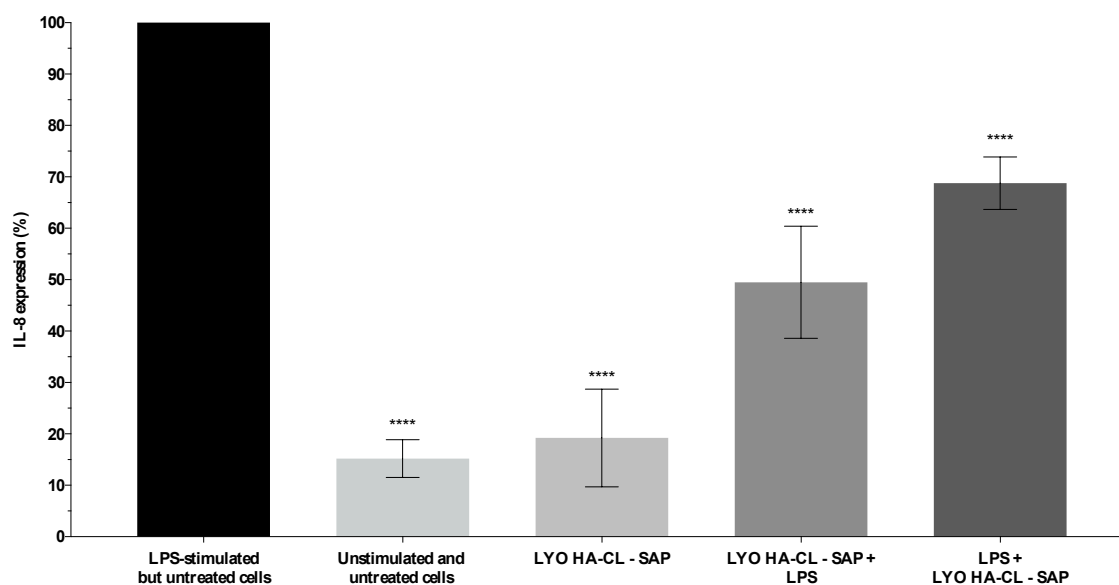


Figure 8.6. Concentration of IL-8 inflammatory cytokine in primary brushed ALI nasal cells supernatant after exposure to: LYO HA CL – SAP; LYO HA CL – SAP then LPS (LYO HA CL – SAP + LPS); LPS and then LYO HA CL – SAP (LPS + LYO HA CL – SAP). IL-8 levels were assessed in comparison to those of LPS-stimulated but untreated cells (positive control, i.e. cells exposed only to 10 ng/mL LPS), and unstimulated and untreated cells (control cells). Data represent mean ± standard deviation (n = 5). Asterisks indicate significant difference from LPS-stimulated but untreated cells (\*\*\*\* $P < 0.0001$ ).

#### 8.4.3. *In vitro* release study: release by Franz's cells and transport across RPMI 2650 cells

Franz's cells were chosen to explore the dissolution and release properties of LYO HA-CL – SAP (Figure 8.7.A), as the thin layer of liquid on the cells membranes permits the progressive hydration of the formulation in a humid environment. This is more representative of the *in vivo* nasal mucus layer with respect to the larger volume of dissolution medium of other release methods. Furthermore, SAP permeation profile was also studied across RPMI 2650 cells grown in the ALI configuration, for 4 hours after LYO HA-CL - SAP deposition in the 3D MC (Figure 8.7.B).

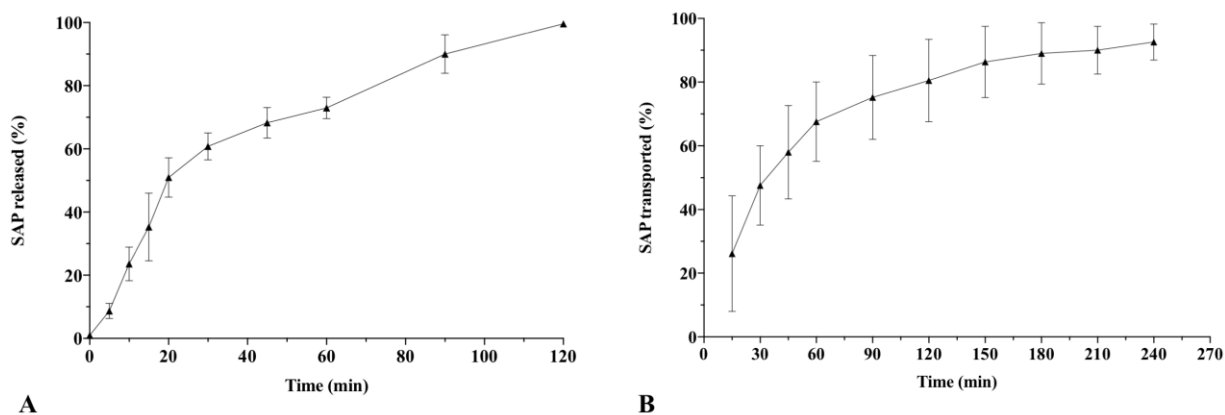


Figure 8.7. *In vitro* release profiles of SAP from LYO HA-CL – SAP: release by Franz's cells (A) and transport across RPMI 2650 cells (B). Data represent mean  $\pm$  SD (n = 3).

Due to its hydrophilicity, SAP rapidly diffused into the medium of the receptor compartment when LYO HA-CL – SAP was deposited on the filter membranes of Franz's cells. After 60 min,  $73.0 \pm 3.4\%$  of the drug was released from the freeze-dried formulation, and after 120 min, the release was completed (Figure 8.7.A). These results could suggest a good *in vivo* dissolution of the formulation in the nasal epithelial lining fluid, enhancing drug transport, bioavailability, and therapeutic efficacy (Vasa et al., 2017).

Figure 8.7.B displays the percentage of SAP transported across RPMI 2650 epithelium as a function of time. During the first hour, LYO HA-CL – SAP exhibited marked permeation properties, with  $67.6 \pm 12.4\%$  of SAP transported. Afterwards, a decreased permeation rate was observed. At the end of the 4 hours, almost all SAP was transported ( $92.6 \pm 5.7\%$ ), as only the  $7.4 \pm 5.7\%$  of SAP remained on the cells (Figure 8.7.B).

SAP release profile was extended when studied on RPMI 2650 cells (**Fig. 7B**) compared to Franz's cells (**Fig. 7A**). This delay was due to the low permeability of the simulated nasal epithelium, and so it was an effect of the cell barrier itself. Moreover, an enhanced mucoadhesive behaviour of hyaluronan on cell tissues could be hypothesized. In fact, HA-CL probably interacted with the mucus layer on the RPMI 2650 cells, absorbing water and thus becoming wet, swelled and gelled. Consequently, the formulation penetrated into the mucus, changed its structure and rheological properties that in turn slowed down drug release (Ugwoke et al., 2005). Hence, LYO HA-CL – SAP could overcome the drawback of a rapid clearance from the nasal cavity, since HA-CL could act not only as carrier for SAP and active ingredient itself, but also as mucoadhesive agent once dissolved in the nasal mucus layer to form a viscous solution/gel. This could potentially prolong the residence time of LYO HA-CL – SAP in the nasal cavity and thus the exposure of the nasal mucosa to the active ingredient (Horváth et al., 2016; Pires et al., 2009).

## 8.5. Conclusions

The present work aimed to develop a novel LYO HA-CL – SAP formulation for the treatment of nasal impairments sustained by inflammation. The dry powder formulation was characterized *in vitro* for its physico-chemical and biological properties. LYO HA-CL – SAP displayed suitable morphology, particle size distribution, mean diameter, thermal properties and *in vitro* aerosol performance for nasal drug delivery. The *in vitro* release/transport study

performed on LYO HA-CL – SAP showed that HA-CL was able to act not only as carrier for SAP and active ingredient itself, but also as mucoadhesive agent. The formulation was shown to be not cytotoxic in the range of SAP concentrations explored (8.0 mM to 60.9 nM), and exhibited wound healing ability on RPMI 2650 cells and anti-inflammatory efficacy on primary nasal epithelial cells. These encouraging results showed that polymer and drug acted in combination to help reduce cell damage. Hence, this preliminary study has opened up potential perspectives for LYO HA-CL – SAP as innovative adjunctive treatment for nasal airway disorders like AR and CRS.

#### **8.6. Disclosure**

The authors declare no conflict of interest.

#### **8.7. Acknowledgements**

This work was supported by a PhD grant to Arianna Fallacara from I.R.A. Srl (Istituto Ricerche Applicate, Usmate-Velate, Monza-Brianza, Italy).

## 8.8. References

- Albano, G.D., Bonanno, A., Cavalieri, L., Ingrassia, E., Di Sano, C., Siena, L., Riccobono, L., Gagliardo, R., Profita M., 2016. Effect of High, Medium, and Low Molecular Weight Hyaluronan on Inflammation and Oxidative Stress in an In Vitro Model of Human Nasal Epithelial Cells. *Mediators Inflamm.*, 8727289.
- Bai, S., Yang, T., Abbruscato, T.J., Ahsan, F., 2008. Evaluation of human nasal RPMI 2650 cells grown at an air-liquid interface as a model for nasal drug transport studies. *J. Pharm. Sci.* 97, 1165-1178.
- Basbaum, C.B., Finkbeiner, W.E., 1988. Airway secretion: a cell-specific analysis. *Horm. Metab. Res.* 20, 661-667.
- Bastacky, J., Lee, C.Y., Goerke, J., Koushafar, H., Yager, D., Kenaga, L., Speed, T.P., Chen, Y., Clements, J.A., 1995. Alveolar lining layer is thin and continuous: low-temperature scanning electron microscopy of rat lung. *J. Appl. Physiol.* 79, 1615-1628.
- Baumeister, P., Huebner, T., Reiter, M., Schwenk-Zieger, S., Harréus, U., 2009. Reduction of oxidative DNA fragmentation by ascorbic acid, zinc and N-acetylcysteine in nasal mucosa tissue cultures. *Anticancer. Res.* 29, 4571-4574.
- Bozdemir, K., Şahin, E., Altintoprak, N., Muluk, N.B., Cengiz, B.P., Acar, M., Cingi, C., 2016. Is resveratrol therapeutic when used to treat allergic rhinitis in rats? *Clin. Invest. Med.* 39, E63-E72.
- Campbell, R.G., 2018. Risks and management of long-term corticosteroid use in chronic rhinosinusitis. *Curr. Opin. Otolaryngol. Head Neck Surg.* 26, 1-7.
- Casale, M., Sabatino, L., Frari, V., Mazzola, F., Dell'Aquila, R., Baptista, P., Mladina, R., Salvinelli, F., 2014. The potential role of hyaluronan in minimizing symptoms and preventing exacerbations of chronic rhinosinusitis. *Am. J. Rhinol. Allergy.* 28, 345-348.
- Casale, M., Vella, P., Moffa, A., Oliveto, G., Sabatino, L., Grimaldi, V., Ferrara, P., Salvinelli, F., 2016. Hyaluronic acid and upper airway inflammation in pediatric population: A systematic review. *Int. J. Pediatr. Otorhinolaryngol.* 85, 22-26.
- Cassandro, E., Chiarella, G., Cavaliere, M., Sequino, G., Cassandro, C., Prasad, S.C., Scarpa, A., Iemma, M., 2015. Hyaluronan in the Treatment of Chronic Rhinosinusitis with Nasal Polyposis. *Indian J. Otolaryngol. Head Neck Surg.* 67, 299-307.
- Cassano, M., Russo, G.M., Granieri, C., Cassano, P., 2016. Cytofunctional changes in nasal ciliated cells in patients treated with hyaluronate after nasal surgery. *Am. J. Rhinol. Allergy.* 30, 83-88.
- Chauhan, B., Gupta, M., Chauhan, K., 2016. Role of antioxidants on the clinical outcome of patients with perennial allergic rhinitis. *Allergy Rhinol. (Providence).* 7, 74-81.

- Chen, Q., Sun, G., Wang, Y., Zhong, W., Shu, X.Z., 2012. The evaluation of two new hyaluronan hydrogels as nasal dressing in the rabbit maxillary sinus. *Am. J. Rhinol. Allergy.* 26, 152-156.
- Cheng, Y.S., Holmes, T.D., Gao, J., Guilmette, R.A., Li, S., Surakitbanharn, Y., Rowlings, C., 2001. Characterization of nasal spray pumps and deposition pattern in a replica of the human nasal airway. *J. Aerosol Med.* 14, 267-280.
- Ciofalo, A., De Vincentiis, M., Zambetti, G., Altissimi, G., Fusconi, M., Greco, A., Ottaviano, G., Magliulo, G., 2017a. Olfactory dysfunction in acute rhinosinusitis: intranasal sodium hyaluronate as adjuvant treatment. *Eur. Arch. Otorhinolaryngol.* 274, 803-808.
- Ciofalo, A., Zambetti, G., Altissimi, G., Fusconi, M., Soldo, P., Gelardi, M., Iannella, G., Pasquariello, B., Magliulo, G., 2017b. Pathological and cytological changes of the nasal mucosa in acute rhinosinusitis: the role of hyaluronic acid as supportive therapy. *Eur. Rev. Med. Pharmacol. Sci.* 21, 4411-4418.
- Citernes, U.R., Beretta, L., Citernes, L., 2015. Cross-linked hyaluronic acid, process for the preparation thereof and use thereof in the aesthetic field. Patent number WO/2015/007773 A1.
- Doub, W.H., Adams, W.P., Wokovich, A.M., Black, J.C., Shen, M., Buhse, L.F., 2012. Measurement of drug in small particles from aqueous nasal sprays by Andersen Cascade Impactor. *Pharm Res.* 29, 3122-3130.
- Elad, D., Wolf, M., Keck, T., 2008. Air-conditioning in the human nasal cavity. *Respir. Physiol. Neurobiol.* 163, 121-127.
- Elmowafy, E., Osman, R., El-Shamy, A.E.-H.A., Awad, G.A.S., 2014. Nasal polysaccharides-glucose regulator microparticles: optimization, tolerability and anti-diabetic activity in rats. *Carbohydr. Polym.* 108, 257-265.
- Emiroglu, G., Ozergin Coskun, Z., Kalkan, Y., Celebi Erdivanli, O., Tumkaya, L., Terzi, S., Özgür, A., Demirci, M., Dursun, E., 2017. The Effects of Curcumin on Wound Healing in a Rat Model of Nasal Mucosal Trauma. *Evid. Based Complement Alternat. Med.* Article ID 9452392., 6.
- Fallacara, A., Baldini, E., Manfredini, S., Vertuani, S., 2018a. Hyaluronic Acid in the Third Millennium. *Polymers* 10, 701.
- Fallacara, A., Busato, L., Pozzoli, M., Ghadiri, M., Xin Ong, H., Young, P.M., Manfredini, S., Traini, D., 2018b. Combination of urea-crosslinked hyaluronic acid and sodium ascorbyl phosphate for the treatment of inflammatory lung diseases: an in vitro study. *Eur. J. Pharm. Sci.* 120, 96-106.
- Fallacara, A., Busato, L., Pozzoli, M., Ghadiri, M., Xin Ong, H., Young, P.M., Manfredini, S., Traini, D., Submitted to *J. Pharm. Sci.* Co-spray-dried urea cross-linked hyaluronic acid and

sodium ascorbyl phosphate as novel inhalable dry powder formulation.

Fallacara, A., Manfredini, S., Durini, E., Vertuani, S., 2017a. Hyaluronic Acid Fillers in Soft Tissue Regeneration. *Facial Plast. Surg.* 33, 87-96.

Fallacara, A., Marchetti, F., Pozzoli, M., Citernes, U.R., Manfredini, S., Vertuani, S., 2018c. Formulation and characterization of native and crosslinked hyaluronic acid microspheres for dermal delivery of sodium ascorbyl phosphate: a comparative study. *Pharmaceutics*. 10 (4).

Fallacara, A., Vertuani, S., Panozzo, G., Pecorelli, A., Valacchi, G., Manfredini, S., 2017b. Novel Artificial Tears Containing Cross-Linked Hyaluronic Acid: An In Vitro Re-Epithelialization Study. *Molecules*. 22.

FDA CDER, 2003. Bioavailability and Bioequivalence Studies for Nasal Aerosols and Nasal Sprays for Local Action.

Foco, A., Gasperlin, M., Kristl, J., 2005. Investigation of liposomes as carriers of sodium ascorbyl phosphate for cutaneous photoprotection. *Int. J. Pharm.* 291, 21-29.

Fokkens, W.J., Lund, V.J., Mullol, J., Bachert, C., Alobid, I., Baroody, F., Cohen, N., Cervin, A., Douglas, R., Gevaert, P., Georgalas, C., Goossens, H., Harvey, R., Hellings, P., Hopkins, C., Jones, N., Joos, G., Kalogjera, L., Kern, B., Kowalski, M., Price, D., Riechelmann, H., Schlosser, R., Senior, B., Thomas, M., Toskala, E., Voegels, R., Wang De, Y., Wormald, P.J., 2012. EPOS 2012: European position paper on rhinosinusitis and nasal polyps 2012. A summary for otorhinolaryngologists. *Rhinology*. 50, 1-12.

Garantziotis, S., Brezina, M., Castelnuovo, P., Drago, L., 2016. The role of hyaluronan in the pathobiology and treatment of respiratory disease. *Am. J. Physiol. Lung Cell Mol. Physiol.* 310, L785-L795.

Gelardi, M., Guglielmi, A.V., De Candia, N., Maffezzoni, E., Berardi, P., Quaranta, N., 2013a. Effect of sodium hyaluronate on mucociliary clearance after functional endoscopic sinus surgery. *Eur. Ann. Allergy Clin. Immunol.* 45, 103-108.

Gelardi, M., Iannuzzi, L., Quaranta, N., 2013b. Intranasal sodium hyaluronate on the nasal cytology of patients with allergic and nonallergic rhinitis. *Int. Forum Allergy Rhinol.* 3, 807-813.

Gelardi, M., Taliente, S., Fiorella, M.L., Quaranta, N., Ciancio, G., Russo, C., Mola, P., Ciofalo, A., Zambetti, G., Caruso Armone, A., Cantone, E., Ciprandi, G., 2016. Ancillary therapy of intranasal T-LysYal® for patients with allergic, non-allergic, and mixed rhinitis. *J. Biol. Regul. Homeost. Agents*. 30, 255-262.

Greiner, A.N., Hellings, P.W., Rotiroti, G., Scadding, G.K., 2011. Allergic rhinitis. *Lancet*. 378, 2112-2222.

Helms, S., Miller, A., 2006. Natural treatment of chronic rhinosinusitis. *Altern. Med. Rev.* 11, 196-207.

Hirst, R.A., Jackson, C.L., Coles, J.L., Williams, G., Rutman, A., Goggin, P.M., Adam, E.C., Page, A., Evans, H.J., Lackie, P.M., O'Callaghan, C., Lucas, J.S., 2014. Culture of primary ciliary dyskinesia epithelial cells at air-liquid interface can alter ciliary phenotype but remains a robust and informative diagnostic aid. *PLoS One*. 9, e89675.

Hong, Z., Guo, Z., Zhang, R., Xu, J., Dong, W., Zhuang, G., Deng, C., 2016. Airborne Fine Particulate Matter Induces Oxidative Stress and Inflammation in Human Nasal Epithelial Cells. *Tohoku J. Exp. Med.* 239, 117-125.

Horváth, T., Bartos, C., Bocsik, A., Kiss, L., Veszeka, S., Deli, M.A., Újhelyi, G., Szabó-Révész, P., Ambrus, R., 2016. Cytotoxicity of Different Excipients on RPMI 2650 Human Nasal Epithelial Cells. *Molecules*. 21, pii:E658.

Hu, H., Li, H., 2018. Prunetin inhibits lipopolysaccharide-induced inflammatory cytokine production and MUC5AC expression by inactivating the TLR4/MyD88 pathway in human nasal epithelial cells. *Biomed. Pharmacother.* 106, 1469-1477.

Jarvis, D., Newson, R., Lotvall, J., Hastan, D., Tomassen, P., Keil, T., Gjomarkaj, M., Forsberg, B., Gunnbjornsdottir, M., Minov, J., Brozek, G., Dahlen, S.E., Toskala, E., Kowalski, M.L., Olze, H., Howarth, P., Krämer, U., Baelum, J., Loureiro, C., Kasper, L., Bousquet, P.J., Bousquet, J., Bachert, C., Fokkens, W., Burney, P., 2012. Asthma in adults and its association with chronic rhinosinusitis: the GA2LEN survey in Europe. *Allergy* 67, 91-98.

Johansson, L., Akerlund, A., Holmberg, K., Melén, I., Bende, M., 2003. Prevalence of nasal polyps in adults: the Skövde population-based study. *Ann. Otol. Rhinol. Laryngol.* 112, 625-629.

Jones, N., 2001. The nose and paranasal sinuses physiology and anatomy. *Adv. Drug Deliv. Rev.* 51, 5-19.

Kippax, P., Suman, J., Williams, G., 2010. Understanding the requirements for effective nasal drug delivery. *Pharm. Technol. Europe*, 58-65.

Kreft, M.E., Jerman, U.D., Lasic, E., Lanisnik Rizner, T., Hevir-Kene, N., Peternel, L., Kristan, K., 2015. The characterization of the human nasal epithelial cell line RPMI 2650 under different culture conditions and their optimization for an appropriate in vitro nasal model. *Pharm. Res.* 32, 665-679.

Lee, D.C., Choi, H., Oh, J.M., Hong, Y., Jeong, S.H., Kim, C.S., Kim, D.K., Cho, W.K., Kim, S.W., Kim, S.W., Cho, J.H., Lee, J., 2018. The effect of urban particulate matter on cultured human nasal fibroblasts. *Int. Forum Allergy Rhinol.* 8, 993-1000.

Lee, M.K., Yoo, J.W., Lin, H., Kim, Y.S., Kim, D.D., Choi, Y.M., Park, S.K., Lee, C.H., Roh, H.J., 2005. Air-liquid interface culture of serially passaged human nasal epithelial cell monolayer for in vitro drug transport studies. *Drug Deliv.* 12, 305-311.

- Li, Y., Schellhorn, H.E., 2007. New developments and novel therapeutic perspectives for vitamin C. *J. Nutr.* 137, 2171-2184.
- Licari, A., Brambilla, I., De Filippo, M., Poddighe, D., Castagnoli, R., Marseglia, G.L., 2017a. The role of upper airway pathology as a co-morbidity in severe asthma. *Expert Rev. Respir. Med.* 11, 855-865.
- Licari, A., Castagnoli, R., Denicolò, C.F., Rossini, L., Marseglia, A., Marseglia, G.L., 2017b. The Nose and the Lung: United Airway Disease? *Front. Pediatr.* 5, 44.
- Marseglia, G.L., Merli, P., Caimmi, D., Licari, A., Labó, E., Marseglia, A., Ciprandi, G., La Rosa, M., 2011. Nasal disease and asthma. *Int. J. Immunopathol. Pharmacol.* 24, 7-12.
- Montoro, J., Sastre, J., Jáuregui, I., Bartra, J., Dávila, I., del Cuvillo, A., Ferrer, M., Mullol, J., Valero, A., 2007. Allergic rhinitis: continuous or on demand antihistamine therapy? *J. Investig. Allergol. Clin. Immunol.* 17, 21-27.
- Monzon, M.E., Casalino-Matsuda, S.M., Forteza, R.M., 2006. Identification of glycosaminoglycans in human airway secretions. *Am. J. Respir. Cell. Mol. Biol.* 34, 135-141.
- Mudway, I.S., Kelly, F.J., 2000. Ozone and the lung: a sensitive issue. *Mol. Aspects Med.* 21, 1-48.
- Muller, L., Brighton, L.E., Carson, J.L., Fischer, W.A., Jaspers, I., 2013. Culturing of human nasal epithelial cells at the air liquid interface. *J. Vis. Exp.* 80, doi: 10.3791/50646.
- Ong, H.X., Traini, D., Bebawy, M., Young, P.M., 2011. Epithelial profiling of antibiotic controlled release respiratory formulations. *Pharm. Res.* 28, 2327-2338.
- Ozsoy, Y., Gungor, S., Cevher, E., 2009. Nasal delivery of high molecular weight drugs. *Molecules* 14, 3754-3779. .
- Patel, R.G., 2017. Nasal Anatomy and Function. *Facial Plast. Surg.* 33, 3-8.
- Petrigni, G., Allegra, L., 2006. Aerosolised hyaluronic acid prevents exercise-induced bronchoconstriction, suggesting novel hypotheses on the correction of matrix defects in asthma. *Pulm. Pharmacol. Ther.* 19, 166-171.
- Pires, A., Fortuna, A., Alves, G., Falcão, A., 2009. Intranasal drug delivery: how, why and what for? *J. Pharm. Pharm. Sci.* 12, 288-311.
- Podoshin, L., Gertner, R., Fradis, M., 1991. Treatment of perennial allergic rhinitis with ascorbic acid solution. *Ear Nose Throat J.* 70, 54-55.
- Pozzoli, M., Ong, H.X., Morgan, L., Sukkar, M., Traini, D., Young, P.M., Sonvico F., 2016a. Application of RPMI 2650 nasal cell model to a 3D printed apparatus for the testing of drug deposition and permeation of nasal products. *Eur. J. Pharm. Biopharm.* 107, 223-233.



- Pozzoli, M., Rogueda, P., Zhu, B., Smith, T., Young, P.M., Traini, D., Sonvico, F., 2016b. Dry powder nasal drug delivery: challenges, opportunities and a study of the commercial Teijin Puvlizer Rhinocort device and formulation. *Drug Dev. Ind. Pharm.* 42, 1660-1668.
- Pozzoli, M., Traini, D., Young, P.M., Sukkar, M.B., Sonvico, F., 2017. Development of a Soluplus budesonide freeze-dried powder for nasal drug delivery. *Drug Dev. Ind. Pharm.* 43, 1510-1518.
- Reichl, S., Becker, K., 2012. Cultivation of RPMI 2650 cells as an in-vitro model for human transmucosal nasal drug absorption studies: optimization of selected culture conditions. *J. Pharm. Pharmacol.* 64, 1621-1630.
- Sagit, M., Erdamar, H., Saka, C., Yalcin, S., Akin, I., 2011. Effect of antioxidants on the clinical outcome of patients with nasal polyposis. *J. Laryngol. Otol.* 125, 811-815.
- Small, P., Kim, H., 2011. Allergic rhinitis. *Allergy Asthma Clin. Immunol.* 7.
- Testa, D., Marcuccio, G., Panin, G., Bianco, A., Tafuri, D., Thyron, F.Z., Nunziata, M., Piombino, P., Guerra, G., Motta, G., 2017. Nasal mucosa healing after endoscopic sinus surgery in chronic rhinosinusitis of elderly patients: role of topic alpha-tocopherol acetate. *Aging Clin. Exp. Res.* 29, 191-195.
- Tiozzo Fasiolo, L., Manniello, M.D., Tratta, E., Buttini, F., Rossi, A., Sonvico, F., Bortolotti, F., Russo, P., Colombo, G., 2018. Opportunity and challenges of nasal powders: drug formulation and delivery. *Eur. J. Pharm. Sci.* 113, 2-17.
- Ugwoke, M.I., Agu, R.U., Verbeke, N., Kinget, R., 2005. Nasal mucoadhesive drug delivery: background, applications, trends and future perspectives. *Adv. Drug Deliv. Rev.* 57, 1640-1665.
- van der Vliet, A., O'Neill, C.A., Cross, C.E., Koostra, J.M., Volz, W.G., Halliwell, B., Louie, S., 1999. Determination of low-molecular-mass antioxidant concentrations in human respiratory tract lining fluids. *Am. J. Physiol.* 276, L289-L296.
- Varricchio, A., Capasso, M., Avvisati, F., Varricchio, A.M., De Lucia, A., Brunese, F.P., Ciprandi, G., 2014. Inhaled hyaluronic acid as ancillary treatment in children with bacterial acute rhinopharyngitis. *J. Biol. Regul. Homeost. Agents.* 28, 537-543.
- Vasa, D.M., Buckner, I.S., Cavanaugh, J.E., Wildfong, P.L., 2017. Improved Flux of Levodopa via Direct Deposition of Solid Microparticles on Nasal Tissue. *AAPS PharmSciTech.* 18, 904-912.
- Wengst, A., Reichl, S., 2010. RPMI 2650 epithelial model and three-dimensional reconstructed human nasal mucosa as in vitro models for nasal permeation studies. *Eur. J. Pharm. Biopharm.* 74, 290-297.
- Wu, D.X., Lee, C.Y., Widdicombe, J.H., Bastacky, J., 1996. Ultrastructure of tracheal surface liquid: low-temperature scanning electron microscopy. *Scanning.* 18, 589-592.

Yoo, J.W., Kim, Y.S., Lee, S.H., Lee, M.K., Roh, H.J., Jhun, B.H., Lee, C.H., Kim, D.D., 2003. Serially passaged human nasal epithelial cell monolayer for in vitro drug transport studies. *Pharm. Res.* 20, 1690-1696.





## CHAPTER 9

### *General conclusions and future perspectives of urea-crosslinked hyaluronic acid*



## 9.1. General conclusions

The main aim of the present work was to investigate the possible pharmaceutical and cosmetic applications of urea-crosslinked hyaluronic acid (HA-CL), a novel promising and versatile polymer consisting of two bioactive, biocompatible and biodegradable molecules: hyaluronic acid (HA) and urea.

Chapter 1 consisted in a brief general introduction, describing the aims of the study and structure of the thesis. Additionally, details regarding the organization of the work were given, presenting the three different host facilities that guaranteed access to all the necessary instrumentations and resources.

In Chapter 2 an overview on HA was proposed. The key features of HA were described in terms of structure, physico-chemical and hydrodynamic properties, biology –occurrence, biosynthesis, degradation, roles, mechanisms of action and receptors. Furthermore, both conventional and recently emerging methods developed for the industrial production of HA and its chemical derivatization were presented. Finally, the medical, pharmaceutical, cosmetic and dietary applications of HA and its derivatives were reviewed, reporting examples of HA-based products which are currently on the market or are undergoing further investigations.

Chapter 3 focused on the hyaluronan derivative object of the present PhD thesis: HA-CL. More precisely, HA-CL synthesis and rheological characterization were reported in accordance to the patent WO/2015/007773 A1 (Citernesi et al., 2015). Additionally, the key features of this innovative polymer intended for aesthetic and cosmetic applications were described.

Therefore, Chapters 1, 2 and 3 reported the necessary basic knowledge to understand the experimental design of the present PhD thesis and the scientific value of the studies performed to investigate the possible applications of HA-CL, described in Chapters 4, 5, 6, 7, and 8.

In Chapter 4, a possible ophthalmic application of HA-CL was described: the novel polymer was used to formulate two prototypes of eye drops (0.02 and 0.4%), which were evaluated as innovative therapy for keratoconjunctivitis sicca. Both HA-CL eye drops were shown to be stable, in terms of macroscopic appearance, pH and viscosity, during a 6 months' study. Moreover, HA-CL, even at the lowest concentration used (0.02%), displayed an interesting re-epithelialization ability –related to cyclin D1 expression- in an *in vitro* study on 2D human corneal cells (HCEpiC) and 3D reconstructed tissues of human corneal epithelium (HCE). Thus, exhibiting safety and efficacy, both formulations showed potential to treat signs and symptoms of keratoconjunctivitis sicca.

Chapter 5 investigated, for the first time, the formulation of HA-CL microspheres (MS) encapsulating sodium ascorbyl phosphate (SAP) for dermal application. Unloaded HA-CL MS, unloaded and SAP-loaded native hyaluronan MS were also prepared as reference formulations. The MS were efficiently produced using an emulsification-solvent evaporation technique. The optimal working conditions were found through a preformulation study which explored the MS features (mean size, particle size distribution, yield, encapsulation efficiency) depending on the emulsification time and on the polymer solutions' properties (pH, viscosity, presence/absence of SAP, native or crosslinked hyaluronan). The optimized MS underwent a more complete physico-chemical characterization: morphological analysis, analysis of the physico-molecular state, analysis of the thermal properties, analysis of the

stability to humidity, solubility test, *in vitro* release studies (dialysis and Franz diffusion cells) and kinetic release studies. This work showed that HA-CL could result in more efficient microsystems -in terms of SAP encapsulation efficiency and release properties- with respect to HA. In future, HA-CL – SAP MS could be potentially improved with the addition of excipients able to further slow down drug release.

Chapter 6 concerned an unprecedented *in vitro* evaluation of the safety and the biological activity of HA-CL and SAP, singularly and in combination, for the treatment of inflammatory lung diseases such as asthma, emphysema and chronic obstructive pulmonary disease. Sample solutions displayed pH, osmolality and viscosity values suitable for pulmonary delivery and showed to be not toxic on lung epithelial Calu-3 cells. A comparative study showed a greater anti-inflammatory and antioxidant activity for the combination HA-CL – SAP, not only with respect to the single HA-CL and SAP, but also with respect to the combination native HA - SAP, and to the single native HA. Additionally, the combination HA-CL - SAP was able to promote tissue re-epithelialization with faster kinetics than the single native HA and SAP, and their combination. In conclusion, the innovative HA-CL - SAP combination showed a high potential as adjunctive therapy of pulmonary disorders sustained by inflammation and oxidative stress.

Considering the promising results reported in Chapter 6, the PhD researches proceeded with the formulation of an inhalable dry powder obtained by co-spray-drying of HA-CL and SAP, described in Chapter 7. The properties of the spray-dried (SD) HA-CL - SAP formulation were compared with a reference formulation consisting of co-spray-dried native HA and SAP. Both the preparations exhibited great yields and encapsulation efficiencies, and were suitable for pulmonary delivery in terms of morphology, mean particle size and size distribution, thermal and humidity stability, *in vitro* aerosolization performance and SAP release/transport across a Calu-3 air-interface model.

Finally, Chapter 8 investigated a possible nasal application of HA-CL. A freeze-dried powder formulation consisting of HA-CL and SAP was prepared and subjected to a physico-chemical characterization of the morphological, dimensional, thermal and *in vitro* release properties. *In vitro* deposition studies showed the suitability of the novel dry powder formulation for nasal drug delivery, and *in vitro* tests on RPMI 2650 nasal cells displayed its safety, wound-healing and anti-inflammatory properties.

Overall, all these research works proved that the novel HA-CL is a multifunctional polymer, showing a number of possible interesting applications both in pharmaceuticals and dermatology/cosmetics. HA-CL displayed enhanced drug carrier ability and intrinsic activity compared to conventional native HA. In some cases, the biological properties of HA-CL could be further improved through its combination with active molecules such as SAP. HA-CL re-epithelializing, antioxidant and anti-inflammatory activities showed its potential as ophthalmic, pulmonary and nasal treatment of inflammatory diseases.

## 9.2. Future perspectives

The researches presented in this PhD thesis have implemented the current knowledge on the potential applications of HA-CL, opening encouraging perspectives. However, they have a preliminary nature and, therefore, further studies should be focused in future in order to:

- investigate the ocular surface residence time, the required dose-frequency and the



potential delivery through the corneal membrane of eye drops containing HA-CL. Additionally, *in vivo* and clinical studies could be extremely helpful to further characterize the bioactivities of HA-CL artificial tears;

- select excipients with the ability to slow down SAP release from HA-CL MS, and study, both *in vitro* and *in vivo*, the safety, the hydration and re-epithelialization efficacy of HA-CL – SAP MS compared to HA – SAP MS;
- study *in vivo* the safety, the bioactivity and the suitability for pulmonary delivery of the SD HA-CL – SAP formulation compared to the SD HA – SAP reference formulation;
- study the *in vivo* suitability for nasal delivery of the freeze-dried formulation consisting of HA-CL and SAP, as well as its safety, wound healing and anti-inflammatory activities;
- find further possible pharmaceutical and cosmetic applications for HA-CL.



# APPENDICES

## A.1. Publications list

### *A.1.1. Journal articles included as thesis chapters*

Fallacara, A., Busato, L., Pozzoli, M., Ghadiri, M., Ong, H.X., Young, P.M., Manfredini, S., Traini, D., 2019. *In vitro* characterization of physico-chemical properties, cytotoxicity, bioactivity of urea-crosslinked hyaluronic acid and sodium ascorbyl phosphate nasal powder formulation. *Int. J. Pharm.*, 558, 341-350.

Fallacara, A., Marchetti, F., Pozzoli, M., Citernes, U.R., Manfredini, S., Vertuani, S., 2018. Formulation and characterization of native and crosslinked hyaluronic acid microspheres for dermal delivery of sodium ascorbyl phosphate: a comparative study. *Pharmaceutics*, 10 (4).

Fallacara, A., Baldini, E., Manfredini, S., Vertuani, S., 2018. Hyaluronic acid in the third millennium. *Polymers* (10)7, 701.

Fallacara, A., Busato, L., Pozzoli, M., Ghadiri, M., Ong, H.X., Young, P.M., Manfredini, S., Traini, D., 2018. Combination of urea-crosslinked hyaluronic acid and sodium ascorbyl phosphate for the treatment of inflammatory lung diseases: An *in vitro* study. *Eur. J. Pharm. Sci.*, 120, 96-106.

Fallacara, A., Vertuani, S., Panozzo, G., Pecorelli, A., Valacchi, G., Manfredini, S., 2017. Novel Artificial Tears Containing Cross-linked Hyaluronic Acid: An *In Vitro* Re-epithelialization study. *Molecules*, 22.



## *In vitro* characterization of physico-chemical properties, cytotoxicity, bioactivity of urea-crosslinked hyaluronic acid and sodium ascorbyl phosphate nasal powder formulation

Arianna Fallacara<sup>a,b</sup>, Laura Busato<sup>a,b</sup>, Michele Pozzoli<sup>a</sup>, Maliheh Ghadiri<sup>a</sup>, Hui Xin Ong<sup>a</sup>, Paul M. Young<sup>a</sup>, Stefano Manfredini<sup>b</sup>, Daniela Traini<sup>a,\*</sup>

<sup>a</sup> Respiratory Technology, Woolcock Institute of Medical Research and Discipline of Pharmacology, Faculty of Medicine and Health, The University of Sydney, 431 Glebe Point Road, Glebe, NSW 2037, Australia

<sup>b</sup> Department of Life Sciences and Biotechnology, University of Ferrara, Via L. Borsari 46, 44121 Ferrara, Italy

### ARTICLE INFO

#### Keywords:

Anti-inflammatory  
Hyaluronic acid  
Nasal diseases  
Sodium ascorbyl phosphate  
Urea-crosslinked hyaluronic acid  
Wound healing

### ABSTRACT

An innovative lyophilized dry powder formulation consisting of urea-crosslinked hyaluronic acid (HA-CL) and sodium ascorbyl phosphate (SAP) – LYO HA-CL – SAP – was prepared and characterized *in vitro* for physico-chemical and biological properties. The aim was to understand if LYO HA-CL – SAP could be used as adjuvant treatment for nasal inflammatory diseases. LYO HA-CL – SAP was suitable for nasal delivery and showed to be not toxic on human nasal septum carcinoma-derived cells (RPMI 2650 cells) at the investigated concentrations. It displayed porous, polygonal particles with unimodal, narrow size distribution, mean geometric diameter of  $328.3 \pm 27.5 \mu\text{m}$ , that is appropriate for nasal deposition with no respirable fraction and 88.7% of particles with aerodynamic diameter  $> 14.1 \mu\text{m}$ . Additionally, the formulation showed wound healing ability on RPMI 2650 cells, and reduced interleukin-8 (IL-8) level in primary nasal epithelial cells pre-induced with lipopolysaccharide (LPS). Transport study across RPMI 2650 cells showed that HA-CL could act not only as carrier for SAP and active ingredient itself, but potentially also as mucoadhesive agent. In conclusion, these results suggest that HA-CL and SAP had anti-inflammatory activity and acted in combination to accelerate wound healing. Therefore, LYO HA-CL – SAP could be a potential adjuvant in nasal anti-inflammatory formulations.

### 1. Introduction

The nose is an olfactory organ, and also represents the first tract of the respiratory system, with pivotal functions: filtration, warming and moistening of the inhaled air; drainage of paranasal sinuses; sneezing; heat regulation; nasopulmonary reflexes. Hence, nasal mucosal health and proper nasal airflow are essential for the accomplishment of nasal functions (Elad et al., 2008; Jones, 2001; Patel, 2017).

Every day, the nasal passages are exposed to several pathogens that could enhance inflammation, oxidative stress, wounding and infection

(Helms and Miller, 2006; Hong et al., 2016). Allergic rhinitis (AR) is one of the most common chronic disease of the nasal mucosa, induced by an Immunoglobulin-E-dependent inflammation due to allergens' exposure (Greiner et al., 2011; Montoro et al., 2007; Small and Kim, 2011). AR can evolve in chronic rhinosinusitis (CRS) (Fokkens et al., 2012; Helms and Miller, 2006; Licari et al., 2017a; Johansson et al., 2003), and AR and CRS frequently coexist with asthma. Indeed, respiratory inflammation may start at one site and extend to another, as upper and lower airways are anatomically, histologically and immunologically linked (Jarvis et al., 2012; Licari et al., 2017a,b;

**Abbreviations:** ALL, air-liquid interface; AR, allergic rhinitis; ATCC, American type cell culture collection; BEGM, bronchial epithelial growth medium; CRS, chronic rhinosinusitis; DMEM, Dulbecco modified eagle medium; DSC, differential scanning calorimetry; Dv10, 10% cumulative volume distribution; Dv50, 50% cumulative volume distribution, i.e. median particle size by volume; Dv90, 90% cumulative volume distribution; EC, 2-l glass expansion chamber; ELISA, enzyme-linked immuno assay; FBS, foetal bovine serum; HA, hyaluronic acid; HA-CL, urea-crosslinked hyaluronic acid; HBSS, Hank's balanced salt solution; HPLC, high-performance liquid chromatography; IC50, half maximal inhibitory concentration; IL-8, interleukin-8; LPS, lipopolysaccharide; LYO HA-CL – SAP, lyophilized formulation of urea-crosslinked hyaluronic acid and sodium ascorbyl phosphate; MC, modified expansion chamber; MEM, minimum essential medium; MTS, methyl tetrazolium salt; NGI, Next Generation Impactor; PBS, phosphate buffered saline; ROS, radical oxygen species; RPMI 2650, human nasal septum carcinoma-derived cells; SAP, sodium ascorbyl phosphate; SEM, scanning electron microscopy; TGA, thermal gravimetric analysis; UDS, unit dose system

\* Corresponding author.

E-mail addresses: [filrnn@unife.it](mailto:filrnn@unife.it) (A. Fallacara), [daniela.traini@sydney.edu.au](mailto:daniela.traini@sydney.edu.au) (D. Traini).

<https://doi.org/10.1016/j.ijpharm.2019.01.012>

Received 26 November 2018; Received in revised form 8 January 2019; Accepted 10 January 2019

Available online 16 January 2019

0378-5173/ Crown Copyright © 2019 Published by Elsevier B.V. All rights reserved.

Marseglia et al., 2011). Therefore, the treatment of AR and CRS also represents an integral part of the management of asthma (Licari et al., 2017a; Marseglia et al., 2011). Intranasal corticosteroids are the mainstay therapy for AR and CRS, exerting an anti-inflammatory action and thus relieving symptoms (Helms and Miller, 2006; Licari et al., 2017a). However, their long-term use may have side effects (Campbell, 2018; Fokkens et al., 2012; Licari et al., 2017a). To limit these complications and drug resistant refractory phenomena, adjunctive therapeutic agents with anti-inflammatory, antioxidant and wound healing activity like resveratrol, alpha-tocopherol (vitamin E), curcumin, N-acetyl-L-cysteine, bromelain, quercetin, beta-carotene (provitamin A), vitamin C (ascorbic acid) and hyaluronic acid (HA) are currently being investigated for their ability to restore and maintain nasal mucosal health and functions (Albano et al., 2016; Baumeister et al., 2009; Bozdemir et al., 2016; Casale et al., 2014, 2016; Cassandro et al., 2015; Chauhan et al., 2016; Ciofalo et al., 2017a,b; Emiroglu et al., 2017; Helms and Miller, 2006; Hong et al., 2016; Horváth et al., 2016; Podoshin et al., 1991; Sagit et al., 2011; Testa et al., 2017). The present study focused on vitamin C and HA derivatives.

Vitamin C represents a major low molecular weight antioxidant of the respiratory tract lining fluid (Bastacky et al., 1995; van der Vliet et al., 1999; Wu et al., 1996). Vitamin C has been shown to scavenge radical oxygen species (ROS), thus protecting the surface of the airway epithelium (Mudway and Kelly, 2000) and intracellular DNA, lipids and proteins from oxidative stress (Li and Schellhorn, 2007). Oral vitamin C supplementation, in combination with other oral antioxidants and intranasal steroids, was found to be beneficial in the management of AR (Chauhan et al., 2016) and nasal polyposis (Sagit et al., 2011). Additionally, intranasal vitamin C was shown to decrease nasal secretions, blockage and edema in patients with AR (Podoshin et al., 1991).

High-molecular weight ( $\geq 1$  MDa) hyaluronic acid (HA) is an important component of the normal airway secretions, produced by sub-mucosal glands and by superficial airway epithelial cells (Basbaum and Finkbeiner, 1988; Fallacara et al., 2018a; Monzon et al., 2006). HA plays a central role in the homeostasis of the whole respiratory apparatus, influencing bio-mechanical forces, hydric balance, cellular functions, growth factors' activity and cytokines' behaviour (Casale et al., 2016; Fallacara et al., 2018a; Petrigli and Allegra, 2006). In the nasal epithelium, HA promotes mucociliary clearance and sustains mucosal surface healing (Gelardi et al., 2013a). Hence, intranasal exogenous HA may represent an anti-inflammatory, antioxidant, and immuno-modulating agent highly beneficial to treat the inflammatory components of AR (Fallacara et al., 2018a; Gelardi et al., 2013b, 2016), CRS (Casale et al., 2014; Cassandro et al., 2015) and other upper respiratory diseases like acute rhinosinusitis (Ciofalo et al., 2017a,b) and bacterial acute rhinopharyngitis (Varricchio et al., 2014). Additionally, intranasal HA enhances the regeneration and the morphofunctional recovery of nasal ciliated cells in patients undergoing surgery, thus promoting rhino-sinusal remodeling (Cassano et al., 2016). The major limitations of HA are its fluid nature and rapid degradation, leading to a short residence time in the nose. Therefore, HA can be crosslinked in order to synthesize novel derivatives with improved mechanical properties and bioactivity (Chen et al., 2012).

The combination of sodium ascorbyl phosphate -SAP, a pro-drug of vitamin C with improved physico-chemical stability- and urea-cross-linked hyaluronic acid -HA-CL, a novel biopolymer with promising bioactivity (Citernes et al., 2015; Fallacara et al., 2017a,b)- has recently shown potential to treat and prevent lung diseases sustained by inflammation and oxidative stress (Fallacara et al., 2018b, submitted for publication). Hence, the present work aimed to study if the combination of SAP and HA-CL could be beneficial as adjuvant therapy to treat inflammatory diseases of the upper airways. A novel nasal dry powder formulation containing SAP and HA-CL was developed using a freeze-dried technique, and characterized for its physico-chemical behaviour, *in vitro* cytotoxicity and bioactivity on human nasal epithelial cells.

## 2. Materials and methods

### 2.1. Materials

Urea-crosslinked hyaluronic acid (HA-CL, molecular weight 2.0–4.0 MDa) was kindly donated by I.R.A. Srl (Istituto Ricerche Applicate, Usmate-Velate, Monza-Brianza, Italy). HA-CL was provided as raw material containing polyethylene glycol, and it was used as supplied. Therefore, a 1% (w/v) 1:1 HA-CL – SAP solution contained also 0.75% (w/v) polyethylene glycol. Sodium ascorbyl phosphate (SAP) was purchased from DSM Nutritional Products Ltd (Segrate, Milano, Italy). Phosphate buffered saline (PBS, pH = 7.4, 0.01 M) used for the physico-chemical characterization of the formulation was supplied by Sigma-Aldrich (Sydney, NSW, Australia). Water was purified by Milli-Q reverse Osmosis (Molsheim, France). Polyamide membrane filters 0.45  $\mu$ m pore size were obtained from Sartorius Biolab Products (Goettingen, Germany), while wax foils were provided by Parafilm M, Bemis Company Inc. (Oshkosh, WI, USA).

The unit dose system (UDS) powder device was purchased from Pfeiffer, Aptar Pharma division (Radolfzell, Germany).

Human nasal septum carcinoma-derived cells (RPMI 2650) were purchased from the American Type Cell Culture Collection (ATCC, Manassas, VA, USA). Snapwell™ cell culture inserts (1.13 cm<sup>2</sup> surface area, polyester, 0.4  $\mu$ m pore size) and 96-well plates were obtained from Corning Costar (Lowell, MA, USA). Disposable cytology brushes (Model BC-202D-2010) were provided by Olympus Australia Pty. Ltd. (Notting Hill, VIC, Australia). All other culture plastics were from Sarstedt (Adelaide, SA, Australia). Minimum essential medium (MEM), PBS for cell cultivation, Hank's balanced salt solution (HBSS), foetal bovine serum (FBS) and 0.25% trypsin – EDTA were all purchased from Gibco by Life Technologies (Sydney, NSW, Australia). Bronchial epithelial growth medium (BEGM) and SingleQuots™ kit were provided by Lonza (Walkersville, MD, USA). Lipopolysaccharide (LPS) from *Escherichia coli*, trans-retinoic acid, non-essential amino acids solution, 200 mM L-glutamine solution were purchased from Sigma-Aldrich (Sydney, NSW, Australia). CellLytic™ buffer was obtained from Invitrogen (Sydney, NSW, Australia). Methyl tetrazolium salt (MTS) reagent -CellTiter 96® Aqueous One Solution Cell Proliferation Assay- for cell viability test was purchased from Promega (Sydney, NSW, Australia). Bovine collagen was provided by Nutacon (Leimuiden, Netherlands). Rat collagen type I and enzyme-linked immuno assay (ELISA) kit for determination of the inflammation marker interleukin-8 (IL-8) were obtained from BD Bioscience (Sydney, NSW, Australia). All solvents were obtained from VWR Prolabo Chemicals (Milan, Italy) and were of HPLC grade.

### 2.2. Preparation of the freeze-dried formulation

HA-CL and SAP were dissolved into 50 mL of milli-Q water kept under constant magnetic stirring, at room temperature, overnight. A 1% (w/v) 1:1 HA-CL – SAP solution was obtained and placed in a –80 °C freezer for 24 h. Then, the solution was lyophilized for 24 h, at –100 °C, with a vacuum degree of 0.1 mbar, using an Alpha 2–4 LSC plus freeze dryer (Martin Christ, Osterode am Harz, Germany) equipped with a rotary vane Vacubrand R26 pump (Wertheim, Germany). No cryoprotectant was added to the formulation. At the end of the lyophilisation process, the sample was stored in a desiccator for 24 h, manually grinded with a spatula and passed through a stainless steel sieve (300  $\mu$ m pore-size).

### 2.3. Physico-chemical characterization

#### 2.3.1. Chemical quantification of SAP by high-performance liquid chromatography

SAP was quantified using a high-performance liquid chromatography (HPLC) method that was adapted from literature (Foco et al.,



2005). A Shimadzu Prominence UFLC system equipped with DGU-20A5R Prominence degassing unit, LC-20 AD solvent delivery unit, SIL-20A HT autosampler and SPD-20A UV/VIS detector was employed (Shimadzu Corporation, Tokyo, Japan). A volume of 50  $\mu$ L of sample was injected using 40:60 (% v/v) acetonitrile:0.3 M phosphate buffer (pH = 4) as mobile phase, at a flow rate of 2.0 mL/min, in isocratic mode with a Luna NH<sub>2</sub> column (5  $\mu$ m, 4.6  $\times$  150 mm) (Phenomenex, Sydney, NSW, Australia). SAP retention time was 6 min. The concentration of SAP was measured at a wavelength of 258 nm from the peak area correlated with a predetermined standard curve over the range 0.1–1000  $\mu$ g/mL ( $R^2 = 1$ ).

### 2.3.2. Morphological analysis

Scanning electron microscopy (SEM) was used to investigate the morphology and surface properties of the lyophilized formulation containing HA-CL and SAP (LYO HA-CL – SAP). The analysis was carried out using a JCM-6000 benchtop scanning electron microscope (Jeol, Tokyo, Japan), operating at 10 kV. Prior to imaging, the sample was deposited on a carbon sticky tape, placed onto aluminium stubs, and gold-coated for 2 min using an automated sputter coater (Smart Coater, Jeol, Tokyo, Japan).

### 2.3.3. Particle size analysis

Particle diameter and particle size distribution of LYO HA-CL – SAP were determined by laser diffraction (Mastersizer 3000, Malvern, Worcestershire, UK). Approximately 10 mg of sample were dispersed in air using the Scirocco Aero-S dry dispersion unit (Malvern, Worcestershire, UK), with a feed pressure of 4 bars, a feed rate of 100% and a total time of analysis set at 3 s. Measurements were carried out in triplicate, with an obscuration value between 0.1% and 15%, and a reference refractive index of 1.33. The maximum particle size for 10, 50 and 90% of the cumulative volume distribution of the sample (defined as Dv10, 50 and 90, respectively) were used to describe particle size. The width of the particle size distribution was expressed by the Span index. Data were reported as mean  $\pm$  standard deviation.

### 2.3.4. Thermal analysis

The thermal response of LYO HA-CL – SAP was assessed using differential scanning calorimetry (DSC – DSC823e; Mettler-Toledo, Schwerzenbach, Switzerland). Roughly 5 mg of sample were weighed, crimp-sealed in DSC standard 40  $\mu$ L aluminium pans and heated at 10  $^{\circ}$ C/min between –20 and 300  $^{\circ}$ C. The endothermic and exothermic peaks were determined using STARe software V.11.0x (Mettler Toledo, Greifensee, Switzerland).

Additionally, the temperature stability and solvent evaporation of the freeze-dried formulation were investigated using the thermal gravimetric analysis (TGA – Mettler-Toledo, Switzerland). Approximately 5 mg of sample were placed onto aluminium crucible pans. The weight loss of the sample was evaluated over a temperature range of 20–400  $^{\circ}$ C, with a scanning rate of 5  $^{\circ}$ C/min, under constant nitrogen gas. Data were analyzed using STARe software V.11.0x (Mettler Toledo, Greifensee, Switzerland) and expressed as the percentage of weight loss with respect to initial sample weight.

### 2.3.5. In vitro SAP release study

Franz's diffusion cells (25 mm internal diameter, multi-station VB6 apparatus, PermeGear Inc., Hellertown, PA, USA) were used to study SAP release profile from LYO HA-CL – SAP, according to a previously published protocol (Ong et al., 2011). Briefly, polyamide membrane filters (0.45  $\mu$ m pore size) were hydrated by sonication in PBS (pH = 7.4, 0.01 M) for 30 min, cut and placed between the receiver and donor compartments of the diffusion cells that were maintained at 37  $\pm$  0.5  $^{\circ}$ C. Samples were placed in the donor compartments in order to have ~5 mg of SAP on the surface of the membranes, which were sealed using a wax foil to prevent evaporation. The receiver compartments were filled with 23 mL of PBS continuously stirred at 150 rpm. At

defined time points (0, 5, 10, 15, 20, 30, 45, 60, 90, 120 min), 0.5 mL of samples were withdrawn from the receptor compartments and replaced with equal volumes of pre-warmed PBS. After 120 min, each filter was washed with 5 mL of PBS and then sonicated with another 5 mL of PBS for 10 min. Samples were assayed for SAP concentration using HPLC. Experiments were performed in triplicate and data were expressed and plotted as mean  $\pm$  standard deviation of the cumulative percentage of SAP released over time.

### 2.3.6. Aerosol performance by cascade impaction

The aerodynamic performance of LYO HA-CL – SAP delivered using the UDS device was investigated using a British Pharmacopoeia Apparatus E – Next Generation Impactor (NGI -Westech W7; Westech Scientific Instruments, Upper Stondon, UK), equipped with a 2-L glass expansion chamber (EC), according to the Food and Drug Administration (FDA) guidance for industry, and as previously reported in literature (FDA CDER, 2003; Pozzoli et al., 2016a,b, 2017).

Considering that the human nose can accommodate about 10–25 mg of powder *per nostril per shot* (Elmowafy et al., 2014), 16 mg of LYO HA-CL – SAP (corresponding to ~5 mg of SAP) were loaded into the UDS device. Briefly, the device was connected to the inlet of the EC, that was assembled on the NGI. A rotary pump (Westech Scientific Instruments, Upper Stondon, UK) was connected to the NGI. The test was performed by actuating the device with an air flow of 15 L/min, calibrated using a flow meter (Model 4040, TSI Precision Measurement Instruments, Aachen, Germany), for 4 s. Each impactor stage was washed with the following volumes of deionized water: EC 25 mL; device, connection tube and first stage 10 mL; all other stages 5 mL. SAP was quantified using the HPLC method. Experiments were carried out in triplicate and data were expressed as mean  $\pm$  standard deviation.

### 2.3.7. In-line geometric aerosol laser diffraction analysis

Laser diffraction (SprayTec™, Malvern Instruments, Worcestershire, UK) was used to measure the geometric particle size distribution of LYO HA-CL – SAP emitted from the UDS device (filled with 16 mg of formulation, corresponding to ~5 mg of SAP). The device was connected to the measurement cell at a fixed angle of 30 $^{\circ}$ , with an extraction flow of 15 L/min. Three independent analyses were performed for 4 s, with an acquisition rate of 2.5 kHz. Results were expressed as mean  $\pm$  standard deviation.

## 2.4. In vitro biological studies on nasal cell models

Cytotoxicity, wound healing activity, drug deposition and transport were investigated using RPMI 2650 human nasal cell line. Additionally, anti-inflammatory activity was explored using primary brushed nasal epithelial cells.

### 2.4.1. Cultivation of RPMI 2650 cell line

RPMI 2650 immortalized human nasal cell line were grown and passaged according to ATCC protocol and as previously described in literature (Bai et al., 2008; Kreft et al., 2015; Pozzoli et al., 2016a,b, 2017; Reichl and Becker, 2012). Briefly, cells between passages 17–25 were cultured in 75 cm<sup>2</sup> flasks containing MEM supplemented with 10% (v/v) FBS, 1% (v/v) non-essential amino acid solution and 2 mM L-glutamine, and maintained in a humidified atmosphere of 95% air, 5% CO<sub>2</sub>, at 37  $^{\circ}$ C.

Liquid covered cultures were obtained by seeding RPMI 2650 cells ( $5 \times 10^4$  cells/well) in a volume of 100  $\mu$ L into 96-well plates, and were used to perform cell viability assay within 24 h from the seeding.

Additionally, an air-liquid interface (ALI) nasal model was established using Snapwell™ cell culture inserts. In brief, inserts were coated with 250  $\mu$ L of 1  $\mu$ g/ml rat collagen type 1 solution in PBS and incubate overnight at 37  $^{\circ}$ C to create the appropriate adherence of the cells to the membrane (Wengst and Reichl, 2010). 200  $\mu$ L of RPMI 2650 nasal cells suspension ( $2.5 \times 10^6$  cell/ml) were seeded on Snapwell™ and after

24 h the medium from the apical compartment was withdrawn, resulting in an ALI model. The medium in the basolateral chamber was replaced 3 times per week. Wound healing and deposition/transport studies were performed 14 days after the seeding.

#### 2.4.2. MTS cytotoxicity assay on RPMI 2650 cells

The *in vitro* cytotoxicity of LYO HA-CL – SAP was assessed on a liquid covered culture of RPMI 2650 cells. Sample solutions with increasing concentrations of the formulation were aseptically prepared, added to the cells and, after 3 days, a MTS assay was performed to measure cellular metabolic activity.

Briefly,  $5 \times 10^4$  cells were seeded per well in a volume of 100  $\mu$ L into 96-well plates. Cells were incubated overnight at 37 °C in a humidified atmosphere with 5% CO<sub>2</sub>. On the second day, 100  $\mu$ L of pre-warmed solutions of LYO HA-CL – SAP were added to each well. The lyophilized formulation was investigated in a SAP concentration range from 8.0 mM to 60.9 nM. Background controls (medium) and untreated controls (untreated cells) were included in the experiment. Plates were incubated for 72 h at 37 °C in a humidified atmosphere with 5% CO<sub>2</sub>. Cells were then analysed for viability. Hence, 20  $\mu$ L of MTS reagent were added to each well and the plates were incubated for another 3 h in the same conditions. Finally, the 96 well-plates were read at 490 nm using a SpectraMax microplate reader. The absorbance values were directly proportional to cell viability (%). Experiments were performed in triplicate. Data were expressed as mean  $\pm$  standard deviation of the % cell viability relative to untreated control, and plotted against SAP concentration (nM) on a logarithmic scale.

#### 2.4.3. Deposition/transport study on RPMI 2650 cells

The aerosol deposition of LYO HA-CL – SAP on RPMI 2650 cell surface was studied using a custom-built 3D printed modified expansion chamber (MC) (Pozzoli et al., 2016a). Prior to the experiment, three inserts were washed with pre-warmed HBSS and fitted into the upper hemisphere of the MC. As described above, a total dose of 16 mg of formulation (corresponding to  $\sim$ 5 mg of SAP, 1 shot/actuation) was delivered with the UDS device into the MC. The cell inserts were then removed from the MC and transferred into a 6-well plate, containing 1.5 mL/well of fresh pre-warmed HBSS. At defined time point (15, 30, 45, 60, 90, 120, 150, 180, 210, 240 min), 200  $\mu$ L of samples were collected from the basal chamber and replaced with the same volume of fresh HBSS buffer. After 4 h, the apical surface of the epithelia was washed twice with 300  $\mu$ L of HBSS in order to collect any remaining drug on the cells. At the end of the experiment, cells were washed with 300  $\mu$ L of HBSS, scraped from the insert membrane, and lysed with 500  $\mu$ L of CellLytic™ buffer in order to quantify intracellular SAP. Samples were centrifuged (10 min, 10,000 $\times$ g, 4 °C) and the supernatants were analyzed for SAP concentration by HPLC. Experiments were performed in triplicate. The initial amount of SAP deposited on the cell layer was calculated as the sum of SAP mass transported, remaining on the epithelium and recovered inside the cells at the end of the experiment. Data were plotted as mean  $\pm$  standard deviation of the cumulative percentage of SAP transported over time.

#### 2.4.4. Physical injury and wound healing assay on RPMI 2650 cells

Wound healing properties of LYO HA-CL – SAP were evaluated on ALI RPMI 2650 cell layer. The cells were mechanically scraped using a sterile 200  $\mu$ L pipette tip to form three homogenous and parallel scratches. After scraping, the wells were allocated into the upper hemisphere of the MC, and the formulation was subsequently deposited on the cell layers as described above. The healing of the layers was monitored via a time-lapse microscopy. Immediately after wounding and deposition, the Snapwells™ plates were transferred to the built-in chamber of a Nikon Eclipse Ti (Nikon, Tokyo, Japan) equipped with Clear State Solution humidifier (Clear State Solution, Mount Waverly, VIC, Australia) and CO<sub>2</sub> controller which provided a humidified CO<sub>2</sub> atmosphere at 37 °C. Images of the scratches were captured by a

CoolSNAP ES2 high resolution digital camera (Photometrics, Tucson, AZ, USA) every 20 min over 24 h. Images were analysed with FIJI (NIH), wound edges were manually selected and wound area was automatically calculated. Experiments were performed in triplicate. Data were expressed as mean  $\pm$  standard deviation of the percentage of wound closed according to the following equation (Eq. (1)):

$$WC = \frac{W_i - W_t}{W_i} \times 100 \quad (1)$$

where WC is the wound closure (%),  $W_i$  is the initial area of wound and  $W_t$  is the area of the wound at certain time.

#### 2.4.5. Sampling, expansion and ALI cultivation of brushed nasal epithelial cells

Nasal cells were obtained from 5 healthy volunteers between the ages of 20 and 30 through nasal brushing biopsies, and cultured according to methodologies as previously described (Muller et al., 2013). Brushings were performed only on volunteers without any upper respiratory tract disease and infection for at least 4 weeks prior to sampling. Briefly, a cytology brush was inserted approximately 5 cm into the volunteers' naris, and the inferior turbinate and the nasal epithelium were gently brushed. Strips of ciliated nasal epithelium were obtained, with each brushing containing up to 10,000 cells.

Prior to cell seeding, the microwell plates, flasks, and Snapwell™ inserts were coated for 1 h with 0.5 mL, 1 mL, and 0.1 mL of 0.3 mg/mL of bovine collagen, respectively, and were air-dried. The strips of ciliated nasal epithelium were grown on collagen-coated tissue culture 12-well plates in BEGM hormonally supplemented with SingleQuots™ for approximately 1 week, changing cell medium every other day. The confluent basal cells were then expanded onto a collagen coated 25 cm<sup>2</sup> flask with the BEGM replaced three times per week. When cultures reached  $\sim$ 80% confluency, the basal cells were detached with 0.25% trypsin – EDTA and seeded with a density of 200,000–250,000 cells per well onto collagen-coated Snapwell™ cell culture inserts. At this stage, the cells were fed with ALI medium made up of 1:1 BEGM:DMEM 4.5 g/L D-glucose including SingleQuots until 100% confluent (into 1–2 days). Primary human basal epithelial cells were then exposed to an ALI interface: to allow for cell differentiation, ALI medium supplemented with additional 100 nM all-trans-retinoic acid was placed only in the basolateral chamber (Hirst et al., 2014; Lee et al., 2005; Yoo et al., 2003). The medium was changed three times per week, and any apical surface liquid or mucus was removed. Cilia started to re-generate after 12 days from the establishment of the ALI conditions, and become visible under the microscope from day 21 ALI.

#### 2.4.6. Pro-inflammatory IL-8 expression in brushed nasal epithelial cells

The expression of the pro-inflammatory cytokine IL-8 was evaluated using the ALI primary nasal cells treated with LYO HA-CL – SAP (150  $\mu$ g/mL), before, after and without LPS exposure. The effect of the formulation on cells was compared with unstimulated and untreated cells (control cells, i.e. cells in culture medium, without LPS and formulations) and LPS-stimulated but untreated cells (positive control, i.e. cells exposed only to 10 ng/mL LPS).

Firstly, LYO HA-CL – SAP was evaluated for its ability to influence IL-8 production in non-inflamed nasal cells. Subsequently, cells were incubated at 37 °C, 5% CO<sub>2</sub>, for 24 h, with a pre-warmed solution of LYO HA-CL – SAP. On the second day, cell culture medium was withdrawn, centrifuged (5 min, 13000 rpm, 4 °C), and analyzed for IL-8 level using a human IL-8 ELISA kit, according to the manufacturer's protocol. The amount of IL-8 released in the samples was quantified using a standard calibration curve obtained with purified recombinant human IL-8 provided with the kit. The limit of detection was 3.1–200 pg/mL.

Then, to test the formulation ability to prevent inflammation, cells were exposed to a pre-warmed solution of LYO HA-CL – SAP, and incubated at 37 °C, 5% CO<sub>2</sub> for 24 h. Afterwards, cells were incubated again for another 24 h, at 37 °C, 5% CO<sub>2</sub>, with 10 ng/mL LPS.



Subsequently, cell culture supernatant was withdrawn, centrifuged (5 min, 13000 rpm, 4 °C), and analyzed for IL-8 level as previously described.

Finally, the anti-inflammatory efficacy of LYO HA-CL – SAP was evaluated by its ability to reduce inflammation in primary ALI nasal cells after induction of IL-8 production by LPS. Hence, cells were incubated with 10 ng/mL LPS for 24 h at 37 °C, in a humidified atmosphere at 5% CO<sub>2</sub>. Subsequently, cells were exposed to a pre-warmed solution of LYO HA-CL – SAP, and after 24 h of incubation in the same conditions, cell culture supernatant was withdrawn, centrifuged (5 min, 13000 rpm, 4 °C), and analyzed for IL-8 concentration as previously described.

### 2.5. Statistical analysis

All the data are presented as mean  $\pm$  standard deviation of a minimum of three independent experiments. Statistical analysis was performed using GraphPad Prism software version 7.0b (GraphPad, San Diego, USA). Wound healing data were analyzed with unpaired *t*-test, while anti-inflammatory response data were analyzed with one-way analysis of variance (ANOVA) followed by Tukey *post hoc* test for multiple comparisons. Differences were considered statistically significant for  $P < 0.05$  (\* $P < 0.05$ , \*\* $P < 0.01$ , \*\*\* $P < 0.001$  and \*\*\*\* $P < 0.0001$ ).

## 3. Results and discussion

Previous studies showed that SAP and HA-CL, when delivered in combination, provide an enhanced effect in controlling lung inflammation and oxidative stress (Fallacara et al., 2018b, submitted for publication). Additionally, emerging data showed the beneficial role in nasal inflammatory diseases for the precursors of these substances –vitamin C (Chauhan et al., 2016; Podoshin et al., 1991; Sagit et al., 2011) and HA (Casale et al., 2014, 2016; Cassandro et al., 2015; Ciofalo et al., 2017a,b; Garantziotis et al., 2016; Gelardi et al., 2013b, 2016; Varricchio et al., 2014). All these evidences strongly supported the present study to develop a novel formulation containing both SAP and HA-CL to enhance treatments for nasal diseases, like AR and CRS. A dry powder formulation was prepared, as powders, being solid dosage forms, are chemically and microbiologically more stable than liquids, and require simpler compositions in excipients (if any) (Tiozzo Fasiolo et al., 2018). Moreover, compared to nasal liquids, nasal powders undergo slower clearances from the nasal cavity, and can be delivered more efficiently by insufflation devices that permit the deposition on a larger surface of the nasal mucosa (Tiozzo Fasiolo et al., 2018). All this can improve drug diffusion, adsorption across the mucosa, and bioavailability (Tiozzo Fasiolo et al., 2018).

### 3.1. Physico-chemical characterization

#### 3.1.1. Morphological analysis

In Fig. 1 the morphology of LYO HA-CL – SAP observed by SEM is presented. The formulation was characterized by porous particles of polygonal shape, with size  $> 50 \mu\text{m}$  and  $< 600 \mu\text{m}$ , that is suitable for nasal delivery (Kippax et al., 2010).

#### 3.1.2. Particle size analysis

Results of laser diffraction analysis of LYO HA-CL – SAP are shown in Fig. 2. A unimodal and narrow dispersion (Span index:  $1.2 \pm 0.0$ ) was observed, with a Dv50 of  $328.3 \pm 27.5 \mu\text{m}$ . Moreover, 10% of LYO HA-CL – SAP particles had a diameter  $\leq 179.0 \pm 17.4 \mu\text{m}$  (Dv10), and 90%  $\leq 566.7 \pm 39.5 \mu\text{m}$  (Dv90). Hence, the freeze-dried formulation appeared to be suitable for nasal delivery as no particle fraction was found to be smaller than  $10 \mu\text{m}$  (Ozsoy et al., 2009; Tiozzo Fasiolo et al., 2018).

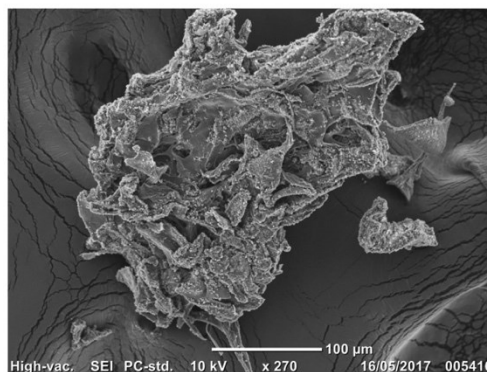


Fig. 1. SEM micrograph of LYO HA-CL – SAP.

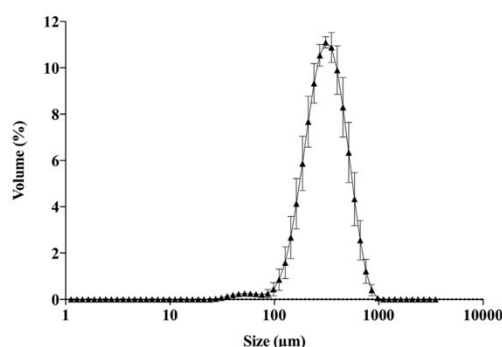


Fig. 2. Particle size distribution of LYO HA-CL – SAP. Data represent mean  $\pm$  SD (n = 3).

#### 3.1.3. Thermal analysis

The thermal behaviour and physical stability of LYO HA-CL – SAP were investigated using DSC and TGA, as shown in Fig. 3.

The DSC thermal profile of LYO HA-CL – SAP was characterized by two wide endothermic peaks: the first at 97 °C, suggesting a dehydration process, and the second at 200 °C, which was attributed to pentylene glycol evaporation (boiling range 198–200 °C) (Fig. 3A). The thermal decomposition of LYO HA-CL – SAP and the formation of a carbonized residue occurred at 240 °C, where a broad exothermic peak was observed. This DSC profile suggested that HA-CL and SAP formed a solid solution/amorphous solid dispersion in the freeze-dried formulation. Such result was in good agreement with previous observations reported for SAP raw material, HA-CL microspheres and other dry powder formulations containing both SAP and HA-CL (Fallacara et al., 2018b, submitted for publication).

TGA thermograph of LYO HA-CL – SAP is displayed in Fig. 3B. Three distinct degradation stages could be observed, with the first stage (20–181 °C, 6.7% w/w of weight loss) that is characteristic of water evaporation; the second (181–246 °C, 22.5% w/w of weight loss, including also the evaporation of pentylene glycol) and the third stages (246–400 °C, 12.8% w/w of weight loss) that are typical of a two-stages polysaccharide degradation.

Hence, the thermal decomposition of HA-CL and SAP occurred simultaneously, as showed by DSC and TGA curves, and confirmed by data previously obtained for HA-CL microspheres containing SAP (Fallacara et al., 2018c).



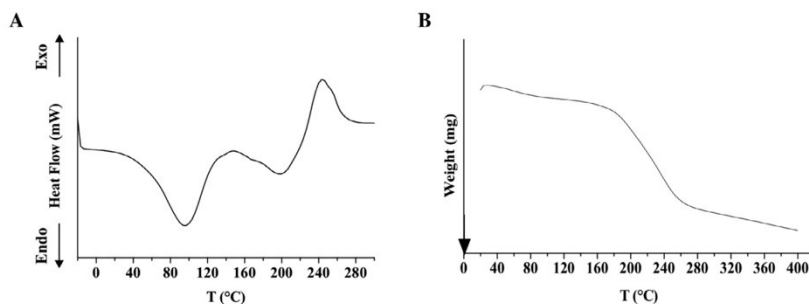


Fig. 3. DSC (A) and TGA (B) thermal profiles of LYO HA-CL – SAP.

### 3.1.4. *In vitro* aerosolization performance

Particle size is a key parameter in defining the deposition pattern of formulations delivered to the nasal mucosa using nasal inhalers and pump sprays. To verify the absence of particles with aerodynamic diameter  $< 10 \mu\text{m}$ , that could reach the lower airways (Cheng et al., 2001; Doub et al., 2012), the FDA draft guidance for industry has suggested to perform impactor and laser diffraction analyses (FDA CDER, 2003). Hence, the aerodynamic efficiency of LYO HA-CL – SAP, delivered with the UDS nasal device, was investigated using the Apparatus E equipped with a FDA 2-L glass EC (FDA CDER, 2003). Additionally, SprayTec™ laser diffraction technique was employed to assess the geometric particle size distribution of the emitted dose from the UDS nasal device.

In Table 1 the *in vitro* aerosolization performance of LYO HA-CL – SAP is presented. Results are presented as the percentage of the drug remaining in the device and deposited in the EC, connection tube, and each stage of the NGI, over the total theoretical amount of drug filled in the device. It was found that the LYO HA-CL – SAP formulation is suitable for nasal drug delivery, with 88.7% of the particles showing an aerodynamic diameter larger than  $14.1 \mu\text{m}$  ( $78.3 \pm 2.7\%$  of the particles in the EC, plus  $0.7 \pm 0.5\%$  in the connection tube and  $9.7 \pm 1.5\%$  in the S1), while the remaining  $11.3 \pm 4.0\%$  of SAP was recovered in the device. As no drug was detected in the lower stages of the NGI, there was no respirable fraction.

The aerosolization performance of the freeze-dried formulation was also characterised by SprayTec™ laser diffraction particle sizing. The SprayTec™ system ensures the characterization of the whole particle size distribution, and detects the dynamics of particle dispersion along with the device reproducibility, while cascade impaction provides information on the aerosol performance of the particles below  $10 \mu\text{m}$ . Table 2 shows the results of SprayTec™ analyses carried out on LYO HA-CL – SAP, which exhibited a geometric diameter that is suitable for nasal delivery. Indeed, the size distribution was unimodal and narrow (Span index:  $1.8 \pm 0.0$ ), with the 90% of particles below  $537.8 \pm 28.8 \mu\text{m}$  and a median diameter of  $243.0 \pm 13.0 \mu\text{m}$ . No particles below  $10 \mu\text{m}$  were detected.

Table 1

Percentage of SAP recovered in each stage of the apparatus E equipped with the 2-l glass EC for nasal delivery. Data are presented as mean  $\pm$  SD (n = 3).

	Amount of SAP recovered (%)	Cut off diameter ( $\mu\text{m}$ )
Device	$11.3 \pm 4.0$	–
EC	$78.3 \pm 2.7$	–
Connection tube	$0.7 \pm 0.5$	–
S1	$9.7 \pm 1.5$	$> 14.1$
S2-S8	–	$< 14.1$
Total recovery	$100.0 \pm 0.0$	–

Table 2

Values of volumetric diameter, Span index and percentage of particles  $\leq 10 \mu\text{m}$  obtained for LYO HA-CL – SAP with SprayTec™ system. Data represent mean  $\pm$  SD (n = 3).

	LYO HA-CL – SAP
Dv(10)	$100.5 \pm 4.5$
Dv(50)	$243.0 \pm 13.0$
Dv(90)	$537.8 \pm 28.8$
Span	$1.8 \pm 0.0$
% V ( $\leq 10 \mu\text{m}$ )	$0.0 \pm 0.0$

### 3.2. *In vitro* studies on nasal cell models

#### 3.2.1. MTS cytotoxicity assay on RPMI 2650 cells

The *in vitro* cytotoxicity of LYO HA-CL – SAP was evaluated using the colorimetric MTS assay. RPMI 2650 cells were incubated for 72 h with solutions of the freeze-dried formulation with SAP concentration ranging from 8.0 mM to 60.9 nM. As displayed in Fig. 4, cells maintained their metabolic activity and were viable after the exposure to the solution with the highest concentration. Since the half maximal inhibitory concentration value (IC50) could not be determined across all the concentration interval examined, LYO HA-CL – SAP could be considered non-toxic for RPMI 2650 cells at the wide concentration range tested. Hence, this study showed for the first time that the novel HA-CL polymer could be safely used for nasal formulations. In fact, HA-CL maintained the excellent safety profile of high molecular weight native HA, which was previously found to be non-toxic even at high concentration – 1% on RPMI 2650 cells (Horváth et al., 2016), 3% on adult

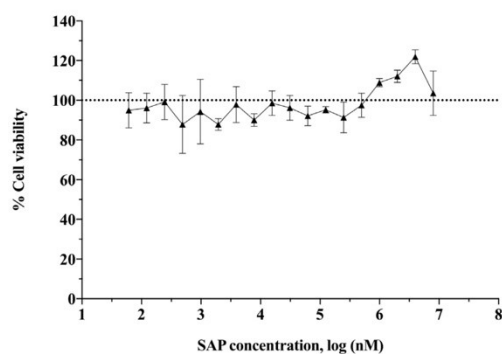


Fig. 4. Viability of RPMI 2650 cells evaluated using MTS assay after 72 h of treatment with LYO HA-CL – SAP. Data represent mean  $\pm$  SD (n = 3).

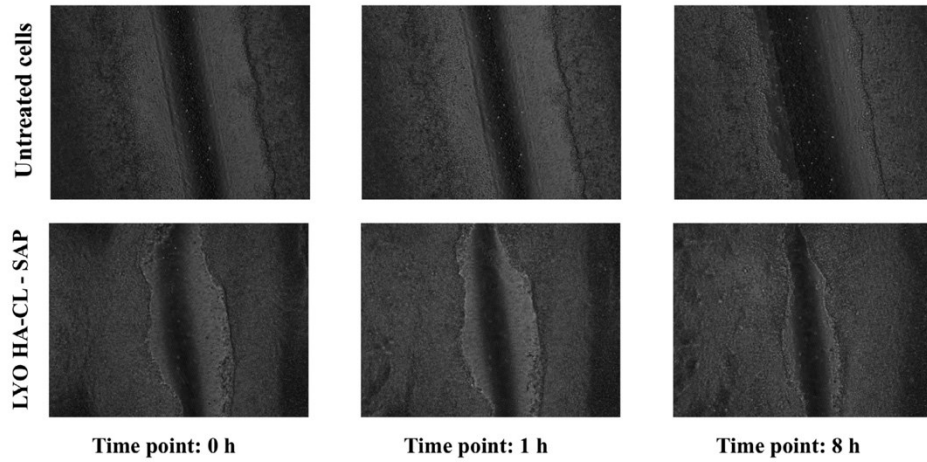


Fig. 5. Wound images of untreated cells and cells treated with LYO HA-CL-SAP at different time points (0, 1, 8 h).

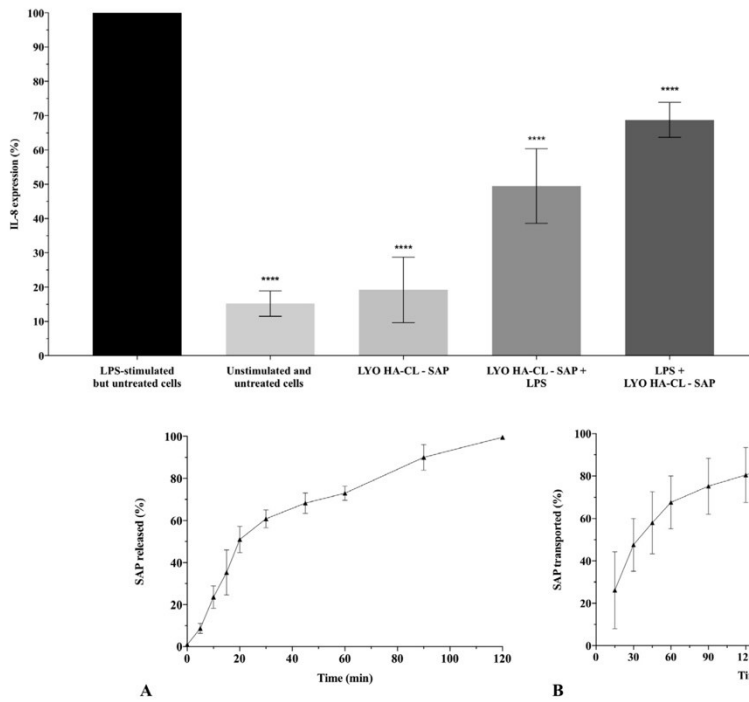


Fig. 7. *In vitro* release profiles of SAP from LYO HA-CL-SAP: release by Franz's cells (A) and transport across RPMI 2650 cells (B). Data represent mean  $\pm$  SD (n = 3).

volunteers affected by rhinosinusitis (Ciofalo et al., 2017a).

### 3.2.2. Wound healing assay on RPMI 2650 cells

Factors such as allergies, prolonged/chronic inflammation, virus and bacterial infections can alter the nasal mucosa homeostasis and,

therefore, can damage or destruct the epithelium. In order to assess the ability of LYO HA-CL-SAP to improve epithelia damage, wound healing assays were performed. Fig. 5 shows images of the wound healing process without and with treatment (LYO HA-CL-SAP) at different time points (0, 1, 8 h). The freeze-dried powder formulation

Fig. 6. Concentration of IL-8 inflammatory cytokine in primary brushed ALI nasal cells supernatant after exposure to: LYO HA CL-SAP; LYO HA CL-SAP then LPS (LYO HA CL-SAP + LPS); LPS and then LYO HA CL-SAP (LPS + LYO HA CL-SAP). IL-8 levels were assessed in comparison to those of LPS-stimulated but untreated cells (positive control, i.e. cells exposed only to 10 ng/mL LPS), and unstimulated and untreated cells (control cells). Data represent mean  $\pm$  standard deviation (n = 5). Asterisks indicate significant difference from LPS-stimulated but untreated cells (\*\*\*\*p < 0.0001).

showed wound healing ability with significant improvement of the wound closure observed at 8 h. Through image analysis, it was calculated that LYO HA-CL – SAP was able to close roughly the  $62 \pm 13\%$  of the wound after 8 h. This closure was significantly different compared to untreated cells ( $P < 0.0001$ ), where the wound closure was only  $13 \pm 4\%$ . Hence, these results provided preliminary evidence that LYO HA-CL – SAP was able to promote the re-epithelialization of RPMI 2650 wounded cells, demonstrating its potential use as adjuvant in nasal anti-inflammatory treatments.

### 3.2.3. Pro-inflammatory IL-8 expression in brushed nasal epithelial cells

IL-8 is a pro-inflammatory cytokine that is able to enhance allergic inflammation. It is highly expressed in many inflammatory diseases of the upper respiratory tract, including AR and CRS (Hu and Li, 2018; Lee et al., 2018). This *in vitro* study investigated the ability of the novel LYO HA-CL – SAP formulation in reducing the expression of IL-8 in primary ALI nasal cells, thus providing an anti-inflammatory activity.

Results showed that IL-8 production was not increased ( $P > 0.05$ ) by the exposure of non-stimulated primary nasal cells to LYO HA-CL – SAP, with IL-8 levels of  $15.2 \pm 3.3\%$  in unstimulated and untreated cells and  $19.2 \pm 8.5\%$  in LYO HA-CL – SAP treated cells (LYO HA-CL – SAP), as showed in Fig. 6. On the contrary, cells exposed to 10 ng/mL LPS that remained untreated exhibited a significant inflammatory response ( $P < 0.0001$ ), with an IL-8 concentration that was 6.5 times higher with respect to unstimulated and untreated cells (Fig. 6).

As depicted in Fig. 6, cell exposure to LYO HA-CL – SAP treatment 24 h prior to stimulation with 10 ng/mL LPS significantly reduced IL-8 production to  $49.5 \pm 9.7\%$  (LYO HA-CL – SAP + LPS), compared to LPS-stimulated but untreated cells ( $100.0 \pm 0.0\%$ ;  $P < 0.0001$ ). Hence, LYO HA-CL – SAP was shown to potentially play a preventive anti-inflammatory action.

Additionally, the anti-inflammatory property of LYO HA-CL – SAP was investigated after stimulation of primary nasal cells with 10 ng/mL LPS 24 h prior to treatment exposure. IL-8 concentration was determined 24 h after the sample addition on the LPS-stimulated cells. LYO HA-CL – SAP showed the ability to reduce IL-8 release compared to LPS-stimulated but untreated cells: more specifically, LYO HA-CL – SAP decreased IL-8 concentration to  $68.8 \pm 4.6\%$  (LPS + LYO HA-CL – SAP) (Fig. 6). Therefore, LYO HA-CL – SAP was found to have a significant anti-inflammatory activity towards inflamed primary nasal cells ( $P < 0.0001$ ) (Fig. 6). These results showed that the freeze-dried powder consisting of HA-CL and SAP could be a suitable formulation to reduce inflammation in upper airway diseases.

### 3.3. *In vitro* release study: release by Franz's cells and transport across RPMI 2650 cells

Franz's cells were chosen to explore the dissolution and release properties of LYO HA-CL – SAP (Fig. 7A), as the thin layer of liquid on the cells membranes permits the progressive hydration of the formulation in a humid environment. This is more representative of the *in vivo* nasal mucus layer with respect to the larger volume of dissolution medium of other release methods. Furthermore, SAP permeation profile was also studied across RPMI 2650 cells grown in the ALI configuration, for 4 h after LYO HA-CL – SAP deposition in the 3D MC (Fig. 7B).

Due to its hydrophilicity, SAP rapidly diffused into the medium of the receptor compartment when LYO HA-CL – SAP was deposited on the filter membranes of Franz's cells. After 60 min,  $73.0 \pm 3.4\%$  of the drug was released from the freeze-dried formulation, and after 120 min, the release was completed (Fig. 7A). These results could suggest a good *in vivo* dissolution of the formulation in the nasal epithelial lining fluid, enhancing drug transport, bioavailability, and therapeutic efficacy (Vasa et al., 2017).

Fig. 7B displays the percentage of SAP transported across RPMI 2650 epithelium as a function of time. During the first hour, LYO HA-CL – SAP exhibited marked permeation properties, with  $67.6 \pm 12.4\%$  of

SAP transported. Afterwards, a decreased permeation rate was observed. At the end of the 4 h, almost all SAP was transported ( $92.6 \pm 5.7\%$ ), as only the  $7.4 \pm 5.7\%$  of SAP remained on the cells (Fig. 7B).

SAP release profile was extended when studied on RPMI 2650 cells (Fig. 7B) compared to Franz's cells (Fig. 7A). This delay was due to the low permeability of the simulated nasal epithelium, and so it was an effect of the cell barrier itself. Moreover, an enhanced mucoadhesive behaviour of hyaluronan on cell tissues could be hypothesized. In fact, HA-CL probably interacted with the mucus layer on the RPMI 2650 cells, absorbing water and thus becoming wet, swelled and gelled. Consequently, the formulation penetrated into the mucus, changed its structure and rheological properties that in turn slowed down drug release (Ugwoko et al., 2005). Hence, LYO HA-CL – SAP could overcome the drawback of a rapid clearance from the nasal cavity, since HA-CL could act not only as carrier for SAP and active ingredient itself, but also as mucoadhesive agent once dissolved in the nasal mucus layer to form a viscous solution/gel. This could potentially prolong the residence time of LYO HA-CL – SAP in the nasal cavity and thus the exposure of the nasal mucosa to the active ingredient (Horváth et al., 2016; Pires et al., 2009).

## 4. Conclusions

The present work aimed to develop a novel LYO HA-CL –SAP formulation for the treatment of nasal impairments sustained by inflammation. The dry powder formulation was characterized *in vitro* for its physico-chemical and biological properties. LYO HA-CL – SAP displayed suitable morphology, particle size distribution, mean diameter, thermal properties and *in vitro* aerosol performance for nasal drug delivery. The *in vitro* release/transport study performed on LYO HA-CL – SAP showed that HA-CL was able to act not only as carrier for SAP and active ingredient itself, but also as mucoadhesive agent. The formulation was shown to be not cytotoxic in the range of SAP concentrations explored (8.0 mM to 60.9 nM), and exhibited wound healing ability on RPMI 2650 cells and anti-inflammatory efficacy on primary nasal epithelial cells. These encouraging results showed that polymer and drug acted in combination to help reduce cell damage. Hence, this preliminary study has opened up potential perspectives for LYO HA-CL – SAP as innovative adjunctive treatment for nasal airway disorders like AR and CRS.

## Disclosure

The authors declare no conflict of interest.

## Acknowledgements

This work was supported by a PhD grant to Arianna Fallacara from I.R.A. Srl (Istituto Ricerche Applicate, Usmate-Velate, Monza-Brianza, Italy).

## References

- Albano, G.D., Bonanno, A., Cavalieri, L., Ingrassia, E., Di, C., Sano, Siena, L., Riccobono, L., Gagliardo, R., Profita, M., 2016. Effect of high, medium, and low molecular weight hyaluronan on inflammation and oxidative stress in an *in vitro* model of Human Nasal Epithelial Cells. *Mediat. Inflamm.* 8727289.
- Bai, S., Yang, T., Abbruscato, T.J., Ahsan, F., 2008. Evaluation of human nasal RPMI 2650 cells grown at an air-liquid interface as a model for nasal drug transport studies. *J. Pharm. Sci.* 97, 1165–1178.
- Basbaum, C.B., Finkbeiner, W.E., 1988. Airway secretion: a cell-specific analysis. *Horm. Metab. Res.* 20, 661–667.
- Bastacky, J., Lee, C.Y., Goerke, J., Koushafar, H., Yager, D., Kenaga, L., Speed, T.P., Chen, Y., Clements, J.A., 1995. Alveolar lining layer is thin and continuous: low-temperature scanning electron microscopy of rat lung. *J. Appl. Physiol.* 79, 1615–1628.
- Baumeister, P., Huebner, T., Reiter, M., Schwenk-Zieger, S., Harréus, U., 2009. Reduction of oxidative DNA fragmentation by ascorbic acid, zinc and N-acetylcysteine in nasal mucosa tissue cultures. *Anticancer Res.* 29, 4571–4574.





- Bozdemir, K., Şahin, E., Altıntoprak, N., Muluk, N.B., Cengiz, B.P., Acar, M., Cingi, C., 2016. Is resveratrol therapeutic when used to treat allergic rhinitis in rats? *Clin. Invest. Med.* 39, E63–E72.
- Campbell, R.G., 2018. Risks and management of long-term corticosteroid use in chronic rhinosinusitis. *Curr. Opin. Otolaryngol. Head Neck Surg.* 26, 1–7.
- Casale, M., Sabatino, L., Frari, V., Mazzola, F., Dell'Aquila, R., Baptista, P., Mladina, R., Salvinelli, F., 2014. The potential role of hyaluronan in minimizing symptoms and preventing exacerbations of chronic rhinosinusitis. *Am. J. Rhinol. Allergy* 28, 345–348.
- Casale, M., Vella, P., Moffa, A., Oliveto, G., Sabatino, L., Grimaldi, V., Ferrara, P., Salvinelli, F., 2016. Hyaluronic acid and upper airway inflammation in pediatric population: a systematic review. *Int. J. Pediatr. Otorhinolaryngol.* 85, 22–26.
- Cassandro, E., Chiarella, G., Cavaliere, M., Sequino, G., Cassandro, C., Prasad, S.C., Scarpa, A., Iemma, M., 2015. Hyaluronan in the treatment of chronic rhinosinusitis with nasal polyposis. *Indian J. Otolaryngol. Head Neck Surg.* 67, 299–307.
- Cassano, M., Russo, G.M., Granieri, C., Cassano, P., 2016. Cytofunctional changes in nasal ciliated cells in patients treated with hyaluronate after nasal surgery. *Am. J. Rhinol. Allergy* 30, 83–88.
- Chauhan, B., Gupta, M., Chauhan, K., 2016. Role of antioxidants on the clinical outcome of patients with perennial allergic rhinitis. *Allergy Rhinol. (Providence)* 7, 74–81.
- Chen, Q., Sun, G., Wang, Y., Zhong, W., Shu, X.Z., 2012. The evaluation of two new hyaluronan hydrogels as nasal dressing in the rabbit maxillary sinus. *Am. J. Rhinol. Allergy* 26, 152–156.
- Cheng, Y.S., Holmes, T.D., Gao, J., Guilmette, R.A., Li, S., Surakitbanharn, Y., Rowlings, C., 2001. Characterization of nasal spray pumps and deposition pattern in a replica of the human nasal airway. *J. Aerosol Med.* 14, 267–280.
- Ciofalo, A., De Vincentis, M., Zambetti, G., Altissimi, G., Fusconi, M., Greco, A., Otaviano, G., Magliulo, G., 2017a. Olfactory dysfunction in acute rhinosinusitis: intranasal sodium hyaluronate as adjuvant treatment. *Eur. Arch. Otorhinolaryngol.* 274, 803–808.
- Ciofalo, A., Zambetti, G., Altissimi, G., Fusconi, M., Soldo, P., Gelardi, M., Iannella, G., Pasquariello, B., Magliulo, G., 2017b. Pathological and cytological changes of the nasal mucosa in acute rhinosinusitis: the role of hyaluronic acid as supportive therapy. *Eur. Rev. Med. Pharmacol. Sci.* 21, 4411–4418.
- Citernesi, U.R., Beretta, L., Citernesi, L., 2015. Cross-linked Hyaluronic Acid, Process for the Preparation Thereof and use Thereof in the Aesthetic Field. Patent number WO/2015/007773 A1.
- Doub, W.H., Adams, W.P., Wokovich, A.M., Black, J.C., Shen, M., Muhse, L.F., 2012. Measurement of drug in small particles from aqueous nasal sprays by Andersen Cascade Impactor. *Pharm. Res.* 29, 3122–3130.
- Elad, D., Wolf, M., Keck, T., 2008. Air-conditioning in the human nasal cavity. *Respir. Physiol. Neurobiol.* 163, 121–127.
- Elmowafy, E., Osman, R., El-Shamy, A.E.-H.A., Awad, G.A.S., 2014. Nasal poly-saccharides-glucose regulator microparticles: optimization, tolerability and anti-diabetic activity in rats. *Carbohydr. Polym.* 108, 257–265.
- Emiroglu, G., Ozerkin Coskun, Z., Kalkan, Y., Celebi Erdivanli, O., Tumkaya, L., Terzi, S., Özgür, A., Demirci, M., Dursun, E., 2017. The effects of curcumin on wound healing in a rat model of nasal mucosal trauma. *Evid. Based Complement Alternat. Med.* 6.
- Fallacara, A., Baldini, E., Manfredini, S., Vertuani, S., 2018a. Hyaluronic acid in the third millennium. *Polymers* 10, 701.
- Fallacara, A., Busato, L., Pozzoli, M., Ghadiri, M., Xin Ong, H., Young, P.M., Manfredini, S., Traini, D., 2018b. Combination of urea-crosslinked hyaluronic acid and sodium ascorbyl phosphate for the treatment of inflammatory lung diseases: an in vitro study. *Eur. J. Pharm. Sci.* 120, 96–106.
- Fallacara, A., Busato, L., Pozzoli, M., Ghadiri, M., Ong, H.X., Young, P.M., Manfredini, S., Traini, D., Co-spray-dried urea cross-linked hyaluronic acid and sodium ascorbyl phosphate as novel inhalable dry powder formulation. *J. Pharm. Sci.*, submitted for publication.
- Fallacara, A., Manfredini, S., Durini, E., Vertuani, S., 2017a. Hyaluronic acid fillers in soft tissue regeneration. *Facial Plast. Surg.* 33, 87–96.
- Fallacara, A., Marchetti, F., Pozzoli, M., Citernesi, U.R., Manfredini, S., Vertuani, S., 2018c. Formulation and characterization of native and crosslinked hyaluronic acid microspheres for dermal delivery of sodium ascorbyl phosphate: a comparative study. *Pharmaceutics* 10 (4).
- Fallacara, A., Vertuani, S., Panozzo, G., Pecorelli, A., Valacchi, G., Manfredini, S., 2017b. Novel artificial tears containing cross-linked hyaluronic acid: an in vitro re-epithelialization study. *Molecules* 22.
- FDA CDER, 2003. Bioavailability and Bioequivalence Studies for Nasal Aerosols and Nasal Sprays for Local Action.
- Foco, A., Gasperlin, M., Kristl, J., 2005. Investigation of liposomes as carriers of sodium ascorbyl phosphate for cutaneous photoprotection. *Int. J. Pharm.* 291, 21–29.
- Fokkens, W.J., Lund, V.J., Mullol, J., Bachert, C., Alobid, I., Baroody, F., Cohen, N., Cervin, A., Douglas, R., Gevaert, P., Gezalas, C., Goossens, H., Harvey, R., Hellings, P., Hopkins, C., Jones, N., Joos, G., Kalogjera, L., Kern, B., Kowalski, M., Pricc, D., Riechelmann, H., Schlosser, R., Senior, B., Thomas, M., Toskala, E., Voegels, R., Wang, D., Y., Wormald, P.J., 2012. EPOS 2012: European position paper on rhinosinusitis and nasal polyps 2012. A summary for otorhinolaryngologists. *Rhinology* 50, 1–12.
- Garantziotis, S., Brezina, M., Castelnovo, P., Drago, L., 2016. The role of hyaluronan in the pathobiology and treatment of respiratory disease. *Am. J. Physiol. Lung Cell Mol. Physiol.* 310, L785–L795.
- Gelardi, M., Guglielmi, A.V., De Candia, N., Maffezzoni, E., Berardi, P., Quaranta, N., 2013a. Effect of sodium hyaluronate on mucociliary clearance after functional endoscopic sinus surgery. *Eur. Ann. Allergy Clin. Immunol.* 45, 103–108.
- Gelardi, M., Iannuzzi, L., Quaranta, N., 2013b. Intranasal sodium hyaluronate on the nasal cytology of patients with allergic and nonallergic rhinitis. *Int. Forum Allergy Rhinol.* 3, 807–813.
- Gelardi, M., Taliente, S., Fiorella, M.L., Quaranta, N., Ciancio, G., Russo, C., Mola, P., Ciofalo, A., Zambetti, G., Caruso Armone, A., Cantone, E., Ciprandi, G., 2016. Ancillary therapy of intranasal T-LysVal\* for patients with allergic, non-allergic, and mixed rhinitis. *J. Biol. Regul. Homeost. Agents* 30, 255–262.
- Greiner, A.N., Hellings, P.W., Rotiroi, G., Scadding, G.K., 2011. Allergic rhinitis. *Lancet* 378, 2112–2222.
- Helms, S., Miller, A., 2006. Natural treatment of chronic rhinosinusitis. *Altern. Med. Rev.* 11, 196–207.
- Hirst, R.A., Jackson, C.L., Coles, J.L., Williams, G., Rutman, A., Goggin, P.M., Adam, E.C., Page, A., Evans, H.J., Lackie, P.M., O'Callaghan, C., Lucas, J.S., 2014. Culture of primary ciliary dyskinesia epithelial cells at air-liquid interface can alter ciliary phenotype but remains a robust and informative diagnostic aid. *PLoS One* 9, e89675.
- Hong, Z., Guo, Z., Zhang, R., Xu, J., Dong, W., Zhuang, G., Deng, C., 2016. Airborne fine particulate matter induces oxidative stress and inflammation in human nasal epithelial cells. *Tohoku J. Exp. Med.* 239, 117–125.
- Horváth, T., Bartos, C., Bocsik, A., Kiss, L., Veszelka, S., Deli, M.A., Újhegyi, G., Szabó-Révész, P., Ambrus, R., 2016. Cytotoxicity of different excipients on RPMI 2650 human nasal epithelial cells. *Molecules* 21, pii:E658.
- Hu, H., Li, H., 2018. Prunetin inhibits lipopolysaccharide-induced inflammatory cytokine production and MUC5AC expression by inactivating the TLR4/MyD88 pathway in human nasal epithelial cells. *Biomed. Pharmacother.* 106, 1469–1477.
- Jarvis, D., Newson, R., Lotvall, J., Hastan, D., Tomassen, P., Keil, T., Gjomarkaj, M., Forsberg, B., Gunnbjornsdottir, M., Minoy, J., Brozek, G., Dahlen, S.E., Toskala, E., Kowalski, M.L., Olze, H., Howarth, P., Krämer, U., Baelum, J., Loureiro, C., Kasper, L., Bousquet, P.J., Bousquet, J., Bachert, C., Fokkens, W., Burney, P., 2012. Asthma in adults and its association with chronic rhinosinusitis: the GA2LEN survey in Europe. *Allergy* 67, 91–98.
- Johansson, L., Akerlund, A., Holmberg, K., Melén, I., Bende, M., 2003. Prevalence of nasal polyps in adults: the Skövde population-based study. *Ann. Otol. Rhinol. Laryngol.* 112, 625–629.
- Jones, N., 2001. The nose and paranasal sinuses physiology and anatomy. *Adv. Drug Deliv. Rev.* 51, 5–19.
- Kippax, P., Suman, J., Williams, G., 2010. Understanding the requirements for effective nasal drug delivery. *Pharm. Technol. Europe* 58–65.
- Kreft, M.E., Jerman, U.D., Lasic, E., Lanisnik Rizner, T., Hevir-Kene, N., Petercel, L., Kristan, K., 2015. The characterization of the human nasal epithelial cell line RPMI 2650 under different culture conditions and their optimization for an appropriate in vitro nasal model. *Pharm. Res.* 32, 665–679.
- Lee, D.C., Choi, H., Oh, J.M., Hong, Y., Jeong, S.H., Kim, C.S., Kim, D.K., Cho, W.K., Kim, S.W., Kim, S.W., Cho, J.H., Lee, J., 2018. The effect of urban particulate matter on cultured human nasal fibroblasts. *Int. Forum Allergy Rhinol.* 8, 993–1000.
- Lee, M.K., Yoo, J.W., Lin, H., Kim, Y.S., Kim, D.D., Choi, Y.M., Park, S.K., Lee, C.H., Roh, H.J., 2005. Air-liquid interface culture of serially passaged human nasal epithelial cell monolayer for in vitro drug transport studies. *Drug Deliv.* 12, 305–311.
- Li, Y., Schellhorn, H.E., 2007. New developments and novel therapeutic perspectives for vitamin C. *J. Nutr.* 137, 2171–2184.
- Licari, A., Brambilla, I., De Filippo, M., Poddighe, D., Castagnoli, R., Marseglia, G.L., 2017a. The role of upper airway pathology as a co-morbidity in severe asthma. *Expert Rev. Respir. Med.* 11, 855–865.
- Licari, A., Castagnoli, R., Denicolò, C.F., Rossini, L., Marseglia, A., Marseglia, G.L., 2017b. The nose and the lung: united airway disease? *Front. Pediatr.* 5, 44.
- Marseglia, G.L., Merli, P., Caimmi, D., Licari, A., Labò, E., Marseglia, A., Ciprandi, G., La Rosa, M., 2011. Nasal disease and asthma. *Int. J. Immunopathol. Pharmacol.* 24, 7–12.
- Montoro, J., Sastre, J., Jáuregui, I., Bartra, J., Dávila, I., del Cuvillo, A., Ferrer, M., Mullol, J., Valero, A., 2007. Allergic rhinitis: continuous or on demand antihistamine therapy? *J. Investig. Allergol. Clin. Immunol.* 17, 21–27.
- Monzon, M.E., Casalino-Matsuda, S.M., Forteza, R.M., 2006. Identification of glycosaminoglycans in human airway secretions. *Am. J. Respir. Cell. Mol. Biol.* 34, 135–141.
- Mudway, I.S., Kelly, F.J., 2000. Ozone and the lung: a sensitive issue. *Mol. Aspects Med.* 21, 1–48.
- Muller, L., Brighton, L.E., Carson, J.L., Fischer, W.A., Jaspers, I., 2013. Culturing of human nasal epithelial cells at the air liquid interface. *J. Vis. Exp.* 80. <https://doi.org/10.3791/50646>.
- Ong, H.X., Traini, D., Bebawy, M., Young, P.M., 2011. Epithelial profiling of antibiotic controlled release respiratory formulations. *Pharm. Res.* 28, 2327–2338.
- Ozsoy, Y., Gungor, S., Cevher, E., 2009. Nasal delivery of high molecular weight drugs. *Molecules* 14, 3754–3779.
- Patel, R.G., 2017. Nasal Anatomy and Function. *Facial Plast. Surg.* 33, 3–8.
- Petrigli, G., Allegra, L., 2006. Aerosolised hyaluronic acid prevents exercise-induced bronchoconstriction, suggesting novel hypotheses on the correction of matrix defects in asthma. *Pulm. Pharmacol. Ther.* 19, 166–171.
- Pires, A., Fortuna, A., Alves, G., Falcão, A., 2009. Intranasal drug delivery: how, why and what for? *J. Pharm. Pharm. Sci.* 12, 288–311.
- Podoshin, L., Gertner, R., Fradis, M., 1991. Treatment of perennial allergic rhinitis with ascorbic acid solution. *Ear Nose Throat J.* 70, 54–55.
- Pozzoli, M., Ong, H.X., Morgan, L., Sukkar, M., Traini, D., Young, P.M., Sonvico, F., 2016a. Application of RPMI 2650 nasal cell model to a 3D printed apparatus for the testing of drug deposition and permeation of nasal products. *Eur. J. Pharm. Biopharm.* 107, 223–233.
- Pozzoli, M., Rogueda, P., Zhu, B., Smith, T., Young, P.M., Traini, D., Sonvico, F., 2016b. Dry powder nasal drug delivery: challenges, opportunities and a study of the commercial Teijin Puvliner Rhinocort device and formulation. *Drug Dev. Ind. Pharm.* 42, 1660–1668.
- Pozzoli, M., Traini, D., Young, P.M., Sukkar, M.B., Sonvico, F., 2017. Development of a Soluplus budesonide freeze-dried powder for nasal drug delivery. *Drug Dev. Ind.*

- Pharm. 43, 1510–1518.
- Reichl, S., Becker, K., 2012. Cultivation of RPMI 2650 cells as an in-vitro model for human transmucosal nasal drug absorption studies: optimization of selected culture conditions. *J. Pharm. Pharmacol.* 64, 1621–1630.
- Sagit, M., Erdamar, H., Saka, C., Yalcin, S., Akin, I., 2011. Effect of antioxidants on the clinical outcome of patients with nasal polyposis. *J. Laryngol. Otol.* 125, 811–815.
- Small, P., Kim, H., 2011. Allergic rhinitis. *Allergy Asthma Clin. Immunol.* 7.
- Testa, D., Marcuccio, G., Panin, G., Bianco, A., Tafuri, D., Thyron, F.Z., Nunziata, M., Piombino, P., Guerra, G., Motta, G., 2017. Nasal mucosa healing after endoscopic sinus surgery in chronic rhinosinusitis of elderly patients: role of topic alpha-tocopherol acetate. *Aging Clin. Exp. Res.* 29, 191–195.
- Tiozzo Fasiolo, L., Manniello, M.D., Tratta, E., Buttini, F., Rossi, A., Sonvico, F., Bortolotti, F., Russo, P., Colombo, G., 2018. Opportunity and challenges of nasal powders: drug formulation and delivery. *Eur. J. Pharm. Sci.* 113, 2–17.
- Ugwoke, M.I., Agu, R.U., Verbeke, N., Kinget, R., 2005. Nasal mucoadhesive drug delivery: background, applications, trends and future perspectives. *Adv. Drug Deliv. Rev.* 57, 1640–1665.
- van der Vliet, A., O'Neill, C.A., Cross, C.E., Koosra, J.M., Volz, W.G., Halliwell, B., Louie, S., 1999. Determination of low-molecular-mass antioxidant concentrations in human respiratory tract lining fluids. *Am. J. Physiol.* 276, L289–L296.
- Varricchio, A., Capasso, M., Avvisati, F., Varricchio, A.M., De Lucia, A., Brunese, F.P., Ciprandi, G., 2014. Inhaled hyaluronic acid as ancillary treatment in children with bacterial acute rhinopharyngitis. *J. Biol. Regul. Homeost. Agents.* 28, 537–543.
- Vasa, D.M., Buckner, I.S., Cavanaugh, J.E., Wildfong, P.L., 2017. Improved flux of levodopa via direct deposition of solid microparticles on nasal tissue. *AAPS PharmSciTech.* 18, 904–912.
- Wengst, A., Reichl, S., 2010. RPMI 2650 epithelial model and three-dimensional reconstructed human nasal mucosa as in vitro models for nasal permeation studies. *Eur. J. Pharm. Biopharm.* 74, 290–297.
- Wu, D.X., Lee, C.Y., Widdicombe, J.H., Bastacky, J., 1996. Ultrastructure of tracheal surface liquid: low-temperature scanning electron microscopy. *Scanning* 18, 589–592.
- Yoo, J.W., Kim, Y.S., Lee, S.H., Lee, M.K., Roh, H.J., Jhun, B.H., Lee, C.H., Kim, D.D., 2003. Serially passaged human nasal epithelial cell monolayer for in vitro drug transport studies. *Pharm. Res.* 20, 1690–1696.

Article

# Formulation and Characterization of Native and Crosslinked Hyaluronic Acid Microspheres for Dermal Delivery of Sodium Ascorbyl Phosphate: A Comparative Study

Arianna Fallacara <sup>1,2,3</sup> , Filippo Marchetti <sup>1</sup>, Michele Pozzoli <sup>2</sup>, Ugo Raffaello Citeresi <sup>3</sup>, Stefano Manfredini <sup>1,4,\*</sup>  and Silvia Vertuani <sup>1,4</sup>

<sup>1</sup> Department of Life Sciences and Biotechnology, Master Course in Cosmetic Science and Technology (COSMAST), University of Ferrara, Via Luigi Borsari 46, 44121 Ferrara (FE), Italy; flrnn@unife.it (A.F.); filippo.marchetti@student.unife.it (F.M.); vrs@unife.it (S.V.)

<sup>2</sup> Respiratory Technology, Woolcock Institute of Medical Research and Discipline of Pharmacology, Faculty of Medicine and Health, The University of Sydney, 431 Glebe Point Road, Glebe, NSW 2037, Australia; michele.pozzoli@sydney.edu.au

<sup>3</sup> I.R.A. Istituto Ricerche Applicate s.r.l., Via Del Lavoro 4a/6, 20865 Usmate-Velate (MB), Italy; citeresi@iralab.it

<sup>4</sup> Ambrosialab Srl, Via Mortara 171, 44121 Ferrara (FE), Italy

\* Correspondence: smanfred@unife.it; Tel.: +39-0532-455-294; Fax: +39-0532-455-378

Received: 27 October 2018; Accepted: 26 November 2018; Published: 1 December 2018



**Abstract:** The present work evaluates for the first time the use of urea-crosslinked hyaluronic acid (HA-CL), a novel derivative of native hyaluronic acid (HA), to produce microspheres (MS) by emulsification-solvent evaporation, for dermal delivery of sodium ascorbyl phosphate (SAP). As the term of comparison, HA MS were prepared. A pre-formulation study—investigation of the effects of polymers solutions properties (pH, viscosity) and working conditions—led to the production of optimized HA-CL MS and HA-CL—SAP MS with: almost unimodal size distributions; mean diameter of  $13.0 \pm 0.7$  and  $9.9 \pm 0.8$   $\mu\text{m}$ , respectively; spherical shape and rough surface; high yield, similar to HA MS and HA-SAP MS ( $\approx 85\%$ ). SAP was more efficiently encapsulated into HA-CL MS ( $78.8 \pm 2.6\%$ ) compared to HA MS ( $69.7 \pm 4.6\%$ ). Physical state, thermal properties, relative moisture stability of HA-CL MS and HA-CL-SAP MS were comparable to those of HA MS and HA-SAP MS. However, HA-CL-SAP MS exhibited an extended drug release compared to HA-SAP MS, despite the same kinetic mechanism—contemporaneous drug diffusion and polymer swelling/dissolution. Therefore, HA-CL formulation showed a greater potential as microcarrier (for encapsulation efficiency and release kinetic), that could be improved, in future, using suitable excipients.

**Keywords:** dermal delivery; drug release; hyaluronic acid; urea-crosslinked hyaluronic acid; microspheres; sodium ascorbyl phosphate

## 1. Introduction

Hyaluronic acid (HA) is a naturally occurring glycosaminoglycan, pervasively diffused in the human body: it is found in the extracellular matrix, skin dermis, eye vitreous, hyaline cartilage, synovial fluid, and umbilical cord. HA is well known for its numerous biological functions [1,2] and its interesting properties such as biocompatibility, biodegradability, and mucoadhesion [3,4]. Moreover, HA has moisturizing, lubricant, and filler actions, and it is involved in wound healing and anti-inflammatory processes [1,3]. For these reasons, hyaluronan has widespread applications in medical, pharmaceutical,



and cosmetic fields, and represents an interesting starting material—frequently combined to other active ingredients or excipients—in tissue engineering, viscosupplementation, and drug delivery [1,3–12]. To design biomaterials with improved physical-chemical, viscoelastic, and biological properties, native HA is often subjected to derivatization or crosslinking [13]. Usually, HA is crosslinked with difunctional molecules of synthetic origin, for example, divinyl sulfone and diglycidyl ether [14,15]. Nevertheless, the recent trend consists in crosslinking the polymer with substances characterized by lower toxicity and intrinsic health activity. The aim is to obtain cross-polymers that can act as multifunctional molecules able to deliver active ingredients and to exert, at the same time, a health action [1]. Toward this end, we are actually investigating the possible pharmaceutical, cosmetic, and aesthetic applications of the new HA crosslinked with urea (HA-CL) [9,16–18]. HA-CL is a recently patented biocompatible and biodegradable polymer, provided with greater consistency and bioactivity with respect to native HA [9,16,18]. This is due to hyaluronan crosslinking with urea, a molecule naturally present in the human body and also employed as active substance. Indeed, urea is widely and safely used in pharmaceutical and cosmetic formulations because it is keratolytic and moisturizing, and thus it enhances cellular regeneration and repair. Urea is useful to treat different diseases, such as dry skin, damaged cutaneous annexes, non-infectious keratopathy, and injured corneal epithelium [19–21]. Hence, HA-CL could be a promising biomaterial for topical treatments requiring simultaneous re-epithelialization and hydration for the resolution of aesthetic/functional skin and mucosae problems [9,16,17].

Biodegradable and mucoadhesive polymers, in the form of microparticulate systems such as microspheres (MS), can accelerate skin wound healing [22] and extend the release of the encapsulated drugs [8,23,24]. Acknowledging the aforementioned facts and properties of HA-CL, we decided to explore for the first time, with this work, the potentiality of HA-CL to formulate drug loaded MS intended for the dermal target. The preparative method chosen was a water-in-oil (w/o) emulsification solvent evaporation technique, and native HA was used as reference polymer, as it has been already employed to produce MS [8,11]. This study has as its goal the provision of the perfect case scenario: to have an active molecule, never loaded before into hyaluronan microcarriers, which could be satisfyingly encapsulated and then freely released by the MS. Therefore, sodium ascorbyl phosphate (SAP) was selected as the model drug for its high hydrophilicity [25] and for its unprecedented encapsulation into hyaluronan MS. Moreover, SAP seemed to be an optimal candidate as it is characterized by good physical–chemical stability instead of ascorbic acid, and by several biological activities which go in synergy with those of HA. Indeed, SAP acts as a radical scavenger, with high capacity to reduce damages caused by photo-oxidation and lipid peroxidation, and it has strong antimicrobial activity on *Propionibacterium acnes*, the major bacterium responsible of acne vulgaris [25,26]. The SAP is a non-irritating prodrug bioconverted by skin enzymes into ascorbic acid, which stimulates collagen synthesis and, therefore, increases skin elasticity [27,28]. Hence, the combination of vitamin C derivatives and hyaluronan could open interesting perspectives. In fact, a recent study reported the safety of an HA sponge system containing a derivative of vitamin C used to reduce and treat scars [27]. Additionally, the delivery of a combination of SAP and HA-CL showed enhanced anti-inflammatory and antioxidant activities with respect to the single SAP and HA-CL: hence, the association of SAP and HA-CL could be suitable as an adjunctive therapy for the treatment of inflammatory pulmonary disorders [18].

In this research, SAP-loaded hyaluronan MS were formulated using the novel urea-crosslinked hyaluronic acid. A pre-formulation study was carried out to obtain optimized MS: particle features such as mean diameter, size distribution, yield (Y%), drug loading (DL%), and encapsulation efficiency (EE%) were investigated in relation to the properties of the starting polymeric solutions and to the emulsification time. The optimized MS were then characterized more in detail for their physical–chemical properties—morphology, physical state, thermal behavior, moisture sorption, and stability—and for their in vitro release profiles. An accurate and itemized theoretical study was performed to understand and explain, with a systematic approach, the mechanisms of release and the experimental features of HA-CL

formulations. Considering that this was the first research describing HA-CL MS, no excipients were added to the formulations, in order to investigate the actual polymer potentiality as microcarrier. Furthermore, all the properties of SAP-loaded as well as unloaded MS of HA-CL were compared to SAP-loaded and unloaded MS of native HA (prepared as reference formulations).

## 2. Materials and Methods

### 2.1. Materials

Native hyaluronic acid (sodium salt, molecular weight 1.2 MDa) and urea-crosslinked hyaluronic acid (molecular weight 2.0–4.0 MDa –raw material containing also pentylene glycol) were kindly given by I.R.A. Srl (Istituto Ricerche Applicate Srl, Usmate-Velate, Monza-Brianza, Italy). Sodium ascorbyl phosphate (known under the trade name STAY-C®50) was purchased from DSM Nutritional Products Ltd. (Segrate, Milano, Italy). Phosphate buffered saline (PBS) and hexane were supplied by Sigma-Aldrich (Schnellendorf, Germany). Mineral oil was obtained from Fagron (Quarto Inferiore, Bologna, Italy). Sorbitan monooleate (Span 80) was provided by Acef (Fiorenzuola D'Arda, Piacenza, Italy).

### 2.2. Preparation of Hyaluronan and Hyaluronan-SAP Solutions (Aqueous Phases)

HA 1% (*w/v*) solution and HA-CL 1% (*w/v*) solution were achieved through a progressive dispersion of the polymers in deionized water, under continuous magnetic stirring (300 rpm). Likewise, hyaluronan-SAP solutions 1% (*w/v*), 1:1, were prepared by dispersing the polymers into SAP water solutions, under constant magnetic stirring (300 rpm). The polymers were allowed to completely hydrate thus forming hydrogels, which were left to swell under moderate stirring, over 12 h, at room temperature, to reach homogeneous appearances. The gels were left at rest for 12 h prior to examinations or use as aqueous phases for MS formulation.

### 2.3. Characterization of Hyaluronan and Hyaluronan-SAP Solutions: pH and Rheology

Firstly, the pH of each hyaluronan aqueous phase was measured in triplicate using a digital pH meter (Docu pH+ meter, Sartorius Mechatronics, Goettingen, Germany).

Secondly, hyaluronan hydrogels were subjected to rheological analyses, performed in triplicate, at  $23 \pm 2$  °C, with a rotational rheometer AR2000 (TA Instruments, New Castle, DE, USA), equipped with an aluminum cone/plate geometry—diameter 40 mm, angle 2°, 64 μm truncation. A solvent trap was used in order to prevent samples dehydration. The rheometer was connected to the Rheology Advantage software (version V7.20) for data analysis.

Flow measurements were performed by a shear rate sweep, under steady state condition: after 1-min equilibration time, the shear rate ( $\dot{\gamma}$ ) was progressively increased from 0.01 to 1000 s<sup>-1</sup>. The gels were compared for their zero-shear-rate viscosity ( $\eta_0$ ), which was determined by fitting the viscosity curves according to the Cross equation [29] (Equation (1)):

$$\eta = \eta_{\infty} + \frac{\eta_0 - \eta_{\infty}}{1 + (C \cdot \dot{\gamma})^n} \quad (1)$$

where  $\eta$  is the viscosity at a given shear rate (Pa.s),  $\dot{\gamma}$  is the shear rate (s<sup>-1</sup>),  $\eta_0$  is the zero-shear-rate viscosity (Pa.s),  $\eta_{\infty}$  is the infinite-shear-rate viscosity (Pa.s),  $C$  is a multiplicative parameter (s) and  $n$  is a dimensionless exponent.

Oscillatory measurements were then taken under the constant stress value of 0.2 Pa, which belonged to the viscoelastic linear regime (defined by a strain sweep test), where the hydrogels could not be subjected to irreversible structural modifications. The experiments were carried out with oscillation frequencies ranging from 0.01 to 100 Hz. The elastic modulus ( $G'$ ) and the viscous modulus ( $G''$ ), measured as a function of the frequency of the stress applied, allowed to evaluate the viscoelastic properties of the gels [30]. More precisely, the samples were compared for their elastic modulus at



1 Hz ( $G'_{1\text{Hz}}$ , quantitative index of elasticity), and for their crossover frequency ( $C_f$ , a frequency where  $G'$  is equal to  $G''$ ).

#### 2.4. Formulation of HA and HA-CL Microspheres Containing or not SAP

HA and HA-CL MS containing or not SAP were produced through a water-in-oil (w/o) emulsification solvent evaporation technique, adapted from the method described by Lim and co-workers [11].

The aqueous phase was added dropwise (flow rate: 0.91 mL/min) into 100 g of mineral oil (oil phase) containing 1% (w/w) sorbitan monooleate as the emulsifying agent, under moderate magnetic stirring (200 rpm), at  $23 \pm 2$  °C. The aqueous phase was then emulsified at 1000 rpm, at  $23 \pm 2$  °C, into the oil phase, using a Silverson L5M A Laboratory Mixer (Silverson Machines, Buckinghamshire, United Kingdom), equipped with a fine emulsor screen workhead. Different emulsification times of 10, 30 and 60 min were investigated. Afterward, moderate magnetic stirring (200 rpm) and mild heating ( $37 \pm 2$  °C) were constantly maintained for 12 h to guarantee the complete evaporation of the dispersed aqueous phase. The MSs thus formed were separated from the oil phase by centrifugation at 4000 rpm, at  $23 \pm 2$  °C, for 30 min (ALC Centrifuge PK110, OPTO-LAB, Concordia sulla Secchia, Modena, Italy). The pellets were resuspended in hexane and filtered under vacuum, at  $23 \pm 2$  °C, using a Millipore glass filtration system, equipped with a polyamide membrane, pore size 0.22  $\mu\text{m}$  (Sartorius, Muggiò, Monza-Brianza, Italy). The collected MSs were finally dried in an oven at  $37 \pm 2$  °C for 12 h.

#### 2.5. MS Yield, Drug Loading, and Encapsulation Efficiency

MS yield (Y%), drug loading (DL%) and drug encapsulation efficiency (EE%) were respectively calculated from Equations (2)–(4)

$$Y\% = \frac{\text{weight of recovered MS}}{\text{weight of polymer* and drug fed initially}} \cdot 100 \quad (2)$$

\* HA-CL was provided as a raw material containing pentylene glycol. Being hydrophilic, this excipient was taken into account for the determination of HA-CL MS Y%, because 1% (w/v) HA-CL solutions contained 0.75% (w/v) pentylene glycol.

$$DL\% = \frac{\text{weight of drug in MS}}{\text{weight of recovered MS}} \cdot 100 \quad (3)$$

$$EE\% = \frac{\text{weight of drug in MS}}{\text{weight of drug fed initially}} \cdot 100 \quad (4)$$

For each MS formulation, all the determinations were performed in triplicate and the results were reported as the mean  $\pm$  standard deviation (SD).

The amount of encapsulated drug was determined by completely dissolving 30 mg of SAP loaded MS in 300 mL of release medium. Drug concentration was then assayed by ultraviolet (UV) spectroscopy (SHIMADZU UV-2600 spectrophotometer, Kyoto, Japan), at 258 nm (wavelength value corresponding to SAP  $\lambda_{\text{max}}$ ), on the basis of a previously plotted calibration curve. Unloaded HA and HA-CL MS were tested to ensure that other components of the formulations were not characterized by UV absorbance at the scanning wavelength.

#### 2.6. Particle Size Analysis

Particle size distributions of HA and HA-CL microspheres containing or not SAP were analyzed using laser diffraction (Malvern Mastersizer 2000, Malvern Instruments Ltd., Malvern, UK). Samples of powder (ca. 10 mg) were dispersed through the Scirocco dry dispersion unit (Malvern, UK) with a feed pressure of 4 bars and a feed rate of 100%. Samples were analyzed in triplicate, with an obscuration value between 0.1% and 15% and a reference refractive index of 1.33. The volume weighted mean

diameters ( $D$  [3,4]) and the median particle size by volume  $Dv50$  were used to describe MS size. Size distributions were evaluated by calculation of samples *Span* values as (Equation (5))

$$Span = \frac{Dv90 - Dv10}{Dv50} \quad (5)$$

where  $Dv90$ ,  $Dv10$ , and  $Dv50$  are respectively the 90%, 10% and 50% cumulative volume distributions. Thus, the *Span* values gave a measure of the ranges of the volume distributions relative to the median diameters.

### 2.7. SEM Morphological Analysis

The morphology (shape and surface) of HA and HA-CL MS containing or not SAP was observed using a field emission scanning electron microscope (Zeiss EVO 40XVP, Carl Zeiss Pty Ltd., Oberkochen, Germany), with an acceleration voltage of 20 kV. Powder samples were deposited on carbon sticky tabs and sputter coated with a thin layer of gold-palladium, under an argon atmosphere, prior to analysis. The samples were then randomly scanned and photographed.

### 2.8. X-ray Powder Diffraction

X-ray diffraction measurements on SAP and SAP-loaded and unloaded MS were performed at 40 kV, 40 mA, with the Bruker AXS D8 Advance Geiger counter equipped with a two-dimensional (2D) gas-filled sealed multiwire detector (scattering-angle resolution of  $0.02^\circ \text{ s}^{-1}$ ). Monochromatized Cu  $K\alpha$  radiation ( $\lambda = 1.54 \text{ \AA}$ ) was used. The analyses were performed in a  $5\text{--}45^\circ 2\theta$  range, at ambient temperature. The intensity vs. scattering angle spectra was obtained after the radial average of the measured 2D isotropic diffraction patterns. Bragg peaks were detected in the wide-angle X-ray diffraction region (WAXD).

### 2.9. Thermal Analysis (DSC and TGA)

The thermal profiles of SAP and MS formulations were studied using differential scanning calorimetry (DSC823e; Mettler-Toledo, Schwerzenbach, Switzerland). Roughly 5 mg of samples were weighted and crimp-sealed in DSC standard 40  $\mu\text{L}$  aluminum pans. Samples were then subjected to a  $10^\circ\text{C}/\text{min}$  temperature ramp between  $-20^\circ\text{C}$  and  $300^\circ\text{C}$ . The endothermic and exothermic peaks were determined using STARe software V.11.0x (Mettler Toledo, Greifensee, Switzerland).

Moreover, the temperature stability and solvent evaporation of each sample were determined using thermal gravimetric analysis (TGA; Mettler-Toledo, Schwerzenbach, Switzerland). Approximately 5 mg of samples were placed on aluminum crucible pans. The weight losses of the samples were assessed by heating the samples from  $20^\circ\text{C}$  to  $400^\circ\text{C}$ , with a scanning rate of  $5^\circ\text{C}/\text{min}$ , under constant nitrogen gas. Data were analyzed using STARe software V.11.0x (Mettler Toledo, Greifensee, Switzerland) and expressed as the percentage of weight loss comparing to initial sample weight.

### 2.10. Dynamic Vapor Sorption (DVS)

The relative moisture sorption and stability of SAP and MS formulations, with respect to humidity, were analyzed by Dynamic Vapor Sorption (DVS). Aluminum sample pans were loaded with 10 mg ca. of samples and then placed in the sample chamber of a DVS (DVS-1, Surface Measurement Systems Ltd., London, UK). Each sample was dried at 0% relative humidity (RH) before being exposed to 10% RH increments for two 0–90% RH cycles ( $25^\circ\text{C}$ ). Equilibrium of moisture sorption was determined, at each humidity step, by a change in mass to time ratio ( $dm/dt$ ) of  $0.0005\% \text{ min}^{-1}$ .

### 2.11. Solubility Test

The solubility of SAP in a release medium (0.01 M PBS, pH = 7.4) was assessed in triplicate by solvent saturation method. An excess amount of SAP was added into tubes containing 2.5 mL of PBS. The tubes were sonicated into a water-bath sonicator at 32 KHz and 32 °C, for 1 h, and then stirred on a thermostated orbital shaker at 120 rpm and 32 °C, for 24 h. The tubes were then centrifuged at 2000 rpm for 5 min. The supernatants were withdrawn, filtered using 0.22 µm polyamide syringe filters, diluted with PBS and analyzed by UV spectroscopy.

### 2.12. In Vitro Drug Release Studies

For topical microcarriers, there are no compendial or standard release methods and apparatuses [31,32]. Therefore, in vitro release profiles of SAP from HA and HA-CL MS were evaluated with two different methodologies, under different experimental conditions.

#### 2.12.1. Dialysis

SAP release profiles were primarily obtained with dialysis method. A calculated amount of each test formulation containing ~10 mg of SAP was placed into a preconditioned dialysis bag (Slide-A-Lyzer G2, 10kDa MWCO, Thermo Fisher Scientific, Rodano, Milano, Italy), and dialyzed against 300 mL PBS (0.01 M, pH = 7.4), a release medium already described in the literature for drug release studies of dermal carriers [31,33,34]. The whole set-up was continuously stirred at 150 rpm and maintained at 32 ± 1 °C to reflect the physiological skin temperature [31]. At predefined time intervals, 1 mL of sample was withdrawn and replaced with an equal volume of warm PBS. The released SAP was quantified by UV spectroscopy. A minimum of three replicates were performed for each test formulation.

#### 2.12.2. Franz Cells

SAP release profiles from hyaluronan MS were also investigated by Franz's cells (25 mm internal diameter, PermeGear Inc., Hellertown, PA, USA). Polyamide filter membranes 0.45 µm pore size (Sartorius Biolab Products, Goettingen, Germany) were hydrated by sonication in deionized water for 30 min, and then cut and mounted between the receiver and donor compartments of the diffusion cells. The whole diffusion cells were put in a thermostatic bath, maintained at 32 ± 1 °C. Test formulations were placed in the donor compartments—in order to have ~2 mg of SAP on the surface of the membranes—which were closed using a wax foil (Parafilm M, Bemis Company Inc., Oshkosh, WI, USA) to prevent evaporation. The receiver compartments were filled with 23 mL PBS (0.01 M, pH = 7.4) and kept under continuous magnetic stirring at 150 rpm. At selected time points, 0.5 mL of samples were withdrawn from the receptor compartment and replaced with equal volumes of warm PBS. Samples were assayed for SAP content using UV spectroscopy. A minimum of three replicates was performed for each formulation. The idea was to get preliminary indications which, if positive, will be used to support a request to the ethics committee for a human skin study.

### 2.13. Drug Release Data Analysis

All the experimental release data were fitted to a series of statistical and kinetic models to evaluate formulations performances and to elucidate their drug release mechanisms, strictly related to the properties of the polymers. This detailed mathematical modeling study was carried out to develop and characterize our novel HA CL MS, in comparison to HA MS, with a systematic approach.

#### 2.13.1. Similarity and Difference Factors for SAP Release Profiles

For each release method used, SAP diffusion across the membranes and SAP release profiles from HA MS and HA CL MS were statistically analyzed and compared using Fit Factors described by Moore and Flanner [35], adopted by the Food and Drug Administration guidance for dissolution



testing in the industry [36]. Fit factors are models widely applied by researchers [37–40] to directly compare the difference between percentage drug released per unit time between a reference and a test formulation. The difference factor ( $f_1$ ) and the similarity factor ( $f_2$ ) were calculated using Equations (6) and (7), respectively

$$f_1 = \left\{ \left[ \frac{\sum_{t=1}^n |R_t - T_t|}{\sum_{t=1}^n R_t} \right] \right\} \cdot 100 \quad (6)$$

$$f_2 = 50 \cdot \log \left\{ \left[ 1 + (1/n) \sum (R_t - T_t)^2 \right]^{-0.5} \cdot 100 \right\} \quad (7)$$

where  $R_t$  and  $T_t$  are percentages of drug released at a certain time point ( $t$ ) from the reference and the test formulation, respectively;  $n$  is the number of dissolution sampling times. The difference factor ( $f_1$ ) calculates the percent difference between the reference and the test curves at each time point thus measuring the relative error between the two curves. The similarity factor ( $f_2$ ) is a logarithmic reciprocal square root transformation of the sum of squared error and is a measurement of the similarity in percentage released between curves. For data analysis, arbitrary descriptors of difference and similarity need to be chosen: curves were considered different with  $f_1 \geq 10$  and  $f_2 \leq 50$ .

### 2.13.2. Analysis of SAP Release Kinetics Using Mathematical Models

SAP release data acquired for HA and HA-CL MS were plotted into four mathematical models corresponding to the known release mechanisms. The linearized form of each function was evaluated using the R2 regression analysis, in order to understand which was the best-fit mathematical model and, therefore, the kinetic process controlling SAP release from hyaluronan MS.

The first model used, called Zero-release kinetic, describes a release mechanism whose rate is independent of the active ingredient concentration, but it is time-dependent [41]. It is described by Equation (8)

$$\frac{Q_t}{Q_\infty} = Kt + Q_0 \quad (8)$$

where  $Q_t/Q_\infty$  is the ratio between the cumulative percentage of drug released at time  $t$  and at infinite time,  $k$  is the zero-order release constant,  $t$  is the time, and  $Q_0$  is the initial quantity of drug in solution due to an immediate releasing process (most times  $Q_0 = 0$ ).

On the contrary, the First order model delineates a process where the release rate is concentration dependent [41]. It is represented by Equation (9)

$$\log \log \frac{Q_t}{Q_\infty} = \log \log Q_0 - kt/2.303 \quad (9)$$

where  $Q_t/Q_\infty$  is the ratio between the cumulative percentage of drug released at time  $t$  and at infinite time,  $k$  is the first-order release constant,  $t$  is the time, and  $Q_0$  is the initial amount of drug in solution.

Also, the Higuchi model was applied [42]. It describes drug release from a matrix system whose swelling is negligible [41,43]. Therefore, the release profile is governed by the properties of the polymeric matrix and by drug solubility, and it is described by the following equation

$$\frac{Q_t}{Q_\infty} = k_H \sqrt{t} + Q_0 \quad (10)$$

where  $Q_t/Q_\infty$  is the ratio between the cumulative percentage of drug released at time  $t$  and at infinite time,  $k$  is the Higuchi release rate constant,  $t$  is the time, and  $Q_0$  is the initial quantity of drug in solution due to an immediate releasing process (most times  $Q_0 = 0$ ).

Finally, the release data were fitted to the Korsmeyer–Peppas model, which describes the drug release from swelling-controlled systems [41,43–46]. In these polymeric systems, both diffusion and dissolution occur together, and they are quite indistinguishable. Korsmeyer–Peppas proposed the following semi-empirical equation

$$\frac{Q_t}{Q_\infty} = kt^n + Q_0 \quad (11)$$

where  $Q_t/Q_\infty$  is the ratio between the cumulative percentage of drug released at time  $t$  and at infinite time,  $k$  is a kinetic constant related to the structural and geometric properties of the system,  $t$  is the time,  $n$  is the release exponent (connected to geometric form), and  $Q_0$  is the initial amount of drug in solution. In this model, the  $n$  value characterizes the release mechanism: Fickian diffusion, i.e., drug diffusive process, is prevalent for  $n \approx 0.43$ ; Case-II transport, i.e., polymer dissolution process, for  $n \approx 0.89$ ; super Case-II transport for  $n > 0.89$ ; anomalous behavior, i.e., a superposition of diffusion and dissolution, for  $0.43 < n < 0.89$ .

#### 2.14. Statistical Analysis

Data are presented as mean  $\pm$  SD of three independent experiments ( $n = 3$ ). Statistical analysis was performed using GraphPad Prism software version 7.0b (GraphPad, San Diego, CA, USA). The tests used were one-way (characterization of hyaluronan solutions) or two-way (characterization of MS during the pre-formulation study) analysis of variance (ANOVA), followed by Tukey post hoc analysis for multiple comparisons. Differences between results were considered statistically significant at  $p < 0.05$ .

### 3. Results and Discussion

#### 3.1. Pre-Formulation Study: Evaluation and Optimization of Microspheres

The present work describes the production and characterization of MS using two different hyaluronans: HA-CL (test polymer) and native HA (reference polymer already employed to formulate microspheres) [10,11]. The aim was to understand if the novel HA-CL could be a promising candidate to obtain MS intended for skin application. It is well known that particles features are affected by the properties of the starting polymer solutions and by factors related to the production method [8,23,47]. In this document, we correlated MS properties to the pH and the rheological behavior of HA aqueous phases, and to the emulsification time. This systematic approach was used in order to facilitate the development of our novel formulations, considering that this was the first study to investigate the novel HA-CL as microcarrier.

All the hyaluronan solutions were characterized by a shear-thinning (Figure 1) and viscoelastic behavior. However, statistical analysis demonstrated that each solution was significantly different ( $p < 0.05$ ) from the others in terms of pH, zero-shear-rate viscosity ( $\eta_0$ ), elastic modulus at 1 Hz ( $G'_{1\text{Hz}}$ ), and crossover frequency (Cf). Indeed, HA type and SAP presence affected the values of pH,  $\eta_0$ ,  $G'_{1\text{Hz}}$ , and Cf (Table 1).

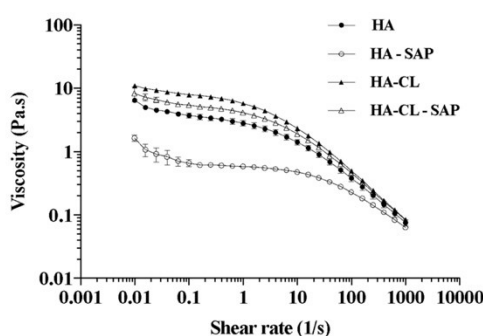


Figure 1. Shear-thinning behavior of hyaluronan solutions: viscosity as a function of shear rate ( $n = 3$ ,  $\pm$  SD).

**Table 1.** Main properties of HA solutions: pH,  $\eta_0$ ,  $G'_{1\text{Hz}}$ ,  $C_f$  ( $n = 3$ ,  $\pm$  SD).

Solution	pH	$\eta_0$ (Pa.s)	$G'_{1\text{Hz}}$ (Pa)	$C_f$ (Hz)
HA	6.8 $\pm$ 0.1	4.2 $\pm$ 0.2	5.5 $\pm$ 0.7	6.2 $\pm$ 1.8
HA-SAP	8.9 $\pm$ 0.1	0.7 $\pm$ 0.0	0.8 $\pm$ 0.0	15.9 $\pm$ 0.4
HA-CL	7.2 $\pm$ 0.0	9.1 $\pm$ 0.3	13.2 $\pm$ 0.6	1.8 $\pm$ 0.0
HA-CL-SAP	8.1 $\pm$ 0.1	6.3 $\pm$ 0.5	9.2 $\pm$ 0.4	3.1 $\pm$ 0.1

As regarding the impact of polymer type, Table 1 shows implemented mechanical properties for HA-CL hydrogel with respect to HA hydrogel (i.e., higher  $\eta_0$  and  $G'_{1\text{Hz}}$ , lower  $C_f$ ). Considering, for example, simple polymeric solutions,  $\eta_0$ ,  $G'_{1\text{Hz}}$  and  $C_f$  were respectively 9.1  $\pm$  0.3 Pa.s, 13.2  $\pm$  0.6 Pa and 1.8  $\pm$  0.0 Hz for HA-CL, and 4.2  $\pm$  0.2 Pa.s, 5.5  $\pm$  0.7 Pa and 6.2  $\pm$  1.8 Hz for HA. This could be ascribed to the different molecular weight of the two polymers (1.2 MDa for native HA, 3.0 MDa for HA-CL), and to the crosslinking of the urea derivative. Indeed, it is well known that the viscosity and the viscoelasticity of hyaluronan solutions increase with increasing polymer molecular weight [48] and crosslinking [13,49]. For the shorter emulsification times investigated (10 and 30 min), the rheological behavior of HA and HA-CL solutions seemed to be reflected in the mean size of the resulting particles. Certainly, Dv50 and D[4,3] values were significantly higher ( $p < 0.05$ ) for HA-CL MS with respect to HA MS produced after the same mixing time (Table 2). After 10 min of emulsification, Dv50 and D[4,3] were respectively 290.0  $\pm$  32.5  $\mu\text{m}$  and 311.0  $\pm$  32.5  $\mu\text{m}$  for HA-CL MS, and 117.7  $\pm$  20.0  $\mu\text{m}$  and 246.0  $\pm$  53.6  $\mu\text{m}$  for HA MS. Moreover, after 30 min of emulsification, Dv50 and D[4,3] were specifically 181.5  $\pm$  3.8  $\mu\text{m}$  and 208.7  $\pm$  6.7  $\mu\text{m}$  for HA-CL MS, and 113.7  $\pm$  19.6  $\mu\text{m}$  and 154.7  $\pm$  27.5  $\mu\text{m}$  for HA MS. Similar findings have already been reported in the literature: bigger particles are generally produced by larger droplets of the precursory  $w/o$  emulsion [8], formed by increasing the solution viscosity [50].

**Table 2.** Effect of emulsification time, polymer type, and SAP presence on MS properties ( $n = 3$ ,  $\pm$  SD).

MS Formulation	Dv50 ( $\mu\text{m}$ )	D[4,3] ( $\mu\text{m}$ )	Span	Y(%)	DL(%)	EE(%)
<i>10 min</i>						
HA	117.7 $\pm$ 20.0	246.0 $\pm$ 53.6	4.2 $\pm$ 0.4	68.6 $\pm$ 1.6	-	-
HA-SAP	71.7 $\pm$ 4.2	121.0 $\pm$ 13.4	4.3 $\pm$ 0.1	75.2 $\pm$ 4.4	39.2 $\pm$ 0.4	59.0 $\pm$ 4.0
HA-CL	290.0 $\pm$ 32.5	311.0 $\pm$ 32.5	1.5 $\pm$ 0.2	56.7 $\pm$ 5.4	-	-
HA-CL-SAP	245.5 $\pm$ 27.6	300.5 $\pm$ 24.7	2.4 $\pm$ 0.5	70.6 $\pm$ 1.1	32.5 $\pm$ 1.4	65.3 $\pm$ 3.5
<i>30 min</i>						
HA	113.7 $\pm$ 19.6	154.7 $\pm$ 27.5	2.9 $\pm$ 0.1	79.4 $\pm$ 2.9	-	-
HA-SAP	54.6 $\pm$ 3.0	63.2 $\pm$ 2.6	2.0 $\pm$ 0.1	81.5 $\pm$ 1.4	39.3 $\pm$ 1.0	64.1 $\pm$ 2.9
HA-CL	181.5 $\pm$ 3.8	208.7 $\pm$ 6.7	2.5 $\pm$ 0.1	76.7 $\pm$ 1.3	-	-
HA-CL-SAP	117.0 $\pm$ 4.2	135.0 $\pm$ 3.5	2.3 $\pm$ 0.0	78.2 $\pm$ 3.3	32.1 $\pm$ 1.0	68.9 $\pm$ 1.0
<i>60 min</i>						
HA	2.5 $\pm$ 0.1	6.3 $\pm$ 0.5	2.9 $\pm$ 0.2	88.4 $\pm$ 1.7	-	-
HA-SAP	2.5 $\pm$ 0.1	3.1 $\pm$ 0.2	2.2 $\pm$ 0.0	84.2 $\pm$ 2.3	41.3 $\pm$ 1.6	69.7 $\pm$ 4.6
HA-CL	13.0 $\pm$ 0.7	21.6 $\pm$ 4.0	2.5 $\pm$ 0.3	85.8 $\pm$ 4.4	-	-
HA-CL-SAP	9.9 $\pm$ 0.8	15.2 $\pm$ 4.0	2.6 $\pm$ 0.2	85.0 $\pm$ 4.8	33.6 $\pm$ 2.3	78.8 $\pm$ 2.6

Concerning the influence of SAP on the properties of HA and HA-CL solutions, it increased the pH, thus causing (as expected [51,52]) a statistically significant ( $p < 0.05$ ) decrease of  $\eta_0$  and  $G'_{1\text{Hz}}$ , and an increase of  $C_f$  (Table 1). In fact, the pH,  $\eta_0$ ,  $G'_{1\text{Hz}}$  and  $C_f$  of HA hydrogel, which were respectively 6.8  $\pm$  0.1, 4.2  $\pm$  0.2 Pa.s, 5.5  $\pm$  0.7 Pa and 6.2  $\pm$  1.8 Hz, changed to 8.9  $\pm$  0.1, 0.7  $\pm$  0.0 Pa.s, 0.8  $\pm$  0.0 Pa and 15.9  $\pm$  0.4 Hz in presence of SAP. A similar trend was observed also for HA-CL solutions: without SAP, the pH,  $\eta_0$ ,  $G'_{1\text{Hz}}$  and  $C_f$  were respectively 7.2  $\pm$  0.0, 9.1  $\pm$  0.3 Pa.s, 13.2  $\pm$  0.6 Pa and 1.8  $\pm$  0.0 Hz; in presence of SAP, these values changed to 8.1  $\pm$  0.1, 6.3  $\pm$  0.5 Pa.s, 9.2  $\pm$  0.4 Pa and 3.1  $\pm$  0.1 Hz. Also, in this case, the rheology of the initial solutions appeared correlated to the dimensional properties of the particles. Indeed, for the same HA type and emulsification time (10 or 30 min), SAP-loaded MS were



smaller than unloaded MS (Table 2), as highlighted by statistical analysis ( $p < 0.05$ ). For example, after a 10 min' emulsification, Dv50 and D[4,3] of HA MS respectively decreased from  $117.7 \pm 20.0 \mu\text{m}$  and  $246.0 \pm 53.6 \mu\text{m}$  to  $71.7 \pm 4.2 \mu\text{m}$  and  $121.0 \pm 13.4 \mu\text{m}$  in presence of SAP. Similarly, Dv50 and D[4,3] of HA-CL MS respectively decreased from  $290.0 \pm 32.5 \mu\text{m}$  and  $311.0 \pm 32.5 \mu\text{m}$  to  $245.5 \pm 27.6 \mu\text{m}$  and  $300.5 \pm 24.7 \mu\text{m}$  in presence of SAP. In the same way, after 30 min of emulsification, HA and HA-CL MS mean size decreased when encapsulating SAP, as reported in Table 2.

In summary, the effect of HA type and SAP presence on MS diameter appeared statistically significant ( $p < 0.05$ ) in the case of 10 and 30 min of emulsification. For MS produced after 60 min of mixing, this effect was negligible. Indeed, particles were all comparable in term of size, regardless of polymer type and SAP loading, with Dv50 ranging from  $2.5 \pm 0.1$  to  $13.0 \pm 0.7 \mu\text{m}$ , and D[4,3] ranging from  $3.1 \pm 0.2$  to  $21.6 \pm 4.0 \mu\text{m}$  (Table 2). Therefore, after 60 min, the side effects due to the differences between hyaluronan solutions were leveled because of a more significative emulsification. Consequently, MS mean diameter and size distribution seemed to be affected not only by the rheology of the starting solution but also by the emulsification time. For each MS formulation, particle diameter was found to be inversely proportional to the emulsification time in the range 10–60 min (Table 2). This correlation was statistically significant ( $p < 0.05$ ), and it was in agreement with previously reported results [47]. Indeed, the higher is the mixing time the smaller are the droplets produced during the emulsification, and, consequently, the final particles. On the contrary, the shorter is the emulsification time, the less fine is the w/o emulsion, and this normally determines the aggregation of aqueous droplets. As already observed [8], also in our study bigger and less uniform-sized MS, with a lower yield, were produced by droplets agglomeration -supposed to occur especially for 10 min' emulsification (Table 2). This drawback could be probably due to the bioadhesivity of the polymers which, when less dispersed, adhere more to the homogenizer workhead. However, by increasing the emulsification time from 10 to 60 min, MS mean size significantly decreased, while particle recovery (Y%) and encapsulation efficiency (EE%) significantly increased ( $p < 0.05$ ) (Table 2). For example, SAP-loaded HA MS could be considered: after 10 min of emulsification, Dv50, D[4,3], Span, Y% and EE% values were respectively  $71.7 \pm 4.2 \mu\text{m}$ ,  $121.0 \pm 13.4 \mu\text{m}$ ,  $4.3 \pm 0.1$ ,  $75.2 \pm 4.4\%$  and  $59.0 \pm 4.0\%$ . After 60 min of emulsification, these values became respectively  $2.5 \pm 0.1 \mu\text{m}$ ,  $3.1 \pm 0.2 \mu\text{m}$ ,  $2.2 \pm 0.0$ ,  $84.2 \pm 2.3\%$  and  $69.7 \pm 4.6\%$ . Considering the parallel increment of particles Y% and EE%, the drug loading (DL%) remained almost constant whatever the emulsification time (around 40% for SAP-loaded HA MS and 33% for SAP-loaded HA-CL MS) (Table 2).

Taking into account the results of this pre-formulation study, the emulsification time of 60 min was chosen as the standard condition to produce optimized MS. Indeed, all the MS formulations produced after 60 min of emulsification were characterized by the highest Y%, ranging from  $84.2 \pm 2.3$  to  $88.4 \pm 1.7\%$  (comparable values). The EE% and DL% were satisfying, even if statistically different ( $p < 0.05$ ) for HA and HA-CL formulations: respectively  $69.7 \pm 4.6\%$  and  $41.3 \pm 1.6\%$  for HA-SAP MS, and  $78.8 \pm 2.6\%$  and  $33.6 \pm 2.3\%$  for HA-CL-SAP MS (Table 2). Particle Dv50 ranging from  $2.5 \pm 0.1$  to  $13.0 \pm 0.7 \mu\text{m}$ , and D[4,3] ranging from  $3.1 \pm 0.2$  to  $21.6 \pm 4.0 \mu\text{m}$  (Table 2) were suitable for dermal target [53,54]. Indeed, to avoid palpable microspheres during application, mean size should be lower than  $50 \mu\text{m}$  [55]: this is essential both in the cosmetic and pharmaceutical field, as it determines the cosmetic elegance of a product [55] and the adherence to a therapy [56]. A statistical comparison revealed no significant difference between the mean size of optimized MS ( $p > 0.05$ ). Moreover, all the optimized formulations showed almost unimodal size distributions (Figure 2), with Span values lower than 3 (Table 2).

Optimized MS underwent a deeper physical-chemical characterization: analysis of morphology, physical and molecular state, thermal properties, relative moisture sorption, and stability, in vitro release properties, and kinetic mechanisms.

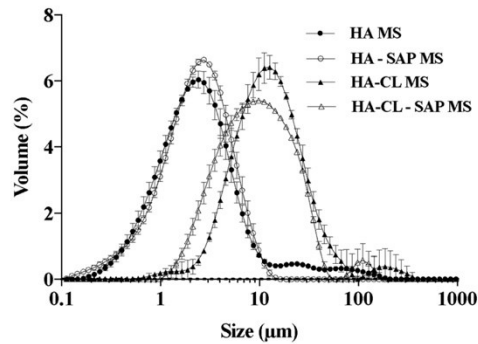


Figure 2. Particle size distribution of hyaluronan MS produced after 60 min of emulsification ( $n = 3, \pm SD$ ).

### 3.2. Characterization of Optimized Microspheres

#### 3.2.1. SEM Morphological Analysis

As regarding particle morphology, all hyaluronan MS encapsulating or not SAP showed a spherical shape. However, polymer typology (HA or HA-CL) influenced MS surface properties. Indeed, SAP-loaded and unloaded HA MS exhibited a regular and smooth surface, while SAP-loaded and unloaded HA-CL MS were characterized by an irregular and rough surface (Figure 3).

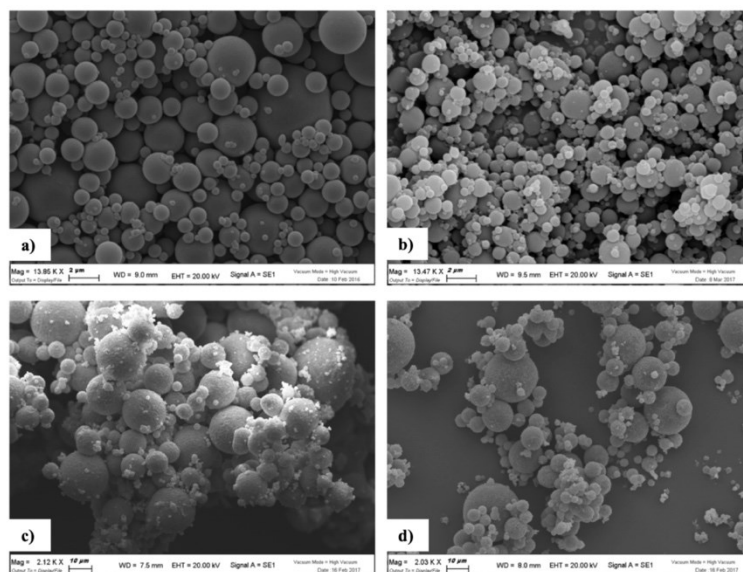


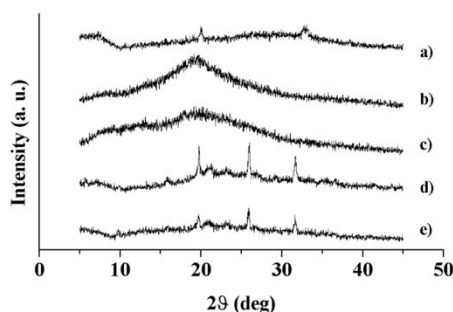
Figure 3. SEM micrographs of hyaluronan MS produced after 60 min of emulsification: HA (a), HA-SAP (b), HA-CL (c), HA-CL-SAP (d).

#### 3.2.2. X-ray Diffraction

Wide angle X-ray diffractometry was performed to investigate the molecular states of MS formulations in comparison to SAP [57]. The diffraction patterns are reported in Figure 4. The WAXD pattern of unloaded HA and HA-CL MS exhibited humps typical of disordered structures, i.e.,



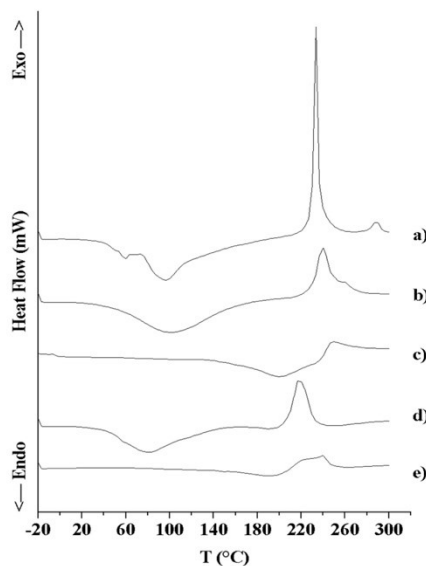
amorphous materials. SAP pattern was characterized by four low intense and broad peaks emerging from a hump at  $2\theta = 7.30, 20.00, 27.32,$  and  $33.12^\circ$ , which can be ascribed to small traits of crystallinity. Indeed, the diffraction intensity is defined by the crystal structure: the higher is the crystallinity degree, the higher is the intensity of the peaks [57]. The diffraction patterns of SAP-loaded MS showed both the main signals of the drug and of the carrier, indicating the permanence of SAP crystalline traits into the amorphous matrixes of HA and HA-CL. However, thermal analyses and DVS study provided evidence and confirmation that the crystallinity of SAP loaded MS was so low to be negligible.



**Figure 4.** X-ray diffraction patterns of: SAP (a), HA MS (b), HA-CL MS (c), HA-SAP MS (d), HA-CL-SAP MS (e).

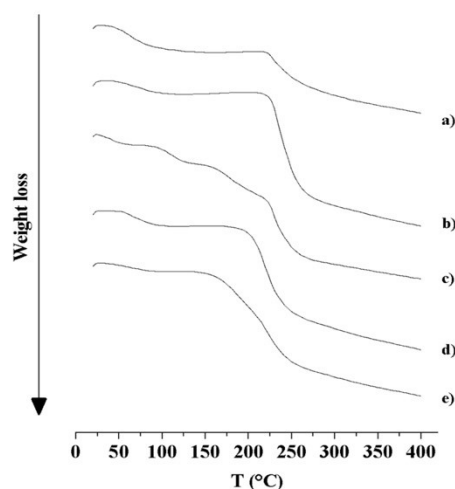
### 3.2.3. Thermal Analysis (DSC and TGA)

DSC and TGA were used to characterize the thermal behavior and stability of the drug and the formulations, providing information on their hydration properties and their physical state [58,59]. Figure 5 shows the DSC thermal profiles of SAP and MS formulations. SAP thermogram (a) was characterized by broad endothermic peaks around  $67^\circ\text{C}$  and  $100^\circ\text{C}$ , which could be associated with the loss of moisture after the initial drying procedure, and by a sharp exothermic peak at  $233^\circ\text{C}$ , due to the melting point with thermal decomposition (as reported in the literature for similar ascorbic acid derivatives [60]). DSC thermal profile of HA MS (b) presented a wide endothermic peak, suggesting a dehydration process around  $103^\circ\text{C}$ , and a broad exothermic peak at  $240^\circ\text{C}$  ascribable to the polymer thermal decomposition and the formation of a carbonized residue. These results were in good agreement with previous observations for native HA [49,61,62]. DSC trace of HA-CL MS (c) exhibited a broad endothermic peak at  $200^\circ\text{C}$ , which could be attributed to pentylene glycol evaporation (boiling range  $198\text{--}200^\circ\text{C}$ ). This was confirmed by pentylene glycol DSC thermal profile (trace not shown). Moreover, HA-CL MS curve showed a wide exothermic peak, due to polymer thermal degradation, at  $250^\circ\text{C}$  (shifted with respect to HA MS, indicating an altered structure due to crosslinking [61]). The thermograms of HA - SAP MS (d) and HA-CL-SAP MS (e) showed the same profile of the corresponding unloaded MS (DSC traces b and d, respectively), but the peaks shifted to lower temperatures (about  $10\text{--}15^\circ\text{C}$  of shift). This evidence, in addition to the reduced intensity of the exothermic peak, suggested an altered microstructure of the polymer matrix due to SAP presence (probable molecular dispersion of SAP inside the microspheres [24]) and the superposition of SAP and hyaluronan thermal degradation phenomena.



**Figure 5.** DSC thermal profiles of: SAP (a), HA MS (b), HA-CL MS (c), HA-SAP MS (d), HA-CL-SAP MS (e).

TGA thermal profiles of SAP and MS formulations are reported in Figure 6. SAP thermogram (a) showed the first region of weight loss (9.6% *w/w*) between ambient temperature and 223 °C (moisture loss), and a second region (20.5% *w/w*) from 223 to 400 °C (melting with decomposition and release of volatile degradation products). TGA curve of HA MS (b) consisted of three distinct degradation stages: the first one (20–223 °C, showing 6.2% *w/w* of weight loss, due to water evaporation); the second (223–269 °C) and the third stages (269–400 °C), typical of a two-stages polysaccharide degradation. In the second stage, the 37.3% *w/w* of weight was lost due to a partial breakage of the molecular structure. Residues of hyaluronan were then degraded in the third stage, characterized by the 12.0% *w/w* of weight loss. Similar findings have already been described in the literature for native HA [63–65]. A comparable TGA profile characterized HA-SAP MS (d), with 10.8% *w/w* of weight loss in the first region (20–208 °C), 26.2% *w/w* in the second (208–258 °C), and 12.0% *w/w* in the third (258–400 °C). For HA-SAP MS the decomposition of polymer and drug seemed to occur at once. TGA thermograms of HA-CL MS (c) and HA-CL-SAP MS (e) presented the two-stages polysaccharide degradation observed also for HA MS formulations (b and d), with an additive stage for pentylene glycol evaporation and more stages for water loss. The more gradual moisture evaporation was due to the water-binding action of pentylene glycol, humectant contained in HA-CL matrix. In detail, TGA trace of HA-CL MS (c) exhibited the following weight loss regions: three stages for water and then pentylene glycol evaporation (20–97 °C, 97–158 °C, 158–223 °C -total weight loss: 26.2% *w/w*), and two stages for HA degradation (223–265 °C, 223–400 °C -total weight loss: 29.5% *w/w*). TGA thermal profile of HA-CL-SAP MS (e) was characterized by two regions for moisture and then pentylene glycol loss (20–154 °C, 154–212 °C, a total weight loss of 21.5% *w/w*), and two regions for HA-CL and SAP decomposition (212–254 °C, 254–400 °C, a total weight loss of 30.3% *w/w*).

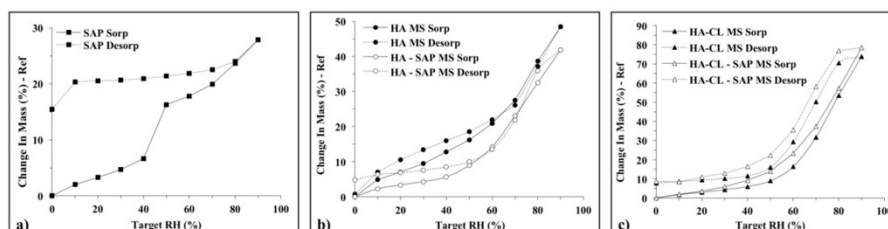


**Figure 6.** TGA thermograms of: SAP (a), HA MS (b), HA-CL MS (c), HA-SAP MS (d), HA-CL-SAP MS (e).

#### 3.2.4. Dynamic Vapor Sorption (DVS)

It is well known that HA is a highly hygroscopic macromolecule, therefore by nature susceptible to moisture sorption and elevated relative humidity (RH) [6,66]. To further characterize hyaluronan MS, and evaluate the effect of SAP encapsulation, the drug, and the formulations were subjected to two 0–90% RH cycles using a DVS. The isotherms of water sorption and desorption for the first humidity ramp (cycle 1) are shown in Figure 7 as a function of the RH%. Following the sorption data of SAP (panel (a)), there was a linear increase of water content starting from the dry powder up to an RH of 40%, where the moisture uptake was 6.6%. A steeper increase of water sorption (+ 9.6%) was observed in the RH range 40–50%. The final total humidity absorbed by SAP was 27.8%. The SAP desorption curve had a very different profile from the SAP sorption curve. A pronounced hysteresis was observed, and at the end of the desorption process, the final retained moisture was 15.4%. On the one hand, this suggested that SAP was not reversible in terms of humidity sorption/desorption, and that water molecules were not easily detached from it, perhaps because of their condensation among the hydrophobic skeleton of the drug. On the other hand, MS formulations (panels (b) and (c)) showed, as previously observed for native HA [67,68], similar trends for their sorption and desorption ramps, and high water-binding capacity due to H-bonds and electrostatic interaction with hyaluronan hydroxyl and carboxylic groups, respectively. Two-stages moisture sorption processes occurred for hyaluronan MS formulations, and this was in agreement with data already reported in the literature for native HA [67,68]. Indeed, in response to RH increment from 0 to 60%, water uptake slowly increased up to 20.9% for HA MS, 14.2% for HA-SAP MS, 16.4% for HA-CL MS, 23.0% for HA-CL-SAP MS (changes in mass similar to that of SAP (+ 17.8%) at 60% RH). However, the final water retention at the end of the sorption process was higher for MS formulations with respect to SAP, as moisture uptake was markedly enhanced for all the formulations in the RH range 60–90%. At 90% RH, the water content was 48.5% for HA MS, 41.9% for HA-SAP MS, 73.8% for HA-CL MS, 78.4% for HA-CL-SAP MS. The higher moisture sorptions observed for HA-CL formulations compared to HA formulations were most likely due to the water-binding ability of urea and pentylene glycol. All the MS formulations displayed hysteresis phenomena: for the same RH value, during the desorption process, samples were characterized by a higher moisture level than during the sorption procedure. However, the hysteresis was reduced with respect to SAP, as well as the final moisture level at the end of the desorption process (0% RH), which was 0.8% for HA MS, 4.9% for HA-SAP MS, 7.8% for HA-CL MS, 8.7% for

HA-CL-SAP MS. Therefore, the encapsulation of SAP into hyaluronan MS produced formulations more reversible in terms of moisture sorption/desorption compared to the pure drug, even if more susceptible to high RH%.



**Figure 7.** DVS isotherms of the first cycle sorption-desorption for: SAP (a), HA MS and HA-SAP MS (b), HA-CL MS and HA-CL-SAP MS (c).

### 3.2.5. SAP Solubility

The solubility of SAP in PBS (0.01 M, pH = 7.4) at 32 °C was  $425.0 \pm 0.9$  mg/mL. This result displayed that sink conditions were guaranteed during the in vitro drug release studies, as SAP concentration, in the case of complete release, could reach values of 0.033 mg/mL in the dialysis tests, and 0.087 mg/mL in the Franz diffusion cell tests.

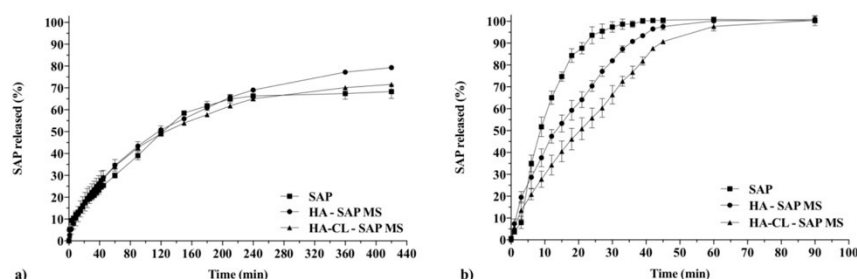
### 3.2.6. In Vitro Drug Release Studies and Kinetic Analysis

One of the most important steps in the study of the efficacy of new delivery systems is the in vitro drug release analysis. Topical carriers are an advanced form of powders for which, so far, there are no compendial or standard release techniques and apparatuses [31,32]. Therefore, several in vitro drug release methods have been used: for example, dialysis [8,12,31,69], Franz cells [23,31,40,70], paddle or basket apparatuses [11,71], flow through cells [8,40]. Variations in the release profiles between different methodologies could be observed [8,31,40], as the methods are different in their working principles. Therefore, during this study, SAP release from HA and HA-CL MS was evaluated with two different in vitro methods: dialysis and Franz diffusion cells. As the control, diffusion tests of free SAP across dialysis and polyamide filter membranes were performed.

Dialysis is a widely used release technique: microspheres are retained into a membrane, while the drug released diffuses firstly from the carrier to the media inside the membrane, and then to an external compartment. Inevitably, the membrane opposes a resistance to the diffusion of drug molecules. This resistance can be limited by using a membrane with an MWCO smaller than the microcarrier size, but importantly bigger than drug molecular weight [72]. Considering hyaluronan MS size and SAP molecular weight (358.08 g/mol), 10kDa MWCO dialysis cassettes were employed in this study. Nevertheless, significant errors were introduced by this release method, as the experimental data did not seem to fully reflect the real release profile of SAP from hyaluronan MS. As previously reported in the literature [72,73], the measured release kinetic seemed to be decreased with respect to the reality: the diffusion rate of free SAP, a highly hydrophilic drug, appeared extremely slow—after 420 min, only the  $68.3 \pm 3.1\%$  of the drug diffused (Figure 8a). Moreover, SAP release profiles from MS appeared controlled by the membranes rather than by the microspheres, as they were almost identical to the diffusion profile of free SAP (Figure 8a). Indeed, a statistical comparison of dialysis data with Moore and Flanner Fit Factors confirmed that all the curves were similar, showing  $f_1 < 10$  and  $f_2 > 50$  (Table 3). Therefore, in this work, the precise release process and kinetic behavior could not be studied using dialysis release method. Similar drawbacks using dialysis technique have already been described in the literature for procaine hydrochloride release from a polymeric carrier: the actual rate of drug release from the delivery system was faster than the rate of diffusion out of the membrane [72]. These results confirm that dialysis could be an unreliable methodology to study drug release from



microcarriers, especially when characterized by a rapid release kinetics [72,73]. Taken together, all these considerations and experimental pieces of evidence can be helpful to optimize, in future, the design of drug release studies for microsystems.



**Figure 8.** Diffusion profile of SAP as free drug and release profile of SAP from HA and HA-CL MS investigated by dialysis (a) and Franz diffusion cells (b).

**Table 3.** Similarity factors ( $f_2$ ) and difference factors ( $f_1$ ) for free SAP and MS formulations

Release Method	Reference Formulation	Test Formulation	$f_1$	$f_2$
Dialysis	SAP	HA-SAP MS	7.9	71.4
	SAP	HA-CL-SAP MS	7.0	74.9
	HA-SAP MS	HA-CL-SAP MS	3.3	82.5
Franz diffusion cell	SAP	HA-SAP MS	15.4	42.7
	SAP	HA-CL-SAP MS	27.4	30.8
	HA-SAP MS	HA-CL-SAP MS	15.1	47.9

Franz diffusion cell tests are probably the most suitable and performed studies to investigate plain drug diffusion and drug release from microparticles intended for dermal and/or mucosal application. Indeed, this model reproduces the conditions encountered on skin and mucosae surface, consenting a slow hydration of the carrier in a humid environment. In vitro release profiles obtained with Franz diffusion cells method were different from those observed with dialysis technique, as displayed by Figure 8. Free SAP diffusion was faster than SAP release from HA MS and HA-CL MS (Figure 8b). More precisely, SAP release from HA-CL MS was significantly extended not only compared to plain SAP but also with respect to HA MS, as proved by Moore and Flanner similarity and difference factors ( $f_1 > 10$  and  $f_2 < 50$ ) (Table 3). For example, after 30 min, the amount of drug released was  $97.4 \pm 2.4\%$  for plain SAP, versus  $81.9 \pm 0.4\%$  and  $66.4 \pm 4.2\%$  for HA MS and HA-CL MS, respectively (Figure 8). A slower drug release was expected with HA-CL MS, considering the higher molecular weight and the implemented mechanical properties of the crosslinked polymer compared to native HA [9,16,74]. The influence of the polymer properties on the release profile was evident, and therefore Franz diffusion cell was found to be a discriminative method to study SAP release kinetic processes.

Among the mathematical templates used to analyze SAP release kinetic from hyaluronan MS, Korsmeyer–Peppas model resulted in the highest  $R^2$  values when compared to Zero order, First order and Higuchi models, for both the formulations (Table 4). The values of the diffusional exponent  $n$  characterizing the release mechanism were 0.709 for HA-SAP MS and 0.712 for HA-CL-SAP MS, suggesting anomalous transport processes [43,46]. SAP release from hyaluronan MS was therefore governed not only by drug diffusion but also by polymer swelling and dissolution. Hyaluronan MS containing SAP behaved as swellable devices composed by hydrophilic polymeric matrixes where a water-soluble drug was dispersed: water penetrated into the polymeric networks, causing their disentanglement and swelling. These phenomena decreased hyaluronan concentration, therefore

enhancing its dissolution at the interface and SAP wettability and diffusion [43,46]. Thus, SAP release was completed in a time frame of about an hour for both the formulations (Figure 8).

**Table 4.** Correlation coefficient for Zero order, First order, Higuchi, and Korsmeyer–Peppas models for SAP dissolution profiles obtained with Franz diffusion cell method.

Formulation	Correlation Coefficient R <sup>2</sup>			
	Zero Order	First Order	Higuchi	Korsmeyer–Peppas
HA–SAP MS	0.729	0.941	0.929	0.993
HA-CL–SAP MS	0.837	0.922	0.960	0.999

#### 4. Conclusions

The present study showed, for the first time and with a systematic approach, that HA-CL could be a promising biopolymer to prepare drug-loaded microspheres with a water-in-oil (w/o) emulsification solvent evaporation technique. Appropriate working conditions led to the production of HA-CL MS and HA-CL–SAP MS characterized by almost unimodal size distributions (*Span* values lower than 3); mean diameter of  $13.0 \pm 0.7$  and  $9.9 \pm 0.8$   $\mu\text{m}$ , respectively (suitable for dermal application); spherical shape and rough surface; high yield—similar to that of HA MS and HA–SAP MS ( $\approx 85\%$ ). SAP could be more efficiently encapsulated into HA-CL MS ( $78.8 \pm 2.6\%$ ) compared to HA–SAP MS ( $69.7 \pm 4.6\%$ ). Physical and molecular state, thermal properties, relative moisture stability of HA-CL MS and HA-CL–SAP MS were comparable to those of HA MS and HA–SAP MS. However, a preliminary Franz diffusion cells test displayed a more extended drug release for HA-CL–SAP MS with respect to HA–SAP MS, despite the same kinetic mechanism (contemporaneous drug diffusion and polymer swelling and dissolution). This underlined that the implemented mechanical properties of the novel HA-CL could result in more efficient microsystems, which could be potentially improved, in future, by the addition of excipients able to further slow down drug release. In vitro studies on skin cells are currently performed to explore SAP release/transport across the cells and the bioactivity of HA-CL MS and HA-CL–SAP MS, in order to understand if they effectively improve hydration and re-epithelialization compared to HA MS and HA–SAP MS.

#### 5. Patent

Fallacara, A.; Vertuani, S.; Manfredini, S.; Citernes, U.R. 2018c. Patent Appl. Filed, n. 102018000008192.

**Author Contributions:** A.F. and S.M. (corresponding author) conceived the study. A.F. designed and performed the experiments, acquired, analyzed, and interpreted the data; wrote the manuscript. F.M. and M.P. contributed to carrying out the experiments, and S.M. participated in the interpretation of the results. S.V. and U.R.C. contributed to revise the manuscript. All authors have given approval to the final version of the manuscript.

**Funding:** This work was supported by a Ph.D. grant (to Arianna Fallacara) from I.R.A. Srl (Istituto Ricerche Applicate Srl, Usmate-Velate, Monza-Brianza, Italy). The authors thank the University of Ferrara and Ambrosialab s.r.l. (Ferrara, Italy, Grant 2016) for the financial support to the running costs of the study.

**Acknowledgments:** Authors gratefully acknowledge the Woolcock Institute of Medical Research and Discipline of Pharmacology, Respiratory Technology—Faculty of Medicine and Health, The University of Sydney (431, Glebe, NSW 2037, Australia)—for the use of facilities and instrumentation. The technical assistance of Gabriele Bertocchi (University of Ferrara) for X-ray analysis is gratefully acknowledged, as well as the English revision of Luigi Mastroianni (State Language High School “Giosuè Carducci” Ferrara, Italy).

**Conflicts of Interest:** The authors declare no conflict of interest. U.R.C. own stocks in I.R.A. srl. The funder had no role in the design of the study; in the collection, analyses, or interpretation of data; in the writing of the manuscript, and in the decision to publish the results.

#### References

1. Fallacara, A.; Baldini, E.; Manfredini, S.; Vertuani, S. Hyaluronic Acid in the Third Millennium. *Polymers* **2018**, *10*, 701. [CrossRef]

2. Laurent, T.C.; Laurent, U.G.B.; Fraser, J.R.E. Functions of hyaluronan. *Ann. Rheum. Dis.* **1995**, *54*, 429–432. [[CrossRef](#)] [[PubMed](#)]
3. Liao, Y.H.; Jones, S.A.; Forbes, B.; Martin, G.P.; Brown, M.B. Hyaluronan: Pharmaceutical characterization and drug delivery. *Drug Deliv.* **2005**, *2*, 327–342. [[CrossRef](#)] [[PubMed](#)]
4. Mayol, L.; Quaglia, F.; Borzacchiello, A.; Ambrosio, L.; La Rotonda, M.I. A novel poloxamers/hyaluronic acid in situ forming hydrogel for drug delivery: Rheological, mucoadhesive and in vitro release properties. *Eur. J. Pharm. Biopharm.* **2008**, *1*, 199–206. [[CrossRef](#)]
5. Benedetti, L.M.; Topp, E.M.; Stella, V.J. Microspheres of hyaluronic acid esters—fabrication methods and in vitro hydrocortisone release. *J. Control. Release* **1990**, *13*, 33–41. [[CrossRef](#)]
6. Casale, M.; Moffa, A.; Sabatino, L.; Pace, A.; Oliveto, G.; Vitali, M.; Baptista, P.; Salvinelli, F. Hyaluronic acid: Perspectives in the upper aero-digestive tract. A systematic review. *PLoS ONE* **2015**, *10*, e0130637. [[CrossRef](#)] [[PubMed](#)]
7. El Kechai, N.; Geiger, S.; Fallacara, A.; Cañero Infante, I.; Nicolas, V.; Ferrary, E.; Huang, N.; Bochot, A.; Agnely, F. Mixtures of hyaluronic acid and liposomes for drug delivery: Phase behavior, microstructure, and mobility of liposomes. *Int. J. Pharm.* **2017**, *523*, 246–259. [[CrossRef](#)]
8. Esposito, E.; Menegatti, E.; Cortesi, R. Hyaluronan-based microspheres as tools for drug delivery: A comparative study. *Int. J. Pharm.* **2005**, *288*, 35–49. [[CrossRef](#)]
9. Fallacara, A.; Manfredini, S.; Durini, E.; Vertuani, S. Hyaluronic acid fillers in soft tissue regeneration. *Facial Plast. Surg.* **2017**, *33*, 87–96. [[CrossRef](#)]
10. Li, Y.; Han, M.; Liu, T.; Cun, D.; Fang, L.; Yang, M. Inhaled hyaluronic acid microparticles extended pulmonary retention and suppressed systemic exposure of a short-acting bronchodilator. *Carbohydr. Polym.* **2017**, *172*, 197–204. [[CrossRef](#)]
11. Lim, S.T.; Martin, G.P.; Berry, D.J.; Brown, M.B. Preparation and evaluation of the in vitro drug release properties and mucoadhesion of novel microspheres of hyaluronic acid and chitosan. *J. Control. Release* **2000**, *66*, 281–292. [[CrossRef](#)]
12. Saadat, E.; Shakor, N.; Gholami, M.; Dorkoosh, F.A. Hyaluronic acid based micelle for articular delivery of triamcinolone, preparation in vitro and in vivo evaluation. *Int. J. Pharm.* **2015**, *489*, 218–225. [[CrossRef](#)] [[PubMed](#)]
13. Shimojo, A.A.; Pires, A.M.; Lichy, R.; Rodrigues, A.A.; Santana, M.H. The crosslinking degree controls the mechanical, rheological, and swelling properties of hyaluronic acid microparticles. *J. Biomed. Mater. Res. A* **2015**, *103*, 730–737. [[CrossRef](#)] [[PubMed](#)]
14. Ramamurthi, A.; Vesely, I. Smooth muscle cell adhesion on cross-linked hyaluronan gels. *J. Biomed. Mater. Res.* **2002**, *60*, 195–205. [[CrossRef](#)] [[PubMed](#)]
15. Tomihata, K.; Ikada, Y. Preparation of cross-linked hyaluronic acid films of low water content. *Biomaterials* **1997**, *18*, 189–195. [[CrossRef](#)]
16. Citernes, U.R.; Beretta, L.; Citernes, L. Crosslinked Hyaluronic Acid, the Process for the Preparation Thereof and Use Thereof in the Aesthetic Field. Patent WO/2015/007773 A1, 22 January 2015.
17. Fallacara, A.; Vertuani, S.; Panozzo, G.; Pecorelli, A.; Valacchi, G.; Manfredini, S. Novel Artificial Tears Containing Cross-Linked Hyaluronic Acid: An In Vitro Re-Epithelialization Study. *Molecules* **2017**, *22*, 2104. [[CrossRef](#)] [[PubMed](#)]
18. Fallacara, A.; Busato, L.; Pozzoli, M.; Ghadiri, M.; Ong, H.X.; Young, P.M.; Manfredini, S.; Traini, D. Combination of urea-crosslinked hyaluronic acid and sodium ascorbyl phosphate for the treatment of inflammatory lung diseases: An in vitro study. *Eur. J. Pharm. Sci.* **2018**, *120*, 96–106. [[CrossRef](#)] [[PubMed](#)]
19. Albèr, C.; Brandner, B.D.; Björklund, S.; Billsten, P.; Corkery, R.W.; Engblom, J. Effects of water gradients and use of urea on skin ultrastructure evaluated by confocal Raman microspectroscopy. *Biochim. Biophys. Acta* **2013**, *1828*, 2470–2478. [[CrossRef](#)]
20. Charlton, J.F.; Schwab, I.R.; Stuchell, R. Topical urea as a treatment for non-infectious keratopathy. *Acta Ophthalmol. Scand.* **1996**, *74*, 391–394. [[CrossRef](#)]
21. Pan, M.; Heinecke, G.; Bernardo, S.; Tsui, C.; Levitt, J. Urea: A comprehensive review of the clinical literature. *Dermatol. Online J.* **2013**, *19*, 20392.
22. Degim, Z. Use of microparticulate systems to accelerate skin wound healing. *J. Drug Target.* **2008**, *16*, 437–448. [[CrossRef](#)] [[PubMed](#)]



23. Abd El-Hameed, M.D.; Kellaway, I.W. Preparation and in vitro characterisation of mucoadhesive polymeric microspheres as intra-nasal delivery systems. *Eur. J. Pharm. Biopharm.* **1997**, *44*, 53–60. [[CrossRef](#)]
24. Kulkarni, A.D.; Bari, D.B.; Surana, S.J.; Pardeshi, C.V. In vitro, ex vivo and in vivo performance of chitosan-based spray-dried nasal mucoadhesive microspheres of diltiazem hydrochloride. *J Drug Deliv. Sci. Technol.* **2016**, *31*, 108–117. [[CrossRef](#)]
25. Khan, H.; Akhtar, N.; Ali, A. Assessment of combined ascorbyl palmitate (AP) and sodium ascorbyl phosphate (SAP) on facial skin sebum control in female healthy volunteers. *Drug Res. (Stuttg)* **2017**, *67*, 52–58. [[CrossRef](#)] [[PubMed](#)]
26. Klock, J.; Ikeno, H.; Ohmori, K.; Nishikawa, T.; Vollhardt, J.; Schehlmann, V. Sodium ascorbyl phosphate shows in vitro and in vivo efficacy in the prevention and treatment of acne vulgaris. *Int. J. Cosmet. Sci.* **2005**, *27*, 171–176. [[CrossRef](#)] [[PubMed](#)]
27. Amirlak, B.; Mahedia, M.; Shah, N. A clinical evaluation of efficacy and safety of hyaluronan sponge with vitamin C versus placebo for scar reduction. *Plast. Reconstr. Surg. Glob. Open* **2016**, *4*, e792. [[CrossRef](#)] [[PubMed](#)]
28. Spiclin, P.; Homar, M.; Zupancic-Valant, A.; Gasperlin, M. Sodium ascorbyl phosphate in topical microemulsions. *Int. J. Pharm.* **2003**, *256*, 65–73. [[CrossRef](#)]
29. Wetton, R.E.; Whorlow, R.W. *Polymer Systems: Deformation and Flow*; Macmillan: London, UK, 1968; ISBN 10 0333062035.
30. Couarraze, G.; Grossiord, J.L. *Initiation à la Rhéologie*; TEC & DOC: Paris, France, 2000; ISBN 2-7430-0285-9.
31. Balzus, B.; Colombo, M.; Sahle, F.F.; Zoubari, G.; Staufenbiel, S.; Bodmeier, R. Comparison of different in vitro release methods used to investigate nanocarriers intended for dermal application. *Int. J. Pharm.* **2016**, *513*, 247–254. [[CrossRef](#)]
32. Lusina Kregar, M.; Durrigl, M.; Rozman, A.; Jelcic, Z.; Cetina-Cizmek, B.; Filipovic-Grcic, J. Development and validation of an in vitro release method for topical particulate delivery systems. *Int. J. Pharm.* **2015**, *485*, 202–214. [[CrossRef](#)]
33. Schlupp, P.; Blaschke, T.; Kramer, K.D.; Höltje, H.D.; Mehnert, W.; Schäfer-Korting, M. Drug release and skin penetration from solid lipid nanoparticles and a base cream: A systematic approach from a comparison of three glucocorticoids. *Skin Pharmacol. Physiol.* **2011**, *24*, 199–209. [[CrossRef](#)]
34. Zoubari, G.; Staufenbiel, S.; Volz, P.; Alexiev, U.; Bodmeier, R. Effect of drug solubility and lipid carrier on drug release from lipid nanoparticles for dermal delivery. *Eur. J. Pharm. Biopharm.* **2017**, *110*, 39–46. [[CrossRef](#)] [[PubMed](#)]
35. Moore, H.H.; Flanner, J.W. Mathematical comparison of dissolution profiles. *Pharm. Technol.* **1996**, *20*, 64–74.
36. Food and Drug Administration. *Guidance for Industry; Dissolution Testing on Immediate Release Solid Oral Dosage Forms*; FDA: Rockville, MD, USA, 1997.
37. Cirri, M.; Roghi, A.; Valleri, M.; Mura, P. Development and characterization of fast-dissolving tablet formulations of glyburide based on solid self-microemulsifying systems. *Eur. J. Pharm. Biopharm.* **2016**, *104*, 19–29. [[CrossRef](#)] [[PubMed](#)]
38. Ong, H.X.; Traini, D.; Bebawy, M.; Young, P.M. Epithelial Profiling of Antibiotic Controlled Release Respiratory Formulations. *Pharm. Res.* **2011**, *28*, 2327–2338. [[CrossRef](#)] [[PubMed](#)]
39. Pozzoli, M.; Traini, D.; Young, P.M.; Sukkar, M.B.; Sonvico, F. Development of a Soluplus budesonide freeze-dried powder for nasal drug delivery. *Drug Dev. Ind. Pharm.* **2017**, *43*, 1510–1518. [[CrossRef](#)] [[PubMed](#)]
40. Salama, R.O.; Traini, D.; Chan, H.K.; Young, P.M. Preparation and characterisation of controlled release co-spray dried drug-polymer microparticles for inhalation 2: Evaluation of in vitro release profiling methodologies for controlled release respiratory aerosols. *Eur. J. Pharm. Biopharm.* **2008**, *70*, 145–152. [[CrossRef](#)] [[PubMed](#)]
41. Costa, P.; Sousa Lobo, J.M. Modeling and comparison of dissolution profiles. *Eur. J. Pharm. Sci.* **2001**, *13*, 123–133. [[CrossRef](#)]
42. Higuchi, T. Rate of release of medicaments from ointment bases containing drugs in suspension. *J. Pharm. Sci.* **1961**, *50*, 874. [[CrossRef](#)]
43. Arifin, D.Y.; Lee, L.Y.; Wang, C.H. Mathematical modelling and simulation of drug release from microspheres: Implication to drug delivery systems. *Adv. Drug Deliv. Rev.* **2006**, *58*, 1274–1325. [[CrossRef](#)]
44. Korsmeyer, R.W.; Peppas, N.A. Effect of the morphology of hydrophilic polymeric matrices on the diffusion and release of water-soluble drugs. *J. Membr. Sci.* **1981**, *9*, 211–227. [[CrossRef](#)]



45. Peppas, N.A. Analysis of fickian and non-fickian drug release from polymers. *Pharm. Acta Helv.* **1985**, *60*, 110–111. [[PubMed](#)]
46. Singhvi, G.; Singh, M. Review: In-vitro drug release characterization models. *Int. J. Pharm. Sci. Res.* **2011**, *2*, 77–84.
47. Liu, Z.; Li, X.; Xiu, B.; Duan, C.; Li, J.; Zhang, X.; Yang, X.; Dai, W.; Johnson, H.; Zhang, H.; et al. A novel and simple preparative method for uniform-sized PLGA microspheres: Preliminary application in antitubercular drug delivery. *Colloids Surf. B Biointerfaces* **2016**, *145*, 679–687. [[CrossRef](#)] [[PubMed](#)]
48. Falcone, S.J.; Palmeri, D.M.; Berg, R.A. Rheological and cohesive properties of hyaluronic acid. *J. Biomed. Mater. Res. A* **2006**, *76*, 721–728. [[CrossRef](#)] [[PubMed](#)]
49. Collins, N.M.; Birkinshaw, C. Physical properties of crosslinked hyaluronic acid hydrogels. *J. Mater. Sci. Mater. Med.* **2008**, *19*, 3335–3343. [[CrossRef](#)] [[PubMed](#)]
50. Ré, M.A.; Messias, L.S.; Schettini, H. The influence of the liquid properties and the atomizing conditions on the physical characteristics of the spray-dried ferrous sulfate microparticles. In Proceedings of the 14th International Drying Symposium (IDS 2004), São Paulo, Brazil, 22–25 August 2004; pp. 1174–1181.
51. Gatej, I.; Popa, M.; Rinaudo, M. Role of pH on hyaluronan behavior in aqueous solution. *Biomacromolecules* **2005**, *6*, 61–67. [[CrossRef](#)] [[PubMed](#)]
52. Maleki, A.; Kjoniksen, A.; Nystrom, B. Effect of pH on the behavior of hyaluronic acid in dilute and semidilute aqueous solutions. *Macromol. Symp.* **2008**, *274*, 131–140. [[CrossRef](#)]
53. Bari, E.; Arciola, C.R.; Vigani, B.; Crivelli, B.; Moro, P.; Marrubini, G.; Sorrenti, M.; Catenacci, L.; Bruni, G.; Chlapanidas, T.; et al. In vitro effectiveness of microspheres based on silk sericin and *Chlorella vulgaris* or *Arthrospira platensis* for wound healing applications. *Materials (Basel)* **2017**, *10*, 983. [[CrossRef](#)] [[PubMed](#)]
54. Ranjan, S.; Fontana, F.; Ullah, H.; Hirvonen, J.; Santos, H.A. Microparticles to enhance delivery of drugs and growth factors into wound sites. *Ther. Deliv.* **2016**, *7*, 711–732. [[CrossRef](#)] [[PubMed](#)]
55. Anonymous. Benzoyl peroxide microsphere formulations: What is the science supporting microsphere vehicle technology and clinical use? *J. Clin. Aesthet. Dermatol.* **2009**, *2*, 46–54.
56. Vertuani, S.; Cvetkovska, A.D.; Zauli, S.; Virgili, A.; Manfredini, S.; Bettoli, V. The topical vehicle as a key factor in the management of the psoriatic patients' therapy. *G. Ital. Dermatol. Venereol.* **2013**, *148*, 679–685.
57. Klug, H.P.; Alexander, L.E. *X-ray Diffraction Procedures for Polycrystalline and Amorphous Materials*, 2nd ed.; John Wiley and Sons: New York, NY, USA, 1974; ISBN 978-0-471-49369-3.
58. Siepmann, J.; Peppas, N.A. Modeling of drug release from delivery systems based on hydroxypropyl methylcellulose. *Adv. Drug Deliv. Rev.* **2001**, *48*, 139–157. [[CrossRef](#)]
59. Yang, S.C.; Zhu, J.B. Preparation and characterization of camptothecin solid lipid nanoparticles. *Drug Dev. Ind. Pharm.* **2002**, *28*, 265–274. [[CrossRef](#)] [[PubMed](#)]
60. Moyano, M.A.; Broussalis, A.M.; Segall, A.I. Thermal analysis of lipoic acid and evaluation of the compatibility with excipients. *J. Therm. Anal. Calorim.* **2010**, *99*, 631–637. [[CrossRef](#)]
61. Collins, M.N.; Birkinshaw, C. Comparison of the effectiveness of four different crosslinking agents with hyaluronic acid hydrogel films for tissue-culture applications. *J. Appl. Polym. Sci.* **2007**, *104*, 3183–3191. [[CrossRef](#)]
62. Kafedjiiski, K.; Jetli, R.K.; Föger, F.; Hoyer, H.; Werle, M.; Hoffer, M.; Bernkop-Schnürch, A. Synthesis and in vitro evaluation of thiolated hyaluronic acid for mucoadhesive drug delivery. *Int. J. Pharm.* **2007**, *343*, 48–58. [[CrossRef](#)] [[PubMed](#)]
63. Lapcik, L.; Otyepková, E.; Lapciková, B.; Otyepka, M.; Vlcek, J.; Kupská, I. Physicochemical analysis of hyaluronic acid powder for cosmetic and pharmaceutical processing. In *Hyaluronic acid for biomedical and pharmaceutical applications*, 1st ed.; Collins, M.N., Ed.; Smithers Rapra Technology: Shropshire, UK, 2014; pp. 89–101, ISBN 10 9781909030770.
64. Lewandowska, K.; Sionkowska, A.; Grabska, S.; Kaczmarek, B. Surface and thermal properties of collagen/hyaluronic acid blends containing chitosan. *Int. J. Biol. Macromol.* **2016**, *92*, 371–376. [[CrossRef](#)] [[PubMed](#)]
65. Réeff, J.; Gaignaux, A.; Goole, J.; De Vriese, C.; Amighi, K. New sustained-release intraarticular gel formulations based on monolein for local treatment of arthritic diseases. *Drug Dev. Ind. Pharm.* **2013**, *39*, 1731–1741. [[CrossRef](#)]
66. Albèr, C.; Engblom, J.; Falkman, P.; Kocherbitov, V. Hydration of hyaluronan: Effects on structural and thermodynamic properties. *J. Phys. Chem. B* **2015**, *119*, 4211–4219. [[CrossRef](#)]

67. Panagopoulou, A.; Vázquez Molina, J.; Kyritsis, A.; Monleón Pradas, M.; Vallés Lluch, A.; Gallego Ferrer, G.; Pissis, P. Glass Transition and Water Dynamics in Hyaluronic Acid Hydrogels. *Food Biophys.* **2013**, *8*, 192–202. [[CrossRef](#)]
68. Servaty, R.; Schiller, J.; Binder, H.; Arnold, K. Hydration of polymeric components of cartilage—An infrared spectroscopic study on hyaluronic acid and chondroitin sulfate. *Int. J. Biol. Macromol.* **2001**, *28*, 121–127. [[CrossRef](#)]
69. Montenegro, L.; Trapani, A.; Fini, P.; Mandracchia, D.; Latrofa, A.; Cioffi, N.; Chiarantini, L.; Giusi, G.P.; Brundu, S.; Puglisi, G. Chitosan nanoparticles for topical co-administration of the antioxidants glutathione and idebenone: Characterization and in vitro release. *Br. J. Pharm. Res.* **2014**, *4*, 2387–2406. [[CrossRef](#)]
70. Alves, A.C.; Ramos, I.I.; Nunes, C.; Magalhães, L.M.; Sklenářová, H.; Segundo, M.A.; Lima, J.L.F.C.; Reis, S. On-line automated evaluation of lipid nanoparticles transdermal permeation using Franz diffusion cell and low-pressure chromatography. *Talanta* **2016**, *146*, 369–374. [[CrossRef](#)] [[PubMed](#)]
71. Dürriegl, M.; Kwokal, A.; Hafner, A.; Šegvi Klari, M.; Dumicic, A.; Cetina-Cižmek, B.; Filipovic-Grcic, J. Spray dried microparticles for controlled delivery of mupirocin calcium: Process-tailored modulation of drug release. *J. Microencapsul.* **2011**, *28*, 108–121. [[CrossRef](#)] [[PubMed](#)]
72. Moreno-Bautista, G.; Tam, K.C. Evaluation of dialysis membrane process for quantifying the in vitro drug-release from colloidal drug carriers. *Colloids Surf. A Physicochem. Eng. Asp.* **2011**, *389*, 299–303. [[CrossRef](#)]
73. Zambito, Y.; Pedreschi, E.; Di Colo, G. Is dialysis a reliable method for studying drug release from nanoparticulate systems?—A case study. *Int. J. Pharm.* **2012**, *434*, 28–34. [[CrossRef](#)] [[PubMed](#)]
74. Garti, N. *Delivery and Controlled Release of Bioactives in Foods and Nutraceuticals*, 1st ed.; Woodhead Publishing: Sawston, UK, 2008; p. 496, ISBN 978-1-84569-145-5.



© 2018 by the authors. Licensee MDPI, Basel, Switzerland. This article is an open access article distributed under the terms and conditions of the Creative Commons Attribution (CC BY) license (<http://creativecommons.org/licenses/by/4.0/>).

Review

# Hyaluronic Acid in the Third Millennium

Arianna Fallacara , Erika Baldini, Stefano Manfredini \* and Silvia Vertuani

Department of Life Sciences and Biotechnology, Master Course in Cosmetic Science and Technology (COSMAST), University of Ferrara, Via L. Borsari 46, 44121 Ferrara, Italy; arianna.fallacara@student.unife.it (A.F.); erika.baldini@student.unife.it (E.B.); vrs@unife.it (S.V.)

\* Correspondence: smanfred@unife.it; Tel.: +39-0532-455294; Fax: +39-0532-455378

Received: 28 May 2018; Accepted: 20 June 2018; Published: 25 June 2018



**Abstract:** Since its first isolation in 1934, hyaluronic acid (HA) has been studied across a variety of research areas. This unbranched glycosaminoglycan consisting of repeating disaccharide units of *N*-acetyl-*D*-glucosamine and *D*-glucuronic acid is almost ubiquitous in humans and in other vertebrates. HA is involved in many key processes, including cell signaling, wound reparation, tissue regeneration, morphogenesis, matrix organization and pathobiology, and has unique physico-chemical properties, such as biocompatibility, biodegradability, mucoadhesivity, hygroscopicity and viscoelasticity. For these reasons, exogenous HA has been investigated as a drug delivery system and treatment in cancer, ophthalmology, arthrology, pneumology, rhinology, urology, aesthetic medicine and cosmetics. To improve and customize its properties and applications, HA can be subjected to chemical modifications: conjugation and crosslinking. The present review gives an overview regarding HA, describing its history, physico-chemical, structural and hydrodynamic properties and biology (occurrence, biosynthesis (by hyaluronan synthases), degradation (by hyaluronidases and oxidative stress), roles, mechanisms of action and receptors). Furthermore, both conventional and recently emerging methods developed for the industrial production of HA and its chemical derivatization are presented. Finally, the medical, pharmaceutical and cosmetic applications of HA and its derivatives are reviewed, reporting examples of HA-based products that currently are on the market or are undergoing further investigations.

**Keywords:** biological activity; crosslinking; drug delivery; cosmetic; food-supplement; functionalization; hyaluronan applications; hyaluronan derivatives; hyaluronan synthases; hyaluronic acid; hyaluronidases; physico-chemical properties

## 1. Introduction and Historical Background of HA

Research on hyaluronic acid (HA) has expanded over more than one century.

The first study that can be referred to regarding HA dates from 1880: the French scientist Portes observed that mucin from vitreous body was different from other mucoids in cornea and cartilage and called it “hyalomucine” [1]. Nevertheless, only in 1934, Meyer and Palmer isolated from bovine vitreous humor a new polysaccharide containing an amino sugar and a uronic acid and named it HA, from “hyaloid” (vitreous) and “uronic acid” [2]. During the 1930s and 1950s, HA was isolated also from human umbilical cord, rooster comb and streptococci [3,4].

The physico-chemical properties of HA were widely studied from the 1940s [5–9], and its chemical structure was solved in 1954 by Meyer and Weissmann [10]. During the second half of the Twentieth Century, the progressive understanding of HA’s biological roles [11–13] determined an increasing interest in its production and development as a medical product for a number of clinical applications. Hence, the extraction processes from animal tissues were progressively optimized, but still carried several problems of purification from unwanted contaminants (i.e., microorganisms, proteins). The first



studies on HA production through bacterial fermentation and chemical synthesis were carried out before the 1970s [1].

The first pharmaceutical-grade HA was produced in 1979 by Balazs, who developed an efficient method to extract and purify the polymer from rooster combs and human umbilical cords [14]. Balazs' procedure set the basis for the industrial production of HA [14]. Since the early 1980s, HA has been widely investigated as a raw material to develop intraocular lenses for implantation, becoming a major product in ophthalmology for its safety and protective effect on corneal endothelium [15–22]. Additionally, HA was found to be beneficial also for the treatment of joint [23–27] and skin diseases [28,29], for wound healing [30–33] and for soft tissue augmentation [34,35]. Since the late 1980s, HA has also been used to formulate drug delivery systems [36–41], and efforts continue still to today to develop HA-based vehicles to improve therapeutic efficacy [42–45]. During the 1990s and 2000s, particular attention was paid to identifying and characterizing the enzymes involved in HA metabolism, as well as developing bacterial fermentation techniques to produce HA with controlled size and polydispersity [1]. Nowadays, HA represents a key molecule in a variety of medical, pharmaceutical, nutritional and cosmetic applications. For this reason, HA is still widely studied to elucidate its biosynthetic pathways and molecular biology, to optimize its biotechnological production, to synthesize derivatives with improved properties and to optimize and implement its therapeutic and aesthetic uses [1,42–44,46–58].

Considering the great interest in HA from different fields, the fast growing number of studies and our interest in this topic, we decided to provide a comprehensive overview regarding HA and its potentialities, giving a concise update on the latest progress. As an example, a search on the most common public databases (i.e., Pubmed, Scopus, Isi Web of Science, ScienceDirect, Google Scholar, ResearchGate and Patent Data Base Questel) with the keyword "hyaluron\*", gave a total of 161,863 hits: 142,575 papers and 19,288 patents. This huge amount of data are continuously growing. Thus, with the aim to give a clearer picture about where researches and applications in the field are going, the present work starts with an update of HA's physico-chemical, structural and hydrodynamic properties and proceeds with the discussion of HA biology: occurrence, biosynthesis (by hyaluronan synthases), degradation (by hyaluronidases and oxidative stress), roles, mechanisms of action and receptors. Furthermore, both conventional and recently-emerging methods developed for the industrial production of HA and its chemical derivatization are described. Finally, the medical, pharmaceutical, cosmetic and dietary applications of HA and its derivatives are reviewed, reporting examples of HA-based products that currently are on the market or are undergoing further investigations.

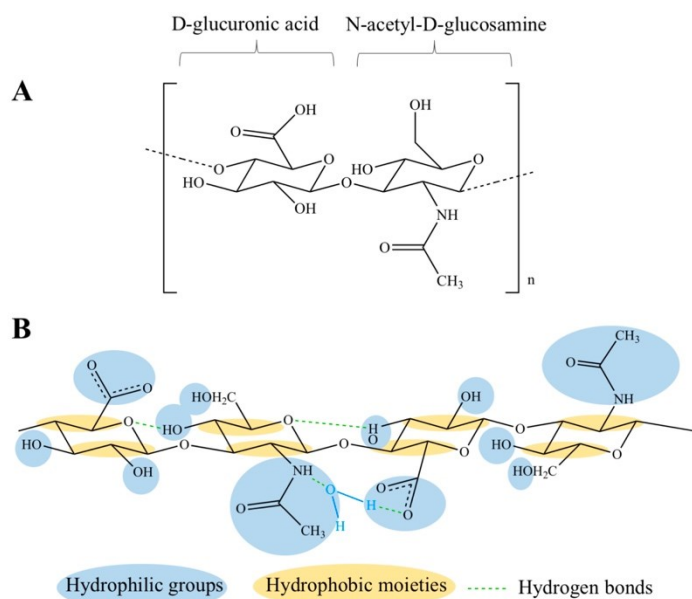
Literature search: we searched the Cochrane Controlled Trials Register (Central), Medline, EMBase and Cinahl from inception to November 2006 using truncated variations of preparation names including brand names combined with truncated variations of terms related to osteoarthritis, all as text. No methodologic filter for controlled clinical trials was applied (the exact search strategy is available from the authors). We entered relevant articles into the Science Citation Index to retrieve reports that have cited these articles, manually searched conference proceedings and textbooks, screened reference lists of all obtained articles and checked the proceedings of the U.S. Food and Drug Administration advisory panel related to relevant approval applications. Finally, we asked authors and content experts for relevant references and contacted manufacturers known to have conducted trials on viscosupplementation.

## 2. Physico-Chemical, Structural and Hydrodynamic Properties of HA

HA is a natural and unbranched polymer belonging to a group of heteropolysaccharides named glycosaminoglycans (GAGs), which are diffused in the epithelial, connective and nervous tissues of vertebrates [46,59,60]. All the GAGs (i.e., HA, chondroitin sulfate, dermatan sulfate, keratin sulfate, heparin sulfate and heparin) are characterized by the same basic structure consisting of disaccharide units of an amino sugar (*N*-acetyl-galactosamine or *N*-acetyl-glucosamine) and a uronic sugar (glucuronic acid, iduronic acid or galactose). However, HA differs as it is not sulfated and it

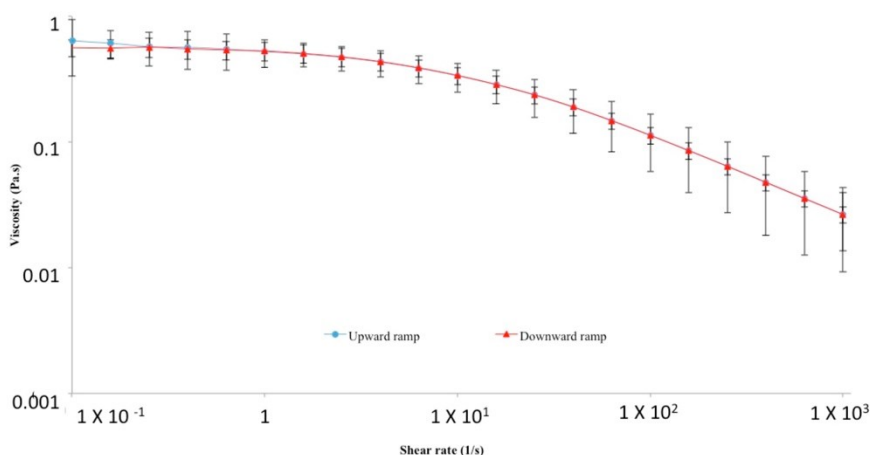
is not synthesized by Golgi enzymes in association with proteins [46,59,60]. Indeed, HA is produced at the inner face of the plasma membrane without any covalent bond to a protein core. Additionally, HA can reach a very high molecular weight (HMW,  $10^8$  Da), while the other GAGs are relatively smaller in size ( $<5 \times 10^4$  Da, usually  $1.5\text{--}2 \times 10^4$  Da) [46,59,60].

The primary structure of HA is a linear chain containing repeating disaccharide units linked by  $\beta$ -1,4-glycosidic bonds. Each disaccharide consists of *N*-acetyl-D-glucosamine and D-glucuronic acid connected by  $\beta$  1,3-glycosidic bonds (Figure 1) [10,61]. When both the monosaccharides are in the  $\beta$  configuration, a very energetically-stable structure is formed, as each bulky functional group (hydroxyl, carboxyl, acetamido, anomeric carbon) is in the sterically-favorable equatorial position, while each small hydrogen atom occupies the less energetically-favorable axial position [62]. Thus, the free rotation around the glycosidic bonds of HA backbone is limited, resulting in a rigid conformation where hydrophobic patches (CH groups) are alternated with polar groups [63,64], which are linked by intra- and inter-molecular hydrogen bonds (H-bonds) (Figure 1) [65]. At physiological pH, each carboxyl group has an anionic charge, which can be balanced with a mobile cation such as  $\text{Na}^+$ ,  $\text{K}^+$ ,  $\text{Ca}^{2+}$  and  $\text{Mg}^{2+}$ . Hence, in aqueous solution, HA is negatively charged and forms salts generally referred to as hyaluronan or hyaluronate [66,67], which are highly hydrophilic and, consequently, surrounded by water molecules. More precisely, as displayed in Figure 1, water molecules link HA carboxyl and acetamido groups with H-bonds that stabilize the secondary structure of the biopolymer, described as a single-strand left-handed helix with two disaccharide residues per turn (two-fold helix) [68]. In aqueous solution, HA two-fold helices form duplexes, i.e., a  $\beta$ -sheet tertiary structure, due to hydrophobic interactions and inter-molecular H-bonds, which enable the aggregation of polymeric chains with the formation of an extended meshwork [64,65].



**Figure 1.** Chemical structures of HA disaccharide unit (A) and HA tetrasaccharide unit where the hydrophilic functional groups and the hydrophobic moieties are respectively evidenced in blue and yellow, while the hydrogen bonds are represented by green dashed lines (B).

The establishment of this network depends on HA molecular weight (MW) and concentration; for example, HMW native HA ( $>10^6$  Da) forms an extended network even at a very low concentration of 1  $\mu\text{g}/\text{mL}$  [64,69]. With increasing MW and concentration, HA networks are strengthened, and consequently, HA solutions display progressively increased viscosity and viscoelasticity [70]. Since hyaluronan is a polyelectrolyte [71], its rheological properties in aqueous solutions are influenced also by ionic strength, pH and temperature [46,70,72]: as these factors increase, HA viscosity declines markedly, suggesting a weakening of the interactions among the polymer chains [73]. In particular, HA is highly sensitive to pH alterations: in acidic and alkaline environments, a critical balance between repulsive and attractive forces occurs [74], and when the pH is lower than four or higher than 11, HA is degraded by hydrolysis [75]. In alkaline conditions, this effect is more pronounced, due to the disruption of H bonds, which take part in the structural organization of HA chains [74,76,77]. Therefore, both the structural properties and the polyelectrolyte character of HA determine its rheological profile [65,73,78,79]. HA solutions are characterized by a non-Newtonian, shear-thinning and viscoelastic behavior. The shear-thinning (or pseudoplastic) profile of HA is due to the breakdown of the inter-molecular hydrogen bonds and hydrophobic interactions under increasing shear rates: HA chains deform and align in the streamlines of flow, and this results in a viscosity decrease [74,78] (Figure 2). Additionally, HA solutions are non-thixotropic: as the shear rate decreases and ends, they recover their original structure and viscosity proceeding through the same intermediate states of the breakdown process [73] (Figure 2). Hence, the breakdown of the polymeric network is transient and reversible. This unique rheological behavior is peculiar and extremely important, as it determines many physiological roles and pharmaceutical, medical, food and cosmetic applications of hyaluronan.



**Figure 2.** Shear-thinning and non-thixotropic behavior of 0.5% HA solution (2 MDa) analyzed using the rotational rheometer AR2000 (TA instruments, New Castle, DE, USA), connected to the Rheology Advantage software (Version V7.20) and equipped with an aluminum cone/plate geometry (diameter 40 mm, angle  $2^\circ$ , 64- $\mu\text{m}$  truncation). The viscosity decreases in response to gradual increases of the shear rate over time (upward ramp), and then, the viscosity increases in response to gradual decreases of the shear rate over time (downward ramp). The initial viscosity is recovered through the same intermediate states of the breakdown process: the breakdown of the polymeric network is transient and reversible, and therefore, the original structure of HA is recovered.



### 3. Biology of HA

#### 3.1. HA Occurrence in Living Organism and Diffusion in the Human Body

Hyaluronan is widely diffused in nature: it is present in humans, animals, such as, rabbits, bovines, roosters, bacteria, such as *Streptococcus equi*, *Streptococcus zooepidermicus*, *Streptococcus equisimilis*, *Streptococcus pyogenes*, *Streptococcus uberis*, *Pasteurella multocida* [49,80–82], algae, such as the green algae *Chlorella* sp. infected by the *Chlorovirus* [49,83], yeasts, such as *Cryptococcus neoformans* [49], and mollusks [84]. However, it is not found in fungi, plants and insects [85].

In the human body, the total content of HA is about 15 g for a 70-kg adult [86]. HA is prevalently distributed around cells, where it forms a pericellular coating, and in the extracellular matrix (ECM) of connective tissues [61,82]. Approximately 50% of the total HA resides in the skin, both in the dermis and the epidermis [82]. Synovial joint fluid and eye vitreous body, being mainly composed of ECM, contain important amounts of hyaluronan: 3–4 mg/mL and 0.1 mg/mL (wet weight), respectively [61,82]. Moreover, HA is also abundant in the umbilical cord (4 mg/mL), where it represents the major component of Wharton's jelly together with chondroitin sulfate [87,88]. The turnover of HA is fast (5 g/day) and is finely regulated through enzymatic synthesis and degradation [86].

#### 3.2. HA Synthesis in the Human Body

In the human body, HA is synthesized as a free linear polymer by three transmembrane glycosyltransferase isoenzymes named hyaluronan synthases, HAS: HAS1, HAS2 and HAS3, whose catalytic sites are located on the inner face of the plasma membrane. HA growing chains are extruded onto the cell surface or into the ECM through the plasma membrane and HAS protein complexes [89,90] (Figure 3). The three HAS isoforms share the 50–71% of their amino acid sequences (55% HAS1/HAS2, 57% HAS1/HAS3, 71% HAS2/HAS3), and indeed, they are all characterized by seven membrane-spanning regions and a central cytoplasmic domain [50,86,89]. However, HAS gene sequences are located on different chromosomes (hCh19-HAS1, hCh8-HAS2 and hCh16-HAS3) [91,92], and the expression and the activity of HAS isoforms are controlled by growth factors, cytokines and other proteins such as kinases in different fashions, which appear cell and tissue specific [50,90,93,94]. Hence, the three HAS genes may respond differently to transcriptional signals: for example, in human fibroblasts like synoviocytes, transforming growth factor  $\beta$  upregulates HAS1 expression, but downregulates HAS3 expression [95]. Moreover, HAS biochemical and synthetic properties are different: HAS1 is the least active isoenzyme and produces HMW hyaluronan (from  $2 \times 10^5$  to  $2 \times 10^6$  Da). HAS2 is more active and synthesizes HA chains greater than  $2 \times 10^6$  Da. It represents the main hyaluronan synthetic enzyme in normal adult cells, and its activity is finely regulated [96]. HAS2 also regulates the developmental and reparation processes of tissue growth, and it may be involved in inflammation, cancer, pulmonary fibrosis and keloid scarring [55,86,97–99]. HAS3 is the most active isoenzyme and produces HA molecules with MW lower than  $3 \times 10^5$  Da [60].

Dysregulation and misregulation of HAS genes' expression result in abnormal production of HA and, therefore, in increased risk of pathological events, altered cell responses to injury and aberrant biological processes such as malignant transformation and metastasis [47,48,50,100].

Even if the exact regulation mechanisms and functions of each HAS isoenzyme have not been fully elucidated yet [96], all the aforementioned studies suggest that HAS are critical mediators of physiological and pathological processes, as they are involved in development, injury and disease.

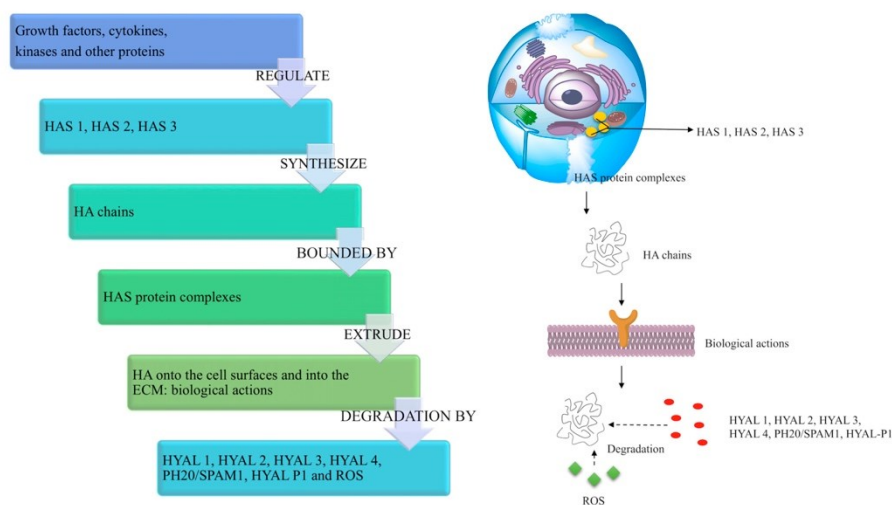


Figure 3. Schematic diagram showing HA key steps from its synthesis to its degradation.

### 3.3. HA Degradation in the Human Body

HA degradation in the human body is accomplished by two different mechanisms: one is specific, mediated by enzymes (hyaluronidases (HYAL)), while the other is nonspecific, determined by oxidative damage due to reactive oxygen species (ROS) (Figure 3). Together, HYAL and ROS locally degrade roughly 30% of the 15 g HA present in the human body. The remaining 70% is catabolized systemically: hyaluronan is mostly transported by the lymph to the lymph nodes, where it is internalized and catabolized by the endothelial cells of the lymphatic vessels. Additionally, a small part of HA is carried to the bloodstream and degraded by liver endothelial cells [50].

HYAL have a pivotal regulatory function in the metabolism of hyaluronan. These enzymes predominantly degrade HA, even if they are able to catabolize also chondroitin sulfate and chondroitin [101]. Randomly cleaving the  $\beta$ -*N*-acetyl-D-glucosaminidic linkages ( $\beta$ -1,4 glycosidic bonds) of HA chains, HYAL are classified as endoglycosidases. In the human genome, six HYAL gene sequences have been identified in two linked triplets: HYAL 1, HYAL 2, HYAL 3 genes, clustered on chromosome 3p21.3; HYAL-4 and PH20/SPAM1 genes, similarly located on chromosome 7p31.3, together with HYAL-P1 pseudogene [102]. HYAL have a consistent amino acid sequence in common: in particular, HYAL 1, HYAL 2, HYAL 3, HYAL 4 and PH20/SPAM1 share about 40% of their identity [101]. The expression of HYAL appears tissue specific. Nowadays, much is still unknown about HYAL activity, functions and posttranslational processing. HYAL-1, HYAL 2 and PH20/SPAM1 are the most characterized human HYAL. Both HYAL-1 and HYAL 2 have an optimal activity at acidic pH ( $\leq 4$ ) [103,104] and are highly expressed in human somatic tissues [102]. HYAL 1 was the first human HYAL to be isolated: it was purified from serum (60 ng/mL) [105] and, successively, from urine [106]. HYAL 1 was found to regulate cell cycle progression and apoptosis: it is the main HYAL expressed in cancers, and therefore, it may regulate tumor growth and angiogenesis [107]. HYAL 1 works together with HYAL 2 to degrade HA, possibly according to the following mechanism, which is still the object of study. HYAL 2 is anchored on the external side of the cell surface: here, it cleaves into oligosaccharides (approximately 25 disaccharide units,  $2 \times 10^4$  Da) and the extracellular HMW HA ( $\geq 10^6$  Da), which is linked to its receptor cluster of differentiation-44 (CD44). These intermediate fragments are internalized, transported first to endosomes and then to lysosomes, where they are degraded into tetrasaccharide units (800 Da) by HYAL-1 [51]. Differently from HYAL-1 and HYAL-2, PH20/SPAM1 shows not only



endoglycosidase activity both at acidic and neutral pH, but also a role in fertilization [108]. Hence, PH20/SPAM1 is unique among HYAL, as it behaves as a multifunctional enzyme.

HMW hyaluronan can also be naturally degraded in the organism by ROS, including superoxide, hydrogen peroxide, nitric oxide, peroxynitrite and hypohalous acids, which are massively produced during inflammatory responses, tissue injury and tumorigenesis [60,109]. The depolymerization of HA occurs through mechanisms of the reaction that are dependent on the ROS species, but always involve the scission of the glycosidic linkages [86,110]. Studies have shown that oxidation-related inflammatory processes, determining HA fragmentation, can increase the risk of injury in the airways and determine loss of viscosity in synovial fluid, with consequent cartilage degeneration, joint stiffness and pain [111–113]. ROS-induced degradation of HA might suggest why its antioxidant activity is one of its possible roles in reducing inflammation; however, so far, this biological function of HA has only been hypothesized, as it is not sufficiently supported by experimental data.

Due to these degradation mechanisms, which continuously occur *in vivo*, it has been estimated that the half-life of HA in the skin is about 24 h, in the eye 24–36 h, in the cartilage 1–3 weeks and in the vitreous humor 70 days [82].

### 3.4. Biological Roles of HA in Relation to Its MW

The equilibrium between HA synthesis and degradation plays a pivotal regulatory function in the human body, as it determines not only the amount, but also the MW of hyaluronan. Molecular mass and circumstances of synthesis/degradation are the key factors defining HA's biological actions [50,51,100]. Indeed, high molecular weight (HMW) and low molecular weight (LMW) hyaluronan can even display opposite effects [51,60], and when they are simultaneously present in a specific tissue, they can exert actions different from the simple sum of those of their separate size-related effects [51].

Extracellular HMW HA ( $\geq 10^6$  Da) is anti-angiogenic, as it is able to inhibit endothelial cell growth [51,60,114]. Additionally, due its viscoelasticity, it acts as a lubricating agent in the synovial joint fluid, thus protecting the articular cartilage [115]. HMW HA has also important and beneficial roles in inflammation, tissue injury and repair, wound healing and immunosuppression: it binds fibrinogen and controls the recruitment of inflammatory cells, the levels of inflammatory cytokines and the migration of stem cells [60,93,114].

During some environmental and pathological conditions, such as asthma, pulmonary fibrosis and hypertension, chronic obstructive pulmonary disease and rheumatoid arthritis, HMW HA is cleaved into LMW HA ( $2 \times 10^4$ – $10^6$  Da), which has been shown to possess pro-inflammatory and pro-angiogenic activities [51,100]. Indeed, LMW hyaluronan is able to stimulate the production of proinflammatory cytokines, chemokines and growth factors [51] and to promote ECM remodeling [50]. Moreover, LMW HA can also induce tumor progression, exerting its influence on cells [51,116] and provoking ECM remodeling.

Both anti- and pro-inflammatory properties have been displayed by oHA and HA fragments ( $\leq 2 \times 10^4$  Da), depending on cell type and disease. Certain studies have shown that oHA are able to reduce Toll-like receptors (TLRs)-mediated inflammation [117], inhibit HA-CD44 activation of kinases [118] and retard the growth of tumors [119]. However, oHA have been also found to promote inflammation in synovial fibroblasts [120], stimulate cell adhesion [121] and enhance angiogenesis during wound healing [53].

Therefore, HA is clearly a key molecule involved in a number of physiological and pathological processes. However, despite the intensive studies carried out so far, still little is known about HA's biological roles, the factors determining HA accumulation in transformed connective tissues and the consequent cancer progression, and much less is known about their dependence on hyaluronan molecular size and localization (intra- or extra-cellular). Further researches focusing on HA molecular biology and mechanisms of action are necessary to clarify all these aspects and may facilitate the development of novel HA-based therapies.

### 3.5. Mechanisms of Action of HA

HA performs its biological actions (Section 3.4.) according to two basic mechanisms: it can act as a passive structural molecule and as a signaling molecule. Both of these mechanisms of action have been shown to be size-dependent [51,86].

The passive mechanism is related to the physico-chemical properties of HMW HA. Due to its macromolecular size, marked hygroscopicity and viscoelasticity, HA is able to modulate tissue hydration, osmotic balance and the physical properties of ECM, structuring a hydrated and stable extracellular space where cells, collagen, elastin fibers and other ECM components are firmly maintained [59,86,88].

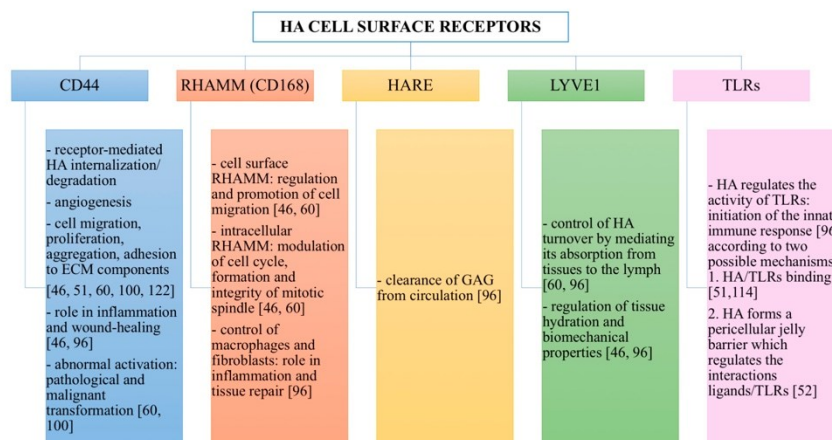
HA also acts as a signaling molecule by interacting with its binding proteins. Depending on HA MW, location and on cell-specific factors (receptor expression, signaling pathways and cell cycle), the binding between HA and its proteins determines opposite actions: pro- and anti-inflammatory activities, promotion and inhibition of cell migration, activation and blockage of cell division and differentiation. All the factors that determine HA activities as a signaling molecule could be related: MW may influence HA uptake by cells and may affect receptor affinity. Additionally, receptor complexes may cluster differently depending on HA MW [51].

HA binding proteins can be distinguished into HA-binding proteoglycans (extracellular or matrix hyaloadherins) and HA cell surface receptors (cellular hyaloadherins) [51]. HA has shown two different molecular mechanisms of interaction with its hyaloadherins. First, HA can interact in an autocrine fashion with its receptors on the same cell [60]. Second, it can behave as a paracrine substance, which binds its receptors on neighboring cells and thus activates different intracellular signal cascades. If HA has an HMW, a single chain can interact simultaneously with several cell surface receptors and can bind multiple proteoglycans. These structures, in turn, can aggregate with additional ECM proteins to form complexes, which can be linked to the cell surface through HA receptors [60,100]. Hence, HA acts as a scaffold that stabilizes the ECM structure not only through its passive structural action, but also through its active interaction with several extracellular hyaloadherins, such as aggrecan (prominent in the cartilage), neurocan and brevican (prominent in the central nervous system) and versican (present in different soft tissues) [60]. For these reasons, pericellular HA is involved in the preservation of the structure and functionality of connective tissues, as well as in their protection from environmental factors [88].

#### HA Cell Surface Receptors

HA interactions with its cell surface receptors mediate three biological processes: signal transduction, formation of pericellular coats and receptor-mediated internalization [60]. The present subsection describes HA cell surface receptors and the biological actions that they control when linked by HA (Figure 4).

The principal receptor for HA is CD44, which is a multifunctional transmembrane glycoprotein. It is expressed in many isoforms diffused in almost all human cell types. CD44 can interact not only with HA, but also with different growth factors, cytokines and extracellular matrix proteins as fibronectin [96]. CD44 intracellular domain interacts with cytoskeleton; hence, when its extracellular domain binds ECM hyaluronan, a link between the cytoskeletal structures and the biopolymer is created [46]. HA-CD44 interaction is involved in a variety of intracellular signaling pathways that control cell biological processes: receptor-mediated hyaluronan internalization/degradation, angiogenesis, cell migration, proliferation, aggregation and adhesion to ECM components [46,51,60,100,122]. Hence, CD44 plays a critical role in inflammation and wound healing [46,96]. However, abnormal activation of HA-CD44 signaling cascades, as well as overexpression and upregulation of CD44 (due to pro-inflammatory cytokines such as interleukin-1, and growth factors such as epidermal growth factors) can result into development of pathological lesions and malignant transformation [60,100]. Indeed, CD44 is overexpressed in many solid tumors, such as pancreatic, breast and lung cancer [54].



**Figure 4.** Summary of HA cell surface receptors and of the actions that they control when linked by HA.

The receptor for HA-mediated cell motility (RHAMM) is also known as CD168, and it was the first isolated cellular hyaloadherin. It exists in several isoforms, which can be present not only in the cell membrane, but also in the cytoplasm and in the nucleus [96]. When linked by HA, cell surface RHAMM mediates and promotes cell migration, while intracellular RHAMM modulates the cell cycle, the formation and the integrity of mitotic spindle [46,60]. Interactions of HA with RHAMM play important roles in inflammation and tissue repair, by triggering a variety of signaling pathways and thus controlling cells such as macrophages and fibroblasts [96].

Hyaluronan receptor for endocytosis (HARE) was initially isolated from endothelial cells in the liver, lymph nodes and spleen and successively found also in endothelial cells of eye, brain, kidney and heart [96]. It is able to bind not only HA, but also other GAGs, with the exception of keratin sulfate, heparin sulfate and heparin. It is involved in the clearance of GAGs from circulation [96].

Furthermore, lymphatic vessel endothelial hyaluronan receptor 1 (LYVE1, a HA-binding protein expressed in lymph vascular endothelium and macrophages) controls HA turnover by mediating its adsorption from tissues to the lymph [60,96]. In this way, LYVE1 is involved in the regulation of tissue hydration and their biomechanical properties [46,96]. Additionally, LYVE1 forms complexes with growth factors, prostaglandins and other tissue mediators, which are implicated in the regulation of lymphangiogenesis and intercellular adhesion [46,96].

Finally, HA is involved in the regulation of the activity of TLRs that, recognizing bacterial lipopolysaccharides and lipopeptides, are able to initiate the innate immune response [96]. Two possible mechanisms have been proposed to explain how HA can influence TLRs. According to the first theory, LMW hyaluronan acts as an agonist for TLR2 and TLR4, thus provoking an inflammatory reaction [51,114]. On the contrary, according to the second theory, hyaluronan does not bind to TLRs, but it is able to regulate TLRs interactions with their ligands through the pericellular jelly barrier that it forms [52]. Indeed, in physiological conditions, HMW HA creates a dense and viscous protective coat around the cells, thus covering surface receptors such as TLRs and limiting their interactions with ligands. During inflammation, an imbalance between HA synthesis and degradation occurs, and this alters the thickness and the viscosity of HA pericellular barrier [52]. More precisely, HA is rapidly degraded due to pH reduction, ROS increase and the possible presence of pathogens producing HYAL [46,109]. Hence, HA MW decreases, reducing the polymer water binding ability and the thickness and the viscosity of its pericellular shield [52]. This results in an increased accessibility of the



cell receptors to their ligands, in the initiation of the innate immune response and in the enhancement of the inflammatory reaction [52]. For this reason, HA can also be involved in the pathogenesis of diseases sustained by immunological processes [46].

#### 4. Industrial Production of HA

The plethora of activities of a food-contained molecule has raised important interest for public health: the global market of HA was USD 7.2 billion in 2016, and it is expected to reach a value of USD 15.4 billion by 2025 [123]. Indeed, hyaluronan is gaining an exponentially growing interest for many pharmaceutical, medical, food and cosmetic applications, due to its important activities—anti-inflammatory, wound healing and immunosuppressive—and its numerous and incomparable biological and physico-chemical properties, such as biocompatibility, biodegradability, non-immunogenicity, mucoadhesivity, hygroscopicity, viscoelasticity and lubricity. Hence, there is a strong interest in optimizing HA production processes to obtain products that fulfill high quality standards and are characterized by great yield and accessible costs. Both the source and the purification process co-occur to determine the characteristics of the produced HA in terms of purity, MW, yield and cost [124,125]. Therefore, producing high quality HA with high yield and less costly methods represents one of the biggest challenges in the field of hyaluronan applied research.

The first production process applied at an industrial scale consisted of HA extraction from animal sources, such as bovine vitreous and rooster combs [46,49,124]. Despite the extraction protocols being improved over the years, this methodology was always hampered by several technical limitations, which led to the production of highly polydispersed HA ( $MW \geq 10^6$  Da) with a low yield [1,46]. This was due to the polymer intrinsic polydispersity, its low concentration in tissues and its uncontrolled degradation caused by the endogenous HYAL and the harsh isolation conditions [46,49]. Additional disadvantages of animal-derived HA were represented by the risk of biological contamination—the presence of proteins, nucleic acids and viruses—and by the high purification costs [46,49,124]. Therefore, alternative methodologies for the industrial production of HA have been developed.

Currently, commercial hyaluronan is principally produced with biotechnology (microbial fermentation). Microorganism-derived HA is biocompatible with the human body because the HA structure is highly conserved among the different species [1,49]. Streptococci strains A and C were the first bacteria used for HA production, and nowadays, many commercial products are derived from *Streptococcus equi* (such as Restylane® by Q-med AB and Juvederm® by Allergan). Optimum bacterial culture conditions to obtain HMW HA ( $3.5\text{--}3.9 \times 10^6$  Da) have been determined at 37 °C, pH 7, in the presence of lactose or sucrose [125,126]. Hyaluronan yield has been optimized up to 6–7 g/L, which is the upper technical limit of the process due to mass transfer limitation caused by the high viscosity of the fermentation broth [1]. As streptococci genera include several human pathogens, an accurate and expensive purification of the produced HA is necessary [46,49]. Hence, other microorganisms have been and are currently investigated to synthesize HA. An ideal microorganism for HA biosynthesis should be generally regarded as safe (GRAS), not secrete any toxins and be able to produce at least  $10^6$  Da HA, as the polymer quality and market value increase with its purity and MW, which affect rheological and biological properties and define suitable applications [49,127]. Since the natural hyaluronan-producing organisms are mostly pathogenic, metabolic engineering currently represents an interesting opportunity to obtain HA from non-pathogenic, GRAS microorganisms. Endotoxin-free HA has already been synthesized by recombinant hosts including *Lactococcus lactis* [128], *Bacillus subtilis* [129], *Escherichia coli* [130] and *Corynebacterium glutamicum* [131]. However, up to now, there has been no heterologous bacterial host producing as much HA as the natural ones. Hence, there is an increasing effort to find an ideal bioreactor for HA production: in addition to bacteria, also eukaryotic organisms such as yeasts, like *Saccharomyces cerevisiae* [132] and *Pichia pastoris* [133], and plant cell cultures, like transformed tobacco-cultured cells [134], have been explored in the last few years.

Finally, to obtain HA of defined MW and narrow polydispersity, other approaches have been used. For example, to produce monodisperse oHA, chemoenzymatic synthesis has been performed [135]. This technique has successfully led to a product commercialized under the name Select HA™ (Hyalose LLC), characterized by a low polydispersity index value. Moreover, other studies have shown the possibility to prepare HA monodisperse fragments by controlling the degradation of HMW hyaluronan using different methods, including acidic, alkaline, ultrasonic and thermal degradation [110].

## 5. Synthetic Modifications of HA

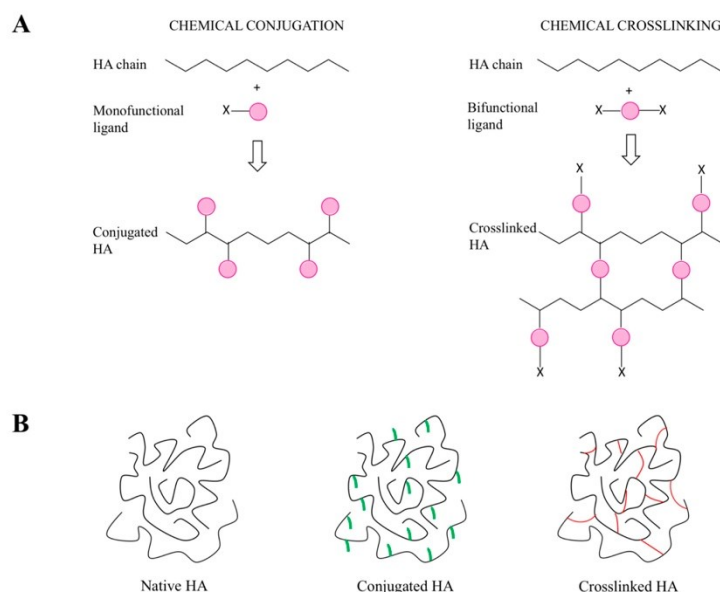
HA has several interesting medical, pharmaceutical, food and cosmetic uses in its naturally-occurring linear form. However, chemical modifications of the HA structure represent a strategy to extend the possible applications of the polymer, obtaining better performing products that can satisfy specific demands and can be characterized by a longer half-life. During the design of novel synthetic derivatives, particular attention is paid to avoiding the loss of native HA properties such as biocompatibility, biodegradability and mucoadhesivity [46].

### 5.1. General Introduction of the Chemical Approaches to Modify HA

HA chemical modifications mainly involve two functional sites of the biopolymer: the hydroxyl (probably the primary alcoholic function of the *N*-acetyl D glucosamine) and the carboxyl groups. Furthermore, synthetic modifications can be performed after the deacetylation of HA *N*-acetyl groups, a strategy that allows one to recover amino functionalities [136]. All these functional groups of HA can be modified through two techniques, which are based on the same chemical reactions, but lead to different products: conjugation and crosslinking (Figure 5). Conjugation consists of grafting a monofunctional molecule onto one HA chain by a single covalent bond, while crosslinking employs polyfunctional compounds to link together different chains of native or conjugated HA by two or more covalent bonds [136]. Crosslinked hyaluronan can be prepared from native HA (direct crosslinking) [56,58,137] or from its conjugates (see below). Conjugation and crosslinking are generally performed for different purposes. Conjugation permits crosslinking with a variety of molecules; to obtain carrier systems with improved drug delivery properties with respect to native HA; to develop pro-drugs by covalently linking active molecules to HA [136]. On the other hand, crosslinking is normally intended to improve the mechanical, rheological and swelling properties of HA and to reduce its degradation rate, in order to develop derivatives with a longer residence time in the site of application and greater release properties [58,138,139]. A recent trend is to conjugate and crosslink HA chains using bioactive molecules in order to develop derivatives with improved and customized activities [58] for a variety of applications in medicine, aesthetics and bioengineering, including cell and molecule delivery, tissue engineering and the development of scaffolds [46,56,58,140–144].

A number of synthetic approaches have been developed to produce conjugated or crosslinked hyaluronan [136].

Generally, HA is chemically modified in the liquid phase. Since it is hydrophilic, several reactions are performed in aqueous media also from its conjugates [145–147]: however, they are pH dependent and, therefore, require acidic or alkaline conditions, which if too strong, can determine HA degradation [75,145]. Other synthetic methods, involving the use of reagents sensitive to hydrolysis, are performed in anhydrous organic solvents such as dimethylsulfoxide (DMSO) [146] or dimethylformamide (DMF) [148]. These approaches necessarily introduce a preparation step to convert native HA into tetrabutylammonium (TBA) salt, soluble in organic ambient [148]: this increases the reaction time and cost, as well as the chances of HA chain fragmentation due to physico-chemical treatments. Additionally, when HA modifications take place in organic solvents, longer final purification processes are necessary [136]. The basic and classic chemistry that underlies the possible modifications of HA functional groups in the liquid phase is overviewed in the following Sections 5.2–5.4.



**Figure 5.** Chemical modifications of HA: conjugation and crosslinking (A). HA forms used for pharmaceutical, medical, food and cosmetic applications: native, conjugated and crosslinked (B).

Generally, HA is chemically modified in the liquid phase. Since it is hydrophilic, several reactions are performed in aqueous media also from its conjugates [145–147]; however, they are pH dependent and, therefore, require acidic or alkaline conditions, which if too strong, can determine HA degradation [75,145]. Other synthetic methods, involving the use of reagents sensitive to hydrolysis, are performed in anhydrous organic solvents such as dimethylsulfoxide (DMSO) [146] or dimethylformamide (DMF) [148]. These approaches necessarily introduce a preparation step to convert native HA into tetrabutylammonium (TBA) salt, soluble in organic ambient [148]: this increases the reaction time and cost, as well as the chances of HA chain fragmentation due to physico-chemical treatments. Additionally, when HA modifications take place in organic solvents, longer final purification processes are necessary [136]. The basic and classic chemistry that underlies the possible modifications of HA functional groups in the liquid phase is overviewed in the following Sections 5.2–5.4.

Since HA derivatives of high quality and purity are necessary to develop injectable products, implantable scaffolds, drug delivery systems and 3D hydrogel matrices encapsulating living cells, techniques for efficient, low-cost and safe modification of HA are continuously being explored [46,147,149]. Hence, in the last few years, several efforts have been made to introduce one-pot reactions that preferably proceed in an aqueous environment, under mild and, possibly, environmentally-friendly conditions, without the use of toxic catalysts and reagents [147,149]. Additionally, alternative approaches to efficiently modify HA have been introduced: solvent-free methods, i.e., reactions in solid phase [57], “click chemistry” syntheses, which are simple and chemoselective, proceeding with fast kinetics in an aqueous environment, under mild conditions, leading to quantitative yields, without appreciable amounts of side products, i.e., the thiol-ene reaction [150], the Diels–Alder cycloaddition [151] and the azide-alkyne cycloaddition [152]; in situ crosslinking of functionalized HA through air oxidation [153]; photo-crosslinking of functionalized HA in the presence of photosensitizers [154,155].



### 5.2. Modification of HA Hydroxyl Groups

By modifying HA's hydroxyl groups, the carboxyl groups remain unchanged, thus preserving HA's natural recognition by its degradative enzymes [136]. Over the years, different derivatives of HA (ethers, hemiacetals, esters and carbamates) have been produced through reactions that occur between the polymeric hydroxyl groups and mono- or bi-functional agents.

Epoxides and bisepoxides like butanediol-diglycidyl ether (BDDE) [137], ethylene glycol-diglycidyl ether, polyglycerol polyglycidyl ether [156], epichlorohydrin and 1,2,7,8 diepoxyoctane [157] have been widely used to synthesize ether derivatives of hyaluronan in alkaline aqueous solution. Currently, HA-BDDE ether represents one of the most marketed HA derivative: it can be obtained through simple synthetic procedures in an aqueous environment, and it is degraded into non-cytotoxic fragments [136]. Other efficient methods to form ether derivatives of HA involve the use of divinyl sulfone (DVS) [158] or ethylene sulfide [159] in basic water.

Many studies showed that hemiacetal bonds can be formed between the hydroxyl groups of HA and glutaraldehyde in an acetone-water medium. Since glutaraldehyde is toxic, particular handling is required during the reaction and purification of the final product [160,161].

The hydroxyl groups of HA can be also esterified by reacting with octenyl succinic anhydride [162] or methacrylic anhydride [163] under alkaline conditions. Alternatively, HA can be converted into a DMSO-soluble salt, which can undergo esterification with activated compounds such as acyl-chloride carboxylates [164].

Finally, the activation of HA hydroxyl groups to cyanate esters, and the subsequent reaction in basic water with amines, allows one to synthesize carbamate derivatives with high degrees of substitution, in a reaction time of only 1 h [165].

### 5.3. Modification of HA Carboxyl Groups

Strategies for the derivatization of HA also involve esterification and amidation, which can be performed after the activation of the polymeric carboxyl groups using different reagents. By modifying HA's carboxyl groups, derivatives more stable to HYAL degradation can be synthesized: hence, if a drug is conjugated on the carboxyl groups of HA, a slow drug release may occur [136].

Esterification can be performed by alkylation of HA carboxyl groups using alkyl halides [166] or tosylate activation [167]. Moreover, HA esters can be synthesized using diazomethane as the activator of the carboxyl groups [168]. All these reactions proceed in DMSO from the TBA salt of HA. Alternatively, HA can undergo esterification also in water using epoxides such as glycidyl methacrylate and excess trimethylamine as a catalyst [169]. The conversion of HA carboxyl groups into less hydrophilic esters represents a strategy to decrease the water solubility of HA, with the aim to reduce its susceptibility to HYAL degradation and enhance its in situ permanence time [46]. A well-known biopolymer synthesized to this end is HA benzyl ester (HYAFF 11), the properties of which are finely regulated by its degree of functionalization [36,170].

Amidation represents a further approach to modify HA: over the years, several synthetic procedures have been developed. However, some of these present important drawbacks: for example, Ugi condensation (useful to crosslink HA chains through diamide linkages) requires a strongly acidic pH (3), the use of formaldehyde, which is carcinogenic, and cyclohexyl isocyanide, which determines a pending undesired cyclohexyl group in the final product [145,160]. HA amidation with 1,1'-carbonyldiimidazole [171] or 2-chloro-1-methylpyridinium iodide [148] as activating agents are performed in DMSO and DMF, respectively: hence, HA conversion into TBA salt and longer purification steps are needed. On the contrary, other methods are based on reaction conditions that meet the modification requirements for HA. Particularly efficient is the activation of HA carboxyl groups by carbodiimide (i.e., *N*-(3-dimethylaminopropyl)-*N*'-ethylcarbodiimide hydrochloride) (EDC) and co-activators such as *N*-hydroxysuccinimide (NHS) or 1-hydroxybenzotriazole in water: proceeding under mild conditions, this reaction does not lead to HA chains' cleavage, and it is suitable also for the derivatization with biopolymers easily susceptible to denaturation, such as protein

or peptides [146,172,173]. Another promising method to synthesize HA derivatives with high grafting yields, in mild conditions, is based on triazine-activated amidation, typically performed with 2-chloro-dimethoxy-1,3,5-triazine [174] or (4-(4,6-dimethoxy-1,3,5-triazin-2-yl)-4-methylmorpholinium (DMTMM) [175]. A recent study made a systematic comparison of EDC/NHS and DMTMM activation chemistry for modifying HA via amide formation in water [175]. The results showed that DMTMM is more efficient than EDC/NHS for ligation of amines to HA and does not require accurate pH control during the reaction to be effective [175]. Using these mild conditions of amidation, it is possible to synthesize highly hydrophilic and biocompatible derivatives, such as urea-crosslinked HA, which has already shown interesting applications in the ophthalmic and aesthetics field [56,58].

#### 5.4. Modification of HA N-Acetyl Groups

The deacetylation of the *N*-acetyl groups of HA recovers amino functionalities, which can then react with activated acids using the same amidation methods described above. However, this approach is not frequently used to synthesize HA derivatives for two main reasons: first of all, even the mildest deacetylation techniques have been shown to induce chain fragmentation [146,171,176]. Moreover, the deacetylation is a strong structural modification, which could importantly change the unique biological properties typical of native HA: indeed, it has been recently found that it reduces the interactions with the receptor CD44 [177].

### 6. Applications of HA and Its Derivatives

Due to their unique biological and physico-chemical properties and to their safety profile, native HA and many of its derivatives represent interesting biomaterials for a variety of medical, pharmaceutical, food and cosmetic applications (Figure 6). Some HA-based products are already on the market and/or have already a consolidated clinical practice, while others are currently undergoing further investigations to confirm their effectiveness. Since the literature concerning HA derivatives and their applications is very extensive, only some examples are reported hereafter.



**Figure 6.** Medical, pharmaceutical, cosmetic and dietary applications of HA and its derivatives.

#### 6.1. Drug Delivery Systems

HA and its derivatives of synthesis represent useful and emerging tools to improve drug delivery. They have been used alone or in combination with other substances to develop pro-drugs, surface-modified liposomes, nanoparticles, microparticles, hydrogel and other drug carriers. All these



delivery systems are undergoing a continuous optimization as they are the object of intensive research. However, the industrialization and extensive clinical application of HA and its derivatives as drug carriers still have a long way to go, as many scientific studies are only at an in vitro experimental stage.

The conjugation of active ingredients to HA is intended to develop pro-drugs with improved physico-chemical properties, stability and therapeutic efficacy compared to free drugs. Considering that hyaluronan has several biological functions, HA-drug conjugates can exert their activities as such. Alternatively, their therapeutic actions are accomplished when the drugs are released, i.e., when the covalent bonds, which link drugs and HA, are broken down in the organism, ideally at the specific target sites. A variety of active ingredients can be conjugated to HA for topical or systemic uses. For example, HA can be conjugated with antidiabetic peptides such as exendin 4: this derivative shows a prolonged half-life, a protracted hypoglycemic effect and improved insulinotropic activity compared to the free exendin 4 in type 2 diabetic mice [178]. However, since HA has a short half-life in the blood, the majority of HA-drug conjugates have been developed for local, i.e., intraarticular, intratumoral, subcutaneous, intravesical and intraperitoneal, rather than systemic administration [179]. For instance, a variety of anti-inflammatory drugs, including hydrocortisone, prednisone, prednisolone and dexamethasone, have been conjugated to HA and investigated for intraarticular therapy of arthritis [166]. Furthermore, a recent study has displayed the potential of an emulsion containing a novel HA-P40 conjugate to treat a mouse model of dermatitis induced by oxazolone [180]. P40 is a particulate fragment isolated from *Corynebacterium granulorum* (actually known as *Propionibacterium acnes*), which has immunomodulatory, antibacterial, antiviral and antitumor properties. The conjugation of P40 to HA successfully prevents its systemic absorption and, therefore, improves its topical therapeutic effect [180]. Other research has shown that conjugation of curcumin with HA represents a strategy to enhance the water solubility and stability of curcumin [181]. Moreover, the HA-curcumin conjugate displays improved healing properties compared to free curcumin and free HA, both in vitro (wound model of human keratinocytes) and in vivo (wound model of diabetic mouse). Hence, HA-conjugated curcumin may be useful to treat diabetic wounds [182]. Finally, the most promising and thoroughly studied conjugations of active ingredients to HA involve antitumoral agents, which can be strategically carried to malignant cells by hyaluronan, as explained in Section 6.2 [179,183].

HA can also be conjugated to phospholipids in order to develop surface-modified liposomes: the chemical modification can be performed prior to liposome formulation [184] or after, on the outside shell [185,186]. Moreover, HA can also be non-covalently linked on the liposome surface: indeed, liposomes can be covered by HA through ionic interaction mechanism [187,188] or the simple lipid film hydration technique [189]. HA-modified liposomes appear to be promising carriers, as they have been shown to enhance the stability of drugs in the bloodstream, prolong their half-life, reduce their systemic toxicity [186], enhance their tissue permeability, sustain their prolonged release [189] and ameliorate their therapeutic effects through synergistic actions [190]. HA-coated liposomes could improve the safety and the efficacy of antitumoral therapies: they appear proficient in mediating site-specific delivery of siRNA [191] and anticancer drugs such as doxorubicin [185], gemcitabine [186], imatinib mesylate [188] and docetaxel [184], via CD44 cell receptors. Additionally, HA-surface-modified liposomes have been investigated as delivery systems also in ophthalmology [189], pneumology [190] and topical treatment of wounds and burns [40].

Another promising type of drug delivery system, which can be formulated with HA and its derivatives of synthesis, is represented by nanoparticles. Hyaluronan can be a constituent element of nanoparticles [192,193], but can also be used to cover nanoparticles, in order to improve the targeting efficiency and the therapeutic action of the encapsulated drugs [194]. HA-nanoparticles are being investigated for a number of administration routes and customized applications: for example, HA-Flt1 peptide conjugate nanoparticles might represent a next-generation pulmonary delivery carrier for dexamethasone in the management of asthma [193], while chitosan nanoparticles coated with HA and containing betamethasone valerate have displayed a great potential for the topical

treatment of atopic dermatitis [194]. Hyaluronan nanoparticles included in polymeric films have shown potential as innovative therapeutic system for the prolonged release of vitamin E for the management of skin wounds [195]. Moreover, the HA-poly(*N*-isopropylacrylamide) conjugate appears to be a promising candidate to treat osteoarthritis: once injected subcutaneously or intra-articularly, it spontaneously forms biocompatible nanoparticles able to control inflammation with a long-lasting action [192]. Finally, other HA surface-modified nanoparticles have been investigated for cancer-targeted therapies [196–198].

Additionally, over the years, HA microspheres and microparticles have been explored as formulations to improve the biomucoadhesive property and the drug release profile and to ameliorate the texturing feeling in the case of dermal formulations. For example, it has been shown that spray-dried HA microspheres allow favorable ofloxacin delivery to the lung via inhalation, determining a superior pharmacological effect compared to free ofloxacin and to other routes of ofloxacin administration [199]. Similarly, inhaled HA microparticles have displayed prolonged pulmonary retention of salbutamol sulfate and reduced systemic exposure and side effects in a rat model [200]. HA microspheres have been evaluated also as possible materials for bone supplementation: indeed, they could be introduced in mineral bone cements to extend the release of active compounds [201]. A recent work has shown the potential of caffeine-loaded HA microparticles dispersed in a lecithin organogel as a dermal formulation for the long-term treatment of cellulite: this drug delivery system is not only effective at repairing cellulite tissue damage, but has also an intrinsic moisturizing action [202]. Besides the microparticles prepared from native HA, the scientific literature also describes microspheres formulated from HA derivatives of synthesis such as hyaluronan benzyl esters [203] and DVS-crosslinked hyaluronan [138] as topical drug delivery systems.

Finally, hydrogels prepared from linear HA and its chemical derivatives are 3D polymeric networks, which can be well-suited systems for topical delivery of cells [204] and many active ingredients, such as anti-inflammatories [44], anti-bacterials [205], antibodies and proteins in general [42]. To implement the mechanical and release properties, HA hydrogels can incorporate thermoresponsive polymers [42] or other drug carriers such as liposomes [43,44]. Up to now, HA hydrogels have shown a great potential for intraocular [42,204], intratympanic [44], intraarticular [206] and dermal delivery [207]. A topical 2.5% HA hydrogel containing 3% diclofenac has been commercialized for the treatment of actinic keratosis under the tradename of Solaraze® (Pharmaderm) in Europe, USA and Canada [207].

## 6.2. Cancer Therapy

It has been shown that the receptor CD44 is overexpressed in a variety of tumor cells, which consequently, display an increase of HA binding and internalization [46,54,208]. Hence, the receptor CD44 has been identified as a potential target in cancer therapy, and hyaluronan, its primary ligand, has been recognized as a powerful tool to develop targeted therapies [54,198]. Many research works have shown that HA can act as a drug carrier and targeting agent at the same time, under the form of polymer-antitumoral conjugates or delivery systems encapsulating anticancer drugs [179]. Additionally, hyaluronan can be employed to design surface-modified nanoparticles [196–198] or liposomes [184–188]. After CD44 receptor-mediated cell internalization, all these HA derivatives are hydrolyzed by intracellular enzymes, and therefore, drugs are released inside the cancer target cells [179]. This should improve the pharmacokinetic profile and the delivery process of many anticancer drugs, overcoming the limitations that reduce their clinical potential, such as low solubility, short *in vivo* half-life, lack of discrimination between healthy and malignant tissues, consequent off-target accumulation and side effects [54,179]. Up to now, there are no HA-antitumoral conjugates and anticancer loaded carriers of HA on the market; however, the promising results of many research works and clinical trials outline their potential and encourage further studies [54,179]. For example, it has been shown that HA-modified polycaprolactone nanoparticles encapsulating naringenin enhance drug uptake by cancer cells *in vitro* and inhibit tumor growth in rat with urethane-induced



lung cancer [198]. Additionally, HA-coated chitosan nanoparticles have been found to promote 5-fluorouracil delivery into tumor cells that overexpress the CD44 receptor [196]. Further studies have displayed that a novel unsaturated derivative of HA [209] and different types of HA-paclitaxel conjugates [179,183] have a great potential as anticancer therapies.

### 6.3. Wound Treatment

As previously explained (Section 3.4.), endogenous HA sustains wound healing and re-epithelialization processes thanks to several actions including the promotion of fibroblast proliferation, migration and adhesion to the wound site, as well as the stimulation of collagen production [210]. For this reason, HA is used in topical formulations (such as Connettivina<sup>®</sup> by Fidia) to treat skin irritations and wounds such as abrasions, post-surgical incisions, metabolic and vascular ulcers and burns [82,210–213]. Currently, HA derivatives [173,182,214,215] and HA-based wound dressings, films or hydrogels enriched with other therapeutic agents [216,217] are being evaluated in order to understand if the cicatrization process could be further enhanced. The wound healing properties of HA and its derivatives are being explored not only in dermatology, but also in other medical fields such as ophthalmology [56,218], otolaryngology [142], rhinology [219] and odontology [220].

### 6.4. Ophthalmologic Surgery and Ophthalmology

HA is a natural component of the human eye: it has been found in vitreous body, lacrimal gland, corneal epithelium and conjunctiva and tear fluid [56]. Therefore, ophthalmic products based on HA are fully biocompatible and do not trigger foreign body reactions [136].

HA solutions are the most used viscosurgical devices to protect and lubricate the delicate eye tissues, replace lost vitreous fluid and provide space for manipulation during ophthalmic interventions [221]. Indeed, the viscosity of HA permits keeping the tissues in place, reducing the risk of displacement, which can potentially compromise both the surgery and the repairing process [46]. The first ophthalmic viscosurgical device containing HA was approved by the FDA in 1980 and is still marketed under the trademark Healon<sup>®</sup> (Abbott).

Moreover, HA is the active ingredient of many eye drops, such as DropStar<sup>®</sup> by Bracco and Lubristil<sup>®</sup> by Eyelab, which, hydrating the ocular surface and improving the quality of vision, are the mainstay to treat diseases such as dry eye syndrome and are useful at increasing the comfortability of contact lenses [56,222,223]. Many studies have proven the safety and the efficacy of native HA solutions as artificial tears [222,224–226]. More recently, also novel derivatives of hyaluronan with improved mechanical and biological properties are being investigated to formulate eye drops with enhanced ocular residence times. For example, promising preliminary results have been obtained with solutions of HA-cysteine ethyl ester [227] and urea-crosslinked HA (HA-CL) [56].

### 6.5. Arthrology

HA is one of the major lubricating agents of the ECM of synovial joint fluid: due to its viscoelasticity, it absorbs mechanical impacts and avoids friction between the bone-ends [61,82,115]. When the synovial fluid is reduced or inflamed, and the HA level decreases, disorders such as rheumatoid arthritis and osteoarthritis occur. Viscosupplementation represents an approach to treat and slow down the progression of these conditions: intraarticular injections of HMW HA, such as Supartz FX<sup>®</sup> by Bioventus and Hyalgan<sup>®</sup> by Fidia, allow maximizing the topical effect and the reduction of pain, as well as minimizing systemic adverse effects [140]. Locally-injected HA has been shown to provide long-term clinical benefits, suggesting that it acts with more than one mechanism [140,228], as the restoration of synovial fluid viscoelasticity is only temporary because HA is degraded within 24 h [229]. Hence, the therapeutic effect of HA intra-articular injection appears prevalently due to biological activities: induction of the synthesis of new HA in synovial cells, stimulation of chondrocyte proliferation and resulting reduction of cartilage degradation [140,228,230].

In order to increase the half-life after injection and, consequently, the therapeutic efficacy, crosslinked HA derivatives have been investigated and introduced on the market (such as Synvisc® by Genzyme) as viscosupplementation agents [140,231].

#### 6.6. Rhinology and Pneumology

Endogenous HMW HA plays a pivotal role in the homeostasis of the upper and the lower airways: it is an important component of the normal airway secretions, exerts anti-inflammatory and anti-angiogenic actions, promotes cell survival and mucociliary clearance, organizes extracellular matrix, stabilizes connective tissues, sustains healing processes and regulates tissues hydration [144,232–234]. Hence, exogenous HMW HA represents a promising therapeutic agent for the treatment of nasal and lung diseases that involve inflammation, oxidative stress and epithelial remodeling, such as allergic and non-allergic rhinitis, asthma, chronic obstructive pulmonary disease and cystic fibrosis [143,233,235–238]. Examples of marketed formulations containing HA to treat respiratory diseases are Ialoclean® (Farma-Derma), a nasal spray to treat nasal dryness and rhinitis and to promote nasal wound healing, Hyaneb® (Chiesi Farmaceutici), a hypertonic saline solution containing HA to hydrate and reduce mucus viscosity in cystic fibrosis patients [239], and Yabro® (Ibsa Farmaceutici), a high viscosity nebulizer solution of HA to treat bronchial hyper-reactivity [143].

#### 6.7. Urology

Recently, the possible therapeutic uses of HA in urology have been explored. Preliminary evidence has shown that intravesical HA, administered alone or in combination with chondroitin sulfate or alpha blockers, could be able to reduce the recurrence of urinary tract infections such as bacterial cystitis, to alleviate the symptoms of these diseases and to protect the mucosa of urinary bladder [240,241]. However, further clinical studies are necessary to confirm the effectiveness of HA treatment in urology.

#### 6.8. Soft Tissue Regeneration

HA skin content decreases with aging, and the most visible effects are the loss of facial skin hydration, elasticity and volume, which are responsible for wrinkles [88]. Over the last few years, HA has been widely used as a biomaterial to develop dermal fillers (DFs), which are class III medical devices that, injected into or under the skin, restore lost volumes and correct facial imperfections such as wrinkles or scars [58]. Being characterized by most of the properties that an ideal DF should have—biocompatibility, biodegradability, viscoelasticity, safety, versatility—HA DFs have become the most popular agents for viscoaugmentation, i.e., for soft tissue contouring and volumizing [58]. Indeed, according to data from the American Society of Plastic Surgeons (ASPS), in 2017, out of a total of 2,691,265 treatments with soft tissue fillers, 2,091,476 were performed with HA DFs [242]. One of the reasons for this success resides in the reversibility of the HA DF effect: they correct wrinkles in a reversible manner, as a hypothetical medical error or complication can be remedied through the injection of HYAL (Vitrace®, ISTA Pharmaceuticals; Hylenex®, Halozyme Therapeutics) [58]. The duration of the corrective effect of HA DFs varies between three and 24 months, depending prevalently on HA concentration, crosslinking (degree and type), the treated area and the individual [58,243]. For example, Hylaform® (Genzyme Biosurgery) contains 4.5–6 mg/mL HA crosslinked with DVS (20% degree), and its effect lasts 3–4 months, while the Juvederm® DFs family (Allergan) contains 18–30 mg/mL HA crosslinked with 9–11% BDDE, and its effect lasts 6–24 months [58]. Finally, DFs that combine BTX-A and HA have been developed to ensure an optimal correction even in patients with extremely deep wrinkles [58].

#### 6.9. Cosmetics

HA represents a moisturizing active ingredient widely used in cosmetic formulations (gels, emulsions or serums) to restore the physiological microenvironment typical of youthful skin. HA-based cosmetics such as Fillerina® (Labo Cosprophar Suisse) claims to restore skin hydration and elasticity:

this is reported to exert an anti-wrinkle effect, although no rigorous scientific proof is able to fully substantiate this claim [82,141,244]. It has to be considered that HA's hydrating effect largely depends on its MW, and its longevity depends on HA stability to hyaluronidases. Indeed, HMW HA mainly works as a film-forming polymer: it reduces water evaporation, with an occlusive-like action. On the other hand, medium MW and LMW HA mainly work by binding moisture from the environment, do to their high hygroscopicity [141,244]. In some cases, this capacity may reverse HA's expected hydrating activity as at a high concentration, HA may even extract humidity from the skin. Furthermore, also sunscreens containing hyaluronan may contribute to maintaining a youthful skin, protecting it against the harmful effects of ultraviolet irradiation, due to the possible free radical scavenging properties of HA [245,246]. The same capability has been demonstrated by dietary intake of HA (Section 6.10).

#### 6.10. Dietary

HA can also represent an interesting ingredient in enriched food and food supplements: it has gained the unofficial designation as a nutri-cosmetic because of its capability to improve skin appearance [247]. For a long time, the fact that HA can cross in its "intact" form the intestinal barrier has been debated; recently, a few studies have appeared in the literature to highlight this question. Kimura et al. have evaluated the degradation and absorption of HA (300 KDa and 2 KDa) after oral ingestion in rats, demonstrating intestinal degradation to oligosaccharides, which are subsequently absorbed in the large intestine, translocated into the blood and distributed in the skin [248]. Orally-ingested LMW HA has shown the opposite effects: some studies have reported inflammatory properties with the activation of the immune response [249], while other research has highlighted the efficacy in reducing knee joint pain without inflammation [250]. Nowadays, the mechanisms at the base of these different actions of LMW ingested HA remain still unclear. In another study, the absorption, distribution and excretion of HMW-labeled (1 MDa) HA were evaluated after oral administration in rats and dogs: for the first time, it was shown that dietary HMW HA can be distributed to connective tissues [251]. In particular, these reproducible results suggest that orally-administered HMW HA may reach joints, bones and skin, even if in small amounts [251], thus highlighting that a rationale may exist in the use of HA-based food supplements designed for joint and skin health.

In these regards, several studies have reported on the safety of HA as a food supplement, confirming its possible use as a food ingredient itself. HA is marketed as a food supplement in the USA, Canada, Europe and Asia (particularly in Korea and Japan) with some difference in the suggested use: to treat joint pain in the USA and in Europe; to treat wrinkles and to moisturize in Japan, even if the involvement of this polymer in the skin moisture retention effect needs to be further elucidated in the future [252]. In the present review, we focused our attention prevalently on studies that exclude complex mixtures, in order to evidence HA's effects alone; however, several research works describe the use of HA as a food ingredient in enriched extracts or mixtures with collagen and other supplements. For example, in a preliminary double-blind, controlled, randomized, parallel trial over 12 weeks, rooster comb extract was added to low fat yoghurt, which was given to mild knee pain patients (n: 40), resulting in significative improvement in muscle strength in men [253]. In another recent clinical study, an oral HA preparation diluted in a cascade fermented organic whole food concentrate supplemented with biotin, vitamin C, copper and zinc (Regulatpro<sup>®</sup> Hyaluron, Dr. Niedermaier<sup>®</sup>) led to a significant cutaneous antiaging effect in twenty female subjects after 40 days of daily consumption [254]. From such mixtures, it is difficult to elucidate HA's specific contribution.

Regarding supplementation with HA alone, some studies have demonstrated a direct correlation between ingestion and body effects. In a recent review, Kawada et al. underlined a number of studies in support of the contribution of ingested HA to hydrate skin, thus improving the quality of life for people who suffer from skin dryness induced by UV, smoking and pollutants, responsible for cutaneous reduction of HA [255]. Indeed, the review of Kawada and coworkers reported that, in different randomized, double-blind, placebo-controlled trials, the amounts of HA ranging from 37.52–240 mg



per day, ingested in a period comprised between four and six weeks, significantly improved cutaneous moistness [255]. These results, as always happens with biopolymers as food supplements, are difficult to correlate with quantitative effects, as polymer sources and MW always vary. However, qualitatively, the correlation between HA consumption and the decrease of skin dryness is evident. The authors suggest that partially-digested HA, regardless of its MW, is adsorbed in the gut, while intact HA is absorbed by the lymphatic system; both are distributed to the skin, where they can work as inducers of fibroblast proliferation and endogenous HA synthesis [255]. In a more recent study, the same authors have investigated, in a double blind, placebo controlled, randomized study of 61 subjects with dry skin, the effects of HA (120 mg/day) of two different MW (800 KDa and 300 KDa) over six weeks [256]. Both the HAs were effective, but the 300-KDa group showed the best improvements in skin dryness and moisture content [256]. Again, Kawada et al., in an experiment on hairless mice, demonstrated that the oral administration of 200 mg/kg body weight per day of two different MW HA (300 KDa and less than 10 KDa) for six weeks reduced epidermal thickness and improved skin hydration upon UV irradiation [257]. The effect was stronger for the less than 10-KDa HA [257]. The authors also demonstrated that the less than 10 KDa orally-administered HA also stimulated HAS2 expression, thus highlighting an overall role of LMW HA in the prevention of skin photoageing with different mechanisms [257]. Thus, combining HA oral treatment with HA topical and injective administration could be very successful in the control of skin ageing. A further study suggesting that orally-administered HA can migrate into the skin of rats, thus possibly reducing skin dryness, was conducted by Oe et al., who demonstrated that about 90% of the ingested HA was absorbed from the digestive tract and was used as an energy source or a structural component [252].

Dietary HA can be beneficial not only for skin, but also for joints, as evidenced by a number of randomized, double-blinded, placebo-controlled studies relative to the treatment of knee pain, relief of synovial effusion or inflammation and improvement of muscular knee strength [258].

#### 6.11. 3D Cell Culture Models

HA and its synthetic derivatives can be used as 3D scaffold structures, which represent physical support systems for in vitro cell culture [259]. Indeed, 3D tissue models can be obtained by culturing cells on pre-fabricated polymeric scaffolds or matrices, designed to simulate the in vivo ECM [259]. Cells attach, migrate and fill the interstices within the scaffold to form 3D cultures [259]. 3D scaffolds can be promising also for in vivo tissue regeneration, reproducing the natural physical and structural environment of living tissue [259]. An example of a cell substrate suitable for a 3D environment, for both in vitro and in vivo research, is represented by HyStem<sup>®</sup> Hydrogels (ESI-BIO<sup>™</sup>).

For example, HA derivatives characterized by aldehyde and hydrazide groups have been used to develop a biomimetic, 3D culture system for poorly-adherent metastatic prostate cancer cells, employed as an in vitro platform to test the efficacy of anticancer drugs [260]. The hyaluronan-3D cell culture system provided a useful interesting alternative to study antineoplastic drugs, with results superior compared to those from conventional 2D monolayers [260]. Another work showed that methacrylated HA is useful to develop in vitro 3D culture models to assess glial scarring in a robust and repeatable way, in order to evaluate, for example, the foreign body response to implants such as electrodes in the central nervous system [261]. Additionally, a recent study highlighted the importance of ink formulation and crosslinking on the printing of stable structures: a dual-crosslinking HA system was evaluated as printable hydrogel ink in biomedicine [262]. It encompassed shear-thinning and self-healing properties through guest-host bonding, and showed an improved cell adhesion after further functionalization (i.e., peptides) [262].

### 7. Conclusions, Future Trends and Perspectives

Figure 7 summarize some of the most common medical, pharmaceutical, cosmetic and dietary applications of HA and its derivatives. The present review underlines the interest of academic and industrial research on HA: a comprehensive overview of this polymer is provided through the

description of its structural, physico-chemical and hydrodynamic properties, occurrence, metabolism, biological roles, mechanisms of action, methods of production and derivatization, pharmaceutical, biomedical, food supplement and cosmetic applications.






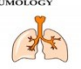




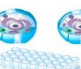
Application	Examples	Beneficial actions and key features	State of the art
<b>DRUG DELIVERY SYSTEMS</b>	 <ul style="list-style-type: none"> <li>- Pro-drugs: HA-<i>uvadin</i> 4 [178], HA-hydrocortisone, HA-prednisone, HA-prednisolone, HA-dexamethasone [166], HA-P40 [180], HA-curcumin [181] conjugates.</li> <li>- Surface modified liposomes: for the delivery of siRNA [191], doxorubicin [185], gemcitabine [186], imatinib mesylate [188], docetaxel [184]; for ophthalmology [189], pneumology [190] and topical treatments of wounds and burns [40].</li> <li>- Nanoparticles: consisting of HA [192, 193] or covered with HA [194]. Pulmonary delivery of dexamethasone to treat asthma [193], skin delivery of betamethasone valerate for atopic dermatitis [194], skin delivery of vitamin E for the management of wounds [195], treatment of osteoarthritis [192], cancer targeted therapies [196-198].</li> <li>- Microspheres and microparticles: pulmonary delivery of ofloxacin [199] and salbutamol sulphate [200], bone supplementation [201], skin delivery of caffeine [202]. Microspheres can be formulated from native HA or from its synthetic derivatives such as HA benzyl esters [203] and DVS-crosslinked HA [138].</li> <li>- Hydrogel: topical delivery of anti-inflammatories [44], anti-bacterials [205], antibodies and proteins [42]. Great potential for intravascular [42, 204], intratympanic [44], intraarticular [206] and dermal delivery [207].</li> </ul>	<ul style="list-style-type: none"> <li>- Development of pro-drugs and derivatives with improved physico-chemical properties, stability, half-life time, and therapeutic efficacy compared to free drugs. Reduction of toxicity.</li> <li>- Development of biocompatible and biodegradable drug delivery systems with intrinsic moisturizing activity.</li> </ul>	<p>Except for gels, the industrialization and extensive clinical application are still a long way to go; many scientific studies are only at an <i>in vitro</i> experimental stage. Example of commercialized hydrogel: Solaraze® (Pharmaderm).</p>
<b>CANCER THERAPY</b>	 <ul style="list-style-type: none"> <li>- Polymer-antitumoral conjugates and delivery systems encapsulating anticancer drugs: <ul style="list-style-type: none"> <li>- HA-modified poly(lactide) nanoparticles encapsulating naringenin [198].</li> <li>- HA-coated chitosan nanoparticles encapsulating 5-fluorouracil [196].</li> <li>- novel unsaturated derivative of HA [209].</li> <li>- HA-polyoxal conjugates [179, 183].</li> </ul> </li> </ul>	<p>HA can act as drug carrier and targeting agent (for CD44 receptor) at the same time [54, 179, 198].</p>	<p>Promising results of many researches and clinical trials: further studies are strongly encouraged to develop marketable products.</p>
<b>WOUND TREATMENT</b>	 <ul style="list-style-type: none"> <li>- HA based wound dressings, films and hydrogels, eventually enriched with other therapeutic agents [216, 217].</li> <li>- Applications in: dermatology, ophthalmology [56, 218], otolaryngology [142], rhinology [219], odontology [220].</li> </ul>	<ul style="list-style-type: none"> <li>- Promotion of fibroblast proliferation, migration and adhesion to the wound site.</li> <li>- Stimulation of collagen production.</li> <li>- Improvement and acceleration of wound healing and re-epithelialization processes: treatment of skin irritations and wounds such as abrasion, post-surgical incisions, metabolic and vascular ulcers, burns [86, 210-213].</li> </ul>	<p>Several products already marketed, such as Comettivina® (Fidia).</p>
<b>OPHTHALMOLOGIC SURGERY AND OPHTHALMOLOGY</b>	 <p>Solutions as viscosurgical devices and eye drops, consisting of native HA or its derivatives, such as HA-cysteine ethyl ester [227] and urea-crosslinked HA [86].</p>	<ul style="list-style-type: none"> <li>- Protection and lubrication of eye tissues, replacement of lost vitreous fluid and creation of space for manipulation during ophthalmic interventions [46, 221].</li> <li>- Hydration of the ocular surface, treatment of dry eye syndrome [86, 222, 223].</li> </ul>	<p>Several products already marketed, such as the viscosurgical device Healon® (Abbott) and the eye drops DropStar® (Bracco) and Lubrifix® (Eyselab). Many studies show the safety and the efficacy of these formulations [222, 224-226].</p>
<b>ARTHRIOLOGY</b>	 <p>Intraarticular injections of native HMW HA and its crosslinked derivatives as viscosupplementation agents [140, 229, 231].</p>	<ul style="list-style-type: none"> <li>- Absorption of mechanical impacts and avoidance of frictions between the bone-ends [61, 82, 113].</li> <li>- Restoration of synovial fluid viscoelasticity [229].</li> <li>- Induction of HA synthesis in synovial cells stimulation of chondrocyte proliferation and resulting reduction of cartilage degradation [140, 228, 230].</li> <li>- Treatment of rheumatoid arthritis and osteoarthritis, with reduction of pain and adverse effects [140].</li> </ul>	<p>Many studies display the safety and the efficacy of HMW HA intraarticular injections. Marketed products: Supartz FX® (Bioscience), Hyalgan® (Fidia) and Synvisc® (Genzyme).</p>
<b>RHINOLOGY AND PNEUMOLOGY</b>	 <p>Nasal sprays, hypertonic saline solution, high viscosity reboiler of HA [143, 239].</p>	<p>HMW HA: promising therapeutic agent for the treatment of nasal and lung diseases that involve inflammation, oxidative stress and epithelial remodeling, such as allergic and non-allergic rhinitis, asthma, chronic obstructive pulmonary disease and cystic fibrosis [143, 233, 235-238].</p>	<p>Many studies display the safety and the efficacy of HMW HA for nasal and lung applications. Marketed products: Lalsciaev® (Farma-Derma), Hyane® (Chiesi Farmaceutici) and Yabco® (Bsa Farmaceutici).</p>
<b>UROLOGY</b>	 <p>Intravesical HA, alone or in combination with chondroitin sulfate or alpha blockers [240, 241].</p>	<p>Reduction of recurrence and symptoms of urinary tract infections such as bacterial cystitis, protection of the mucosa of urinary bladder [240, 241].</p>	<p>Preliminary evidences; further clinical studies are necessary to confirm the effectiveness of HA treatment in urology.</p>
<b>SOFT TISSUE REGENERATION</b>	 <p>Injectable dermal fillers (DFs, class III medical devices) consisting of gels of native HA or HA derivatives—such as DVS-crosslinked HA and BDEE crosslinked HA [88].</p>	<p>Injected into or under the skin, restore lost volumes and correct facial imperfections such as wrinkle or scars [88]. Biocompatibility, biodegradability, viscoelasticity, safety, versatility, reversibility: HA DFs are the most popular DFs [88, 242].</p>	<p>Many studies show the safety and the efficacy of HMW HA as DFs. Marketed products: Hyalform® (Genzyme-Biosurgery) and Juvederm® (Allergan).</p>
<b>COSMETICS</b>	 <p>Several cosmetic formulations: gels, emulsions and serums.</p>	<ul style="list-style-type: none"> <li>- Restoration of the physiological microenvironment typical of youthful skin. Hydration depending on HA MW: HMW HA forms films with an occlusive-like action; medium MW and LMW HA bind moisture from the environment.</li> <li>- Possible antiwrinkle effect [82, 141, 144].</li> <li>- Possible protection from UV irradiation due to the possible free-radical scavenging properties [45, 246].</li> </ul>	<p>Several marketed products, such as Fillerina® (Labo Cosmoprof Suisse).</p>
<b>DIETARY</b>	 <ul style="list-style-type: none"> <li>- HA contained in enriched food and food supplements.</li> <li>- HA as <i>nutri-cosmetic</i>.</li> <li>- HA as food ingredient itself.</li> </ul>	<ul style="list-style-type: none"> <li>- Dietary HMW HA can be distributed to connective tissues: it can reach joints, bones and skin [251].</li> <li>- Some studies have underlined that also LMW HA may reduce knee joint pain [250].</li> <li>- Relief of synovial effusion and inflammation, and improvement of muscular knee strength [258].</li> </ul>	<p>HA is marketed as food supplement in Canada, USA, Europe (joint pain), and in Japan (treatment of wrinkles) [252]. Example of marketed product: Regulatpro® Hyaluron, Dr. Niedermair®. Several researches are being performed: randomized, double-blinded, placebo-controlled studies [248-258].</p>
<b>3D cell culture</b>	 <p>HA and its synthetic derivatives as 3D scaffold structures for <i>in vitro</i> cell culture and for <i>in vivo</i> tissue regeneration [259-262].</p>	<ul style="list-style-type: none"> <li>- Stimulation of the <i>in vitro</i> ECM and reproduction of the natural physical and structural environment of living tissues [259].</li> <li>- <i>In vitro</i> platform to test the efficacy of drugs with results superior compared to those from conventional 2D monolayers [260].</li> </ul>	<p>Example of marketed product: HySens® Hydrogels (ESI - BICO™).</p>

Figure 7. Summary of the medical, pharmaceutical, cosmetic and dietary applications of HA and its derivatives, reporting some examples, the beneficial actions, the key features and the state of the art.

During the last few decades, HA has shown great success due to its numerous and unique properties, such as biodegradability, biocompatibility, mucoadhesivity, hygroscopicity and viscoelasticity, and to the broad spectrum of chemical modifications that it can undergo, allowing the development of derivatives with specific targeting and long-lasting drug delivery. Several *in vitro* and *in vivo* studies have shown the beneficial actions of HA treatment, with anti-inflammatory, wound healing, chondroprotective, antiangiogenic, anti-ageing and immunosuppressive effects, among others [51,56,60,115]. This supported the development of a great number of HA-based commercial products: from native HA for ophthalmic and arthritic therapies, to food supplement, esthetic and cosmetic formulations. More recently, also some chemical derivatives of HA have received FDA approval and have been successfully introduced on the market, especially as DFs. As a proof of the great potential of this molecule in terms of real benefits for health, we also conducted (on 20 April 2018) a search on the patent database Questel (Paris, France), which resulted in the following table (Table 1) that illustrates the interest toward hyaluronan.

**Table 1.** Data on hyaluronan patents resulting from the database Questel (Paris, France).

Total	13,684
Alive	8749
Dead	4935
<b>1st application year</b>	<b>unknown</b>
After 2015	2717
2011–2015	4568
2006–2010	2647
2001–2005	1694
Before 2001	2058

In our opinion, although hyaluronan displays a great number of potential applications, further investigations and technological improvements are required, as there are still some questions to be answered and some issues to be addressed. First of all, many aspects of HA metabolism, receptor clustering and affinity still need to be explored to understand the different biological actions that hyaluronan has through changes in MW fully. Additional insight needs to be gained in understanding whether there is a relation between HA size and localization and how concomitant use of different HA sizes may modulate signaling. The comprehension of all these mechanisms could provide opportunities to extend and improve hyaluronan pharmaceutical, biomedical, cosmetics and food supplements applications, obtaining more targeted effects. Towards this aim, the key mechanisms that control MW during HA biotechnological synthesis should be clarified to develop methods to produce more uniform size-defined HA. Additionally, progresses in metabolic engineering are necessary to improve HA yield and find biosynthetic strategies with good sustainability and acceptable production cost. Furthermore, the preparation of hyaluronan chemical derivatives needs to be optimized, using strategies such as one-pot reactions, chemo-selective synthesis, solvent-free methods and “click chemistry” approaches. Furthermore, the reproducibility of HA derivatives during scale-up, their pharmacokinetic and pharmacodynamic properties must be improved to allow their successful commercialization. Finally, all the HA-based next generation products, such as innovative crosslinked derivatives, polymer-drug conjugates and delivery systems, should be developed, enabling high biocompatibility, prolonged half-life and improved *in situ* permanence: hence, *in vivo* and clinical studies are required to characterize their safety and efficacy fully. Nevertheless, to date, recent *in vitro* research works have shown promising results, which open encouraging perspectives for safe and health uses of these novel derivatives: for example, HA-CL has displayed high biocompatibility towards human corneal and lung epithelial cell, as well as interesting anti-inflammatory, antioxidant and wound healing properties [56,263].



**Acknowledgments:** This work was supported by a PhD grant (to Arianna Fallacara) from I.R.A. Srl (Istituto Ricerche Applicate, Usmate-Velate, Monza-Brianza, Italy) and by Ambrosialab Srl (Ferrara, Italy, Grant 2017 to Stefano Manfredini and Silvia Vertuani).

**Conflicts of Interest:** The authors declare no conflict of interest.

### Abbreviations

BDDE	butanediol-diglycidyl ether
CD44	cluster of differentiation-44
CDMT	2-chloro-dimethoxy-1,3,5-triazine
DFs	dermal fillers
DMF	dimethylformamide
DMTMM	4-(4,6-dimethoxy-1,3,5-triazin-2-yl)-4-methylmorpholinium
DMSO	dimethylsulfoxide
DVS	divinyl sulfone
ECM	extracellular matrix
EDC	<i>N</i> -(3-dimethylaminopropyl)- <i>N</i> '-ethylcarbodiimide hydrochloride
HA	hyaluronic acid; hyaluronate; hyaluronan
HA-CL	urea-crosslinked hyaluronic acid
HARE	hyaluronan receptor for endocytosis
HAS	hyaluronan synthases
H-bonds	hydrogen bonds
HYAL	hyaluronidases
HMW	high molecular weight
GAGs	glycosaminoglycans
GRAS	generally regarded as safe
LYVE1	lymphatic vessel endothelial hyaluronan receptor 1
LMW	low molecular weight
MW	molecular weight
NHS	<i>N</i> -hydroxysuccinimide
oHA	oligosaccharides of hyaluronic acid
RHAMM	receptor for HA-mediated cell motility
ROS	reactive oxygen species
TBA	tetrabutylammonium
TLRs	Toll-like receptors

### References

- Boeriu, C.G.; Springer, J.; Kooy, F.K.; van den Broek, L.A.M.; Eggink, G. Production methods for hyaluronan. *Int. J. Carbohydr. Chem.* **2013**, *2013*, 14. [[CrossRef](#)]
- Meyer, K.; Palmer, J.W. The polysaccharide of the vitreous humor. *J. Biol. Chem.* **1934**, *107*, 629–634.
- Kendall, F.E.; Heidelberger, M.; Dawson, M.H. A serologically inactive polysaccharide elaborated by mucoid strains of group a hemolytic streptococcus. *J. Biol. Chem.* **1937**, *118*, 61–69.
- Boas, N.F. Isolation of hyaluronic acid from the cock's comb. *J. Biol. Chem.* **1949**, *181*, 573–575. [[PubMed](#)]
- Kaye, M.A.; Stacey, M. Observations on the chemistry of hyaluronic acid. *Biochem. J.* **1950**, *2*, 13. [[PubMed](#)]
- Meyer, K. Highly viscous sodium hyaluronate. *J. Biol. Chem.* **1948**, *176*, 993–994. [[PubMed](#)]
- Varga, L. Studies on hyaluronic acid prepared from the vitreous body. *J. Biol. Chem.* **1955**, *217*, 651–658. [[PubMed](#)]
- Fletcher, E.; Jacobs, J.H.; Markham, R.L. Viscosity studies on hyaluronic acid of synovial fluid in rheumatoid arthritis and osteoarthritis. *Clin. Sci.* **1955**, *14*, 653–660. [[PubMed](#)]
- Blumberg, B.S.; Ogston, A.G.; Lowther, D.A.; Rogers, H.J. Physicochemical properties of hyaluronic acid formed by *Streptococcus haemolyticus*. *Biochem. J.* **1958**, *70*, 1–4. [[CrossRef](#)] [[PubMed](#)]
- Weissmann, B.; Meyer, K. The structure of hyalobiuronic acid and of hyaluronic acid from umbilical cord. *J. Am. Chem. Soc.* **1954**, *76*, 1753–1757. [[CrossRef](#)]

11. Meyer, K. The biological significance of hyaluronic acid and hyaluronidase. *Physiol. Rev.* **1947**, *27*, 335–359. [[CrossRef](#)] [[PubMed](#)]
12. Ogston, A.G.; Stanier, J.E. The physiological function of hyaluronic acid in synovial fluid; viscous, elastic and lubricant properties. *J. Physiol.* **1953**, *119*, 244–252. [[CrossRef](#)]
13. Pinkus, H.; Perry, E.T. The influence of hyaluronic acid and other substances on tensile strength of healing wounds. *J. Investig. Dermatol.* **1953**, *21*, 365–374. [[CrossRef](#)] [[PubMed](#)]
14. Balazs, E.A. Ultrapure Hyaluronic Acid and the Use Thereof. U.S. Patent 4,141,973, 27 February 1979.
15. Miller, D.; Stegmann, R. Use of Na-hyaluronate in anterior segment eye surgery. *J. Am. Intraocul. Implant Soc.* **1980**, *6*, 13–15. [[CrossRef](#)]
16. Binkhorst, C.D. Advantages and disadvantages of intracameral Na-hyaluronate (Healon) in intraocular lens surgery. *Doc. Ophthalmol.* **1981**, *50*, 233–235. [[CrossRef](#)] [[PubMed](#)]
17. Binkhorst, C.D. Inflammation and intraocular pressure after the use of Healon in intraocular lens surgery. *J. Am. Intraocul. Implant Soc.* **1980**, *6*, 340–341. [[CrossRef](#)]
18. Percival, P. Results of a clinical trial of sodium hyaluronate in lens implantation surgery. *J. Am. Intraocul. Implant Soc.* **1985**, *11*, 257–259. [[CrossRef](#)]
19. Graue, E.L.; Polack, F.M.; Balazs, E.A. The protective effect of Na-hyaluronate to corneal endothelium. *Exp. Eye Res.* **1980**, *31*, 119–127. [[CrossRef](#)]
20. Percival, P. Protective role of Healon during lens implantation. *Trans. Ophthalmol. Soc. UK* **1981**, *101*, 77–78. [[PubMed](#)]
21. Regnault, F.; Bregat, P. Treatment of severe cases of retinal detachment with highly viscous hyaluronic acid. *Mod. Probl. Ophthalmol.* **1974**, *12*, 378–383. [[PubMed](#)]
22. Kanski, J.J. Intravitreal hyaluronic acid injection. A long-term clinical evaluation. *Br. J. Ophthalmol.* **1975**, *59*, 255–256. [[CrossRef](#)] [[PubMed](#)]
23. Auer, J.A.; Fackelman, G.E.; Gingerich, D.A.; Fetter, A.W. Effect of hyaluronic acid in naturally occurring and experimentally induced osteoarthritis. *Am. J. Vet. Res.* **1980**, *41*, 568–574. [[PubMed](#)]
24. Namiki, O.; Toyoshima, H.; Morisaki, N. Therapeutic effect of intra-articular injection of high molecular weight hyaluronic acid on osteoarthritis of the knee. *Int. J. Clin. Pharmacol. Ther. Toxicol.* **1982**, *20*, 501–507. [[PubMed](#)]
25. Leardini, G.; Perbellini, A.; Franceschini, M.; Mattara, L. Intra-articular injections of hyaluronic acid in the treatment of painful shoulder. *Clin. Ther.* **1988**, *10*, 521–526. [[PubMed](#)]
26. Dougados, M.; Nguyen, M.; Listrat, V.; Amor, B. High molecular weight sodium hyaluronate (hyalectin) in osteoarthritis of the knee: A 1 year placebo-controlled trial. *Osteoarthr. Cartil.* **1993**, *1*, 97–103. [[CrossRef](#)]
27. Jones, A.C.; Patrick, M.; Doherty, S.; Doherty, M. Intra-articular hyaluronic acid compared to intra-articular triamcinolone hexacetonide in inflammatory knee osteoarthritis. *Osteoarthr. Cartil.* **1995**, *3*, 269–273. [[CrossRef](#)]
28. Juhlin, L. Hyaluronan in skin. *J. Intern. Med.* **1997**, *242*, 61–66. [[CrossRef](#)] [[PubMed](#)]
29. Pavicic, T.; Gauglitz, G.G.; Lersch, P.; Schwach-Abdellaoui, K.; Malle, B.; Korting, H.C.; Farwick, M. Efficacy of cream-based novel formulations of hyaluronic acid of different molecular weights in anti-wrinkle treatment. *J. Drugs Dermatol.* **2011**, *10*, 990–1000. [[PubMed](#)]
30. Abatangelo, G.; Martelli, M.; Vecchia, P. Healing of hyaluronic acid-enriched wounds: Histological observations. *J. Surg. Res.* **1983**, *35*, 410–416. [[CrossRef](#)]
31. Doillon, C.J.; Silver, F.H. Collagen-based wound dressing: Effects of hyaluronic acid and fibronectin on wound healing. *Biomaterials* **1986**, *7*, 3–8. [[CrossRef](#)]
32. Hellström, S.; Laurent, C. Hyaluronan and healing of tympanic membrane perforations. An experimental study. *Acta Otolaryngol. Suppl.* **1987**, *442*, 54–61. [[CrossRef](#)] [[PubMed](#)]
33. King, S.R.; Hickerson, W.L.; Proctor, K.G. Beneficial actions of exogenous hyaluronic acid on wound healing. *Surgery* **1991**, *109*, 76–84. [[PubMed](#)]
34. Duranti, F.; Salti, G.; Bovani, B.; Calandra, M.; Rosati, M.L. Injectable hyaluronic acid gel for soft tissue augmentation. A clinical and histological study. *Dermatol. Surg.* **1998**, *24*, 1317–1325. [[CrossRef](#)] [[PubMed](#)]
35. Lin, K.; Bartlett, S.P.; Matsuo, K.; LiVolsi, V.A.; Parry, C.; Hass, B.; Whitaker, L.A. Hyaluronic acid-filled mammary implants: An experimental study. *Plast. Reconstr. Surg.* **1994**, *94*, 306–315. [[CrossRef](#)] [[PubMed](#)]
36. Benedetti, L.M.; Topp, E.M.; Stella, V.J. Microspheres of hyaluronic acid esters—Fabrication methods and in vitro hydrocortisone release. *J. Control. Release* **1990**, *13*, 33–41. [[CrossRef](#)]

37. Lim, S.T.; Martin, G.P.; Berry, D.J.; Brown, M.B. Preparation and evaluation of the in vitro drug release properties and mucoadhesion of novel microspheres of hyaluronic acid and chitosan. *J. Control. Release* **2000**, *66*, 281–292. [[CrossRef](#)]
38. Moreira, C.A.J.; Armstrong, D.K.; Jelliffe, R.W.; Moreira, A.T.; Woodford, C.C.; Liggett, P.E.; Trousdale, M.D. Sodium hyaluronate as a carrier for intravitreal gentamicin. An experimental study. *Acta Ophthalmol.* **1991**, *69*, 45–49. [[CrossRef](#)]
39. Morimoto, K.; Yamaguchi, H.; Iwakura, Y.; Morisaka, K.; Ohashi, Y.; Nakai, Y. Effects of viscous hyaluronate-sodium solutions on the nasal absorption of vasopressin and an analogue. *Pharm. Res.* **1991**, *8*, 471–474. [[CrossRef](#)] [[PubMed](#)]
40. Yerushalmi, N.; Arad, A.; Margalit, R. Molecular and cellular studies of hyaluronic acid-modified liposomes as bioadhesive carriers for topical drug delivery in wound healing. *Arch. Biochem. Biophys.* **1994**, *313*, 267–273. [[CrossRef](#)] [[PubMed](#)]
41. Camber, O.; Edman, P. Sodium hyaluronate as an ophthalmic vehicle: Some factors governing its effect on the ocular absorption of pilocarpine. *Curr. Eye Res.* **1989**, *8*, 563–567. [[CrossRef](#)] [[PubMed](#)]
42. Egbu, R.; Brocchini, S.; Khaw, P.T.; Awwad, S. Antibody loaded collapsible hyaluronic acid hydrogels for intraocular delivery. *Eur. J. Pharm. Biopharm.* **2018**, *124*, 95–103. [[CrossRef](#)] [[PubMed](#)]
43. El Kechai, N.; Geiger, S.; Fallacara, A.; Cañero Infante, I.; Nicolas, V.; Ferrary, E.; Huang, N.; Bochot, A.; Agnely, F. Mixtures of hyaluronic acid and liposomes for drug delivery: Phase behavior, microstructure and mobility of liposomes. *Int. J. Pharm.* **2017**, *523*, 246–259. [[CrossRef](#)] [[PubMed](#)]
44. El Kechai, N.; Mamelle, E.; Nguyen, Y.; Huang, N.; Nicolas, V.; Chaminade, P.; Yen-Nicolaÿ, S.; Gueutin, C.; Granger, B.; Ferrary, E.; et al. Hyaluronic acid liposomal gel sustains delivery of a corticoid to the inner ear. *J. Control. Release* **2016**, *226*, 248–257. [[CrossRef](#)] [[PubMed](#)]
45. Xie, Y.; Upton, Z.; Richards, S.; Rizzi, S.C.; Leavesley, D.I. Hyaluronic acid: Evaluation as a potential delivery vehicle for vitronectin: Growth factor complexes in wound healing applications. *J. Control. Release* **2011**, *153*, 225–232. [[CrossRef](#)] [[PubMed](#)]
46. Knopf-Marques, H.; Pravda, M.; Wolfova, L.; Velebny, V.; Schaaf, P.; Vrana, N.E.; Lavallo, P. Hyaluronic Acid and Its Derivatives in Coating and Delivery Systems: Applications in Tissue Engineering, Regenerative Medicine and Immunomodulation. *Adv. Healthc. Mater.* **2016**, *5*, 2841–2855. [[CrossRef](#)] [[PubMed](#)]
47. Adamia, S.; Pilarski, P.M.; Belch, A.R.; Pilarski, L.M. Aberrant splicing, hyaluronan synthases and intracellular hyaluronan as drivers of oncogenesis and potential drug targets. *Curr. Cancer Drug Targets* **2013**, *13*, 347–361. [[CrossRef](#)] [[PubMed](#)]
48. Adamia, S.; Maxwell, C.A.; Pilarski, L.M. Hyaluronan and hyaluronan synthases: Potential therapeutic targets in cancer. *Curr. Drug Targets Cardiovasc. Haematol. Disord.* **2005**, *5*, 3–14. [[CrossRef](#)] [[PubMed](#)]
49. De Oliveira, J.D.; Carvalho, L.S.; Gomes, A.M.; Queiroz, L.R.; Magalhães, B.S.; Parachin, N.S. Genetic basis for hyper production of hyaluronic acid in natural and engineered microorganisms. *Microb. Cell Fact.* **2016**, *15*, 119. [[CrossRef](#)] [[PubMed](#)]
50. Heldin, P.; Lin, C.Y.; Kolliopoulos, K.; Chen, Y.H.; Skandalis, S.S. Regulation of hyaluronan biosynthesis and clinical impact of excessive hyaluronan production. *Matrix Biol.* **2018**. [[CrossRef](#)] [[PubMed](#)]
51. Cyphert, J.M.; Trempus, C.S.; Garantziotis, S. Size matters: Molecular weight specificity of hyaluronan effects in cell biology. *Int. J. Cell Biol.* **2015**, *2015*, 563818. [[CrossRef](#)] [[PubMed](#)]
52. Ebid, R.; Lichtnekert, J.; Anders, H.J. Hyaluronan is not a ligand but a regulator of toll-like receptor signaling in mesangial cells: Role of extracellular matrix in innate immunity. *ISRN Nephrol.* **2014**, *2014*. [[CrossRef](#)] [[PubMed](#)]
53. Gao, F.; Yang, C.X.; Mo, W.; Liu, Y.W.; He, Y.Q. Hyaluronan oligosaccharides are potential stimulators to angiogenesis via RHAMM mediated signal pathway in wound healing. *Clin. Investig. Med.* **2008**, *31*, E106–E116. [[CrossRef](#)]
54. Mattheolabakis, G.; Milane, L.; Singh, A.; Amiji, M.M. Hyaluronic acid targeting of CD44 for cancer therapy: From receptor biology to nanomedicine. *J. Drug Target.* **2015**, *23*, 605–618. [[CrossRef](#)] [[PubMed](#)]
55. Supp, D.M.; Hahn, J.M.; McFarland, K.L.; Glaser, K. Inhibition of hyaluronan synthase 2 reduces the abnormal migration rate of keloid keratinocytes. *J. Burn Care Res.* **2014**, *35*, 84–92. [[CrossRef](#)] [[PubMed](#)]
56. Fallacara, A.; Vertuani, S.; Panozzo, G.; Pecorelli, A.; Valacchi, G.; Manfredini, S. Novel Artificial Tears Containing Cross-Linked Hyaluronic Acid: An In Vitro Re-Epithelialization Study. *Molecules* **2017**, *22*, 2104. [[CrossRef](#)] [[PubMed](#)]



57. Larrañeta, E.; Henry, M.; Irwin, N.J.; Trotter, J.; Perminova, A.A.; Donnelly, R.F. Synthesis and characterization of hyaluronic acid hydrogels crosslinked using a solvent-free process for potential biomedical applications. *Carbohydr. Polym.* **2018**, *181*, 1194–1205. [CrossRef] [PubMed]
58. Fallacara, A.; Manfredini, S.; Durini, E.; Vertuani, S. Hyaluronic acid fillers in soft tissue regeneration. *Facial Plast. Surg.* **2017**, *33*, 87–96. [CrossRef] [PubMed]
59. Fraser, J.R.; Laurent, T.C.; Laurent, U.B. Hyaluronan: Its nature, distribution, functions and turnover. *J. Intern. Med.* **1997**, *242*, 27–33. [CrossRef] [PubMed]
60. Girish, K.S.; Kemparaju, K. The magic glue hyaluronan and its eraser hyaluronidase: A biological overview. *Life Sci.* **2007**, *80*, 1921–1943. [CrossRef] [PubMed]
61. Laurent, T.C.; Fraser, J.R. Hyaluronan. *FASEB J.* **1992**, *6*, 2397–2404. [CrossRef] [PubMed]
62. Hascall, V.C.; Laurent, T.C. Hyaluronan: Structure and Physical Properties. GlycoForum—Hyaluronan Today Website. 1997. Available online: <http://glycoforum.gr.jp/science/hyaluronan/HA01/HA01E.html> (accessed on 22 February 2018).
63. Scott, J.E. Secondary structures in hyaluronan solutions: Chemical and biological implications. *Ciba Found. Symp.* **1989**, *143*, 6–15. [PubMed]
64. Scott, J.E.; Cummings, C.; Brass, A.; Chen, Y. Secondary and tertiary structures of hyaluronan in aqueous solution, investigated by rotary shadowing-electron microscopy and computer simulation. Hyaluronan is a very efficient network-forming polymer. *Biochem. J.* **1991**, *274*, 699–705. [CrossRef] [PubMed]
65. Scott, J.E.; Heatley, F. Hyaluronan forms specific stable tertiary structures in aqueous solution: A <sup>13</sup>C NMR study. *Proc. Natl. Acad. Sci. USA* **1999**, *96*, 4850–4855. [CrossRef] [PubMed]
66. Laurent, T. The biology of hyaluronan. Introduction. *Ciba Found. Symp.* **1989**, *143*, 1–20. [PubMed]
67. Balazs, E.A.; Laurent, T.C.; Jeanloz, R.W. Nomenclature of hyaluronic acid. *Biochem. J.* **1986**, *235*, 903. [CrossRef] [PubMed]
68. Heatley, F.; Scott, J.E. A water molecule participates in the secondary structure of hyaluronan. *Biochem. J.* **1988**, *254*, 489–493. [CrossRef] [PubMed]
69. Scott, J.E. Supramolecular organization of extracellular matrix glycosaminoglycans, in vitro and in the tissues. *FASEB J.* **1992**, *6*, 2639–2645. [CrossRef] [PubMed]
70. Kobayashi, Y.; Okamoto, A.; Nishinari, K. Viscoelasticity of hyaluronic acid with different molecular weights. *Biorheology* **1994**, *31*, 235–244. [CrossRef] [PubMed]
71. Cleland, R.L. Ionic polysaccharides. II. Comparison of polyelectrolyte behavior of hyaluronate with that of carboxymethyl cellulose. *Biopolymers* **1968**, *6*, 1519–1529. [CrossRef] [PubMed]
72. Balazs, E.A. The physical properties of synovial fluid and the special role of hyaluronic acid. In *Disorders of the Knee*; Helfet, A.J., Ed.; J.B. Lippincott Company: Philadelphia, PA, USA, 1974; pp. 63–75.
73. Rwei, S.P.; Chen, S.W.; Mao, C.F.; Fang, H.W. Viscoelasticity and wearability of hyaluronate solutions. *Biochem. Eng. J.* **2008**, *40*, 211–217. [CrossRef]
74. Lapčík, L.J.; Lapčík, L.; De Smedt, S.; Demeester, J.; Chabreck, P. Hyaluronan: Preparation, Structure, Properties, and Applications. *Chem. Rev.* **1998**, *98*, 2663–2684. [CrossRef]
75. Maleki, A.; Kjøniksen, A.L.; Nystrom, B. Effect of pH on the behavior of hyaluronic acid in dilute and semidilute aqueous solutions. *Macromol. Symp.* **2008**, *274*, 131–140. [CrossRef]
76. Ghosh, S.; Kobal, I.; Zquette, D.; Reed, W.F. Conformational contraction and hydrolysis of hyaluronate in sodium hydroxide solutions. *Macromolecules* **1993**, *26*, 4685–4693. [CrossRef]
77. Morris, E.R.; Rees, D.A.; Welsh, E.J. Conformation and dynamic interactions in hyaluronate solutions. *J. Mol. Biol.* **1980**, *138*, 383–400. [CrossRef]
78. Pisárčik, M.; Bakoš, D.; Čeppan, M. Non-Newtonian properties of hyaluronic acid aqueous solution. *Colloids Surf. A Physicochem. Eng. Asp.* **1995**, *97*, 197–202. [CrossRef]
79. Gura, E.; Hüchel, M.; Müller, P.J. Specific degradation of hyaluronic acid and its rheological properties. *Polym. Degrad. Stab.* **1998**, *59*, 297–302. [CrossRef]
80. DeAngelis, P.L.; Jing, W.; Drake, R.R.; Achyuthan, A.M. Identification and molecular cloning of a unique hyaluronan synthase from *Pasteurella multocida*. *J. Biol. Chem.* **1998**, *273*, 8454–8458. [CrossRef] [PubMed]
81. Balazs, E.A.; Leshchiner, E.; Larsen, N.E.; Band, P. Applications of hyaluronan and its derivatives. In *Biotechnological Polymers*; Gebelein, C.G., Ed.; Technomic: Lancaster, UK, 1993; pp. 41–65.
82. Schiraldi, C.; La Gatta, A.; De Rosa, M. Biotechnological Production and Application of Hyaluronan. In *Biopolymers*; Elnashar, M., Ed.; IntechOpen: London, UK, 2010; Available online: <https://www.intechopen>.

- com/books/biopolymers/biotechnological-production-characterization-and-application-of-hyaluronan (accessed on 20 June 2018).
83. DeAngelis, P.L. Hyaluronan synthases: Fascinating glycosyltransferases from vertebrates, bacterial pathogens, and algal viruses. *Cell. Mol. Life Sci.* **1999**, *56*, 670–682. [[CrossRef](#)] [[PubMed](#)]
  84. Volpi, N.; Maccari, F. Purification and characterization of hyaluronic acid from the mollusc bivalve *Mytilus galloprovincialis*. *Biochimie* **2003**, *85*, 619–625. [[CrossRef](#)]
  85. Kogan, G.; Soltés, L.; Stern, R.; Gemeiner, P. Hyaluronic acid: A natural biopolymer with a broad range of biomedical and industrial applications. *Biotechnol. Lett.* **2007**, *29*, 17–25. [[CrossRef](#)] [[PubMed](#)]
  86. Volpi, N.; Schiller, J.; Stern, R.; Soltés, L. Role, metabolism, chemical modifications and applications of hyaluronan. *Curr. Med. Chem.* **2009**, *16*, 1718–1745. [[CrossRef](#)] [[PubMed](#)]
  87. Sobolewski, K.; Bańkowski, E.; Chyczewski, L.; Jaworski, S. Collagen and glycosaminoglycans of Wharton's jelly. *Biol. Neonate* **1997**, *71*, 11–21. [[CrossRef](#)] [[PubMed](#)]
  88. Robert, L.; Robert, A.M.; Renard, G. Biological effects of hyaluronan in connective tissues, eye, skin, venous wall. Role in aging. *Pathol. Biol.* **2010**, *58*, 187–198. [[CrossRef](#)] [[PubMed](#)]
  89. Weigel, P.H.; Hascall, V.C.; Tammi, M. Hyaluronan synthases. *J. Biol. Chem.* **1997**, *272*, 13997–14000. [[CrossRef](#)] [[PubMed](#)]
  90. Itano, N.; Kimata, K. Mammalian hyaluronan synthases. *IUBMB Life* **2002**, *54*, 195–199. [[CrossRef](#)] [[PubMed](#)]
  91. Spicer, A.P.; McDonald, J.A. Characterization and molecular evolution of a vertebrate hyaluronan synthase gene family. *J. Biol. Chem.* **1998**, *273*, 1923–1932. [[CrossRef](#)] [[PubMed](#)]
  92. Itano, N.; Sawai, T.; Yoshida, M.; Lenas, P.; Yamada, Y.; Imagawa, M.; Shinomura, T.; Hamaguchi, M.; Yoshida, Y.; Ohnuki, Y.; et al. Three isoforms of mammalian hyaluronan synthases have distinct enzymatic properties. *J. Biol. Chem.* **1999**, *274*, 25085–25092. [[CrossRef](#)] [[PubMed](#)]
  93. Jiang, D.; Liang, J.; Noble, P.W. Hyaluronan in tissue injury and repair. *Annu. Rev. Cell Dev. Biol.* **2007**, *23*, 435–461. [[CrossRef](#)] [[PubMed](#)]
  94. Vigetti, D.; Viola, M.; Karousou, E.; De Luca, G.; Passi, A. Metabolic control of hyaluronan synthases. *Matrix Biol.* **2014**, *35*, 8–13. [[CrossRef](#)] [[PubMed](#)]
  95. Stuhlmeier, K.M.; Pollaschek, C. Differential effect of transforming growth factor beta (TGF-beta) on the genes encoding hyaluronan synthases and utilization of the p38 MAPK pathway in TGF-beta-induced hyaluronan synthase 1 activation. *J. Biol. Chem.* **2004**, *279*, 8753–8760. [[CrossRef](#)] [[PubMed](#)]
  96. Vigetti, D.; Karousou, E.; Viola, M.; Deleonibus, S.; De Luca, G.; Passi, A. Hyaluronan: Biosynthesis and signaling. *Biochim. Biophys. Acta* **2014**, *1840*, 2452–2459. [[CrossRef](#)] [[PubMed](#)]
  97. Zhang, Z.; Tao, D.; Zhang, P.; Liu, X.; Zhang, Y.; Cheng, J.; Yuan, H.; Liu, L.; Jiang, H. Hyaluronan synthase 2 expressed by cancer-associated fibroblasts promotes oral cancer invasion. *J. Exp. Clin. Cancer Res.* **2016**, *35*, 181. [[CrossRef](#)] [[PubMed](#)]
  98. Li, Y.; Liang, J.; Yang, T.; Monterrosa Mena, J.; Huan, C.; Xie, T.; Kurkciyan, A.; Liu, N.; Jiang, D.; Noble, P.W. Hyaluronan synthase 2 regulates fibroblast senescence in pulmonary fibrosis. *Matrix Biol.* **2016**, *55*, 35–48. [[CrossRef](#)] [[PubMed](#)]
  99. Zhang, H.; Tsang, J.Y.; Ni, Y.B.; Chan, S.K.; Chan, K.F.; Cheung, S.Y.; Tse, G.M. Hyaluronan synthase 2 is an adverse prognostic marker in androgen receptor-negative breast cancer. *J. Clin. Pathol.* **2016**, *69*, 1055–1062. [[CrossRef](#)] [[PubMed](#)]
  100. Toole, B.P. Hyaluronan: From extracellular glue to pericellular cue. *Nat. Rev. Cancer* **2004**, *4*, 528–539. [[CrossRef](#)] [[PubMed](#)]
  101. Stern, R.; Jedrzejewski, M.J. Hyaluronidases: Their genomics, structures, and mechanisms of action. *Chem. Rev.* **2006**, *106*, 818–839. [[CrossRef](#)] [[PubMed](#)]
  102. Csoka, A.B.; Frost, G.I.; Stern, R. The six hyaluronidase-like genes in the human and mouse genomes. *Matrix Biol.* **2001**, *20*, 499–508. [[CrossRef](#)]
  103. Lokeshwar, V.B.; Rubinowicz, D.; Schroeder, G.L.; Forgacs, E.; Minna, J.D.; Block, N.L.; Nadj, M.; Lokeshwar, B.L. Stromal and epithelial expression of tumor markers hyaluronic acid and HYAL1 hyaluronidase in prostate cancer. *J. Biol. Chem.* **2001**, *276*, 11922–11932. [[CrossRef](#)] [[PubMed](#)]
  104. Lepperdinger, G.; Strobl, B.; Kreil, G. HYAL2, a human gene expressed in many cells, encodes a lysosomal hyaluronidase with a novel type of specificity. *J. Biol. Chem.* **1998**, *273*, 22466–22470. [[CrossRef](#)] [[PubMed](#)]
  105. Frost, G.I.; Csoka, A.B.; Wong, T.; Stern, R. Purification, cloning, and expression of human plasma hyaluronidase. *Biochem. Biophys. Res. Commun.* **1997**, *236*, 10–15. [[CrossRef](#)] [[PubMed](#)]

106. Csoka, A.B.; Frost, G.I.; Wong, T.; Stern, R. Purification and microsequencing of hyaluronidase isozymes from human urine. *FEBS Lett.* **1997**, *417*, 307–310. [CrossRef]
107. Stern, R. Hyaluronidases in cancer biology. *Semin. Cancer Biol.* **2008**, *18*, 275–280. [CrossRef] [PubMed]
108. Cherr, G.N.; Yudin, A.I.; Overstreet, J.W. The dual functions of GPI-anchored PH-20: Hyaluronidase and intracellular signaling. *Matrix Biol.* **2001**, *20*, 515–525. [CrossRef]
109. Soltés, L.; Mendichi, R.; Kogan, G.; Schiller, J.; Stankovska, M.; Arnhold, J. Degradative action of reactive oxygen species on hyaluronan. *Biomacromolecules* **2006**, *7*, 659–668. [CrossRef] [PubMed]
110. Stern, R.; Kogan, G.; Jedrzejak, M.J.; Soltés, L. The many ways to cleave hyaluronan. *Biotechnol. Adv.* **2007**, *25*, 537–557. [CrossRef] [PubMed]
111. Monzon, M.E.; Fregien, N.; Schmid, N.; Falcon, N.S.; Campos, M.; Casalino-Matsuda, S.M.; Forteza, R.M. Reactive oxygen species and hyaluronidase 2 regulate airway epithelial hyaluronan fragmentation. *J. Biol. Chem.* **2010**, *285*, 26126–26134. [CrossRef] [PubMed]
112. Schiller, J.; Arnhold, J.; Arnold, K. Contribution of reactive oxygen species to cartilage degradation in rheumatic diseases: Molecular pathways, diagnosis and potential therapeutic strategies. *Curr. Med. Chem.* **2003**, *10*, 2123–2145. [CrossRef] [PubMed]
113. Schiller, J.; Arnhold, J.; Arnold, K. Action of hypochlorous acid on polymeric components of cartilage. Use of <sup>13</sup>C NMR spectroscopy. *Z. Naturforsch. C* **1995**, *50*, 721–728. [PubMed]
114. Jiang, D.; Liang, J.; Noble, P.W. Hyaluronan as an immune regulator in human diseases. *Physiol. Rev.* **2011**, *91*, 221–264. [CrossRef] [PubMed]
115. Tamer, T.M. Hyaluronan and synovial joint: Function, distribution and healing. *Interdiscip. Toxicol.* **2013**, *6*, 111–125. [CrossRef] [PubMed]
116. Wu, M.; Cao, M.; He, Y.; Liu, Y.; Yang, C.; Du, Y.; Wang, W.; Gao, F. A novel role of low molecular weight hyaluronan in breast cancer metastasis. *FASEB J.* **2015**, *29*, 1290–1298. [CrossRef] [PubMed]
117. Kim, M.Y.; Muto, J.; Gallo, R.L. Hyaluronic acid oligosaccharides suppress TLR3-dependent cytokine expression in a TLR4-dependent manner. *PLoS ONE* **2013**, *8*, e72421. [CrossRef] [PubMed]
118. Misra, S.; Toole, B.P.; Ghatak, S. Hyaluronan constitutively regulates activation of multiple receptor tyrosine kinases in epithelial and carcinoma cells. *J. Biol. Chem.* **2006**, *281*, 34936–34941. [CrossRef] [PubMed]
119. Toole, B.P.; Ghatak, S.; Misra, S. Hyaluronan oligosaccharides as a potential anticancer therapeutic. *Curr. Pharm. Biotechnol.* **2008**, *9*, 249–252. [CrossRef] [PubMed]
120. Campo, G.M.; Avenoso, A.; D’Ascola, A.; Prestipino, V.; Scuruchi, M.; Nastasi, G.; Calatroni, A.; Campo, S. 4-mer hyaluronan oligosaccharides stimulate in ammation response in synovial broblasts in part via TAK-1 and in part via p38-MAPK. *Curr. Med. Chem.* **2013**, *20*, 1162–1172. [CrossRef] [PubMed]
121. Yang, C.; Cao, M.; Liu, H.; He, Y.; Xu, J.; Du, Y.; Liu, Y.; Wang, W.; Cui, L.; Hu, J.; et al. The high and low molecular weight forms of hyaluronan have distinct effects on CD44 clustering. *J. Biol. Chem.* **2012**, *287*, 43094–43107. [CrossRef] [PubMed]
122. Turley, E.A.; Noble, P.W.; Bourguignon, LY. Signaling properties of hyaluronan receptors. *J. Biol. Chem.* **2002**, *277*, 4589–4592. [CrossRef] [PubMed]
123. Research, G.V. Hyaluronic Acid Market Size Worth USD 15.4 Billion by 2025 | CAGR: 8.8%. Available online: <https://www.grandviewresearch.com/press-release/global-hyaluronic-acid-market> (accessed on 8 March 2018).
124. Shiedlin, A.; Bigelow, R.; Christopher, W.; Arbabi, S.; Yang, L.; Maier, R.V.; Wainwright, N.; Childs, A.; Miller, R.J. Evaluation of hyaluronan from different sources: Streptococcus zooepidemicus, rooster comb, bovine vitreous, and human umbilical cord. *Biomacromolecules* **2004**, *5*, 2122–2127. [CrossRef] [PubMed]
125. Rangaswamy, V.; Jain, D. An efficient process for production and purification of hyaluronic acid from Streptococcus equi subsp. zooepidemicus. *Biotechnol. Lett.* **2008**, *30*, 493–496. [CrossRef] [PubMed]
126. Kim, J.H.; Yoo, S.J.; Oh, D.K.; Kweon, Y.G.; Park, D.W.; Lee, C.H.; Gil, G.H. Selection of a Streptococcus equi mutant and optimization of culture conditions for the production of high molecular weight hyaluronic acid. *Enzyme Microb. Technol.* **1996**, *19*, 440–445. [CrossRef]
127. Liu, L.; Liu, Y.; Li, J.; Du, G.; Chen, J. Microbial production of hyaluronic acid: Current state, challenges, and perspectives. *Microb. Cell Fact.* **2011**, *10*. [CrossRef] [PubMed]
128. Kaur, M.; Jayaraman, G. Hyaluronan production and molecular weight is enhanced in pathway-engineered strains of lactate dehydrogenase-deficient Lactococcus lactis. *Metab. Eng. Commun.* **2016**, *3*, 15–23. [CrossRef] [PubMed]



129. Chien, L.J.; Lee, C.K. Enhanced hyaluronic acid production in *Bacillus subtilis* by coexpressing bacterial hemoglobin. *Biotechnol. Prog.* **2007**, *23*, 1017–1022. [[CrossRef](#)] [[PubMed](#)]
130. Yu, H.; Stephanopoulos, G. Metabolic engineering of *Escherichia coli* for biosynthesis of hyaluronic acid. *Metab. Eng.* **2008**, *10*, 24–32. [[CrossRef](#)] [[PubMed](#)]
131. Cheng, F.; Gong, Q.; Yu, H.; Stephanopoulos, G. High-titer biosynthesis of hyaluronic acid by recombinant *Corynebacterium glutamicum*. *Biotechnol. J.* **2016**, *11*, 574–584. [[CrossRef](#)] [[PubMed](#)]
132. DeAngelis, P.L.; Achyuthan, A.M. Yeast-derived recombinant DG42 protein of *Xenopus* can synthesize hyaluronan in vitro. *J. Biol. Chem.* **1996**, *271*, 23657–23660. [[CrossRef](#)] [[PubMed](#)]
133. Jeong, E.; Shim, W.Y.; Kim, J.H. Metabolic engineering of *Pichia pastoris* for production of hyaluronic acid with high molecular weight. *J. Biotechnol.* **2014**, *185*, 28–36. [[CrossRef](#)] [[PubMed](#)]
134. Rakkhumkaew, N.; Shibatani, S.; Kawasaki, T.; Fujie, M.; Yamada, T. Hyaluronan synthesis in cultured tobacco cells (BY-2) expressing a chlorovirus enzyme: Cytological studies. *Biotechnol. Bioeng.* **2013**, *110*, 1174–1179. [[CrossRef](#)] [[PubMed](#)]
135. DeAngelis, P.L. Monodisperse hyaluronan polymers: Synthesis and potential applications. *Curr. Pharm. Biotechnol.* **2008**, *9*, 246–248. [[CrossRef](#)] [[PubMed](#)]
136. Schanté, C.E.; Zuber, G.; Herlin, C.; Vandamme, T.F. Chemical modifications of hyaluronic acid for the synthesis of derivatives for a broad range of biomedical applications. *Carbohydr. Polym.* **2011**, *85*, 469–489. [[CrossRef](#)]
137. Malson, T.; Lindqvist, B. Gels of Crosslinked Hyaluronic Acid for Use as a Vitreous Humor Substitute. International Publication No. WO1986000079 A1, 3 January 1986.
138. Shimajo, A.A.; Pires, A.M.; Lichy, R.; Rodrigues, A.A.; Santana, M.H. The crosslinking degree controls the mechanical, rheological, and swelling properties of hyaluronic acid microparticles. *J. Biomed. Mater. Res. A* **2015**, *103*, 730–737. [[CrossRef](#)] [[PubMed](#)]
139. Collins, M.N.; Birkinshaw, C. Physical properties of crosslinked hyaluronic acid hydrogels. *J. Mater. Sci. Mater. Med.* **2008**, *19*, 3335–3343. [[CrossRef](#)] [[PubMed](#)]
140. Bowman, S.; Awad, M.E.; Hamrick, M.W.; Hunter, M.; Fulzele, S. Recent advances in hyaluronic acid based therapy for osteoarthritis. *Clin. Transl. Med.* **2018**, *7*, 6. [[CrossRef](#)] [[PubMed](#)]
141. Nobile, V.; Buonocore, D.; Michelotti, A.; Marzatico, F. Anti-aging and filling efficacy of six types hyaluronic acid based dermo-cosmetic treatment: Double blind, randomized clinical trial of efficacy and safety. *J. Cosmet. Dermatol.* **2014**, *13*, 277–287. [[CrossRef](#)] [[PubMed](#)]
142. Kaur, K.; Singh, H.; Singh, M. Repair of tympanic membrane perforation by topical application of 1% sodium hyaluronate. *Indian J. Otolaryngol. Head Neck Surg.* **2006**, *58*, 241–244. [[PubMed](#)]
143. Gelardi, M.; Iannuzzi, L.; Quaranta, N. Intranasal sodium hyaluronate on the nasal cytology of patients with allergic and nonallergic rhinitis. *Int. Forum Allergy Rhinol.* **2013**, *3*, 807–813. [[CrossRef](#)] [[PubMed](#)]
144. Gelardi, M.; Guglielmi, A.V.; De Candia, N.; Maffezzoni, E.; Berardi, P.; Quaranta, N. Effect of sodium hyaluronate on mucociliary clearance after functional endoscopic sinus surgery. *Eur. Ann. Allergy Clin. Immunol.* **2013**, *45*, 103–108. [[PubMed](#)]
145. Maleki, A.; Kjøniksen, A.L.; Nyström, B. Characterization of the chemical degradation of hyaluronic acid during chemical gelation in the presence of different cross-linker agents. *Carbohydr. Res.* **2007**, *342*, 2776–2792. [[CrossRef](#)] [[PubMed](#)]
146. Bulpitt, P.; Aeschlimann, D. New strategy for chemical modification of hyaluronic acid: Preparation of functionalized derivatives and their use in the formation of novel biocompatible hydrogels. *J. Biomed. Mater. Res.* **1999**, *47*, 152–169. [[CrossRef](#)]
147. Lim, D.G.; Prim, R.E.; Kang, E.; Jeong, S.H. One-pot synthesis of dopamine-conjugated hyaluronic acid/polydopamine nanocomplexes to control protein drug release. *Int. J. Pharm.* **2018**, *542*, 288–296. [[CrossRef](#)] [[PubMed](#)]
148. Magnani, A.; Rappuoli, R.; Lamponi, S.; Barbucci, R. Novel polysaccharide hydrogels: Characterization and properties. *Polym. Adv. Technol.* **2000**, *11*, 488–495. [[CrossRef](#)]
149. Sigen, A.; Xu, Q.; McMichael, P.; Gao, Y.; Li, X.; Wang, X.; Greiser, U.; Zhou, D.; Wang, W. A facile one-pot synthesis of acrylated hyaluronic acid. *Chem. Commun.* **2018**, *54*, 1081–1084.

150. Felgueiras, H.P.; Wang, L.M.; Ren, K.F.; Querido, M.M.; Jin, Q.; Barbosa, M.A.; Ji, J.; Martins, M.C. Octadecyl chains immobilized onto hyaluronic acid coatings by thiol-ene “click chemistry” increase the surface antimicrobial properties and prevent platelet adhesion and activation to polyurethane. *ACS Appl. Mater. Interfaces* **2017**, *9*, 7979–7989. [[CrossRef](#)] [[PubMed](#)]
151. Smith, L.J.; Taimoory, S.M.; Tam, R.Y.; Baker, A.E.G.; Binth Mohammad, N.; Trant, J.F.; Shoichet, M.S. Diels-Alder Click-Cross-Linked Hydrogels with Increased Reactivity Enable 3D Cell Encapsulation. *Biomacromolecules* **2018**, *19*, 926–935. [[CrossRef](#)] [[PubMed](#)]
152. Fu, S.; Dong, H.; Deng, X.; Zhuo, R.; Zhong, Z. Injectable hyaluronic acid/poly(ethylene glycol) hydrogels crosslinked via strain-promoted azide-alkyne cycloaddition click reaction. *Carbohydr. Polym.* **2017**, *169*, 332–340. [[CrossRef](#)] [[PubMed](#)]
153. Shu, X.Z.; Liu, Y.; Luo, Y.; Roberts, M.C.; Prestwich, G.D. Disulfide cross-linked hyaluronan hydrogels. *Biomacromolecules* **2002**, *3*, 1304–1311. [[CrossRef](#)] [[PubMed](#)]
154. Bencherif, S.A.; Srinivasan, A.; Horkay, F.; Hollinger, J.O.; Matyjaszewski, K.; Washburn, N.R. Influence of the degree of methacrylation on hyaluronic acid hydrogels properties. *Biomaterials* **2008**, *29*, 1739–1749. [[CrossRef](#)] [[PubMed](#)]
155. Donnelly, P.E.; Chen, T.; Finch, A.; Brial, C.; Maher, S.A.; Torzilli, P.A. Photocrosslinked tyramine-substituted hyaluronate hydrogels with tunable mechanical properties improve immediate tissue-hydrogel interfacial strength in articular cartilage. *J. Biomater. Sci. Polym. Ed.* **2017**, *28*, 582–600. [[CrossRef](#)] [[PubMed](#)]
156. Yui, N.; Okano, T.; Sakurai, Y. Inflammation responsive degradation of crosslinked hyaluronic acid gels. *J. Control. Release* **1992**, *22*, 105–116.
157. Zhao, X. Process for the Production of Multiple Cross-Linked Hyaluronic Acid Derivatives. International Publication No. WO/2000/046253, 10 August 2000.
158. Collins, M.; Birkinshaw, C. Comparison of the effectiveness of four different crosslinking agents with hyaluronic acid hydrogel films for tissue-culture applications. *J. Appl. Polym. Sci.* **2007**, *104*, 3183–3191. [[CrossRef](#)]
159. Serban, M.; Yang, G.; Prestwich, G. Synthesis, characterization and chondroprotective properties of a hyaluronan thioethyl ether derivative. *Biomaterials* **2008**, *29*, 1388–1399. [[CrossRef](#)] [[PubMed](#)]
160. Crescenzi, V.; Francescangeli, A.; Taglienti, A.; Capitani, D.; Mannina, L. Synthesis and partial characterization of hydrogels obtained via glutaraldehyde crosslinking of acetylated chitosan and of hyaluronan derivatives. *Biomacromolecules* **2003**, *4*, 1045–1054. [[CrossRef](#)] [[PubMed](#)]
161. Tomihata, K.; Ikada, Y. Crosslinking of hyaluronic acid with glutaraldehyde. *J. Polym. Sci. Part A Polym. Chem.* **1997**, *35*, 3553–3559. [[CrossRef](#)]
162. Toemmeras, K.; Eenschooten, C. Aryl/Alkyl Succinic Anhydride Hyaluronan Derivatives. International Publication No. WO/2007/033677, 29 March 2007.
163. Seidlits, S.K.; Khaing, Z.Z.; Petersen, R.R.; Nickels, J.D.; Vanscoy, J.E.; Shear, J.B.; Schmidt, C.E. The effects of hyaluronic acid hydrogels with tunable mechanical properties on neural progenitor cell differentiation. *Biomaterials* **2010**, *31*, 3930–3940. [[CrossRef](#)] [[PubMed](#)]
164. Pravata, L.; Braud, C.; Boustta, M.; El Ghzaoui, A.; Toemmeras, K.; Guillaumie, F.; Schwach-Abdellaoui, K.; Vert, M. New amphiphilic lactic acid oligomer-hyaluronan conjugates: Synthesis and physicochemical characterization. *Biomacromolecules* **2008**, *9*, 340–348. [[CrossRef](#)] [[PubMed](#)]
165. Mlcochová, P.; Bystrický, S.; Steiner, B.; Machová, E.; Koós, M.; Velebný, V.; Krcmár, M. Synthesis and characterization of new biodegradable hyaluronan alkyl derivatives. *Biopolymers* **2006**, *82*, 74–79. [[CrossRef](#)] [[PubMed](#)]
166. Della Valle, F.; Romeo, A. Esters of Hyaluronic Acid. U.S. Patent 4,851,521, 25 July 1989.
167. Huin-Amargier, C.; Marchal, P.; Payan, E.; Netter, P.; Dellacherie, E. New physically and chemically crosslinked hyaluronate (HA)-based hydrogels for cartilage repair. *J. Biomed. Mater. Res. A* **2006**, *76*, 416–424. [[CrossRef](#)] [[PubMed](#)]
168. Hirano, K.; Sakai, S.; Ishikawa, T.; Avcı, F.Y.; Linhardt, R.J.; Toida, T. Preparation of the methyl ester of hyaluronan and its enzymatic degradation. *Carbohydr. Res.* **2005**, *340*, 2297–2304. [[CrossRef](#)] [[PubMed](#)]
169. Prata, J.E.; Barth, T.A.; Bencherif, S.A.; Washburn, N.R. Complex fluids based on methacrylated hyaluronic acid. *Biomacromolecules* **2010**, *11*, 769–775. [[CrossRef](#)] [[PubMed](#)]



170. Benedetti, L.; Cortivo, R.; Berti, T.; Berti, A.; Pea, F.; Mazzo, M.; Moras, M.; Abatangelo, G. Biocompatibility and biodegradation of different hyaluronan derivatives (Hyaff) implanted in rats. *Biomaterials* **1993**, *14*, 1154–1160. [[CrossRef](#)]
171. Bellini, D.; Topai, A. Amides of Hyaluronic Acid and the Derivatives Thereof and a Process for Their Preparation. International Application No. PCT/IB1999/001254, 13 January 2000.
172. Kaczmarek, B.; Sionkowska, A.; Kozłowska, J.; Osyczka, A.M. New composite materials prepared by calcium phosphate precipitation in chitosan/collagen/hyaluronic acid sponge cross-linked by EDC/NHS. *Int. J. Biol. Macromol.* **2018**, *107*, 247–253. [[CrossRef](#)] [[PubMed](#)]
173. Kirk, J.F.; Ritter, G.; Finger, I.; Sankar, D.; Reddy, J.D.; Talton, J.D.; Nataraj, C.; Narisawa, S.; Millán, J.L.; Cobb, R.R. Mechanical and biocompatible characterization of a cross-linked collagen-hyaluronic acid wound dressing. *Biomatter* **2013**, *3*, pii: E25633. [[CrossRef](#)] [[PubMed](#)]
174. Bergman, K.; Elvingson, C.; Hilborn, J.; Svensk, G.; Bowden, T. Hyaluronic acid derivatives prepared in aqueous media by triazine-activated amidation. *Biomacromolecules* **2007**, *8*, 2190–2195. [[CrossRef](#)] [[PubMed](#)]
175. D'Este, M.; Eglin, D.; Alini, M. A systematic analysis of DMTMM vs EDC/NHS for ligation of amines to hyaluronan in water. *Carbohydr. Polym.* **2014**, *108*, 239–246. [[CrossRef](#)] [[PubMed](#)]
176. Crescenzi, V.; Francescangeli, A.; Segre, A.; Capitani, D.; Mannina, L.; Renier, D.; Bellini, D. NMR structural study of hydrogels based on partially deacetylated hyaluronan. *Macromol. Biosci.* **2002**, *2*, 272–279. [[CrossRef](#)]
177. Bhattacharya, D.; Svehkarev, D.; Souček, J.J.; Hill, T.K.; Taylor, M.A.; Natarajan, A.; Mohs, A.M. Impact of structurally modifying hyaluronic acid on CD44 interaction. *J. Mater. Chem. B.* **2017**, *5*, 8183–8192. [[CrossRef](#)] [[PubMed](#)]
178. Kong, J.H.; Oh, E.J.; Chae, S.Y.; Lee, K.C.; Hahn, S.K. Long acting hyaluronate—Exendin 4 conjugate for the treatment of type 2 diabetes. *Biomaterials* **2010**, *31*, 4121–4128. [[CrossRef](#)] [[PubMed](#)]
179. Mero, A.; Campisi, M. Hyaluronic acid bioconjugates for the delivery of bioactive molecules. *Polymers* **2014**, *6*, 346–369. [[CrossRef](#)]
180. Mangano, K.; Veralito, F.; Mammana, S.; Mariano, A.; De Pasquale, R.; Meloscia, A.; Bartollino, S.; Guerra, G.; Nicoletti, F.; Di Marco, R. Evaluation of hyaluronic acid-P40 conjugated cream in a mouse model of dermatitis induced by oxazolone. *Exp. Ther. Med.* **2017**, *14*, 2439–2444. [[CrossRef](#)] [[PubMed](#)]
181. Manju, S.; Sreenivasan, K. Conjugation of curcumin onto hyaluronic acid enhances its aqueous solubility and stability. *J. Colloid Interface Sci.* **2011**, *359*, 318–325. [[CrossRef](#)] [[PubMed](#)]
182. Sharma, M.; Sahu, K.; Singh, S.P.; Jain, B. Wound healing activity of curcumin conjugated to hyaluronic acid: In vitro and in vivo evaluation. *Artif. Cells Nanomed. Biotechnol.* **2018**, *46*, 1009–1017. [[CrossRef](#)] [[PubMed](#)]
183. Chen, Y.; Peng, F.; Song, X.; Wu, J.; Yao, W.; Gao, X. Conjugation of paclitaxel to C-6 hexanediamine-modified hyaluronic acid for targeted drug delivery to enhance antitumor efficacy. *Carbohydr. Polym.* **2018**, *181*, 150–158. [[CrossRef](#)] [[PubMed](#)]
184. Nguyen, V.D.; Zheng, S.; Han, J.; Le, V.H.; Park, J.O.; Park, S. Nanohybrid magnetic liposome functionalized with hyaluronic acid for enhanced cellular uptake and near-infrared-triggered drug release. *Colloids Surf. B. Biointerfaces* **2017**, *154*, 104–114. [[CrossRef](#)] [[PubMed](#)]
185. Hayward, S.L.; Wilson, C.L.; Kidambi, S. Hyaluronic acid-conjugated liposome nanoparticles for targeted delivery to CD44 overexpressing glioblastoma cells. *Oncotarget* **2016**, *7*, 34158–34171. [[CrossRef](#)] [[PubMed](#)]
186. Han, N.K.; Shin, D.H.; Kim, J.S.; Weon, K.Y.; Jang, C.Y.; Kim, J.S. Hyaluronan-conjugated liposomes encapsulating gemcitabine for breast cancer stem cells. *Int. J. Nanomed.* **2016**, *11*, 1413–1425. [[CrossRef](#)] [[PubMed](#)]
187. Chi, Y.; Yin, X.; Sun, K.; Feng, S.; Liu, J.; Chen, D.; Guo, C.; Wu, Z. Redox-sensitive and hyaluronic acid functionalized liposomes for cytoplasmic drug delivery to osteosarcoma in animal models. *J. Control. Release* **2017**, *261*, 113–125. [[CrossRef](#)] [[PubMed](#)]
188. Negi, L.M.; Jaggi, M.; Joshi, V.; Ronodip, K.; Talegaonkar, S. Hyaluronan coated liposomes as the intravenous platform for delivery of imatinib mesylate in MDR colon cancer. *Int. J. Biol. Macromol.* **2015**, *73*, 222–235. [[CrossRef](#)] [[PubMed](#)]
189. Moustafa, M.A.; Elnaggar, Y.S.R.; El-Refaie, W.M.; Abdallah, O.Y. Hyalugel-integrated liposomes as a novel ocular nanosized delivery system of fluconazole with promising prolonged effect. *Int. J. Pharm.* **2017**, *534*, 14–24. [[CrossRef](#)] [[PubMed](#)]

190. Manconi, M.; Manca, M.L.; Valenti, D.; Escribano, E.; Hillaireau, H.; Fadda, A.M.; Fattal, E. Chitosan and hyaluronan coated liposomes for pulmonary administration of curcumin. *Int. J. Pharm.* **2017**, *525*, 203–210. [[CrossRef](#)] [[PubMed](#)]
191. Leite Nascimento, T.; Hillaireau, H.; Vergnaud, J.; Rivano, M.; Deloménie, C.; Courilleau, D.; Arpicco, S.; Suk, J.S.; Hanes, J.; Fattal, E. Hyaluronic acid-conjugated lipoplexes for targeted delivery of siRNA in a murine metastatic lung cancer model. *Int. J. Pharm.* **2016**, *514*, 103–111. [[CrossRef](#)] [[PubMed](#)]
192. Maudens, P.; Meyer, S.; Seemayer, C.A.; Jordan, O.; Allémann, E. Self-assembled thermoresponsive nanostructures of hyaluronic acid conjugates for osteoarthritis therapy. *Nanoscale* **2018**, *10*, 1845–1854. [[CrossRef](#)] [[PubMed](#)]
193. Kim, H.; Park, H.T.; Tae, Y.M.; Kong, W.H.; Sung, D.K.; Hwang, B.W.; Kim, K.S.; Kim, Y.K.; Hahn, S.K. Bioimaging and pulmonary applications of self-assembled Flt1 peptide-hyaluronic acid conjugate nanoparticles. *Biomaterials* **2013**, *34*, 8478–8490. [[CrossRef](#)] [[PubMed](#)]
194. Pandey, M.; Choudhury, H.; Gunasegaran, T.A.P.; Nathan, S.S.; Md, S.; Gorain, B.; Tripathy, M.; Hussain, Z. Hyaluronic acid-modified betamethasone encapsulated polymeric nanoparticles: Fabrication, characterisation, in vitro release kinetics, and dermal targeting. *Drug Deliv. Transl. Res.* **2018**. [[CrossRef](#)] [[PubMed](#)]
195. Pereira, G.G.; Detoni, C.B.; Balducci, A.G.; Rondelli, V.; Colombo, P.; Guterres, S.S.; Sonvico, F. Hyaluronate nanoparticles included in polymer films for the prolonged release of vitamin E for the management of skin wounds. *Eur. J. Pharm. Sci.* **2016**, *83*, 203–211. [[CrossRef](#)] [[PubMed](#)]
196. Wang, T.; Hou, J.; Su, C.; Zhao, L.; Shi, Y. Hyaluronic acid-coated chitosan nanoparticles induce ROS-mediated tumor cell apoptosis and enhance antitumor efficiency by targeted drug delivery via CD44. *J. Nanobiotechnol.* **2017**, *15*, 7. [[CrossRef](#)] [[PubMed](#)]
197. Cho, H.J.; Yoon, H.Y.; Koo, H.; Ko, S.H.; Shim, J.S.; Lee, J.H.; Kim, K.; Kwon, I.C.; Kim, D.D. Self-assembled nanoparticles based on hyaluronic acid-ceramide (HA-CE) and Pluronic® for tumor-targeted delivery of docetaxel. *Biomaterials* **2011**, *32*, 7181–7190. [[CrossRef](#)] [[PubMed](#)]
198. Parashar, P.; Rathor, M.; Dwivedi, M.; Saraf, S.A. Hyaluronic acid decorated naringenin nanoparticles: Appraisal of chemopreventive and curative potential for lung cancer. *Pharmaceutics* **2018**, *10*. [[CrossRef](#)] [[PubMed](#)]
199. Hwang, S.M.; Kim, D.D.; Chung, S.J.; Shim, C.K. Delivery of ofloxacin to the lung and alveolar macrophages via hyaluronan microspheres for the treatment of tuberculosis. *J. Control. Release* **2008**, *129*, 100–106. [[CrossRef](#)] [[PubMed](#)]
200. Li, Y.; Han, M.; Liu, T.; Cun, D.; Fang, L.; Yang, M. Inhaled hyaluronic acid microparticles extended pulmonary retention and suppressed systemic exposure of a short-acting bronchodilator. *Carbohydr. Polym.* **2017**, *172*, 197–204. [[CrossRef](#)] [[PubMed](#)]
201. Fatnassi, M.; Jacquart, S.; Brouillet, F.; Rey, C.; Combes, C.; Girod Fullana, S. Optimization of spray-dried hyaluronic acid microspheres to formulate drug-loaded bone substitute materials. *Powder Technol.* **2014**, *255*, 44–51. [[CrossRef](#)]
202. Simsolo, E.E.; Eroğlu, İ.; Tanrıverdi, S.T.; Özer, Ö. Formulation and evaluation of organogels containing hyaluronan microparticles for topical delivery of caffeine. *AAPS PharmSciTech* **2018**, *19*, 1367–1376. [[CrossRef](#)] [[PubMed](#)]
203. Esposito, E.; Menegatti, E.; Cortesi, R. Hyaluronan-based microspheres as tools for drug delivery: A comparative study. *Int. J. Pharm.* **2005**, *288*, 35–49. [[CrossRef](#)] [[PubMed](#)]
204. Koivusalo, L.; Karvinen, J.; Sorsa, E.; Jönkkäri, I.; Väliaho, J.; Kallio, P.; Ilmarinen, T.; Miettinen, S.; Skottman, H.; Kellomäki, M. Hydrazone crosslinked hyaluronan-based hydrogels for therapeutic delivery of adipose stem cells to treat corneal defects. *Mater. Sci. Eng. C Mater. Biol. Appl.* **2018**, *85*, 68–78. [[CrossRef](#)] [[PubMed](#)]
205. Luo, Y.; Kirker, K.R.; Prestwich, G.D. Cross-linked hyaluronic acid hydrogel films: New biomaterials for drug delivery. *J. Control. Release* **2000**, *69*, 169–184. [[CrossRef](#)]
206. Kroin, J.S.; Kc, R.; Li, X.; Hamilton, J.L.; Das, V.; van Wijnen, A.J.; Dall, O.M.; Shelly, D.A.; Kenworth, T.; Im, H.J. Intraarticular slow-release triamcinolone acetate reduces allodynia in an experimental mouse knee osteoarthritis model. *Gene* **2016**, *591*, 1–5. [[CrossRef](#)] [[PubMed](#)]

207. Pirard, D.; Vereecken, P.; Mélot, C.; Heenen, M. Three percent diclofenac in 2.5% hyaluronan gel in the treatment of actinic keratoses: A meta-analysis of the recent studies. *Arch. Dermatol. Res.* **2005**, *297*, 185–189. [[CrossRef](#)] [[PubMed](#)]
208. Gao, Y.; Foster, R.; Yang, X.; Feng, Y.; Shen, J.K.; Mankin, H.J.; Hornicek, F.J.; Amiji, M.M.; Duan, Z. Up-regulation of CD44 in the development of metastasis, recurrence and drug resistance of ovarian cancer. *Oncotarget* **2015**, *6*, 9313–9326. [[CrossRef](#)] [[PubMed](#)]
209. Buffa, R.; Šedová, P.; Basarabová, I.; Bobula, T.; Procházková, P.; Vágnerová, H.; Dolečková, I.; Moravčíková, S.; Hejlová, L.; Velebný, V. A new unsaturated derivative of hyaluronic acid—Synthesis, analysis and applications. *Carbohydr. Polym.* **2017**, *163*, 247–253. [[CrossRef](#)] [[PubMed](#)]
210. Aya, K.L.; Stern, R. Hyaluronan in wound healing: Rediscovering a major player. *Wound Repair Regen.* **2014**, *22*, 579–593. [[CrossRef](#)] [[PubMed](#)]
211. Tagliagambe, M.; Elstrom, T.A.; Ward, D.B. Hyaluronic Acid Sodium Salt 0.2% Gel in the Treatment of a Recalcitrant Distal Leg Ulcer: A Case Report. *J. Clin. Aesthet. Dermatol.* **2017**, *10*, 49–51. [[PubMed](#)]
212. Neuman, M.G.; Nanau, R.M.; Oruña-Sanchez, L.; Coto, G. Hyaluronic acid and wound healing. *J. Pharm. Pharm. Sci.* **2015**, *18*, 53–60. [[CrossRef](#)] [[PubMed](#)]
213. Rueda López, J.; Segovia Gómez, T.; Guerrero Palmero, A.; Bermejo Martínez, M.; Muñoz Bueno, A.M. Hyaluronic acid: A new trend to cure skin injuries an observational study. *Rev. Enferm.* **2005**, *28*, 53–57. [[PubMed](#)]
214. Shi, L.; Zhao, Y.; Xie, Q.; Fan, C.; Hilborn, J.; Dai, J.; Ossipov, D.A. Moldable Hyaluronan Hydrogel Enabled by Dynamic Metal-Bisphosphonate Coordination Chemistry for Wound Healing. *Adv. Healthc. Mater.* **2018**, *7*. [[CrossRef](#)] [[PubMed](#)]
215. Li, H.; Xue, Y.; Jia, B.; Bai, Y.; Zuo, Y.; Wang, S.; Zhao, Y.; Yang, W.; Tang, H. The preparation of hyaluronic acid grafted pullulan polymers and their use in the formation of novel biocompatible wound healing film. *Carbohydr. Polym.* **2018**, *188*, 92–100. [[CrossRef](#)] [[PubMed](#)]
216. Berce, C.; Muresan, M.S.; Soritau, O.; Petrushev, B.; Tefas, L.; Rigo, I.; Ungureanu, G.; Catoi, C.; Irimie, A.; Tomuleasa, C. Cutaneous wound healing using polymeric surgical dressings based on chitosan, sodium hyaluronate and resveratrol. A preclinical experimental study. *Colloids Surf. B Biointerfaces* **2018**, *163*, 155–166. [[CrossRef](#)] [[PubMed](#)]
217. Sanad, R.A.; Abdel-Bar, H.M. Chitosan-hyaluronic acid composite sponge scaffold enriched with Andrographolide-loaded lipid nanoparticles for enhanced wound healing. *Carbohydr. Polym.* **2017**, *173*, 441–450. [[CrossRef](#)] [[PubMed](#)]
218. Wirostko, B.; Mann, B.K.; Williams, D.L.; Prestwich, G.D. Ophthalmic Uses of a Thiol-Modified Hyaluronan-Based Hydrogel. *Adv. Wound Care* **2014**, *3*, 708–716. [[CrossRef](#)] [[PubMed](#)]
219. Cassano, M.; Russo, G.M.; Granieri, C.; Cassano, P. Cytofunctional changes in nasal ciliated cells in patients treated with hyaluronate after nasal surgery. *Am. J. Rhinol. Allergy* **2016**, *30*, 83–88. [[CrossRef](#)] [[PubMed](#)]
220. Dahiya, P.; Kamal, R. Hyaluronic acid: A boon in periodontal therapy. *N. Am. J. Med. Sci.* **2013**, *5*, 309–315. [[CrossRef](#)] [[PubMed](#)]
221. Neumayer, T.; Prinz, A.; Findl, O. Effect of a new cohesive ophthalmic viscosurgical device on corneal protection and intraocular pressure in small-incision cataract surgery. *J. Cataract Refract. Surg.* **2008**, *34*, 1362–1366. [[CrossRef](#)] [[PubMed](#)]
222. Vandermeer, G.; Chamy, Y.; Pisella, P.J. Comparison of objective optical quality measured by double-pass aberrometry in patients with moderate dry eye: Normal saline vs. artificial tears: A pilot study. *J. Fr. Ophthalmol.* **2018**, *41*, e51–e57. [[CrossRef](#)] [[PubMed](#)]
223. Carracedo, G.; Villa-Collar, C.; Martin-Gil, A.; Serramito, M.; Santamaria, L. Comparison Between Viscous Teardrops and Saline Solution to Fill Orthokeratology Contact Lenses Before Overnight Wear. *Eye Contact Lens.* **2017**. [[CrossRef](#)] [[PubMed](#)]
224. Johnson, M.E.; Murphy, P.J.; Boulton, M. Effectiveness of sodium hyaluronate eyedrops in the treatment of dry eye. *Graefe's Arch. Clin. Exp. Ophthalmol.* **2006**, *244*, 109–112. [[CrossRef](#)] [[PubMed](#)]
225. Aragona, P.; Papa, V.; Micali, A.; Santocono, M.; Milazzo, G. Long term treatment with sodium hyaluronate-containing artificial tears reduces ocular surface damage in patients with dry eye. *Br. J. Ophthalmol.* **2002**, *86*, 181–184. [[CrossRef](#)] [[PubMed](#)]



226. Ho, W.T.; Chiang, T.H.; Chang, S.W.; Chen, Y.H.; Hu, F.R.; Wang, I.J. Enhanced corneal wound healing with hyaluronic acid and high-potassium artificial tears. *Clin. Exp. Optom.* **2013**, *96*, 536–541. [CrossRef] [PubMed]
227. Laffleur, F.; Dachs, S. Development of novel mucoadhesive hyaluronic acid derivate as lubricant for the treatment of dry eye syndrome. *Ther. Deliv.* **2015**, *6*, 1211–1219. [CrossRef] [PubMed]
228. Ghosh, P.; Guidolin, D. Potential mechanism of action of intra-articular hyaluronan therapy in osteoarthritis: Are the effects molecular weight dependent? *Semin. Arthritis Rheum.* **2002**, *32*, 10–37. [CrossRef] [PubMed]
229. Brown, T.J.; Laurent, U.B.; Fraser, J.R. Turnover of hyaluronan in synovial joints: Elimination of labelled hyaluronan from the knee joint of the rabbit. *Exp. Physiol.* **1991**, *76*, 125–134. [CrossRef] [PubMed]
230. Greenberg, D.D.; Stoker, A.; Kane, S.; Cockrell, M.; Cook, J.L. Biochemical effects of two different hyaluronic acid products in a co-culture model of osteoarthritis. *Osteoarthr. Cartil.* **2006**, *14*, 814–822. [CrossRef] [PubMed]
231. Sun, S.F.; Hsu, C.W.; Lin, H.S.; Liou, I.H.; Chen, Y.H.; Hung, C.L. Comparison of single intra-articular injection of novel hyaluronan (HYA-JOINT Plus) with synvisc-one for knee osteoarthritis: A randomized, controlled, double-blind trial of efficacy and safety. *J. Bone Joint Surg. Am.* **2017**, *99*, 462–471. [CrossRef] [PubMed]
232. Monzon, M.E.; Casalino-Matsuda, S.M.; Forteza, R.M. Identification of glycosaminoglycans in human airway secretions. *Am. J. Respir. Cell Mol. Biol.* **2006**, *34*, 135–141. [CrossRef] [PubMed]
233. Garantziotis, S.; Brezina, M.; Castelnovo, P.; Drago, L. The role of hyaluronan in the pathobiology and treatment of respiratory disease. *Am. J. Physiol. Lung Cell Mol. Physiol.* **2016**, *310*, L785–L795. [CrossRef] [PubMed]
234. Gerdin, B.; Hällgren, R. Dynamic role of hyaluronan (HYA) in connective tissue activation and inflammation. *J. Intern. Med.* **1997**, *242*, 49–55. [CrossRef] [PubMed]
235. Furnari, M.L.; Termini, L.; Traverso, G.; Barrale, S.; Bonaccorso, M.R.; Damiani, G.; Piparo, C.L.; Collura, M. Nebulized hypertonic saline containing hyaluronic acid improves tolerability in patients with cystic fibrosis and lung disease compared with nebulized hypertonic saline alone: A prospective, randomized, double-blind, controlled study. *Ther. Adv. Respir. Dis.* **2012**, *6*, 315–322. [CrossRef] [PubMed]
236. Gavina, M.; Luciani, A.; Vilella, V.R.; Esposito, S.; Ferrari, E.; Bressani, I.; Casale, A.; Bruscia, E.M.; Maiuri, L.; Raia, V. Nebulized hyaluronan ameliorates lung inflammation in cystic fibrosis mice. *Pediatr. Pulmonol.* **2013**, *48*, 761–771. [CrossRef] [PubMed]
237. Petrigli, G.; Allegra, L. Aerosolised hyaluronic acid prevents exercise-induced bronchoconstriction, suggesting novel hypotheses on the correction of matrix defects in asthma. *Pulm. Pharmacol. Ther.* **2006**, *19*, 166–171. [CrossRef] [PubMed]
238. Turino, G.M.; Ma, S.; Lin, Y.Y.; Cantor, J.O. The therapeutic potential of hyaluronan in COPD. *Chest* **2017**. [CrossRef] [PubMed]
239. Nenna, R.; Papasso, S.; Battaglia, M.; De Angelis, D.; Petrarca, L.; Felder, D.; Salvadei, S.; Berardi, R.; Roberti, M.; Papoff, P.; et al. 7% hypertonic saline and hyaluronic acid and in the treatment of infants mild-moderate bronchiolitis. *Eur. Respir. J.* **2011**, *38*, 1717.
240. Goddard, J.C.; Janssen, D.A.W. Intravesical hyaluronic acid and chondroitin sulfate for recurrent urinary tract infections: Systematic review and meta-analysis. *Int. Urogynecol. J.* **2017**. [CrossRef] [PubMed]
241. Ząbkowski, T.; Jurkiewicz, B.; Saracyn, M. Treatment of recurrent bacterial cystitis by intravesical instillations of hyaluronic acid. *Urol. J.* **2015**, *12*, 2192–2195. [PubMed]
242. American Society of Plastic Surgeons. 2017 Plastic Surgery Statistics Report. Available online: <https://www.plasticsurgery.org/documents/News/Statistics/2017/plastic-surgery-statistics-report-2017.pdf> (accessed on 8 March 2018).
243. Muhn, C.; Rosen, N.; Solish, N.; Bertucci, V.; Lupin, M.; Dansereau, A.; Weksberg, F.; Remington, B.K.; Swift, A. The evolving role of hyaluronic acid fillers for facial volume restoration and contouring: A Canadian overview. *Clin. Cosmet. Investig. Dermatol.* **2012**, *5*, 147–158. [CrossRef] [PubMed]
244. Janiš, R.; Pata, V.; Egner, P.; Pavlačková, J.; Zapletalová, A.; Kejlová, K. Comparison of metrological techniques for evaluation of the impact of a cosmetic product containing hyaluronic acid on the properties of skin surface. *Biointerphases* **2017**, *12*, 021006. [CrossRef] [PubMed]

245. Trommer, H.; Wartewig, S.; Böttcher, R.; Pöpl, A.; Hoentsch, J.; Ozegowski, J.H.; Neubert, R.H. The effects of hyaluronan and its fragments on lipid models exposed to UV irradiation. *Int. J. Pharm.* **2003**, *254*, 223–234. [CrossRef]
246. Hašová, M.; Crhák, T.; Safránková, B.; Dvořáková, J.; Muthný, T.; Velebný, V.; Kubala, L. Hyaluronan minimizes effects of UV irradiation on human keratinocytes. *Arch. Dermatol. Res.* **2011**, *303*, 277–284. [CrossRef] [PubMed]
247. Drealos, Z.D. Nutrition and enhancing youthful-appearing skin. *Clin. Dermatol.* **2010**, *28*, 400–408. [CrossRef] [PubMed]
248. Kimura, M.; Maeshima, T.; Kubota, T.; Kurihara, H.; Masuda, Y.; Nomura, Y. Adsorption of orally administered hyaluronan. *J. Med. Food* **2016**, *19*, 1172–1179. [CrossRef] [PubMed]
249. Zgheib, C.; Xu, J.; Liechty, K.W. Targeting Inflammatory Cytokines and Extracellular Matrix Composition to Promote Wound Regeneration. *Adv. Wound Care* **2014**, *3*, 344–355. [CrossRef] [PubMed]
250. Sato, T.; Iwaso, H. An effectiveness study of hyaluronic acid [Hyabest® (J)] in the treatment of osteoarthritis of the knee on the patients in the United States. *J. New Rem. Clin.* **2009**, *58*, 260–269.
251. Balogh, L.; Polyak, A.; Mathe, D.; Kiraly, R.; Thuroczy, J.; Terez, M.; Janoki, G.; Ting, Y.; Bucci, L.R.; Schauss, A.G. An effectiveness study of hyaluronic acid [Hyabest® (J)] in the treatment of osteoarthritis of the knee on the patients in the United States. *J. Agric. Food Chem.* **2008**, *56*, 10582–10593. [CrossRef] [PubMed]
252. Oe, M.; Mitsugi, K.; Odanaka, W.; Yoshida, H.; Matsuoka, R.; Seino, S.; Kanemitsu, T.; Masuda, Y. Dietary hyaluronic acid migrates into the skin of rats. *Sci. World J.* **2014**, *2014*, 378024. [CrossRef] [PubMed]
253. Solà, R.; Valls, R.M.; Martorell, I.; Giral, M.; Pedret, A.; Taltavull, N.; Romeu, M.; Rodríguez, À.; Moriña, D.; Lopez de Frutos, V.; Montero, M.; et al. A low-fat yoghurt supplemented with a rooster comb extract on muscle joint function in adults with mild knee pain: A randomized, double blind, parallel, placebo-controlled, clinical trial of efficacy. *Food Funct.* **2015**, *6*, 3531–3539. [CrossRef] [PubMed]
254. Göllner, I.; Voss, W.; von Hehn, U.; Kammerer, S. Ingestion of an Oral Hyaluronan Solution Improves Skin Hydration, Wrinkle Reduction, Elasticity, and Skin Roughness: Results of a Clinical Study. *J. Evid. Based Complement. Altern. Med.* **2017**, *22*, 816–823. [CrossRef] [PubMed]
255. Kawada, C.; Yoshida, T.; Yoshida, H.; Matsuoka, R.; Sakamoto, W.; Odanaka, W.; Sato, T.; Yamasaki, T.; Kanemitsu, T.; Masuda, Y.; et al. Ingested hyaluronan moisturizes dry skin. *Nutr. J.* **2014**, *13*, 70. [CrossRef] [PubMed]
256. Kawada, C.; Yoshida, T.; Yoshida, H.; Sakamoto, W.; Odanaka, W.; Sato, T.; Yamasaki, T.; Kanemitsu, T.; Masuda, Y.; Urushibata, O. Ingestion of hyaluronans (molecular weights 800 k and 300 k) improves dry skin conditions: A randomized, double blind, controlled study. *J. Clin. Biochem. Nutr.* **2015**, *56*, 66–73. [CrossRef] [PubMed]
257. Kawada, C.; Kimura, M.; Masuda, Y.; Nomura, Y. Oral administration of hyaluronan prevents skin dryness and epidermal thickening in ultraviolet irradiated hairless mice. *J. Photochem. Photobiol. B* **2015**, *153*, 215–221. [CrossRef] [PubMed]
258. Oe, M.; Tashiro, T.; Yoshida, H.; Nishiyama, H.; Masuda, Y.; Maruyama, K.; Koikeda, T.; Maruya, R.; Fukui, N. Oral hyaluronan relieves knee pain: A review. *Nutr. J.* **2016**, *15*, 11. [CrossRef] [PubMed]
259. Larson, B. 3D Cell Culture: A Review of Current Techniques. 2015. Available online: <http://mktg.biotek.com/news/2015/Fall/featured-application.html> (accessed on 14 June 2018).
260. Gurski, L.A.; Jha, A.K.; Zhang, C.; Jia, X.; Farach-Carson, M.C. Hyaluronic acid-based hydrogels as 3D matrices for in vitro evaluation of chemotherapeutic drugs using poorly adherent prostate cancer cells. *Biomaterials* **2009**, *30*, 6076–6085. [CrossRef] [PubMed]
261. Jeffery, A.F.; Churchward, M.A.; Mushahwar, V.K.; Todd, K.G.; Elias, A.L. Hyaluronic acid-based 3D culture model for in vitro testing of electrode biocompatibility. *Biomacromolecules* **2014**, *15*, 2157–2165. [CrossRef] [PubMed]
262. Ouyang, L.; Highley, C.B.; Rodell, C.B.; Sun, W.; Burdick, J.A. 3D Printing of Shear-Thinning Hyaluronic Acid Hydrogels with Secondary Cross-Linking. *ACS Biomater. Sci. Eng.* **2016**, *2*, 1743–1751. [CrossRef]
263. Fallacara, A.; Busato, L.; Pozzoli, M.; Ghadiri, M.; Ong, H.X.; Young, P.M.; Manfredini, S.; Traini, D. Combination of urea-crosslinked Hyaluronic acid and sodium ascorbyl phosphate for the treatment of inflammatory lung diseases: An in vitro study. *Eur. J. Pharm. Sci.* **2018**, *120*, 96–106. [CrossRef] [PubMed]



© 2018 by the authors. Licensee MDPI, Basel, Switzerland. This article is an open access article distributed under the terms and conditions of the Creative Commons Attribution (CC BY) license (<http://creativecommons.org/licenses/by/4.0/>).



Contents lists available at ScienceDirect

European Journal of Pharmaceutical Sciences

journal homepage: [www.elsevier.com/locate/ejps](http://www.elsevier.com/locate/ejps)

## Combination of urea-crosslinked hyaluronic acid and sodium ascorbyl phosphate for the treatment of inflammatory lung diseases: An *in vitro* study

Arianna Fallacara<sup>a,b</sup>, Laura Busato<sup>a,b</sup>, Michele Pozzoli<sup>a</sup>, Maliheh Ghadiri<sup>a</sup>, Hui Xin Ong<sup>a</sup>, Paul M. Young<sup>a</sup>, Stefano Manfredini<sup>b</sup>, Daniela Traini<sup>a,\*</sup>

<sup>a</sup> Respiratory Technology, Woolcock Institute of Medical Research and Discipline of Pharmacology, Sydney Medical School, The University of Sydney, 431 Glebe Point Road, Glebe, NSW 2037, Australia

<sup>b</sup> Department of Life Sciences and Biotechnology, University of Ferrara, Via L. Borsari 46, 44121 Ferrara, Italy.



### ARTICLE INFO

#### Keywords:

Anti-inflammatory  
Antioxidant  
Hyaluronic acid  
Sodium ascorbyl phosphate  
Urea-crosslinked hyaluronic acid  
Wound healing

### ABSTRACT

This *in vitro* study evaluated, for the first time, the safety and the biological activity of a novel urea-crosslinked hyaluronic acid component and sodium ascorbyl phosphate (HA-CL – SAP), singularly and/or in combination, intended for the treatment of inflammatory lung diseases. The aim was to understand if the combination HA-CL – SAP had an enhanced activity with respect to the combination native hyaluronic acid (HA) – SAP and the single SAP, HA and HA-CL components. Sample solutions displayed pH, osmolality and viscosity values suitable for lung delivery and showed to be not toxic on epithelial Calu-3 cells at the concentrations used in this study. The HA-CL – SAP displayed the most significant reduction in interleukin-6 (IL-6) and reactive oxygen species (ROS) levels, due to the combined action of HA-CL and SAP. Moreover, this combination showed improved cellular healing (wound closure) with respect to HA – SAP, SAP and HA, although at a lower rate than HA-CL alone. These preliminary results showed that the combination HA-CL - SAP could be suitable to reduce inflammation and oxidative stress in lung disorders like acute respiratory distress syndrome, asthma, emphysema and chronic obstructive pulmonary disease, where inflammation is prominent.

### 1. Introduction

The airway epithelium is directly exposed to the external environment and, consequently, it is strongly responsive to exogenous toxic substances like cigarette smoke, biophysical and biological stresses. All these factors, in combination with genetic predisposition and age, are involved in the pathogenesis of bronchopulmonary diseases. Respiratory pathologies - like asthma, chronic obstructive pulmonary disease (COPD), emphysema, acute respiratory distress syndrome (ARDS) and cystic fibrosis - affect millions of people every year and are amongst the main causes of mortality (Burney et al., 2015; Crotty Alexander et al., 2015; Ferkol and Schraufnagel, 2014; World Health Organization, 2017; Yang et al., 2017). Furthermore, patients require more effective treatments, as numerous of them will become non-responsive to the conventional corticosteroid therapy (Barnes, 2013;

Jiang and Zhu, 2016). Considering that inflammation and oxidative stress represent the principal mechanisms underlying the development and progression of many lung diseases (Kleniewska and Pawliczak, 2017; MacNee, 2001; Moldoveanu et al., 2009; Nichols and Chmiel, 2015; Oudijk et al., 2003), the use of anti-inflammatory and antioxidant compounds as adjunctive therapy could be a promising approach to restore and maintain normal lung functions, possibly by reducing drug resistant refractory phenomena. To this end, several recent researches have investigated the therapeutic value of naturally occurring biomolecules –such as vitamins, hyaluronan, polyphenols, and herbal active compounds - and of their derivatives (Bharara et al., 2016; Garantziotis et al., 2016; Li and Li, 2016; Park et al., 2016; Pincikova et al., 2017; Yeo et al., 2017; Zemmouri et al., 2017).

Vitamin C (i.e. ascorbic acid) is a physiological low-molecular weight antioxidant. In the lung, it is able to regulate the innate immune

**Abbreviations:** ALL, air-liquid interface; ARDS, acute respiratory distress syndrome; COPD, chronic obstructive pulmonary disease; DCF, dichlorofluorescein; DCFH-DA, 2',7'-dichlorofluorescein diacetate; ELISA, enzyme-linked immuno assay; FBS, foetal bovine serum; H<sub>2</sub>O<sub>2</sub>, hydrogen peroxide; HA, hyaluronic acid; HA-CL, urea-crosslinked hyaluronic acid; IC50, half maximal inhibitory concentration; IL-6, interleukin-6; IL-8, interleukin-8; LDH, lactate dehydrogenase; LPS, lipopolysaccharide; MTS, methyl tetrazolium salt; PBS, phosphate buffer saline; ROS, reactive oxygen species; SAP, sodium ascorbyl phosphate; TEER, transepithelial electrical resistance;  $\eta_0$ , zero-shear rate viscosity

\* Corresponding author.

**E-mail addresses:** flrnn@unife.it (A. Fallacara), laura01.busato@student.unife.it (L. Busato), michele.pozzoli@sydney.edu.au (M. Pozzoli), maliheh.ghadiri@sydney.edu.au (M. Ghadiri), ong.hui@sydney.edu.au (H.X. Ong), paul.young@sydney.edu.au (P.M. Young), mv9@unife.it (S. Manfredini), daniela.traini@sydney.edu.au (D. Traini).

<https://doi.org/10.1016/j.ejps.2018.04.042>

Received 24 November 2017; Received in revised form 16 March 2018; Accepted 27 April 2018

Available online 30 April 2018

0928-0987 / © 2018 Elsevier B.V. All rights reserved.



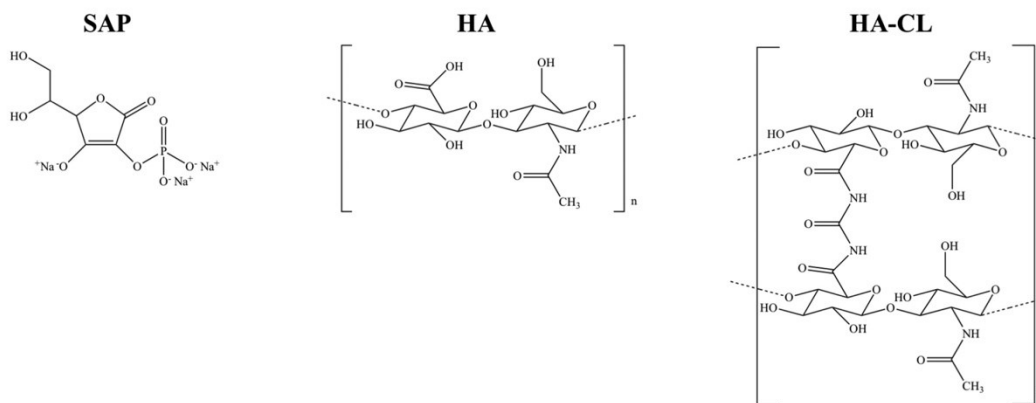


Fig. 1. Chemical structures of SAP, HA and HA-CL.

system, maintain host defence and function of the airway epithelial barrier (Li and Li, 2016). Indeed, vitamin C reduces the oxidative stress provoked by inhaled pollutants or irritants, thus limiting cellular damage induced by inflammatory-derived oxidants at the air-lung interface (Larsson et al., 2015). Moreover, vitamin C supplementation reduces acute lung inflammatory response, thus exhibiting a potential preventive and therapeutic role (Silva Bezerra et al., 2006). High doses of intravenous vitamin C with antioxidant and anti-inflammatory properties have been shown to be efficient as adjunctive therapy for recurrent ARDS (Bharara et al., 2016). Although the use of vitamin C to treat pulmonary impairments is still investigational, many studies have suggested its benefits against lung infections (Hemilä and Louhiala, 2007), COPD (Pirabbasi et al., 2016), asthma attacks, bronchial hyper-sensitivity (Hemilä, 2013) and smoke-induced pulmonary emphysema (Koike et al., 2014).

Sodium ascorbyl phosphate (SAP, Fig. 1) is a salt form of ascorbic acid 2-phosphate, and it is a hydrophilic derivative of vitamin C characterized by improved physico-chemical stability. SAP has already shown important antioxidant properties for dermal application (Klock et al., 2005; Spiclin et al., 2003). Additionally, even if to a lesser extent in comparison to magnesium ascorbyl phosphate (another salt of ascorbic acid 2-phosphate), SAP has been shown to stimulate collagen synthesis in cultures of human dermal fibroblasts (Geesin et al., 1993). Hence, SAP may be involved in wound healing processes like magnesium ascorbyl phosphate, which was found to be able not only to promote collagen synthesis (Amirlak et al., 2016; Geesin et al., 1993), but also to increase cell motility and fibroblast proliferation during skin reparation (Duarte et al., 2009; Stumpf et al., 2011).

Hyaluronic acid (HA, Fig. 1) is a biocompatible, biodegradable, visco-elastic and mucoadhesive glycosaminoglycan consisting of repeating dimeric units of D-glucuronic acid and N-acetyl-D-glucosamine (Fallacara et al., 2017a; Kakehi et al., 2003; Liao et al., 2005; Mayol et al., 2008; Toole, 2004). In humans, HA is ubiquitous, and in the lung its total content under physiological condition is approximately 160 mg (Turino and Cantor, 2003). Specifically, in the lung, the high-molecular-weight of HA exerts anti-inflammatory and anti-angiogenic actions, promotes cell survival, organizes extracellular matrix, stabilizes connective tissues, regulates hydration and water homeostasis (Garantziotis et al., 2016; Gerdin and Hällgren, 1997). Due to all these physico-chemical and biological properties, exogenous HA represents a promising multifunctional agent for the treatment of lung diseases, as it can be used as a drug carrier with intrinsic therapeutic potential (Garantziotis et al., 2016; Li et al., 2017; Martinelli et al., 2017; Surendrakumar et al., 2003). Emerging studies support the use of high-

molecular-weight (> 1 MDa) HA to treat airway diseases whose pathogenesis involves inflammation, oxidative stress and epithelial remodelling (Allegra et al., 2008; Buonpensiero et al., 2010; Cantor et al., 2005, 2011; Furnari et al., 2012; Garantziotis et al., 2016; Gavina et al., 2013; Jiang et al., 2005, 2010; Lennon and Singleton, 2011; Maiz Carro et al., 2012; Petrigli and Allegra, 2006; Savani et al., 2001; Souza-Fernandes et al., 2006; Venge et al., 1996). Two inhalation products containing HA as active ingredient are currently marketed: Hyaneb® (Chiesi Farmaceutici, IT) and Yabro® (Ibsa Farmaceutici, IT). Hyaneb® is a hypertonic saline solution containing HA (molecular-weight 0.5 MDa, 0.1% w/v) to hydrate and consequently, reduce mucus viscosity in cystic fibrosis patients (Nenna et al., 2011). Yabro®, on the other hand, is a high viscosity nebuliser solution of hyaluronan (molecular-weight 0.8–1 MDa, 0.3% w/v) to treat bronchial hyper-reactivity due to irritants inhalation or physical stress (Gelardi et al., 2013).

To improve hyaluronan activity and potential for its use as therapeutic agent, several derivatives have been synthesized (Williams et al., 2017). In this study, a novel urea-crosslinked hyaluronic acid (HA-CL, Fig. 1) was investigated for pulmonary application. HA-CL is a patented (Citernes et al., 2015, WO/2015/007773 A1) biocompatible and biodegradable polymer, with enhanced consistency in comparison to native HA (Citernes et al., 2015, WO/2015/007773 A1; Fallacara et al., 2017a), due to its crosslinking with urea, a molecule naturally occurring and therapeutically employed as hydrating and re-epithelializing agent (Albèr et al., 2013; Charlton et al., 1996; Pan et al., 2013).

In this context, the focus of the present *in vitro* bio-investigation was to evaluate the cytotoxicity and the bioactivity - anti-inflammatory, antioxidant and wound healing properties - of these components, vitamin C and hyaluronic acid (HA) derivatives, used singularly and in combination, on Calu-3 lung carcinoma derived epithelia cells.

## 2. Materials and methods

### 2.1. Materials

Native hyaluronic acid (HA, *i.e.* sodium hyaluronate, molecular weight 1.2 MDa) and urea-crosslinked hyaluronic acid (HA-CL, molecular weight 2.0–4.0 MDa – raw material containing also pentylene glycol) were kindly donated by IRAlab (Usmate Velate, Monza-Brianza, Italy) and used as supplied. Sodium ascorbyl phosphate (SAP) was purchased from DSM Nutritional Products Ltd. (Segrate, Milano, Italy). Calu-3 cells were supplied by American Type Cell Culture Collection (ATCC, Rockville, USA). Transwell® polyester cell inserts (0.33 cm<sup>2</sup>



surface area, 0.4 µm pore size) were obtained from Corning by Sigma-Aldrich (Australia). Triton®X-100, L-ascorbic acid, 2',7'-dichlorofluorescein diacetate (DCFH-DA), lipopolysaccharide (LPS) from *Escherichia coli*, non-essential amino acids solution, 200 mM L-glutamine solution were purchased from Sigma-Aldrich (Milan, Italy, and Sydney, Australia). Other cell culture reagents including Dulbecco's Modified Eagle's medium/F-12, phosphate buffer saline (PBS) and foetal bovine serum (FBS) were obtained from Gibco by ThermoFisher Scientific (Sydney, Australia). Hydrogen Peroxide (H<sub>2</sub>O<sub>2</sub>) 6% (w/v) was supplied by Gold Cross (Spring Hill, Australia). Methyl tetrazolium salt (MTS) reagent - CellTiter 96® Aqueous One Solution Cell Proliferation Assay - and lactate dehydrogenase (LDH) assay kit - RayBio LDH-Cytotoxicity assay kit II - for cell viability tests were purchased from Promega (Sydney, Australia) and RayBiotech (Kirrawee, Australia), respectively. Collagen Type I and enzyme-linked immuno assay (ELISA) kits for determination of the inflammation markers interleukin-6 (IL-6) and interleukin-8 (IL-8) were obtained from BD Bioscience (Sydney, Australia). Water was purified by Milli-Q reverse Osmosis (Molsheim, France).

## 2.2. Preparation and physico-chemical characterization of hyaluronan and SAP samples

To evaluate the *in vitro* cytotoxicity and biological activities of the novel combinations HA-CL – SAP and HA – SAP on Calu-3 lung cells, sample solutions were aseptically prepared. SAP was employed with a concentration of 0.45% (w/v), since high doses of ascorbate are necessary to obtain a significant therapeutic activity (Bharara et al., 2016; Li and Li, 2016). Hyaluronan was used at 0.15% (w/v), a concentration similar to those of commercially available products for inhalation (0.1–0.3% w/v) (Gelardi et al., 2013; Nenna et al., 2011), and ideal to improve drug bioavailability from lung compared to simple drug solutions (Morimoto et al., 2001). Thus, hyaluronan-SAP (0.15–0.45% w/v) solutions<sup>1</sup> were formulated by dissolving polymers and drug into 10 mL of FBS-free cell culture medium that was kept under constant and gentle magnetic stirring overnight, at room temperature. In the same way, 0.45% (w/v) SAP, 0.15% (w/v) HA and 0.15% (w/v) HA-CL<sup>1</sup> solutions were prepared as comparison.

Before performing the biological study, all the solutions were subjected to physico-chemical characterization.

pH and osmolality were assessed using a Docu-pH<sup>+</sup> meter (Sartorius Mechatronics, Goettingen, Germany) and a 5500 Vapor Pressure Osmometer (Wescor, Logan, United States). Viscosity analyses were carried out at 37 ± 2 °C with a rotational rheometer AR2000 (TA instruments, New Castle, USA) connected to the Rheology Advantage software (version V7.20). The rheometer was equipped with an aluminium cone/plate geometry –diameter 40 mm, angle 2°, 64 µm truncation-, and with a solvent trap to prevent samples dehydration. Shear rate sweep tests were carried out under steady state condition: after 1-min equilibration time, the shear rate ( $\dot{\gamma}$ ) was progressively increased from 0.01 to 1000 s<sup>-1</sup>. Zero-shear rate viscosity ( $\eta_0$ ) of the solutions was determined by fitting the viscosity curves according to the Cross equation (Cross, 1968) (Eq. (1)):

$$\eta = \eta_{\infty} + \frac{\eta_0 - \eta_{\infty}}{1 + (C \cdot \dot{\gamma})^n} \quad (1)$$

where  $\eta$  is the viscosity at a given shear rate (Pa·s),  $\dot{\gamma}$  is the shear rate (s<sup>-1</sup>),  $\eta_0$  is the zero-shear rate viscosity (Pa·s),  $\eta_{\infty}$  is the infinite-shear rate viscosity (Pa·s),  $C$  is a multiplicative parameter (s) and  $n$  is a dimensionless exponent. Data are reported as mean ± standard deviations of three independent analyses. As control, pH, osmolality and viscosity of cell culture medium alone were assayed as well.

<sup>1</sup> Note: HA-CL was provided as raw material containing pentylene glycol. Therefore, 0.15% (w/v) HA-CL solutions contained also 0.11% (w/v) pentylene glycol.

## 2.3. Cell culture

The lung epithelia cancer derived Calu-3 cell line was chosen as *in vitro* respiratory model. This cell line has been well characterized and reflects the main characteristics and secretory activity of the airway epithelium when grown at an air-liquid interface (ALI) (Haghi et al., 2010). The ALI model allows for cell differentiation in terms of mucus secretion, tight junction generation and protein expressions to mimic the physiological conditions (Haghi et al., 2010).

Calu-3 cells were cultured between passages 38 to 43 in 75 cm<sup>2</sup> flasks containing Dulbecco's Modified Eagle's medium/F-12 enriched with 10% (v/v) foetal bovine serum (FBS), 1% (v/v) non-essential amino acids solution and 1% (v/v) L-glutamine solution. Cells were maintained in a humidified 95% air, 5% CO<sub>2</sub> atmosphere, at 37 °C, until confluency was reached. The medium was replaced three times a week and cells were passaged according to American Type Culture Collection Recommendations - ATCC guidelines.

## 2.4. LDH and MTS cytotoxicity assays

The *in vitro* cytotoxicities of hyaluronan-SAP (0.15–0.45% w/v) solutions and their single components - 0.45% (w/v) SAP, 0.15% (w/v) HA and 0.15% (w/v) HA-CL - were evaluated on Calu-3 cells by performing a LDH test. A commercial LDH assay kit was used to quantify the amount of LDH released into the cell culture medium, directly related to cell membrane damage. Extracellular LDH in the medium was measured by a coupled enzymatic reaction in which LDH catalysed lactate conversion into pyruvate, thus provoking the final production of formazan, a dye whose intensity was directly correlated with the number of cells lysed (Chan et al., 2013). Briefly, Calu-3 cells were seeded with a density of 5 × 10<sup>4</sup> cells/well in a volume of 100 µL into a 96 well-plate. Cells were incubated overnight at 37 °C in a humidified atmosphere at 5% CO<sub>2</sub>. Supernatant was replaced with 100 µL of pre-warmed treatments, and cells incubated at the same conditions for another 24 h. Background controls (medium), negative controls (untreated cells) and positive controls (cells treated with 1% w/v Triton®X-100) were included in the experiment. 10 µL of cell culture supernatant was withdrawn and transferred into a new 96 well-plate, followed by the addition of 100 µL of reaction mixture from LDH kit. After 30 min of light-protected incubation at room temperature, LDH activity was quantified by measuring the absorbance with a SpectraMax microplate reader at 450 nm. Experiments were performed in triplicate. Cytotoxicity was calculated according to the following equation (Eq. 2), and presented as the percentage of LDH leakage of each treatment compared to the positive control:

$$LDH \text{ release (\%cell death)} = \frac{\text{Test sample} - \text{negative control}}{\text{Positive control} - \text{negative control}} \times 100 \quad (2)$$

A MTS assay was also performed on Calu-3 cells to measure cytotoxicity on cellular metabolic activity as a function of HA – SAP and HA-CL – SAP solution concentrations. MTS assay is a colorimetric test based on tetrazolium reduction into formazan. This reaction occurs only in metabolic active cells (Riss et al., 2004). Briefly, 100 µL of 5 × 10<sup>4</sup> cells/well were seeded into a 96 well-plate. Cells were incubated overnight at 37 °C in a humidified atmosphere at 5% CO<sub>2</sub>. On the second day, 100 µL of pre-warmed treatments were added to the seeded cells with progressively diluted concentration. Indeed, maintaining hyaluronan-SAP ratio constant to 1–3, a concentration range from 12.6 mM SAP (which corresponded to a solution containing 0.15% hyaluronan and 0.45% SAP) to 1.5 µM SAP was tested. Background controls (medium) and untreated controls (untreated cells) were included in the experiment. After 24 h of incubation with treatments at 37 °C, in a humidified atmosphere at 5% CO<sub>2</sub>, Calu-3 cells were incubated for another 4 h, in the same conditions, with 20 µL of MTS solution. Finally, the 96 well-plate was read at 490 nm using a

SpectraMax microplate reader. The absorbance values were directly proportional to cell viability (%). Experiments were performed in triplicate. Data were expressed as % cell viability relative to untreated control, and plotted against SAP concentration (nM) on a logarithmic scale.

Considering the results of the cytotoxicity tests, all the following biological assays were performed with the most concentrated solutions: 0.15–0.45% (w/v) HA – SAP and HA-CL – SAP, 0.45% (w/v) SAP, 0.15% (w/v) HA and (w/v) HA-CL.

### 2.5. Evaluation of epithelial barrier integrity

The epithelial barrier function was studied using an electrically-based method, consisting of transepithelial electrical resistance (TEER) measurements. Briefly, Calu-3 cells were seeded on Transwell polyester inserts at density of  $1.65 \times 10^5$  cell/insert, and maintained in a humidified 95% air, 5% CO<sub>2</sub> atmosphere, at 37 °C. After 24 h, the apical chamber medium was removed and the cells were maintained in the basolateral chamber, where the medium was replaced every alternate day with 600 µL of fresh medium to establish an ALI model over 12–14 days. 200 µL of treatments - 0.15–0.45% (w/v) hyaluronan-SAP, 0.45% (w/v) SAP, 0.15% (w/v) HA and 0.15% (w/v) HA-CL solutions - were added to the apical side, and after 4 h the resistance was measured using a EVOM voltohmmeter (World Precision Instrument, Sarasota, USA) connected to STX-2 chopstick electrodes. Blank controls (cell-free inserts containing medium) and untreated controls (inserts of cells in medium) were included in the study. Experiments were performed in triplicate. TEER ( $\Omega\text{cm}^2$ ) was calculated from the measured potential resistance difference ( $\Omega$ ) between the apical and basolateral sides, normalized by subtracting the blank insert and multiplying by the area of the Transwell inserts, according to the following equation (Eq. 3):

$$TEER (\Omega\text{cm}^2) = (Resistance_{test} - Resistance_{blank}) \times 0.33 \quad (3)$$

### 2.6. Pro-inflammatory markers expression

The expressions of the pro-inflammatory cytokines, IL-6 and IL-8, were evaluated in Calu-3 cells treated with 0.15–0.45% (w/v) hyaluronan-SAP, 0.45% (w/v) SAP, 0.15% (w/v) HA and 0.15% (w/v) HA-CL solutions.

The effects of test solutions were compared with untreated cells and positive controls, i.e. cells exposed to 10 ng/mL LPS. In this experiment, 1 mL of  $5 \times 10^5$  cells/well was seeded into a 24-well plate. Cells were incubated overnight at 37 °C in a humidified atmosphere at 5% CO<sub>2</sub>. On the second day, cell culture medium was withdrawn and replaced with 1 mL of pre-warmed treatments. Calu-3 were then incubated for 24 h at 37 °C, in a humidified atmosphere at 5% CO<sub>2</sub>, to allow for the production of IL-6 and IL-8. After that, cell culture supernatant was collected, centrifuged (5 min, 13,000 rpm, 4 °C) and analysed for IL-6 and IL-8 levels using human IL-6 and IL-8 ELISA kits, according to the manufacturer's instructions. The amounts of cytokines released in the test samples were determined using standard calibration curves obtained with purified recombinant human IL-6 and IL-8 provided with the kit. The limits of detection were 4.7–300 pg/mL for IL-6 and 3.1–200 pg/mL for IL-8. Experiments were performed in triplicate.

The anti-inflammatory efficacy of the samples was evaluated by their ability to reduce inflammation in Calu-3 cells after induction of inflammatory cytokines production by LPS. Calu-3, seeded into a 24-well plate as previously described, were incubated with 10 ng/mL LPS for 24 h at 37 °C, in a humidified atmosphere at 5% CO<sub>2</sub>. Cells were subsequently treated with hyaluronan and/or SAP solutions and, after 24 h of incubation, cell culture supernatant was withdrawn, centrifuged (5 min, 13,000 rpm, 4 °C) and analysed for IL-6 and IL-8 levels as previously described.

### 2.7. Analysis of intracellular reactive oxygen species (ROS)

Oxidative stress was evaluated by quantification of intracellular ROS produced by Calu-3 cells treated with 0.15–0.45% (w/v) hyaluronan-SAP, 0.45% (w/v) SAP, 0.15% (w/v) HA and 0.15% (w/v) HA-CL solutions, with and without LPS induction. ROS levels were determined by conversion of the non-fluorescent DCFH-DA into the fluorescent dichlorofluorescein (DCF).

Briefly, 100 µL of Calu-3 cells were seeded with a density of  $5 \times 10^4$  cells/well into a 96 well-plate, incubated overnight at 37 °C in a humidified atmosphere at 5% CO<sub>2</sub>. Afterwards, Calu-3 were incubated in the dark for 30 min (37 °C, 5% CO<sub>2</sub>) with 100 µL of 5 µM DCFH-DA (Wu and Yotnda, 2011). Then, DCFH-DA containing medium was removed and 100 µL of treatment was added to DCFH-DA-loaded cells, protected from light. Background controls (medium), untreated and unlabelled controls (untreated and unlabelled cells), untreated controls (untreated cells), negative controls (cells treated with 1 mM L-ascorbic acid) and positive controls (cells treated with 0.03% H<sub>2</sub>O<sub>2</sub>) were included in the experiment. After 10 min of incubation (37 °C, 5% CO<sub>2</sub>), cell supernatant was withdrawn and transferred into a 96-well plate for fluorescence analysis by a SpectraMax microplate reader with excitation filter set at 485 nm and emission filter set at 520 nm. Experiments were performed in triplicate and results were expressed as % of ROS production relative to untreated control.

The antioxidant activity of the samples was also investigated by their ability to reduce oxidative stress in Calu-3 cells after induction of ROS production by 10 ng/mL LPS.

### 2.8. Electric cell-substrate impedance sensing (ECIS) wound healing assay

The ECIS system (ECIS Z0, Applied Biophysics, NY, USA) was used to apply an electrical current to create a wound on the Calu-3 monolayer and investigate the healing process over time. Briefly, 500 µL of Calu-3 cells were seeded at  $5 \times 10^5$  cells/well in collagen coated 8W1E arrays (Applied Biophysics, NY, USA) and allowed to grow for 24 h, directly contacting the gold film surface of the microelectrode – 250 µm diameter. Culture medium was used as electrolyte. Once the cells reached confluency, an elevated electrical field (2000 µA, 60 s, 100 kHz) was applied to wound the epithelial layer. Subsequently, cell debris were washed with sterile PBS and 300 µL of the different pre-warmed treatments were added to each well: 0.15–0.45% (w/v) hyaluronan-SAP, 0.45% (w/v) SAP, 0.15% (w/v) HA and 0.15% (w/v) HA-CL solutions. Wounded but untreated cells were also included in the experiment as control. The study was carried out in an incubator at 37 °C, with a humidified 5% CO<sub>2</sub> atmosphere. After wounding, resistance ( $\Omega$ ) across the cell layer was measured every 5 min for > 30 h, and data were collected and analysed using the ECIS software, according to the principle of ECIS measurements (Balasubramanian et al., 2008; Stolwijk et al., 2015). Resistance was normalized by dividing the resistance values from electrodes confluent with cells by the corresponding quantities for the cell-free electrodes.

### 2.9. Statistical analysis

Data are presented as mean  $\pm$  standard deviation of three independent experiments. Statistical analysis was performed using GraphPad Prism software version 7.0 b (GraphPad, San Diego, USA). One-way analysis of variance (ANOVA) followed by Tukey *post hoc* test for multiple comparisons was used to determine statistical significance (\*P < 0.05, \*\*P < 0.01, \*\*\*P < 0.001 and \*\*\*\*P < 0.0001).

## 3. Results and discussion

Both hyaluronic acid (Allegra et al., 2008; Buonpensiero et al., 2010; Cantor et al., 2005, 2011; Furnari et al., 2012; Garantziotis et al., 2016; Gavina et al., 2013; Jiang et al., 2005; Lennon and Singleton,



2011; Maiz Carro et al., 2012; Petrigni and Allegra, 2006; Savani et al., 2001; Souza-Fernandes et al., 2006; Venge et al., 1996) and vitamin C (Berger and Oudemans-van Straaten, 2015; Bharara et al., 2016; Bracher et al., 2012; Fisher et al., 2012; Garcia-Larsen et al., 2016; Gupta et al., 2016; Hemila, 2014; Jin et al., 2016; Li and Li, 2016; Park et al., 2016; Sawyer et al., 1989) have shown potential as adjunctive treatments for lung diseases with inflammatory and oxidative components. Therefore, the present *in vitro* study was devised to investigate the safety and efficacy of the novel hyaluronan – SAP on Calu-3 human epithelial cells. More specifically, the biological activity of SAP combined with HA-CL with urea, a recently synthesized promising polymer (Citernesi et al., 2015, WO/2015/007773 A1; Fallacara et al., 2017a; Fallacara et al., 2017b), has been investigated. This novel combination was evaluated in comparison to the native HA – SAP, and to the single components SAP, HA and HA-CL, to understand if an enhanced activity was present, and whether the crosslinked polymer had an added therapeutic value. Prior to any anti-inflammatory, antioxidant and wound healing tests, the potential cytotoxicity effect of hyaluronan and SAP (in combination and as single components) towards Calu-3 epithelia was evaluated. Moreover, the physico-chemical behaviour of the sample solutions was examined.

### 3.1. Physico-chemical properties of hyaluronan and SAP solutions

Prior to the biological study, the physico-chemical behaviour of the test solutions was analysed to evaluate the samples suitability for direct delivery on the lung epithelium (Forbes et al., 2000). To achieve optimal physico-chemical properties for airway tolerability, test formulations should have a pH close to neutrality (7.4) and an osmolality between 150 and 550 mosm/Kg, although small variations can be tolerated (Alhanout et al., 2011; Wong-Beringer et al., 2005).

As shown in Table 1, samples displayed an almost neutral pH for lung epithelium. More precisely, HA and HA-CL did not affect the pH of Calu-3 medium, which remained constant at 7.7. The addition of SAP to cell medium increased the pH to 8.1, regardless of the presence of hyaluronan. Nevertheless, these pH variations were not significant for Calu-3 tolerability, as all the solutions were biocompatible, as confirmed by the subsequent viability results. In regards to the sample's osmolality, all the test solutions showed values ranging between  $312.0 \pm 1.7$  (HA) and  $363.0 \pm 0.0$  mOsm/Kg (HA-CL – SAP) - Table 1 - that is also suitable for lung delivery.

Another important physico-chemical parameter that was assessed was viscosity, as it affects drug absorption rate. Previous studies reported that sodium hyaluronate solutions, being viscous and mucoadhesive, were able to control and enhance the absorption of drugs and, hence, improve their pharmacological availability from the lung, compared to the less viscous drugs solutions (Morimoto et al., 2001; Yamamoto et al., 2004). As shown in Table 1, 0.15–0.45% (w/v) HA – SAP and HA-CL – SAP solutions were more viscous ( $4.5 \pm 0.2$  and  $5.5 \pm 1.0$  mPa-s, respectively) than 0.45% (w/v) SAP solution ( $1.0 \pm 0.0$  mPa-s) -  $P < 0.0001$ . Indeed, HA and HA-CL acted as rheological agents, significantly increasing ( $P < 0.0001$ ) the viscosity of the cell culture medium from  $1.4 \pm 0.0$  to  $8.2 \pm 0.3$  and

$12.1 \pm 0.8$  mPa-s, respectively. Therefore, hyaluronate solutions seemed to be promising vehicle for pulmonary delivery of SAP, as they might be useful to guarantee high local drug concentration.

### 3.2. LDH and MTS cytotoxicity assays

The cytotoxicity of hyaluronan and/or SAP solutions on Calu-3 cells was evaluated via changes in cell membrane damage (LDH assay) and cell metabolic activity (MTS assay).

Sample solutions of HA – SAP, HA-CL – SAP, SAP, HA and HA-CL, at the selected concentrations of 0.15% (w/v) hyaluronan and 0.45% (w/v) SAP, respectively, were added to Calu-3 cells which underwent a LDH assay after 24 h. As displayed in Fig. 2A, none of these samples showed LDH release, thus indicating that treated Calu-3 cells maintained viability ( $P > 0.05$ ). On the contrary, cells exposure to 1% Triton<sup>®</sup>X-100, a toxic compound used as positive control, significantly increased LDH release in comparison with untreated cells control ( $P < 0.0001$ ), confirming cell death as expected. Thus, all the test samples, at the selected concentrations, showed to be non-toxic on the Calu-3 epithelial cells.

To further confirm these results, Calu-3 cells were incubated for 24 h with HA – SAP and HA-CL – SAP solutions characterized by concentration ranging from 1.5  $\mu$ M to 12.6 mM SAP, and by a constant 1–3 polymer-drug ratio. Viability was assessed using a MTS assay. As shown in Fig. 2B, Calu-3 cells were viable after treatment with HA – SAP and HA-CL – SAP solutions within the wide range of concentrations investigated. The half maximal inhibitory concentration (IC<sub>50</sub>) values could not be determined across this concentration interval and, therefore, both the hyaluronan - SAP associations were considered safe for Calu-3 epithelium even with the highest concentration (Fig. 2B).

### 3.3. Evaluation of epithelial barrier integrity

A quantitative measurement of Calu-3 epithelium barrier integrity was performed after 4 h of exposure to 0.15–0.45% (w/v) HA – SAP and HA-CL – SAP, 0.45% (w/v) SAP, 0.15% (w/v) HA and HA-CL solutions. As displayed in Fig. 3, TEER results obtained from the chopstick method showed no significant change ( $P > 0.05$ ) between control untreated cells ( $511 \pm 26 \Omega \text{cm}^2$ ) and cells treated with HA – SAP ( $500 \pm 15 \Omega \text{cm}^2$ ), HA-CL – SAP ( $519 \pm 32 \Omega \text{cm}^2$ ), SAP ( $500 \pm 22 \Omega \text{cm}^2$ ), HA ( $545 \pm 28 \Omega \text{cm}^2$ ) and HA-CL ( $541 \pm 13 \Omega \text{cm}^2$ ), respectively. All the normalized resistance values were thus comparable and no treatment affected the integrity of Calu-3 epithelial monolayer under the time scale and the conditions studied. Hence, subsequent efficacy studies can be performed confidently within the concentrations evaluated.

### 3.4. Pro-inflammatory markers expression

Airway inflammation is a biological response stimulated by several factors –such as genetic factors, endogenous substances, inhalation of exogenous irritants, cigarette smoke and pollutants, environmental factors-, and it represents the most important cause of the progression of acute and chronic lung disorders (MacNee, 2001; Oudijk et al., 2003; Wouters et al., 2007). During lung inflammation, different types of inflammatory cells are activated whereby cytokines, and inflammatory mediators such as IL-6 and IL-8 are released, exacerbating tissue irritations (Tulbah et al., 2016).

IL-6 is a pleiotropic cytokine, with important biological effects on inflammation, immunity and stress (Doganci et al., 2005). IL-6 was found to be overproduced during lung inflammatory processes in response to irritants and viruses, and in asthmatic and COPD patients (Rincon and Irvin, 2012). These evidences suggest that IL-6 plays an active role in the pathogenesis of inflammatory pulmonary diseases with different pathways, involving genetic mechanisms and an increased release of pro-inflammatory cytokines like interleukin-13

**Table 1**  
Physico-chemical properties (pH, osmolality and viscosity) of: 0.15–0.45% (w/v) HA – SAP and HA-CL – SAP, 0.45% (w/v) SAP, 0.15% (w/v) HA and HA-CL solutions (n = 3  $\pm$  StDev).

Test solution	pH	Osmolality (mOsm/Kg)	Viscosity (mPa-s)
Calu-3-medium	7.7 $\pm$ 0.0	310.0 $\pm$ 2.0	1.4 $\pm$ 0.0
HA - SAP	8.1 $\pm$ 0.0	347.0 $\pm$ 1.0	4.5 $\pm$ 0.2
HA-CL - SAP	8.1 $\pm$ 0.0	363.0 $\pm$ 0.0	5.5 $\pm$ 1.0
SAP	8.1 $\pm$ 0.0	351.0 $\pm$ 1.0	1.0 $\pm$ 0.0
HA	7.7 $\pm$ 0.0	312.0 $\pm$ 1.7	8.2 $\pm$ 0.3
HA-CL	7.7 $\pm$ 0.0	335.3 $\pm$ 0.6	12.1 $\pm$ 0.8

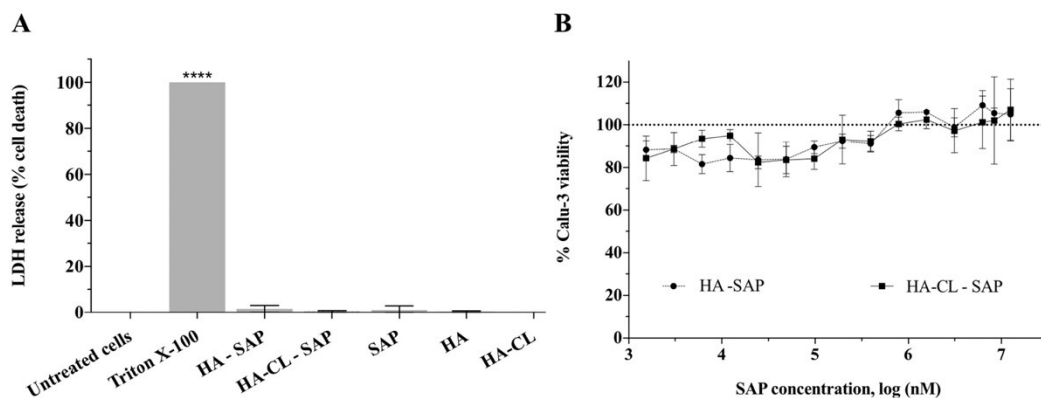


Fig. 2. Viabilities of Calu-3 cells evaluated using: (A) LDH assay and (B) MTS assay after 24 h of treatment with sample solutions. Data represent mean  $\pm$  standard deviation (n = 3). Asterisks indicate significant difference from control untreated cells (\*\*\*\*P < 0.0001).

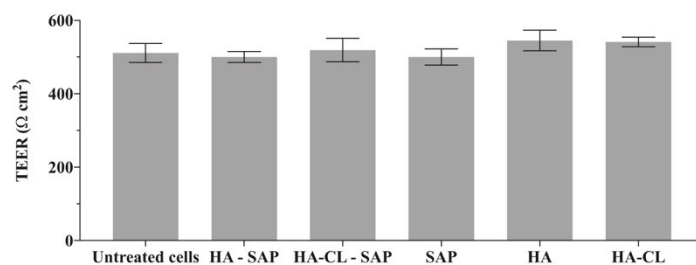


Fig. 3. Transepithelial electrical resistance (TEER, normalized resistance values) of Calu-3 cells after 4 h of treatment with 0.15–0.45% (w/v) hyaluronan-SAP, 0.45% (w/v) SAP, 0.15% (w/v) HA and HA-CL solutions compared to untreated cells (control). Data represent mean  $\pm$  standard deviation (n = 3).

(responsible of mucus secretion) (Rincon and Irvin, 2012) and eotaxin (Ammit et al., 2007).

IL-8 is a potent neutrophil attractant and activator, which is over-expressed in lung diseases like ARDS (Allen and Kurdowska, 2014), COPD, cystic fibrosis and asthma (Mortaz et al., 2011; Ovreik et al., 2011). IL-8 is regulated *via* multiple signalling pathways which involve nuclear factor NF- $\kappa$ B, epidermal growth factor receptor, and MAP kinases, all implicated in the pathogenesis of lung inflammatory diseases (Ovreik et al., 2011).

As previously discussed, emerging data have shown that high-molecular weight hyaluronan can be used as therapeutic agent in inflammatory airway diseases (Allegra et al., 2008; Buonpensiero et al., 2010; Cantor et al., 2005, 2011; Furnari et al., 2012; Garantziotis et al., 2016; Gavina et al., 2013; Jiang et al., 2005; Lennon and Singleton, 2011; Maiz Carro et al., 2012; Petrigli and Allegra, 2006; Savani et al., 2001; Souza-Fernandes et al., 2006; Venge et al., 1996). Therefore, this *in vitro* study investigated if the novel HA-CL compound could provide enhanced anti-inflammatory activity than that of native HA, especially when in combination with SAP.

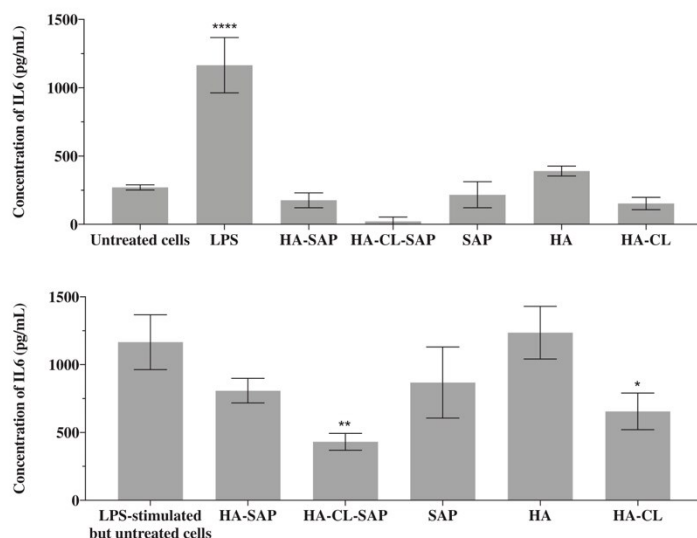
Results showed that HA-CL did not influence IL-8 production, even if combined with SAP, both in non-inflamed and inflamed Calu-3 cells (data not shown). Similarly, IL-6 release was not affected in non-inflamed Calu-3 cells treated with hyaluronan and/or SAP solutions (Fig. 4). On the contrary, exposure to 10 ng/mL LPS significantly increased (P < 0.0001) IL-6 production from 270.7  $\pm$  18.7 pg/mL (untreated cells control) to 1165.7  $\pm$  202.0 pg/mL, as expected (Fig. 4). This was due to the inflammatory effects of LPS, an endotoxin located on the outer membrane of bacteria - such as *Escherichia coli*,

*Staphylococcus aureus* and *Pseudomonas aeruginosa* - (Pier, 2007; Rietschel et al., 1994), responsible of pathological processes, which aggravates chronic lung disorders during a respiratory infection (Cakir et al., 2003).

The anti-inflammatory properties of the test solutions were investigated after stimulation of Calu-3 cells with 10 ng/mL LPS 24 h prior to treatments exposure. IL-6 concentrations were determined 24 h after samples addition on the stimulated Calu-3 cells. With the exception of HA, which maintained an IL-6 level similar to that of non-treated LPS-induced Calu-3 cells (1165.7  $\pm$  202.0 pg/mL), all other treatments showed the ability to reduce IL-6 release (Fig. 5). More specifically, HA - SAP reduced IL-6 concentration to 808.3  $\pm$  90.7 pg/mL, SAP to 868.1  $\pm$  262.1 pg/mL, HA-CL and HA-CL - SAP even to 655.3  $\pm$  135.0 and 431.3  $\pm$  61.7 pg/mL, respectively. Therefore, HA-CL was found to have a statistically significant anti-inflammatory activity towards inflamed Calu-3 cells (P < 0.05), and an enhanced anti-inflammatory effect when combined with SAP (Fig. 5) -P < 0.01.

As oxidative stress is responsible for lung inflammation, both directly and indirectly (Krishna et al., 1998; MacNee, 2001; Santus et al., 2014; Teramoto et al., 1996; Zuo et al., 2013), it was assumed that the antioxidant properties of SAP could improve the anti-inflammatory effect of hyaluronan. This enhanced effect was more evident in the case of HA-CL, probably due to its crosslinking with urea - an active molecule which enhances cellular regeneration and reparation (Albèr et al., 2013; Charlton et al., 1996; Pan et al., 2013) - and, therefore, to its higher molecular weight (2.0–4.0 MDa) in comparison to the native HA (1.2 MDa) from which it was synthesized. Indeed, the biological properties of hyaluronan depend on its size, where only high-molecular





**Fig. 4.** Concentration of IL-6 inflammatory cytokine in unstimulated Calu-3 cells supernatant after 24 h of exposure to 0.15–0.45% (w/v) hyaluronan-SAP, 0.45% (w/v) SAP, 0.15% (w/v) HA and HA-CL solutions, evaluated in comparison to untreated cells and cells treated with 10 ng/mL LPS (positive control). Data represent mean  $\pm$  standard deviation (n = 3). Asterisks indicate significant difference from untreated cells control (\*\*\*\*P < 0.0001).

**Fig. 5.** Concentration of IL-6 inflammatory cytokine in Calu-3 cells supernatant stimulated with 10 ng/mL LPS and then exposed for 24 h to 0.15–0.45% (w/v) hyaluronan-SAP, 0.45% (w/v) SAP, 0.15% (w/v) HA and HA-CL solutions, evaluated in comparison to untreated LPS-stimulated cells (control). Data represent mean  $\pm$  standard deviation (n = 3). Asterisks indicate significant difference from untreated cells control (\*P < 0.05 and \*\*P < 0.01).

weight HA (> 1.0MDa) has shown anti-inflammatory properties (Garantziotis et al., 2016).

### 3.5. Analysis of intracellular ROS

The respiratory system is continually exposed to irritants, dusts, cigarette smoke, pollutants, viruses and bacteria, which cause the production of oxidant species (Holgate, 2011). When the imbalance between pro-oxidants and endogenous antioxidants moves in favour of pro-oxidant molecules, oxidative stress increases (Birben et al., 2012) and stimulates the production of pro-inflammatory mediators, responsible of ROS release by macrophages activation (Kirkham and Rahman, 2006). Thus, oxidative stress and inflammation engages in an endless cycle, which plays an important role in the pathogenesis of lung diseases (Corrigan and Kay, 1991; Kirkham and Rahman, 2006; MacNee, 2001). Considering that both HA and vitamin C seem to have potential as adjunctive treatments of lung diseases with inflammatory and oxidative components, and that SAP has good antioxidant properties when administered topically (Khan et al., 2017; Klock et al., 2005; Spiclin et al., 2003), this study investigated their ability to induce and reduce oxidative stress in Calu-3 cells. Intracellular ROS were quantified after cells treatment with combinations of 0.15–0.45% (w/v) hyaluronan-SAP, and were compared to ROS levels detected in cells exposed to 0.45% (w/v) SAP, 0.15% (w/v) HA and HA-CL, ascorbic acid (negative control), H<sub>2</sub>O<sub>2</sub> (positive control), and untreated cells control.

Results in Fig. 6 showed that hyaluronan and/or SAP solutions did not induce oxidative stress in Calu-3 cells (without LPS stimulation). On the contrary, hyaluronan and/or SAP solutions reduced the basal level of intracellular ROS, compared to untreated cells. Indeed, both the hyaluronan-SAP combinations significantly decreased ROS concentrations compared to untreated cells: HA – SAP to  $57.9 \pm 2.4\%$  (P < 0.001), and HA-CL – SAP to  $23.2 \pm 2.9\%$  (P < 0.0001) (Fig. 6A), respectively. Thus, HA-CL – SAP displayed an activity comparable to that of the negative control ascorbic acid ( $41.3 \pm 3.4\%$ ), and an improved effect with respect to HA – SAP and of the single SAP ( $55.9 \pm 5.9\%$ ), HA ( $82.3 \pm 8.0\%$ ) and HA-CL ( $51.3 \pm 1.0\%$ ) (Fig. 6B), respectively. These data showed an enhanced antioxidant effect due to HA-CL combination with SAP, with HA-CL – SAP

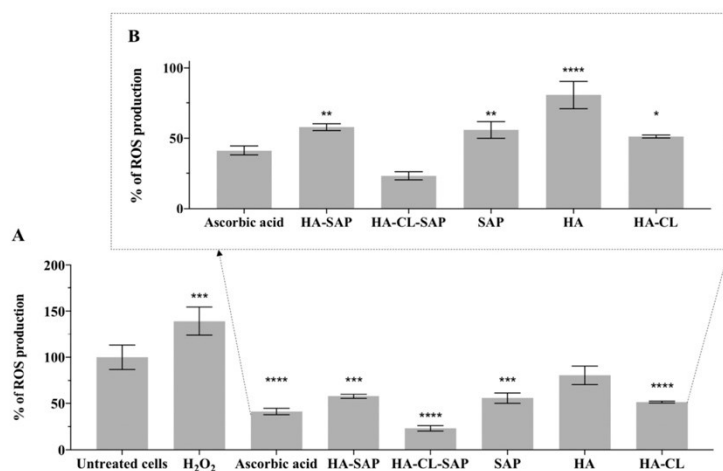
appearing to be the best treatment to provide a potential preventive antioxidant action. On the other hand, the treatment with H<sub>2</sub>O<sub>2</sub> as a positive control resulted in a significant and damaging (Grommes et al., 2012) overproduction of ROS ( $139.1 \pm 15.3\%$ ) (Fig. 6A).

The antioxidant activity of the samples was then studied for their ability to decrease ROS levels in inflamed Calu-3 cells that have been stimulated with 10 ng/mL LPS. All the test solutions significantly reduced ROS production in Calu-3 cells compared to untreated inflamed cells, as displayed in Fig. 7A. More precisely, the combination HA-CL – SAP showed a ROS release of  $84.4 \pm 0.6\%$ , which was significantly lower than those of the association HA – SAP ( $93.2 \pm 1.5\%$ ), and of the single SAP ( $95.7 \pm 0.9\%$ ), HA ( $90.1 \pm 0.4\%$ ) and HA-CL ( $87.9 \pm 0.7\%$ ) (Fig. 7B), respectively. Hence, HA-CL – SAP showed to be the most promising treatment with the highest antioxidant activity.

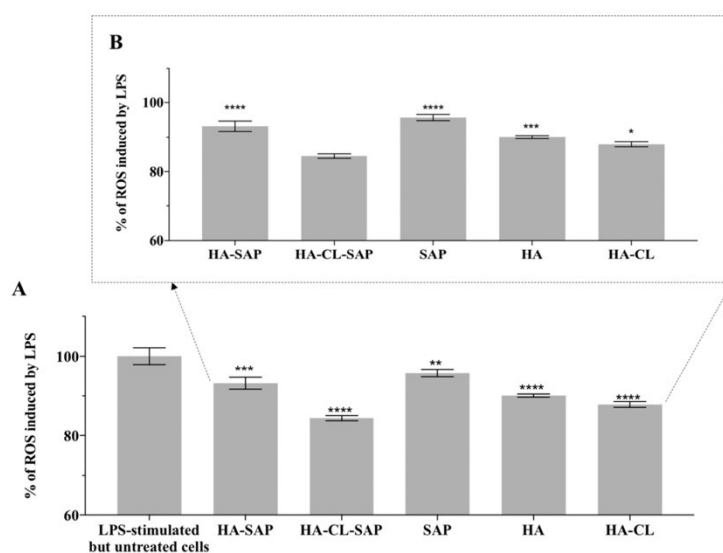
### 3.6. Electric cell-substrate impedance sensing wound healing assay

Although the use of vitamin C and its derivatives to treat lung injury is still investigational, it has been shown that their antioxidant activity attenuates tissue damage and positively affects the functions of airway epithelial barrier (Bharara et al., 2016; Li and Li, 2016). Relative to HA, several studies reported that it plays a crucial role in the reparation and regeneration of lung (Jiang et al., 2005, 2010) and many other tissues, such as skin (Murphy et al., 2017; Papakonstantinou et al., 2012), tympanic membrane (Teh et al., 2012) and corneal epithelium (Gomes et al., 2004; Lee et al., 2015; Wu et al., 2013). Considering the strict correlation between tissue damage, inflammation and oxidative stress, hyaluronan's role in wound healing process cannot be precisely ascribed to any single one of its properties, but it is rather due to the combination of its protective effects (Chen and Abatangelo, 1999; Frenkel, 2014). Hence, the promising results of the anti-inflammatory and antioxidant tests performed during this *in vitro* study lead to the investigation of the wound healing ability. In a previous *in vitro* study, it was demonstrated that the novel HA-CL could induce tissue re-epithelialization (Fallacara et al., 2017b). Nevertheless, this was the first study to evaluate on Calu-3 cells the wound healing efficacy of the combinations 0.15–0.45% (w/v) HA – SAP and HA-CL – SAP, in comparison to the single 0.45% (w/v) SAP, 0.15% (w/v) HA and HA-CL.

As displayed in Fig. 8, resistance decreased sharply upon wounding



**Fig. 6.** Oxidative effects of 0.15–0.45% (w/v) hyaluronan-SAP, 0.45% (w/v) SAP, 0.15% (w/v) HA, 0.15% (w/v) HA-CL solutions, and controls (untreated cells, 0.03% H<sub>2</sub>O<sub>2</sub>, 1 mM L-ascorbic acid) on intracellular ROS production (%) in Calu-3 cells. Data represent mean  $\pm$  standard deviation (n = 3). Asterisks indicate significant differences from untreated cells control (A) and from HA-CL - SAP (B), with \*P < 0.05, \*\*P < 0.01, \*\*\*P < 0.001 and \*\*\*\*P < 0.0001.



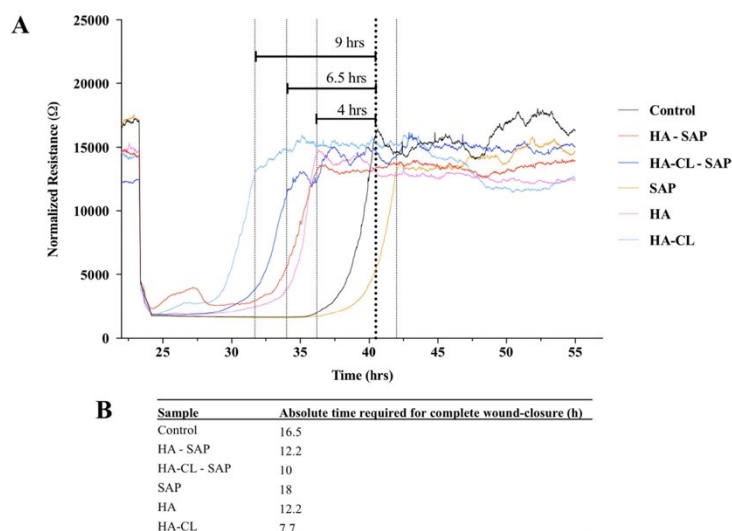
**Fig. 7.** Intracellular ROS production (%) in Calu-3 cells stimulated with 10 ng/mL LPS and then exposed to 0.15–0.45% (w/v) hyaluronan-SAP, 0.45% (w/v) SAP, 0.15% (w/v) HA and HA-CL solutions, evaluated in comparison to untreated control (stimulated but untreated cells). Data represent mean  $\pm$  standard deviation (n = 3). Asterisks indicate significant differences from untreated cells control (A) and from HA-CL - SAP (B), with \*P < 0.05, \*\*P < 0.01, \*\*\*P < 0.001 and \*\*\*\*P < 0.0001.

of the Calu-3 epithelia (after 24 h), and then progressively increased during the healing process to reach a plateau when tissues integrity was completely restored. Our results confirmed the importance of the wound healing activity of hyaluronan (Chen and Abatangelo, 1999; Frenkel, 2014; Jiang et al., 2005, 2010). Indeed, with the exception of SAP, all the treatments increased the rate of wound closure in comparison with untreated wounds (control), which showed a total re-epithelialization after 16.5 h. More precisely, HA - SAP and HA were able to heal the wound almost 4 h before control cells, while HA-CL - SAP and HA-CL 6.5 and 9 h before, respectively (Fig. 8). Therefore, although the combination HA-CL - SAP showed improved healing properties in comparison to HA, SAP and the association HA - SAP, the fastest wound closure ability was exhibited by the single HA-CL, which restored epithelial integrity in 7.7 h. This assay demonstrated that HA-

CL had improved wound healing properties compared to native HA, and that hyaluronan and SAP, used in combination, did not enhance the re-epithelialization of Calu-3 wounded cells.

#### 4. Conclusions

The present *in vitro* study investigated the safety and efficacy of the novel combination HA-CL - SAP in comparison to the association HA - SAP, intended for the treatment and possible prevention of lung diseases with inflammatory and oxidative components. To determine if the combination of the new HA-CL with SAP had an enhanced activity, and if the crosslinked polymer had an enhanced activity with respect to the native compound, the single SAP, HA and HA-CL components were tested. The samples displayed physico-chemical properties (pH,



**Fig. 8.** Wound healing ability of 0.15–0.45% (w/v) hyaluronan-SAP, 0.45% (w/v) SAP, 0.15% (w/v) HA and HA-CL solutions on Calu-3 monolayers wounded with an electrical current (2000  $\mu$ A, 60 s, 100 kHz) applied using the ECIS system. For each sample, the time required for wound closure (vertical dashed line) was calculated as difference from the time employed by control cells (wounded but untreated – vertical dashed line in bold) (A) and additionally reported as absolute time to restore epithelial integrity (B).

osmolality and viscosity) suitable for the airway, and showed to maintain viability and epithelial integrity of Calu-3 cells in the broad range of concentration explored (1.5  $\mu$ M to 12.6 mM). The association HA-CL – SAP showed the highest anti-inflammatory and antioxidant activity, indicating that polymer and drug worked in combination to reduce IL-6 and ROS levels, and that the crosslinked hyaluronan provided further benefits compared to the native one. Although the fastest kinetic of wound closure was exhibited by the single HA-CL, the combination HA-CL – SAP showed improved healing properties with respect to the association HA – SAP and to its single components. Therefore, these results provided preliminary evidence that HA-CL and SAP, if delivered in combination, could be suitable as adjunctive therapy for inflammatory pulmonary disorders.

#### Disclosure

The authors declare no conflict of interest.

#### Acknowledgements

This work was supported by a PhD grant (to Arianna Fallacara) from IRAlab Srl (Usmate-Velate, Monza-Brianza, Italy). The authors thank the University of Ferrara (Ferrara, Italy, Grant Fir 2016 to Silvia Vertuani) and Ambrosialab s.r.l. (Ferrara, Italy, Grant 2016 to Stefano Manfredini) for the financial support.

#### References

- Albèr, C., Brandner, B.D., Björklund, S., Billsten, P., Corkery, R.W., Engblom, J., 2013. Effects of water gradients and use of urea on skin ultrastructure evaluated by confocal Raman microspectroscopy. *Biochim. Biophys. Acta* 1828, 2470–2478.
- Alhanout, K., Brunel, J.M., Dubus, J.C., Rolain, J.M., Andrieu, V., 2011. Suitability of a new antimicrobial aminosterol formulation for aerosol delivery in cystic fibrosis. *J. Antimicrob. Chemother.* 66, 2797–2800.
- Allegra, L., Abraham, W.M., Fasano, V., Petrigli, G., 2008. Methacholine challenge in asthmatics is protected by aerosolised hyaluronan at high (1,000 kDa) but not low (300 kDa) molecular weight. *G. Ital. Mal. Torace* 62, 297–301.
- Allen, T.C., Kurdowska, A., 2014. Interleukin 8 and acute lung injury. *Arch. Pathol. Lab. Med.* 138, 266–269.
- Amirlak, B., Mahedia, M., Shah, N., 2016. A clinical evaluation of efficacy and safety of hyaluronan sponge with vitamin C versus placebo for scar reduction. *Plast. Reconstr. Surg. Glob. Open.* 4, e792.

- Ammit, A.J., Moir, L.M., Oliver, B.G., Hughes, J.M., Alkhoury, H., Ge, Q., Burgess, J.K., Black, J.L., Roth, M., 2007. Effect of IL-6 trans-signaling on the pro-remodeling phenotype of airway smooth muscle. *Am. J. Phys. Lung Cell. Mol. Phys.* 292, L199–L206.
- Balasubramanian, L., Yip, K.P., Hsu, T.H., Lo, C.M., 2008. Impedance analysis of renal vascular smooth muscle cells. *Am. J. Phys. Cell Phys.* 295, C954–C965.
- Barnes, P.J., 2013. Corticosteroid resistance in patients with asthma and chronic obstructive pulmonary disease. *J. Allergy Clin. Immunol.* 131, 636–645.
- Berger, M.M., Oudemans-van Straaten, H.M., 2015. Vitamin C supplementation in the critically ill patient. *Curr. Opin. Clin. Nutr. Metab. Care* 18, 193–201.
- Bharara, A., Grossman, C., Grinnan, D., Syed, A., Fisher, B., DeWilde, C., Natarajan, R., Fowler, A.A., 2016. Intravenous vitamin C administered as adjunctive therapy for recurrent acute respiratory distress syndrome. *Case Rep. Crit. Care.* <http://dx.doi.org/10.1155/2016/8560871>.
- Birben, E., Sahiner, U.M., Sackesen, C., Erzurum, S., Kalayci, O., 2012. Oxidative stress and antioxidant defense. *World Allergy Organ. J.* 5, 9–19.
- Bracher, A., Doran, S.F., Squadrito, G.L., Postlethwait, E.M., Bowen, L., Matalon, S., 2012. Targeted aerosolized delivery of ascorbate in the lungs of chlorine-exposed rats. *J. Aerosol Med. Pulm. Drug Deliv.* 25, 333–341.
- Buonpensiero, P., De Gregorio, F., Sepe, A., Di Pasqua, A., Ferri, P., Siano, M., Terlizzi, V., Raia, V., 2010. Hyaluronic acid improves “pleasantness” and tolerability of nebulized hypertonic saline in a cohort of patients with cystic fibrosis. *Adv. Ther.* 27, 870–878.
- Burney, P., Jarvis, D., Perez-Padilla, R., 2015. The global burden of chronic respiratory disease in adults. *Int. J. Tuberc. Lung Dis.* 19, 10–20.
- Cakir, O., Oruc, A., Eren, S., Buyukbayram, H., Erdinc, L., Eren, N., 2003. Does sodium nitroprusside reduce lung injury under cardiopulmonary bypass? *Eur. J. Cardiothorac. Surg.* 23, 1040–1045.
- Cantor, J.O., Cerreta, J.M., Ochoa, M., Ma, S., Chow, T., Grunig, G., Turino, G.M., 2005. Aerosolized hyaluronan limits airspace enlargement in a mouse model of cigarette smoke-induced pulmonary emphysema. *Exp. Lung Res.* 31, 417–430.
- Cantor, J.O., Cerreta, J.M., Ochoa, M., Ma, S., Liu, M., Turino, G.M., 2011. Therapeutic effects of hyaluronan on smoke-induced elastic fiber injury: does delayed treatment affect efficacy? *Lung* 189, 51–56.
- Chan, F.K.M., Moriawaki, K., De Rosa, M.J., 2013. Detection of necrosis by release of lactate dehydrogenase (LDH) activity. In: *Methods in Molecular Biology*. Clifton, N.J. 979, pp. 65–70.
- Charlton, J.F., Schwab, I.R., Stuchell, R., 1996. Topical urea as a treatment for non-infectious keratopathy. *Acta Ophthalmol. Scand.* 74, 391–394.
- Chen, W.Y., Abatangelo, G., 1999. Functions of hyaluronan in wound repair. *Wound Repair Regen.* 7, 79–89.
- Citernes, U.R., Beretta, L., Citernes, L., 2015. Cross-linked hyaluronic acid, process for the preparation thereof and use thereof in the aesthetic field. Patent number: WO/2015/007773 A1.
- Corrigan, C., Kay, A., 1991. The roles of inflammatory cells in the pathogenesis of asthma and chronic obstructive pulmonary disease. *Am. Rev. Respir. Dis.* 143, 1165–1168.
- Cross, M.M., 1968. *Polymer Systems: Deformation and Flow*. Wetton RE, Whorlow RW. Crotty Alexander, L.E., Shin, S., Hwang, J.H., 2015. Inflammatory diseases of the lung induced by conventional cigarette smoke: a review. *Chest* 148, 1307–1322.
- Doganci, A., Sauer, K., Karwot, R., Finotto, S., 2005. Pathological role of IL-6 in the experimental allergic bronchial asthma in mice. *Clin. Rev. Allergy Immunol.* 28, 257–270.



- Duarte, T.L., Cooke, M.S., Jones, G.D., 2009. Gene expression profiling reveals new protective roles for vitamin C in human skin cells. *Free Radic. Biol. Med.* 46, 78–87.
- Fallacara, A., Manfredini, S., Durini, E., Vertuani, S., 2017a. Hyaluronic acid fillers in soft tissue regeneration. *Facial Plast. Surg.* 33, 87–96.
- Fallacara, A., Vertuani, S., Panozzo, G., Pecorelli, A., Valacchi, G., Manfredini, S., 2017b. Novel artificial tears containing cross-linked hyaluronic acid: an in vitro re-epithelialization study. *Molecules* 22.
- Ferkol, T., Schraufnagel, D., 2014. The global burden of respiratory disease. *Ann. Am. Thorac. Soc.* 11, 404–406.
- Fisher, B.J., Kraskauskas, D., Martin, E.J., Farkas, D., Wegelin, J.A., Brophy, D., Ward, K.R., Voelkel, N.F., Fowler 3rd, A.A., Natarajan, R., 2012. Mechanisms of attenuation of abdominal sepsis induced acute lung injury by ascorbic acid. *Am. J. Phys. Lung Cell. Mol. Phys.* 303, L20–L32.
- Forbes, B., Hashmi, N., Martin, G.P., Lansley, A.B., 2000. Formulation of inhaled medicines: effect of delivery vehicle on immortalized epithelial cells. *J. Aerosol Med.* 13, 281–288.
- Frenkel, J.S., 2014. The role of hyaluronan in wound healing. *Int. Wound J.* 11, 159–163.
- Furnari, M.L., Termini, L., Traverso, G., Barrale, S., Bonaccorso, M.R., Damiani, G., Piparo, C.L., Collura, M., 2012. Nebulized hypertonic saline containing hyaluronic acid improves tolerability in patients with cystic fibrosis and lung disease compared with nebulized hypertonic saline alone: a prospective, randomized, double-blind, controlled study. *Thorax* 67, 315–322.
- Garantziotis, S., Brezina, M., Castelnovo, P., Drago, L., 2016. The role of hyaluronan in the pathobiology and treatment of respiratory disease. *Am. J. Phys. Lung Cell. Mol. Phys.* 310, L785–L795.
- García-Larsen, V., Del Giacco, S.R., Moreira, A., Bonini, M., Charles, D., Reeves, T., Carlsen, K.H., Hahtela, T., Bonini, S., Fonseca, J., Agache, I., Papadopoulos, N.G., Delgado, L., 2016. Asthma and dietary intake: an overview of systematic reviews. *Allergy* 71, 433–442.
- Gavina, M., Luciani, A., Vilella, V.R., Esposito, S., Ferrari, E., Bressani, I., Casale, A., Bruscia, E.M., Mairui, L., Raia, V., 2013. Nebulized hyaluronan ameliorates lung inflammation in cystic fibrosis mice. *Pediatr. Pulmonol.* 48, 761–771.
- Geesin, J.C., Gordon, J.S., Berg, R.A., 1993. Regulation of collagen synthesis in human dermal fibroblasts by the sodium and magnesium salts of ascorbyl-2-phosphate. *Skin Pharmacol.* 6, 65–71.
- Gelardi, M., Iannuzzi, L., Quaranta, N., 2013. Intranasal sodium hyaluronate on the nasal cytology of patients with allergic and nonallergic rhinitis. *Int. Forum Allergy Rhinol.* 3, 807–813.
- Gerdin, B., Hällgren, R., 1997. Dynamic role of hyaluronan (HYA) in connective tissue activation and inflammation. *J. Intern. Med.* 242, 49–55.
- Gomes, J.A.P., Amankwah, R., Powell-Richards, A., Dua, H.S., 2004. Sodium hyaluronate (hyaluronic acid) promotes migration of human corneal epithelial cells in vitro. *Br. J. Ophthalmol.* 88.
- Grommes, J., Vijayan, S., Drechsler, M., Hartwig, H., Morgelin, M., Dembinski, R., Jacobs, M., Koepfel, T.A., Binnebösel, M., Weber, C., Soehnle, O., 2012. Simvastatin reduces endotoxin-induced acute lung injury by decreasing neutrophil recruitment and radical formation. *PLoS One* 7, e38917.
- Gupta, I., Ganguly, S., Rozanas, C.R., Stuehr, D.J., Panda, K., 2016. Ascorbate attenuates pulmonary emphysema by inhibiting tobacco smoke and Rtp801-triggered lung protein modification and proteolysis. *Proc. Natl. Acad. Sci. U. S. A.* 113, E4208–E4217.
- Haghi, M., Young, P.M., Traini, D., Jaiswal, R., Gong, J., Bewawy, M., 2010. Time- and passage-dependent characteristics of a Calu-3 respiratory epithelial cell model. *Drug Dev. Ind. Pharm.* 36, 1207–1214.
- Hemilä, H., 2013. Vitamin C and common cold-induced asthma: a systematic review and statistical analysis. *Allergy, Asthma Clin. Immunol.* 9, 46.
- Hemilä, H., 2014. The effect of vitamin C on bronchoconstriction and respiratory symptoms caused by exercise: a review and statistical analysis. *Allergy, Asthma Clin. Immunol.* 10, 58.
- Hemilä, H., Louhiala, P., 2007. Vitamin C may affect lung infections. *J. R. Soc. Med.* 100, 495–498.
- Holgate, S.T., 2011. The sentinel role of the airway epithelium in asthma pathogenesis. *Immunol. Rev.* 242, 205–219.
- Jiang, Z., Zhu, L., 2016. Update on molecular mechanisms of corticosteroid resistance in chronic obstructive pulmonary disease. *Pulm. Pharmacol. Ther.* 37, 1–8.
- Jiang, D., Liang, J., Fan, J., Yu, S., Chen, S., Luo, Y., Prestwich, G.D., Mascarenhas, M.M., Garg, H.G., Quinn, D.A., Homer, R.J., Goldstein, D.R., Bucala, R., Lee, P.J., Medzhitov, R., Noble, P.W., 2005. Regulation of lung injury and repair by Toll-like receptors and hyaluronan. *Nat. Med.* 11, 1173–1179.
- Jiang, D., Liang, J., Noble, P.W., 2010. Regulation of non-infectious lung injury, inflammation, and repair by the extracellular matrix glycosaminoglycan hyaluronan. *Anat. Rec. (Hoboken)* 293, 982–985.
- Jin, X., Su, R., Li, R., Song, L., Chen, M., Cheng, L., Li, Z., 2016. Amelioration of particulate matter-induced oxidative damage by vitamin C and quercetin in human bronchial epithelial cells. *Chemosphere* 144, 459–466.
- Kakehi, K., Kinoshita, M., Yasueda, S., 2003. Hyaluronic acid: separation and biological implications. *J. Chromatogr. B Anal. Technol. Biomed. Life Sci.* 797, 347–355.
- Khan, H., Akhtar, N., Ali, A., 2017. Assessment of combined ascorbyl palmitate (AP) and sodium ascorbyl phosphate (SAP) on facial skin sebum control in female healthy volunteers. *Drug Res. (Stuttg)* 67, 52–58.
- Kirkham, P., Rahman, I., 2006. Oxidative stress in asthma and COPD: antioxidants as a therapeutic strategy. *Pharmacol. Ther.* 111, 476–494.
- Kleniewska, P., Pawliczak, R., 2017. The participation of oxidative stress in the pathogenesis of bronchial asthma. *Biomed. Pharmacother.* 94, 100–108.
- Klock, J., Ikeno, H., Ohmori, K., Nishikawa, T., Vollhardt, J., Schehlmann, V., 2005. Sodium ascorbyl phosphate shows in vitro and in vivo efficacy in the prevention and treatment of acne vulgaris. *Int. J. Cosmet. Sci.* 27, 171–176.
- Koike, K., Ishigami, A., Sato, Y., Hirai, T., Yuan, Y., Kobayashi, E., Tobino, K., Sato, T., Sekiya, M., Takahashi, K., Fukuchi, Y., Maruyama, N., Seyama, K., 2014. Vitamin C prevents cigarette smoke-induced pulmonary emphysema in mice and provides pulmonary restoration. *Am. J. Respir. Cell Mol. Biol.* 50, 347–357.
- Krishna, M.T., Madden, J., Teran, L.M., Biscione, G.L., Lau, L.C., Withers, N.J., Sandström, T., Mudway, I., Kelly, F.J., Walls, A., Frew, A.J., Holgate, S.T., 1998. Effects of 0.2 ppm ozone on biomarkers of inflammation in bronchoalveolar lavage fluid and bronchial mucosa of healthy subjects. *Eur. Respir. J.* 11, 1294–1300.
- Larsson, N., Rankin, G.D., Bicer, E.M., Roos-Engstrand, E., Pourazar, J., Blomberg, A., Mudway, I.S., Behndig, A.F., 2015. Identification of vitamin C transporters in the human airways: a cross-sectional in vivo study. *BMJ Open* 5, e006979.
- Lee, J.S., Lee, S.U., Che, C.Y., Lee, J.E., 2015. Comparison of cytotoxicity and wound healing effect of carboxymethylcellulose and hyaluronic acid on human corneal epithelial cells. *Int. J. Ophthalmol.* 8, 215–221.
- Lennon, F.E., Singleton, P.A., 2011. Role of hyaluronan and hyaluronan-binding proteins in lung pathobiology. *Am. J. Phys. Lung Cell. Mol. Phys.* 301, L137–L147.
- Li, Y., Li, G., 2016. Is vitamin C beneficial to patients with CAP? *Curr. Infect. Dis. Rep.* 18, 24.
- Li, Y., Han, M., Liu, T., Cun, D., Fang, L., Yang, M., 2017. Inhaled hyaluronic acid microparticles extended pulmonary retention and suppressed systemic exposure of a short-acting bronchodilator. *Carbohydr. Polym.* 172, 197–204.
- Liao, Y.H., Jones, S.A., Forbes, B., Martin, G.P., Brown, M.B., 2005. Hyaluronan: pharmaceutical characterization and drug delivery. *Drug Deliv.* 12, 327–342.
- MacNee, W., 2001. Oxidative stress and lung inflammation in airways disease. *Eur. J. Pharmacol.* 429, 195–207.
- Maiz Carro, L., Lamas Ferreira, A., Ruiz de Valbuena Maiz, M., Wagner Struwing, C., Gabilondo Alvarez, G., Suarez Cortina, L., 2012. Tolerance of two inhaled hypertonic saline solutions in patients with cystic fibrosis. *Med. Clin. (Barc.)* 138, 57–59.
- Martinelli, F., Balducci, A.G., Kumar, A., Sonvico, F., Forbes, B., Bettini, R., Buttini, F., 2017. Engineered sodium hyaluronate respirable dry powders for pulmonary drug delivery. *Int. J. Pharm.* 517, 286–295.
- Mayol, L., Quaglia, F., Borzacchiello, A., Ambrosio, L., La Rotonda, M.I., 2008. A novel poloxamers/hyaluronic acid in situ forming hydrogel for drug delivery: rheological, mucoadhesive and in vitro release properties. *Eur. J. Pharm. Biopharm.* 70, 199–206.
- Moldoveanu, B., Otmishi, P., Jani, P., Walker, J., Sarmiento, S., Guardiola, J., Saad, M., Yu, J., 2009. Inflammatory mechanisms in the lung. *J. Inflamm. Res.* 2, 1–11.
- Morimoto, K., Metsugi, K., Katsumata, H., Iwanaga, K., Kakemi, M., 2001. Effects of low-viscosity sodium hyaluronate preparation on the pulmonary absorption of rh-insulin in rats. *Drug Dev. Ind. Pharm.* 27, 365–371.
- Mortaz, E., Henricks, P.A., Kraneveld, A.D., Givi, M.E., Garsen, J., Folkerts, G., 2011. Cigarette smoke induces the release of CXCL8 from human bronchial epithelial cells via TLRs and induction of the inflammasome. *Biochim. Biophys. Acta* 1812, 1104–1110.
- Murphy, S.V., Skardal, A., Song, L., Sutton, K., Haug, R., Mack, D.L., Jackson, J., Soker, S., Atala, A., 2017. Solubilized anionic membrane hyaluronic acid hydrogel accelerates full-thickness wound healing. *Stem Cells Transl. Med.* 6, 2020–2032.
- Nenna, R., Papasso, S., Battaglia, M., De Angelis, D., Petrarca, L., Felder, D., Salvadei, S., Berardi, R., Roberti, M., Papoff, P., Moretti, C., Midulla, F., 2011. 7% hypertonic saline and hyaluronic acid and in the treatment of infants mild-moderate bronchiolitis. *Eur. Respir. J.* 38, 1717.
- Nichols, D.P., Chmiel, J.F., 2015. Inflammation and its genesis in cystic fibrosis. *Pediatr. Pulmonol.* 50, S539–56.
- Oudijk, E.D., Lammers, J.J., Koenderman, L., 2003. Systemic inflammation in chronic obstructive pulmonary disease. *Eur. Respir. J.* 22, 58–138.
- Ovevik, J., Refsnes, M., Totlandsdal, A.L., Holme, J.A., Schwarzer, P.E., Låg, M., 2011. TACE/TGF- $\alpha$ /EGFR regulates CXCL8 in bronchial epithelial cells exposed to particulate matter components. *Eur. Respir. J.* 38, 1189–1199.
- Pan, M., Heinecke, G., Bernardo, S., Tsui, C., Levitt, J., 2013. Urea: a comprehensive review of the clinical literature. *Dermatol. Online J.* 19.
- Papakonstantinou, E., Roth, M., Karakiulakis, G., 2012. Hyaluronic acid: a key molecule in skin aging. *Dermatoendocrinol.* 4, 253–258.
- Park, H.J., Byun, M.K., Kim, H.J., Kim, J.Y., Kim, Y.L., Yoo, K.H., Chun, E.M., Jung, J.Y., Lee, S.H., Ahn, C.M., 2016. Dietary vitamin C intake protects against COPD: the Korea National Health and Nutrition Examination Survey in 2012. *Int. J. Chron. Obstruct. Pulmon. Dis.* 11, 2721–2728.
- Petrigli, G., Allegra, L., 2006. Aerosolised hyaluronic acid prevents exercise-induced bronchoconstriction, suggesting novel hypotheses on the correction of matrix defects in asthma. *Pulm. Pharmacol. Ther.* 19, 166–171.
- Pier, G.B., 2007. *Pseudomonas aeruginosa* lipopolysaccharide: a major virulence factor, initiator of inflammation and target for effective immunity. *Int. J. Med. Microbiol.* 297, 277–295.
- Pincikova, T., Paquin-Proulx, D., Sandberg, J.K., Flodström-Tullberg, M., Hjelt, L., 2017. Vitamin D treatment modulates immune activation in cystic fibrosis. *Clin. Exp. Immunol.* 189, 359–371.
- Pirabbasi, E., Shahar, S., Manaf, Z.A., Rajab, N.F., Manap, R.A., 2016. Efficacy of ascorbic acid (vitamin C) and N-acetylcysteine (NAC) supplementation on nutritional and antioxidant status of male chronic obstructive pulmonary disease (COPD) patients. *J. Nutr. Sci. Vitaminol. (Tokyo)* 62, 54–61.
- Rietschel, E.T., Kirikae, T., Schade, F.U., Mamat, U., Schmidt, G., Loppnow, H., Ulmer, A.J., Zähringer, U., Seydel, U., Di Padova, F., Schreier, M., Brade, H., 1994. Bacterial endotoxin: molecular relationships of structure to activity and function. *FASEB J.* 8, 217–225.
- Rincon, M., Irvin, C.G., 2012. Role of IL-6 in asthma and other inflammatory pulmonary diseases. *Int. J. Biol. Sci.* 8, 1281–1290.
- Riss, T.L., Moravec, R.A., Niles, A.L., Duellman, S., Benink, H.A., Worzella, T.J., Minor, L.,



2004. Cell viability assays. In: Sittampalam, G.S., Coussens, N.P., Brimacombe, K., Grossman, A., Arkin, M., Auld, D., Austin, C., Baell, J., Bejcek, B., Chung, T.D.Y., Dahlin, J.L., Devanaryan, V., Foley, T.L., Glicksman, M., Hall, M.D., Hass, J.V., Ingles, J., Iversen, P.W., Kahl, S.D., Kales, S.C., Lal-Nag, M., Li, Z., McGee, J., McManus, O., Riss, T., Trask Jr.O.J., Weidner, J.R., Xia, M., Xu, X. (Eds.), *Assay Guidance Manual*, Bethesda (MD), <http://dx.doi.org/10.1590/S1806-83242009000300006>.
- Santus, P., Corsico, A., Solidoro, P., Braidò, F., Di Marco, F., Scichilone, N., 2014. Oxidative stress and respiratory system: pharmacological and clinical reappraisal of N-acetylcysteine. *COPD* 11, 705–717.
- Savani, R.C., Cao, G., Pooler, P.M., Zaman, A., Zhou, Z., DeLisser, H.M., 2001. Differential involvement of the hyaluronan (HA) receptors CD44 and receptor for HA-mediated motility in endothelial cell function and angiogenesis. *J. Biol. Chem.* 276, 36770–36778.
- Sawyer, M.A.J., Mike, J.J., Chavin, K., 1989. Antioxidant therapy and survival in ARDS. *Crit. Care Med.* 17.
- Silva Bezerra, F., Valença, S.S., Lanzetti, M., Pimenta, W.A., Castro, P., Gonçalves Koatz, V.L., Porto, L.C., 2006. Alpha-tocopherol and ascorbic acid supplementation reduced acute lung inflammatory response by cigarette smoke in mouse. *Nutrition* 22, 1192–1201.
- Souza-Fernandes, A.B., Pelosi, P., Rocco, P.R., 2006. Bench-to-bedside review: the role of glycosaminoglycans in respiratory disease. *Crit. Care* 10, 237.
- Spiclin, P., Homar, M., Zupanic-Valant, A., Gasperlin, M., 2003. Sodium ascorbyl phosphate in topical microemulsions. *Int. J. Pharm.* 256, 65–73.
- Stolwijk, J.A., Matrougui, K., Renken, C.W., Trebak, M., 2015. Impedance analysis of GPCR-mediated changes in endothelial barrier function: overview and fundamental considerations for stable and reproducible measurements. *Pflugers Arch.* 467, 2193–2218.
- Stumpf, U., Michaelis, M., Klassert, D., Cinatl, J., Altrichter, J., Windolf, J., Hergenröther, J., Scholz, M., 2011. Selection of proangiogenic ascorbate derivatives and their exploitation in a novel drug-releasing system for wound healing. *Wound Repair Regen.* 19, 597–607.
- Surendrakumar, K., Martyn, G.P., Hodgson, E.C., Jansen, M., Blair, J.A., 2003. Sustained release of insulin from sodium hyaluronate based dry powder formulations after pulmonary delivery to beagle dogs. *J. Control. Release* 91, 385–394.
- Teh, B.M., Shen, Y., Friedland, P.L., Atlas, M.D., Marano, R.J., 2012. A review on the use of hyaluronic acid in tympanic membrane wound healing. *Expert. Opin. Biol. Ther.* 12, 23–36.
- Teramoto, S., Shu, C.Y., Ouchi, Y., Fukuchi, Y., 1996. Increased spontaneous production and generation of superoxide anion by blood neutrophils in patients with asthma. *J. Asthma* 33, 149–155.
- Toole, B.P., 2004. Hyaluronan: from extracellular glue to pericellular cue. *Nat. Rev. Cancer* 4, 528–539.
- Tulbah, A.S., Ong, H.X., Lee, W.H., Colombo, P., Young, P.M., Traini, D., 2016. Biological effects of simvastatin formulated as pMDI on pulmonary epithelial cells. *Pharm. Res.* 33, 92–101.
- Turino, G.M., Cantor, J.O., 2003. Hyaluronan in respiratory injury and repair. *Am. J. Respir. Crit. Care Med.* 167, 1169–1175.
- Venge, P., Pedersen, B., Hakansson, L., Hallgren, R., Lindblad, G., Dahl, R., 1996. Subcutaneous administration of hyaluronan reduces the number of infectious exacerbations in patients with chronic bronchitis. *Am. J. Respir. Crit. Care Med.* 153, 312–316.
- Williams, D.L., Wirotko, B.M., Gum, G., Mann, B.K., 2017. Topical cross-linked HA-based hydrogel accelerates closure of corneal epithelial defects and repair of stromal ulceration in companion animals. *Invest. Ophthalmol. Vis. Sci.* 58, 4616–4622.
- Wong-Beringer, A., Lambros, M.P., Beringer, P.M., Johnson, D.L., 2005. Suitability of caspofungin for aerosol delivery: physicochemical profiling and nebulizer choice. *Chest* 128, 3711–3716.
- World Health Organization, 2017. *World Health Statistics 2017: Monitoring Health for the SDGs, Sustainable Development Goals*. World Health Organization, Geneva.
- Wouters, E.F., Groenewegen, K.H., Dentener, M.A., Vernooy, J.H., 2007. Systemic inflammation in chronic obstructive pulmonary disease: the role of exacerbations. *Proc. Am. Thorac. Soc.* 4, 626–634.
- Wu, D., Yotnda, P., 2011. Production and detection of reactive oxygen species (ROS) in cancers. *J. Vis. Exp.* 57 (pii: 3357).
- Wu, C.L., Chou, H.C., Li, J.M., Chen, Y.W., Chen, J.H., Chen, Y.H., Chan, H.L., 2013. Hyaluronic acid-dependent protection against alkali-burned human corneal cells. *Electrophoresis* 34, 388–396.
- Yamamoto, A., Yamada, K., Muramatsu, H., Nishinaka, A., Okumura, S., Okada, N., Fujita, T., Muranishi, S., 2004. Control of pulmonary absorption of water-soluble compounds by various viscous vehicles. *Int. J. Pharm.* 282, 141–149.
- Yang, I.V., Lozupone, C.A., Schwartz, D.A., 2017. The environment, epigenome, and asthma. *J. Allergy Clin. Immunol.* 140, 14–23.
- Yeo, S.C.M., Fenwick, P.S., Barnes, P.J., Lin, H.S., Donnelly, L.E., 2017. Isorhapontigenin, a bioavailable dietary polyphenol, suppresses airway epithelial cell inflammation through a corticosteroid-independent mechanism. *Br. J. Pharmacol.* 174, 2043–2059.
- Zemmouri, H., Sekiou, O., Ammar, S., El Feki, A., Bouaziz, M., Messarah, M., Boumendjel, A., 2017. *Urtica dioica* attenuates ovalbumin-induced inflammation and lipid peroxidation of lung tissues in rat asthma model. *Pharm. Biol.* 55, 1561–1568.
- Zuo, L., Otenbaker, N.P., Rose, B.A., Salisbury, K.S., 2013. Molecular mechanisms of reactive oxygen species-related pulmonary inflammation and asthma. *Mol. Immunol.* 56, 57–63.